



**RT-100 Type B Cask
Safety Analysis Report
Docket Number 71-9365**

Revision 7

December 5, 2018



This Part 71 Application for Approval of RT-100 Type B Cask Package for Radioactive Material represents Robatel Technologies, LLC approach to its business as applied to the specifications of this submittal. This Application requests that the Nuclear Regulatory Commission respects the proprietary information and withholds it from public disclosure subject to the provisions of 10 CFR 2.390. All detailed drawings are considered proprietary information.

TABLE OF CONTENTS

1. GENERAL INFORMATION.....	1-1
1.1 Introduction.....	1-1
1.2 Package Description.....	1-3
1.2.1 Packaging.....	1-3
1.2.1.1 Overall Dimensions	1-3
1.2.1.2 Weight	1-4
1.2.1.3 Containment Features	1-4
1.2.1.4 Neutron and Gamma Shielding Features	1-4
1.2.1.5 Shielding Features for Personnel Barriers	1-4
1.2.1.6 Criticality Control Features.....	1-4
1.2.1.7 Structural Features – Lifting and Tie-Down Devices	1-4
1.2.1.8 Structural Features – Impact Limiters.....	1-5
1.2.1.9 Structural Features – Internal Supporting or Positioning Features.....	1-5
1.2.1.10 Structural Features – Outer Shell or Outer Packaging.....	1-5
1.2.1.11 Structural Features – Packaging Closure Device.....	1-6
1.2.1.12 Structural Features – Heat Transfer Features	1-6
1.2.1.13 Structural Features – Packaging Markings	1-6
1.2.1.14 Additional Information	1-6
1.2.2 Contents	1-6
1.2.2.1 Identification and Maximum Quantity of Radioactive Material	1-7
1.2.2.2 Identification and Maximum Quantity of Fissile Material	1-7
1.2.2.3 Physical and Chemical Form – Density, Moisture Content and Moderators	1-7
1.2.2.3.1 Ion-Exchange Resins.....	1-7
1.2.2.3.2 Filters.....	1-8
1.2.2.3.3 Secondary Containers.....	1-8
1.2.2.4 Location and Configuration	1-8
1.2.2.5 Use of Non-Fissile Materials as Neutron Absorbers/Moderators	1-8
1.2.2.6 Chemical/Galvanic/Gas Generation	1-8
1.2.2.7 Maximum Weight of Contents and Payload	1-9
1.2.2.8 Maximum Decay Heat.....	1-9
1.2.2.9 Loading Restrictions.....	1-10
1.2.2.10 Contents for the Certificate of Compliance	1-10

1.2.3 Special Requirements for Plutonium	1-10
1.2.4 Operational Features	1-10
1.3 Engineering Drawings and Additional Information	1-11
1.3.1 Engineering Drawings	1-11
1.3.2 Conformance to Approved Design	1-11
1.3.3 Referenced Pages	1-11
1.3.4 Special Fabrication Procedures	1-11
1.3.5 Package Category	1-11
1.3.6 Supplemental Information.....	1-11
1.4 Appendix.....	1-12
1.5 References	1-27
2. STRUCTURAL EVALUATION	2-1
2.1 Description of Structural Design	2-1
2.1.1 Discussion	2-3
2.1.1.1 Containment Boundary	2-4
2.1.2 Design Criteria	2-4
2.1.2.1 Cask Body Criteria (except Bolts and O-Rings)	2-5
2.1.2.2 Bolts.....	2-5
2.1.2.3 Lead	2-6
2.1.2.4 Foam.....	2-6
2.1.3 Weights and Centers of Gravity	2-6
2.1.4 Identification of Codes and Standards for Package Design	2-7
2.2 Materials	2-8
2.2.1 Material Properties and Specifications	2-8
2.2.2 Chemical, Galvanic, or Other Reactions.....	2-10
2.2.2.1 Component Material Categories.....	2-10
2.2.2.1.1 Stainless/Nickel Alloy Steels	2-11
2.2.2.1.2 Nonferrous Metals.....	2-11
2.2.2.1.3 Shielding Materials	2-11
2.2.2.1.4 Criticality Control Material.....	2-12
2.2.2.1.5 Energy Absorbing Material	2-12
2.2.2.1.6 Cellular Foam and Insulation.....	2-12
2.2.2.1.7 Lubricant and Grease.....	2-12

2.2.2.1.8 O-Rings.....	2-12
2.2.2.1.9 Secondary Containers and Shoring	2-12
2.2.2.1.10 Filters.....	2-12
2.2.2.2 General Effects of Identified Reactions	2-12
2.2.2.3 Adequacy of the Cask Operating Procedures.....	2-13
2.2.2.4 Effects of Reaction Products.....	2-13
2.2.3 Effects of Radiation on Materials	2-13
2.3 Fabrication and Examination.....	2-13
2.3.1 Fabrication	2-13
2.3.2 Examination	2-13
2.4 General Requirements for All Packages.....	2-14
2.4.1 Minimum Package Size	2-14
2.4.2 Tamper-Indicating Feature.....	2-14
2.4.3 Positive Closure.....	2-14
2.5 Lifting and Tie-Down Standards for All Packages	2-14
2.5.1 Lifting Devices.....	2-14
2.5.1.1 Lifting Design Criteria.....	2-15
2.5.1.2 Lifting Device Descriptions	2-15
2.5.1.3 Lifting Device Evaluations	2-15
2.5.1.3.1 Cask Body Lifting Evaluation.....	2-15
2.5.1.3.1.1 Lifting Pocket Design Features	2-16
2.5.1.3.1.2 Lifting Pocket Tear-out Stresses	2-17
2.5.1.3.1.3 Lifting Pocket Bearing Stresses	2-18
2.5.1.3.1.4 Lifting Pocket Weld Stresses	2-18
2.5.1.3.1.5 Lifting Pocket Average Pure Shear	2-20
2.5.1.3.1.6 Summary of Results	2-20
2.5.1.3.2 Primary Lid Lifting Evaluation.....	2-21
2.5.1.3.2.1 Primary Lid Lifting Ring Working Loads	2-21
2.5.1.3.2.2 Primary Lid Thread Engagement	2-22
2.5.1.3.3 Secondary Lid Lifting Evaluation	2-23
2.5.1.3.3.1 Lifting Ring Working Load	2-23
2.5.1.3.3.2 Secondary Lid Thread Engagement	2-23
2.5.1.3.4 Upper Impact Limiter Lifting Evaluation.....	2-24

2.5.1.3.4.1 Lifting Ring Working Load	2-24
2.5.1.3.4.2 Impact Limiter Thread Engagement.....	2-25
2.5.1.3.5 Lower Impact Limiter Lifting Evaluation	2-26
2.5.1.3.5.1 Attachment Bolt Stresses	2-26
2.5.1.3.5.2 Lower Impact Limiter Thread Engagement.....	2-27
2.5.2 Tie-down Devices.....	2-28
2.5.2.1 Tie-down Load Calculation	2-28
2.5.2.2 Tie-down Force Calculation.....	2-29
2.5.2.3 Tie-Down Arm Evaluation	2-33
2.5.2.4 Tie-down Arm & Plate Weld Evaluation.....	2-34
2.5.2.4.1 Tie Down Arm-to-Plate Weld Stress	2-35
2.5.2.4.2 Tie Down Plate-to-Outer Shell Weld Stress	2-35
2.5.2.5 Tie-Down Evaluation Summary.....	2-36
2.6 Normal Conditions of Transport.....	2-36
2.6.1 Heat	2-37
2.6.1.1 Summary of Pressures and Temperatures.....	2-37
2.6.1.2 Differential Thermal Expansion.....	2-38
2.6.1.3 Stress Calculations	2-38
2.6.1.4 Comparison with Allowable Stresses	2-38
2.6.2 Cold	2-38
2.6.3 Reduced External Pressure.....	2-39
2.6.4 Increased External Pressure	2-39
2.6.5 Vibration	2-39
2.6.5.1 Vibration Evaluation of the RT-100 Cask Primary Lid Bolts.....	2-39
2.6.5.2 Vibration Evaluation of the RT-100 Cask Secondary Lid Bolts	2-41
2.6.6 Water Spray.....	2-42
2.6.7 Free Drop	2-42
2.6.7.1 Methodology	2-42
2.6.7.2 Finite Element Analysis.....	2-42
2.6.7.2.1 Model Description.....	2-43
2.6.7.2.2 Boundary Conditions.....	2-48
2.6.7.3 Side Drop	2-53
2.6.7.4 End Drop.....	2-61
2.6.8 Corner Drop	2-69

2.6.9 Compression.....	2-69
2.6.10 Penetration	2-69
2.7 Hypothetical Accident Conditions.....	2-69
2.7.1 Free Drop	2-69
2.7.1.1 End Drop.....	2-71
2.7.1.1.1 End Drop Evaluation	2-71
2.7.1.1.2 Lead Slump Evaluation	2-71
2.7.1.1.2.1 Elastic Deformation.....	2-71
2.7.1.1.2.2 Plastic Deformation with Maximum Gap	2-71
2.7.1.2 Side Drop	2-82
2.7.1.3 Corner Drop	2-90
2.7.1.4 Oblique Drops	2-92
2.7.1.5 Summary of Results	2-94
2.7.2 Crush.....	2-94
2.7.3 Puncture	2-94
2.7.3.1 Lid Puncture.....	2-94
2.7.3.1.1 Lid Puncture Boundary Conditions	2-94
2.7.3.1.2 Lid Puncture Results	2-95
2.7.3.2 Cask Side Puncture.....	2-97
2.7.3.2.1 Cask Side Puncture Minimum Wall Thickness.....	2-97
2.7.3.2.2 Cask Sidewall Bending Stresses	2-97
2.7.3.3 Lead Deformation during Side Puncture	2-98
2.7.3.3.1 Outer Shell Stiffness.....	2-98
2.7.3.3.2 Lead Stiffness.....	2-99
2.7.3.3.3 Inner Shell Stiffness	2-99
2.7.3.3.4 Lead Deformation due to Puncture Load.....	2-99
2.7.4 Thermal.....	2-102
2.7.4.1 Summary of Pressures and Temperatures.....	2-102
2.7.4.2 Differential Thermal Expansion.....	2-102
2.7.4.3 Stress Calculations	2-102
2.7.4.3.1 Bolt stresses during fire accident	2-102
2.7.4.3.2 Pressure stress during fire accident	2-102
2.7.4.4 Comparison with Allowable Stresses	2-102
2.7.5 Immersion – Fissile Material.....	2-104

2.7.6 Immersion – All Package	2-104
2.7.7 Deep Water Immersion Test (for Type B Packages Containing More than 10^5 A2)	2-104
2.7.8 Summary of Damage	2-104
2.8 Accident Conditions for Air Transport of Plutonium.....	2-104
2.9 Accident Conditions for Fissile Material Packages for Air Transport	2-104
2.10 Special Form	2-104
2.11 Fuel Rods	2-104
2.12 Appendix – Impact Limiter Analysis.....	2-105
2.12.1 Assumptions.....	2-105
2.12.2 Analysis Inputs	2-105
2.12.2.1 Cask Assembly	2-105
2.12.2.2 Foam Material Properties.....	2-107
2.12.2.2.1 Density.....	2-107
2.12.2.2.2 Crush Strength.....	2-107
2.12.2.3 Temperatures.....	2-107
2.12.3 Methodology	2-108
2.12.3.1 Numerical Integration.....	2-109
2.12.3.2 Crush Strength.....	2-110
2.12.3.3 Crush Force.....	2-113
2.12.3.3.1 End-Drop Case.....	2-114
2.12.3.3.2 Side-Drop Case	2-116
2.12.3.3.3 Corner-Drop Case	2-119
2.12.4 Calculations.....	2-123
2.12.4.1 RT-100 Cask Drop Analysis	2-123
2.12.4.1.1 Calculation for Drop Height of 9.0 m.....	2-123
2.12.4.1.1.1 HAC End-Drop Case	2-124
2.12.4.1.1.2 HAC Side-Drop Case	2-127
2.12.4.1.1.3 HAC Corner-Drop Case.....	2-130
2.12.4.1.2 Calculation for Drop Height of 0.3 m.....	2-134
2.12.4.1.2.1 NCT End-Drop Case	2-134
2.12.4.1.2.2 NCT Side-Drop Case.....	2-137
2.12.4.1.2.3 NCT Corner-Drop Case.....	2-140
2.12.4.2 Pin Puncture	2-143

2.12.4.3 Confirmatory Testing - 3/10 Scale Cask.....	2-144
2.12.4.3.1 End-Drop	2-146
2.12.4.3.2 Corner-Drop.....	2-148
2.12.4.3.3 Side-Drop.....	2-150
2.12.5 Discussion of Test Results	2-152
2.12.6 Summary of Accelerations	2-152
2.13 Appendix – Closure Bolt Evaluation	2-161
2.13.1 Methodology	2-161
2.13.2 Loads	2-161
2.13.2.1 Internal Pressure Loads.....	2-161
2.13.2.1.1 Internal Pressure Loads for Primary Lid Closure Bolts.....	2-161
2.13.2.1.2 Internal Pressure Load for Secondary Lid Closure Bolts	2-163
2.13.2.2 Temperature Loads	2-164
2.13.2.2.1 Temperature Loads for Primary Lid Closure Bolts	2-164
2.13.2.2.2 Temperature Loads for Secondary Lid Closure Bolts	2-165
2.13.2.3 Bolt Preloads	2-165
2.13.2.3.1 Bolt Preload for Primary Lid Closure Bolts.....	2-165
2.13.2.3.2 Bolt Preload for Secondary Lid Closure Bolts.....	2-166
2.13.2.4 Impact Loads	2-167
2.13.2.4.1 Dynamic Load Factors.....	2-167
2.13.2.4.2 End Drop Loads	2-170
2.13.2.4.2.1 Primary Lid Bolts	2-170
2.13.2.4.2.2 Secondary Lid Bolts	2-174
2.13.2.4.3 Corner Drop Evaluations	2-177
2.13.2.4.4 Side Drop Evaluations	2-178
2.13.2.5 Puncture Loads	2-178
2.13.2.5.1 End Puncture	2-178
2.13.2.5.1.1 Primary Lid Bolts	2-178
2.13.2.5.1.2 Secondary Lid Bolts	2-182
2.13.2.5.2 Side Puncture	2-185
2.13.2.6 External Pressure.....	2-185
2.13.2.6.1 Primary Lid Bolts	2-186
2.13.2.6.2 Secondary Lid Bolts	2-187
2.13.2.7 Gasket Seating Load.....	2-188

2.13.3 Load Combinations.....	2-188
2.13.3.1 Primary Lid Closure Bolt Evaluation under Normal Conditions of Transport.....	2-189
2.13.3.2 Secondary Lid Closure Bolt Evaluation under Normal Conditions of Transport	2-194
2.13.3.3 Primary Lid Closure Bolt Evaluation under Hypothetical Accident Conditions	2-198
2.13.3.4 Secondary Lid Closure Bolt Evaluation under Hypothetical Accident Conditions....	2-202
2.13.4 Seal Integrity	2-206
2.13.4.1 Primary Lid Seals	2-206
2.13.4.2 Secondary Lid Seals	2-206
2.13.5 Vent Port Cover Plate O-Ring and Bolt Evaluation	2-207
2.13.5.1 Vent Port Cover Plate O-Ring Evaluation	2-207
2.13.5.1.1 O-ring Sealing Force	2-207
2.13.5.1.2 Vent Port Cover Plate Preload	2-208
2.13.5.1.3 Factor of Safety to Maintain a Tight Seal.....	2-208
2.13.5.2 Bolt Evaluation.....	2-209
2.13.5.2.1 Thread Engagement.....	2-209
2.13.5.2.2 Thread Shear Evaluation.....	2-209
2.13.5.2.3 Load to Break Bolt	2-210
2.14 Appendix – Fabrication Stress Evaluation	2-210
2.14.1 Lead Pour	2-211
2.14.1.1 Cask Shell Geometry	2-211
2.14.1.2 Stresses Resulting from Lead Pour.....	2-211
2.14.2 Cool-down.....	2-212
2.14.2.1 Hoop (Circumferential) Stresses	2-212
2.14.2.2 Axial Stress	2-214
2.14.2.3 Effects of Temperature Differential during Cool-down	2-215
2.14.3 Lead Creep	2-215
2.15 Appendix – Seal Region Stress Evaluation	2-215
2.15.1 Seal Region Post-Processing Methodology	2-215
2.15.2 Stress Concentration Factors.....	2-216
2.15.3 Seal Region Stress Results.....	2-216
2.15.4 Displacement Results.....	2-216
2.16 References	2-228
3. THERMALEVALUATION	3-1

3.1 Description of Thermal Design	3-3
3.1.1 Design Features	3-3
3.1.1.1 RT-100 Description	3-3
3.1.1.2 RT-100 Dimensions.....	3-4
3.1.2 Content's Decay Heat	3-4
3.1.3 Summary Tables of Temperatures.....	3-5
3.1.4 Summary Tables of Maximum Pressures	3-7
3.2 Material Properties and Component Specifications	3-7
3.2.1 Material Properties	3-8
3.2.2 Component Specifications	3-11
3.2.3 Content Properties	3-12
3.3 Thermal Evaluation under Normal Conditions of Transport	3-13
3.3.1 Heat and Cold.....	3-14
3.3.1.1 Load Cases.....	3-14
3.3.1.2 Analytical Model.....	3-16
3.3.1.3 Analysis Results	3-19
3.3.2 Maximum Normal Operating Pressure	3-29
3.3.2.1 Calculation Method	3-29
3.3.2.2 Pressure Due to the Initially Sealed Air in the Cavity	3-29
3.3.2.3 Pressure Due to the Water Vapor in the Cask.....	3-29
3.3.2.4 Pressure Due to Generation of Gas	3-30
3.3.2.5 Total Pressure.....	3-30
3.4 Thermal Evaluation under Hypothetical Accident Conditions	3-31
3.4.1 HAC Fire Analysis—Pin Puncture Damage to Top Impact Limiter	3-31
3.4.1.1 Initial Conditions—Pin Puncture Damage to Top Impact Limiter.....	3-31
3.4.1.2 HAC Fire and Cool-down Analysis—Pin Puncture Damage to Top Impact Limiter	3-31
3.4.1.3 HAC Fire Analysis Results—Pin Puncture Damage to Top Impact Limiter.....	3-32
3.4.2 HAC Fire Evaluation—Pin Puncture Damage to the Side of the Cask Body	3-43
3.4.2.1 Initial Condition—Pin Puncture Damage to the Side of the Cask Body	3-43
3.4.2.2 HAC Fire Analysis—Pin Puncture Damage to the Side of the Cask Body	3-44
3.4.2.3 HAC Fire and Cool-down Analysis—Pin Puncture Damage to the Side of the Cask Body.....	3-44

3.4.3 Maximum Temperatures and Pressure.....	3-57
3.4.3.1 Maximum Temperatures.....	3-57
3.4.3.2 Maximum Accident Condition Pressure.....	3-57
3.4.3.2.1 Calculation Method.....	3-58
3.4.3.2.2 Pressure Due to the Initially Sealed Air in the Cavity.....	3-58
3.4.3.2.3 Pressure Due to the Water Vapor in the Cask.....	3-58
3.4.3.2.4 Pressure Due to Generation of Gas.....	3-58
3.4.3.2.5 Total Pressure.....	3-59
3.4.3.2.6 Total Pressure Accounting for Combustion of Contents.....	3-59
3.4.4 Maximum Thermal Stress.....	3-60
3.4.5 Accident Conditions for Fissile Material Packages for Air Transport.....	3-60
3.5 Appendix.....	3-61
3.6 References.....	3-70
4. CONTAINMENT.....	4-1
4.1 Description of Containment System.....	4-1
4.1.1 Containment Vessel.....	4-1
4.1.2 Containment Penetration.....	4-3
4.1.3 Welds and Seals.....	4-5
4.1.4 Closure.....	4-5
4.1.5 Cavity Volume, Conditions, and Contents.....	4-6
4.2 Allowable Leakage Rates at Test Conditions.....	4-7
4.3 Leakage Rate Test for Type B Packages.....	4-8
4.3.1 Determination of Equivalent Reference Leakage Rate for Helium Gas.....	4-9
4.3.2 Determination of Equivalent Reference Leakage Rate for Air.....	4-15
4.4 Hydrogen Gas Generation.....	4-16
4.4.1 Determination of Bounding G Values.....	4-17
4.4.1.1 G Values for Waste and Secondary Container Materials.....	4-17
4.4.1.2 Calculation of Effective G Values.....	4-19
4.4.1.3 Operating Temperature G Value Adjustment.....	4-20
4.4.2 Hydrogen Gas Generation by Radiolysis.....	4-22
4.4.3 Hydrogen Generation – Radiolysis in Waste, Water and Polyethylene Container.....	4-24
4.4.4 Hydrogen Gas Generation – Simplified Model used to develop Loading Curve.....	4-31
4.4.5 Hydrogen Gas Generation – Analytical Model used for Detailed Analysis.....	4-34

4.5 Appendix.....	4-37
4.6 References.....	4-48
5. SHIELDING EVALUATION.....	5-1
5.1 Description of Shielding Design	5-5
5.1.1 Design Features	5-5
5.1.2 Summary Table of Maximum Radiation Levels	5-5
5.2 Source Specification.....	5-6
5.2.1 Gamma Source	5-6
5.2.2 Neutron Source.....	5-7
5.3 Shielding Model	5-8
5.3.1 Configuration of Source and Shielding.....	5-8
5.3.1.1 Source Term.....	5-9
5.3.1.2 NCT Model.....	5-9
5.3.1.3 HAC Model.....	5-9
5.3.2 Material Properties	5-17
5.4 Shielding Evaluation.....	5-19
5.4.1 Methods	5-19
5.4.1.1 MCNP6 Analysis.....	5-19
5.4.1.2 Dose Rate Response Calculation.....	5-19
5.4.1.3 Maximum allowed source strength density	5-23
5.4.1.4 Variance Reduction	5-24
5.4.2 Input and Output Data	5-24
5.4.3 Flux-to-Dose Rate Conversion.....	5-24
5.4.4 External Radiation Levels.....	5-26
5.4.4.1 MCNP6 Statistics Evaluation.....	5-27
5.4.4.1.1 Tally Statistics Diagnostics.....	5-27
5.4.4.1.2 Fractional Standard Deviation of Individual Tally Segments.....	5-27
5.4.4.2 Media Composition and Density	5-29
5.4.4.2.1 Effect of Media Composition.....	5-29
5.4.4.2.2 Effect of Media Density	5-30
5.4.4.3 Shielding Evaluation Uncertainty	5-31
5.4.4.3.1 Calculation of Dose Rates	5-31
5.4.4.3.1.1 Radiation Source Generation	5-31

5.4.4.3.1.2 Cross Section Data	5-32
5.4.4.3.1.3 Radiation Transport Codes	5-32
5.4.4.3.2 Attenuation from other material (i.e. secondary containers) not included in shielding analysis	5-32
5.4.4.3.3 Nominal Media Bulk Density	5-33
5.4.4.4 Loading Table	5-33
5.4.4.5 Dose Rates for Maximum Radionuclide Loading	5-34
5.5 Appendix.....	5-50
5.5.1 List of Gamma Radionuclides with Greater than 1 Day Half Life	5-50
5.5.2 Gamma Radionuclide Responses	5-52
5.5.3 Radionuclide Maximum Ci/g Loading Limits	5-68
5.5.4 Process Description for Calculating Maximum Allowed Source Strength Density	5-76
5.6 References.....	5-77
6. CRITICALITY EVALUATION.....	6-1
7. PACKAGE OPERATIONS.....	7-1
7.1 Package Loading	7-3
7.1.1 Preparation for Loading	7-3
7.1.1.1 Upper Impact Limiter Removal	7-5
7.1.1.2 Optional Loading Steps	7-5
7.1.1.3 Removal of Quick-Disconnect Valve Cover Plate	7-5
7.1.1.4 Removal of the Primary Lid.....	7-6
7.1.1.5 Removal of the Secondary Lid.....	7-6
7.1.2 Loading of the RT-100	7-7
7.1.2.1 Content Loading.....	7-7
7.1.2.2 Primary Lid Replacement	7-8
7.1.2.3 Secondary Lid Replacement	7-8
7.1.2.4 Quick-Disconnect Valve Cover Plate Replacement	7-9
7.1.3 Preparation for Transport.....	7-9
7.1.3.1 Replacement of Upper Impact Limiter	7-10
7.1.3.2 Verification for Transport.....	7-11
7.2 Package Unloading	7-11
7.2.1 Receipt of Package from Carrier	7-11
7.2.2 Removal of Contents	7-12

8.1.4.4 Quick Disconnect Valve Cover Plate Containment O-Rings Helium Leak Testing	8-11
8.1.5 Component and Material Tests.....	8-13
8.1.5.1 Foam.....	8-14
8.1.5.2 O-Ring	8-14
8.1.5.3 Ceramic Paper	8-15
8.1.5.4 Fusible Plugs	8-15
8.1.5.5 Carbon Steel and Alloy Steel Fasteners.....	8-16
8.1.5.6 Stainless Steel Fasteners	8-18
8.1.5.7 Thread Inserts.....	8-20
8.1.5.8 Quick Disconnect Valve.....	8-21
8.1.6 Shielding Tests	8-21
8.1.7 Thermal Tests.....	8-22
8.1.8 Miscellaneous Tests.....	8-22
8.2 Maintenance Program.....	8-22
8.2.1 Structural and Pressure Tests	8-22
8.2.2 Leakage Tests.....	8-23
8.2.2.1 Periodic and Maintenance Leak Test.....	8-23
8.2.2.2 Pre-Shipment Leak Test – Gas Pressure Rise Option.....	8-23
8.2.2.3 Pre-Shipment Leak Test – Gas Pressure Drop Option	8-26
8.2.3 Component and Material Tests.....	8-28
8.2.3.1 Routine Component Inspection.....	8-28
8.2.3.2 Annual Component Inspection.....	8-29
8.2.4 Thermal Tests.....	8-29
8.2.5 Miscellaneous Tests.....	8-30
8.3 Appendix.....	8-31
8.3.1 Summary of Leak Test Requirements	8-31
8.3.2 Minimum Lead Thickness and Gap Determination.....	8-32
8.3.2.1 Explanation of the Gap Between Lead and the External Shell	8-32
8.3.2.2 Conclusion	8-37
8.4 References.....	8-38

List of Figures

Figure 1-1	Information Flow for General Information	1-2
Figure 1.2.1-1	RT-100 Cask Package Artist Concept	1-3
Figure 2-1	Information Flow for the Structural Review	2-2
Figure 2.5.1-1	RT-100 Lifting Pocket Dimensions	2-17
Figure 2.5.1-2	Weld Geometry	2-19
Figure 2.5.2-1	RT-100 Tie-Down Arm Geometry	2-31
Figure 2.5.2-2	RT-100 Tie-Down Free Body Diagrams	2-32
Figure 2.6.7-1	RT-100 Solid Model	2-45
Figure 2.6.7-2	RT-100 Finite Element Model	2-46
Figure 2.6.7-3	Gap Elements Used to Represent the Impact Limiters for Side and End Drop Configurations	2-47
Figure 2.6.7-4	Bolt Pre-load Using ANSYS Pre-Tension Elements (PRETS179)	2-51
Figure 2.6.7-5	Pressure Distribution Used to Simulate the Contents	2-52
Figure 2.6.7-6	RT-100 NCT Side Drop Stress Intensity Results	2-55
Figure 2.6.7-7	RT-100 Inner Shell NCT Side Drop Stress Intensity Results	2-56
Figure 2.6.7-8	RT-100 Outer Shell NCT Side Drop Stress Intensity Results	2-57
Figure 2.6.7-9	RT-100 Flange NCT Side Drop Stress Intensity Results	2-58
Figure 2.6.7-10	RT-100 Outer Lid NCT Side Drop Stress Intensity Results	2-59
Figure 2.6.7-11	RT-100 Inner Lid NCT Side Drop Stress Intensity Results	2-60
Figure 2.6.7-12	RT-100 NCT Bottom Drop Stress Intensity Results	2-63
Figure 2.6.7-13	RT-100 Inner Shell NCT End Drop Stress Intensity Results	2-64
Figure 2.6.7-14	RT-100 Outer Shell NCT End Drop Stress Intensity Results	2-65
Figure 2.6.7-15	RT-100 Flange NCT End Drop Stress Intensity Results	2-66
Figure 2.6.7-16	RT-100 Outer Lid NCT End Drop Stress Intensity Results	2-67
Figure 2.6.7-17	RT-100 Inner Lid NCT End Drop Stress Intensity Results	2-68
Figure 2.7.1-1	RT-100 HAC End Drop Stress Intensity Results	2-75
Figure 2.7.1-2	RT-100 Inner Shell HAC End Drop Stress Intensity Results	2-76
Figure 2.7.1-3	RT-100 Outer Shell HAC End Drop Stress Intensity Results	2-77
Figure 2.7.1-4	RT-100 Flange HAC End Drop Stress Intensity Results	2-78
Figure 2.7.1-5	RT-100 Outer Lid HAC End Drop Stress Intensity Results	2-79
Figure 2.7.1-6	RT-100 Inner Lid HAC End Drop Stress Intensity Results	2-80
Figure 2.7.1-7	RT-100 Lead Slump	2-81
Figure 2.7.1-8	RT-100 HAC Side Drop Stress Intensity Results	2-84

Figure 2.7.1-9	RT-100 Inner Shell HAC Side Drop Stress Intensity Results.....	2-85
Figure 2.7.1-10	RT-100 Outer Shell HAC Side Drop Stress Intensity Results	2-86
Figure 2.7.1-11	RT-100 Flange HAC Side Drop Stress Intensity Results	2-87
Figure 2.7.1-12	RT-100 Outer Lid HAC Side Drop Stress Intensity Results.....	2-88
Figure 2.7.1-13	RT-100 Inner Lid HAC Side Drop Stress Intensity Results	2-89
Figure 2.7.3-1	RT-100 ANSYS Puncture Model.....	2-96
Figure 2.7.3-2	RT-100 Pin Puncture Stress Intensity Results	2-96
Figure 2.7.3-3	RT-100 Side Puncture Details.....	2-101
Figure 2.12.2-1	Schematic of the RT100 impact limiters	2-106
Figure 2.12.3-1	Example Crush Strength-Strain Curve	2-113
Figure 2.12.3-2	Cask configuration at impact (End-Drop).....	2-114
Figure 2.12.3-3	Cask configuration when velocity becomes zero (End-Drop)	2-115
Figure 2.12.3-4	Diagram for contact area calculation (End-Drop)	2-115
Figure 2.12.3-5	Cask configuration at impact (Side-Drop).....	2-117
Figure 2.12.3-6	Cask configuration when velocity becomes zero (Side-Drop).....	2-117
Figure 2.12.3-7	Diagram of Contact Zones	2-118
Figure 2.12.3-8	Cask Configuration at Impact (Corner-Drop)	2-119
Figure 2.12.3-9	Cask configuration when velocity becomes zero (Corner-Drop).....	2-120
Figure 2.12.3-10	Typical Unit Cell Configuration	2-121
Figure 2.12.3-11	Crush sequence of two foam cell	2-122

Proprietary Information Content Withheld Under 10 CFR 2.390(b)

 Proprietary Information Content Withheld Under 10 CFR 2.390(b)

Figure 2.13.4-1	Compression Set vs. Temperature	2-207
Figure 2.15.4-1	Stress Intensity Contour Plot of Primary Lid Following End Drop.	2-219
Figure 2.15.4-2	Stress Intensity Contour Plot of the Primary Seal Region	2-220
Figure 2.15.4-3	Lid Seal Geometry	2-221
Figure 2.15.4-4	Primary Lid Sealing Surface Displacement during Side drop	2-222
Figure 2.15.4-5	Secondary Lid Sealing Surface Displacement during Side drop.....	2-223
Figure 2.15.4-6	Primary Lid Sealing Surface Displacement during End drop	2-224
Figure 2.15.4-7	Secondary Lid Sealing Surface Displacement during End drop	2-225
Figure 2.15.4-8	Primary Lid Sealing Surface Displacement during Puncture.....	2-226
Figure 2.15.4-9	Secondary Lid Sealing Surface Displacement during Puncture.....	2-227
Figure 3-1	Information Flow for the Thermal Review	3-2
Figure 3.3.1-1	RT-100 ANSYS Finite Element Model Volumes	3-17
Figure 3.3.1-2	RT-100 ANSYS Normal Condition Finite Element Mesh.....	3-18
Figure 3.3.1-3	Temperature Contour Plot of Package—Hot Case 1	3-19
Figure 3.3.1-4	Temperature Contour Plot of Cask Body—Hot Case 1	3-20
Figure 3.3.1-5	Temperature Contour Plot of Inner Shell Surface—Hot Case 1	3-21
Figure 3.3.1-6	Temperature Contour Plot of Lead Shielding—Hot Case 1	3-22
Figure 3.3.1-7	Temperature Contour Plot of Package—Hot Case 2.....	3-23

Figure 3.3.1-8	Temperature Contour Plot of Cask Body—Hot Case 2.....	3-24
Figure 3.3.1-9	Temperature Contour Plot of Package—Cold Case 1	3-25
Figure 3.3.1-10	Temperature Contour Plot of Cask Body—Cold Case 1	3-26
Figure 3.3.1-11	Temperature Contour Plot of Package—Cold Case 2	3-27
Figure 3.3.1-12	Temperature Contour Plot of Cask Body Cold Case 2.....	3-28
Figure 3.4.1-1	Temperature Contour Plot of Package Pre-Fire Fire Condition—HAC Pin Damage on Top Impact Limiter	3-33
Figure 3.4.1-2	Temperature Contour Plot of Cask Body Pre-Fire Condition—HAC Pin Damage on Top Impact Limiter	3-34
Figure 3.4.1-3	Temperature Contour Plot of Inner Shell Pre-Fire Condition—HAC Pin Damage on Top Impact Limiter	3-35
Figure 3.4.1-4	Temperature Contour Plot of Package at the End of Fire—HAC Pin Damage on Top Impact Limiter.....	3-36
Figure 3.4.1-5	Temperature Contour Plot of Cask Body at the End of Fire—HAC Pin Damage on Top Impact Limiter	3-37
Figure 3.4.1-6	Temperature Contour Plot of Package after Cool-Down—HAC Pin Damage on Top Impact Limiter.....	3-38
Figure 3.4.1-7	Temperature Contour Plot of Cask Body after Cool-Down—HAC Pin Damage on Top Impact Limiter	3-39
Figure 3.4.1-8	Time-History Plot of Critical Package Components—HAC Pin Damage on Top Impact Limiter	3-40
Figure 3.4.1-9	Time-History Enhanced View Plot of Critical Package Components—HAC Pin Damage on Top Impact Limiter	3-41
Figure 3.4.1-10	Maximum Temperature of the Inner Shell—HAC Pin Damage on Top Impact Limiter	3-42
Figure 3.4.1-11	Maximum Temperature of Lead Shielding—HAC Pin Damage on Top Impact Limiter	3-43
Figure 3.4.2-1	Cask Model-HAC Pin Damage on Cask Body Side.....	3-45
Figure 3.4.2-2	Temperature Contour Plot of Package Pre-Fire Condition—HAC Pin Damage on Cask Body Side	3-46
Figure 3.4.2-3	Temperature Contour Plot of Cask Body Pre-Fire Condition—HAC Pin Damage on Cask Body Side	3-47
Figure 3.4.2-4	Temperature Contour Plot of Inner Shell Pre-Fire Condition—HAC Pin Damage on Cask Body Side	3-48

Figure 3.4.2-5	Temperature Contour Plot of Package at the End of Fire—HAC Pin Damage on Cask Body Side	3-49
Figure 3.4.2-6	Temperature Contour Plot of Cask Body at the End of Fire—HAC Pin Damage on Cask Body Side	3-50
Figure 3.4.2-7	Temperature Contour Plot of Package after Cool-Down—HAC Pin Damage on Cask Body Side	3-51
Figure 3.4.2-8	Temperature Contour Plot of Cask Body After Cool-Down—HAC Pin Damage on Cask Body Side	3-52
Figure 3.4.2-9	Time-History Plot of Critical Package Components—HAC Pin Damage on Cask Body Side	3-53
Figure 3.4.2-10	Time-History Enhanced View Plot of Critical Package Components—HAC Pin Damage on Cask Body Side	3-54
Figure 3.4.2-11	Maximum Temperature of the Inner Shell—HAC Pin Damage on Cask Body Side	3-55
Figure 3.4.2-12	Maximum Temperature of Lead Shielding—HAC Pin Damage on Cask Body Side	3-56
Figure 4-1	Information Flow for the Containment Review	4-2
Figure 4.1.2-1	Illustration of Containment Boundary	4-4
Figure 4.3.1-1	Allowable Air/Helium Mixture Test Leakage Rates	4-12
Figure 4.3.1-2	Allowable Helium Test Leakage Rates	4-13
Figure 4.4.4-1	Package Loading Curve for Hydrogen Generation – Decay Heat Limit Versus Waste Volume	4-32
Figure 5-1	Information Flow for the Shielding Evaluation	5-4
Figure 5.3.1-1	NCT Model 1 & 2	5-11
Figure 5.3.1-2	NCT Model Tally Surfaces for Dose Rate Response Estimation	5-12
Figure 5.3.1-3	HAC Model 1	5-13
Figure 5.3.1-4	HAC Model 2	5-14
Figure 5.3.1-5	HAC Model General Tally Surfaces	5-15
Figure 5.3.1-6	HAC Model Surface Tally	5-16
Figure 5.4.1-1	Fe-59 Spectrum Grouped into Generic Energy Lines	5-21
Figure 5.4.4-1	Fluctuation in Radial Dose Rates (Cs-137)	5-28
Figure 5.4.4-2	Summary of Calculated Dose Rate Margins	5-31
Figure 5.4.4-3	Example of Media Density Effect	5-33
Figure 5.4.4-4	NCT Maximum Gamma Dose Rates for Co-60 Content at 1.00 g/cc	5-35

Figure 7-1	Information Flow for the Operating Procedures Review.....	7-2
Figure 7.1.1-1	Preparation for Loading Process Flowchart.....	7-4
Figure 7.1.2-1	Loading of the RT-100 Process Flowchart.....	7-7
Figure 7.1.3-1	Preparation for Transport Process Flowchart.....	7-10
Figure 7.4.2-1	Lifting Yoke Arm Positioned on Cask	7-15
Figure 7.4.2-2	Lifting Yoke Connections.....	7-15
Figure 7.4.2-3	Lifting Yoke Secured with Locking Pin.....	7-15
Figure 7.4.2-4	Assembled Cask Ready to Lift.....	7-15
Figure 7.4.4-1	Example Trailer Illustration.....	7-17
Figure 7.4.4-2	Loading of the RT-100 on Transportation Trailer.....	7-17
Figure 7.5-1	Package Loading Curve for Hydrogen Generation – Decay Heat Limit Versus Waste Volume.....	7-21
Figure 8-1	Information Flow for the Acceptance Tests and Maintenance Program Review	8-1
Figure 8.1.4-1	Cask Body Containment Boundary Test Apparatus.....	8-5
Figure 8.1.4-2	Primary Lid Assembly Containment Boundary Test Apparatus.....	8-6
Figure 8.1.4-3	Test Apparatus for Measuring the Helium Leak Rate through the Quick Disconnect Valve	8-10
Figure 8.1.4-4	Alternate Test Apparatus for Measuring the Helium Leak Rate through the Quick Disconnect Valve	8-10
Figure 8.1.4-5	Test Apparatus for Measuring the Helium Leak Rate through the Quick Disconnect Valve Cover Plate	8-12
Figure 8.1.4-6	Alternate Test Apparatus for Measuring the Helium Leak Rate through the Quick Disconnect Valve Cover Plate	8-12
Figure 8.3.2-1	Lead Solidification Diagram.....	8-33
Figure 8.3.2-2	Effect of temperature on the physical properties of AISI 301 stainless steel.....	8-35

List of Tables

Table 2.1.2-1	Load Combinations for RT-100 Cask Body Analyses	2-5
Table 2.1.2-2	Structural Design Criteria for RT-100.....	2-5
Table 2.1.3-1	Assembly Weights and Center of Gravity Locations.....	2-7
Table 2.2.1-1	Cask Temperature-Dependent Material Properties	2-9
Table 2.2.1-2	Cask Temperature-Independent Material Properties	2-10
Table 2.2.1-3	Allowable Stresses for Cask Body Materials.....	2-10
Table 2.5.1-1	Summary of Results for Lifting Assembled Cask.....	2-21
Table 2.5.2-1	Tie-down Arms Horizontal Angles	2-29
Table 2.5.2-2	Calculated Values for Tie-Down Arms	2-33
Table 2.5.2-3	Calculated Forces for Tie-Down Arms.....	2-33
Table 2.6.7-1	NCT Side Drop Stress Summary	2-54
Table 2.6.7-2	NCT End Drop Stress Summary	2-62
Table 2.7.1-1	Deceleration Loadings in RT-100 Cask Body Finite Element Analyses.....	2-70
Table 2.7.1-2	HAC End Drop Stress Summary.....	2-74
Table 2.7.1-3	HAC Side Drop Stress Summary	2-83
Table 2.7.1-4	Corner Drop Component Accelerations	2-90
Table 2.7.1-5	HAC Corner Drop Stress Summary	2-91
Table 2.7.3-1	HAC Pin Puncture Stress Summary	2-95
Table 2.7.4-1	HAC Pressure Stress Summary.....	2-103
Table 2.12.3-1	Foam Crush Strength Coefficients	2-112
Table 2.12.4-1	Maximum Decelerations Summary for 9.0 m End-Drop Case	2-127
Table 2.12.4-2	Maximum Crush Depths for 9.0 m End-Drop Case	2-127
Table 2.12.4-3	Maximum Decelerations Summary for 9.0 m Side-Drop Case.....	2-130
Table 2.12.4-4	Maximum Crush Depths for 9.0 m Side-Drop Case	2-130
Table 2.12.4-5	Maximum Decelerations for 9.0 m Corner-Drop Case.....	2-133
Table 2.12.4-6	Maximum Crush Depths for 9.0 m Corner-Drop Case.....	2-133
Table 2.12.4-7	Maximum Decelerations for 0.3 m End-drop Case.....	2-137
Table 2.12.4-8	Maximum Crush Depths for 0.3 m End-drop Case.....	2-137
Table 2.12.4-9	Maximum Decelerations for 0.3 m Side-drop Case	2-140
Table 2.12.4-10	Maximum Crush Depths for 0.3 m Side-Drop Case	2-140
Table 2.12.4-11	Maximum Decelerations for 0.3 m Corner-Drop Case.....	2-143
Table 2.12.4-12	Maximum Crush Depths for 0.3 m Corner-Drop Case.....	2-143
Table 2.12.4-13	Actual Test Conditions - 3/10 Scale Cask Drop Tests.....	2-145

Table 2.12.4-14	Foam Densities - 3/10 Scale Cask Drop Tests	2-145
Table 2.12.4-15	Predicted and Actual Deceleration and Crush Depth - 3/10 Scale Cask End-Drop	2-146
Table 2.12.4-16	Predicted and Actual Deceleration and Crush Depth - 3/10 Scale Cask Corner-Drop	2-148
Table 2.12.4-17	Predicted and Actual Deceleration and Crush Depth - 3/10 Scale Cask Side-Drop	2-150
Table 2.12.5-1	Comparison of 3/10th Scale Drop Test Results and Analytical Method	2-152
Table 2.12.6-1	Design Decelerations for Subsequent Cask Body Analysis	2-153
Table 2.13.2-1	Closure Bolt Loads for 9.0 m Corner-Drop	2-178
Table 2.13.3-1	Primary Lid Bolt Load Summary	2-189
Table 2.13.3-2	Secondary Lid Bolt Load Summary	2-189
Table 2.14.2-1	Lead Shrinkage Evaluation Results	2-214
Table 2.15.4-1	Stress Concentration Factors	2-217
Table 2.15.4-2	Sealing Surface Stress Summary	2-217
Table 2.15.4-3	Lid Seal Groove Region Stresses	2-217
Table 2.15.4-4	HAC Seal Region Displacement	2-218
Table 3.1.3-1	RT-100 Maximum Normal Condition Temperature Summary	3-6
Table 3.1.3-2	RT-100 Maximum Calculated Temperature of Cask under HAC with Pin Puncture Damage on Top Impact Limiter	3-6
Table 3.1.3-3	RT-100 Maximum Calculated Temperature of Cask under HAC with Pin Puncture Damage at the Side of the Cask Body	3-7
Table 3.1.4-1	RT-100 Summary of Maximum Normal and Hypothetical Accident Condition Pressures	3-7
Table 3.2.1-1	Temperature-Independent Material Properties	3-9
Table 3.2.1-2	Temperature-Dependent Material Properties—Stainless Steel 304	3-10
Table 3.2.1-3	Temperature-dependent Material Properties—Lead	3-11
Table 3.2.1-4	Temperature-dependent Material Properties—Ceramic Paper	3-11
Table 3.2.2-1	Component Specifications – Minimum and Maximum Temperatures	3-12
Table 3.2.3-1	Maximum Temperature Limits for RT-100 Content Materials	3-13
Table 4.1.4-1	Bolt Torque Requirements	4-6
Table 4.1.5-1	Cask Cavity Dimensions	4-6
Table 4.1.5-2	Cask Cavity Volume	4-6
Table 4.1.5-3	Parameters for Normal Transport and Accident Conditions	4-7

Table 4.3-1	Leakage Tests of the RT-100 Package	4-9
Table 4.3.1-1	Helium and Air Viscosity	4-11
Table 4.3.1-2	Allowable Helium Test Leakage Rates, cm ³ /sec.....	4-14
Table 4.4-1	G Values (Molecules/100eV) for Potential Content Materials	4-18
Table 4.4-2	Effective G Values (Molecules/100eV) for Potential Content Materials	4-19
Table 4.4-3	Activation Energy	4-20
Table 4.4-4	Bounding G Values for Contents at Maximum NCT Temperature.....	4-21
Table 4.4-5	Effective G Values and Corresponding α Values for Contents.....	4-26
Table 4.4.3-6	Secondary Container Volumes and Allowable Shoring Volume	4-30
Table 4.4.4-1	Conditions and Justifications for using Package Loading Curve (Figure 4.4.4-1)	4-33
Table 4.4.5-1	Conditions for Shipper to use the Detailed Analysis.....	4-35
Table 4.4.5-2	G-values and α -Fractions for a Range of Alpha/Gamma Decay Heat Distributions.....	4-36
Table 5.1.2-1	Summary Table of External Radiation Levels (Exclusive Use).....	5-6
Table 5.2.1-1	One Curie Co-60 Gamma Source Term	5-7
Table 5.3-1	Model Shielding Thicknesses	5-8
Table 5.3.2-1	RT-100 Material Composition Summary	5-18
Table 5.4.3-1	ANSI/ANS 6.1.1-1977 – Gamma Flux-to-Dose Conversion Factors	5-25
Table 5.4.4-1	Maximum Dose Rates and Responsible Radionuclides	5-26
Table 5.4.4-2	Media Composition Comparison	5-29
Table 5.4.4-3	Media Density Comparison	5-30
Table 5.4.4-4	NCT Dose Rate Responses Due to Bremsstrahlung.....	5-32
Table 5.4.4-5	NCT Gamma Dose Rates for the Maximum Radionuclide Loading.....	5-36
Table 5.4.4-6	HAC Gamma Dose Rates for the Maximum Radionuclide Loading	5-43
Table 5.5.1-1	List of Gamma Radionuclides with Greater Than 1 Day Half Life.....	5-50
Table 5.5.2-1	NCT Gamma Dose Rate Responses (mrem/hr/Ci).....	5-52
Table 5.5.2-2	HAC Gamma Dose Rate Responses (mrem/hr/Ci)	5-60
Table 5.5.3-1	Radionuclide Maximum Ci/g Loading Limits based on Gamma Response	5-68
Table 7.4.5-1	Lid Bolt Tightening Torques.....	7-18
Table 7.4.5-2	Tightening Torques - Other Parts.....	7-18
Table 7.5.1-1	Conditions for using Package Loading Curve (Excerpt from Table 4.4.4-1)	7-21
Table 7.5.1-2	Secondary Container and Allowable Shoring Volumes (Excerpt from Table 4.4.3-6)	7-22

Table 7.5.2-1	Conditions for Shipper to use the Detailed Analysis (From Table 4.4.5-1).....	7-24
Table 7.5.2-2	G-values and α -Fractions for a Range of Alpha/Gamma Decay Heat Distributions (Excerpt from Table 4.4.5-2)	7-25
Table 7.6.1-1	RT-100 Loading Table Illustration.....	7-31
Table 7.6.1-2	Turkey Point Loading Table Example.....	7-34
Table 7.6.1-3	St. Lucie Loading Table Example.....	7-36
Table 7.6.1-4	Maximum Co-60 Loading Table Example	7-37
Table 7.6.1-5	Failed Loading Table Example	7-37
Table 7.6.1-6	Radionuclide Activity Concentration Limits	7-38
Table 8.1.5-1	Material Specifications for O-Rings.....	8-14
Table 8.1.5-2	Basic Requirements for O-Rings.....	8-14
Table 8.1.5-3	Supplementary Requirements for O-Rings	8-15
Table 8.1.5-4	Critical Characteristics of Ceramic Paper.....	8-15
Table 8.1.5-5	Materials and Reference Standards for Carbon Steel and Alloy Steel Fasteners	8-16
Table 8.1.5-6	Chemical Composition for Carbon Steel and Alloy Steel Fasteners	8-17
Table 8.1.5-7	Mechanical Properties of Carbon Steel and Alloy Steel Fasteners	8-18
Table 8.1.5-8	Materials and Reference Standards for Stainless Steel Fasteners	8-19
Table 8.1.5-9	Chemical Composition for Stainless Steel Fasteners	8-19
Table 8.1.5-10	Mechanical Properties of Stainless Steel Fasteners.....	8-19
Table 8.1.5-11	Chemical Composition for Stainless Steel Bars.....	8-20
Table 8.1.5-12	Mechanical Properties of Stainless Steel Bars	8-20
Table 8.1.5-13	Chemical Composition for Threaded Inserts	8-21
Table 8.1.5-14	Mechanical Properties of Threaded Inserts.....	8-21
Table 8.2.2-1	Volume of the Interspaces between the O-rings	8-24
Table 8.3-1	RT-100 Leakage Test Types	8-31
Table 8.3-2	Allowable Helium Leakage Rates	8-31

List of Attachments

Attachment 1.4-1	RT100 NM 1000 Rev. F — Bill of Material.....	1-13
Attachment 1.4-2	RT100 PE 1001-1 Rev. H — Robatel Transport Package RT-100 General Assembly Sheet 1/2	1-19
Attachment 1.4-3	RT100 PE 1001-2 Rev. H — Robatel Transport Package RT-100 General Assembly Sheet 2/2	1-20
Attachment 1.4-4	RT100 PRS 1011 Rev. E — Robatel Transport Package RT-100 Cask Sub Assembly Weld Map Cask Body	1-21
Attachment 1.4-5	RT100 PRS 1013 Rev. C — Robatel Transport Package RT-100 Cask Sub Assembly Weld Map Secondary Lid.....	1-22
Attachment 1.4-6	RT100 PRS 1031 Rev. D — Robatel Transport Package RT-100 Cask Sub Assembly Weld Map Lower Impact Limiter	1-23
Attachment 1.4-7	RT100 PRS 1032 Rev. D — Robatel Transport Package RT-100 Cask Sub Assembly Weld Map Upper Impact Limiter.....	1-24
Attachment 1.4-8	102885 MD 1031-06 Rev. F — Robatel Transport Package RT-100 Sub Assembly Fabrication Drawing Impact Limiter Foam.....	1-25
Attachment 1.4-9	RT-100 Cask as Prepared for Transport with Approximate Trailer Dimensions	1-26
Attachment 2.12-1	General Plastics Foam Product Information Sheets	2-154
Attachment 3.5-1	EPDM Temperature Specifications	3-61
Attachment 3.5-2	Seal Material EPDM Working Temperature.....	3-62
Attachment 3.5-3	Water Vapor Pressure Reference (80°C).....	3-63
Attachment 3.5-4	Water Vapor Pressure Reference (150°C).....	3-66
Attachment 4.5-1	EPDM Temperature Specifications	4-37
Attachment 4.5-2	Seal Material EPDM Working Temperature.....	4-38
Attachment 4.5-3	Seal Material EPDM Helium gas permeation rate	4-39
Attachment 4.5-4	Seal Material EPDM Characteristics With Respect to Damage by Radiation and Hardness Concerns	4-41
Attachment 4.5-5	Additional Support Information about EPDM Resistance to Radiation Up to 5x10 ⁸ Rads While Retaining Reasonable Flexibility and Strength, Hardness and Very Good Compression Set Resistance.....	4-45

1. GENERAL INFORMATION

ROBATEL Technologies, LLC (RT) submits this Application and Safety Analysis Report (SAR), Revision 7, to the Nuclear Regulatory Commission (NRC) to renew the Certificate of Compliance (CoC) No. 9365, Revision No. 1 for the Model RT-100 Type B(U) Cask Package (RT-100).

This application is intended to meet the NRC regulation 10 CFR Part 71, and the Canadian Nuclear Safety Commission (CNSC) regulation SOR/2000-208, and was prepared following the guidance of NUREG 1886. The RT-100 package and the SAR meet the more stringent of the two codes.

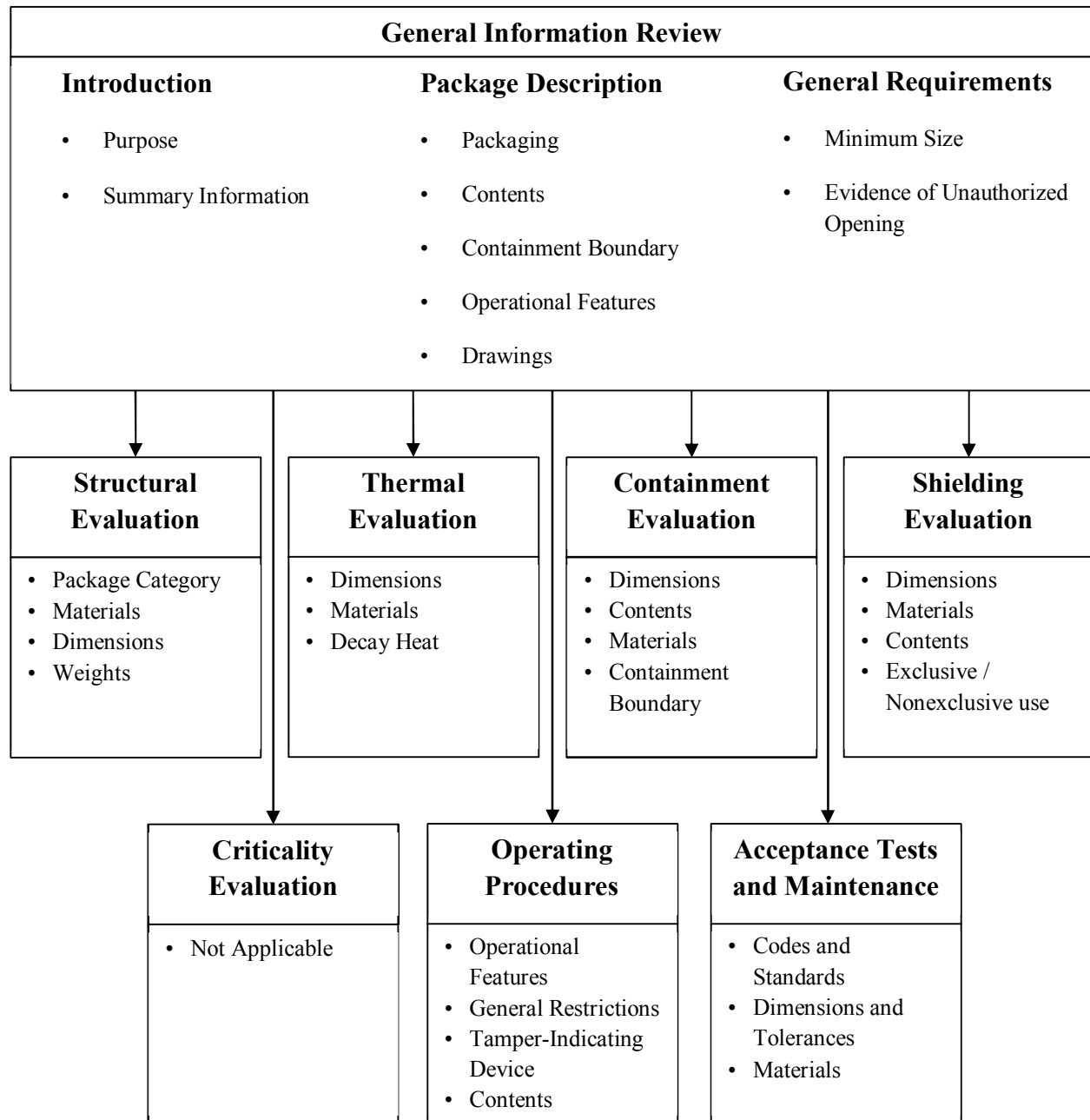
Chapter 1 of the SAR provides General Information that feeds information to later sections in this application according to Figure 1-1 on the following page. The RT-100 meets the following general requirements for all packages:

- The smallest overall dimension of the RT-100 is not less than 10 cm (4 in.).
- The outside of the RT-100 incorporates a feature that, while intact, is evidence that the package has not been opened by unauthorized persons.

1.1 Introduction

The purpose of this application is to request the renewal of the CoC for the Model No. RT-100 type B(U) cask, for package and transport contaminated spent resins and spent filters.

This application does not request the packaging and/or transport of fissile material in quantities exceeding those exempted from consideration in accordance with 10 CFR 71.15 [Ref. 2] and thus, the Criticality Safety Index (CSI) is non-applicable.

Figure 1-1 Information Flow for General Information

1.2 Package Description

Section 1.2 provides a summary of all design aspects of the RT-100. A general arrangement of the RT-100 cask is included in Appendix 1.4. The general arrangement depicts the package dimensions and the materials of construction. Figure 1.2.1-1 shows the major components of the RT-100 as an exploded artist view with the various components labeled.

1.2.1 Packaging

Section 1.2.1 provides details regarding overall dimensions, weight, containment, shielding, criticality, structural features, heat transfer features and package markings.

1.2.1.1 Overall Dimensions

The package consists of a stainless-steel and lead cylindrical shipping cask with a pair of cylindrical foam-filled impact limiters installed on each end. The package configuration is shown in Figure 1.2.1-1.

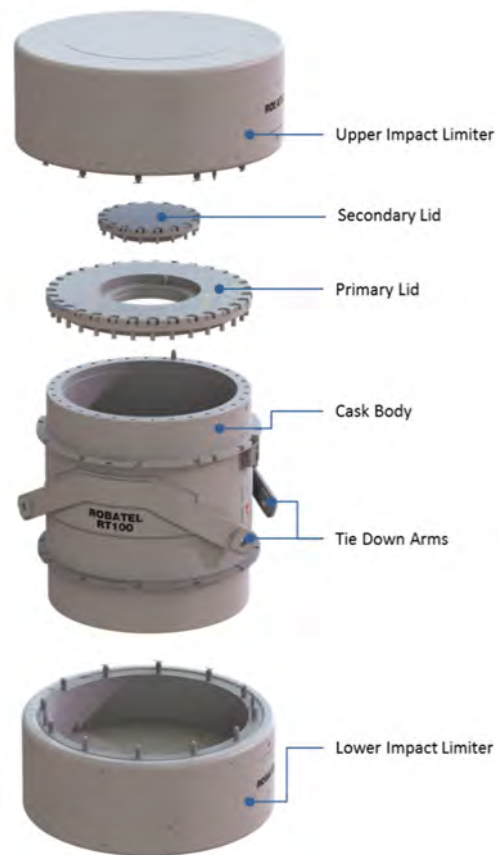


Figure 1.2.1-1 RT-100 Cask Package Artist Concept

The internal cavity dimensions are 1730 mm in diameter and 1956 mm high. The cylindrical cask body is comprised of a 35 mm thick outer stainless-steel shell and a 30 mm thick inner stainless-steel plate. The annular space between the shells is filled with 90 mm thick lead.

The base of the cask consists of a 30 mm thick stainless steel outer bottom plate, a 75 mm thick gamma shield of poured lead, and a 50 mm thick stainless steel inner bottom forging.

The primary lid consists of a 210 mm thick stainless steel forging. The primary lid is fastened to the cask body with thirty-two (32) M48 hex head bolts.

The secondary lid is made of 100 mm thick stainless steel plate, a 60 mm thick lead gamma shield and a 10 mm thick stainless steel plate. The secondary lid is attached to the primary lid with eighteen (18) M36 hex head bolts.

1.2.1.2 Weight

The maximum gross weight of the RT-100 including impact limiters is 41,500 kg (including the maximum payload weight of 6,804 kg). The maximum (empty) weight of the RT-100 including impact limiters is 34,696 kg.

1.2.1.3 Containment Features

The containment vessel of the RT-100 cask consists of the inner shell, the bottom forging, the top flange, the primary lid, the primary lid inner O-ring, the stainless steel vent port cover plate and its inner O-ring, the secondary lid and the secondary lid inner O-ring. The containment system prevents leakage of radioactive material from the cask cavity and allows pre-shipment leakage testing of the assembled cask configuration.

1.2.1.4 Neutron and Gamma Shielding Features

The RT-100 is not designed to carry fissile material or neutron sources (except typical small quantities consistent with contaminated resins and filters as discussed in Chapter 5) and thus, provision of neutron shielding is not required for the RT-100.

In regards to gamma shielding, the RT-100 cask walls provide a shield thickness of 90 mm of lead and 70 mm of stainless steel including the thermal shield plate of 5 mm thickness (65 mm used for HAC analysis). The cask bottom end provides a shield thickness of 75 mm of lead and 80 mm of stainless steel. The top end provides a shield thickness of 210 mm of stainless steel for the primary lid and a shield thickness of 60 mm of lead and 110 mm of stainless steel for the secondary lid. Contents are limited such that the radiological shielding provided assures compliance with U.S. Department of Transportation (DOT) regulatory requirements.

1.2.1.5 Shielding Features for Personnel Barriers

The RT-100 does not require the use of personnel barriers to meet 10 CFR 71 dose rate limits.

1.2.1.6 Criticality Control Features

The RT-100 contents are resins and filters from commercial nuclear power plants that contain only trace quantities of fissile radionuclides. As such, the contents meet the requirements of 10 CFR 71.15 [Ref. 2] and are exempt from classification as fissile material. As a result, the RT-100 does not require any criticality control features.

1.2.1.7 Structural Features – Lifting and Tie-Down Devices

The RT-100 cask employs lifting devices that are a structural part of the package. Two lifting pockets are welded to the cylindrical cask body as shown in Drawing RT100 PE 1001-02, Rev. H (Chapter 1, Appendix 1.4, Attachment 1.4-3). The pockets engage the arms of a separate lifting yoke used to lift the package. When not in use for package lifting, the pockets are rendered inoperable so they cannot be inadvertently used as cask tie-downs. Removable lifting lugs are

utilized for removal and handling of the primary and secondary lids, as well as the impact limiters. Refer to Chapter 2, Section 2.5.1 for a detailed analysis of the structural integrity of the lifting devices.

Two tie-down arms are welded to the external cask shell and are considered a structural part of the package. When not in use for package tie-down, the arms' holes are rendered inoperable preventing the tie-down arms from being used to lift the packaging. Refer to Chapter 2, Section 2.5.2 for a detailed analysis of the structural integrity of the tie-down arms.

1.2.1.8 Structural Features – Impact Limiters

The impact limiters have an outside diameter of 2587 mm. The lower impact limiter extends 494 mm beyond the base of the cask. The upper impact limiter extends 498 mm beyond the cask primary lid. The impact limiter external shells are stainless-steel, allowing them to withstand large plastic deformation without fracturing. The volume inside the shell is filled with crushable shock-absorbing and thermal-insulating polyurethane foam. The polyurethane is preformed and inserted into the shell to the void space. The use of preformed foam ensures homogeneous density. Several different foam densities are used to customize the shock absorbing performance of the impact limiters during hypothetical accident conditions. The rationale for use of preformed foam blocks and the use of different foam densities is presented in detail in Chapter 2, Section 2.2.

The impact limiters are attached to the cask via two stainless-steel bolt ring flanges located on the exterior cask body. The flanges are welded along the cask circumference and considered a structural part of the package. Each impact limiter is equipped with twelve (12) M36 studs and attached to the bolt ring using twelve (12) M36 stainless steel hex head nuts. The purpose of the bolt rings and bolts are to ensure the impact limiters remain attached to the cask body for all Normal Conditions of Transport (NCT) and Hypothetical Accident Conditions (HAC) events. Additionally, use of bolt rings facilitates removal of the impact limiters during loading and unloading operations.

1.2.1.9 Structural Features – Internal Supporting or Positioning Features

The RT-100 cask interior has no supporting or positioning features. The waste contents shall be pre-packaged in liners and placed into the cask cavity. Waste liners may require appropriate shoring to prevent movement during transit. It is the responsibility of the shipper to provide shoring that meets DOT requirements.

1.2.1.10 Structural Features – Outer Shell or Outer Packaging

The external surface of the cylindrical cask body is comprised of a 35 mm thick stainless-steel outer shell.

1.2.1.11 Structural Features – Packaging Closure Device

The chief packaging closure device is the primary lid that consists of a 210 mm thick stainless steel forging as described in Section 1.2.1.1. The primary lid is fastened to the cask body with thirty-two (32) M48 hex head bolts.

The secondary lid also represents a closure device for the cask and is made of 100 mm thick stainless steel plate with lead shielding and another stainless steel plate as described in Section 1.2.1.1. The secondary lid is attached to the primary lid with eighteen (18) M36 hex head bolts.

1.2.1.12 Structural Features – Heat Transfer Features

The RT-100 relies on the insulating properties of the impact limiter polyurethane foam and the cask body ceramic fiber thermal shield to minimize heat input during the hypothetical fire accident event. See Chapter 3, Section 3.4 for details.

There are no special features designed to dissipate heat from the cask.

1.2.1.13 Structural Features – Packaging Markings

The side of the cask body is marked with the Model Number of the cask “RT-100”, the Certificate of Compliance No., Empty Weight, Type B(U)-96, UN 2916 and other required data.

1.2.1.14 Additional Information

- RT-100 cask has one configuration as depicted in the engineering drawings provided in Appendix 1.4, Attachments 1.4-1 thru 1.4-8.
- The RT-100 has no receptacles.
- Pressure test ports are provided between the twin O-rings for the primary lid, between the O-rings for the secondary lid, and between the O-rings for the vent port cover plate. These ports facilitate leak testing of the package in accordance with ANSI N14.5-2014 [Ref. 1].
- The vent port is provided for venting pressures within the containment cavity which may be generated during transport and prior to lid removal. Each port is sealed with an EPDM O-ring. Specification information for all O-rings is contained in Chapter 4, Section 4.1.3.
- The RT-100 does not rely on any coolants to perform its function of providing safe transportation of its radioactive contents.
- There are no external/internal protrusions other than the tie-down arms previously described.

1.2.2 Contents

The authorized contents of the RT-100 are generally described in Section 1.2.2. The radioactive contents are described to the extent required to demonstrate compliance with 10 CFR 71

requirements relating to the structural, thermal and shielding performance of the cask.

1.2.2.1 Identification and Maximum Quantity of Radioactive Material

The contents of the RT-100 cask are limited to contaminated resins and filters containing byproduct or otherwise radioactive nuclear material.

The maximum quantity of material is defined as a Type B quantity of radioactive materials not to exceed 3000 A₂. The activity of beta, gamma and neutron emitting radionuclides will not exceed the limits established in the shielding evaluation provided in Chapter 5 and using the procedure presented in Chapter 7.

1.2.2.2 Identification and Maximum Quantity of Fissile Material

The RT-100 will not transport fissile material exceeding the quantities exempt in 10 CFR 71.15 [Ref. 2]. Thus, Section 1.2.2.2 is non-applicable.

1.2.2.3 Physical and Chemical Form – Density, Moisture Content and Moderators

The type/form of material is defined as byproduct, source, or special nuclear material in the form of resins, filters, and mixtures of resins/filters. These materials are contained within secondary container(s). The chemical form of the contents is resins and filter media containing radioactive materials. The radioactive content of the resins and filters is considered to be in the form of dispersible solids. There are no contents in powdered form. The contents may include the metal housings associated with the media.

1.2.2.3.1 Ion-Exchange Resins

Single or mixed bed ion exchange resins are used in deep bed filter demineralizers for reduction of particulate matter and dissolved contaminants in utility power plant condensates. Radioactive waste systems in nuclear power plants include ion exchange systems for the removal of trace quantities of radioactive nuclides from water that will be released to the environment. The primary resin system used is the mixed bed.

Conventional ion exchange resins consist of a cross-linked polymer matrix with a relatively uniform distribution of ion-active sites throughout the structure. Ion exchange resin materials are sold as spheres or sometimes granules with a specific size and uniformity to meet the needs of a particular application. Ion exchange resins can contain up to 66% water when delivered from the manufacturer. This is essentially the same moisture content within the resin when delivered for disposal. The majority are prepared in spherical (bead) form, either as conventional resin with a polydispersed particle size distribution from about 0.3 mm to 1.2 mm (50-16 mesh) or as uniform particle sized (UPS) resin with all beads in a narrow particle size range. In the water swollen state, ion exchange resins typically show a specific gravity of 1.1-1.5. The bulk density as installed in a column includes a normal 35-40 percent voids volume for a spherical

conventional resin product. Bulk densities in the range of 560-960 g/l (35-60 lb/ft³) are typical for wet resinous products [Ref. 7].

The contents are limited by the maximum overall weight limit of 6,804 kg as described in Section 1.2.1.2. The radioactive inventory of the contents are limited as a function of the activity concentration as described in Chapter 5.

1.2.2.3.2 Filters

Filters packaged in the secondary liner are designed for use in a nuclear power plant's primary water chemistry; therefore, the housings are a non-corrosive and non-reactive material. Filter housings may be stainless steel or a thermoplastic such as polyethylene or polypropylene. They are designed to filter radioactive material from the water, and thus are acceptable for use in a radiation environment. The filter housings do not interact with the secondary container and therefore do not interact with the RT-100 metal cavity.

1.2.2.3.3 Secondary Containers

Secondary containers may be constructed of carbon steel or stainless steel, or a thermoplastic such as polyethylene or polypropylene. The secondary containers are used to package resins or filters generated by nuclear power plants. There is a long history of transportation of these resins and filters via typical polyethylene or metal liners in metal casks by the nuclear power industry and other low-level waste generators. Secondary containers are required to be passively vented within the cask cavity during shipment. The RT-100 stainless steel inner cavity does not interact with polyethylene or metal liners typically used in the nuclear industry for the shipment of resins and filters. Secondary containers may be positioned or braced within the cavity using shoring. This shoring may be constructed of carbon steel or stainless steel, wood, or a thermoplastic material or any combination thereof.

1.2.2.4 Location and Configuration

The contents shall be packaged in secondary containers. Except for close fitting contents, shoring is placed between the secondary containers and the cask cavity liner to prevent movement during accident conditions. Providing appropriate shoring is the responsibility of the shipper.

1.2.2.5 Use of Non-Fissile Materials as Neutron Absorbers/Moderators

The RT-100 does not contain non-fissile materials as neutron absorbers/moderators.

1.2.2.6 Chemical/Galvanic/Gas Generation

Chemical Reaction and Galvanic Reactions

The contents do not include materials that may cause any significant chemical, galvanic, or other reaction.

Gas Generation

Secondary packages containing water and/or organic substances may generate combustible gases via radioanalytical reactions. A maximum molar quantity of 5% hydrogen by volume at standard temperature and pressure is allowed. The time duration is calculated as twice the expected shipment time.

Determination of hydrogen generation is made using the methods in NUREG/CR-6673 [Ref. 5], “*Hydrogen Generation in TRU Waste Transportation Packages*”, and supplemented with data from EPRI NP-5977 [Ref. 6], “*Radwaste Radiolytic Gas Generation Literature Review*”. NUREG/CR-6673 provides equations that allow prediction of the hydrogen concentration as a function of time for simple nested enclosures and for packages containing multiple contents packaged within multiple nested confinement layers. The inputs to these equations include the bounding effective $G(H_2)$ -value for the contents, the $G(H_2)$ -values for the packaging material(s), the void volume in the containment vessel and in the confinement layers (when applicable), the temperature when the package was sealed, the temperature of the package during transport, and the contents decay heat. EPRI NP-5799 provides G-Values for a wide range of ion exchange resins [Ref. 6].

For any package delivered to a carrier for transport, the secondary container is prepared for shipment in the same manner in which the determination for gas generation is made. Shipment period begins when the package is prepared (sealed) and is completed within a time period that is one half the time used in the hydrogen generation calculation. It is the shipper’s responsibility to ensure that hydrogen generation in the cavity will be below 5% by volume, representing the lower flammability limit for hydrogen. The maximum allowable shipping time is not restricted for any other reason. Detailed discussion of the hydrogen generation calculations are provided in Chapter 4, Section 4.4, and Chapter 7, Section 7.5.

Secondary packages with radioactive contents less than Low Specific Activity (LSA) and shipped within 10 days of preparation (or within 10 days of venting the secondary container) do not require a determination of hydrogen gas generation or a restriction on shipping time.

1.2.2.7 Maximum Weight of Contents and Payload

All contents shall be packaged in a secondary container (liner). The maximum gross weight of payload is 6,804 kg including the secondary container (liner).

1.2.2.8 Maximum Decay Heat

The maximum decay heat of the RT-100 contents is 200 watts.

1.2.2.9 Loading Restrictions

Contents that are prohibited include explosives, non-radioactive pyrophoric materials, and corrosives (pH less than 2 or greater than 12.5). Pyrophoric radionuclides may be present only in residual amounts less than 1% by weight. Materials that may auto-ignite or undergo phase transformation at temperatures less than 140 °C, with the exception of water, are not included in the contents. As required by 10 CFR 71.43(d) [Ref. 2], the contents do not include materials that may cause any significant chemical, galvanic, or other reactions.

1.2.2.10 Contents for the Certificate of Compliance

The type and form of material is defined as byproduct, source, or special nuclear material in the form of dewatered or grossly dewatered resins, spent filters, or mixtures of resins/filters, contained within secondary container(s). Secondary containers are required to be passively vented within the cask cavity during shipment. The maximum bulk density of the contents may not exceed 1.0 g/cm³. The maximum quantity of payload material including contents, secondary containers, and shoring is limited to 6,804 kg. The maximum quantity of material is defined as a Type B quantity of radioactive materials not to exceed 3000 A₂. The activity of alpha, beta, gamma and neutron emitting radionuclides does not exceed the limits established in the shielding evaluation provided in Chapter 5 and using the loading table provided in Appendix 7.6, Section 7.6.1. The contents may include fissile materials provided at least one of the paragraphs (a) through (f) of 10 CFR 71.15 [Ref. 2] is met.

1.2.3 Special Requirements for Plutonium

The RT-100 will not contain plutonium in solid form. Therefore, the requirements of 10 CFR 71.63 [Ref. 2] specifying that more than 0.74 TBq (20 Ci) of plutonium must be in solid form do not apply.

1.2.4 Operational Features

The RT-100 has no complex operational requirements. The various valves, connections, openings, seals and containment boundaries are depicted in the drawings provided in Appendix 1.4, Attachments 1.4-1 through 1.4-8. There are no piping systems associated with the RT-100 cask.

1.3 Engineering Drawings and Additional Information

Appendix 1.4 contains the engineering drawings (Attachments 1.4-1 thru 1.4-8) and additional information associated with the RT-100.

1.3.1 Engineering Drawings

The RT-100 drawings are enclosed in Appendix 1.4, Attachments 1.4-1 thru 1.4-8, and contain the following information:

- Safety features (primary and secondary lids, seals, bolts, containment boundary, and shielding)
- Materials list, dimensions, vent and leak test ports and weld inspection requirements
- Weld joint requirements
- Details of gasket joints

Appendix 1.4 does not include detailed construction drawings.

1.3.2 Conformance to Approved Design

The RT-100 cask will be fabricated in accordance with the drawings referenced in the CoC.

1.3.3 Referenced Pages

All referenced pages are generally available to the public.

1.3.4 Special Fabrication Procedures

Fabrication of the RT-100 involves standard cask fabrication techniques.

1.3.5 Package Category

The RT-100 is categorized as a Type B(U)-96 Package.

1.3.6 Supplemental Information

This application contains no supplemental information.

1.4 Appendix

Appendix 1.4 contains Proprietary Information that Robatel requests be withheld from public disclosure under 10 CFR 2.390. This request is in accordance with the Robatel Affidavit and as requested in 10 CFR 2.390.

Attachment 1.4-1 RT100 NM 1000 Rev. F — Bill of Material

**Attachment 1.4-2 RT100 PE 1001-1 Rev. H — Robatel Transport Package RT-100
General Assembly Sheet 1/2**

**Attachment 1.4-3 RT100 PE 1001-2 Rev. H — Robatel Transport Package RT-100
General Assembly Sheet 2/2**

**Attachment 1.4-4 RT100 PRS 1011 Rev. E — Robatel Transport Package RT-100
Cask Sub Assembly Weld Map Cask Body**

**Attachment 1.4-5 RT100 PRS 1013 Rev. C — Robatel Transport Package RT-100
Cask Sub Assembly Weld Map Secondary Lid**

**Attachment 1.4-6 RT100 PRS 1031 Rev. D — Robatel Transport Package RT-100
Cask Sub Assembly Weld Map Lower Impact Limiter**

**Attachment 1.4-7 RT100 PRS 1032 Rev. D — Robatel Transport Package RT-100
Cask Sub Assembly Weld Map Upper Impact Limiter**

**Attachment 1.4-8 102885 MD 1031-06 Rev. F — Robatel Transport Package RT-100
Sub Assembly Fabrication Drawing Impact Limiter Foam**

**Attachment 1.4-9 RT-100 Cask as Prepared for Transport with Approximate Trailer
Dimensions**

Proprietary Information Content Withheld Under 10 CFR 2.390(b)

Proprietary Information Content Withheld Under 10 CFR 2.390(b)

Proprietary Information Content Withheld Under 10 CFR 2.390(b)

Proprietary Information Content Withheld Under 10 CFR 2.390(b)

Proprietary Information Content Withheld Under 10 CFR 2.390(b)

Proprietary Information Content Withheld Under 10 CFR 2.390(b)

Proprietary Information Content Withheld Under 10 CFR 2.390(b)

Proprietary Information Content Withheld Under 10 CFR 2.390(b)

Proprietary Information Content Withheld Under 10 CFR 2.390(b)

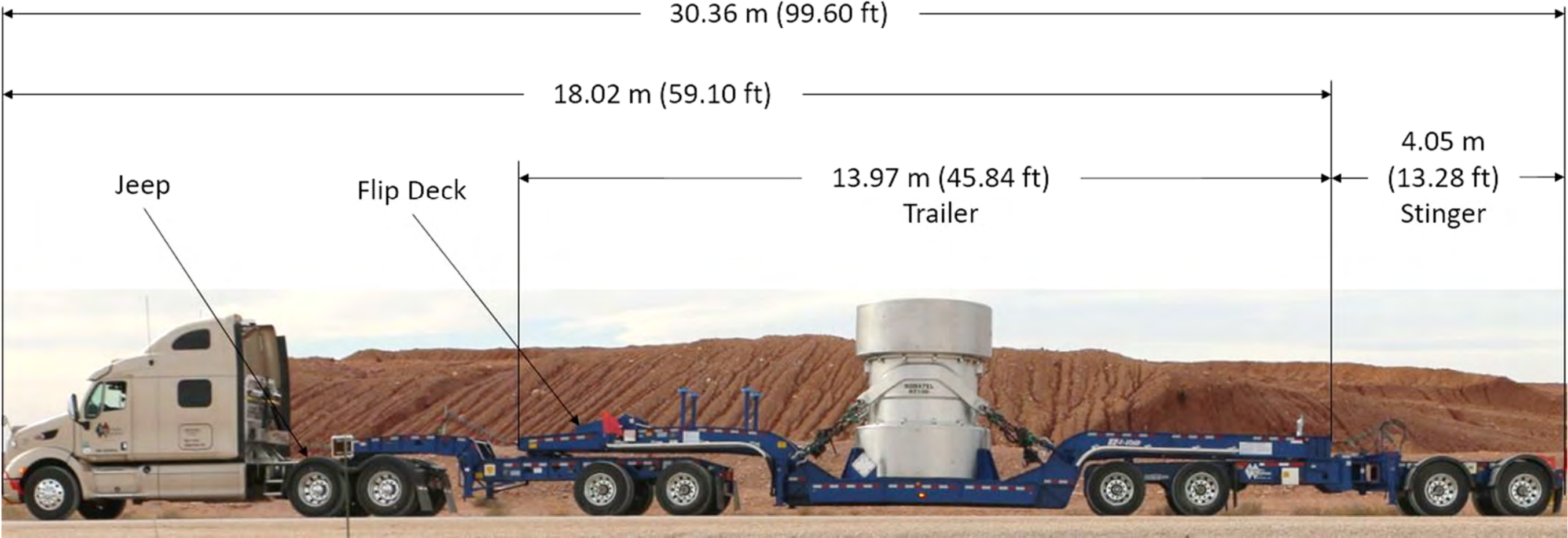
Proprietary Information Content Withheld Under 10 CFR 2.390(b)

Proprietary Information Content Withheld Under 10 CFR 2.390(b)

Proprietary Information Content Withheld Under 10 CFR 2.390(b)

Proprietary Information Content Withheld Under 10 CFR 2.390(b)

Attachment 1.4-9 RT-100 Cask as Prepared for Transport with Approximate Trailer Dimensions



1.5 References

1. Robatel Technologies, LLC, Quality Assurance Program for Packaging and Transportation of Radioactive Material, 10 CFR 71 Subpart H, Rev. 2, Dated November 10, 2017 and NRC Approved on March 21, 2012
2. U.S. Nuclear Regulatory Commission, 10 CFR Part 71--PACKAGING AND TRANSPORTATION OF RADIOACTIVE MATERIAL

71.15	71.43(d)	71.63
-------	----------	-------
3. Robatel Technologies, LLC Application and Safety Analysis Report, Revision 6, for the Model RT-100 Cask Package, dated May 15, 2015.
4. ANSI N14.5-2014, "American National Standard for Radioactive Materials – Leakage Tests on Packages for Shipment," American National Standards Institute, Inc., 11 West 42nd Street, New York, NY, www.ansi.org.
5. NUREG/CR-6673, "Hydrogen Generation in TRU Waste Transportation Packages," Anderson, B., Sheaffer, M., & Fischer, L., Lawrence Livermore National Laboratory, Livermore, CA, May 2000.
6. EPRI NP-5977, "Radwaste Radiolytic Gas Generation Literature Review", Electric Power Research Institute, September 1988.
7. Resin and Filter Handbook – Primers and Product Information

This page is intentionally left blank.

2. STRUCTURAL EVALUATION

Chapter 2 describes the structural evaluation for the RT-100 under the RT Quality Assurance Program [Ref. 1] and summarizes the results to demonstrate compliance with the structural requirements of 10 CFR Part 71 [Ref. 2]. These evaluations follow nuclear industry standards [Refs. 3 – 20]. Chapter 1 General Information and Chapter 3 Thermal Evaluation provide input to the Chapter 2 Structural Evaluation; furthermore, these three chapters feed information to later Chapters of the SAR as demonstrated in Figure 2-1 on the following page.

The RT-100 structural performance under 10 CFR Part 71 [Ref. 2] Normal Conditions of Transport (NCT) and Hypothetical Accident Conditions (HAC) significantly affects the package ability to meet the thermal, containment, shielding and subcriticality requirements. Consequently, results from the structural evaluation are used in the thermal, containment, and shielding evaluations (Note: criticality issues are not applicable to the RT-100).

The foremost structural requirement of the RT-100 is to withstand NCT and HAC loadings with sufficient structural integrity to maintain shielded containment. Evaluations in the following sections demonstrate the RT-100 package design satisfies these requirements. Before presenting these detailed evaluations, a general description of the RT-100 cask design is provided and includes complete specifications for the containment boundary.

2.1 Description of Structural Design

Major design features that govern the structural performance of the RT-100 under NCT and HAC conditions are the impact limiters (upper and lower) and the cask body including the impact limiter attachment rings, bolting ring, primary and secondary lids, lifting pockets and tie-down arms. These features are sufficiently designed so that the structural response of the RT-100 exceeds all 10 CFR 71 [Ref. 2] requirements.

Appendix 1.4 (Attachment 1.4-2 thru 1.4-8) shows the general assembly drawings of the RT-100 Cask Package. The major components are identified and include the impact limiters and cask body. As subsequently discussed in Section 2.1.1.1, the package containment boundary is defined by the inner surfaces of the cask body, and the primary and secondary lids. Shielding is provided by the following features:

- Cask bottom and sidewall that contain 75 and 90 mm lead layers, respectively
- 210 mm thick stainless steel primary lid
- 170 mm (nominally) stainless steel secondary lid with embedded 60 mm thick lead layer

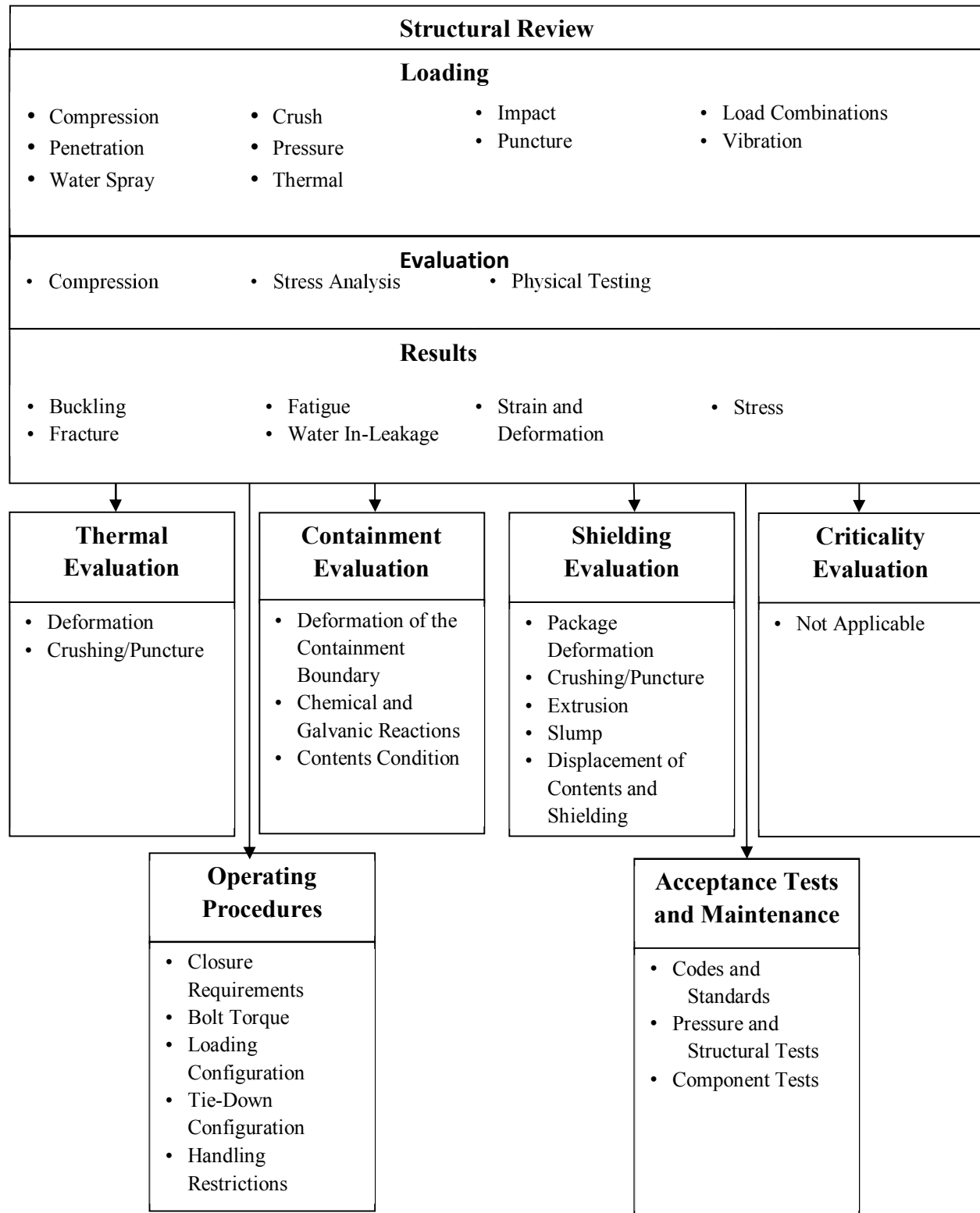


Figure 2-1 Information Flow for the Structural Review

2.1.1 Discussion

The RT-100 cask body is a cylindrical container with an outside diameter of 2060 mm and an overall height of 2321 mm (including lids). The sidewalls are nominally 165 mm thick, consist of a 90 mm thick lead layer encased by 30 mm thick internal and 35 mm thick external (ASTM A240, Type 304) stainless steel shells, have a 5 mm thick ceramic insulation layer, and have an outer 5 mm thick protective shell (ASTM A240, Type 304L stainless steel). The cask sidewall design varies from the above description in the following areas:

- Regions of the cask body encompassed by the impact limiters
- Impact limiter attachment rings
- Lifting pocket locations
- Tie-down arm attachment pads.

The specific sidewall configuration at each of these locations is further described and fully considered in all subsequent evaluations.

The bottom end of the cask body consists of a 75 mm thick lead layer encased by a 50 mm thick (ASTM A240, Type 304L) stainless steel bottom forging on top, and a 30 mm thick external stainless steel bottom plate underneath. The bottom forging is connected to the inner shell with full penetration welds. The bottom plate is connected to the outer shell with a full penetration weld.

The top end of the cask body consists of an upper forging (ASTM A240, Type 304L), and two lids (primary and secondary, both ASTM A240, Type 304L). The upper forging is connected to the inner shell with full penetration welds. The upper forging is connected to the cask outer shell with full penetration welds. Thirty-two (32) M48×2d threaded holes for securing the primary lid are equally spaced along the upper forging top surface. The upper forging top surface also provides a seating surface for the primary lid seals. The primary lid is nominally 210 mm thick.

The primary lid has thirty-two (32) clearance holes near its outer periphery for the M48 bolts (ASTM A354 Gr. BD or equivalent), which secure it to the bolting ring. These clearance holes are sufficiently counter-bored to preclude direct impact to the M48 bolts during a drop. Additionally, the primary lid has a central 737 mm diameter through-hole with a 2016 mm OD × 82 mm deep counter-bore. The counter-bore surface has eighteen (18) M36×2d equally spaced threaded holes for securing the secondary lid and also provides a seating surface for the secondary lid seals. The secondary lid is nominally 170 mm thick with an embedded 60 mm thick lead layer. The secondary lid has eighteen (18) clearance holes near its outer periphery for the M36 bolts (ASTM A354 Gr. BD or equivalent) used to attach it to the primary lid. The primary and secondary lids have one vent port each which allows for leakage monitoring.

The impact limiters are cylindrically-shaped components that surround the top and bottom ends of the cask as shown in Chapter 1, Figure 1.2.1-1. Each impact limiter has twelve (12) M36 studs. The impact limiters are attached to the cask with these studs that pass through clearance holes in the top and bottom impact limiter attachment rings, and accept M36 stainless steel nuts. The

impact limiters are comprised of segmented polyurethane foam blocks encased in relatively thin stainless steel outer coverings. The outer coverings are 4 mm thick except near the cask surface where the thickness is 10 mm. During NCT and HAC tests, the impact limiters are designed to protect the cask by absorbing energy and for providing thermal insulation.

2.1.1.1 Containment Boundary

As shown in Chapter 4, Figure 4.1.2-1 (“Illustration of Containment Boundary”), the containment boundary of the RT-100 cask is defined by the following specific features of the cask body and the primary and secondary lid.

- Bottom forging at the bottom end of the cask
- Inner shell that forms the wall of the cask with a full penetration weld
- Full penetration weld between the inner bottom forging and the inner shell bottom
- Top forging at the top of the cask
- Full penetration weld between the upper forging and inner shell top
- Primary lid and inner O-ring
- Vent port cover plate and inner O-ring
- Secondary lid and inner O-ring

2.1.2 Design Criteria

The RT-100 design satisfies the NCT requirements of 10 CFR 71.71 [Ref. 2], and HAC requirements of 10 CFR 71.73 [Ref. 2]. Furthermore, the design complies with “General Standards for All Packages” as specified in 10 CFR 71.43 [Ref. 2], and the “Lifting and Tie-Down Standards” specified in 10 CFR 71.45 [Ref. 2]. These criteria are demonstrated in Sections 2.5.1 and 2.5.2.

The design criteria used in the qualification of the RT-100 were selected based on guidance provided in Regulatory Guide 7.6 [Ref. 4]. Regulatory Guide 7.6 provides design criteria based on the ASME B&PV Code, Section III [Ref. 7], and is intended for Type B packages used to transport irradiated fuel assemblies. Therefore, allowable stresses values for NCT Service Level A Limits and HAC Service Level D Limits are conservatively adopted from Regulatory Guide 7.6 [Ref. 4] for the qualification of the RT-100 cask body.

Allowable stresses are derived from the Stress Intensity values appropriate to ASME B&PV Code, Section III, Subsection ND [Ref. 7]. Stress Intensity values based on Subsection ND are presented in Table 2.2.1-1.

The load combinations used in performing the structural evaluations of the RT-100 cask are in accordance with Regulatory Guide 7.8 [Ref. 3]. Load combinations for the RT-100 cask body analysis are summarized in Table 2.1.2-1.

Table 2.1.2-1 Load Combinations for RT-100 Cask Body Analyses

LOAD		NORMAL		ACCIDENT			
Reg. Guide 7.8 Load Combinations		A		D			
		1	2	1	2	3	4
Dead Weight	With maximum contents	X	X	X	X	X	X
Thermal Stresses	Hot	X		X		X	
	Cold		X		X		X
Internal Pressure	Normal	X	X	X	X		
	Accident (fire)					X	X
Drop/Impact	0.3 Meters	X	X				
Drop/Impact	9 Meters			X	X		

2.1.2.1 Cask Body Criteria (except Bolts and O-Rings)

The criteria for the cask shells and lids are developed per Regulatory Guide 7.6 Regulatory Position 2 [Ref. 4]. (The tie-down arms are also fabricated from stainless steel but their criteria are developed separately in Section 2.5.2). Table 2.1.2-2 provides a summary of the allowable stress limits defined in Regulatory Guide 7.6.

Table 2.1.2-2 Structural Design Criteria for RT-100

Reg. Guide 7.6 Service Level	Stress Criteria	Notes
Normal conditions: Service Level A	$P_m \leq S_m$	(1)(2)
	$P_m + P_b \leq 1.5 S_m$	(2)
	$P_m + P_b + Q \leq 3 S_m$	(3)
Accident conditions: Service Level D	$P_m \leq 2.4 S_m$ or $0.7 S_u$ (whichever is less)	(4)
	$P_m + P_b \leq 3.6 S_m$ or $1.0 S_u$ (whichever is less)	(4)
	Total Stress $< 2 S_u$	(5)

1. Regulatory Guide 7.6 [Ref. 4], Regulatory Position 1
2. Regulatory Guide 7.6, Regulatory Position 2
3. Regulatory Guide 7.6, Regulatory Position 4
4. Regulatory Guide 7.6, Regulatory Position 6
5. Regulatory Guide 7.6, Regulatory Position 7

2.1.2.2 Bolts

The allowable stresses under NCT (per NUREG/CR-6007 [Ref. 10]) are:

$$f_t < S_m$$

$$f_t^{\max} < 3S_m \text{ if } S_u < 689 \text{ MPa}$$

$$< 2.7S_m \text{ if } S_u > 689 \text{ MPa}$$

$$P_m + P_b + \text{residual torsion} < S_m$$

where

$$f_t = \text{average tensile stress}$$

f_t^{\max} = maximum tensile stress under combined tension and bending, and all other terms are as previously defined.

The allowable stresses under NCT (per NUREG/CR-6007 [Ref. 10]) are:

$$\begin{aligned} f_t &< F_{tb} \\ f_v &< F_{vb} \\ \left(\frac{f_t}{F_{tb}} \right)^2 + \left(\frac{f_v}{F_{vb}} \right)^2 &< 1.0 \end{aligned}$$

where

f_v = average shear stress
 F_{tb} = allowable average tensile stress
 = Min (0.7Su, Sy) at temperature
 F_{vb} = allowable average shear stress
 = Min (0.42Su, 0.6Sy) at temperature and all other terms are as previously defined.

2.1.2.3 Lead

The structural integrity of the RT-100 cask does not depend on lead strength and thus, no lead strength criteria are specified. Mechanical and thermal properties which are important to the RT-100 cask structural performance are discussed in Sections 2.2, 2.14, and 3.2

2.1.2.4 Foam

Criteria of the polyurethane foam used in the impact limiters are provided in Appendix 2.12 Impact Limiter Evaluation.

2.1.3 Weights and Centers of Gravity

The nominal RT-100 weights and centers of gravity are shown in Table 2.1.3-1. Refer to RT100 PE 1001-1 Rev. H – Robatel Transport Package RT-100 General Assembly Sheet 1/2 (Chapter 1, Appendix 1.4, Attachment 1.4-2) for identification of assemblies and centers of gravity data. These weights are utilized in the structural evaluation presented in this chapter.

With the exception of the impact limiter, all analyses are performed with no less than a minimum gross weight of 41,500 kg. The impact limiter calculation is performed using 41,000 kg. The reason for this is that the max crush is obtained by using the minimum density of the foam. The calculation package RTL-001-CALC-ST-0401 Rev. 6 [Ref. 40] calculates the maximum g-load using both 41,500 kg and 41,000 kg. It is shown that max g-load is obtained using a gross weight of 41,000 kg. Thus, the impact limiter calculation is performed using a gross weight of 41,000 kg.

Table 2.1.3-1 Assembly Weights and Center of Gravity Locations

Assembly³	Nominal Weight (kg)	Center of Gravity³ (mm)
Lower Impact Limiter	2,450	516
Cask Body	24,500	1,446
Primary Lid w/ bolts	3,670	2,716
Secondary Lid w/ bolts	870	2,737
Upper Impact Limiter	2,550	2,812
Total Assembly Empty	34,040	1,650
Payload	6,805 ¹	1,434 min. ³ 1,826 max. ³
Total Assembly with payload	40,845 ²	1,620 min. ³ 1,676 max. ³

Notes: 1. Maximum.

2. A minimum weight of 41,000 kg was used in all structural evaluations.

3. Value determined using payload center of gravity at 10% of cask interior height below or above the cask interior geometric centerline.

As shown in Table 2.1.3-1, the center of gravity of the empty RT-100 cask is approximately 1650 mm above the bottom of the cask. This location is just 20 mm lower than the 1630 mm elevation of the center of the inner cavity. Further, the maximum payload weight is less than 17% ($= 6,805/40,845 \times 100\%$) of the loaded cask weight. Thus, payload weight and/or center of gravity variations will not result in large changes to the loaded RT-100 cask center of gravity. Indeed, locating the payload center of gravity within 10% of the cavity internal height above or below the cavity centerline elevation moves the loaded RT-100 cask center of gravity by no more than +/- 28 mm. Such minor variations are insignificant during either NCT or HAC.

2.1.4 Identification of Codes and Standards for Package Design

Since the package is used to transport contents with 3,000 A₂ (as defined in 10 CFR 71.4 [Ref. 2]), the RT-100 cask is a Type B Category II package per Regulatory Guide 7.11 [Ref. 5]. The codes and standards used in the design of the RT-100 cask are selected based on guidance provided in Regulatory Guide 7.6 [Ref. 4 and NUREG/CR-3854 [Ref. 6] for packages transporting Category II contents.

Per NUREG/CR-3854 [Ref. 6], the package containment system is fabricated in accordance with the ASME Code, Section III, Subsection ND [Ref. 7], and the tie-downs are fabricated in accordance with Subsection NF [Ref. 8]. These codes are applicable to the RT-100 cask design as they were developed for components of similar material as well as, for similar loading operations and potential package failures.

Several regulatory guides and NUREGs are used to design and evaluate the RT-100 package. Regulatory Guide 7.8 [Ref. 3] is used in identifying the load combinations to be used in package design evaluation. Regulatory Guide 7.6 [Ref. 4] is used to determine the design criteria. NUREG/CR-4554 [Ref. 9] is used in evaluating buckling of the containment vessel.

NUREG/CR-6007 [Ref. 10] is followed for the bolt evaluations.

2.2 Materials

Material properties used in the RT-100 cask structural analyses are shown in Tables 2.2.1-1, 2.2.1-2, and 2.2.1-3. Material properties for the structural analyses of the polyurethane foam used in the impact limiter evaluations are provided in Appendix 2.12. Properties of both cask materials and foam used in the thermal analyses are provided in Section 3.2.1.

2.2.1 Material Properties and Specifications

Structural components of the cask body are specified to be ASME A240 Type 304/304L steel, with the exception of the tie-down straps, which are ASME A240 UNS No. S31803 (Type 316) stainless steel. The primary and secondary lids are ASME A240 Type 304/304L steel, and the M36 and M48 bolts used to secure the lids are fabricated to meet the critical characteristics given in Chapter 8. These materials meet the requirements of ASME Section III, Subsection ND [Ref. 7]. Strength properties for these materials are presented in Table 2.2.1-1 using material information taken from ASME Section II-D [Ref. 31]. Table 2.2.1-2 provides density and Poisson's ratio values also from ASME Section II-D.

The shielding is specified to be ASTM B-29 lead. The lead properties are provided in NUREG/CR-0481 [Ref. 11] and are presented in Table 2.2.1-2.

EPDM (material designation per ASTM D1418) is used for all O-rings as part of the containment boundary. They serve as one of the boundaries for the cask. These O-rings have a usable temperature range going from -50°C up to 150°C; this temperature range meets or exceeds both NCT and HAC requirements.

RT verifies that all the materials of structural components have sufficient fracture toughness to preclude brittle fracture under NCT and HAC. Regulatory Guides 7.11 [Ref. 5] and 7.12 [Ref. 16] are used to provide criteria for fracture toughness. RT shall procure all materials under the RT Quality Assurance Program [Ref. 1] with the specifications for each material. Regulatory Guides 7.11 and 7.12 do not apply to the RT-100; use of Stainless Steel ASTM A-240 type 304, ASTM A-240 type 304L, and ASTM A-240 UNS S31803 precludes brittle fracture under both NCT and HAC.

RT verifies that all material properties are appropriate for the load conditions specified in Regulatory Guide 7.6 [Ref. 4] and temperatures at which allowable stress limits are defined are consistent with minimum and maximum service temperatures. Allowable stresses based on Regulatory Guide 7.6 [Ref. 4] at the bounding NCT temperature of 100°C are provided in Table 2.2.1-3. Allowable stress intensities at other temperatures considered to be the bounding condition for a specific case are defined as needed in the section where that analysis is presented.

RT verifies that all the force-deformation properties for impact limiters are based on appropriate test conditions and temperature. Test parameters for qualifying the foam material are identified in Chapter 2, Appendix 2.13.

Table 2.2.1-1 Cask Temperature-Dependent Material Properties

Material	Temperature (°C)	Yield Strength (S _y)	Tensile Strength (S _u)	Design Stress Intensity (S _m)	Young's Modulus (GPa)	Coefficient of Thermal Expansion (10 ⁻⁶ /°C)
		(MPa)				
ASME SA-240 Type 304/304L (Dual Certified)	-30	207	517	138	198	—
	20	207	517	138	195	15.3
	65	184	496	138	192	15.8
	100	170	485	138	189	16.2
	150	154	456	138	186	16.6
	200	144	442	129	183	17.0
	250	135	437	122	179	17.4
ASME SA-240 Type 304L	-30	172	483	115	198	—
	20	172	483	115	195	15.3
	65	157	463	115	192	15.8
	100	146	452	115	189	16.2
	150	132	421	115	186	16.6
	200	121	406	110	183	17.0
	250	114	398	103	179	17.4
ASME SA-240 Type 316L	-30	172	483	115	198	—
	20	172	483	115	195	15.3
	65	157	471	106	192	15.8
	100	145	467	96.3	189	16.2
	150	131	441	87.4	186	16.6
	200	121	429	81.2	183	17.0
	250	114	426	76.0	179	17.4
ASME SA-240 UNS No. S31803	-30	448	621	207 = S _u /3	211	—
	20	448	621	207	205	15.3
	65	418	620	207	200	15.8
	100	395	619	206	194	16.2
	150	370	598	199	190	16.6
	200	354	577	193	186	17.0
	250	344	564	188	183	17.4
ASME SA-354 Grade BD (Bolting material)	-30	896	1030	343 = S _u /3	199	—
	20	896	1030	343	202	11.5
	65	855	1030	343	199	11.8
	100	816	1030	343	197	12.1
	150	792	1030	343	194	12.4
	200	768	1030	343	191	12.7
	250	737	1030	343	188	13.0
ASME SA-479, ER308	-30 to 40	205	515	—	—	—
ASTM B-29 Lead	-29	—	—	—	16.75	28.2
	20	—	—	—	15.67	28.9
	50	—	—	—	14.94	29.4
	100	—	—	—	13.73	30.2
	150	—	—	—	12.74	31.2
	200	—	—	—	11.80	32.6
	250	—	—	—	10.70	34.1

**Table 2.2.1-2 Cask Temperature-Independent Material Properties
ASME [Ref. 31]**

Material	Density (kg/m ³)	Poisson's Ratio
ASME SA-240 Type 304/304L (Dual Certified)	8030	0.31
ASME SA-240 UNS No. S31803	8030	0.31
ASME SA-354 Grade BD (Bolting material)	7750	0.30
ASTM B-29 Lead	11300	0.40

Table 2.2.1-3 Allowable Stresses for Cask Body Materials

Design Criteria		Material				
		ASME SA-240 Type 304/304L (Dual Certified)	ASME SA-240 Type 304L	ASME SA-240 Type 316L	ASME SA-240 UNS No. S31803	ASME SA-354 Grade BD
		MPa	MPa	MPa	MPa	MPa
Yield Stress, S_y		170	146	145	395	816
Tensile Strength, S_u		485	452	467	619	1030
Design Stress Intensity, S_m		138	115	96.3	206	299
Normal Conditions	P_m	138	115	96.3	206	299
	$P_m + P_b$	207	173	144	309	449
	$P_m + P_b + Q$	414	345	289	618	897
Hypothetical Accident Conditions	P_m	331	276	231	433	718
	$P_m + P_b$	485	414	347	619	1030
	Total Stress	970	904	934	1238	2060

2.2.2 Chemical, Galvanic, or Other Reactions

The materials used in the fabrication and operation of the RT-100, including coatings, lubricants, and cleaning agents, are evaluated to determine whether chemical, galvanic, or other reactions among the materials, contents, and environments can occur. All phases of operation, loading, unloading, handling, storage, and transportation, are considered (in conjunction with the procedures described in Chapter 7) for the environments that may be encountered under normal, off-normal, or accident conditions. Based on the evaluation, there are no potential reactions that could adversely affect the overall integrity of the cask or the structural integrity and retrievability of the contents from the cask. The evaluation conforms to the guidelines of NRC Bulletin 96-04, "Chemical, Galvanic, or Other Reactions in spent Fuel Storage and Transportation Casks," dated July 5, 1996 [Ref. 52], and demonstrates that the RT-100 cask meets the requirements of 10 CFR 71.43(d) [Ref. 2].

2.2.2.1 Component Material Categories

The component materials evaluated are categorized based on similarity of physical and chemical properties and/or on similarity of component functions. The categories of materials that are considered are as follows:

- Stainless/nickel alloy steels
- Nonferrous metals
- Shielding materials
- Criticality control materials
- Energy absorbing materials
- Cellular foams and insulations
- Lubricants and greases
- O-rings
- Secondary Containers and Shoring
- Filters

These categories are evaluated based on the environment to which they could be exposed during operation or use of the RT-100.

The RT-100 component materials are not reactive among themselves, with the cask's contents, nor with the cask's operating environments during any phase of normal, or accident condition loading, unloading, handling, storage or transportation operations. No reactions occur, and no gases or other corrosion byproducts are generated.

2.2.2.1.1 Stainless/Nickel Alloy Steels

No reaction of the cask components (stainless or nickel alloy) is expected in any environment. During the fabrication process of the RT-100 ridges and crevices on the external surfaces are reduced through the finishing process and the external surface is passivated to prevent corrosion.

Galvanic corrosion between the stainless steels and nickel alloy steels does not occur due to the lack of effective electrochemical potential difference between these metals. No coatings are applied to the stainless steel or nickel alloy steels.

There is no potential for a reaction between stainless steel and any silicone products, fluorocarbon elastomers, dry film lubricants, blended polytetrafluoroethylene (PTFE), or ethylene glycol.

Based on the foregoing discussion, there are no potential reactions expected with the stainless steel cask components.

2.2.2.1.2 Nonferrous Metals

There are no nonferrous metals used in the RT-100. Therefore, no electrochemical driving potential exists.

2.2.2.1.3 Shielding Materials

The primary shielding materials used in the RT-100 is lead which is completely enclosed and sealed in stainless steel. Therefore, there are no potential reactions associated with the cask shielding materials.

2.2.2.1.4 Criticality Control Material

The RT-100 does not contain materials for criticality control. Therefore, no potential reactions associated with these materials exist.

2.2.2.1.5 Energy Absorbing Material

The RT-100 utilizes polyurethane foam for energy absorption in the impact limiters. The foam is completely enclosed (sealed) in stainless steel and there are no potential reactions between the foam and the stainless steel shells. The foam is cured, cut, and machined prior to installation. During fabrication the machined foam blocks are inserted into the impact limiter stainless steel shell. During the welding process backing strips, high temperature heat tape, and rock wool are used to protect the foam. Therefore, no potential reactions associated with the energy absorbing material exists.

2.2.2.1.6 Cellular Foam and Insulation

The RT-100 does not utilize cellular foam or insulation. Therefore, no potential reactions associated with the cellular foam or insulation exists.

2.2.2.1.7 Lubricant and Grease

The dry film lubricants used with the RT-100 meet the performance and general compositional requirements of the nuclear power industry. These lubricants are used primarily on threaded/mechanical connection surfaces. These lubricants are insoluble in most solutions. There are no potential reactions associated with these lubricants or grease.

2.2.2.1.8 O-Rings

The RT-100 utilizes seals formed from EPDM. EPDM is a synthetic rubber elastomer. Elastomer O-rings are used for transport cask applications because of their excellent short-term sealing capabilities, ease of handling, and more economical cost. Seal and gasket materials have stable, non-reactive compositions. There are no potential reactions associated with the RT-100 seal materials.

2.2.2.1.9 Secondary Containers and Shoring

Secondary containers and shoring features may be constructed of carbon steel, stainless steel, wood, or a thermoplastic such as polyethylene or polypropylene.

2.2.2.1.10 Filters

Filters shipped for disposal may be constructed from stainless steel or thermoplastic such as polyethylene or polypropylene.

2.2.2.2 General Effects of Identified Reactions

No significant potential galvanic or other reactions have been identified for the RT-100. Therefore, no adverse conditions can result during any phase of cask operations for NCT or HAC.

2.2.2.3 Adequacy of the Cask Operating Procedures

Based on the results of this evaluation, it is concluded that the RT-100 operating controls and procedures presented in Chapter 7 are adequate to minimize occurrence of hazardous conditions.

2.2.2.4 Effects of Reaction Products

No significant potential chemical, galvanic, or other reactions are identified for the RT-100. Therefore, the overall integrity of the cask and the structural integrity and retrievability of the contents are not adversely affected for any cask operations throughout the design basis life of the cask. Based on the evaluation, no significant reactions are identified and thus, there is no change in cask properties, no binding of mechanical surface, and no degradation of any safety components either directly or indirectly.

2.2.3 Effects of Radiation on Materials

Gamma radiation has no significant effect on metal and therefore, the radiation produced by the contained radioactivity does not cause any measurable damage to the cask metallic components (stainless steel, carbon steel and lead).

For seals, the absorbed dose in a year is expected to be below 350 rad which is significantly below the polymer damage threshold of 1×10^5 rad. Additional support information about EPDM resistance to radiation up to 5×10^8 rads while retaining reasonable flexibility and strength, hardness and very good compression set resistance is provided by an IEEE paper [Ref. 54].

For the ceramic thermal shield, the absorbed dose is expected to be below 350 rad. However, ceramic materials are insensitive to gamma radiation damage and thus, the ceramic thermal shield is expected to be unaffected by radiation.

2.3 Fabrication and Examination

The following subsections provide a summary description of fabrication and examination of the RT-100. A more detailed description is provided in subsequent sections of the SAR.

2.3.1 Fabrication

The RT-100 packaging is designed as a category II container, as mentioned in Section 2.1.4. Fabrication and procurement of the containment components is based on ASME B&PV code, section III, Subsection ND [Ref. 7]. The other components (non-containment) are fabricated based on ASME B&PV code, Section III, subsection NF [Ref.8]. See Sections 2.1.2 and 2.1.4 for additional information.

2.3.2 Examination

Examination of the RT-100 during and after fabrication is conducted in accordance with the requirements of the ASME B&PV code, Section III, Subsection ND-5000 [Ref. 7]. The non-containment components examination is conducted in accordance with the requirements of ASME B&PV Code, Section III, Subsection ND-5000 or NF5000 [Ref. 8]. See Chapter 8, Sections 8.1 and 8.2 for additional information.

2.4 General Requirements for All Packages

The RT-100 meets or exceeds all the requirements in 10 CFR 71.43 [Ref 2]. Also, the RT-100 meets the general package requirements Regulatory Guide 7.9 [Ref. 49] as listed below:

- Smallest overall dimension is greater than 10 cm (4 in).
- Outside of the cask incorporates a feature, such as a seal, that is not readily breakable and that, while intact, would be evidence that the package has not been opened by unauthorized persons.
- Cask includes a containment system closed by a positive fastening device that cannot be opened unintentionally or by a pressure that may arise within the package.

The following sections describe compliance of the RT-100 with these requirements.

2.4.1 Minimum Package Size

This section is not applicable since the RT-100 has dimensions larger than 10 cm (4 inches). The smallest overall dimension of the cask body is the outer diameter, which is over 200 cm.

2.4.2 Tamper-Indicating Feature

The RT-100 upper impact limiter covers the upper end of the cask including the primary and secondary lids, which prevents access to the cask lids. Therefore, tamper-indicating devices are attached to the impact limiter aligning pin. Impact limiters are installed on the cask body following the lid closure operation. Once the impact limiters are installed on the cask body, the attachment nuts are threaded on the attaching studs and hand-tightened (drop testing has shown that torquing of the attachment bolts is not necessary). A tamper-indicating seal is installed on the aligning pin of the upper impact limiter to ensure that removal of the impact limiter by unauthorized individuals can be detected.

2.4.3 Positive Closure

The RT-100 design includes a containment system that is bounded by the inner shell, primary lid, secondary lid, and vent port cover plate. Each lid and the cover plate are secured to the cask body by multiple bolts. These bolts are tightened during the loading process to a set torque value that cannot be inadvertently loosened. Additionally, the stress analysis of the bolts presented in Section 2.6.7 demonstrates that the bolts can maintain positive closure during operation.

2.5 Lifting and Tie-Down Standards for All Packages

The RT-100 lifting and tie-down components are evaluated structurally in the following sections. The lifting and tie-down requirements are as specified in 10 CFR 71.45 [Ref. 2].

2.5.1 Lifting Devices

The primary lifting device for the RT-100 is the set of two lifting pockets that are welded to the outer shell of the cask. After removal of the impact limiters, the lifting pockets are designed to allow the loaded cask to be lifted using a lifting yoke. The primary and secondary lids and the upper/lower impact limiters are fitted with threaded bolt holes; these bolt holes provide for attachment of lifting rings that are used in lifting each component.

2.5.1.1 Lifting Design Criteria

Lifting attachments that are a structural part of the RT-100 cask are designed with a minimum safety factor of three against yielding when used to lift the package. The lifting devices are also designed so that any failure of the lifting device under excessive load would not impair the ability of the RT-100 to meet other requirements of 10 CFR 71.45 [Ref. 2]. The design weights used in the lifting evaluation are as follows:

- Fully loaded RT-100 with maximum contents and the lower impact limiter is 41,500 kg
- Primary lid with secondary lid in place is 4,505 kg
- Secondary lid is 857 kg
- Upper impact limiter is 2,541 kg
- Lower impact limiter is 2,448 kg

2.5.1.2 Lifting Device Descriptions

In this section, the following RT-100 components are evaluated for lifting:

- Lifting Pockets
- Primary Lid
- Secondary Lid
- Lower Impact Limiter
- Upper Impact Limiter

The lifting pockets are utilized to lift the assembled cask; the bounding configuration is the cask loaded with the maximum payload weight and the lower impact limiter attached. Additionally, the primary and secondary lids and the upper and lower impact limiters are evaluated for lifts using removable lifting rings.

2.5.1.3 Lifting Device Evaluations

In the following sections, each device used for lifting is evaluated for stress. The details of each evaluation are presented including the worst-case stress results and safety factors. Additional details supporting these calculations are provided in Calculation Package RTL-001-CALC-ST-0201, Rev. 5 [Ref. 33].

2.5.1.3.1 Cask Body Lifting Evaluation

The cask is lifted by using the two lifting pockets that are welded to the cask exterior sidewall on opposite sides of the cask body. The assembled and loaded cask is lifted with the upper impact limiter removed to accommodate the connection between the lift yoke and the lifting pockets. The cask lifting load is the total weight of the fully assembled cask, including the payload, but with the upper impact limiter load removed. The upper impact limiter is lifted separately. The lifting pockets are evaluated for the tear-out stress, bearing stress, and weld stress due to the required lifting activities. The lifting pockets are also evaluated for pure shear stress as described in ASME Section III Subsection NF [Ref. 8].

A Dynamic Load Factor (DLF) of 1.35 is applied to the lift forces that act on the cask components during movement. ANSI N14.6 [Ref. 56] requires additional safety features for handling of critical loads. One option identified is to apply increased stress design factors on the load-bearing members; however, the standard does not recommend a value for the stress design factor. The German Nuclear Safety Standards Commission provides standard KTA-3905 for lifting loads in nuclear power plants. [Ref. 57] This standard requires a live load factor of 1.35 for dead weight lifts. This calculation uses the KTA-3905 live load factor value as the dynamic load factor. The dynamic load factor is applied to all load bearing members.

2.5.1.3.1.1 Lifting Pocket Design Features

The lifting pockets are manufactured from blocks of ASTM A240 Dual Certified Type 304/304L stainless steel that are welded to opposite sides of the outer shell of the cask body, also manufactured from ASTM A240 Type 304/304L stainless steel. The weld material is SA-279 Grade ER308 UNS S30880. The welds extend down both sides and along the bottom of the lifting pockets, forming a “U” shape. The lifting pockets have a cutout that allows the lifting yoke to pass downward and through the lifting pocket. The connection is completed with a rectangular shaped retaining pin that is inserted through cutouts in both the lifting pocket and the lifting yoke. Figure 2.5.1-1 provides the configuration and dimensions of the lifting pockets and shows the cutouts for the lifting yoke and retaining pin. The design loads and material strengths of the lifting pocket base metal and weld materials are as follows:

Total Lifted Cask Weight	$W = 41,500 - 2,541 \text{ kg} = 38,959 \Rightarrow \text{use } 39,500 \text{ kg}$
Dynamic Load Factor	$DLF = 1.35$
Number of Lifting Pockets	$n_p = 2$
Gravitational Acceleration	$g = 9.81 \text{ m/s}^2$
Vertical Shear Load	$PV = \frac{W \times DLF \times g}{n_p} = \frac{39500 \times 1.35 \times 9.81}{2} \times \frac{1 \text{ kN}}{1000 \text{ N}}$ $= 261.6 \text{ kN pocket}$
Lifting Pocket Yield Strength	$S_y = 199 \text{ MPa}$
Lifting Pocket Tensile Strength	$S_u = 511 \text{ MPa}$
Factor of Safety on Yield Strength	$F_{sy} = 3$
Factor of Safety on Tensile Strength	$F_{su} = 5$

The critical dimensions for the weld evaluation are as follows. These dimensions ignore the dimensions of the welds.

Lifting Pocket Length	$L_p = 191 \text{ mm} = 0.191 \text{ m}$
Lifting Pocket Edge Distance	$d_p = 55 \text{ mm} = 0.055 \text{ m}$
Lifting Pocket Eye Length	$L_e = 84 \text{ mm} = 0.084 \text{ m}$
Retaining Pin Dimensions	$W_p = 60 \text{ mm} = 0.060 \text{ m}$ $H_p = 80 \text{ mm} = 0.080 \text{ m}$

The “eye” refers to the rectangular cutout in the lifting pocket for the retaining pin and the eye length is the vertical height of the eye. The lifting pocket length is the distance from the horizontal centerline of the retaining pin eye to the top of the lifting pocket. The lifting pocket edge distance refers to the vertical height of the recessed cap on the lifting pocket.

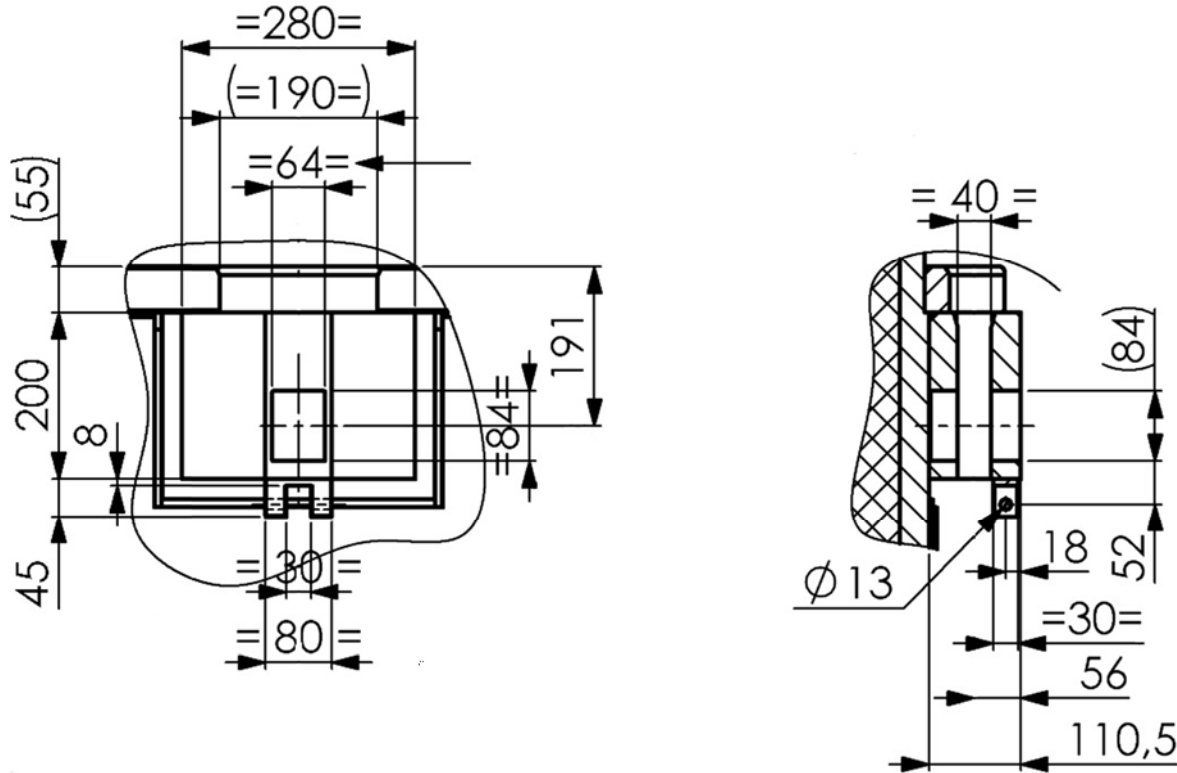


Figure 2.5.1-1 RT-100 Lifting Pocket Dimensions

2.5.1.3.1.2 Lifting Pocket Tear-out Stresses

The lifting pockets are used for lifting the assembled and loaded cask body, without the upper impact limiter, and are rendered inoperable by removing the lifting attachment from the lifting pocket during transport. The lifting pockets are considered to be a structural part of the package with respect to lifting and shall be designed for the factor of safety against yielding and ultimate stresses. A lifting yoke is used to lift the assembled cask body and to ensure that the lifting straps or cables remain parallel to the body of the cask during lifting operations. The tear-out stresses for the lifting pocket retaining pin hole are as follows:

$$\text{Lifting Eye Tear-out distance } d_{to} = L_p - d_p - \frac{L_e}{2} = 0.191 - 0.055 - \frac{0.084}{2} \\ = 0.094 \text{ m}$$

$$\text{Lifting Pocket Thickness } t_p = 110.5 - 40 = 70.5 \text{ mm} = 0.071 \text{ m}$$

$$\text{Lifting eye Tear-out Area } A_{to} = d_{to} \times t_p = 0.094 \times 0.071 \\ = 0.00663 \text{ m}^2$$

The tear-out stresses for the lifting pocket are calculated:

Nominal Tear-out Stress $\tau_{to} = \frac{P_V}{2 \times A_{to}} = \frac{261.6}{2 \times 0.00663} = 19734 \frac{kN}{m^2} = 19.7 MPa$

Allowable Yield Stress

$$\sigma_y = 0.6 \times S_{yL} = 119 MPa$$

Allowable Ultimate Stress

$$\sigma_u = 0.6 \times S_{uL} = 307 MPa$$

Factor of Safety on Yield Strength

$$FS = \frac{\sigma_y}{\tau_{to}} = \frac{119}{19.7} = 6.05 > 3.0$$

Factor of Safety on Tensile Strength

$$FS = \frac{\sigma_u}{\tau_{to}} = \frac{307}{19.7} = 15.54 > 5.0$$

2.5.1.3.1.3 Lifting Pocket Bearing Stresses

The bearing stress in the lifting pocket from the lift yoke retaining pin is calculated as follows. The acceptance criterion for the pocket bearing stress are the yield strength of the material.

Lifting Pocket Bearing Area

$$A_b = W_p \times t_p = 0.06 \times 0.071 = 0.00423 m^2$$

Nominal Bearing Stress

$$\tau_b = \frac{P_V}{A_b} = \frac{261.6}{0.00423} = 61834 \frac{kN}{m^2} = 61.8 MPa$$

Factor of Safety on Yield Strength

$$FS = \frac{S_y}{\tau_b} = \frac{199}{61.8} = 3.22 > 1.0$$

2.5.1.3.1.4 Lifting Pocket Weld Stresses

The stresses in the welds (attaching the lifting pocket to the cask outer shell) are found by applying the shear load from the lifting pockets to the weld around the perimeter of the plate. Based on the safety factors for the lifting pocket, yielding controls the weld evaluation. The stresses and allowables are determined as described in “Design of Welded Structures” [Ref. 25] and Calculation Package RTL-001-CALC-ST-0201, Rev. 5 [Ref. 33]

Conservatively, the upper section of the pocket is considered to take the full lifting load. The lifting pocket is seal welded to and bears upon the cask bolting ring. The lifting load is therefore shared between the lifting pocket weld and the bolting ring. Conservatively, the full load is considered to be taken by the lifting pocket weld only.

The stresses in the welds attaching the lifting pocket to the cask outer shell are found by applying the shear load from the lifting pockets to the weld around the perimeter of the lifting pocket. Based on the safety factors for the lifting pocket, yielding controls the weld evaluation. The welds on the lifting pockets are evaluated as a line force on the weld as described in “Design of Welded Structures” [Ref. 25] (Refer to pages 7.4-6 and 7, Tables 4 and 5). Since the cask is lifted using a yoke that maintains the force in a vertical direction, there are no bending or twisting loads, so the section Modulus and the polar moment of inertia are zero and can be ignored. The weld geometry is provided in Figure 2.5.1-2

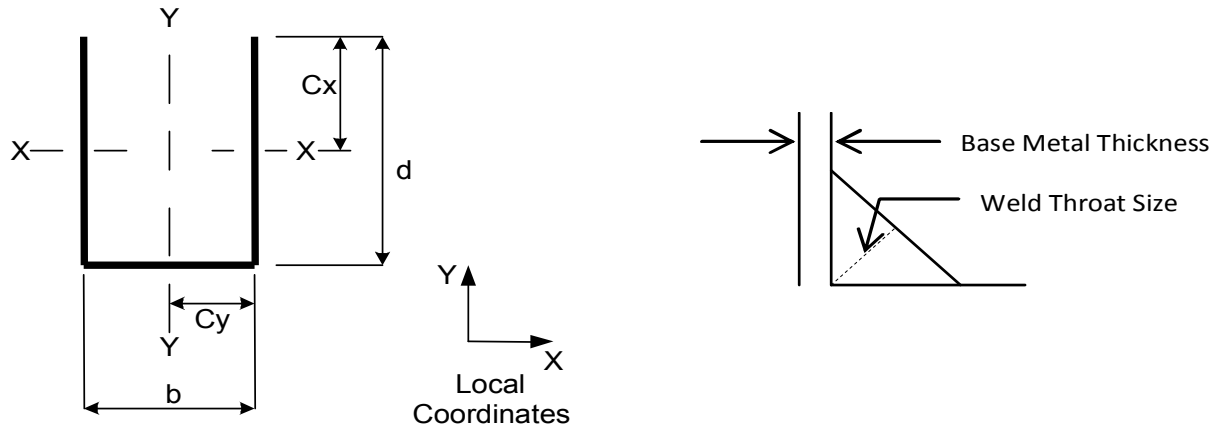


Figure 2.5.1-2 Weld Geometry

Weld properties are as follows:

Length of horizontal weld	$b = 0.28 \text{ m}$
Length of vertical weld	$d = 0.20 \text{ m}$
Weld Length	$A_w = b + 2d = 0.68 \text{ m}$
Weld Throat Size	$T_w = 0.015 \text{ m}$
Base Metal (Cask Wall) Thickness T_c	0.035 m

The force acting on the weld is:

$$f_{vy} = \frac{F_y}{A_w} = \frac{261.6}{0.68} = 384.71 \frac{\text{kN}}{\text{m}}$$

$$\begin{aligned} \text{Yield Weld Allowable } \tau_{wya} &= 0.6 \times S_{wy} \times T_w \times 1000 \\ &= 0.6 \times 205 \times 0.015 \times 1000 = 1845 \text{ kN/m} \end{aligned}$$

$$\begin{aligned} \text{Tensile Weld Allowable } \tau_{wya} &= 0.6 \times S_{wu} \times T_w \times 1000 \\ &= 0.6 \times 515 \times 0.015 \times 1000 = 4635 \text{ kN/m} \end{aligned}$$

Yield Cask Allowable

$$\begin{aligned} \tau_{cya} &= \frac{0.6 \times S_{cy} \times T_c \times 1000}{0.7071} = \frac{0.6 \times 199 \times 0.035 \times 1000}{0.7071} \\ &= 5910 \text{ kN/m} \end{aligned}$$

Tensile Cask Allowable

$$\tau_{cua} = \frac{0.6 \times S_{cu} \times T_c \times 1000}{0.7071} = \frac{0.6 \times 511 \times 0.036 \times 1000}{0.7071}$$

$$= 15176 \text{ kN/m}$$

Weld Yield FS

$$= \frac{\tau_{wya}}{f_w} = \frac{1845}{384.71} = 4.80 > 3.0$$

Weld Tensile FS

$$= \frac{\tau_{wua}}{f_w} = \frac{4635}{384.71} = 12.05 > 5.0$$

Cask Yield FS

$$= \frac{\tau_{cya}}{f_w} = \frac{5910}{384.71} = 15.36 > 3.0$$

Cask Ultimate FS

$$= \frac{\tau_{cua}}{f_w} = \frac{15176}{384.71} = 39.45 > 5.0$$

2.5.1.3.1.5 Lifting Pocket Average Pure Shear

The lifting pocket average pure shear is evaluated in accordance with ASME Section III Subsection NF [Ref. 8] Subparagraph 3223.2 and is limited to $0.6 S_m$. The factor of safety is determined by comparing the pure shear to the lifting pocket tear out stress. For the lifting pocket weld evaluation, the average pure shear is evaluated as follows.

Cask Membrane Strength

$$S_m = 115 \text{ MPa}$$

Cask Allowable Pure Shear

$$S_{ap} = 0.6 \times S_m = 0.6 \times 115 = 69.0 \text{ MPa}$$

FS for Cask Pure Shear

$$= \frac{S_{ap}}{\tau_{to}} = \frac{69.0}{19.7} = 3.50 > 1.0 \text{ cask pure shear is OK}$$

2.5.1.3.1.6 Summary of Results

Table 2.5.1-1 provides a summary of the Factors of Safety for each of the lifting conditions that are evaluated for the assembled RT-100. The table shows that all of the lifting conditions meet the required factor of safety greater than 3.0 against yield and the factor of safety greater than 5.0 against ultimate stress for the tear out and weld stress and a greater than 1.0 for the bearing stresses and average pure shear.

Table 2.5.1-1 Summary of Results for Lifting Assembled Cask

Lifting Condition Evaluated	Factor of Safety	
	Yield (> 3)	Ultimate (>5)
Lifting Pocket Tear-out Stresses	6.05	15.54
Lifting Pocket Weld Stresses: Weld	4.80	12.05
Lifting Pocket Weld Stresses: Cask	15.36	39.45
	Factor of Safety (>1)	
Lifting Pocket Bearing Stresses	3.22	N/A
Lifting Pocket Average Pure Shear	3.50	

2.5.1.3.2 Primary Lid Lifting Evaluation

The primary lid is evaluated for the working load limit in the lifting rings and for the tear-out stresses in the lid from the lifting activities. The lifting rings for the primary lid can only be used when the cask lid is separated from the cask body. The secondary cask lid is also removable, so the primary lid may be lifted with the secondary lid attached or separated from the primary lid. Conservatively, the combined primary and secondary lid is used for the lifting evaluation. The primary lid design information is:

Primary Lid Weight	$W_{PL} = 3648 \text{ kg, assume } 3700 \text{ kg}$
Secondary Lid Weight	$W_{SL} = 857 \text{ kg, assume } 900 \text{ kg}$
Total Lid Lifting Weight	$W_L = 3700 + 900 = 4600 \text{ kg}$
Number of Lifting Rings	$n_r = 3$
Dynamic Load Factor	$DLF = 1.35$

2.5.1.3.2.1 Primary Lid Lifting Ring Working Loads

The lifting rings on the primary lid are only used for lifting when the lid is detached from the cask body, and are rendered inoperable by removing the rings from the lid when the cask is assembled. The rings are therefore not considered to be a structural part of the package and do not need to be designed for the factor of safety against yielding.

Lifting Ring Load	$P_r = \frac{W_L \times DLF}{n_r} = \frac{4600 \times 1.35}{3} = 2070 \text{ kg}$
Ring Working Load Limit	$P_{r,max} = 3000 \text{ kg}$
Factor of Safety	$FS = \frac{P_{r,max}}{P_r} = \frac{3000}{2070} = 1.45 > 1.0$

2.5.1.3.2.2 Primary Lid Thread Engagement

The minimum required thread engagement length is determined in accordance with “Machinery’s Handbook [Ref. 27]. The primary lid is manufactured from ASTM A240 Type 304L SS material. This material is weaker than the M20 lifting ring material (ASTM A-354 Gr. BD), so failure will occur at the root of the primary lid material threads. The minimum required thread engagement length that prevents primary lid material failure is:

$$\text{Minimum Engagement Length } L_e = \frac{S_{bt} \times 2 \times A_b}{S_{ct} \times \pi \times n \times D_{s,min} \times \left[\frac{1}{2 \times n} + 0.57735 \times (D_{s,min} - E_{n,max}) \right]}$$

Where

S_{bt} = Bolt External Thread Tensile Strength, MPa

A_b = Stress Area of Bolt External Threads, mm²

S_{ct} = Cask Internal Thread Tensile Strength, MPa n = Number of threads per millimeter

$D_{s,min}$ = Minimum Major Bolt Diameter, mm

$E_{n,max}$ = Maximum Pitch Diameter of Internal Thread, mm

Solving the equation for Minimum Engagement Length, L_e :

$$\begin{aligned} \text{Minimum Engagement Length} \\ L_e &= \frac{150,000 \times 2 \times 0.38}{69,000 \times \pi \times 10.16 \times 0.773 \times \left[\frac{1}{2 \times 10.16} + 0.57735 \times (0.773 - 0.699) \right]} \\ &= 0.73 \text{ in} = 18.5 \text{ mm} \end{aligned}$$

Where

$S_{bt} = 1030 \text{ MPa} = 150,000 \text{ psi}$

$A_b = 245.0 \text{ mm}^2 = 0.38 \text{ in}^2$

$S_{Lt} = 470 \text{ MPa} = 69,000 \text{ psi}$

$p = \text{Thread Pitch} = 2.5 \text{ mm} = 0.098 \text{ in}$

$n = \frac{1}{p} = \frac{1}{0.098} = 10.16 \text{ Threads/inch}$

$D_{s,min} = 19.623 \text{ mm} = 0.773 \text{ in}$

$E_{n,max} = 17.744 \text{ mm} = 0.699 \text{ in}$

The available thread engagement, L_{ep} , is 32 mm. Therefore, the factor of safety is:

$$FS = \frac{L_{ep}}{L_e} = \frac{32.0}{18.5} = 1.73 > 1.0$$

The lifting ring configuration is acceptable for the applied loads. In the unlikely event that failure does occur in the lid threads, no adverse effects on the RT-100 will occur since the threads are outside the cask containment boundary.

2.5.1.3.3 Secondary Lid Lifting Evaluation

The secondary lid is lifted using a set of three lifting rings that attach to threaded holes in the top surface of the lid. Although the maximum evaluated weight of the secondary lid lift includes only the secondary lid, the hardware is the same as that used for the primary lid. The combined primary and secondary lid are evaluated for lifting in Section 2.5.1.3.2. This section evaluates the working load limit in the lifting rings and for the minimum thread engagement in the lid during lifting activities. The secondary lid design information is:

Secondary Lid Weight	$W_{SL} = 857 \text{ kg}$, assume 900 kg
Number of Lifting Rings	$n_r = 3$
Dynamic Load Factor	$DLF = 1.35$

2.5.1.3.3.1 Lifting Ring Working Load

The lifting rings on the secondary lid are only used for lifting when the lid is detached from the cask and are rendered inoperable by removing the rings from the lid when the cask is assembled. The rings are therefore not considered to be a structural part of the package and do not need to be designed for the factor of safety against yielding.

Lifting Ring Load

$$P_r = \frac{W_{SL} \times DLF}{n_r} = \frac{900 \times 1.35}{3} = 405 \text{ kg}$$

Ring Working Load Limit

$$P_{r,max} = 3000 \text{ kg}$$

Factor of Safety

$$FS = \frac{P_{r,max}}{P_r} = \frac{3000}{405} = 7.4 > 1.0$$

2.5.1.3.3.2 Secondary Lid Thread Engagement

The minimum required thread engagement length is determined in accordance with “Machinery’s Handbook” [Ref. 27]. The secondary lid is manufactured from ASTM A240 Type 304L SS material. This material is weaker than the M20 lifting ring material (ASTM A-354 Gr. BD), so failure will occur at the root of the secondary lid material threads. The minimum required thread engagement length that prevents secondary lid material failure is:

$$\text{Minimum Engagement Length } L_e = \frac{S_{bt} \times 2 \times A_b}{S_{ct} \times \pi \times n \times D_{s,min} \times \left[\frac{1}{2 \times n} + 0.57735 \times (D_{s,min} - E_{n,max}) \right]}$$

S_{bt} = Bolt External Thread Tensile Strength, MPa

A_b = Stress Area of Bolt External Threads, mm²

S_{ct} = Cask Internal Thread Tensile Strength, MPa n = Number of threads per millimeter

$D_{s,min}$ = Minimum Major Bolt Diameter, mm

$E_{n,max}$ = Maximum Pitch Diameter of Internal Thread, mm

Solving the equation for Minimum Engagement Length, L_e :

Minimum Engagement Length

$$L_e = \frac{150,000 \times 2 \times 0.38}{69,000 \times \pi \times 10.16 \times 0.773 \times \left[\frac{1}{2 \times 10.16} + 0.57735 \times (0.773 - 0.699) \right]}$$

$$= 0.73 \text{ in} = 18.5 \text{ mm}$$

Where

$$\begin{aligned} S_{bt} &= 1030 \text{ MPa} = 150,000 \text{ psi} \\ A_b &= 245.0 \text{ mm}^2 = 0.38 \text{ in}^2 \\ S_{Lt} &= 470 \text{ MPa} = 69,000 \text{ psi} \\ p &= \text{Thread Pitch} = 2.5 \text{ mm} = 0.098 \text{ in} \\ n &= \frac{1}{p} = \frac{1}{0.098} = 10.16 \text{ Threads/inch} \\ D_{s,min} &= 19.623 \text{ mm} = 0.773 \text{ in} \\ E_{n,max} &= 17.744 \text{ mm} = 0.699 \text{ in} \end{aligned}$$

The available thread engagement, L_{ep} , is 32 mm. Therefore, the factor of safety is:

$$FS = \frac{L_{ep}}{L_e} = \frac{32.0}{18.5} = 1.73 > 1.0$$

Therefore, the secondary lid lifting ring configuration is acceptable for the required loads.

2.5.1.3.4 Upper Impact Limiter Lifting Evaluation

The upper impact limiter is lifted using a set of three lifting rings that attach to threaded holes in the top surface of the limiter. The lifting rings are designed to remove the impact limiter from the cask body and not to lift the cask body while still attached. In the following sections, the impact limiter is evaluated for the working load limit in the lifting ring and the lifting ring thread engagement. The upper impact limiter design information is:

Secondary Lid Weight	$W_{UL} = 2541 \text{ kg}$, assume 2700 kg
Number of Lifting Rings	$n_r = 3$
Dynamic Load Factor	DLF = 1.35

2.5.1.3.4.1 Lifting Ring Working Load

The lifting rings on the upper impact limiter are used only for lifting when the impact limiter is detached from the cask body; the rings are rendered inoperable by removing the rings from the impact limiter when the cask is assembled. Since the rings are not considered a structural part of the package, they do not need to be designed for the factor of safety against yielding.

Lifting Ring Load

$$P_r = \frac{W_{UL} \times DLF}{n_r} = \frac{2700 \times 1.35}{3} = 1215 \text{ kg}$$

Ring Working Load Limit

$$P_{r,max} = 3000 \text{ kg}$$

Factor of Safety

$$FS = \frac{P_{r,max}}{P_r} = \frac{3000}{1215} = 2.47 > 1.0$$

2.5.1.3.4.2 Impact Limiter Thread Engagement

The minimum required thread engagement length to prevent impact limiter material failure is determined in accordance with “Machinery’s Handbook” [Ref. 27]. The upper impact limiter is manufactured from ASTM A240 Dual Certified Type 304/304L material. This material is weaker than the M20 lifting ring material (ASTM A-354 Gr. BD), so failure will occur at the root of the upper impact limiter material threads. The minimum required thread engagement length that prevents upper impact limiter material failure is:

$$\text{Minimum Engagement Length } L_e = \frac{S_{bt} \times 2 \times A_b}{S_{ct} \times \pi \times n \times D_{s,min} \times \left[\frac{1}{2 \times n} + 0.57735 \times (D_{s,min} - E_{n,max}) \right]}$$

 S_{bt} = Bolt External Thread Tensile Strength, MPa A_b = Stress Area of Bolt External Threads, mm² S_{ct} = Cask Internal Thread Tensile Strength, MPa n = Number of threads per millimeter $D_{s,min}$ = Minimum Major Bolt Diameter, mm $E_{n,max}$ = Maximum Pitch Diameter of Internal Thread, mmSolving the equation for Minimum Engagement Length, L_e :

Minimum Engagement Length

$$L_e = \frac{150,000 \times 2 \times 0.38}{69,000 \times \pi \times 10.16 \times 0.773 \times \left[\frac{1}{2 \times 10.16} + 0.57735 \times (0.773 - 0.699) \right]}$$

$$= 0.73 \text{ in} = 18.5 \text{ mm}$$

Where

$$S_{bt} = 1030 \text{ MPa} = 150,000 \text{ psi}$$

$$A_b = 245.0 \text{ mm}^2 = 0.38 \text{ in}^2$$

$$\begin{aligned}
 S_{Lt} &= 470 \text{ MPa} = 69,000 \text{ psi} \\
 p &= \text{Thread Pitch} = 2.5 \text{ mm} = 0.098 \text{ in} \\
 n &= \frac{1}{p} = \frac{1}{0.098} = 10.16 \text{ Threads/inch} \\
 D_{s,min} &= 19.623 \text{ mm} = 0.773 \text{ in} \\
 E_{n,max} &= 17.744 \text{ mm} = 0.699 \text{ in}
 \end{aligned}$$

The available thread engagement, L_{ep} , is 32 mm. Therefore, the factor of safety is:

$$FS = \frac{L_{ep}}{L_e} = \frac{32.0}{18.5} = 1.73 > 1.0$$

Therefore, the upper impact limiter lifting ring configuration is acceptable for the required loads.

2.5.1.3.5 Lower Impact Limiter Lifting Evaluation

The lower impact limiter is lifted using three of the threaded bolt studs that are utilized to attach the lower limiter to the cask body. As such, it cannot be lifted while attached to the cask body. The lower impact limiter is evaluated for the bolt stresses and for minimum thread engagement in the lower impact limiter during lifting activities. The lower impact limiter design information is:

Lower Impact Limiter Weight	$W_{LL} = 2448 \text{ kg, assume } 2600 \text{ kg}$
Number of Lifting Rings	$n_r = 3$
Dynamic Load Factor	$DLF = 1.35$
Gravitational Acceleration	$g = 9.81 \text{ m/s}^2$

2.5.1.3.5.1 Attachment Bolt Stresses

The bolts on the lower impact limiter are only used for lifting when the lower impact limiter is detached from the cask body, and are rendered inoperable by securing them to the cask body as part of the assembled cask. The bolts are therefore not considered to be a structural part of the package with respect to lifting and do not need to be designed for the factor of safety against yielding. Since the arrangement of the cables or straps used to lift the lower impact limiter may vary, the total lifting load is conservatively considered simultaneously in the vertical and horizontal directions.

Bolt Tension	$T = \frac{W_{LL} \times DLF \times g}{n_b} = \frac{2600 \times 1.35 \times 9.81}{3} = 11477.7 \text{ N}$
Bolt Shear	$V = \frac{W_{LL} \times DLF \times g}{n_b} = \frac{2600 \times 1.35 \times 9.81}{3} = 11477.7 \text{ N}$
Bolt Stress Area	$A_b = 0.000817 \text{ m}^2$
Bolt Tensile Stress	$\sigma_1 = \frac{T}{A_b} = \frac{11477.7}{0.000817 \times 1000} = 14048.6 \frac{\text{kN}}{\text{m}^2} = 14.0 \text{ MPa}$

$$\begin{aligned}
 \text{Bolt Shear Stress } \tau &= \frac{V}{A_b} = \frac{11477.7}{0.000817 \times 1000} = 14048.6 \frac{\text{kN}}{\text{m}^2} = 14.0 \text{ MPa} \\
 \text{Maximum Principal Stress } \sigma_{p1} &= \frac{1}{2} \times \left[\sigma_1 + \sqrt{\sigma_1^2 + 4 \times \tau^2} \right] \\
 &= \frac{1}{2} \times \left[14.0 + \sqrt{14.0^2 + 4 \times 14.0^2} \right] = 22.7 \text{ MPa} \\
 \text{Minimum Principal Stress } \sigma_{p2} &= \frac{1}{2} \times \left[\sigma_1 - \sqrt{\sigma_1^2 + 4 \times \tau^2} \right] \\
 &= \frac{1}{2} \times \left[14.0 - \sqrt{14.0^2 + 4 \times 14.0^2} \right] = -8.7 \text{ MPa} \\
 \text{Maximum Shear Stress } \tau_{\max} &= \frac{\sigma_{p1} - \sigma_{p2}}{2} = \frac{22.7 - (-8.7)}{2} = 15.7 \text{ MPa} \\
 \text{Bolt Yield Stress } S_y &= 896.3 \text{ MPa} \\
 \text{Allowable Shear Stress } S_a &= 0.6 \times S_y = 537.6 \text{ MPa} \\
 \text{Factor of Safety } FS &= \frac{S_a}{\tau_{\max}} = \frac{537.6}{15.7} = 34.2 > 3.0
 \end{aligned}$$

2.5.1.3.5.2 Lower Impact Limiter Thread Engagement

The minimum required thread engagement length to prevent impact limiter material failure is determined in accordance with “Machinery’s Handbook”, 26th Edition [Ref. 27]. Since the constants in the equation assume U.S. customary units, the metric units used in this calculation are converted for determination of the required engagement length. The minimum required thread engagement length that prevents upper impact limiter material failure is:

$$\text{Minimum Engagement Length } L_e = \frac{S_u \times 2 \times A_b}{S_{ct} \times \pi \times n \times D_{s,\min} \times \left[\frac{1}{2 \times n} + 0.57735 \times (D_{s,\min} - E_{n,\max}) \right]}$$

S_{bt} = Bolt External Thread Tensile Strength, MPa

A_b = Stress Area of Bolt External Threads, mm²

S_{ct} = Cask Internal Thread Tensile Strength, MPa n = Number of threads per millimeter

$D_{s,\min}$ = Minimum Major Bolt Diameter, mm

$E_{n,\max}$ = Maximum Pitch Diameter of Internal Thread, mm

Solving the equation for Minimum Engagement Length, L_e :

$$\begin{aligned}
 \text{Minimum Engagement Length} \\
 L_e &= \frac{150,000 \times 2 \times 1.27}{69,000 \times \pi \times 6.35 \times 1.396 \left[\frac{1}{2 \times 6.35} + 0.57735 \times (1.396 - 1.313) \right]} \\
 &= 1.56 \text{ in} = 39.5 \text{ mm}
 \end{aligned}$$

Where

$$\begin{aligned}
 S_{bt} &= 1030 \text{ MPa} = 150,000 \text{ psi} \\
 A_b &= 817.0 \text{ mm}^2 = 1.27 \text{ in}^2 \\
 S_{Lt} &= 470 \text{ MPa} = 69,000 \text{ psi} \\
 p &= \text{Thread Pitch} = 4.0 \text{ mm} = 0.157 \text{ in} \\
 n &= \frac{1}{p} = \frac{1}{0.157} = 6.35 \text{ Threads/inch} \\
 D_{s,min} &= 35.465 \text{ mm} = 1.396 \text{ in} \\
 E_{n,max} &= 33.342 \text{ mm} = 1.313 \text{ in}
 \end{aligned}$$

The available thread engagement, L_{ep} , is 75 mm. Therefore, the factor of safety is

$$FS = \frac{L_{ep}}{L_e} = \frac{75.0}{39.5} = 1.90 > 1.0$$

Therefore, the lower impact limiter lifting ring configuration is acceptable for the required loads.

2.5.2 Tie-down Devices

The RT-100 cask utilizes two sets of tie down arms, as shown in Chapter 7, Figure 7.4.4-1. These tie-down arms are welded to two different tie-down plates that in turn are welded to the outer shell of the cask body. Each set of arms on opposite sides of the cask are designed to cross over and securely position the cask, and to absorb the latitudinal, longitudinal and vertical forces required by 10 CFR 71.45 [Ref. 2]. The tie-down arms and plates are a structural part of the package, and must withstand the following loads without impairing the safety of the cask:

- Two (2) times the loaded weight of the cask in the vertical direction
- Ten (10) times the loaded weight of the cask in the direction of travel
- Five (5) times the loaded weight of the cask transverse to the direction of travel

These loads are considered to act simultaneously on the cask and the tie-down arms.

The lifting pockets on the cask body are the only other parts of the cask that could possibly be used to tie down the cask. As such, these pockets are rendered inoperable for tie-down during transport by ensuring that the lift yoke retaining pins are installed in place prior to transport.

2.5.2.1 Tie-down Load Calculation

The maximum forces applicable in each of the three loading directions are calculated in this section. This calculation is accomplished by using the mass of the fully loaded cask along with the gravitational acceleration and the vertical, longitudinal and lateral factors specified in 10 CFR 71.45 [Ref. 2]. The loaded weight of the cask is specified in Chapter 1, Section 1.2.1.2.

Gravitational Acceleration:	$g = 9.81 \text{ m/s}^2$
Cask Mass:	$M_c = 34696 \text{ kg}$
Payload Mass:	$M_p = 7060 \text{ kg}$
Total Mass:	$M = M_c + M_p = 34696 \text{ kg, assume } 42000 \text{ kg}$

Total Weight:	$W = M_g = 412.02 \text{ kN}$
Vertical Acceleration	$d_v = 2$
Axial Acceleration	$d_a = 10$
Transverse Acceleration	$d_L = 5$
Vertical Load	$P_y = M \times g \times d_v = 824 \text{ kN}$
Axial Load	$P_a = M \times g \times d_a = 4120.2 \text{ kN}$
Transverse Load	$P_L = M \times g \times d_L = 2060.1 \text{ kN}$

2.5.2.2 Tie-down Force Calculation

The geometric configuration of the tie-down system is designed so that the resultant tie-down arm tensile loads are tangent to the cask surface in order to minimize the effects of out-of-plane stresses in the cask shell. Figure 2.5.2-1 and Figure 2.5.2-2 illustrate the details of the tie-down system geometry. Shear stops are utilized to convert some of the cask loads into turning moments that are restricted by the tie-down arms. As shown on drawing RT PE 1001-1Rev. F – Robatel Transport Package RT-100 General Assembly Sheet 1/2 (Chapter 1, Appendix 1.4, Attachment 1.4-2), the tie-down arms have slightly different angles in the front and rear of the casks. These differences are summarized in Table 2.5.2-1. The horizontal angles from the cask body to each arm varies from 40° and 44° on one end of the cask and 37° and 41° on the other.

Table 2.5.2-1 Tie-down Arms Horizontal Angles

Load	Arms in Tension	Angles	Average Angle
Longitudinal	L & M (Rear)	44 and 40	42
	Q & R (Front)	37 and 41	39
Lateral	M & R	40 and 41	40.5
	L & Q	44 and 37	40.5
Vertical	L, M, Q, R	44, 40, 37, 41	40.5

The analytical model for determining the reaction loads required to prevent rotation and translation of the package due to the 10 CFR 71.45 [Ref. 2] applied loads is shown in Figure 2.5.2-1 and Figure 2.5.2-2. The evaluation is bounded by analyzing the high average angle (42°) caused by longitudinal forces on the tie-down arms on the rear of the cask, and the low average angle (32°) caused by longitudinal forces on the tie-down arms on the front of the cask. The shear stop forces at the bottom of the package are represented by the orthogonal components of a single force vector, S , making an angle of γ with the global y -axis. The stresses in the members are determined by considering the component loads ($10W$, $5W$, and $2W$) individually and superimposing the results. The geometry of the arms has a slight asymmetry so that the tie downs can cross one another; this slight asymmetry is ignored and average dimensions are used for calculation purposes. A detailed force analysis is conducted using the dimensions and notations shown in the figures; other terms are defined below:

W : weight of cask, kN

T_x : tensile force in member 2 and 3 resulting from $5W$ load, kN

T_y : tensile force in member 1 and 2 resulting from $10W$ load, kN

- T_z : tensile force in each member resulting from 2W load, kN
 $T_{1,2,3,4}$: total tensile force in subscripted member, kN
 F_x : total force in the x direction resulting from 5W load, kN
 F_y : total force in the y direction resulting from 10W load, kN
 L : Effective length of tie-down arm, i.e. distance between tie-down tangent point and center of tie-down attachment eye, mm

The forces are derived in detail in Calculation Package RTL-001-CALC-ST-0202, Rev. 4 [Ref. 34] and are developed via summing the moments about the center of gravity. A summary of the values calculated using Figure 2.5.2-1 and Figure 2.5.2-2 are provided in Table 2.5.2-2. The maximum calculated forces using these values is provided in Table 2.5.2-3. The results show that the front arms with the lower horizontal angle are subjected to the greater forces. The evaluation of the longitudinal loads on the two front tie-down arms bounds the evaluation of all other load conditions on the cask. The tension calculations and safety margin evaluations contained in the following sections focuses on the front tie-down arms.

Unit: mm

 $R = \text{impac limiter radius} = 2587/2$ $r = \text{cask radius} = (2040+60)/2$ $d = \text{cask C.G. elev.} = 1648$ $t = \text{avg. tie-down eye elev.} = 1429$ $L = \text{total length from the tangent point of the tie-down arm (to the cask body) to the tie-down eye}$ $x' = \text{avg. tie-down eye X axis offset}$ $y' = \text{avg. tie-down eye Y axis offset}$ $z' = \text{cask tangent elev.}$ $a = L \cos\theta \sin\phi$ $b = L \cos\theta \cos\phi$ $c = L \sin\theta$

weight	412.02	KN
R	1293.5	mm
r	1050	mm
d	1648	mm
t	1429	mm
L	605	mm
θ	0.514872	rad
ϕ	0.733038	rad
a	352.3409	mm
b	391.3142	mm
c	297.9163	mm
x'	427.9612	mm
y'	1093.901	mm
z'	1726.916	mm

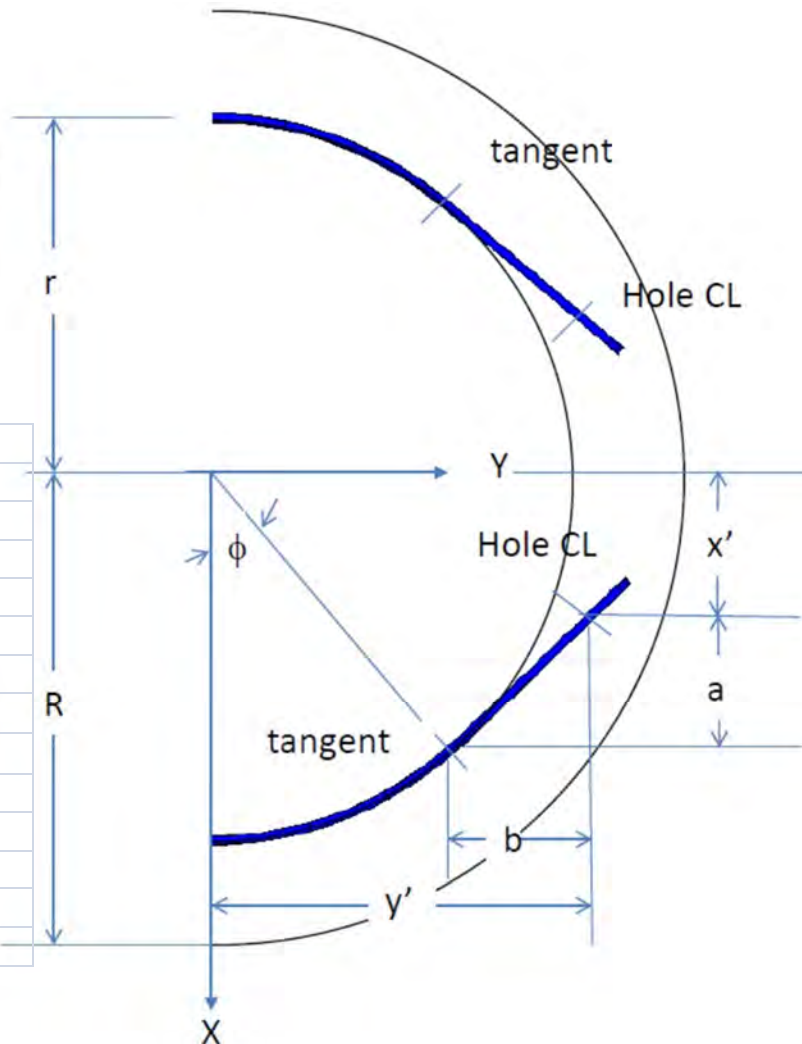


Figure 2.5.2-1 RT-100 Tie-Down Arm Geometry



Table 2.5.2-2 Calculated Values for Tie-Down Arms

	Rear Arms		Front Arms	
Φ	$(44^\circ \& 40^\circ) = > 0.733038$	rad	$(41^\circ \& 37^\circ) = > 0.680678$	rad
a	351.47	mm	365.61	mm
b	390.34	mm	451.49	mm
c	297.18	mm	328.69	mm
L	$(616 + 591)/2 = 603.5$	mm	$(682 + 653)/2 = 667.5$	mm
x'	451.13	mm	473.71	mm
y'	1113.01	mm	1131.16	mm
z'	1726.18	mm	1757.59	mm

(Note: these values calculated using parameters as defined in Figure 2.5.2-1 and Figure 2.5.2-2)

Table 2.5.2-3 Calculated Forces for Tie-Down Arms

	Rear Arms		Front Arms	
T _x	1361.26	kN	1430.82	kN
T _y	1609.56	kN	1571.40	kN
T _z	418.36	kN	418.36	kN
T _{max}	3389.18	kN	3420.58	kN
F _{xx}	474.56	kN	492.68	kN
F _{yy}	2038.07	kN	1994.43	kN
F _n	2925.80	kN	2956.73	kN
F _f	146.29	kN	147.84	kN
S _x	204.57	kN	213.28	kN
S _y	953.61	kN	931.10	kN

2.5.2.3 Tie-Down Arm Evaluation

The maximum tie-down arm load of 3420.58 kN is determined as described in Section 2.5.2.2 above. This load is applied to the tie-down arm design to ensure that stresses are within allowable limits. As show in the drawings presented in (Chapter 1, Appendix 1.4, Attachments 1.4-2 through 1.4-8) the tie-down arm is reinforced in the portion containing the attachment hole. This reinforcement ensures that the loads in this area of reduced cross-section can be transmitted safely into the rest of the tie-down arm. Stresses for the tie-down arm and its connection to the exterior cask shell are calculated as follows:

Arm Tension Stress at HoleArm Cross-Sectional Area at Hole, $A_{\text{net}} = 11,450 \text{ mm}^2$ Arm Tension Stress, $\sigma_{\text{net}} = T_{\text{max}} / A_{\text{net}} = 298.74 \text{ MPa}$ Stress Allowable, $\sigma_{\text{allow}} = 437.2 \text{ MPa}$ (@50°C per Table 2.2.1-1)Factor of Safety, $FS = \sigma_{\text{allow}} / \sigma_{\text{net}} = 437.2 / 298.74 = 1.46 > 1.0$ Arm Bearing Stress at HoleArm Bearing Area at Hole, $A_{\text{bear}} = 7,650 \text{ mm}^2$ Arm Tension Stress, $\sigma_{\text{net}} = T_{\text{max}} / A_{\text{bear}} = 447.13 \text{ MPa}$

Stress Allowable, $\sigma_{\text{allow}} = 1.35 \times 437.2 \text{ MPa} = 590.2 \text{ MPa}$ (@50°C per Table
2.2.1-1) Factor of Safety, $FS = \sigma_{\text{allow}} / \sigma_{\text{net}} = 590.2 / 447.13 = \underline{1.32} > 1.0$

Arm Tear-Out Stress at Hole

Arm Tear-out Area, $A_{\text{tear}} = 18,700 \text{ mm}^2$

Arm Tear-out Stress, $\tau_{\text{tear}} = T_{\text{max}} / A_{\text{tear}} = 182.92 \text{ MPa}$

Tear-out Stress Allowable, $\tau_{\text{allow}} = 0.6 \times 437.2 = 262.3 \text{ MPa}$

Factor of Safety, $FS = \tau_{\text{allow}} / \tau_{\text{tear}} = 262.3 / 182.92 = \underline{1.43} > 1.0$

Arm Tension Stress at Main Cross Section

Arm Area, $A_{\text{arm}} = 9,100 \text{ mm}^2$

Arm Tear-out Stress, $\sigma_{\text{arm}} = T_{\text{max}} / A_{\text{arm}} = 375.89 \text{ MPa}$

Tear-out Stress Allowable, $\sigma_{\text{allow}} = 437.2 \text{ MPa}$

Factor of Safety, $FS = \sigma_{\text{allow}} / \sigma_{\text{arm}} = 437.2 / 375.89 = \underline{1.16} > 1.0$

As shown in the summary above, the stresses in the limiting tie-down arm are below the yield stress allowables.

2.5.2.4 Tie-down Arm & Plate Weld Evaluation

The stresses in the welds attaching the tie-down arms to the tie-down plates and the plates to the cask body are found by applying the loads from the attachment arms to the weld around the perimeter of the plates. The maximum load on the tie-down arm welds are the sum of the loads in two connecting arms. Thus, from inspection of Figure 2.5.2-2, the maximum tie-down arm load is calculated as follows:

Tie-down Arm Weld Force, $F_{\text{total}} = 2T_x + T_y + 2T_z = 5269.76 \text{ kN}$

Weld axial load $F_x = F_{\text{total}} \times (b / L) = 3564.43 \text{ kN}$

Weld vertical load $F_y = F_{\text{total}} \times (c / L) = 2594.96 \text{ kN}$

Weld transverse load $F_z = F_{\text{total}} \times (a / L) = 2886.42 \text{ kN}$

Arm tensile strength: 437.2 MPa

Cask tensile strength: 199.3 MPa

Weld tensile strength: 450 MPa, weld between tie-down arm and plate [Ref. 34]

420 MPa, weld between tie-down plate and cask [Ref. 34]

The weld length, b , is 1583.36 mm, the weld height “ d ” for the tie- down arm plate is the 260 mm height of the arm, and weld height “ d ” for the weld between tie- down plate and cask body is 388.03 mm (Calculation Package RTL-001-CALC-ST-0202 Rev. 4 [Ref. 34]). These dimensions and loads are used in the following weld stress calculations.

2.5.2.4.1 Tie Down Arm-to-Plate Weld Stress

The stresses in the welds attaching the tie-down arm to the tie-down plate are found by applying the weld loads as specified in Section 2.5.2.4. The stresses and allowables are determined as described in “Design of Welded Structures” [Ref. 25] and Calculation Package RTL-001-CALC-ST-0202, Rev. 4 [Ref. 34].

Weld properties are as follows:

$$b = 1.583 \text{ m}$$

$$d = 0.260 \text{ m}$$

$$C_y = b/2 = 0.79 \text{ m}$$

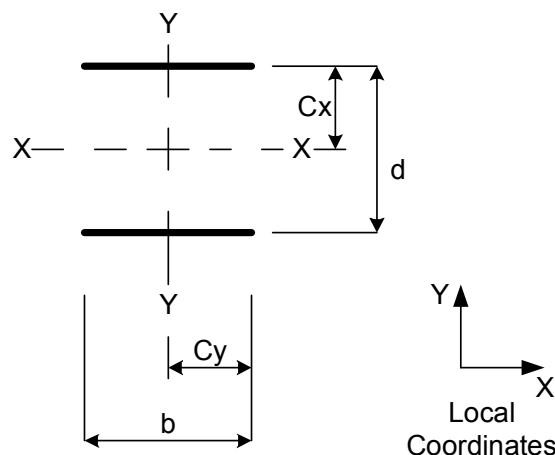
$$C_x = d/2 = 0.13 \text{ m}$$

$$A_w = 2 \times b = 3.172 \text{ m}^2/\text{m}$$

$$S_x = b \times d = 0.41 \text{ m}^3/\text{m}$$

$$S_y = b^2/3 = 0.84 \text{ m}^3/\text{m}$$

$$J_w = b (3d^2 + b^2) / 6 = 0.71 \text{ m}^4/\text{m}$$



$$\text{Weld Throat Size} = 0.022 \text{ m}$$

Weld stress is calculated as follows:

$$f_t = (F_z / A_w) + (M_x / S_x) + (M_y / S_y) = 911.69 \text{ kN/m}$$

$$f_{vy} = (F_y / A_w) + ((M_z \times C_y) / J_w) = 819.63 \text{ kN/m}$$

$$f_{vx} = (F_x / A_w) + ((M_z \times C_x) / J_w) = 1125.85 \text{ kN/m}$$

$$f_w = (f_t^2 + f_{vy}^2 + f_{vx}^2)^{1/2} = 1664.49 \text{ kN/m}$$

$$\text{Weld Allowable Stress} = 0.6 \times F_w \times \text{Weld Size} \times 1000 = 5940 \text{ kN/m}$$

$$\text{Weld Metal Factor of Safety, FS} = 5940 / 1664.49 = \underline{3.56} > 1.0$$

$$\text{Tie-Down Arm Shear Allowable} = 0.6 \times F_w \times \text{Weld Size} / 0.7071 \times 1000 = 8158 \text{ kN/m}$$

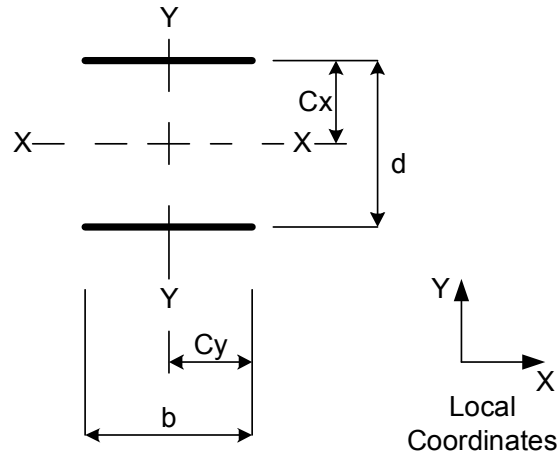
$$\text{Tie-Down Arm Factor of Safety, FS} = 8158 / 1664.49 = \underline{4.90} > 1.0$$

2.5.2.4.2 Tie Down Plate-to-Outer Shell Weld Stress

The stresses in the welds attaching the tie-down plate to the cask outer shell are found by applying the weld loads as specified in Section 2.5.2.4. The stresses and allowables are determined as described in “Design of Welded Structures” [Ref. 25] and Calculation Package RTL-001-CALC-ST-0202, Rev. 4 [Ref. 34].

Weld properties are as follows:

$$\begin{aligned}
 b &= 1.583 \text{ m} \\
 d &= 0.388 \text{ m} \\
 C_y &= b/2 = 0.79 \text{ m} \\
 C_x &= d/2 = 0.19 \text{ m} \\
 A_w &= 2 \times b = 3.172 \text{ m}^2/\text{m} \\
 S_x &= b \times d = 0.615 \text{ m}^3/\text{m} \\
 S_y &= b^2/3 = 0.84 \text{ m}^3/\text{m} \\
 J_w &= b (3d^2 + b^2) / 6 = 0.78 \text{ m}^4/\text{m}
 \end{aligned}$$



Weld Throat Size = 0.017 m

Weld stress is calculated as follows:

$$\begin{aligned}
 f_t &= (F_z / A_w) + (M_x / S_x) + (M_y / S_y) = 911.69 \text{ kN/m} \\
 f_{vy} &= (F_y / A_w) + ((M_z \times C_y) / J_w) = 819.63 \text{ kN/m} \\
 f_{vx} &= (F_x / A_w) + ((M_z \times C_x) / J_w) = 1125.85 \text{ kN/m} \\
 f_w &= (f_t^2 + f_{vy}^2 + f_{vx}^2)^{1/2} = 1664.49 \text{ kN/m}
 \end{aligned}$$

Weld Allowable Stress = $0.6 \times F_w \times \text{Weld Size} \times 1000 = 4284 \text{ kN/m}$

Weld Metal Factor of Safety, FS = $4284 / 1664.49 = 2.57 > 1.0$

Outer Shell Shear Allowable = $0.6 \times F_w \times \text{Weld Size} / 0.7071 \times 1000 = 2.875 \text{ kN/m}$

Outer Shell Factor of Safety, FS = $2875 / 1664.49 = 1.73 > 1.0$

2.5.2.5 Tie-Down Evaluation Summary

As shown in the previous sections, all components of the tie-down components that are a structural part of the cask maintain positive safety margins when subjected to the simultaneous loadings specified in 10 CFR 71.45 [Ref. 2]. The smallest factor of safety is 1.16 against tie-down arm tension. Under excessive loading, the failure of the tie-down system occurs by yielding in the tie-down arm. This failure does not impair the package's ability to meet other regulatory requirements since the tie-down arms are welded to a plate that is in-turn welded to the cask body. Damage to the tie-down arm does not damage any component integral to the cask body and therefore, does not compromise the cask body shell.

2.6 Normal Conditions of Transport

This Section describes the RT-100 evaluation for the normal conditions of transport specified in 10 CFR 71.71[Ref. 2]. The requirements of 10 CFR 71.71 state that the RT-100 shall be structurally adequate for the following normal conditions of transport:

- Heat
- Cold
- Reduced external pressure

- Increased external pressure
- Vibration
- Water spray, free drop
- Corner drop
- Compression, and
- Penetration.

During the free drop analyses, the cask impact orientation evaluated is the orientation that inflicts the maximum damage to the cask. Also, the requirements of 10 CFR 71.71 [Ref. 2] specify that the evaluation of the RT-100 for the normal conditions of transport be evaluated at the most unfavorable ambient temperature in the range from -29°C to +100°C. The normal conditions of transport evaluations presented in this section show that the package satisfies the applicable performance requirements specified in the 10 CFR 71.71 [Ref. 2]. The scale drop testing and analytical analyses demonstrate that there is no decrease in the RT-100 Cask Package effectiveness as follows:

- No loss or dispersal of contents
- No structural changes reducing the effectiveness of components required for shielding, for heat transfer, or for maintaining subcriticality or containment
- No changes to the package affecting its ability to withstand HAC.

The normal conditions evaluations described in the following sections are performed in accordance with the design criteria and load combinations as identified in Section 2.1.2. Each of the following subsections addresses each normal conditions requirement.

2.6.1 Heat

The RT-100 cask body and closure lids are analyzed for structural adequacy in accordance with the thermal evaluation of the RT-100 for the temperatures specified in 10 CFR 71.71(c)(1) [Ref. 2] is presented in Chapter 3. The thermal evaluation demonstrates that the cask component temperatures are maintained within their safe operating ranges for all normal conditions of transport. The following subsections discuss the structural evaluation of the RT-100 using the appropriate component temperatures as determined in Chapter 3.

2.6.1.1 Summary of Pressures and Temperatures

The pressures and temperatures occurring in the RT-100 as a result of the 10 CFR 71 [Ref. 2] normal conditions of transport thermal conditions are an important consideration for the structural evaluations presented in this chapter. The internal pressure induces stresses on the containment system; the temperatures affect the selection of temperature-dependent material properties as well as, the internal pressures that occur as a result of the ambient temperatures and solar insolation specified in 10 CFR 71.71 [Ref.2]. The material properties utilized are based on the maximum calculate temperatures of each component or higher temperatures which are conservative.

The maximum normal operating pressure evaluation for the RT-100 is presented in Chapter, 3 Section 3.3.2. As described in this section, the calculated maximum pressure for normal

conditions is 182.71 kPa (26.5 psia). For conservatism, the structural evaluations involving internal pressure use a maximum normal operating condition pressure of 342.7 kPa (49.7 psia or 35 psig).

The maximum component temperatures in the RT-100 for normal conditions are presented in Chapter 3, Table 3.1.3-1 “RT-100 Maximum Normal Condition Temperature Summary” (Found in Chapter 3). The temperatures are utilized to determine the stress allowables used in the structural evaluation for the normal conditions of transport.

2.6.1.2 Differential Thermal Expansion

As shown in Chapter 3, Table 3.1.3-1, the temperatures of the components of the cask differ by only a few degrees under normal conditions of transport thermal ambient conditions. This difference is due in part to the relatively low decay heat of the contents. The RT-100 is evaluated for differential thermal expansion as described in Section 2.6.7 in combination with normal pressure and inertial loads under the following conditions:

- Ambient temperature, 38°C
- Initial temperature, 38°C
- Heat transfer to ambient by natural convection, still air
- Heat transfer to ambient by radiation
- Steady-state solar insolation
- Internal heat load as a uniform heat flux, 13.04 W/m²

2.6.1.3 Stress Calculations

Regulatory Guide 7.6 [Ref. 4] requires that the range of primary plus secondary stress intensities during normal conditions of transport be less than 3.0 S_m. To evaluate this condition, the range of primary plus secondary stresses for the combined normal events (including heat, cold, normal operating pressure, 0.3-m end drop, and 0.3-m side drop conditions) are analyzed using the finite element model presented in 2.6.7.2.

2.6.1.4 Comparison with Allowable Stresses

The combined stress results are presented in Tables 2.6.7-1 and 2.6.7-2. Since the margins of safety are all positive, the RT-100, therefore, satisfies the requirements of 10 CFR 71.71(c)(1) [Ref. 2] for the heat (normal transport) condition.

2.6.2 Cold

The RT-100 cask body and closure lids are analyzed for structural adequacy in accordance with the thermal evaluation of the RT-100 for the temperatures specified in 10 CFR 71.71(c)(2) [Ref. 2] is presented in Chapter 3. The thermal evaluation demonstrates that the RT-100 component temperatures are maintained within their safe operating ranges for all normal conditions of transport. Using the same methodology presented in Section 2.6.1, the RT-100 is evaluated for cold conditions. The following thermal case is used to calculate the thermal stress under cold conditions:

- Ambient temperature, -40°C
- Initial temperature, -40°C

- Heat transfer to ambient by natural convection, still air
- Heat transfer to ambient by radiation
- No solar insolation, in shade
- Internal heat load as a uniform heat flux, 13.04 W/m²

The combined stress results are presented in Tables 2.6.7-1 and 2.6.7-2. Since the margins of safety are all positive, the RT-100, therefore, satisfies the requirements of 10 CFR 71.71(c)(2) [Ref. 2] for the cold (normal transport) condition.

2.6.3 Reduced External Pressure

The drop in atmospheric pressure to 24 kPa (3.5 psia), as specified in 10 CFR 71.71(c)(3) [Ref. 2], effectively results in an additional internal pressure in the cask of 77 kPa (11.2 psig). This additional pressure has a negligible effect on the RT-100 because, in Section 2.6.1.1, the cask is analyzed for a normal transport conditions internal pressure of 241 kPa (35 psig). Maximum internal pressure is included in combination with internal loads (see Tables 2.6.7-1 and 2.6.7-2). Since the margins of safety are all positive, the RT-100 satisfies the requirements of 10 CFR 71.71(c)(3) for reduced external pressure.

2.6.4 Increased External Pressure

An increased external pressure of 20 psia (5.3 psig external pressure), as specified in 10 CFR 71.71(c)(4) [Ref. 2], has a negligible effect on the RT-100 because of the thick outer shell and end closures of the cask. Section 2.6.7 addresses many different loading cases which exceed these prescribed external pressure requirements. Therefore, the requirements of 10 CFR 71.71(c)(4) [Ref. 4] are satisfied.

2.6.5 Vibration

10 CFR 71.71 (c)(5) [Ref.4] requires that “vibration normally incident to transport” be evaluated. The RT-100 package consists of thick section materials that are unaffected by vibration normally incident to transport, such as over the road vibrations.

2.6.5.1 Vibration Evaluation of the RT-100 Cask Primary Lid Bolts

The RT-100 may be subjected to a cycle range typically associated with high-cycle fatigue ($> 10^8$ cycles). Therefore, the endurance limit of the material for the high cycle fatigue can be approximated by using a 60% reduction, r_h , of the ultimate tensile strength (AISC [Ref. 26]) with an additional 10% reduction r_g , for the connection surface (Machinery’s Handbook [Ref. 27]). Thus the endurance limit for the material is:

$$S_a = (1 - r_h) \times (1 - r_g) \times S_{ub}$$

where:

$$\begin{aligned} S_{ub} &= \text{Bolt Ultimate Stress} \\ &= 1030 \text{ MPa} \quad (\text{ASTM A354 Grade B, Table 2.2.1-3}) \end{aligned}$$

$$\begin{aligned}
 S_a &= (1 - 0.60) \times (1 - 0.10) \times 1030 \\
 &= 370.8 \text{ MPa}
 \end{aligned}$$

NUREG-0128 [Ref. 30] gives the following RMS vibration load factors for the road travel:

$$\begin{aligned}
 f_v &= \text{Vertical Vibration Load Factor} \\
 &= 0.52
 \end{aligned}$$

$$\begin{aligned}
 f_L &= \text{Longitudinal Vibration Load Factor} \\
 &= 0.27
 \end{aligned}$$

$$\begin{aligned}
 f_t &= \text{Transverse Vibration Load Factor} \\
 &= 0.19
 \end{aligned}$$

The RT-100 is transported in the vertical orientation. The cask lid is subjected to vibration in the vertical direction. A notch factor, f_N , of 3.0 is used and is conservative (AISC [Ref. 26]). The vibration stress in the bolts is:

$$s_y = \frac{F_b \times f_N}{A_b}$$

where:

$$\begin{aligned}
 F_b &= \text{Bolt Force due to Vibration} \\
 &= \frac{f_v \times W_{Lp} \times g}{N_b}
 \end{aligned}$$

$$\begin{aligned}
 A_b &= \text{Bolt Stress Area} \\
 &= 1470 \text{ mm}^2 \quad \quad \quad [\text{Ref. 27}]
 \end{aligned}$$

$$\begin{aligned}
 W_{Lp} &= \text{Cask Lid Weight} \\
 &= 3648 \text{ kg, use } 3650 \text{ kg}
 \end{aligned}$$

$$\begin{aligned}
 N_b &= \text{Number of Bolts} \\
 &= 32
 \end{aligned}$$

$$\begin{aligned}
 F_b &= \frac{0.52 \times 3650 \times 9.81}{32} \times \frac{1 \text{ kN}}{1000 \text{ N}} \\
 &= 0.58 \text{ kN}
 \end{aligned}$$

$$\begin{aligned}
 s_v &= \frac{0.58 \times 3.0}{0.001470} \times \frac{1 \text{ MPa}}{1000 \frac{\text{kN}}{\text{m}^2}} \\
 &= 1.19 \text{ MPa} \ll S_a = 370.8 \text{ MPa}
 \end{aligned}$$

Since the stress in the bolts is well below the endurance limit of the material, the primary lid bolts are not subjected to transportation-related fatigue damage during their service life.

The maximum shock loading coefficient for the three orthogonal directions is specified as 2.9 (NUREG-0128 [Ref. 30]). The RT-100 primary lid is subjected to shock loading during transport. The primary lid closure bolts are shown to withstand a 125g impact load (Section 2.13.3.3), which is much larger than the 2.9W shock loading during transport. Therefore, the primary lid closure bolts are acceptable for shock loading by comparison.

2.6.5.2 Vibration Evaluation of the RT-100 Cask Secondary Lid Bolts

Per Section 2.6.5.1, the components of the package are in the high-cycle fatigue range ($> 10^8$ cycles). The endurance limit of the material for the high cycle fatigue for the secondary lid bolts is the same as for the primary lid bolts. The RT-100 lid is subjected to vibration in the vertical direction. A notch factor, f_N , of 3.0 is used and is conservative (AISC [Ref. 26]). The vibration stress in the bolts is:

$$s_v = \frac{F_b \times f_N}{A_b}$$

where:

$$F_b = \text{Bolt Force due to Vibration}$$

$$= \frac{f_v \times W_{Lp} \times g}{N_b}$$

$$A_b = \text{Bolt Stress Area}$$

$$= 817 \text{ mm}^2 \quad [\text{Ref. 27}]$$

$$W_{Ls} = \text{Cask Lid Weight}$$

$$= 857 \text{ kg}$$

$$N_b = \text{Number of Bolts}$$

$$= 18$$

All other quantities are defined in Section 2.6.5.1

$$F_b = \frac{0.52 \times 857 \times 9.81}{18} \times \frac{1 \text{ kN}}{1000 \text{ N}}$$

$$= 0.24 \text{ kN}$$

$$s_v = \frac{0.24 \times 3.0}{0.000817} \times \frac{1 \text{ MPa}}{1000 \text{ kN/m}^2}$$

$$= 0.89 \text{ MPa} \ll S_a = 370.8 \text{ MPa}$$

Since the stress in the bolts is well below the endurance limit of the material, the secondary lid bolts are not subjected to transportation-related fatigue damage during their service life.

The maximum shock loading coefficient for the three orthogonal directions is specified as 2.9 (NUREG-0128 [Ref. 30]). The cask primary lid is subjected to shock loading during transport. The secondary lid closure bolts have been shown to withstand a 125g impact load (Section 2.12.4.1), which is much larger than the 2.9W shock loading during transport. Therefore, the secondary lid closure bolts are acceptable for shock loading by comparison.

The RT-100 satisfies the requirements for normal vibration incident to transport as required by 10 CFR 71.71(c)(5) [Ref. 2].

2.6.6 Water Spray

Water causes negligible corrosion of the stainless shell of the RT-100. The cask contents are protected in the sealed cavity. A water spray as specified in 10 CFR 71.71(c)(6) [Ref. 2] has no adverse impact on the package. The cask surface temperature specified during the water spray is between 38°C and -29°C. Consequently, the induced thermal stress in the cask components is less than the thermal stresses that occur during the extreme temperature conditions for normal transport. Therefore, the requirements of 10 CFR 71.71(c)(6) [Ref. 2] are satisfied.

2.6.7 Free Drop

The RT-100 is shown to meet the free drop requirements of 10 CFR 71.71 [Ref. 2] through a combination of classic calculations, finite element analyses and scale model drop testing (RTL-001-CALC-ST-0402, Rev. 4 [Ref. 35]). The evaluations include the qualification of the RT-100 cover bolt design for the combined effects of free drop impact force, internal pressures, thermal stress, O-ring compression force, and bolt preload following the methodology of NUREG/CR-6007 [Ref. 10] (Appendix 2.13). The combined effects of inertial loads, internal pressures, and thermal stress are considered for packaging components.

2.6.7.1 Methodology

The RT-100 is designed in accordance with Regulatory Guide 7.6 [Ref. 4]. The design criteria for NCT and HAC are presented in Table 2.1.2-2. Load combinations for the structural analysis of shipping casks for radioactive materials are defined by Regulatory Guide 7.8 [Ref. 3]. The load combinations for all normal and accident conditions and corresponding ASME service levels are shown in Table 2.1.2-1. Material properties used in this evaluation are presented in Section 2.2.1. Stress intensities caused by pressure, thermal expansion, and mechanical loads are combined before comparing to ASME, Section III, Subsection ND [Ref. 7] stress allowables, which are listed in Table 2.2.1-3.

2.6.7.2 Finite Element Analysis

The finite element code ANSYS [Ref. 28] is used to generate a three-dimensional model of the RT-100 and to determine its response to normal conditions of transport (NCT) and hypothetical accident conditions (HAC) (Section 2.7.1). Specifically, a one-half (180°) 3D model of the RT-100 inner and outer shells, outer and inner lids, bottom plate and lead shields is constructed using ANSYS [Ref. 28] solid elements. The interaction between components is modeled using gap elements. Stability of the model is assured by using weak springs. Boundary conditions are

applied to the model simulating the loading conditions the cask will experience during normal and accident transport conditions. Pressure loads are applied to the cask inner shell to simulate bounding contents loads and internal pressurization. Thermal stresses are calculated using input temperatures from the NCT thermal analyses. Bolt preloads are applied to represent the bolt torque at the time the cask is readied for shipment. Post-processing is accomplished by linearizing the stress across locations where maximum stresses are calculated. The analyses assume linear elastic behavior of the cask. Therefore, calculated stress intensities are compared to appropriate allowables (Table 2.2.1-1) and the margin of safety is calculated.

2.6.7.2.1 Model Description

Finite element analysis methods are used to perform the stress evaluation of the RT-100 for normal and accident free drop conditions. Each drop condition is analyzed using a three-dimensional finite element model using the computational modeling software ANSYS [Ref. 28]. Figure 2.6.7-1 shows the major components of the RT-100 represented in the model including the inner and outer shells, flange, bottom plate, primary and secondary lids, and closure bolts.

As shown in Figure 2.6.7-1, the model (which corresponds to half (180°) of the cask body) is generated by de-featuring the SolidWorks® solid model used to develop the manufacturing drawings and exporting the model to a .STEP file format. The .STEP file is imported directly into ANSYS [Ref.28] where the finite element model is developed following the guidance presented in ISG-21 [Ref. 53]. The resulting finite element model of the cask body is represented using solid elements, contact elements, mass elements and spring/damper elements (Figure 2.6.7-2).

The solid portion of the model is constructed using ANSYS solid (SOLID185) elements. Surface-to-surface contact elements are used to simulate the interaction between adjacent components. Specifically, contact between the cask shells and lead shielding are modeled using CONTAC174/TARGE170 surface-to-surface contact elements with zero friction, which allows the lead to float between the inner and outer shells. Contact elements are also used to bond dissimilarly meshed components. To simulate the impact limiters, the interaction between the cask body and impact limiters is modeled using CONTAC52 gap elements (Figure 2.6.7-3), which acts as a compression only element. The size of the CONTAC52 gaps is determined from nominal dimensions between the impact limiter and cask body. Spring elements (COMBIN14) are inserted automatically during the solution to help stabilize the model. ANSYS [Ref. 28] assigns low spring stiffness so their presence does not adversely affect the accuracy of the solution.

Finite element model verification and mesh density study are presented in Appendix A.4 of Calculation Package RTL-001-CALC-ST-0402, Rev. 4 [Ref. 35]. During the development of the finite element model each part and interface was considered on an individual basis. The RT-100 outer shell was meshed using the sweep method and the element size was varied until there was a sufficient number of elements across the shell thickness. The element ratio was reviewed to ensure adequate results. To test a component, in this case the outer shell, the ends were fixed and a pressure load was applied to the inner surface and a solution was obtained. If a singularity or discontinuity was noted, the mesh was refined until uniform results were obtained. As a second check, a hand calculation was performed on to ensure that the stress calculated by ANSYS

[Ref. 28] is giving expected results. Hoop stresses were also calculated and compared to the results. As the model was developed the same philosophy was applied to the intersection of the shell and bottom plate. Using Roark's equations ("Roark's Formulas for Stress and Strain" [Ref. 29]), the interface stress was checked to ensure the bending stress was in the expected range.

The choice of element type was evaluated by running a series of sensitivity studies. For this case, a high order 8-node brick element was chosen over brick element with mid-side nodes. This choice was made because of the relatively thin section of the RT-100 shell versus the length, which made it possible to increase the total number of elements without compromising the run time performance. Several cases were run to vary the total mesh density to see how the stress results varied versus performance of the model. In the extreme case, an overly dense mesh produced excessively long run times and un-converged solutions. Models with low mesh densities that were too low resulted in unrealistic stress results. After numerous runs a balance was found between consistent results and model performance with variations in stress results of less than 1% when comparing high mesh densities to adequate mesh densities. Therefore, it was concluded that the cask model was a quality model and met the intent of ISG-21 [Ref. 53].

At the time the analyses were performed, analyses were generally compared to models previously generated for other 10 CFR 71 [Ref. 2] cask designs. The results of the RT-100 cask analysis are consistent with these previous designs and where peak stress are expected. Additionally, confirmatory scale model testing of the RT-100 demonstrated that the methods used to calculate the cask accelerations and impact limiter deformation are consistent with the drop test results. Therefore, the inertial loads applied to the cask body are conservative.

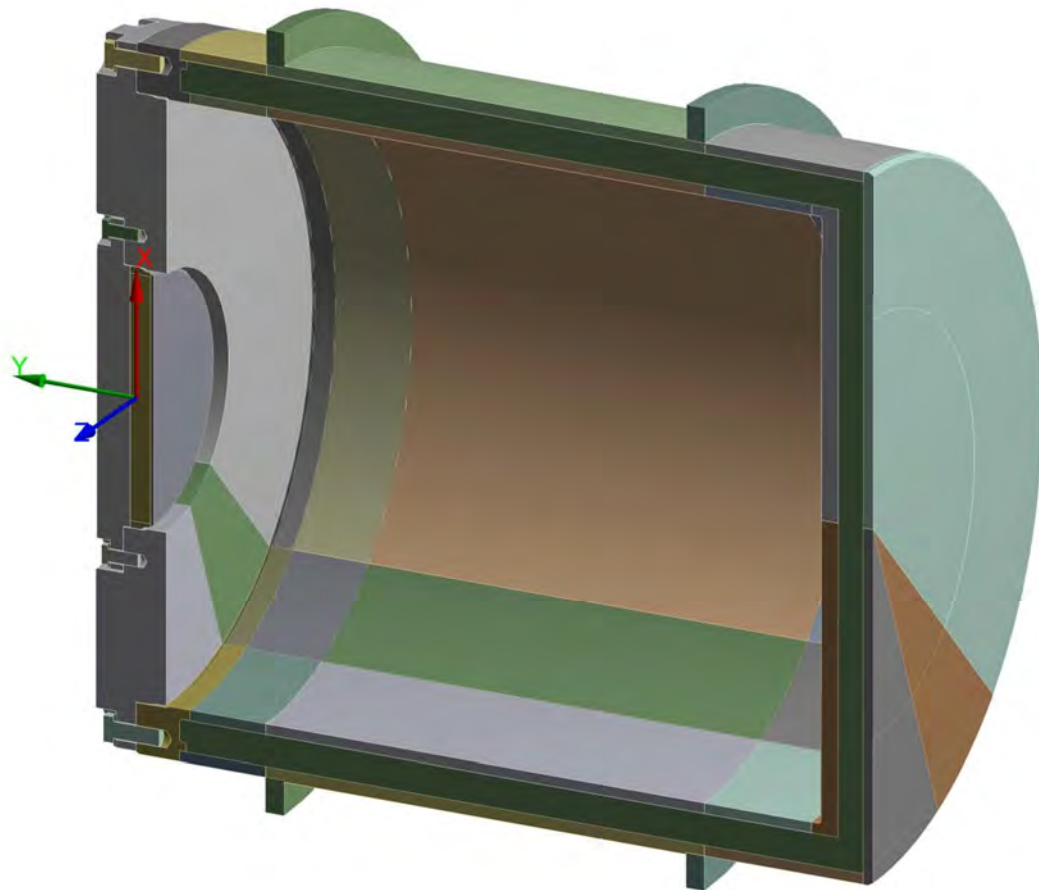


Figure 2.6.7-1 RT-100 Solid Model

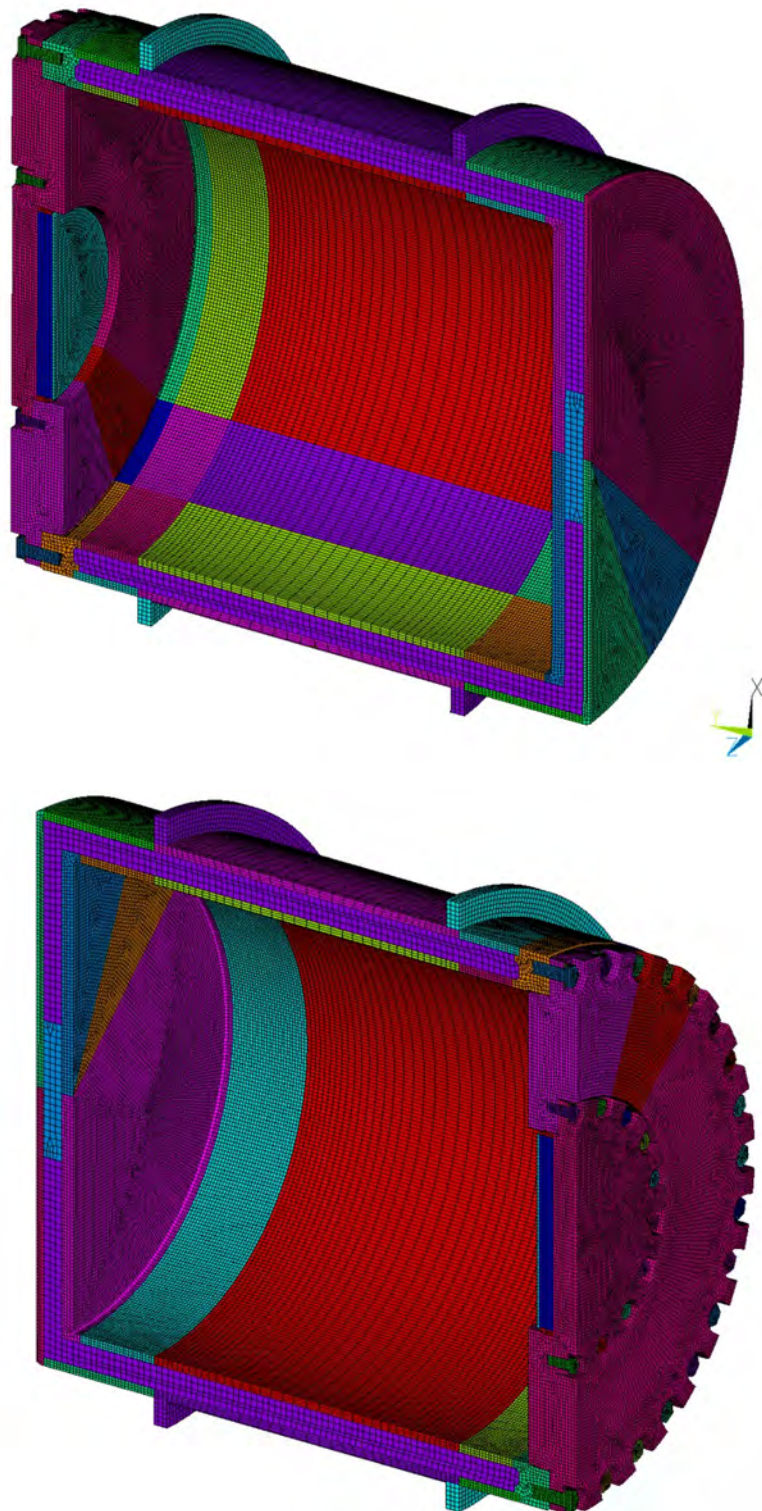


Figure 2.6.7-2 RT-100 Finite Element Model

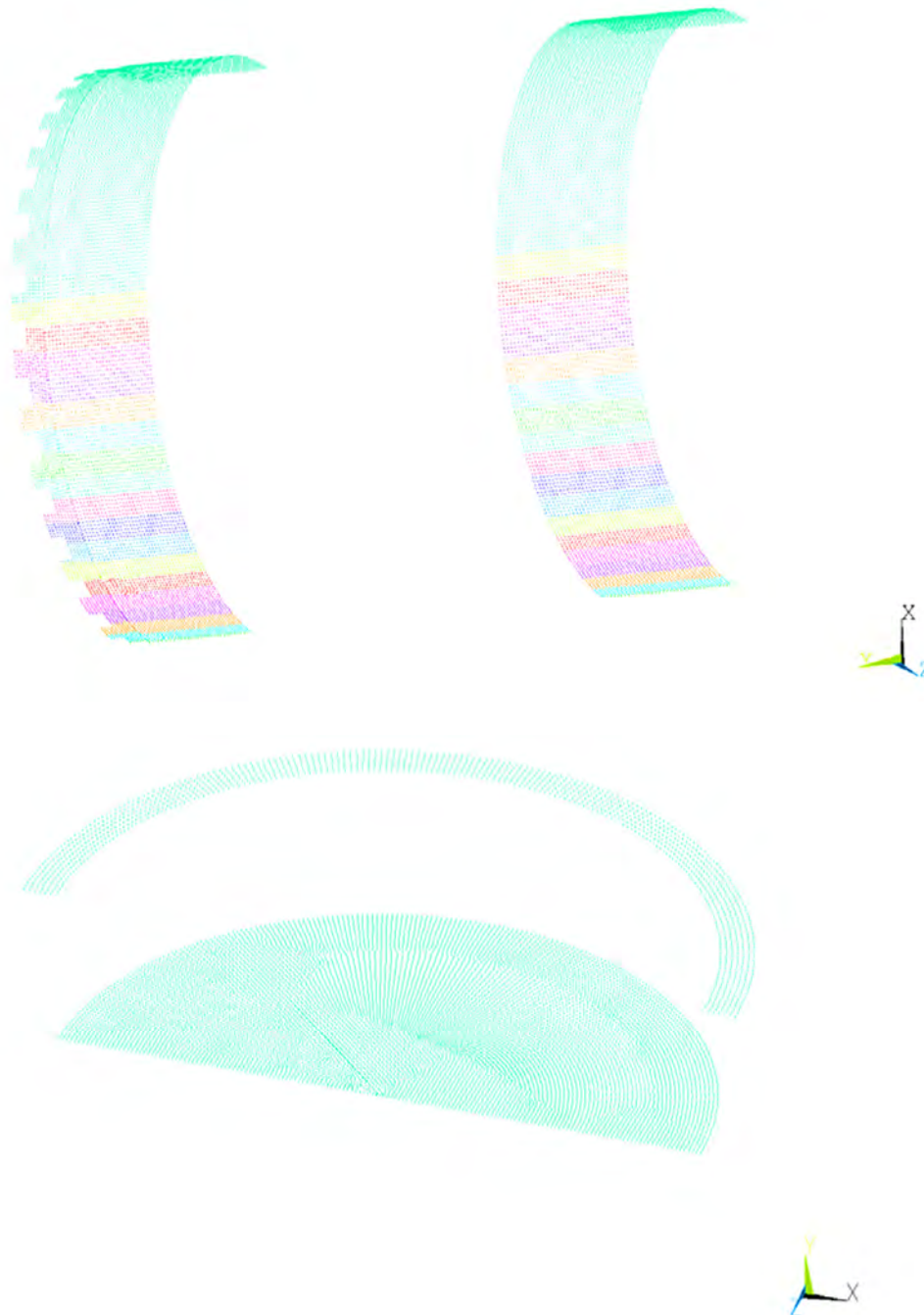


Figure 2.6.7-3 Gap Elements Used to Represent the Impact Limiters for Side and End Drop Configurations

2.6.7.2.2 Boundary Conditions

Boundary conditions are applied to the model to simulate the loading conditions the RT-100 experiences during NCT and HAC. The five categories of cask loading considered in the free drop event are closure lid bolt preload, internal pressure load, thermal load, inertial body load and displacement.

- Closure Lid Bolt Preload: The required total bolt preloads on the cask outer and inner lid bolts are 130.6 kN and 72.2 kN, respectively (10). To apply the bolt preload ANSYS [Ref. 28] pre-tension elements (PRETS179) are used to define the 3-D pre-tension section within the meshed bolt. The PRETS179 element uses a single translation degree of freedom to define pretension direction (Figure 2.6.7-4). The pretension Section is modeled by a set of pretension elements defined by the bolt shaft.
- Pressure Loading: A pressure of 241 kPa (35 psig) is used to envelope the maximum normal operating pressure for all impact loadings considered (Calculation Package RTL-001-CALC-TH-0102, Rev. 6 [Ref. 42]). For accident conditions, a pressure value of 588 kPa (85.3 psig) is used to represent the pressure experienced during fire conditions (Calculation Package RTL-001-CALC-TH-0202, Rev. 6 [Ref. 43]). The internal pressure load is applied as an equivalent static pressure load uniformly applied on the interior surface of the cask.
- Pressure loading contents—cask end drop: For the end drop analyses, the content weight is assumed to be uniformly distributed on the cask end and over an area determined by the inside diameter of the RT-100. Therefore, one-half the contents weight of 6,804 kg (15,000 lb) is applied to the cask inner shell bottom plate. The contents pressure load is multiplied by the appropriate g-load to accurately represent the 304.8 mm (1-foot) and 9144 mm (30-foot) end drop. The pressure value is conservatively multiplied by 1.05 to account for the difference between the solid model surface and the tessellated area of the element mesh.
- Pressure loading contents—side drop: For the side drop condition, the contact area between the contents and the cask cavity is approximately 180° (90° on each side of the drop centerline). The inertial load produced by the 6,804 kg (15,000 lb) contents weight is represented as an equivalent static pressure applied on the interior surface of the RT-100. The pressure is uniformly distributed along the cavity length and is varied in the circumferential direction as a cosine distribution. The pressure value is conservatively multiplied by 1.05 to account for the difference between the solid model surface and the tessellated area of the element mesh. The maximum pressure occurs at the impact centerline; the pressure decreases to zero at locations that are 90° either side of the impact centerline, as illustrated in Figure 2.6.7-5. The following formula is used to determine the contents pressures for the side drop analyses, which

vary around the circumference.

This method uses a summation scheme to approximate the integration of the cosine-shaped pressure distribution:

$$F_{\text{total}} = \sum_{i=1}^{18} P_{\text{max}} A_i \cos(\theta_i) \cos(\theta'_i)$$

$$F_{\text{total}} = 6,804/2 \text{ kg}$$

Where

P_{max} = maximum pressure (at impact centerline)

θ_i = average angle of subtended arc of i^{th} element measured from centerline at point of impact to obtain vertical component of pressure

i = i^{th} circumferential sector

θ'_i = normalized angle to peak at 0° and to be zero at 90°

A_i = i^{th} circumferential area over which the pressure is applied

Gap elements are defined at both ends of the cask to simulate the pressure applied by the impact limiters during side drop conditions. This is accomplished by defining the gap stiffness as a cosine function from a maximum value $175 \times 10^6 \text{ N/m}$ ($1 \times 10^6 \text{ lb/in}$) at the center line to $15.3 \times 10^6 \text{ N/m}$ ($87,156 \text{ lb/in}$) at 85° from the center line of impact, and a minimal value $175 \times 10^3 \text{ N/m}$ (100 lb/in) from 90° to 180° . The load distribution that results from the crushing of the impact limiter is shown in Figure 2.6.7-3.

- Thermal: According to Regulatory Guide 7.8 [Ref. 3], four credible thermal conditions must be considered

Condition 1 – Hot Case 1:

- a. Ambient temperature, 38°C
- b. Initial temperature, 38°C
- c. Heat transfer to ambient by natural convection, still air
- d. Heat transfer to ambient by radiation
- e. Steady-state Solar insolation
- f. Internal heat load as a uniform heat flux, 13.04 W/m^2

Condition 2 – Hot Case 2:

- a. Ambient temperature, 38°C
- b. Initial temperature, 38°C
- c. Heat transfer to ambient by natural convection, still air
- d. Heat transfer to ambient by radiation
- e. No solar insolation, in shade
- f. Internal heat load as uniform heat flux, 13.04 W/m^2

Condition 3 – Cold Case 1:

- a. Ambient temperature, -40°C
- b. Initial temperature, -40°C
- c. Heat transfer to ambient by natural convection, still air
- d. Heat transfer to ambient by radiation
- e. No solar insolation, in shade
- f. Internal heat load as a uniform heat flux, 13.04 W/m²

Condition 4 – Cold Case 2:

- a. Ambient temperature, -29°C
- b. Initial temperature, -29°C
- c. Heat transfer to ambient by natural convection, still air
- d. Heat transfer to ambient by radiation
- e. No solar insolation
- f. Internal heat load as a uniform heat flux, 13.04 W/m²

Heat Conditions 1 and 3 bound the differential the worst case thermal expansion between dissimilar materials. Therefore, Heat Conditions 2 and 4 are not considered.

The cask temperature distributions calculated for Conditions 1 and 3 are used as inputs to the ANSYS [Ref. 28] analyses. The ANSYS analyses determine the stresses arising from the thermal expansion of the cask from its initial 21°C condition, including the effects of the differential thermal growth within the components; these effects are a result of the temperature difference across the cask walls. The cask temperature distributions are also used to determine the values of the temperature-dependent material properties.

The temperatures for the structural analysis are obtained from the results file and database file of the thermal analysis by writing the results to an ASCII file using the ANSYS BFINT command. Nodes for the structural model are transferred to the same coordinate system as used by the thermal run and the thermal results are interpolated for each thermal condition.

- Inertial body load: The inertial effects, which occur during impact, are represented by equivalent static forces, in accordance with the D'Alembert's principle. The inertial body load includes the weight of the empty cask and the weight of the cavity contents. Accelerations are calculated in Appendix 2.13. An acceleration of 44g and 52g are applied to the model to simulate end drop and side drop conditions, respectively. The inertial load is applied to the cask body using the ANSYS ACEL command equivalent to the normal and accident conditions accelerations corresponding to the 0.3 meter and 9 meter drop cases. Since the lead shield is attached to the steel shells with frictionless contact elements, the lead represents the largest physical load applied to the cask structure.

- Displacement boundary conditions: Displacement boundary conditions are applied to enforce symmetry at the cut boundary of the 3D model. All nodes on the symmetry plane are fixed in the UZ direction. The overall model is stabilized by the gap elements (CONTAC52) that represent the impact limiter, which are connected to the cask body with the outer nodes or “ground” nodes representing the impact limiter fixed.

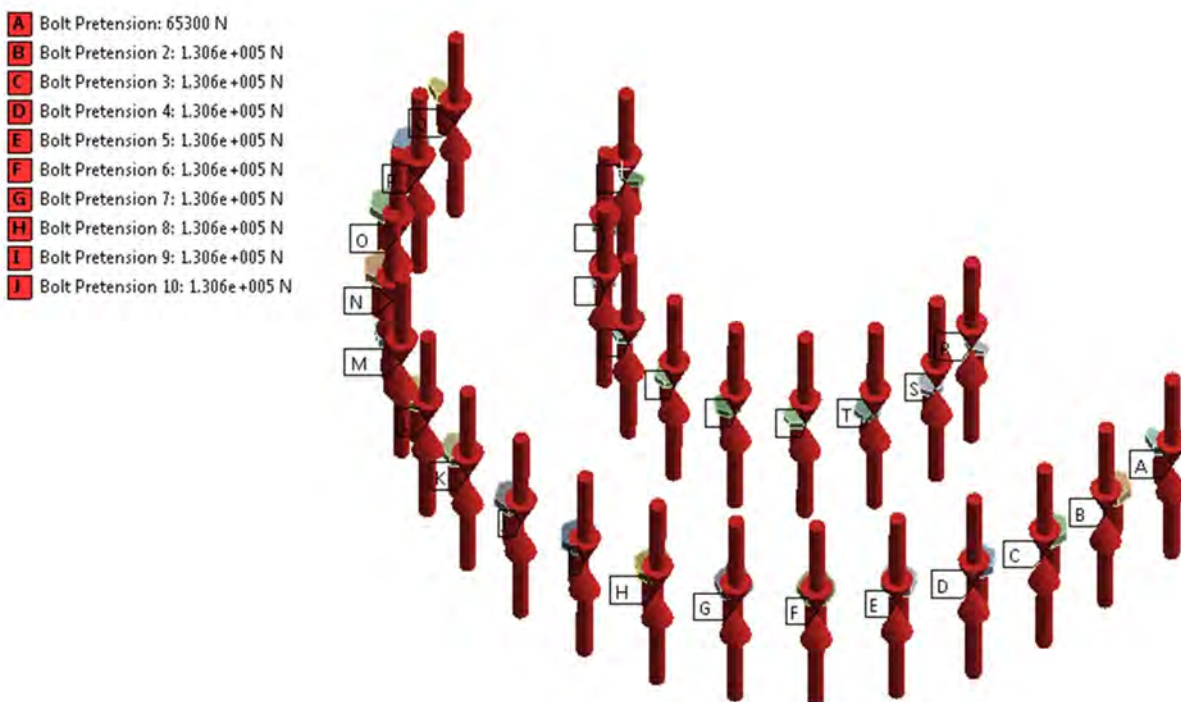


Figure 2.6.7-4 Bolt Pre-load Using ANSYS Pre-Tension Elements (PRETS179)

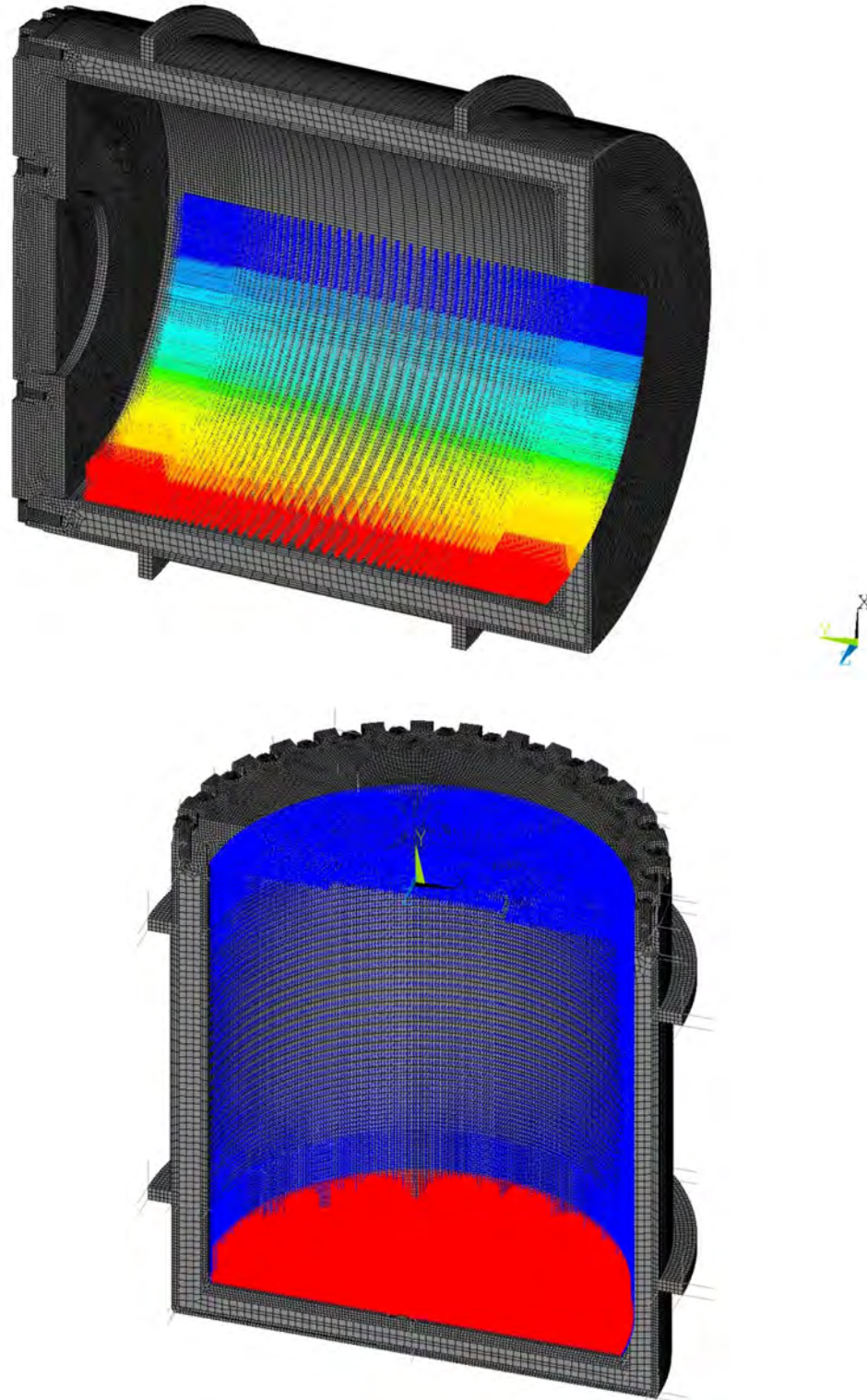


Figure 2.6.7-5 Pressure Distribution Used to Simulate the Contents

2.6.7.3 Side Drop

In accordance with the requirements of 10 CFR 71.71 [Ref. 2], the RT-100 is structurally evaluated for the normal condition of transport 0.3 meter side-drop. During the 0.3 meter side-drop event, the cask (equipped with an impact limiter over each end) falls a distance of 0.3 meter onto a flat, unyielding, horizontal surface. The cask strikes the surface in a horizontal position, thereby resulting in a side impact of the cask. The types of loading involved in a side-drop event are lid closure bolt preload, internal pressure load, thermal load, and inertial body load.

Stress results for the 0.3 meter side drop combined loading conditions discussed previously are documented in Table 2.6.7-1. The table documents the primary membrane (P_m), primary membrane plus primary bending (P_m+P_b), primary membrane plus primary bending plus secondary peak stress (P_m+P_b+Q) in accordance with the criteria presented in Regulatory Guide 7.6 [Ref. 4].

As shown in Table 2.6.7-1, the margins of safety are positive when compared to the stress intensity for each category. The most critically stressed component in the system is the inner lid. The minimum margin of safety is found to be +0.8 for primary membrane plus bending stress intensity. The locations of the critical sections correspond to the maximum stress location shown in Figures 2.6.7.3-1 through 2.6.7.3-11. The minimum margin of safety for primary plus secondary stress intensity is +1.5.

Table 2.6.7-1 NCT Side Drop Stress Summary

Component and Stress State		Stress Location	ANSYS Results (MPa)				RG 7.6 Allowable Stress	Margin of Safety (1)
			S1	S2	S3	SINT		
INNER SHELL	P_m		5.0	-3.8	-31.6	36.6	138	2.8
	$P_m + P_b$	Inside	5.3	-3.8	-31.4	36.7	207	4.6
		Center	5.0	-3.8	-31.6	36.6	207	4.7
		Outside	4.7	-3.8	-31.8	36.5	207	4.7
	Hot $P_m + P_b + Q$	Inside	5.3	-3.8	-31.4	36.7	414	10.3
		Center	5.0	-3.8	-31.6	36.6	414	10.3
		Outside	4.7	-3.8	-31.8	36.5	414	10.3
	Cold $P_m + P_b + Q$	Inside	5.3	-3.8	-31.4	36.7	414	10.3
		Center	5.0	-3.8	-31.6	36.6	414	10.3
		Outside	4.7	-3.8	-31.8	36.5	414	10.3
OUTER SHELL	P_m		4.3	-3.8	-32.3	36.6	138	2.8
	$P_m + P_b$	Inside	4.4	-3.8	-32.2	36.5	207	4.7
		Center	4.3	-3.8	-32.3	36.6	207	4.7
		Outside	4.2	-3.9	-32.5	36.7	207	4.6
	Hot $P_m + P_b + Q$	Inside	4.4	-3.8	-32.2	36.5	414	10.3
		Center	4.3	-3.8	-32.3	36.6	414	10.3
		Outside	4.2	-3.9	-32.5	36.7	414	10.3
	Cold $P_m + P_b + Q$	Inside	4.4	-3.8	-32.2	36.5	414	10.3
		Center	4.3	-3.8	-32.3	36.6	414	10.3
		Outside	4.2	-3.9	-32.5	36.7	414	10.3
FLANGE	P_m		4.1	-3.9	-32.9	37.0	138	2.7
	$P_m + P_b$	Inside	4.1	-3.9	-32.7	36.8	207	4.6
		Center	4.1	-3.9	-32.9	37.0	207	4.6
		Outside	4.1	-4.0	-33.0	37.1	207	4.6
	Hot $P_m + P_b + Q$	Inside	4.1	-3.9	-32.7	36.8	414	10.2
		Center	4.1	-3.9	-32.9	37.0	414	10.2
		Outside	4.1	-4.0	-33.0	37.1	414	10.2
	Cold $P_m + P_b + Q$	Inside	4.1	-3.9	-32.7	36.8	414	10.2
		Center	4.1	-3.9	-32.9	37.0	414	10.2
		Outside	4.1	-4.0	-33.0	37.1	414	10.2
OUTER LID	P_m		18.4	-0.3	-18.4	36.8	138	2.7
	$P_m + P_b$	Inside	51.6	9.5	7.4	44.3	207	3.7
		Center	18.4	-0.3	-18.4	36.8	207	4.6
		Outside	-8.9	-12.7	-47.7	38.8	207	4.3
	Hot $P_m + P_b + Q$	Inside	62.8	-15.8	-41.9	104.7	414	3.0
		Center	11.4	-12.5	-39.4	50.8	414	7.1
		Outside	12.9	-2.4	-41.7	54.5	414	6.6
	Cold $P_m + P_b + Q$	Inside	116.0	61.8	27.6	88.4	414	3.7
		Center	30.1	5.4	-17.7	47.8	414	7.7
		Outside	-4.4	-13.7	-55.0	50.7	414	7.2
INNER LID	P_m		-1.5	-2.6	-56.9	55.4	138	1.5
	$P_m + P_b$	Inside	-4.2	-19.9	-121.3	117.1	207	0.8
		Center	-1.5	-2.6	-56.9	55.4	207	2.7
		Outside	15.9	7.2	0.3	15.7	207	12.2
	Hot $P_m + P_b + Q$	Inside	2.4	-31.7	-161.7	164.1	414	1.5
		Center	15.2	2.8	-58.4	73.6	414	4.6
		Outside	13.5	-5.2	-23.7	37.2	414	10.1
	Cold $P_m + P_b + Q$	Inside	-8.8	-28.7	-148.7	140.0	414	2.0
		Center	4.1	-0.2	-58.8	62.9	414	5.6
		Outside	19.5	4.7	-6.9	26.4	414	14.7

Note: (1) The margin of safety is the ratio of Allowable Stress and the Stress Intensity (SINT) minus 1.

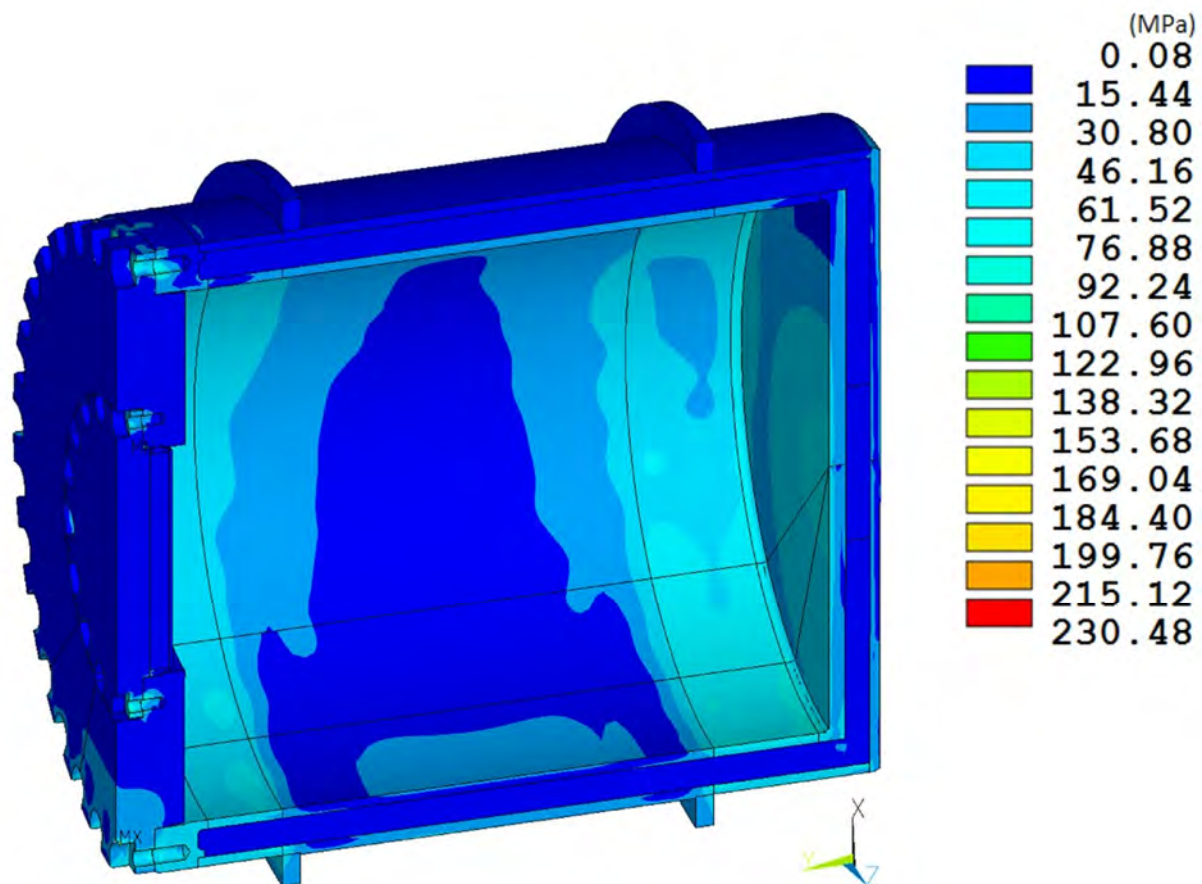


Figure 2.6.7-6 RT-100 NCT Side Drop Stress Intensity Results

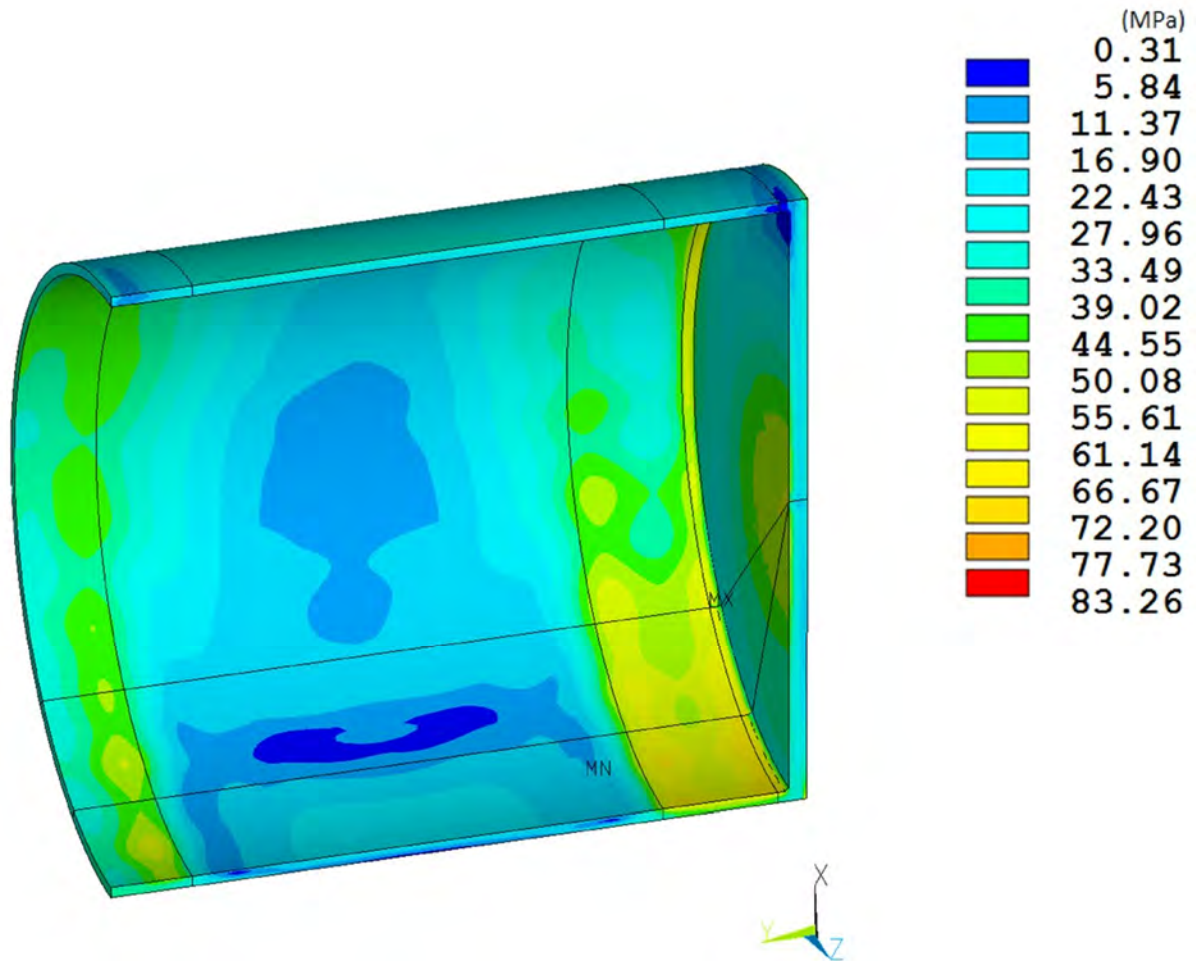


Figure 2.6.7-7 RT-100 Inner Shell NCT Side Drop Stress Intensity Results

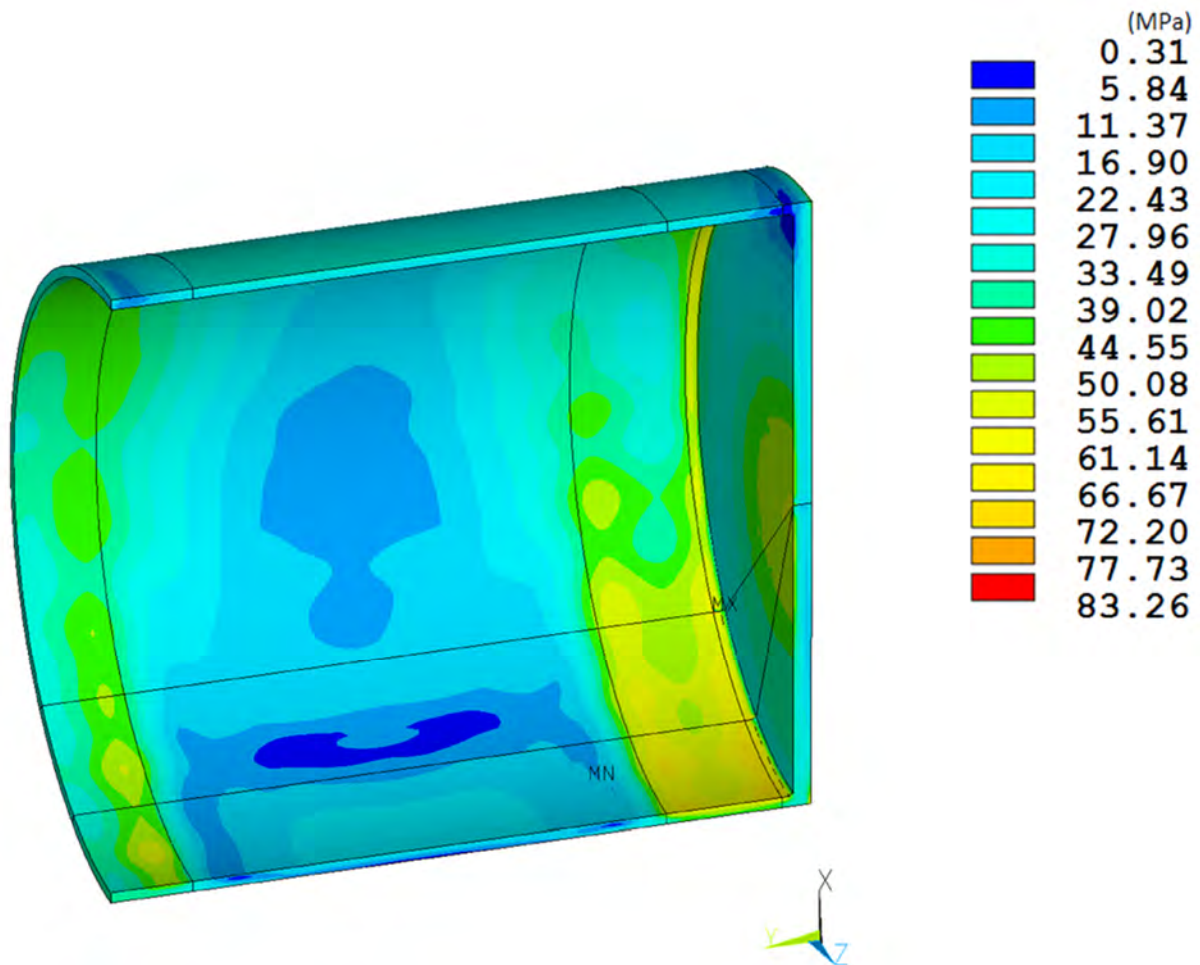


Figure 2.6.7-8 RT-100 Outer Shell NCT Side Drop Stress Intensity Results

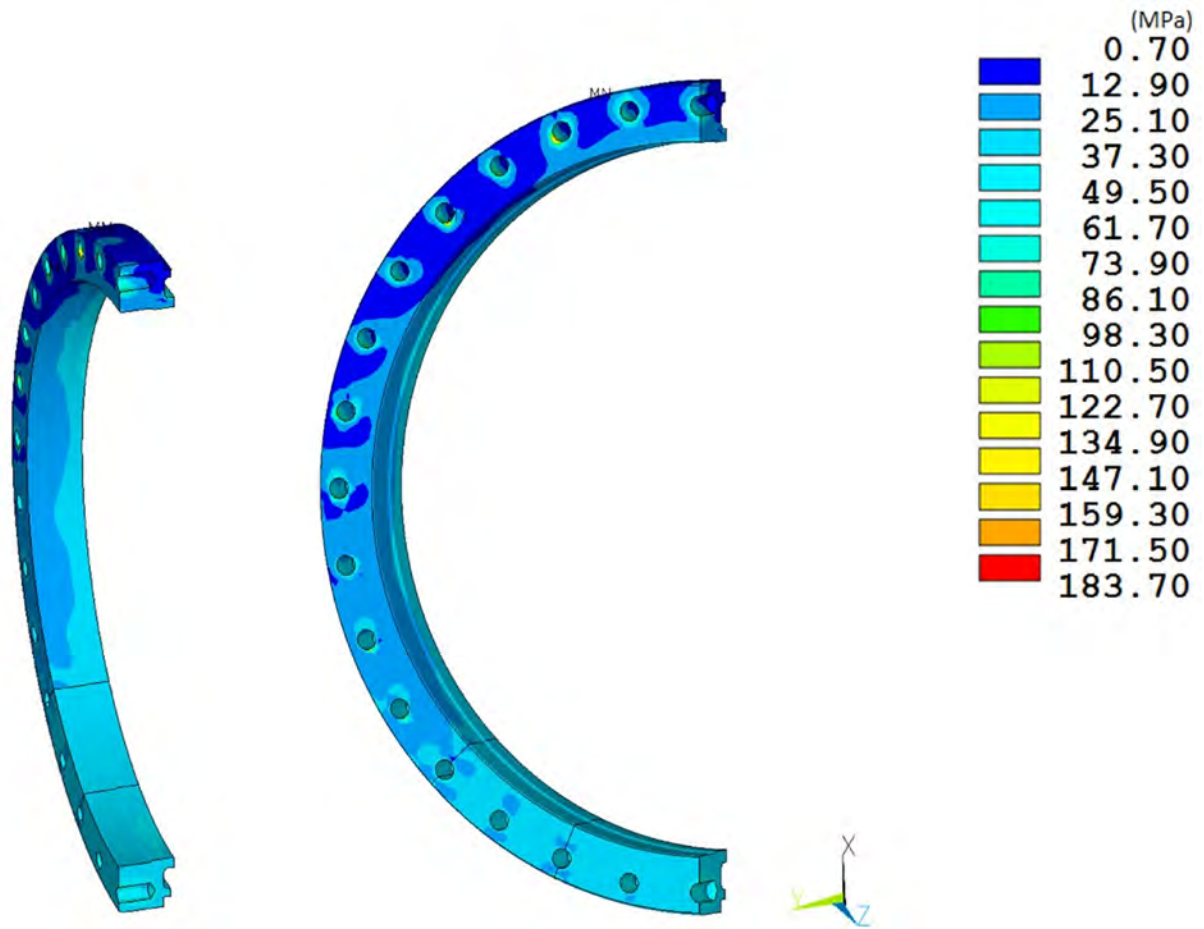


Figure 2.6.7-9 RT-100 Flange NCT Side Drop Stress Intensity Results

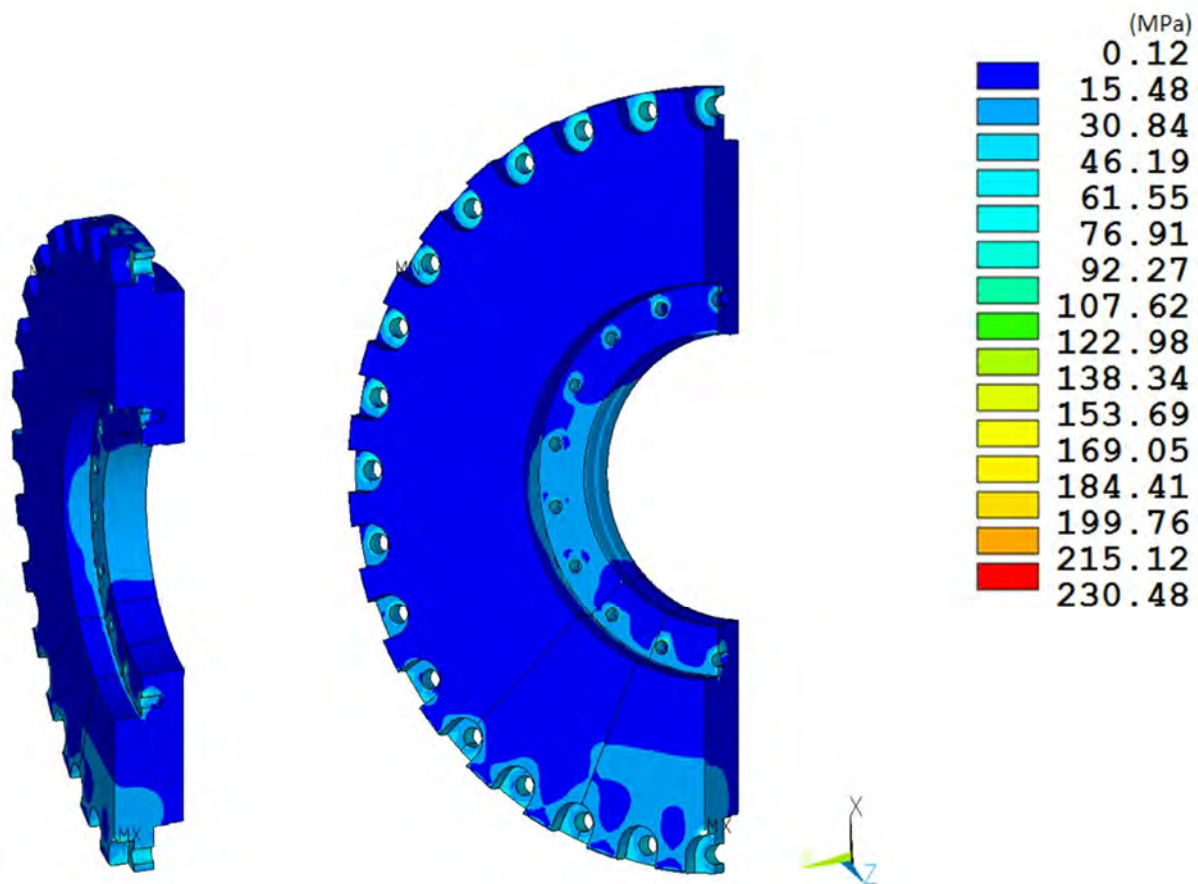


Figure 2.6.7-10 RT-100 Outer Lid NCT Side Drop Stress Intensity Results

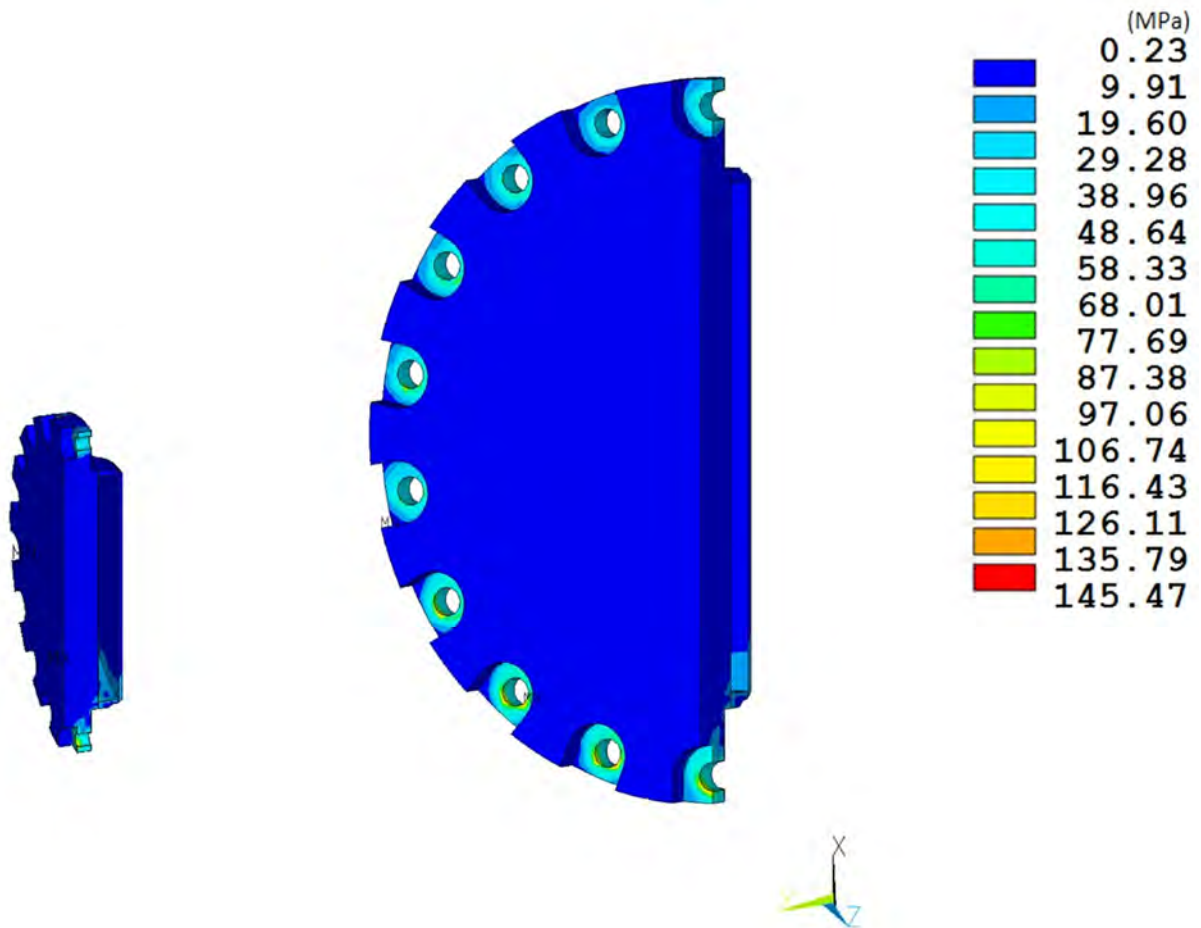


Figure 2.6.7-11 RT-100 Inner Lid NCT Side Drop Stress Intensity Results

2.6.7.4 End Drop

In accordance with the requirements of 10 CFR 71.71 [Ref. 2], the Universal Transport Cask is structurally evaluated for the normal condition of transport 0.3 m end-drop. In this event, the cask (equipped with an impact limiter over each end) falls a distance of 0.3 m onto a flat, unyielding, horizontal surface. The cask strikes the surface in a vertical position; consequently, an end impact on the bottom end or top end of the cask occurs.

As discussed previously, stress results for the 1-ft top and bottom-end drop combined loading conditions are documented in Table 2.6.7-2. The table documents the primary membrane (P_m), primary membrane plus primary bending (P_m+P_b), primary membrane plus primary bending plus secondary peak stress (P_m+P_b+Q) in accordance with the criteria presented in Regulatory Guide 7.6 [Ref. 4].

As shown in the Table 2.6.7-2, the margins of safety for the primary stress intensity category are positive for all of the 0.3 m top-end drop conditions. The most critically stressed component in the system is the cask flange region due to the bending of the flange due to the inertial load imposed by the cask lids. The minimum margin of safety is found to be +2.4 for primary membrane plus bending stress intensity. The locations of the critical sections correspond to the maximum stress location shown in Figure 2.6.7-12 through Figure 2.6.7-17. The minimum margin of safety for primary plus secondary stress intensity is +0.2.

Table 2.6.7-2 NCT End Drop Stress Summary

Component and Stress State		Stress Location	ANSYS Results (MPa)				RG 7.6 Allowable Stress	Margin of Safety (1)
			S1	S2	S3	SINT		
INNER SHELL	P_m		2.7	1.2	-7.8	10.5	138	12.1
	P_m + P_b	<i>Inside</i>	2.7	2.0	-12.2	14.9	207	12.9
		<i>Center</i>	2.7	1.2	-7.8	10.5	207	18.7
		<i>Outside</i>	2.9	0.2	-3.6	6.6	207	30.5
	Hot P_m + P_b + Q	<i>Inside</i>	2.7	2.0	-12.2	14.9	414	26.8
		<i>Center</i>	2.7	1.2	-7.8	10.5	414	38.3
		<i>Outside</i>	2.9	0.2	-3.6	6.6	414	61.9
	Cold P_m + P_b + Q	<i>Inside</i>	2.7	2.0	-12.2	14.9	414	26.8
		<i>Center</i>	2.7	1.2	-7.8	10.5	414	38.3
		<i>Outside</i>	2.9	0.2	-3.6	6.6	414	61.9
OUTER SHELL	P_m		6.5	-0.9	-3.4	9.9	138	12.9
	P_m + P_b	<i>Inside</i>	7.5	1.0	-2.7	10.2	207	19.3
		<i>Center</i>	6.5	-0.9	-3.4	9.9	207	19.9
		<i>Outside</i>	6.9	0.7	-9.0	15.9	207	12.0
	Hot P_m + P_b + Q	<i>Inside</i>	113.3	39.9	-63.2	176.5	414	1.3
		<i>Center</i>	22.5	-10.9	-16.7	39.2	414	9.5
		<i>Outside</i>	25.4	0.5	-33.5	58.9	414	6.0
	Cold P_m + P_b + Q	<i>Inside</i>	10.7	0.5	-4.5	15.3	414	26.1
		<i>Center</i>	18.7	5.7	-4.7	23.5	414	16.6
		<i>Outside</i>	10.4	2.4	-9.5	19.9	414	19.8
FLANGE	P_m		5.9	1.5	-12.3	18.1	138	6.6
	P_m + P_b	<i>Inside</i>	0.1	-3.3	-19.5	19.6	207	9.5
		<i>Center</i>	5.9	1.5	-12.3	18.1	207	10.4
		<i>Outside</i>	20.1	6.3	-13.6	33.7	207	5.1
	Hot P_m + P_b + Q	<i>Inside</i>	48.0	24.1	-219.4	267.4	414	0.5
		<i>Center</i>	12.9	-5.7	-23.8	36.6	414	10.3
		<i>Outside</i>	74.0	34.2	-53.9	127.9	414	2.2
	Cold P_m + P_b + Q	<i>Inside</i>	32.8	-42.6	-105.1	137.9	414	2.0
		<i>Center</i>	14.2	2.1	-24.1	38.3	414	9.8
		<i>Outside</i>	92.7	71.4	-36.7	129.4	414	2.2
OUTER LID	P_m		-0.9	-4.0	-14.6	13.7	138	9.1
	P_m + P_b	<i>Inside</i>	-7.7	-17.0	-52.6	45.0	207	3.6
		<i>Center</i>	-0.9	-4.0	-14.6	13.7	207	14.1
		<i>Outside</i>	24.2	9.0	5.1	19.0	207	9.9
	Hot P_m + P_b + Q	<i>Inside</i>	280.5	36.7	-55.4	336.0	414	0.2
		<i>Center</i>	35.3	20.9	-4.7	40.0	414	9.3
		<i>Outside</i>	41.6	16.7	-56.7	98.3	414	3.2
	Cold P_m + P_b + Q	<i>Inside</i>	-35.0	-71.0	-163.6	128.5	414	2.2
		<i>Center</i>	14.0	4.5	-14.8	28.8	414	13.4
		<i>Outside</i>	21.6	-0.3	-22.2	43.8	414	8.4

Table 2.6.7-2 (Continued)

Component and Stress State		Stress Location	ANSYS Results (MPa)				RG 7.6 Allowable Stress	Margin of Safety (1)
			S1	S2	S3	SINT		
NCT	P _m		5.7	-2.3	-35.4	41.1	138	2.4
	P _m + P _b	Inside	-6.5	-10.3	-67.7	61.3	207	2.4
		Center	5.7	-2.3	-35.4	41.1	207	4.0
		Outside	20.8	6.0	-6.5	27.3	207	6.6
	Hot P _m + P _b + Q	Inside	-14.6	-27.5	-112.1	97.5	414	3.2
		Center	28.9	11.0	-26.3	55.2	414	6.5
		Outside	18.9	-8.7	-36.5	55.3	414	6.5
	Cold P _m + P _b + Q	Inside	-18.9	-23.7	-93.0	74.1	414	4.6
		Center	9.7	-1.3	-39.2	49.0	414	7.4
		Outside	23.4	3.1	-13.5	36.8	414	10.2

Note: The margin of safety is the ratio of the Allowable Stress and the Stress Intensity (SINT) minus 1.

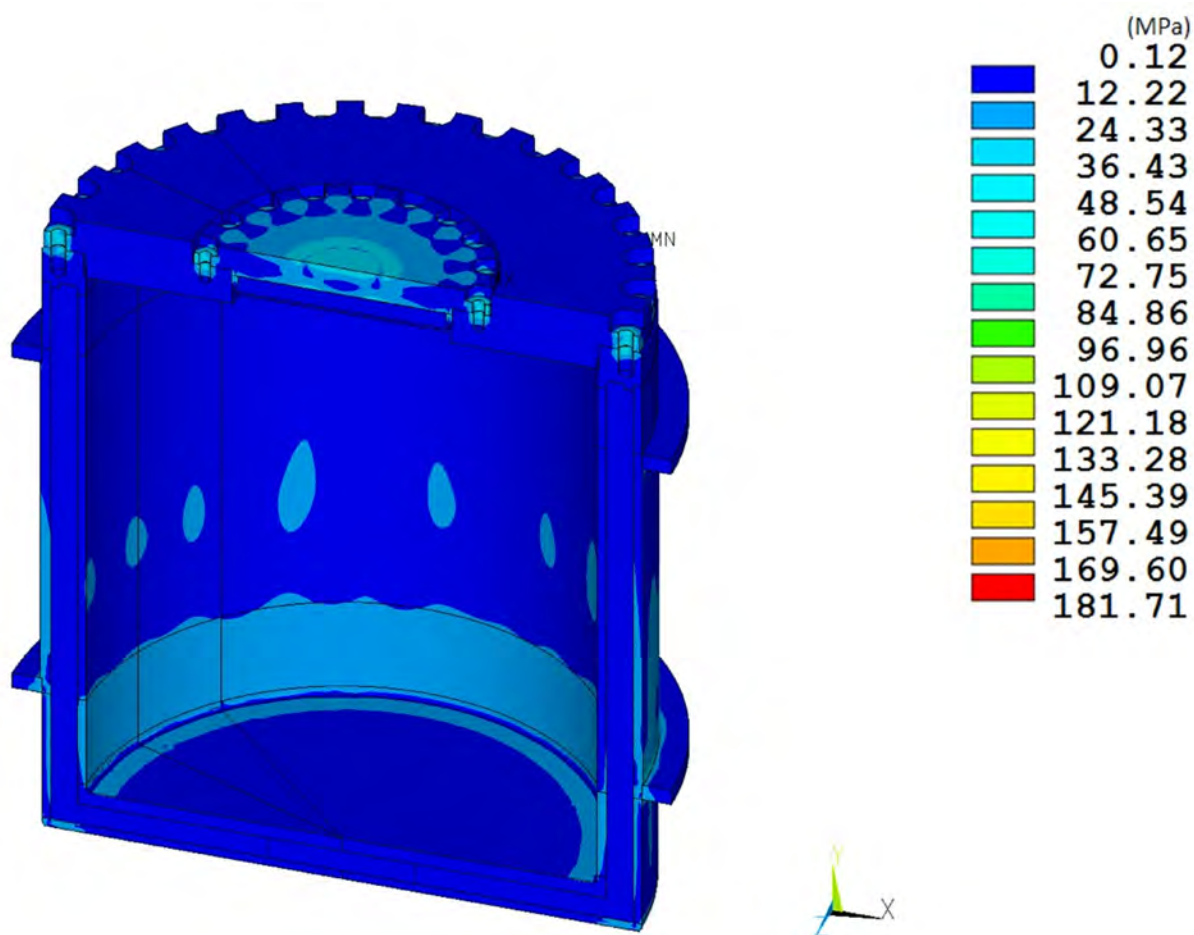


Figure 2.6.7-12 RT-100 NCT Bottom Drop Stress Intensity Results

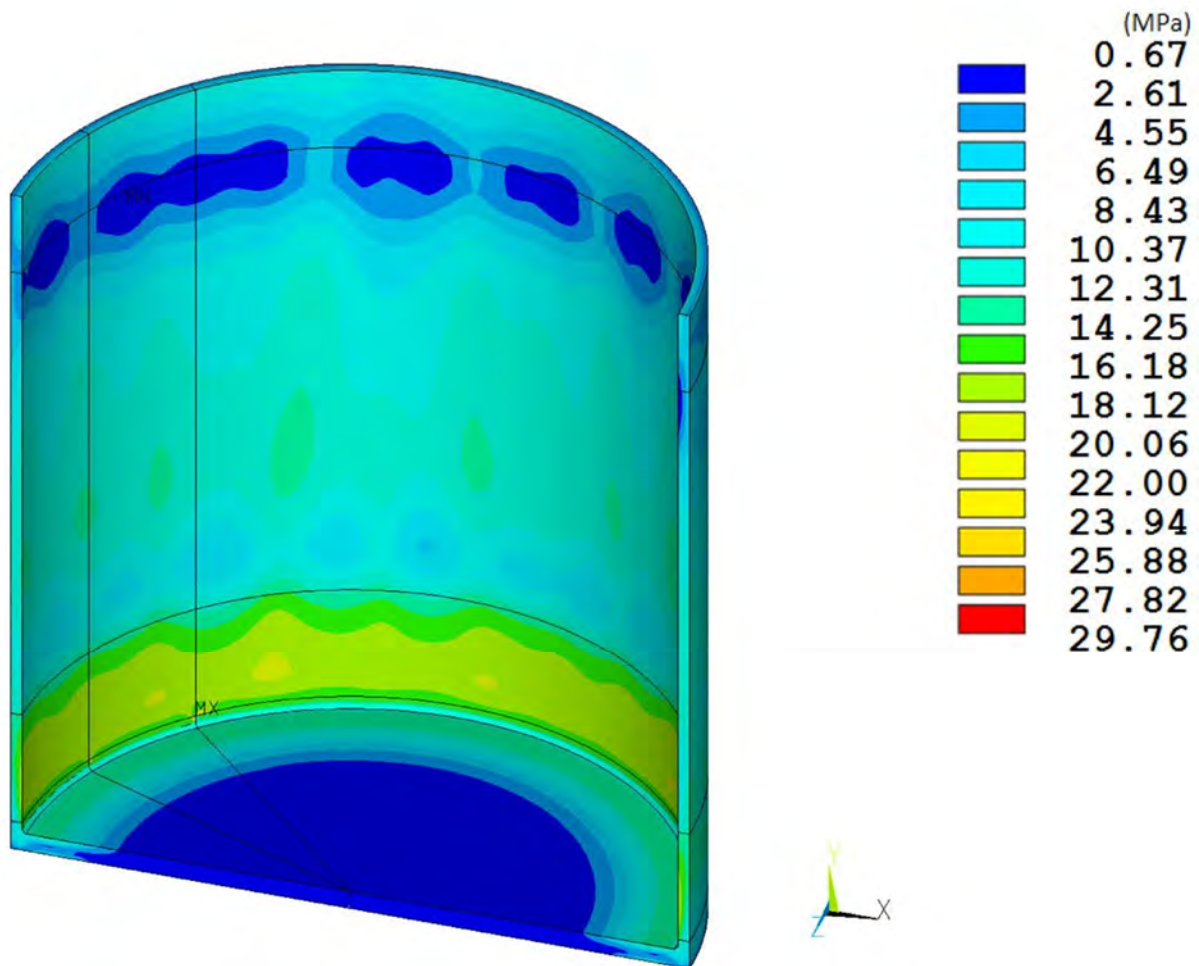


Figure 2.6.7-13 RT-100 Inner Shell NCT End Drop Stress Intensity Results

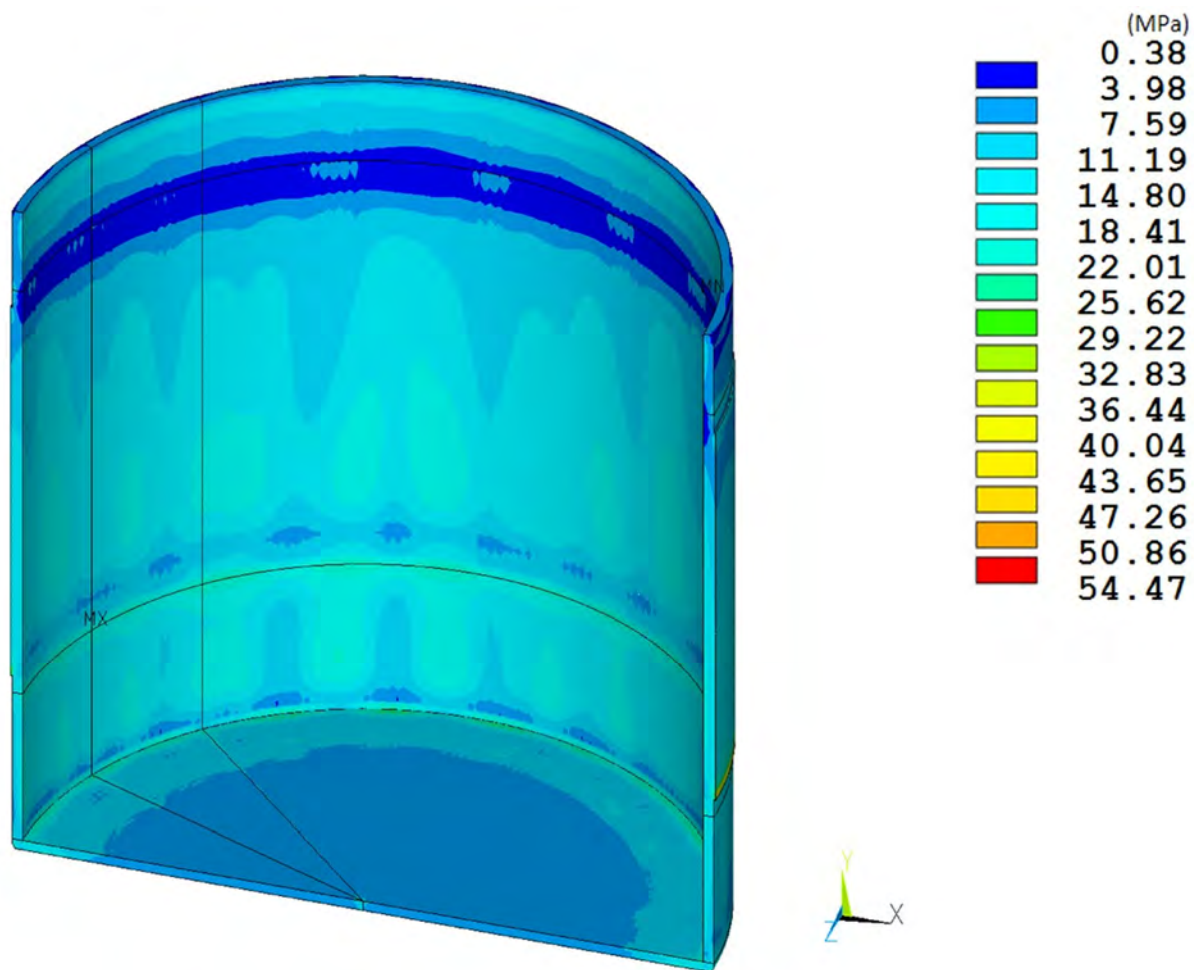


Figure 2.6.7-14 RT-100 Outer Shell NCT End Drop Stress Intensity Results

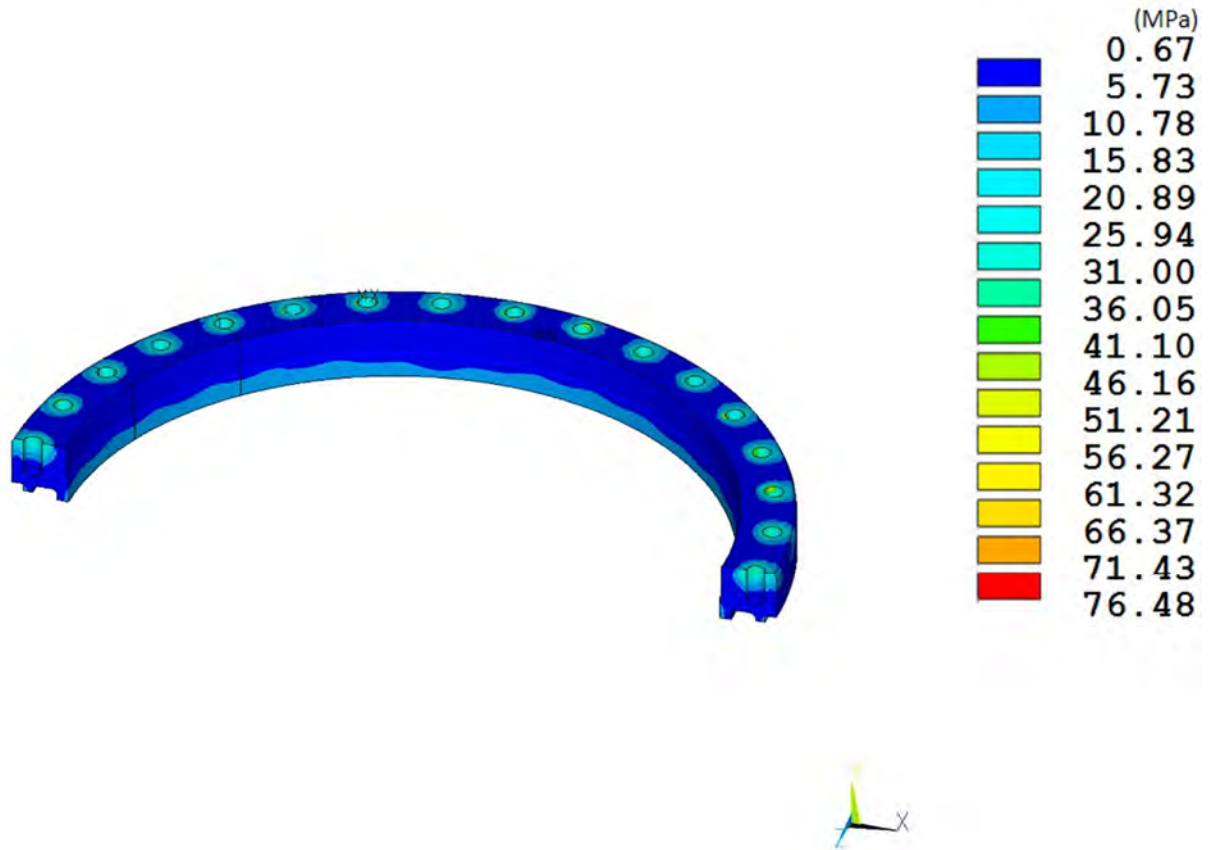


Figure 2.6.7-15 RT-100 Flange NCT End Drop Stress Intensity Results

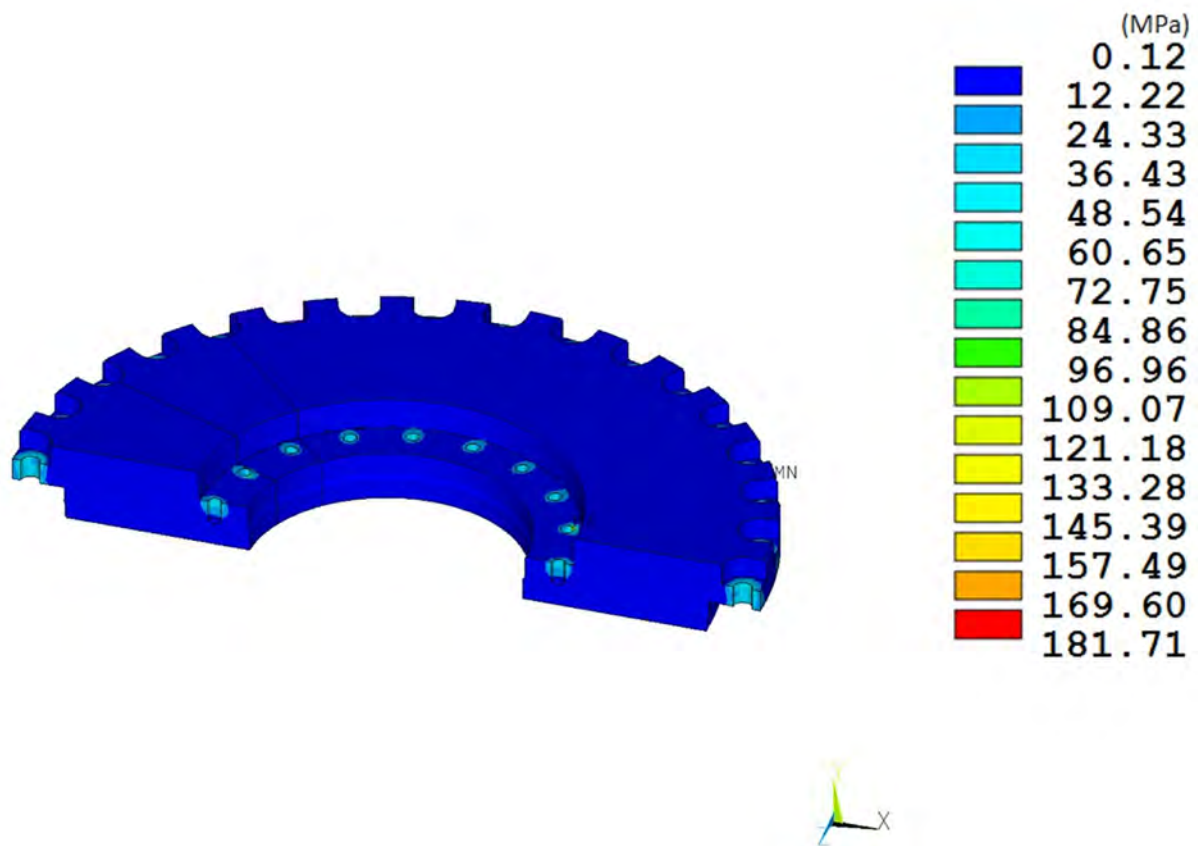


Figure 2.6.7-16 RT-100 Outer Lid NCT End Drop Stress Intensity Results

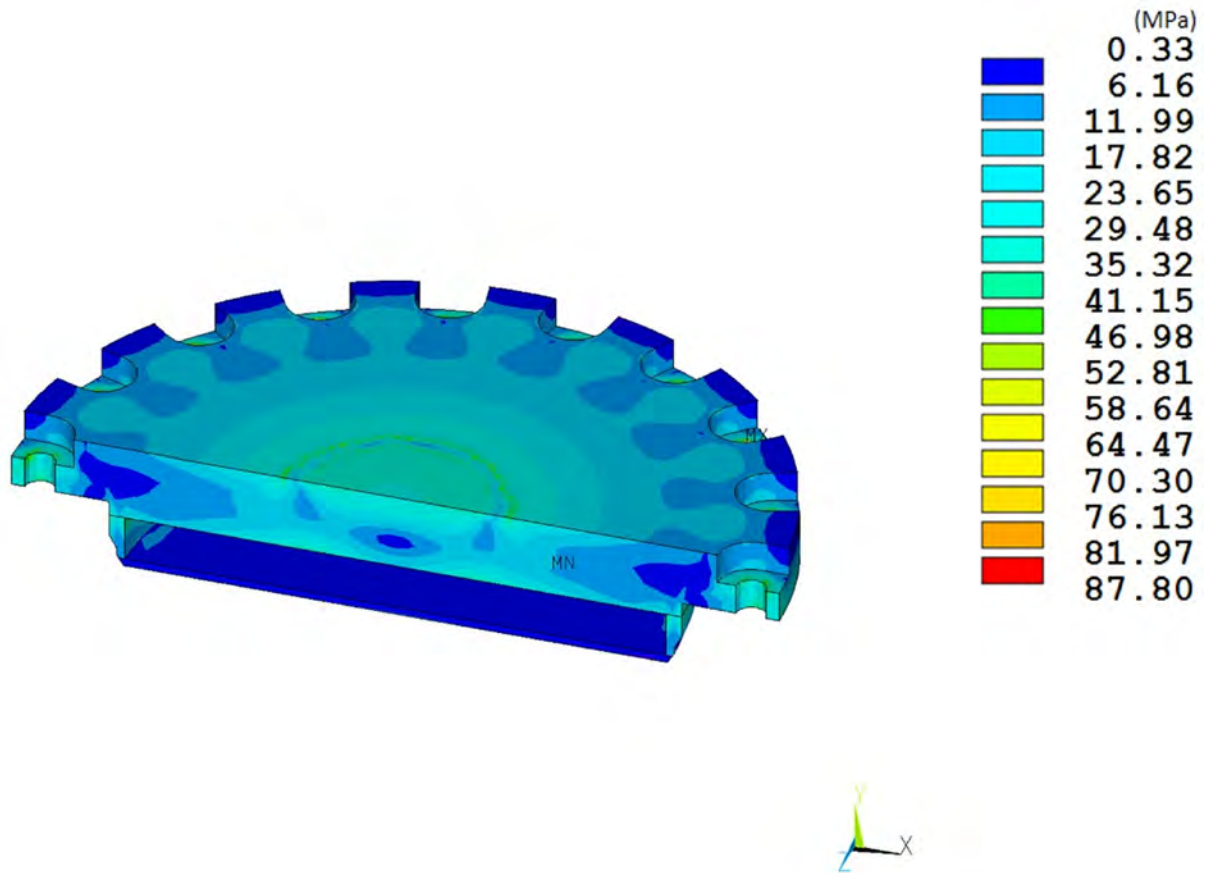


Figure 2.6.7-17 RT-100 Inner Lid NCT End Drop Stress Intensity Results

2.6.8 Corner Drop

The RT-100 is composed of materials other than fiberboard or wood. Also, the weight of the RT-100 exceeds 100 kg. According to 10 CFR 71.71(c)(8) [Ref. 2], the corner drop test is not applicable to the RT-100.

2.6.9 Compression

According to 10 CFR 71.71(c)(9) [Ref. 2], the compression test is not applicable to the RT-100 because the package weight is greater than 5,000 kg.

2.6.10 Penetration

According to 10 CFR 71.71(c)(10) [Ref. 2], a penetration test involving a 13-lb (6-kg) penetration cylinder dropped from a height of 1 m is required for evaluation of packages during normal conditions of transport. However, Regulatory Guide 7.8 [Ref. 3] states that “the penetration test of 10 CFR 71.71 [Ref. 2] is not considered by the NRC staff to have structural significance for large shipping casks (except for unprotected valves and rupture disks) and is not considered as a general requirement.” A penetration test is not performed since the RT-100 has no unprotected valves or rupture disks that could be affected by normal conditions of transport.

2.7 Hypothetical Accident Conditions

The RT-100 Cask meets the standards specified in 10 CFR 71.51 [Ref. 2] when subjected to the conditions and tests specified in 10 CFR 71.73 [Ref. 2] for hypothetical accidents. In accordance with 10 CFR 71.73 [Ref. 2], the RT-100 is structurally evaluated for hypothetical accident scenarios of free drop, puncture, fire, crush, and water immersion. In the free-drop and puncture analyses, the cask impact orientation evaluated is the one that inflicts the maximum damage to the cask. The most unfavorable ambient temperature condition during operation in the range from -40°C to 38°C is assumed. The following sections contain the evaluation of the cask for structural integrity under the hypothetical accident conditions.

2.7.1 Free Drop

The RT-100 Cask is required by 10 CFR 71.73(c)(1) [Ref. 2] to demonstrate structural adequacy for a free drop through a distance of 9 meters onto a flat, unyielding, horizontal surface. The cask payload is oriented to strike the surface to inflict the maximum damage. In determining the orientation that produces the maximum damage, the cask is evaluated for impact orientations in which the cask strikes the impact surface on its bottom end and side. Evaluation of each drop orientation is performed by using finite element analysis techniques. A complete description of the 3-D model used to analyze the cask body is presented in Section 2.6.7.2. The results of each drop orientation listed above are presented in this section. The impact limiters are evaluated in Appendix 2.12 for all loading conditions and orientations. These analyses provide the inertial loads (maximum “g-loads”) imparted to the cask for each drop orientation (Table 2.12.6-1). Cask body decelerations used in NCT and HAC finite element analyses are shown in Table 2.7.1-1.

Table 2.7.1-1 Deceleration Loadings in RT-100 Cask Body Finite Element Analyses

Case	End Drop (g)	Side Drop (g)
HAC (Drop Height = 9.0 m)	123	226
NCT (Drop Height = 0.3 m)	44	52

The mass of the contents is considered when evaluating impact and environmental temperature for the drop is between -40°C and 38°C. For the accident condition, stresses arising from thermal expansion are not considered. However, for determination of properties, the temperatures are considered. The mean normal operating pressure of 241 (kPa) 35 psig is applied in the finite element models to produce the bounding critical stress condition in conjunction with the other loads previously discussed. A separate analysis evaluates the stresses associated with the accident pressure of 588 kPa (85.3 psig) that results from the regulatory fire event. Closure lid bolt preload is considered (Appendix 2.13 and Section 2.6.7.2.2) and fabrication stresses are discussed (Appendix 2.14). The following method and assumptions are adopted in all the hypothetical accident drop analyses:

The following sections contain the evaluation of the RT-100 for impact orientations in which the cask strikes the impact surface on its bottom end and side. The impact conditions (in accordance with Regulatory Guide 7.8 [Ref. 3] and the categories of load to be considered for the hypothetical accident conditions) are similar to those for the 0.3 meter free drops under normal conditions of transport as discussed in Section 2.6.7. Therefore, the discussions in the following sections refer to Section 2.6.7 wherever applicable.

Three categories of load—closure lid bolt preload, internal pressure, and inertial body loads—are considered on the cask. The inertia loads imposed upon the cask by the impact limiter result from the mass of the entire assembly being acted upon by a design deceleration value of 123 g for the 30-ft end-drop case. The closure lid bolt preload, internal pressure load, and contents loads considered for the 30-ft end-drop condition are similar to those considered for 1-ft end-drop condition in Section 2.6.7.2, with the exception that thermal stresses are not considered for accident conditions. The material properties of the components are considered to be temperature dependent.

The allowable stress limits criteria are discussed in Section 2.6.7.1. These criteria are used to determine the allowable stresses for each cask component, conservatively using the maximum operating temperature within a given component to determine the allowable stress throughout that component. For cask body analyses presented in this section, the maximum heat conditions (thermal condition 1) are 38°C ambient temperature, maximum decay heat load, and maximum solar insolation.

During fabrication of the RT-100, thermal stresses can be introduced in the inner and outer shells as a result of pouring molten lead between them. Residual stresses may be induced in the inner shell (containment boundary) and the outer shell due to shrinkage of the lead shielding subsequent to lead pouring operations; however, these stresses are relieved early in the life of the cask because of the low creep strength of lead. Therefore, the effects of stresses resulting from the cask fabrication processes are considered negligible. Further discussion of fabrication stresses is

provided in Appendix 2.14.

2.7.1.1 End Drop

In accordance with the requirements of 10 CFR 71.73(c)(1) [Ref. 2], the RT-100 is structurally evaluated for the 30-foot end-drop condition. In this hypothetical accident, the cask including the payload, spacer (if appropriate), and the impact limiters falls 30 feet onto a flat, unyielding, horizontal surface. The cask strikes the surface in a vertical position and results in an end impact on the bottom of the cask. The types of loading involved in an end-drop accident are closure lid bolt preload, internal pressure, and inertial body load. Section 2.6.7.2 describes the application of each loading condition.

2.7.1.1.1 End Drop Evaluation

In accordance with the requirements of 10 CFR 71.73(c)(1) [Ref. 2], the RT-100 is structurally evaluated for the 30-foot end-drop condition. In this hypothetical accident, the cask including the payload and the impact limiters falls 30 feet onto a flat, unyielding, horizontal surface. The cask strikes the surface in a vertical upright position. For the RT-100 cask, the bottom end drop is bounding. In the bottom down position, the prying load on the closure bolts is maximized.

Stress results for the 9-meter bottom end drop combined are documented in Table 2.7.1-2. The table documents the primary membrane (P_m), primary membrane plus primary bending (P_m+P_b) stresses in accordance with the criteria presented in Regulatory Guide 7.6 [Ref. 4].

As shown in Table 2.7.1-2, the margins of safety when compared to the stress intensity for each category are positive. The most critically stressed component in the system is the flange; this result is due to bending as a result of the inertial loads on the cask lids. The minimum margin of safety is found to be +1.5 for primary membrane plus bending stress intensity. The locations of the critical sections correspond to the maximum stress location shown in Figure 2.7.1-1 through Figure 2.7.1-6.

2.7.1.1.2 Lead Slump Evaluation

The following sections provide the lead slump evaluation of the RT-100. During an end drop accident, the shielding capability of the RT-100 cask may be reduced as a result of lead slump.

2.7.1.1.2.1 Elastic Deformation

The maximum lead slump occurs during the previously analyzed bottom end drop in Section 2.7.1.1.1. The relative displacement is obtained from the finite element analysis. Figure 2.7.1-7 shows the exaggerated displacement plot under this drop orientation. The total elastic displacement of the lead column is 1.62 mm.

2.7.1.1.2.2 Plastic Deformation with Maximum Gap

Maximum plastic deformation of the lead shield occurs when the package experiences extreme cold conditions prior to the end drop. During extreme cold conditions, the contraction of the lead shield forms a small gap at the top of the lead column. The reduced height of the lead shield due to contraction is:

$$h_{\text{lead}} = h_{\text{lead}} (1 + \alpha \Delta T) = 2037.4 \text{ mm}$$

Where,

$h_{\text{lead}} = 2040.9 \text{ mm}$	Initial height of lead shield at 21.1°C
$\alpha = 2.78 \times 10^{-5} \text{ mm/mm/}^\circ\text{C}$	Coefficient of thermal expansion for lead at -40°C
$\Delta T = -40^\circ\text{C} - 21.1^\circ\text{C} = -61.1^\circ\text{C}$	Temperature difference

The reduced height of the annular column formed by the steel shells due to contraction is:

$$h_{\text{steel}} = h_{\text{steel}} (1 + \alpha \Delta T) = 2039.0 \text{ mm}$$

Where,

$h_{\text{steel}} = 2040.9 \text{ mm}$	Initial height of annular column at 21.1°C
$\alpha = 1.48 \times 10^{-5} \text{ mm/mm/}^\circ\text{C}$	Coefficient of thermal expansion for steel at -40°C
$\Delta T = -40^\circ\text{C} - 21.1^\circ\text{C} = -61.1^\circ\text{C}$	Temperature difference

Radial Thermal Expansion

In addition to the gap formed in the axial direction, radial gaps also form during extreme cold conditions. For this evaluation, the interference fit between the cask inner shell and lead shield is ignored because during thermal contraction, the lead applies pressure to the steel inner shell. Since the yield strength of lead is low compared to the steel shell, the lead will conform to the shape of the inner shell. Therefore, the lead volume is not lost during the contraction process and the physical gap between lead and outer shell if any will be significantly less than the values predicted in this calculation. The reduced outside radius of the lead shield at -40°C is:

$$r_o = r_{\text{outer}} (1 + \alpha \Delta T) = 983.3 \text{ mm}$$

Where,

$r_{\text{outer}} = 985.0 \text{ mm}$	Initial outside radius of lead shield = inner radius of steel outer shell at 21.1°C
$\alpha = 2.78 \times 10^{-5} \text{ mm/mm/}^\circ\text{C}$	Coefficient of thermal expansion for lead at -40°C
$\Delta T = -40^\circ\text{C} - 21.1^\circ\text{C} = -61.1^\circ\text{C}$	Temperature difference

The change in inside radius of lead shield at -40°C:

$$r_i = r_{\text{inner}} (1 + \alpha \Delta T) = 893.6 \text{ mm}$$

Where,

$r_{\text{inner}} = 895.1 \text{ mm}$	Inner radius of lead shield at 21.1°C
$\alpha = 2.78 \times 10^{-5} \text{ mm/mm/}^\circ\text{C}$	Coefficient of thermal expansion for lead at -40°C
$\Delta T = -40^\circ\text{C} - 21.1^\circ\text{C} = -61.1^\circ\text{C}$	Temperature difference

The reduced inside radius of the outer steel shell at -40°C:

$$r_o = r_{\text{int}} (1 + \alpha \Delta T) = 984.1 \text{ mm}$$

Where,

$r_{\text{int}} = 985.0 \text{ mm}$	Inner radius of steel outer shell at 21.1°C
-------------------------------------	---

$$\begin{aligned}\alpha &= 1.48 \times 10^{-5} \text{ mm/mm/}^{\circ}\text{C} && \text{Coefficient of thermal expansion for steel at } -40^{\circ}\text{C} \\ \Delta T &= -40^{\circ}\text{C} - 21.1^{\circ}\text{C} = -61.1^{\circ}\text{C} && \text{Temperature difference}\end{aligned}$$

The change in outside radius of inner steel shell is at -40°C :

$$r_i = r_{\text{inner}} (1 + \alpha \Delta T) = 894.3 \text{ mm}$$

Where,

$$\begin{aligned}r_{\text{inner}} &= 895.1 \text{ mm} && \text{Inner radius of lead shield at } 21.1^{\circ}\text{C} \\ \alpha &= 1.48 \times 10^{-5} \text{ mm/mm/}^{\circ}\text{C} && \text{Coefficient of thermal expansion for steel at } -40^{\circ}\text{C} \\ \Delta T &= -40^{\circ}\text{C} - 21.1^{\circ}\text{C} = -61.1^{\circ}\text{C} && \text{Temperature difference}\end{aligned}$$

Lead Shield Volume

The previous section shows that the relative contraction of materials during extreme cold conditions results in a small gap between the lead shield and outer steel shell. The small gap formed in the radial directions is sufficient to allow the lead shield to slump during an HAC bottom impact. Following exposure to extreme cold conditions (-40°C), the available volume of the lead column is:

$$V_f = A_f \times h_c = 1.0784 \times 10^9 \text{ mm}^3$$

Where,

$$\begin{aligned}A_f &= \pi (r_o^2 - r_i^2) = 5.293 \times 10^5 \text{ mm}^2 && \text{Cross-sectional area of lead shield} \\ r_o &= 983.3 \text{ mm} && \text{Outside radius of lead shield at } -40^{\circ}\text{C} \\ r_i &= 893.6 \text{ mm} && \text{Inner radius of lead shield at } -40^{\circ}\text{C} \\ h_c &= 2037.4 \text{ mm} && \text{Height of lead column at } -40^{\circ}\text{C}\end{aligned}$$

The cross sectional area of the annulus between the inner and outer shells following exposure to extreme cold conditions (-40°C) is:

$$A_i = \pi (r_o^2 - r_i^2) = 5.3013 \times 10^5 \text{ mm}^2$$

Where,

$$\begin{aligned}r_o &= 984.1 \text{ mm} && \text{Inside radius of steel outer shell at } -40^{\circ}\text{C} \\ r_i &= 894.3 \text{ mm} && \text{Outside radius of steel inner shell } -40^{\circ}\text{C}\end{aligned}$$

Lead Slump

Accounting for the contraction of the steel shells and lead shield the reduced height of the lead column based on the net gap is:

$$h_{\text{final}} = V_f / A_i = 2034.2 \text{ mm}$$

Subtracting the reduced height of the lead column from the height of the annular region and ignoring the elastic deformation, the lead slump is:

$$h_{\text{slump}} = h_{\text{steel}} - h_{\text{final}} = 2039.0 - 2034.2 = 4.8 \text{ mm}$$

Table 2.7.1-2 HAC End Drop Stress Summary

Component and Stress State	Stress Location	ANSYS Results				RG 7.6 Allowable Stress	Margin of Safety (1)
		S1	S2	S3	SINT		
INNER SHELL		MPa	MPa	MPa	MPa	MPa	
Pm		7.5	5.7	-30.9	38.4	331	7.6
Pm + Pb	<i>Inside</i>	12.8	6.5	-51.3	64.1	496	6.7
	<i>Center</i>	7.5	5.7	-30.9	38.4	496	11.9
	<i>Outside</i>	8.2	-0.5	-11.2	19.4	496	24.6
OUTER SHELL		MPa	MPa	MPa	MPa	MPa	
Pm		10.7	0.1	-22.0	32.8	331	9.1
Pm + Pb	<i>Inside</i>	7.2	-0.2	-26.3	33.5	496	13.8
	<i>Center</i>	10.7	0.1	-22.0	32.8	496	14.2
	<i>Outside</i>	14.2	0.5	-17.8	32.0	496	14.5
FLANGE		MPa	MPa	MPa	MPa	MPa	
Pm		-5.2	-11.9	-19.5	14.3	331	22.2
Pm + Pb	<i>Inside</i>	-5.9	-13.2	-20.2	14.2	496	33.8
	<i>Center</i>	-5.2	-11.9	-19.5	14.3	496	33.8
	<i>Outside</i>	4.7	-14.9	-23.9	28.6	496	16.3
OUTER LID		MPa	MPa	MPa	MPa	MPa	
Pm		10.1	-2.3	-30.1	40.3	331	7.2
Pm + Pb	<i>Inside</i>	-29.7	-48.1	-104.5	74.8	496	5.6
	<i>Center</i>	10.1	-2.3	-30.1	40.3	496	11.3
	<i>Outside</i>	68.5	45.1	24.1	44.4	496	10.2
INNER LID		MPa	MPa	MPa	MPa	MPa	
Pm		45.2	31.4	9.3	35.9	331	8.2
Pm + Pb	<i>Inside</i>	47.0	-14.6	-143.5	190.4	496	1.6
	<i>Center</i>	45.2	31.4	9.3	35.9	496	12.8
	<i>Outside</i>	172.0	77.5	33.6	138.4	496	2.6

Note: (1) The margin of safety is the ratio of the Allowable Stress and the Stress Intensity (SINT) minus 1.

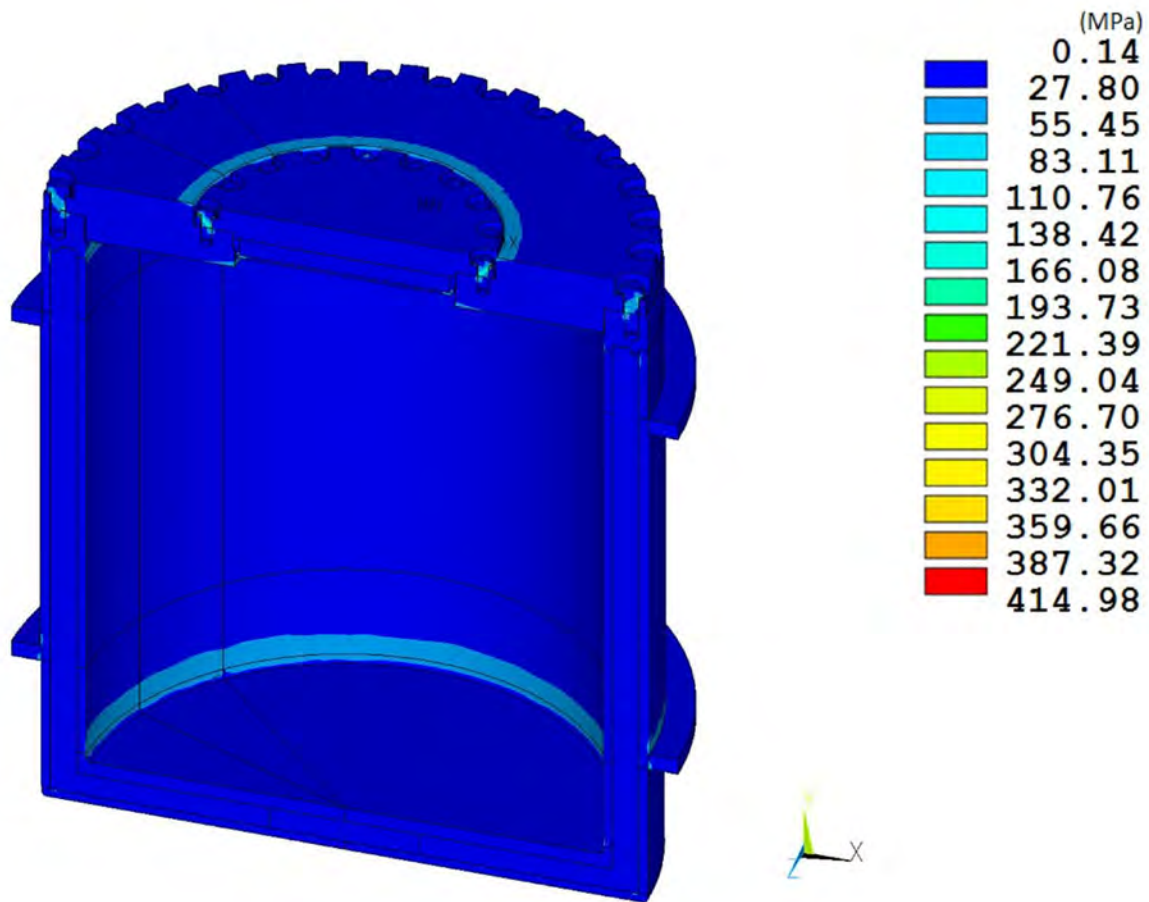


Figure 2.7.1-1 RT-100 HAC End Drop Stress Intensity Results

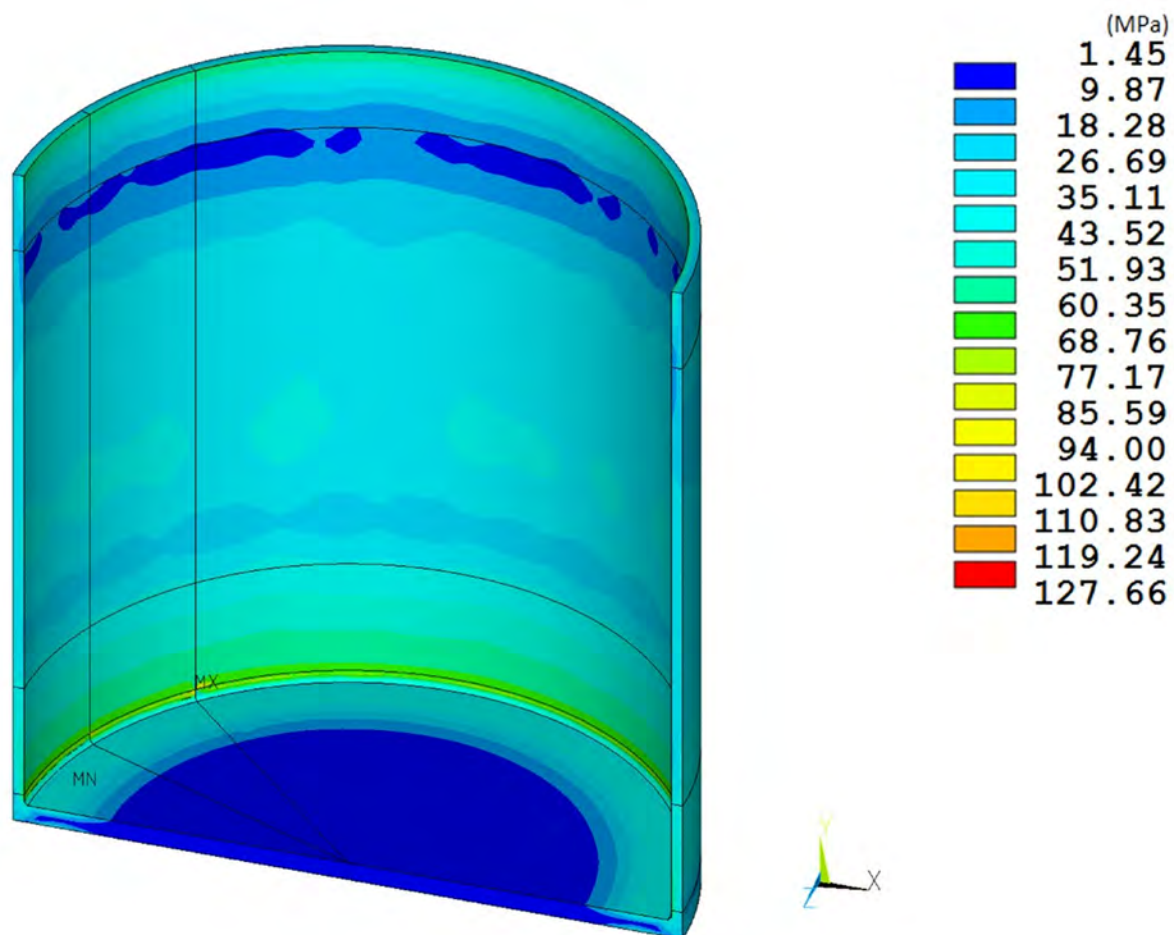


Figure 2.7.1-2 RT-100 Inner Shell HAC End Drop Stress Intensity Results

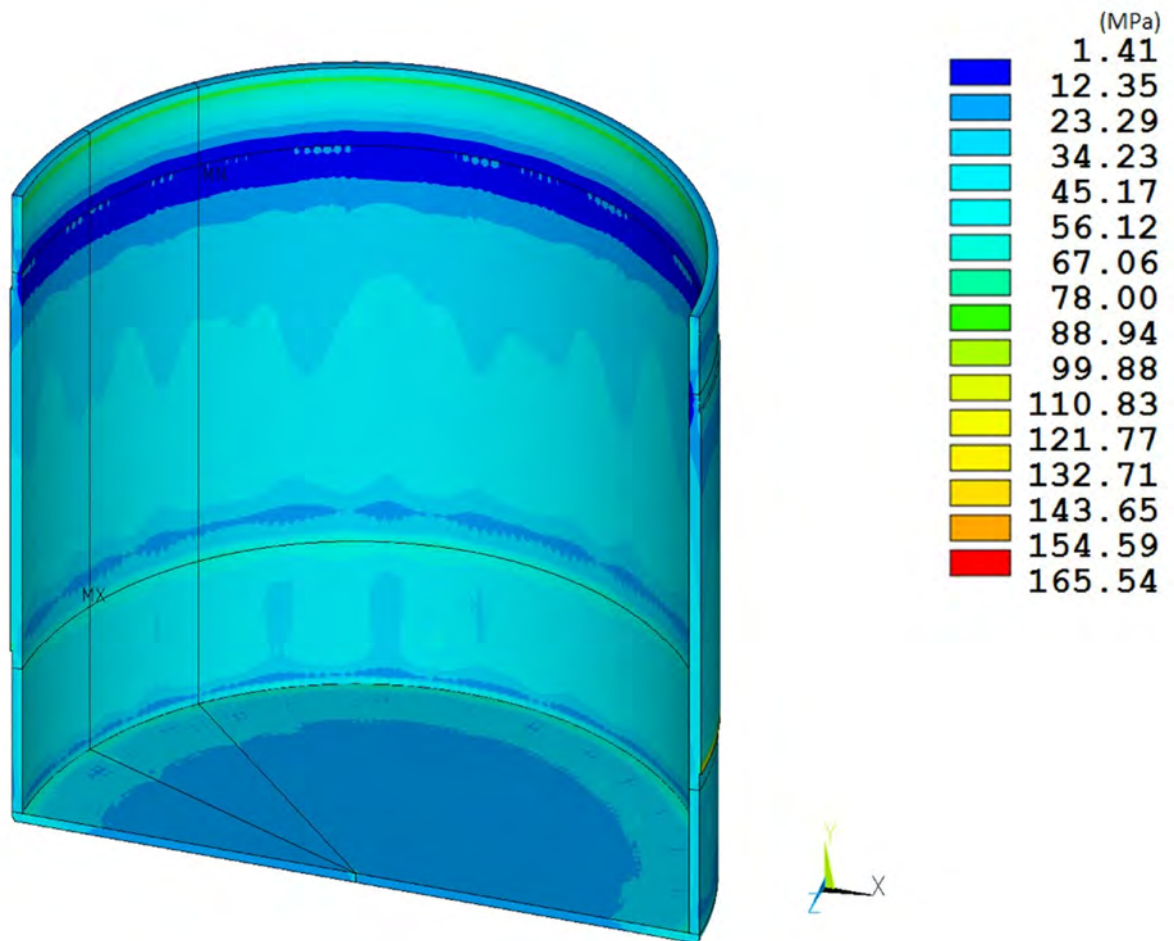


Figure 2.7.1-3 RT-100 Outer Shell HAC End Drop Stress Intensity Results

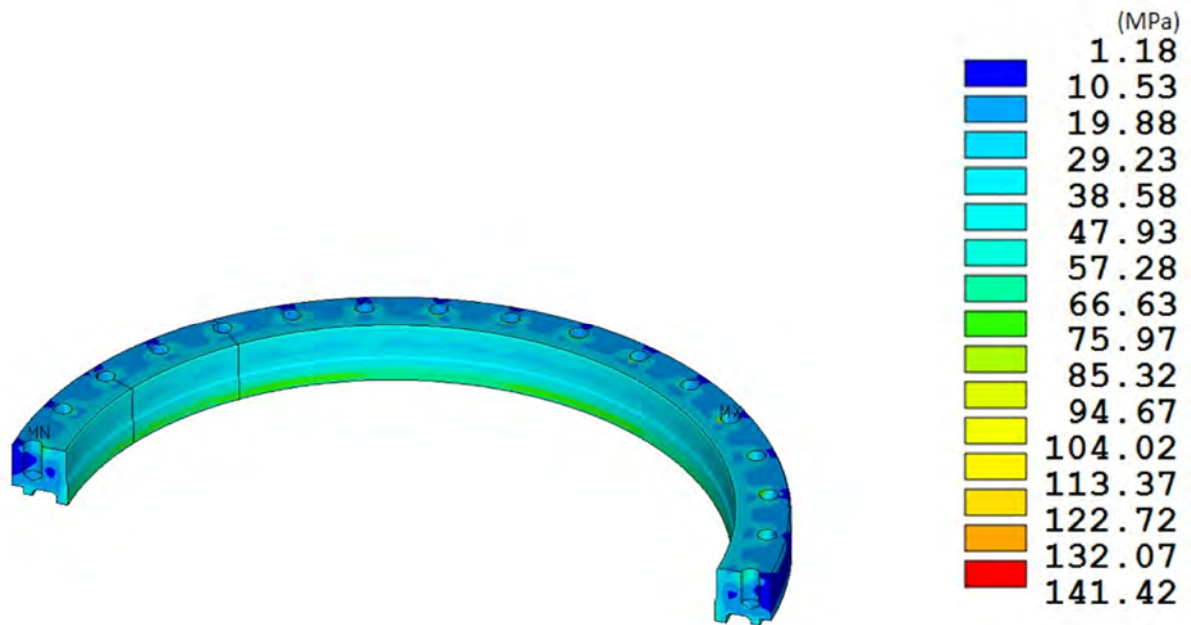


Figure 2.7.1-4 RT-100 Flange HAC End Drop Stress Intensity Results

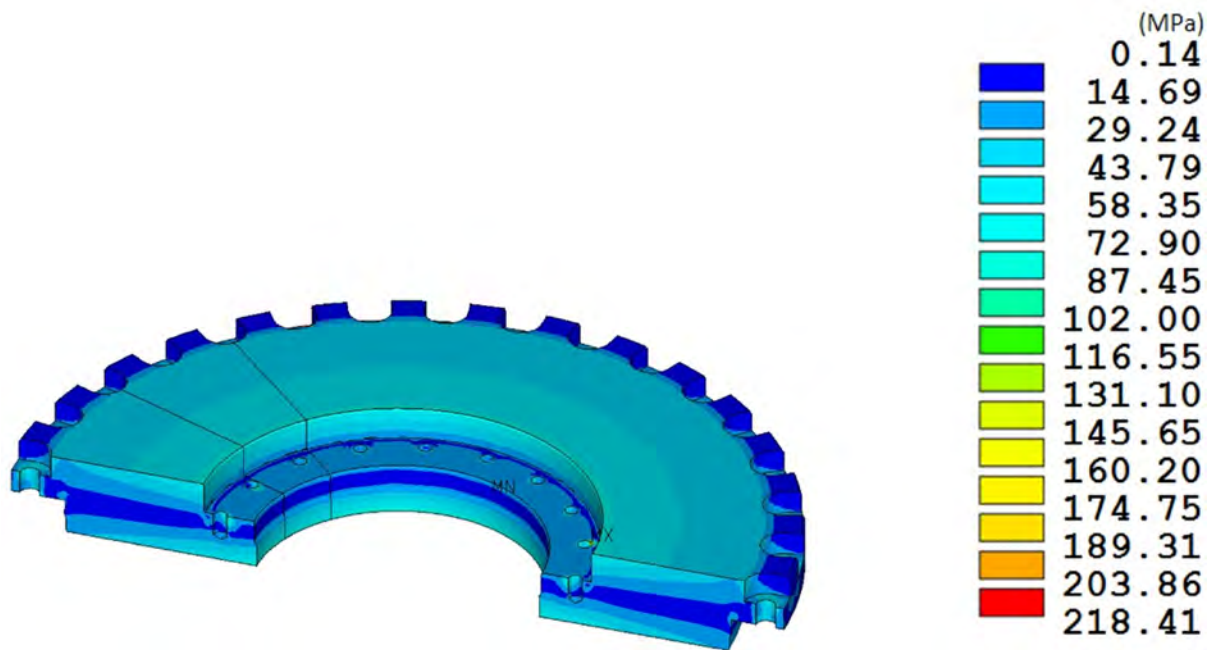


Figure 2.7.1-5 RT-100 Outer Lid HAC End Drop Stress Intensity Results

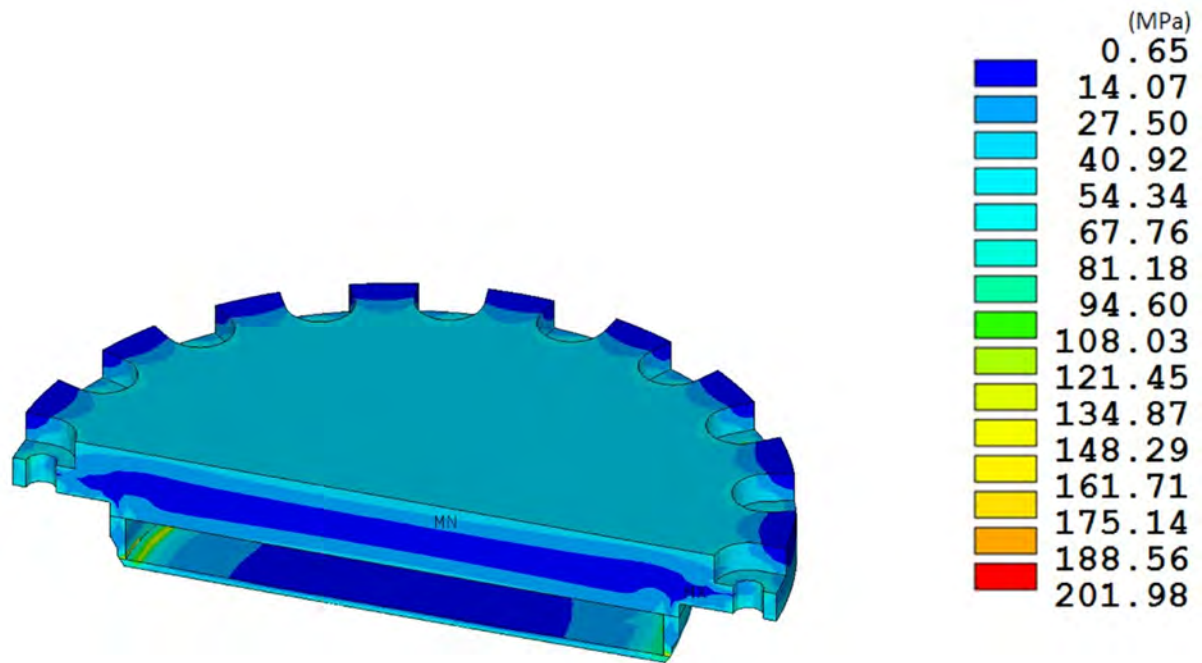


Figure 2.7.1-6 RT-100 Inner Lid HAC End Drop Stress Intensity Results

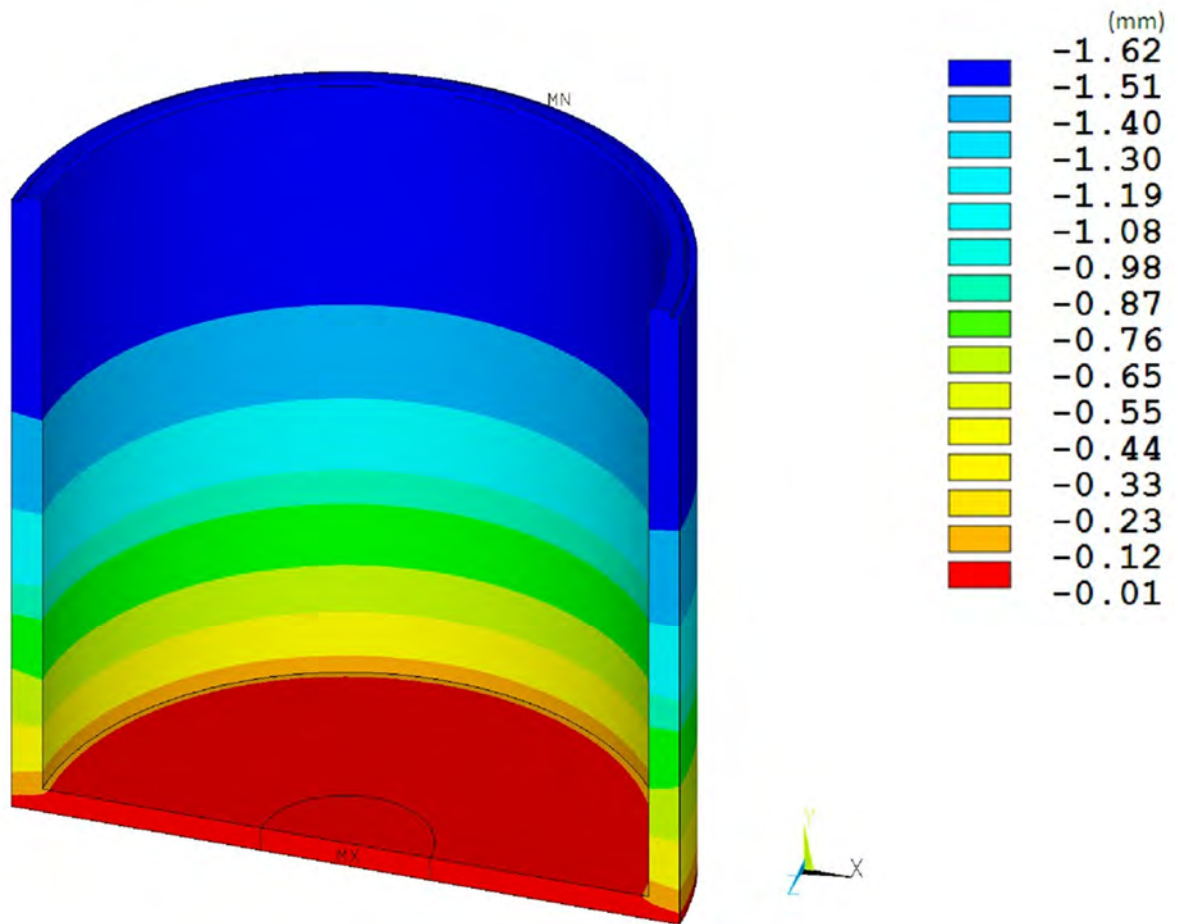


Figure 2.7.1-7 RT-100 Lead Slump

2.7.1.2 Side Drop

In accordance with the requirements of 10 CFR 71.73(c)(1) [Ref. 2], the RT-100 is structurally evaluated for the hypothetical accident 30-foot side drop condition. In this event, the cask including the payload and impact limiters falls 30 feet onto a flat, unyielding, horizontal surface. The package strikes the surface in a horizontal position resulting in a side impact. The types of loading involved in a side drop accident are closure lid bolt preload, internal pressure, and inertial body load.

As previously discussed, stress results for the 9-meter side drop combined loading conditions are documented in Table 2.7.1-3. The table documents the primary membrane (P_m), primary membrane plus primary bending (P_m+P_b), stresses in accordance with the criteria presented in Regulatory Guide 7.6 [Ref. 4].

As shown in Table 2.7.1-3, the margins of safety are positive when compared to the stress intensity for each category. The most critically stressed component in the system is the cask outer shell; this condition is due to ovalization of the cask body and the inertial load of the lead shield. The minimum margin of safety is found to be +0.2 for primary membrane plus bending stress intensity. The locations of the critical sections correspond to the maximum stress location shown in Figure 2.7.1-8 through Figure 2.7.1-13.

Table 2.7.1-3 HAC Side Drop Stress Summary

Component and Stress State	Stress Location	ANSYS Results				RG 7.6 Allowable Stress	Margin of Safety (1)
		S1	S2	S3	SINT		
INNER SHELL		MPa	MPa	MPa	MPa	MPa	
Pm		19.1	-13.7	-140.4	159.6	331	1.1
Pm + Pb	Inside	20.0	-13.9	-139.7	159.7	496	2.1
	Center	19.1	-13.7	-140.4	159.6	496	2.1
	Outside	18.3	-13.5	-141.3	159.6	496	2.1
OUTER SHELL		MPa	MPa	MPa	MPa	MPa	
Pm		-14.2	-129.8	-201.4	187.1	331	0.8
Pm + Pb	Inside	-66.9	-166.2	-472.2	405.3	496	0.2
	Center	-14.2	-129.8	-201.4	187.1	496	1.7
	Outside	73.5	36.5	-95.5	169.0	496	1.9
FLANGE		MPa	MPa	MPa	MPa	MPa	
Pm		17.1	-12.5	-145.1	162.2	331	1.0
Pm + Pb	Inside	16.9	-12.6	-144.6	161.5	496	2.1
	Center	17.1	-12.5	-145.1	162.2	496	2.1
	Outside	17.3	-12.4	-145.5	162.8	496	2.0
OUTER LID		MPa	MPa	MPa	MPa	MPa	
Pm		95.6	0.3	-104.9	200.5	331	0.7
Pm + Pb	Inside	289.3	35.4	-7.0	296.3	496	0.7
	Center	95.6	0.3	-104.9	200.5	496	1.5
	Outside	-34.4	-94.7	-206.7	172.3	496	1.9
INNER LID		MPa	MPa	MPa	MPa	MPa	
Pm		-4.3	-14.3	-164.4	160.1	331	1.1
Pm + Pb	Inside	-20.9	-70.1	-371.6	350.6	496	0.4
	Center	-4.3	-14.3	-164.4	160.1	496	2.1
	Outside	64.8	33.1	-1.4	66.3	496	6.5

Note: (1) The margin of safety is the ratio of the Allowable Stress and the Stress Intensity (SINT) minus 1.

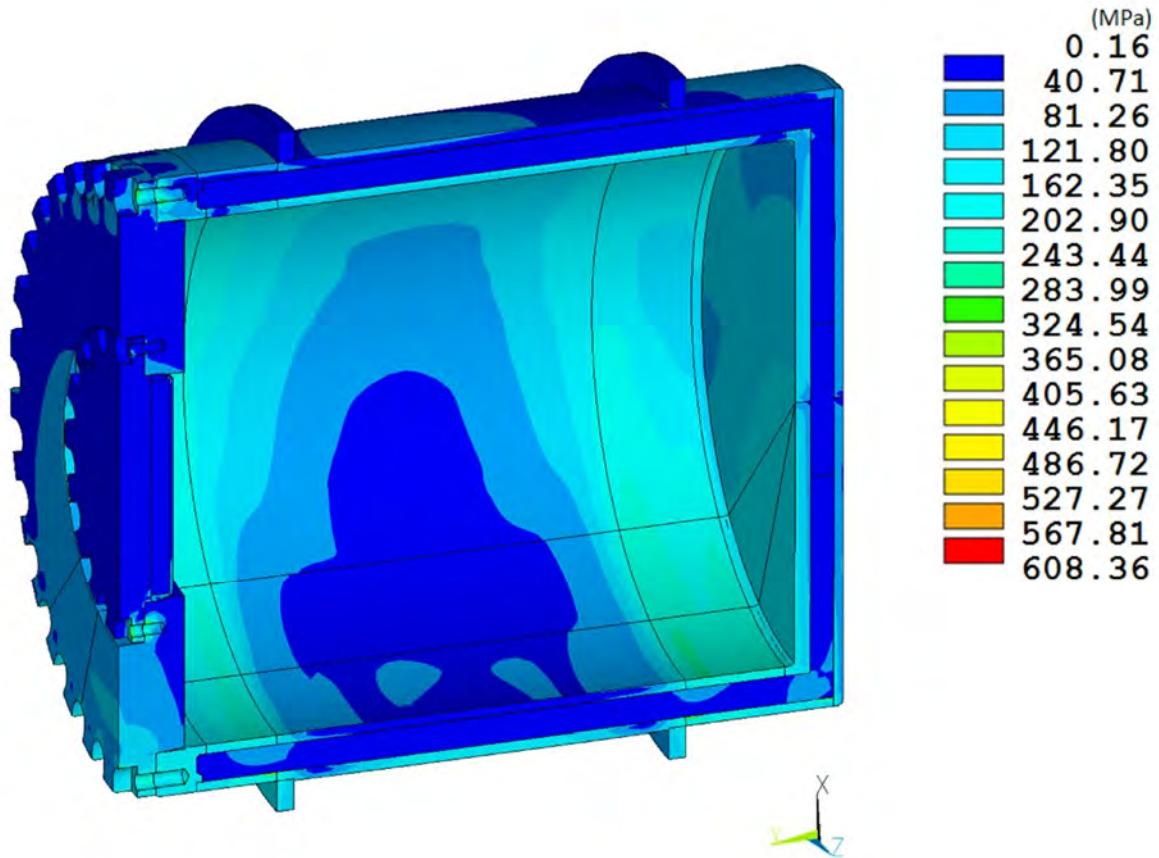


Figure 2.7.1-8 RT-100 HAC Side Drop Stress Intensity Results

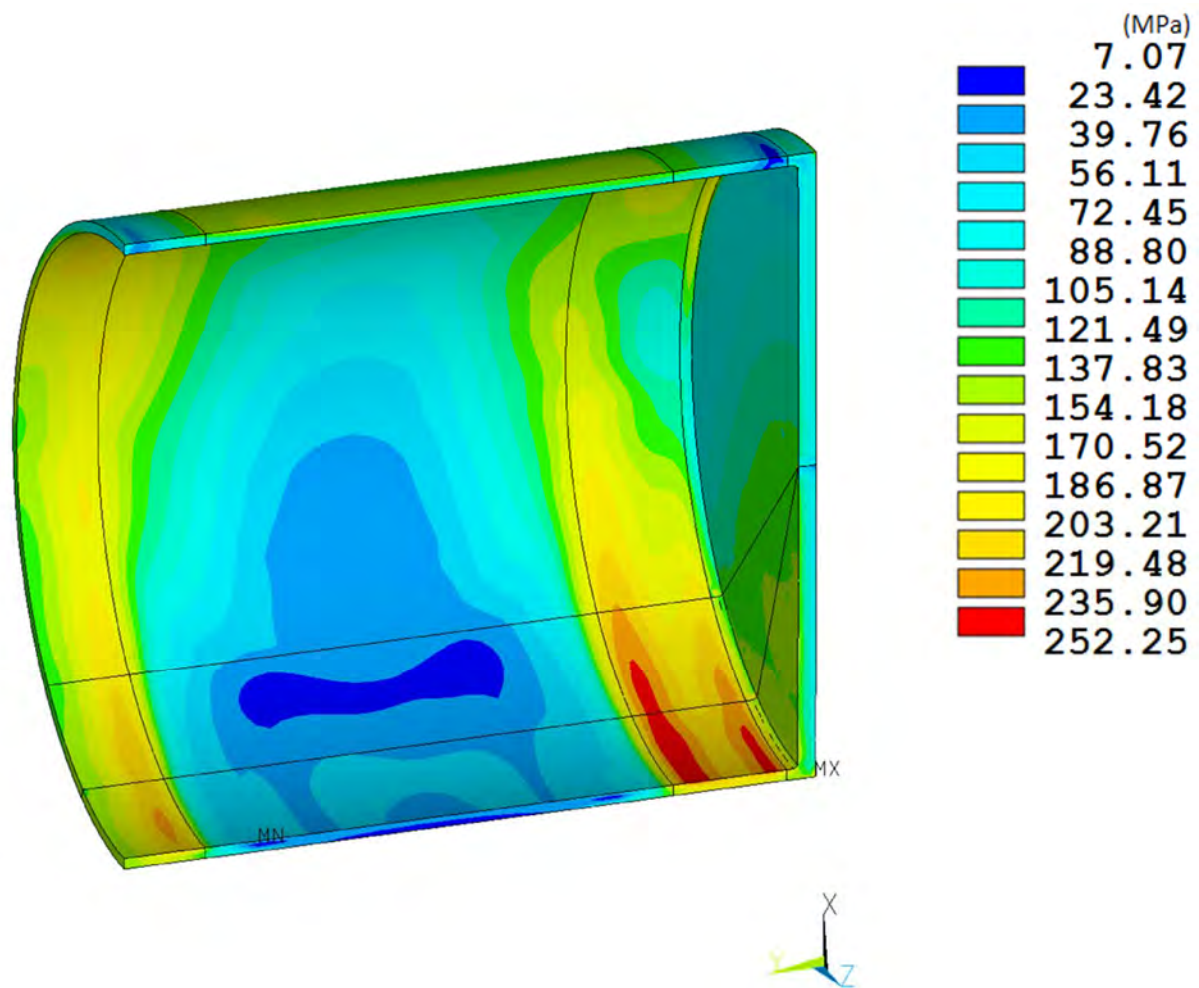


Figure 2.7.1-9 RT-100 Inner Shell HAC Side Drop Stress Intensity Results

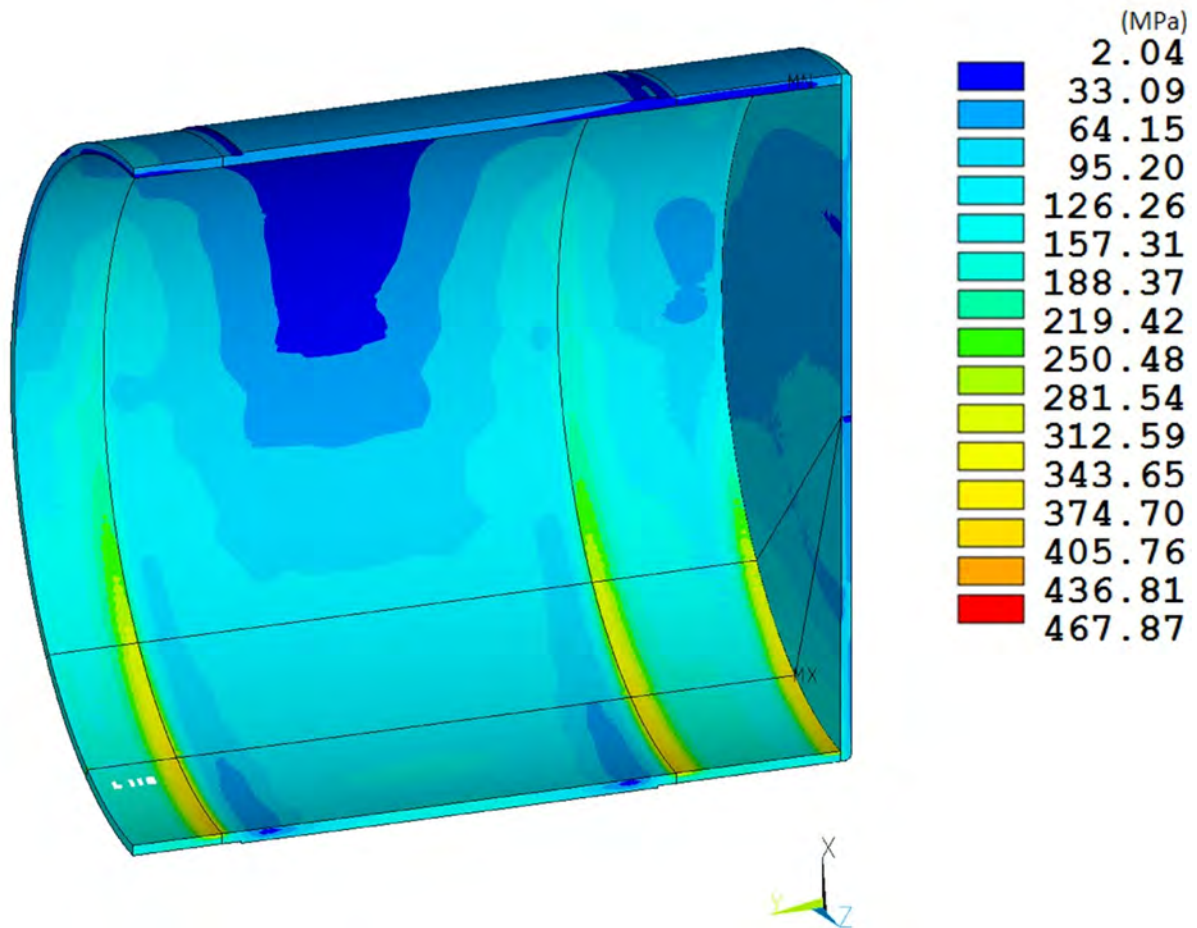


Figure 2.7.1-10 RT-100 Outer Shell HAC Side Drop Stress Intensity Results

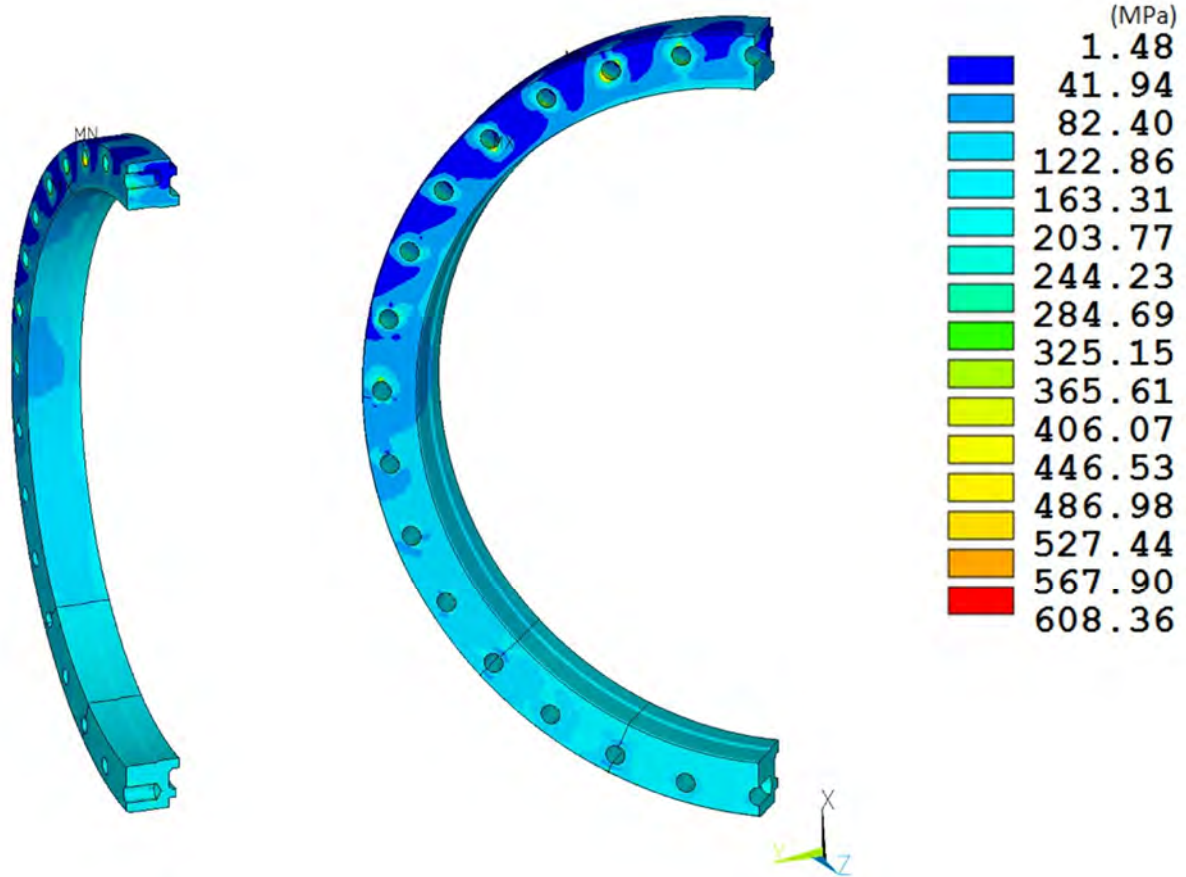


Figure 2.7.1-11 RT-100 Flange HAC Side Drop Stress Intensity Results

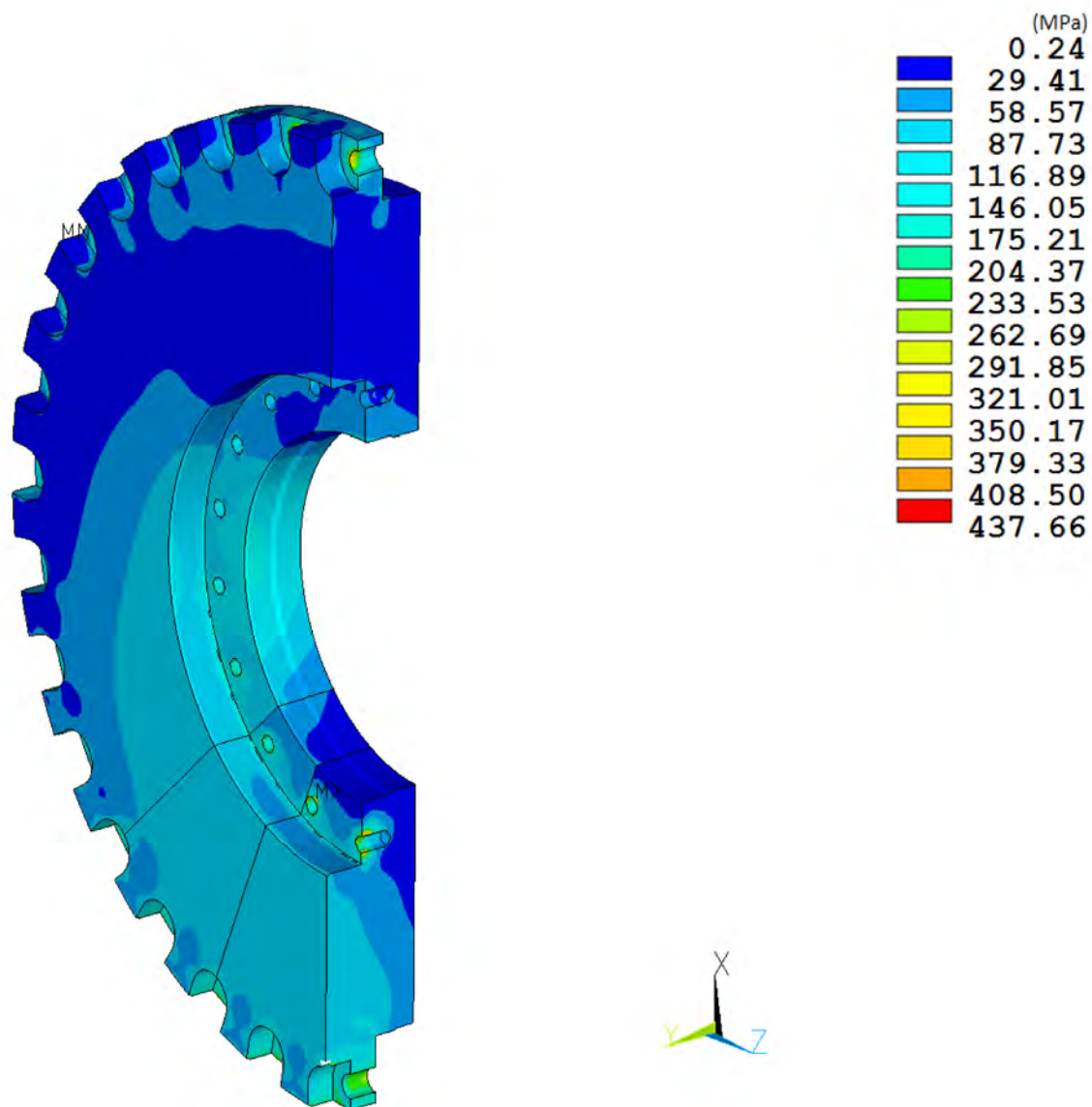


Figure 2.7.1-12 RT-100 Outer Lid HAC Side Drop Stress Intensity Results

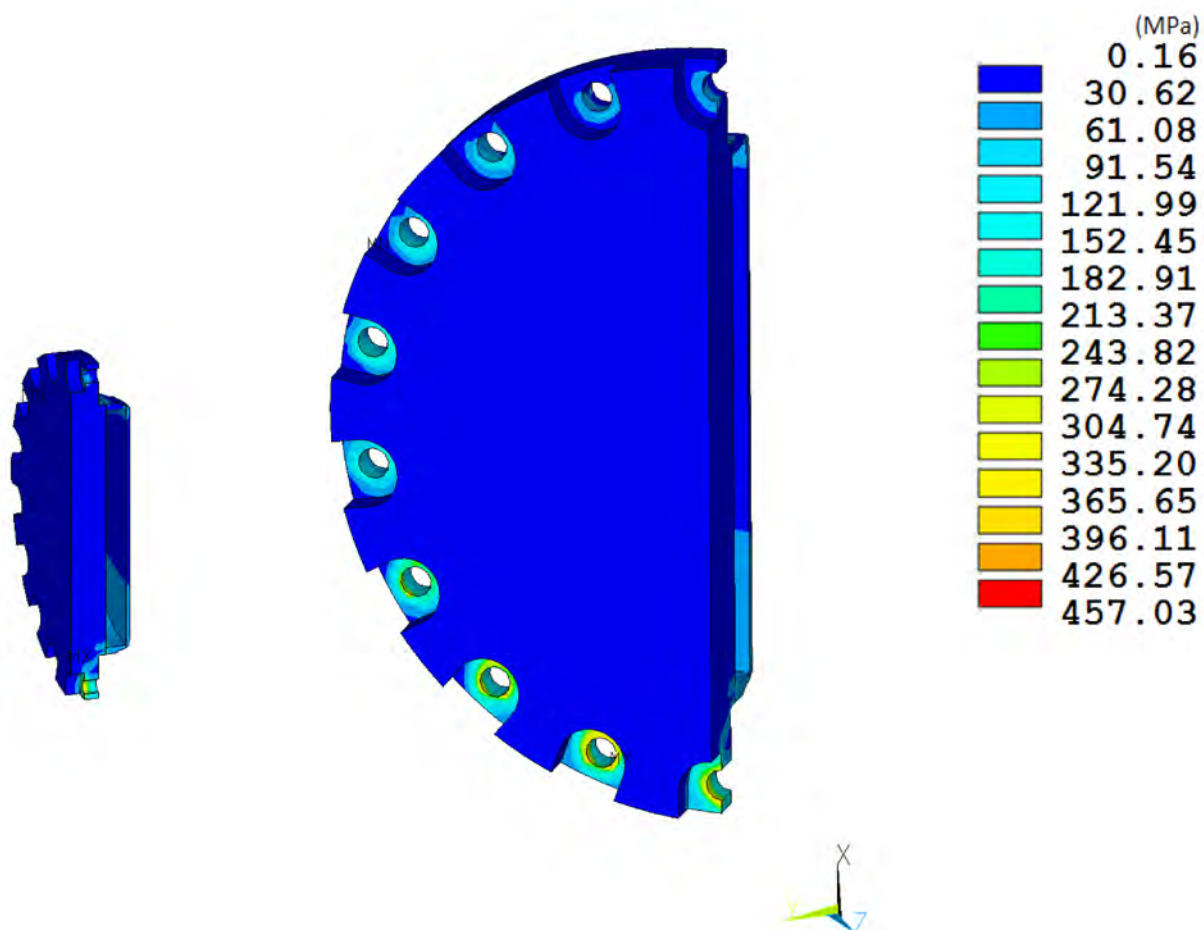


Figure 2.7.1-13 RT-100 Inner Lid HAC Side Drop Stress Intensity Results

2.7.1.3 Corner Drop

In accordance with the requirements of 10 CFR 71.73(c)(1) [Ref. 2], the RT-100 is structurally evaluated for the hypothetical accident 30-foot corner drop condition. Based on the impact limiter analysis provided in Appendix 2.12, Table 2.7.1-4 demonstrates that the end and side drop accelerations bound the CG over corner drop acceleration.

Table 2.7.1-4 Corner Drop Component Accelerations

Side Drop Acceleration (g)	End Drop Acceleration (g)	Corner Drop Acceleration (g)	Corner Drop Axial Component (g)	Corner Drop Lateral Component (g)
226	123	116	91.4	71.4

To evaluate the stresses generated in the RT-100 during the corner drop (38° from vertical), the ANSYS [Ref. 28] stress results for the side and end drop evaluations are scaled by the ratio of the end and side drop accelerations and the corner drop axial and lateral component accelerations. Once scaled, the resulting axial and lateral component stresses are summed and compared to the allowable stress intensity.

Stress results for the 9-meter corner drop combined loading conditions are documented in Table 2.7.1-5. The table documents the primary membrane (P_m), primary membrane plus primary bending (P_m+P_b) stresses in accordance with the criteria presented in Regulatory Guide 7.6 [Ref. 4].

As shown in Table 2.7.1-5, the margins of safety when compared to the stress intensity for each category are positive. The most critically stressed component in the system is the inner lid. The minimum margin of safety is found to be +1.0 for primary membrane plus bending stress intensity.

Table 2.7.1-5 HAC Corner Drop Stress Summary

Stress State	End Drop SINT	Side Drop SINT	Corner SINT	RG 7.6 Allowable Stress	Margin of Safety(1)
INNER SHELL	MPa	MPa	MPa	MPa	
P_m	38.4	159.6	79.0	331	3.2
P_m + P_b	64.1	159.7	98.1	496	4.1
	38.4	159.6	79.0	496	5.3
	19.4	159.6	64.9	496	6.7
OUTER SHELL	MPa	MPa	MPa	MPa	
P_m	32.8	187.1	83.5	331	3.0
P_m + P_b	33.5	405.3	153.0	496	2.2
	32.8	187.1	83.5	496	4.9
	32.0	169.0	77.2	496	5.4
FLANGE	MPa	MPa	MPa	MPa	
P_m	14.3	162.2	61.9	331	4.4
P_m + P_b	14.2	161.5	61.6	496	7.1
	14.3	162.2	61.9	496	7.0
	28.6	162.8	72.7	496	5.8
OUTER LID	MPa	MPa	MPa	MPa	
P_m	40.3	200.5	93.3	331	2.5
P_m + P_b	74.8	296.3	149.2	496	2.3
	40.3	200.5	93.3	496	4.3
	44.4	172.3	87.4	496	4.7
INNER LID	MPa	MPa	MPa	MPa	
P_m	35.9	160.1	77.3	331	3.3
P_m + P_b	190.4	350.6	252.3	496	1.0
	35.9	160.1	77.3	496	5.4
	138.4	66.3	123.8	496	3.0

Note: (1) The margin of safety is the ratio of the Allowable Stress and the Stress Intensity (SINT) minus 1.

2.7.1.4 Oblique Drops

In accordance with the requirements of 10 CFR 71.73(c)(1) [Ref. 2], the RT-100 is structurally evaluated for the hypothetical accident 30-foot oblique drop condition. Based on the following analysis, the cask velocities and stresses generated by an oblique-angle drop are bounded by those produced by the side drop. For a shallow angle drop, it is assumed that no energy is absorbed by the first impact limiter that contacts the impact surface, which causes all of the rotational inertia generated by the cask into the second impact limiter. The analysis is performed according to the following basic inertial equations in “Standard Handbook for Mechanical Engineers, 7th Edition” [Ref. 51]

Assumptions:

- The rotational inertia of the cask is approximated by a solid cylinder
- The cask does not slide along the impact surface
- No gravitational acceleration is assumed to occur after initial contact of the cask with the impact surface

The equation for the rotational inertia of a cylinder is:

$$I_{cyl} = I_{cyl} = \frac{1}{4} \times M \times \left(r^2 + \frac{l^2}{3} \right)$$

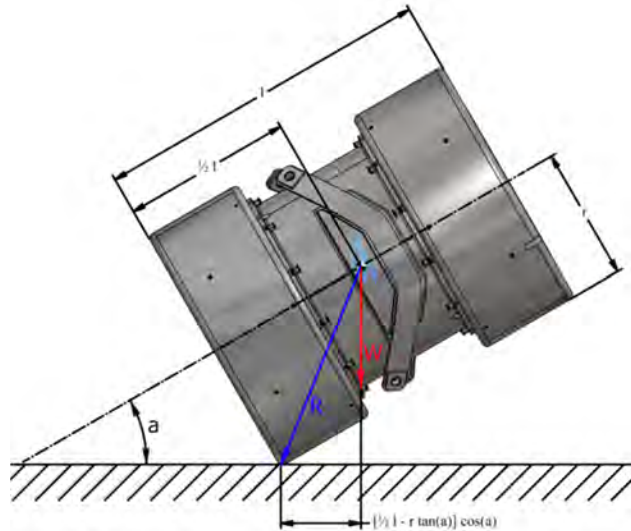
Where M = mass of cask

r = radius of cask

l = length of cask

R = distance from CG to corner of impact limiter

a = angle of the cask at impact



For this configuration, the angular momentum of the cask before impact, L_1 , is represented by:

$$L_1 = M \times v_1 \times \left(\frac{l}{2} - \tan(a) \right) \times \cos(a)$$

Where v_1 = impact velocity

After impact the angular momentum, L_2 , of the cask is:

$$L_2 = I_{imp} \times \omega_2$$

Where $I_{imp} = I_{cyl} + M \times R^2$

ω_2 = angular velocity of cask following impact

Substituting the rotational inertia for a cylinder, I_{cyl} :

$$I_{imp} = M \times \left(\frac{r^2}{4} + \frac{l^2}{12} + R^2 \right)$$

Because no external moments are applied to the cask, angular momentum is conserved.

Therefore:

$$L_1 = L_2$$

Substituting:

$$M \times v_1 \times \left(\frac{1}{2} - r \times \tan(a) \right) \times \cos(a) = M \times \left(\frac{r^2}{4} + \frac{l^2}{12} + R^2 \right) \times \omega_2$$

Solving for the angular velocity, ω_2 , gives:

$$\omega_2 = v_1 \times \frac{\left(\frac{1}{2} - r \times \tan(a) \right) \times \cos(a)}{\frac{r^2}{4} + \frac{l^2}{12} + R^2}$$

The maximum angular velocity occurs when the impact angle equals zero. Therefore, the velocity of the secondary impact is:

$$v_s = l \times \omega_2$$

Substituting the angular velocity:

$$v_s = l \times v_1 \times \frac{\left(\frac{1}{2} - r \times \tan(a) \right) \times \cos(a)}{\frac{r^2}{4} + \frac{l^2}{12} + R^2}$$

The limiting case occurs when the secondary impact velocity equals the initial impact velocity.

Therefore:

$$v_s = v_1 \text{ when the angle } a = 0$$

Solving:

$$1 = \frac{\frac{l^2}{2}}{\frac{r^2}{4} + \frac{l^2}{12} + R^2}$$

From the figure above:

$$R^2 = \frac{l^2}{4} + r^2$$

Substituting and solving:

$$\frac{l^2}{2} = \frac{r^2}{4} + \frac{l^2}{12} + \frac{l^2}{4} + r^2 \Rightarrow \frac{4}{12}l^2 = \frac{5}{4}r^2 \Rightarrow \frac{l^2}{r^2} = 7.5 \Rightarrow \frac{l}{r} = 2.74$$

Therefore:

$$\frac{l}{D} = 1.37$$

Where D = diameter of cask

This evaluation shows that cask designs with a length-to-diameter ratio greater than 1.37 may result in oblique impact velocities greater than the side drop. However, the length of the

RT-100 is 3316 mm and the diameter is 2587 mm for a length-to-diameter ratio of 1.28. Therefore, impact velocities and resulting stresses in the RT-100 during the oblique drop event are less than those experienced during the side drop.

2.7.1.5 Summary of Results

Structural analyses are performed for the RT-100 for hypothetical accident conditions free drop conditions. To evaluate the RT-100, 3D ANSYS [Ref. 28] is used to analyze the governing drop cases. All structural members have a positive margin of safety under worst case loading conditions. It is concluded that the RT-100 is structurally adequate for the HAC free drop conditions. Therefore, the requirements of 10 CFR 71.73(c)(1) [Ref. 2] have been satisfied.

2.7.2 Crush

In accordance with the requirements of 10 CFR 71.73(c)(2) [Ref. 2], the RT-100 is to be subjected to a dynamic crush test by evaluating the package on essentially unyielding horizontal surface so as to suffer maximum damage by the drop of a 500-kg mass from 9 m onto the package. The mass must consist of a solid mild steel plate 1 m × 1 m and must fall in a horizontal attitude. The crush test is required only when the specimen has a mass not greater than 500 kg, and overall density not greater than 1000 kg/m³ based on external dimension. The crush condition is not applicable since the RT-100 weighs more than 500 kg and overall density is greater than 1000 kg/m³.

2.7.3 Puncture

In accordance with the requirements of 10 CFR 71.73(c)(3) [Ref. 2] related to puncture (hypothetical accident condition), the RT-100 Cask is analyzed for structural adequacy (Calculation Package RTL-001-CALC-ST-0403 Rev. 4 [Ref. 36]). The cask is assumed to be in a horizontal position and dropped 1 m onto a 15 cm diameter, mild steel bar, oriented vertically on an unyielding surface. The structural evaluation of the RT-100 is performed by classical elastic analysis and finite element analysis methods.

2.7.3.1 Lid Puncture

Finite element analysis methods are used to perform the stress evaluation of the RT-100 for the end puncture conditions. The end puncture is analyzed using a three-dimensional finite element model using the computational modeling software ANSYS [Ref. 28]. To simplify the pin puncture analysis, only the upper end of the cask is considered for this evaluation. Figure 2.7.3-1 shows the pin puncture model.

2.7.3.1.1 Lid Puncture Boundary Conditions

The puncture load is applied to a 152 mm (6 in) diameter region which corresponds to a 152 mm diameter pin. The load is simulated with an evenly distributed pressure load equal to the dynamic flow stress of the pin; the dynamic flow stress is taken to be 324 MPa (47,000 psi). As discussed in the cask body analysis, the preload torque is included as an initial condition. In addition, the maximum normal operating pressure of 241 KPa (35 psig) is applied to the interior surface of the RT-100.

2.7.3.1.2 Lid Puncture Results

Stress results for the 1-meter pin puncture combined loading conditions are documented in Table 2.7.3-1. The table documents the primary membrane (P_m), primary membrane plus primary bending ($P_m + P_b$) stresses in accordance with the criteria presented in Regulatory Guide 7.6 [Ref. 4]. Stresses are linearized across critical sections to determine the membrane and bending stresses and subsequently, are compared with allowable stress intensities.

As shown in Table 2.7.3-1, the margins of safety are positive when compared to the stress intensity for each category. The most critically stressed component in the system is the flange; this condition is due to bending as a result of the pin puncture probe striking the center of the lid. The minimum margin of safety is found to be +0.2 for primary membrane plus bending stress intensity. The locations of critical section correspond to the maximum stress location are shown in Figure 2.7.3-2.

Table 2.7.3-1 HAC Pin Puncture Stress Summary

Stress State	Location	S1	S2	S3	SINT	RG 7.6 Allowable Stress	Margin of Safety
INNER LID		MPa	MPa	MPa	MPa	MPa	
P_m		-108.6	-109.8	-191.5	82.9	331	3.0
P_m + P_b	<i>Inside</i>	383.4	382.9	-37.7	421.1	485	0.2
	<i>Center</i>	-108.6	-109.8	-191.5	82.9	485	4.9
	<i>Outside</i>	-342.9	-602.3	-603.3	260.4	485	0.9

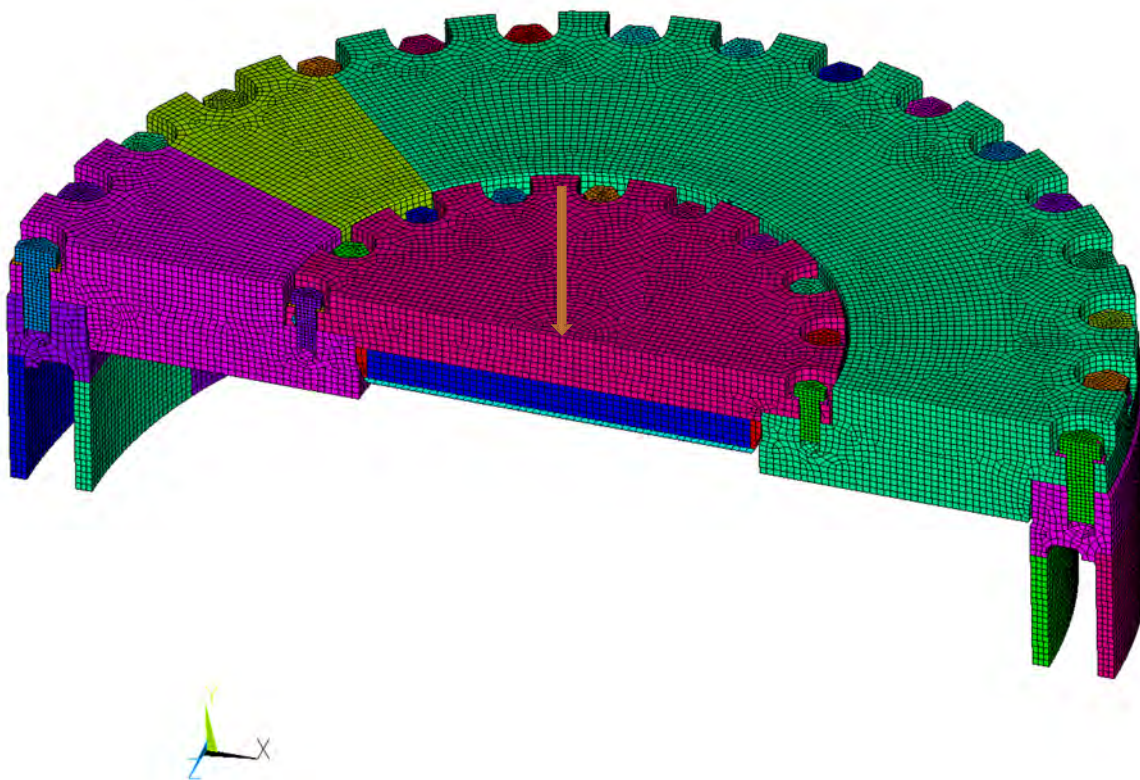


Figure 2.7.3-1 RT-100 ANSYS Puncture Model

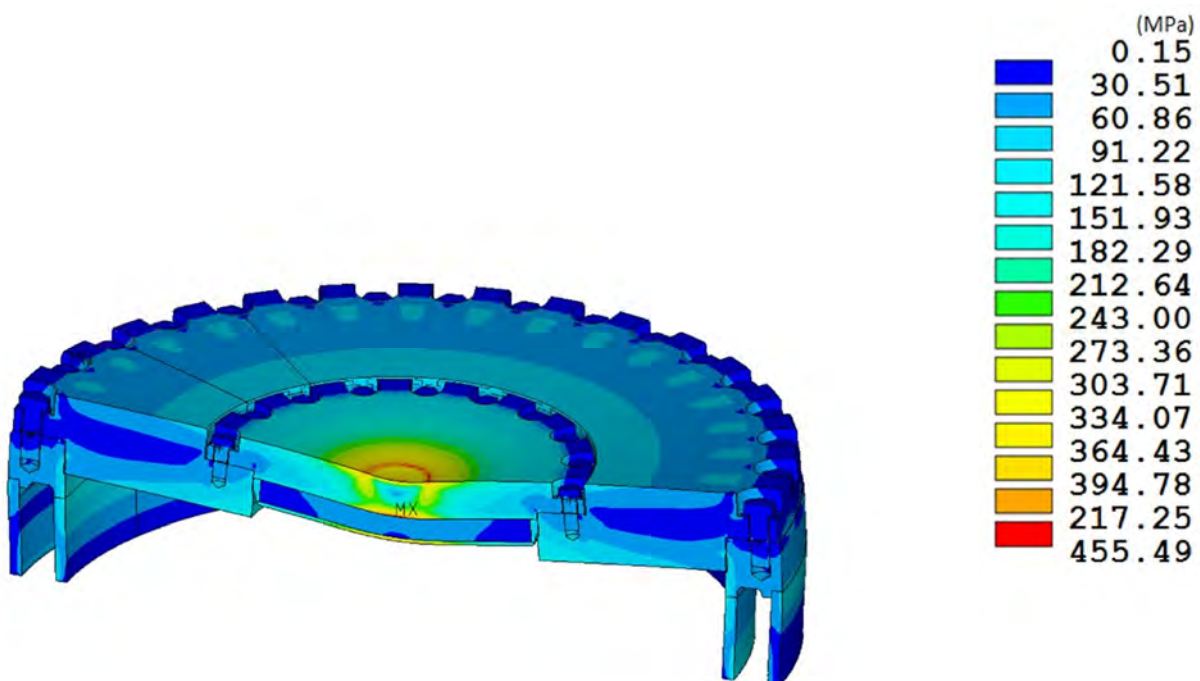


Figure 2.7.3-2 RT-100 Pin Puncture Stress Intensity Results

2.7.3.2 Cask Side Puncture

The following sections describe the cask side puncture analysis.

2.7.3.2.1 Cask Side Puncture Minimum Wall Thickness

A series of pin puncture tests (performed at Oak Ridge National Laboratory) are used to develop an empirical equation to determine the stress in the outer wall of a multi-wall cask as a function of the mass of the cask and the thickness of the cask outer wall material. This equation (Nelm's equation [Ref. 59]) applies to steel-lead-steel cask wall construction and is used to demonstrate pin puncture adequacy for casks with stainless steel walls; this equation has been the basis for the puncture analysis of several previously licensed casks. Solving Nelm's equation [Ref.59] for the RT-100 outer shell:

$$t = \left(\frac{W}{S} \right)^{0.71} = 1.16 \text{ in (29mm)} < 35 \text{ mm}$$

where,

$$W = 92,594 \text{ lb (42,000 kg), maximum gross weight of the package}$$

$$S = 75,000 \text{ psi (517.1 MPa), ultimate tensile strength of the outer shell}$$

Nelm's equation [Ref. 59] shows that the cask outer shell is sufficient to resist puncture.

2.7.3.2.2 Cask Sidewall Bending Stresses

When the cask sidewall impacts the puncture pin, the bending force is:

$$\sigma_b = \frac{M \times c}{I} = 15.3 \text{ MPa}$$

Conservatively assuming the compressive and tensile stresses occur at the same location, the stress intensity is doubled to 30.6 MPa. Therefore, the factor of safety is:

$$FS = \frac{517.1}{30.6} = 15.7 > 1$$

where,

$$M = \frac{F_i \times m}{4} = 1589.2 \text{ kN-m, moment due to impact force}$$

$$m = \frac{L}{2} = 1.16 \text{ m, moment arm resulting from impact}$$

$$L = h_{\text{tot}} - h_U - h_L = 2.32 \text{ m, sidewall length}$$

$$h_{\text{tot}} = 3312.8 \text{ mm, cask total height}$$

$$h_U = 498 \text{ mm, upper impact limiter height}$$

$$h_L = 494 \text{ mm, lower impact limiter height}$$

$$F_i = K_s \times A_i = 5478.2 \text{ kN, impact force}$$

$$K_s = 324 \text{ MPa, dynamic flow stress for mild steel (3)}$$

$$A_i = \frac{\pi}{4} \times d_p^2 = 0.0177 \text{ m}^2, \text{ puncture probe area}$$

$$d_p = 0.15 \text{ m, puncture probe diameter}$$

Therefore, the RT-100 sidewall successfully resists the regulatory puncture drop.

2.7.3.3 Lead Deformation during Side Puncture

Following the postulated side puncture of The RT-100, the cask may experience localized deformation in the outer shell. Behind this localized deformation a slight flattening may occur, and results in shielding loss. To quantify this loss, the local stiffness of the cask wall is determined to calculate the energy absorbed by the package. To calculate the total deformation of the lead shield, it is conservatively assumed that the available potential energy of the 1 meter puncture drop is converted to strain energy.

The maximum deformation occurs during postulated puncture event when the cask strikes the puncture probe approximately mid-span on the cask outer shell. Figure 2.7.3-3 shows the side puncture details. For the purposes of this evaluation, the cask is considered a closed cylinder subjected to a concentrated load at the mid-span. The deformation is obtained from Table 31, Case 9 of “Roark’s Formulas for Stress and Strain, 6th Edition” [Ref. 29]. The deflection of the outer shell due to the applied load is:

$$y = \frac{P}{Et} \left[0.48 \times \left(\frac{L}{R} \right)^{0.5} \times \left(\frac{R}{t} \right)^{1.22} \right]$$

where:

L = length of the cylinder

R = mean radius of the shell

P = applied load

E = Young’s modulus

Solving for the stiffness

$$k = \frac{P}{y} = \frac{Et}{\left[0.48 \times \left(\frac{L}{R} \right)^{0.5} \times \left(\frac{R}{t} \right)^{1.22} \right]}$$

The RT-100 is considered a composite cylinder comprised of an outer shell, lead shield, and inner shell. The resulting stiffness of each component is shown below.

2.7.3.3.1 Outer Shell Stiffness

$$k_1 = \frac{1.989 \times 10^{10} \times 3.505 \times 10^{-2}}{\left[0.48 \times \left(\frac{1.946}{1.003} \right)^{0.5} \times \left(\frac{1.003}{3.505 \times 10^{-2}} \right)^{1.22} \right]} = 1.743 \times 10^7 \text{ N/m}$$

where:

L = 1.946 m

R = 1.003 m

$$\begin{aligned}
 t &= 3.505 \times 10^{-2} \text{ m} \\
 P &= 6.972 \times 10^8 \text{ N} \\
 E &= 1.989 \times 10^{10} \text{ Pa}
 \end{aligned}$$

2.7.3.3.2 Lead Stiffness

$$k_2 = \frac{1.602 \times 10^9 \times 8.992 \times 10^{-2}}{\left[0.48 \times \left(\frac{1.946}{9.401 \times 10^{-1}} \right)^{0.5} \times \left(\frac{9.401 \times 10^{-1}}{8.992 \times 10^{-2}} \right)^{1.22} \right]} = 1.191 \times 10^7 \text{ N/m}$$

where:

$$\begin{aligned}
 L &= 1.946 \text{ m} \\
 R &= 9.401 \times 10^{-1} \text{ m} \\
 t &= 8.992 \times 10^{-2} \text{ m} \\
 P &= 1.441 \times 10^8 \text{ N} \\
 E &= 1.602 \times 10^9 \text{ Pa}
 \end{aligned}$$

2.7.3.3.3 Inner Shell Stiffness

$$k_3 = \frac{1.989 \times 10^{10} \times 1.905 \times 10^{-2}}{\left[0.48 \times \left(\frac{1.946}{8.801 \times 10^{-1}} \right)^{0.5} \times \left(\frac{8.801 \times 10^{-1}}{1.905 \times 10^{-2}} \right)^{1.22} \right]} = 4.945 \times 10^6 \text{ N/m}$$

where:

$$\begin{aligned}
 L &= 1.946 \text{ m} \\
 R &= 8.801 \times 10^{-1} \text{ m} \\
 t &= 1.905 \times 10^{-2} \text{ m} \\
 P &= 3.789 \times 10^8 \text{ N} \\
 E &= 1.989 \times 10^{10} \text{ Pa}
 \end{aligned}$$

2.7.3.3.4 Lead Deformation due to Puncture Load

The effective stiffness of the composite section of the cask is:

$$k_{\text{eff}} = k_1 + k_2 + k_3 = 3.428 \times 10^7 \text{ N/m}$$

The energy absorbed during impact is:

$$U = \frac{1}{2} k_{\text{eff}} \times \delta^2$$

Assuming the energy absorbed is equal to the total potential energy, the potential energy is calculated as:

$$\text{P.E.} = W \times h$$

Setting the energy absorbed during impact equal to the total potential energy the outer shell deformation is:

$$\frac{1}{2} k_{\text{eff}} \times \delta^2 = W \times h \Rightarrow \delta = \sqrt{\frac{2(W \times h)}{k_{\text{eff}}}} = 0.050 \text{ m}$$

where:

$$W = 42,000 \text{ kg}$$

$$H = 1.016 \text{ m}$$

The deformation of the lead is calculated from the ratio of the effective stiffness and lead stiffness:

$$\delta_{\text{lead}} = \delta \times \frac{k_2}{k_{\text{eff}}} = 0.017 \text{ m}$$

Although the deformation is comprised of an elastic and inelastic component, the entire deformation is conservatively assumed to be permanent.

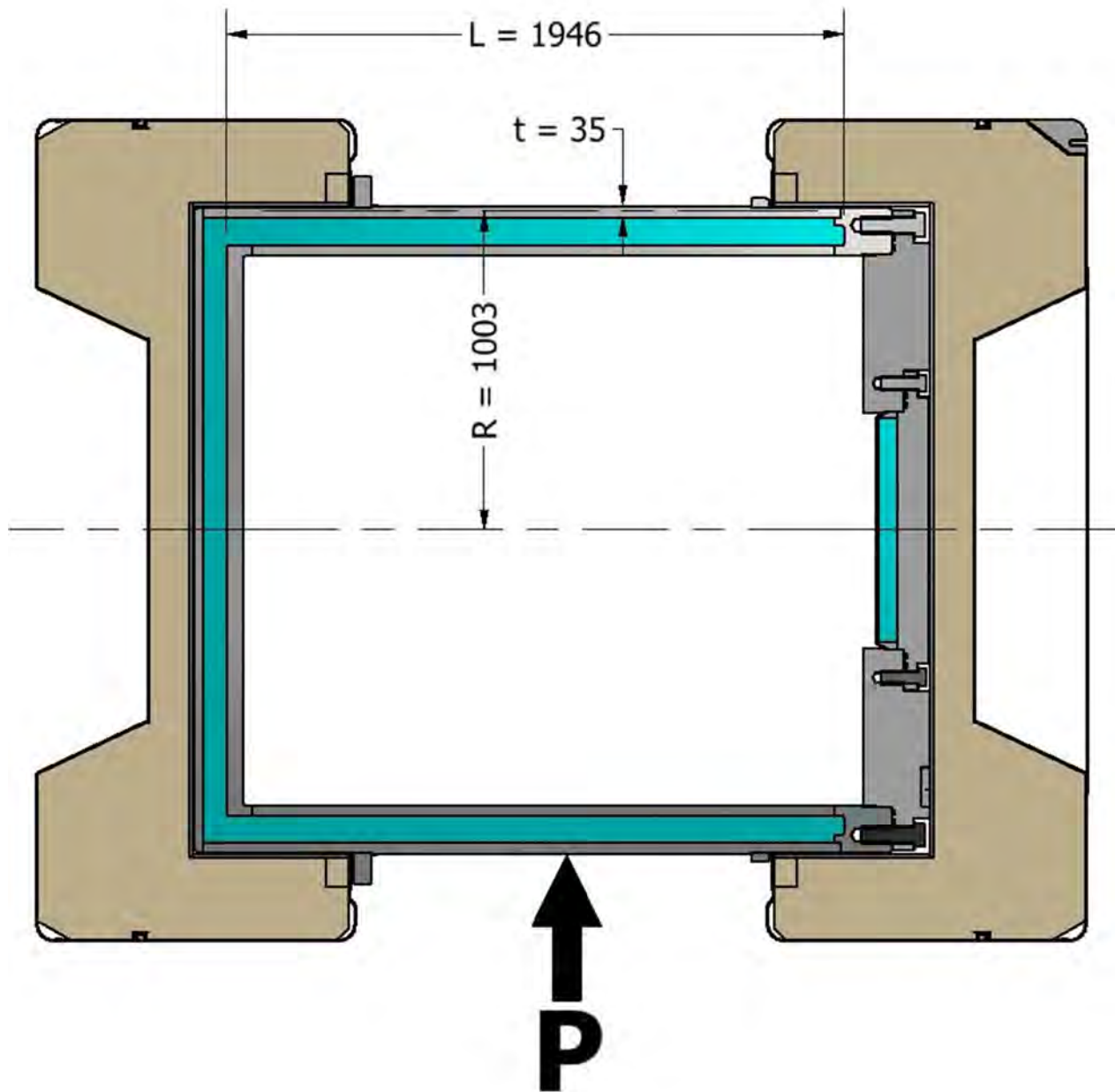


Figure 2.7.3-3 RT-100 Side Puncture Details

2.7.4 Thermal

For hypothetical accident conditions, the RT-100 cask body provides protection and containment of the contents. Thermal expansion of the bolts is evaluated to ensure the containment boundary is maintained. Similarly, the cask body is evaluated for pressures associated with the fire accident; during the accident, the cask is assumed to be subjected to a fire that produces a surrounding environment of 800°C for a period of 30 minutes. The thermal evaluation of the hypothetical fire transient is presented Section in 3.4.

2.7.4.1 Summary of Pressures and Temperatures

Cask components temperatures under varying conditions are evaluated using the ANSYS finite element computer code [Ref. 28]. The cask cavity pressure is estimated based on the surface averaged temperature of the inner shell at the cavity side. The detail of the thermal analyses is documented in Chapter 3, Section 3.1. Table 3.1.3-1 presents the normal condition maximum temperature along with the maximum surface averaged temperature of inner shell surface at the cavity side. Chapter 3, Table 3.1.3-2 presents the maximum temperatures under hypothetical accident conditions along with the maximum surface averaged temperature of inner shell surface at the cavity side. The surface averaged temperature of the inner shell at the cavity side is used to predict the gas pressure inside the cask; Chapter 3, Table 3.1.4-1 summarizes the maximum NCT and HAC pressures.

2.7.4.2 Differential Thermal Expansion

For the RT-100 Cask, the closure bolts are the only components of concern during the fire accident that may experience thermal expansion. The bolting evaluation in Appendix 2.13 evaluates the effects of thermal expansion on the closure bolts.

2.7.4.3 Stress Calculations

The following Section evaluates the stresses in the bolts and cask body during hypothetical accident conditions.

2.7.4.3.1 Bolt stresses during fire accident

The bolt stress evaluation is presented in Appendix 2.13. The evaluation shows that the bolt stresses are less than the allowables. Therefore, the bolts continue to provide a tight seal and containment is maintained.

2.7.4.3.2 Pressure stress during fire accident

In accordance with the requirements of 10 CFR 71.73(c)(4), the RT-100 Cask is structurally evaluated when subjected to an accident internal pressure of 689.4 kPa (100 psia). The pressure is based upon an average cask temperature of 73.1°C. For conservatism, the stress intensity values are compared to allowable stress values at 150°C. To obtain pressure stress results, a uniform internal pressure is applied to the ANSYS finite element model.

2.7.4.4 Comparison with Allowable Stresses

The accident pressure stresses are presented in Table 2.7.4-1. The table documents the primary membrane (P_m), primary membrane and plus primary bending (P_m+P_b) stresses in accordance with the criteria presented in Regulatory Guide 7.6. As Table 2.7.4-1 shows, the margins of

safety are positive when compared to the stress intensity for each category. The most critically stressed component in the system is the inner lid; this condition is due to prying load at the interface of the closure bolt and lid. The minimum margin of safety is found to be +6.4 for primary membrane plus bending stress intensity. The margins of safety are all positive and thus, the RT-100 satisfies the requirements of 10CFR71.73(c)(4) for thermal HAC.

Table 2.7.4-1 HAC Pressure Stress Summary

Component and Stress State	Stress Location	ANSYS Results				RG 7.6 Allowable Stress	Margin of Safety (1)
		S1	S2	S3	SINT		
INNER SHELL		MPa	MPa	MPa	MPa	MPa	
Pm		1.2	0.0	-1.0	2.2	331	Large
Pm + Pb	<i>Inside</i>	1.2	0.0	-1.1	2.3	496	Large
	<i>Center</i>	1.2	0.0	-1.0	2.2	496	Large
	<i>Outside</i>	1.2	0.0	-0.9	2.1	496	Large
OUTER SHELL		MPa	MPa	MPa	MPa	MPa	
Pm		1.2	0.0	-0.7	1.9	331	Large
Pm + Pb	<i>Inside</i>	1.2	0.0	-0.7	2.0	496	Large
	<i>Center</i>	1.2	0.0	-0.7	1.9	496	Large
	<i>Outside</i>	1.2	0.0	-0.6	1.8	496	Large
FLANGE		MPa	MPa	MPa	MPa	MPa	
Pm		1.2	0.0	-0.4	1.6	331	Large
Pm + Pb	<i>Inside</i>	1.2	0.0	-0.5	1.7	496	Large
	<i>Center</i>	1.2	0.0	-0.4	1.6	496	Large
	<i>Outside</i>	1.2	0.0	-0.4	1.5	496	Large
OUTER LID		MPa	MPa	MPa	MPa	MPa	
Pm		1.1	0.1	-0.2	1.3	331	Large
Pm + Pb	<i>Inside</i>	1.1	0.1	-0.3	1.4	496	Large
	<i>Center</i>	1.1	0.1	-0.2	1.3	496	Large
	<i>Outside</i>	1.0	0.1	-0.2	1.2	496	Large
INNER LID		MPa	MPa	MPa	MPa	MPa	
Pm		0.2	-2.1	-36.5	36.7	331	Large
Pm + Pb	<i>Inside</i>	-2.1	-6.2	-64.0	61.9	496	Large
	<i>Center</i>	0.2	-2.1	-36.5	36.7	496	Large
	<i>Outside</i>	4.1	2.0	-10.6	14.7	496	Large

2.7.5 Immersion – Fissile Material

This Section is not applicable. The RT-100 does not have any fissile material subject to the requirements of 10 CFR 71.55 [Ref. 2].

2.7.6 Immersion – All Package

According to the requirements of 10 CFR 71.73(c)(6) [Ref.2], a package must be subjected to water pressure that is equivalent to: immersion under a head of water of at least 15 meters for a period of 8 hours. Also, 10 CFR 71.61 [Ref. 2] requires that a package's undamaged containment system be able to withstand an external water pressure of 2000 kPa for a period of not less than one hour without collapse, buckling or in-leakage of water. The outer lid is shown to be structurally adequate for a maximum external dynamic crush pressure of the top impact limiter. Therefore, the RT-100 satisfies all of the immersion requirements for a package that is used for the international shipment of radioactive materials.

2.7.7 Deep Water Immersion Test (for Type B Packages Containing More than 10^5 A₂)

This Section is not applicable. The RT-100 is limited to a maximum of 3000 A₂.

2.7.8 Summary of Damage

The analytical results reported in Section 2.7.1 through 2.7.7 indicate that the damage incurred by the RT-100 during the hypothetical accident is minimal, and such damage does not diminish the cask ability to maintain the containment boundary. A 9-meter drop or a 1-meter pin puncture accident may damage the outer shell and result in a localized reduction in shielding ability. However, the shielding remains intact to satisfy the accident shielding criteria. Based on the analyses of Section 2.7 through 2.7.7, the RT-100 fulfills the structural and shielding requirements of 10 CFR 71 [Ref. 2] for all of the hypothetical accident conditions.

2.8 Accident Conditions for Air Transport of Plutonium

This Section is not applicable. The RT-100 cask is not to be used to transport Plutonium by air transport.

2.9 Accident Conditions for Fissile Material Packages for Air Transport

This Section is not applicable. The RT-100 is limited by 10 CFR 71 [Ref. 2] for quantities of fissile material. However, the RT-100 is not used to transport any fissile material by air transport.

2.10 Special Form

This Section is not applicable. The RT-100 is not to be used to transport special form materials as specified in 10 CFR 71.75 [Ref. 2].

2.11 Fuel Rods

This Section is not applicable. The RT-100 is not to be used to transport fuel rods.

Proprietary Information Content Withheld Under 10 CFR 2.390(b)

Proprietary Information Content Withheld Under 10 CFR 2.390(b)

Proprietary Information Content Withheld Under 10 CFR 2.390(b)

Proprietary Information Content Withheld Under 10 CFR 2.390(b)

Proprietary Information Content Withheld Under 10 CFR 2.390(b)

Proprietary Information Content Withheld Under 10 CFR 2.390(b)

Proprietary Information Content Withheld Under 10 CFR 2.390(b)

Proprietary Information Content Withheld Under 10 CFR 2.390(b)

Proprietary Information Content Withheld Under 10 CFR 2.390(b)

Proprietary Information Content Withheld Under 10 CFR 2.390(b)

Proprietary Information Content Withheld Under 10 CFR 2.390(b)

Proprietary Information Content Withheld Under 10 CFR 2.390(b)

Proprietary Information Content Withheld Under 10 CFR 2.390(b)

Proprietary Information Content Withheld Under 10 CFR 2.390(b)

Proprietary Information Content Withheld Under 10 CFR 2.390(b)

Proprietary Information Content Withheld Under 10 CFR 2.390(b)

Proprietary Information Content Withheld Under 10 CFR 2.390(b)

Proprietary Information Content Withheld Under 10 CFR 2.390(b)

Proprietary Information Content Withheld Under 10 CFR 2.390(b)

Proprietary Information Content Withheld Under 10 CFR 2.390(b)

Proprietary Information Content Withheld Under 10 CFR 2.390(b)

Proprietary Information Content Withheld Under 10 CFR 2.390(b)

Proprietary Information Content Withheld Under 10 CFR 2.390(b)

Proprietary Information Content Withheld Under 10 CFR 2.390(b)

Proprietary Information Content Withheld Under 10 CFR 2.390(b)

Proprietary Information Content Withheld Under 10 CFR 2.390(b)

Proprietary Information Content Withheld Under 10 CFR 2.390(b)

Proprietary Information Content Withheld Under 10 CFR 2.390(b)

Proprietary Information Content Withheld Under 10 CFR 2.390(b)

Proprietary Information Content Withheld Under 10 CFR 2.390(b)

Proprietary Information Content Withheld Under 10 CFR 2.390(b)

Proprietary Information Content Withheld Under 10 CFR 2.390(b)

Proprietary Information Content Withheld Under 10 CFR 2.390(b)

Proprietary Information Content Withheld Under 10 CFR 2.390(b)

Proprietary Information Content Withheld Under 10 CFR 2.390(b)

Proprietary Information Content Withheld Under 10 CFR 2.390(b)

Proprietary Information Content Withheld Under 10 CFR 2.390(b)

Proprietary Information Content Withheld Under 10 CFR 2.390(b)

Proprietary Information Content Withheld Under 10 CFR 2.390(b)

Proprietary Information Content Withheld Under 10 CFR 2.390(b)

Proprietary Information Content Withheld Under 10 CFR 2.390(b)

Proprietary Information Content Withheld Under 10 CFR 2.390(b)

Proprietary Information Content Withheld Under 10 CFR 2.390(b)

Proprietary Information Content Withheld Under 10 CFR 2.390(b)

Proprietary Information Content Withheld Under 10 CFR 2.390(b)

Proprietary Information Content Withheld Under 10 CFR 2.390(b)

Proprietary Information Content Withheld Under 10 CFR 2.390(b)

Proprietary Information Content Withheld Under 10 CFR 2.390(b)

Proprietary Information Content Withheld Under 10 CFR 2.390(b)

Proprietary Information Content Withheld Under 10 CFR 2.390(b)

Proprietary Information Content Withheld Under 10 CFR 2.390(b)

Proprietary Information Content Withheld Under 10 CFR 2.390(b)

Proprietary Information Content Withheld Under 10 CFR 2.390(b)

RT-100 Safety Analysis Report, Rev. 7

Proprietary Information

Content Withheld

Under 10 CFR 2.390(b)

Proprietary Information Content Withheld Under 10 CFR 2.390(b)

Proprietary Information Content Withheld Under 10 CFR 2.390(b)

Proprietary Information Content Withheld Under 10 CFR 2.390(b)

2.13 Appendix – Closure Bolt Evaluation

The RT-100 package is designed with two sets of closure bolts: 18 M36 hex head bolts at the secondary lid and 32 M48 hex head bolts at the primary lid. These two sets of bolts are credited with maintaining positive closure of the package under all accident conditions. The purpose of this evaluation is to structurally qualify these bolts for the loadings associated with the normal conditions of transport and the hypothetical accident conditions.

2.13.1 Methodology

Bolt loadings under the various normal and accident conditions are determined in accordance with the recommendations of NUREG/CR-6007 [Ref.10]. Stresses resulting from these loads are compared with the design criteria in Section 2.1.2.2. Note that in many cases, calculations are made using exact values, not the rounded numbers shown in intermediate steps. In certain situations, the numbers displayed may not be capable of providing the exact final solution. Using the exact numbers, however, provides the most accurate solution possible. Calculation Package RTL-001-CALC-ST-0203, Rev. 6 [Ref. 60] provides additional information.

2.13.2 Loads

The following loads are evaluated in this section:

- Internal pressure loads
- Temperature loads
- Bolt preload
- Impact loads
- Puncture loads
- External pressure loads
- Gasket seating load

These loads are combined per NUREG/CR-6007 [Ref. 10] in Section 2.13.3.

2.13.2.1 Internal Pressure Loads

Per Table 4.3 of NUREG/CR-6007 [Ref. 10], the forces and moments generated under the internal pressure load are a tensile load F_{ap} , a shear load F_{sp} , a fixed edge closure force F_{fp} , and a fixed edge closure moment M_{fp} . These factors are evaluated for the primary and secondary lid bolts.

2.13.2.1.1 Internal Pressure Loads for Primary Lid Closure Bolts

The tensile force per bolt due to internal pressure, F_{ap} , is:

$$F_{ap} = \frac{\pi x D_{lg}^2 x (P_{li} - P_{lo})}{4 x N_b}$$

where,

$$\begin{aligned}
 D_{lg} &= \text{Outer Seal Diameter} \\
 &= 1835 \text{ mm} \\
 N_b &= \text{Number of Bolts} \\
 &= 32 \\
 P_{li} &= \text{Internal Pressure} \\
 &= 35 \text{ psi} = 241.3 \text{ kN/m}^2 \quad \text{use } 250 \text{ kN/m}^2 \quad (\text{Calc TH-102}) \\
 P_{lo} &= \text{External Pressure} \\
 &= 0 \text{ kN/m}^2 \quad (\text{conservative})
 \end{aligned}$$

Thus,

$$F_{ap} = \frac{(1.835)^2 \times (250 - 0)}{4 \times 32} = 20.7 \text{ kN/bolt}$$

The shear force per bolt due to internal pressure F_{sp} is:

$$F_{sp} = \frac{\pi \times E_t \times t_t \times (P_{li} - P_{lo}) \times D_{lb}^2}{2 \times N_b \times E_c \times t_c \times (1 - N_{ul})}$$

where,

$$\begin{aligned}
 E_l &= \text{Primary Lid Material Elastic Modulus, it means the} \\
 &\quad (\text{SA 240 TYP304/304L}) \\
 &= 195 \text{ GPa at } 20^\circ \text{ C} \quad (\text{Table 2.2.1-1}) \\
 D_{lb} &= \text{Primary Lid Bolt Circle Diameter} \\
 &= 1920 \text{ mm} \\
 N_{ul} &= \text{Primary Lid Material Poisson's} \\
 &\quad \text{Ratio, (SA 240 TYPE 304/304L)} \\
 &= 0.31 \quad (\text{Table 2.2.1-2}) \\
 E_c &= \text{Cask Material Elastic Modulus,} \\
 &\quad (\text{SA 240 TYPE 304/304L}) \\
 &= 195 \text{ GPa at } 20^\circ \text{ C} \quad (\text{Table 2.2.1-1}) \\
 t_l &= \text{Primary Lid Thickness} \\
 &= 210 \text{ mm} \\
 t_c &= \text{Cask Wall Thickness} \\
 &= 65 \text{ mm (neglecting lead)}
 \end{aligned}$$

The remaining terms are as previously defined. However, this expression for shear force does not apply to the RT-100 cask design because the *maximum* gap between the lid and cask body (4 mm = 1741 – 1737) per RT100 PE 1001-1 Rev. H, Detail 1, Chapter 1, Appendix 1.4, Attachment 1.4-2) is less than the *minimum* gap between the bolt clearance holes and bolt shank (5.5 mm = 52.5- 47) per RT100 PE 1001-1 Rev. H (Chapter1, Appendix 1.4, Attachment 1.4-2) and Machinery's Handbook [Ref. 27]). Thus, the RT-100 primary lid bolts are not subjected to any shear loads. Therefore,

$$F_{sp} = 0.0 \text{ kN/bolt.}$$

The fixed edge closure force F_{fp} and moment M_{fp} are:

$$F_{fp} = \frac{D_{lb} \times (P_{li} - P_{lo})}{4} = \frac{1.920 \times (250 - 0)}{4} = 120.0 \text{ kN/m}$$

and,

$$M_{fp} = \frac{(P_{li} - P_{lo}) \times D_{lb}^2}{32} = \frac{(250 - 0) \times 1.920^2}{32} = 28.8 \text{ kN-m/m}$$

2.13.2.1.2 Internal Pressure Load for Secondary Lid Closure Bolts

The secondary lid closure bolt forces and moments are determined using the same methodology as shown for the primary lid bolts (Section 2.13.2.1.1), except that the secondary lid features are incorporated.

The tensile force per bolt due to internal pressure F_{as} is:

$$F_{as} = \frac{\pi \times D_{lg}^2 \times (P_{li} - P_{lo})}{4 \times N_b}$$

where,

$$\begin{aligned} D_{lg} &= \text{Outer Seal Diameter} \\ &= 850 \text{ mm} \\ N_b &= \text{Number of Bolts} \\ &= 18 \\ P_{li} &= \text{Internal Pressure} \\ &= 35 \text{ psi} = 241.3 \text{ kN/m}^2 \text{ use } 250 \text{ kN/m}^2 \text{ [Ref. 38]} \\ P_{lo} &= \text{External Pressure} \\ &= 0 \text{ kN/m}^2 \text{ (conservative)} \end{aligned}$$

Thus,

$$\begin{aligned} F_{as} &= \frac{\pi \times (0.850)^2 \times (250 - 0)}{4 \times 18} \\ &= 7.9 \text{ kN/bolt} \end{aligned}$$

The *maximum* gap between the lid and cask body (just 4 mm = 748 – 744) is less than the *minimum* gap between the bolt clearance holes and bolt shank (5.5 mm = 40.5- 35). As with the primary lid (Section 2.13.2.1.1), the shear force per bolt due to internal pressure F_{ss} is:

$$F_{ss} = 0.0 \text{ kN/bolt.}$$

The fixed edge closure force F_{fs} and moment M_{fs} are:

$$F_{fs} = \frac{D_{lb} \times (P_{li} - P_{lo})}{4}$$

and,

$$M_{fs} = \frac{(P_{li} - P_{lo}) \times D_{lb}^2}{32}$$

where, D_{lb} = Secondary Lid Bolt Diameter
= 926 mm

All other terms are previously defined. Thus,

$$F_{fs} = \frac{D_{lb} \times (P_{li} - P_{lo})}{4} = \frac{0.926 \times (250 - 0)}{4} = 57.9 \text{ kN/m}$$

and,

$$M_{fs} = \frac{(P_{li} - P_{lo}) \times D_{lb}^2}{32} = \frac{(250 - 0) \times 0.926^2}{32} = 6.7 \text{ kN-m/m}$$

2.13.2.2 Temperature Loads

Temperature differentials and/or differences in the thermal-expansion coefficients of the joint components induce bolt loads. These forces are evaluated Per Table 4.4 of NUREG/CR-6007, [Ref. 10].

2.13.2.2.1 Temperature Loads for Primary Lid Closure Bolts

The tensile force per bolt due to temperature F_{atp} is:

$$F_{atp} = 0.25 \times \pi \times D_b \times E_b \times (\alpha_l \times T_l - \alpha_b \times T_b)$$

where,

D_b = Nominal Bolt diameter
= 48 mm
 E_b = Bolt Material Elastic Modulus,
(SA 354 Grade BD)
= 202 GPa at 20° C (Table 2.2.1-1)

$$\begin{aligned}
 \alpha_l &= \text{Primary Lid Material Coefficient of Thermal Expansion} \\
 &= 16.6 \times 10^{-6} \text{ m/m/}^\circ\text{C} \quad (\text{Table 2.2.1-1}) \\
 \alpha_b &= \text{Bolt Material Coefficient of Thermal Expansion} \\
 &= 11.5 \times 10^{-6} \text{ m/m/}^\circ\text{C} \quad (\text{Table 2.2.1-1}) \\
 T_l &= \text{Maximum Primary Lid Temperature} \\
 &\quad \text{under NCT conditions} \\
 &= 71^\circ\text{C (conservatively use } 100^\circ\text{C)} \quad (\text{Table 3.1.3-1}) \\
 T_b &= \text{Minimum Bolt Temperature} \\
 &\quad \text{under NCT conditions} \\
 &= -20^\circ\text{C} \quad (10 \text{ CFR } 71.71 [\text{Ref. 2}])
 \end{aligned}$$

Thus,

$$\begin{aligned}
 F_{atp} &= 0.25 \times \pi \times 0.048^2 \times 202 \times 10^6 \times (16.6 \times 10^{-6} \times 100 - 11.5 \times 10^{-6} \times -20) \\
 &= 690.9 \text{ kN/bolt}
 \end{aligned}$$

Shear force per bolt due to temperature F_{stp} is considered zero because the clamped components (primary lid and cask forged ring) have essentially the same temperature.

2.13.2.2.2 Temperature Loads for Secondary Lid Closure Bolts

The secondary lid closure bolt forces are determined using the same methodology as shown for the primary lid bolts (Section 2.13.2.2.1) and incorporating the secondary lid geometry, material properties and temperatures. Only the bolt diameter in the previous equation must be changed since the primary and secondary lids are constructed of the same materials and experience essentially the same temperature. The secondary bolt diameter is 36 mm. Thus, the tensile force per unit bolt due to temperature F_{stl} is:

$$\begin{aligned}
 F_{atl} &= 0.25 \times \pi \times 0.036^2 \times 202 \times 10^6 \times (16.6 \times 10^{-6} \times 100 - 11.5 \times 10^{-6} \times -20) \\
 &= 388.6 \text{ kN/bolt}
 \end{aligned}$$

As with the primary lid, the shear force per bolt due to temperature F_{sts} is considered zero since the clamped components (primary and secondary lids) have essentially the same temperature.

2.13.2.3 Bolt Preloads

Tightening torques for the primary and secondary lid bolts are respectively, 850 N-m +/-10 % and 350 +/-10 % per Chapter 7, Table 7.4.5-1. The method of analysis is described in Table 4.1 of NUREG/CR-6007 [Ref.10].

2.13.2.3.1 Bolt Preload for Primary Lid Closure Bolts

The primary lid bolt preload F_{pl} is determined as follows (Table 4.1 of NUREG/CR-6007 [Ref. 10]):

$$F_{pl} = \frac{T}{K_L \times D_b}$$

$$\begin{aligned}
 D_b &= \text{Nominal Bolt diameter} \\
 &= 48 \text{ mm} \\
 K &= \text{Nut Factor for empirical relation between} \\
 &\quad \text{applied torque and the achieved preload} \\
 &= 0.15 \text{ (lubricated) minimum (EPRI Good} \\
 &\quad \text{0.30 (dry) maximum (Bolting Practices)} \\
 T &= \text{Applied Torque} \\
 &= 850 \text{ N-m } \pm 10\%
 \end{aligned}$$

To determine maximum preload F_{plmax} for the primary lid bolts, minimum nut factor, K , of 0.15 (lubricated) and maximum tightening torque of 940 N-m (conservatively bounds the 850 N-m +10% maximum):

$$\begin{aligned}
 F_{pl} &= \frac{T}{K_L \times D_b} = \frac{940}{0.15 \times 0.048} \times \frac{1 \text{ kN}}{1000 \text{ N}} \\
 &= 130.6 \text{ kN}
 \end{aligned}$$

The residual torsion moment M_{rl} is:

$$\begin{aligned}
 M_{rl} &= 0.5 \times T_{max} = 0.5 \times 940 \\
 &= 470 \text{ N-m}
 \end{aligned}$$

The residual tensile bolt force F_{arl} is

$$F_{arl} = F_{plmax} = 130.6 \text{ kN}$$

2.13.2.3.2 Bolt Preload for Secondary Lid Closure Bolts

The maximum secondary lid bolt preload F_{psmax} is determined in a manner similar to the primary bolt lids (Section 2.13.2.3.1). Thus,

$$F_{pl} = \frac{T}{K_L \times D_b}$$

where,

$$\begin{aligned}
 D_b &= \text{Nominal Bolt diameter} \\
 &= 36 \text{ mm} \\
 T &= \text{Applied Torque} \\
 &= 350 \text{ N-m } \pm 10\%
 \end{aligned}$$

Other terms are as previously defined. The maximum preload F_{psmax} for the secondary lid bolts is obtained by using a nut factor K of 0.15 (lubricated) and a tightening torque of 390 N-m (conservatively bounding the 350 N-m+10% maximum).

$$F_{psmax} = \frac{T_{max}}{K_L \times D_b} = \frac{390}{0.15 \times 36} = 72.2 \text{ kN}$$

The residual tensile bolt force M_{rs} is:

$$M_{rs} = 0.5 \times T_{max} = 0.5 \times 390 = 195.0 \text{ N-m}$$

The residual tensile bolt force F_{ars} is

$$F_{ars} = F_{psmax} = 72.2 \text{ kN}$$

2.13.2.4 Impact Loads

Maximum tension and shear loads in the closure bolts due to the regulatory impact drops are evaluated in accordance with NUREG/CR-6007 [Ref. 10]. Using the NUREG terminology, the primary lid bolts are evaluated as closure bolts for an *unprotected* lid, and the secondary bolts are evaluated as components of a *protected* lid. This approach means the primary bolt evaluation includes the impact or inertial forces of the entire cask; the secondary lid bolts are evaluated only for the forces due to the inertia of the secondary lid.

2.13.2.4.1 Dynamic Load Factors

Drop impact loadings are generally considered triangular or half-sine loadings; NUREG/CR-3966 [Ref. 17] presents dynamic load factor (DLF) charts for either pulse shape. For this analysis, results are compared and loading with the higher DLF is utilized.

Dynamic load factors for triangular and half sine loadings are shown in Figures 2.3 and Figure 2.15 of NUREG/CR-3966 [Ref. 17]. This information is presented as graphs where the DLF is the ordinate and t_d/T is the abscissa. The latter quantity t_d/T is the ratio of the impact duration t_d and the natural period of the impacting object T .

The period of the lids T is considered for bolt closure analyses. T is determined by the lid's lowest mode frequency.

Dynamic Load Factors for Primary Lid Closure Bolts

To determine the primary lid frequency, the primary lid and secondary lid are considered a single simply-supported flat circular plate. Thus, (Table 36, Case 11a of "Roark's Formulas for Stress and Strain" [Ref. 29]):

Resonant Frequency of Primary Lid (with secondary lid attached):

$$f_l = \frac{4.99}{2\pi} \sqrt{\frac{D g_c}{w r^4}}$$

where,

$$\begin{aligned} D &= \text{Lid Flexural Rigidity} \\ &= \frac{E_1 t_1^3}{12(1 - \nu_1^2)} \\ g_c &= \text{conversion factor} \\ &= 1000 \text{ kg-mm/s}^2\text{-N} \\ w &= \text{weight per unit area} \\ r &= \text{lid bolt radius} \\ &= D_{lb}/2 \\ &= 960 \text{ mm} \end{aligned}$$

RT100 PE 1001-1, Rev. H Appendix 1.4, the primary lid weighs 3648 kg and the secondary lid weighs 857 kg. Thus,

$$\begin{aligned} W &= \frac{(3648 + 857)}{\pi \cdot 960^2} \\ &= 0.001556 \text{ kg/mm}^2 \end{aligned}$$

D may be determined from previously defined values:

$$\begin{aligned} D &= \frac{195 \times 10^3 \times 210^3}{12 \times (1 - 0.31^2)} \\ &= 1.665 \times 10^{11} \text{ N-mm} \end{aligned}$$

The frequency of the primary lid (with attached secondary lid) is:

$$\begin{aligned} f_l &= 0.7942 \times \sqrt{\frac{1.665 \times 10^{11} \times 1000}{0.001556 \times 960^4}} \\ &= 282 \text{ Hz} \end{aligned}$$

The period of the primary lid is equal to $1/f_l$, or $T = 1/282 = 0.00354$ s. Impact durations for the NCT and HAC impacts range from 0.012 s to 0.045 s (RTL-001-CALC-ST-0401, Rev. 6 [Ref.40]). Thus, the smallest value of the ratio t_d/T is 3.389 and the largest is 12.71. With these values, the maximum DLF is determined from Figures 2.3 and 2.15 (NUREG/CR-3966 [Ref.17]) to be less than 1.15. Thus, it is concluded that the DLF for the primary lid bolts may be conservatively bounded by a value of 1.15 for both NCT and HAC drops.

Dynamic Load Factors for Secondary Lid Closure Bolts

To determine the secondary lid frequency, the secondary lid is considered a simply-supported flat circular plate. Thus, (Table 36, Case 11a of “Roark’s Formulas for Stress and Strain” [Ref. 29]):

Resonant Frequency of Secondary Lid:

$$f_l = 0.7942 \sqrt{\frac{D g_c}{w r^4}}$$

where,

$$\begin{aligned} D &= \text{Lid Flexural Rigidity} \\ &= \frac{E_1 t_1^3}{12(1 - \nu_1^2)} \\ g_c &= \text{conversion factor} \\ &= 1000 \text{ kg-mm/s}^2\text{-N} \\ w &= \text{weight per unit area} \\ r &= \text{lid bolt radius} \\ &= D_{lb}/2 \\ &= 463 \text{ mm} \end{aligned}$$

The secondary lid weighs 857 kg. Furthermore,

$$\begin{aligned} E_1 &= \text{Secondary Lid Material Elastic Modulus, (SA 240 TYPE 304/304L)} \\ &= 195 \text{ GPa at } 20^\circ \text{ C} \quad (\text{Table 2.2.1-1}) \\ D_{lb} &= \text{Secondary Lid Bolt Circle Diameter} \\ &= 926 \text{ mm} \\ \nu_{ul} &= \text{Secondary Lid Material Poisson’s Ratio, (SA 240 TYPE 304/304L)} \\ &= 0.31 \quad (\text{Table 2.2.1-2}) \\ t_1 &= \text{Secondary Lid Thickness} \\ &= 110 \text{ mm (stainless steel only)} \end{aligned}$$

Thus,

$$\begin{aligned} w &= \frac{857}{\pi \cdot 463^2} \\ &= 0.001272 \text{ kg/mm}^2 \end{aligned}$$

D may be determined from previously defined values:

$$D = \frac{195 \times 10^3 \times 110^3}{12 \times (1 - 0.31^2)}$$

$$= 2.395 \times 10^{10} \text{ N-mm}$$

The frequency of the secondary lid is:

$$f_l = 0.7942 \times \sqrt{\frac{2.395 \times 10^{10} \times 1000}{0.001272 \times 463^4}}$$

$$= 508 \text{ Hz}$$

The period of the secondary lid is equal to $1/f_l$, or $T = 1/508 = 0.00197$ s. Impact durations for the NCT and HAC impacts range from 0.012 s to 0.045 s (RTL-001-CALC-ST-0401, Rev. 6 [Ref.40]). Thus, the value of t_d/T is 4.6 or more. With this value, the maximum DLF can be determined from Figures 2.3 and 2.15 (NUREG/CR-6007 [Ref. 10]) to be approaching unity. For consistency with the primary lid bolt analyses, the DLF for the secondary lid bolts is set conservatively to 1.15 for both NCT and HAC drops.

2.13.2.4.2 End Drop Loads

The following subsections detail calculations for the end drop load.

2.13.2.4.2.1 Primary Lid Bolts

Impact loads in the primary lid bolts due to an end drop are determined using the formulas for evaluating bolt forces/moments generated by impact load applied to an unprotected closure in Table 4.5 of NUREG/CR-6007 [Ref. 10]. An acceleration of 125 g is used in this analysis (which bounds the 123 g maximum reported in Section 2.12.4.1).

The non-prying tensile bolt force per primary lid bolt F_{tp} is:

$$F_{tp} = \frac{1.34 \sin(x_i) DLF a_i (W_L + W_c) g}{N_b}$$

where,

x_i	=	End Drop Impact Angle
	=	90°
DLF	=	1.15 (Section 2.13.2.4.1)
a_i	=	Maximum Impact Acceleration
	=	123 g (use 125 g) [Ref. 40]
W_L	=	Closure Lid Weight
	=	3648 kg (use 3650 kg)
W_c	=	Cask Payload Weight
	=	6804 kg (use 7000kg)
N_b	=	Number of Bolts

$$= 32$$

Thus,

$$F_{tp} = \frac{1.34 \times \sin(90.0) \times 1.15 \times 125 \times (3650 + 7000) \times 9.81}{32} \times \frac{1 \text{ kN}}{1000 \text{ N}}$$

$$= 628.9 \text{ kN/bolt}$$

As discussed in Section 2.13.2.1.1, the RT-100 primary lid bolts are not subjected to any shear loads. Thus,

$$F_{sp} = 0.0 \text{ kN/bolt.}$$

The fixed edge closure lid force F_f is:

$$F_f = \frac{1.34 \times \sin(x_i) \times DLF \times a_i \times (W_L + W_c) \times g}{\pi \times D_{lb}}$$

where,

$$D_{lb} = \text{Primary Lid Bolt Diameter}$$

$$= 1920 \text{ mm}$$

The remaining terms are as previously defined. Thus,

$$F_f = \frac{1.34 \times \sin(90.0) \times 1.15 \times 125 \times (3650 + 7000) \times 9.81}{\pi \times 1.920} \times \frac{1 \text{ kN}}{1000 \text{ N}}$$

$$= 3336.4 \text{ kN/m}$$

The fixed edge closure lid moment M_f is:

$$M_f = \frac{1.34 \times \sin(x_i) \times DLF \times a_i \times (W_L + W_c) \times g}{\pi \times 8}$$

All other terms are as previously defined. Thus,

$$M_f = \frac{1.34 \times \sin(90.0) \times 1.15 \times 125 \times (3650 + 7000) \times 9.81}{\pi \times 8} \times \frac{1 \text{ kN}}{1000 \text{ N}}$$

$$= 800.7 \text{ kN-m/m}$$

The additional tensile bolt force per bolt F_{tp} caused by the prying action of the primary lid is (Table 2.1 of NUREG/CR-6007 [Ref. 10]):

$$F_{tp} = \left(\frac{\pi \times D_{lb}}{N_b} \right) \times \left[\frac{\frac{2 \times M_f}{D_{lo} - D_{lb}} - C1 \times (B - F_f) - C2 \times (B - P)}{C1 + C2} \right]$$

where,

P = Bolt Preload per unit Length of Bolt Circle

$$= F_{plmax} \times \frac{N_b}{\pi \times D_{lb}} B$$

= Non-prying Tensile Bolt Force

= MAX(F_f , P)

C1 = Force Constant

= 1.0

C2 = Second Force Constant

$$= \left(\frac{8}{3 \times (D_{lo} - D_{lb})^2} \right) \times \left[\frac{E_l \times t_l^3}{1 - N_{ul}} + \frac{(D_{lo} - D_{li}) \times E_{lf} \times t_{lf}^3}{D_{lb}} \right] \\ \times \left(\frac{L_b}{N_b \times D_b^2 \times E_b} \right)$$

D_{lo} = Closure Lid Diameter at Outer Edge

= 2016 mm

D_{li} = Closure Lid Diameter at Inner Edge

= 1730 mm

t_{lf} = Closure Lid Flange Thickness

= 120 mm

E_{lf} = Primary Lid Flange Material Elastic Modulus,
(SA 240 TYPE 304/304L)

L_b = Bolt length between the top and bottom surfaces of the closure lid
at the bolt circle

= 67 mm

Other terms are as previously defined. Thus,

$$C2 = \left(\frac{8}{3 \times (D_{lo} - D_{lb})^2} \right) \times \left[\frac{E_l \times t_l^3}{1 - N_{ul}} + \frac{(D_{lo} - D_{li}) \times E_{lf} \times t_{lf}^3}{D_{lb}} \right] \times \left(\frac{L_b}{N_b \times D_b^2 \times E_b} \right)$$

$$C2 = \left(\frac{8}{3 \times (2.016 - 1.920)^2} \right) \\ \times \left[\frac{195 \times 10^6 \times 0.210^3}{1 - 0.31} + \frac{(2.016 - 1.730) \times 195 \times 10^6 \times 0.120^3}{1.920} \right] \\ \times \left(\frac{0.067}{32 \times 0.048^2 \times 202 \times 10^6} \right)$$

$$C2 = 3.47$$

$$P = \frac{130.6 \times \frac{32}{\pi \times 1.920}}{1}$$

$$= 692.9 \text{ kN/m}$$

and

$$F_{tp} = \left(\frac{\pi \times 1.920}{32} \right) \times \left[\frac{2 \times 800.7}{2.016 - 1.920} - 1 \times (3336.4 - 3336.4) - 3.47 \times (3336.4 - 692.9) \right] \frac{1}{1 + 3.47}$$

$$= 316.2 \text{ kN/bolt}$$

The total tension force F_a is

$$F_a = F_t + F_{tp}$$

$$= 628.9 + 316.2$$

$$= 945.1 \text{ kN/bolt}$$

The shear force F_s is 0.

The maximum bending moment generated by the applied loads M_{bb} is:

$$M_{bb} = \left(\frac{\pi \times D_{lb}}{N_b} \right) \times \left(\frac{Kb}{Kb + K1} \right) \times Mf$$

where,

$$Kb = \left(\frac{N_b}{L_b} \right) \times \left(\frac{E_b}{D_{lb}} \right) \times \left(\frac{D_b^4}{64} \right)$$

$$= \left(\frac{32}{0.067} \right) \times \left(\frac{202 \times 10^6}{1.920} \right) \times \left(\frac{0.048^4}{64} \right)$$

$$= 4,167 \text{ kN}$$

$$K1 = \frac{E_l \times t_l^3}{3 \times \left[(1 - N_{ul}^2) + (1 - N_{ul})^2 \times \left(\frac{D_{lb}}{D_{lo}} \right)^2 \right] \times D_{lb}}$$

$$= \frac{195 \times 10^6 \times 0.210^3}{3 \times \left[(1 - 0.31^2) + (1 - 0.31)^2 \times \left(\frac{1.920}{2.016} \right)^2 \right] \times 1.920}$$

$$= 234,719 \text{ kN}$$

Thus,

$$M_{bb} = \left(\frac{\pi \times D_{lb}}{N_b} \right) \times \left(\frac{Kb}{Kb + Kl} \right) \times Mf$$

$$= \left(\frac{\pi \times 1.920}{32} \right) \times \left(\frac{4167}{4167 + 234719} \right) \times 800.7$$

$$= 2.6 \text{ kN-m}$$

2.13.2.4.2.2 Secondary Lid Bolts

Impact loads in the secondary lid bolts due to an end drop are determined similarly as for the primary lid bolts in Section 2.13.2.4.2.1.

The non-prying tensile bolt force per secondary lid bolt F_{ts} is:

$$F_{ts} = \frac{1.34 \times \sin(x_i) \times DLF \times a_i \times (W_L + W_{cs}) \times g}{N_b}$$

where,

$$\begin{aligned} x_i &= \text{End Drop Impact Angle} \\ &= 90^\circ \\ DLF &= 1.15 \quad (\text{Section 2.13.2.4.1}) \\ a_i &= \text{Maximum Impact Acceleration} \\ &= 123 \text{ g} \quad (\text{use } 125 \text{ g}) \quad [\text{Ref. 40}] \\ W_L &= \text{Closure Lid Weight} \\ &= 857 \text{ kg} \quad (\text{use } 860 \text{ kg}) \\ W_{cs} &= \text{Payload Weight borne by Secondary Lid} \\ N_b &= \text{Number of Bolts} \\ &= 18 \end{aligned}$$

Since the payload weight is assumed to be evenly distributed across both the primary and secondary lids, the weight borne by the secondary lid can be obtained by multiplying the payload weight by the ratio of areas, i.e.,

$$W_{cs} = \frac{A_s}{A_p} \times W_c = \left(\frac{D_s}{D_p} \right)^2 \times W_c$$

$$= \left(\frac{0.785}{3.192} \right) \times 7000$$

$$= 1674 \text{ kg}$$

Thus,

$$F_{ts} = \frac{1.34 \times \sin(90.0) \times 1.15 \times 125 \times (860 + 1674) \times 9.81}{18} \times \frac{1 \text{ kN}}{1000 \text{ N}}$$

$$= 266.0 \text{ kN/bolt}$$

As discussed in Section 2.13.2.1.1.2, the RT-100 secondary lid bolts are not subjected to any shear loads. Thus,

$$F_s = 0.0 \text{ kN/bolt}$$

The fixed edge closure lid force F_f is:

$$F_f = \frac{1.34 \times \sin(x_i) \times DLF \times a_i \times (W_L + W_{cs}) \times g}{\pi \times D_{lb}}$$

where,

$$D_{lb} = \text{Secondary Lid Bolt Diameter}$$

$$= 926 \text{ mm}$$

The remaining terms are as previously defined. Thus,

$$F_f = \frac{1.34 \times \sin(90.0) \times 1.15 \times 125 \times (860 + 1674) \times 9.81}{\pi \times 0.926} \times \frac{1 \text{ kN}}{1000 \text{ N}}$$

$$= 1646.1 \text{ kN/m}$$

The fixed edge closure lid moment M_f is:

$$M_f = \frac{1.34 \times \sin(x_i) \times DLF \times a_i \times (W_L + W_{cs}) \times g}{\pi \times 8}$$

where all terms are as previously defined. Thus,

$$M_f = \frac{1.34 \times \sin(90.0) \times 1.15 \times 125 \times (860 + 1674) \times 9.81}{\pi \times 8} \times \frac{1 \text{ kN}}{1000 \text{ N}}$$

$$= 190.5 \text{ kN-m/m}$$

The additional tensile bolt force per bolt F_{tp} caused by the prying action of the secondary lid is (Table 2.1 of NUREG/CR-6007 [Ref. 10]):

$$F_{tp} = \left(\frac{\pi \times D_{lb}}{N_b} \right) \times \left[\frac{\frac{2 \times M_f}{D_{lo} - D_{lb}} - C1 \times (B - F_f) - C2 \times (B - P)}{C1 + C2} \right]$$

$$= 173.5 \text{ kN/bolt}$$

where,

P = Bolt Preload per unit Length of Bolt Circle

$$= F_{plmax} \times \frac{N_b}{\pi \times D_{lb}} = 72.2 \times \frac{18}{\pi \times 0.926}$$

$$= 446.7 \text{ kN/m}$$

B = Non-prying Tensile Bolt Force

$$= \text{MAX}(F_f, P)$$

C1 = Force Constant

$$= 1.0$$

C2 = Second Force Constant

$$= \left(\frac{8}{3 \times (D_{lo} - D_{lb})^2} \right) \times \left[\frac{E_l \times t_l^3}{1 - N_{ul}} + \frac{(D_{lo} - D_{li}) \times E_{lf} \times t_{lf}^3}{D_{lb}} \right]$$

$$\times \left(\frac{L_b}{N_b \times D_b^2 \times E_b} \right)$$

$$= 1.79$$

D_{lo} = Closure Lid Diameter at Outer Edge

$$= 1000 \text{ mm}$$

D_{li} = Closure Lid Diameter at Inner Edge

$$= 745 \text{ mm}$$

t_{lf} = Closure Lid Flange Thickness

$$= 80 \text{ mm}$$

E_{lf} = Secondary Lid Flange Material Elastic Modulus,
(SA 240 TYPE 304/304L)

$$= 195 \text{ GPa at } 20^\circ\text{C} \quad (\text{Table 2.2.1-1})$$

L_b = Bolt length between the top and bottom surfaces of the
Closure lid at the bolt circle

$$= 43 \text{ mm}$$

The total tension force of F_a is:

$$\begin{aligned}
 F_a &= F_t + F_{tp} \\
 &= 266.0 + 173.5 \\
 &= 439.5 \text{ kN/bolt}
 \end{aligned}$$

The shear force F_s is 0.

The maximum bending moment generated by the applied loads M_{bb} is (Table 2.2 NUREG/CR-6007 [Ref. 10]):

$$\begin{aligned}
 M_{bb} &= \left(\frac{\pi \times D_{lb}}{N_b} \right) \times \left(\frac{Kb}{Kb + K1} \right) \times Mf \\
 Kb &= \left(\frac{N_b}{L_b} \right) \times \left(\frac{E_b}{D_{lb}} \right) \times \left(\frac{D_b^4}{64} \right) \\
 &= \left(\frac{18}{0.043} \right) \times \left(\frac{202 \times 10^6}{0.926} \right) \times \left(\frac{0.036^4}{64} \right) \\
 &= 2,396.5 \text{ kN} \\
 K1 &= \frac{E_l \times t_l^3}{3 \times \left[(1 - N_{ul}^2) + (1 - N_{ul})^2 \times \left(\frac{D_{lb}}{D_{lo}} \right)^2 \right] \times D_{lb}} \\
 &= \frac{195 \times 10^6 \times 0.110^3}{3 \times \left[(1 - 0.31^2) + (1 - 0.31)^2 \times \left(\frac{0.926}{1.000} \right)^2 \right] \times 0.926} \\
 &= 71,203 \text{ kN}
 \end{aligned}$$

Thus,

$$\begin{aligned}
 M_{bb} &= \left(\frac{\pi \times D_{lb}}{N_b} \right) \times \left(\frac{Kb}{Kb + K1} \right) \times Mf \\
 &= \left(\frac{\pi \times 0.926}{18} \right) \times \left(\frac{2.40}{2.40 + 71.20} \right) \times 190.5 \\
 &= 1.0 \text{ kN-m}
 \end{aligned}$$

2.13.2.4.3 Corner Drop Evaluations

The closure bolt evaluations for the corner drop impact are conducted very similarly to the end drop analyses in Section 2.13.2.1.2. The cask body acceleration is changed and the impact angle

x_i is set equal to 52.5° (corresponding to a 37.5° angle between cask axis and vertical line).

Additionally, an acceleration of 120 g is used in this analysis (which bounds the 116 g maximum reported in Section 2.12.4.1). Results are summarized in Table 2.13.2-1.

Table 2.13.2-1 Closure Bolt Loads for 9.0 m Corner-Drop

BOLT/LOCATION	Non-Prying Tensile Force, F_t (kN/bolt)	Prying Force, F_{tp} (kN/m)	Bending Moment, M_{bb} (kN-m/bolt)	Shear Force, F_s (kN/bolt)
M48x170 Bolts /Primary Lid	479.0	265.0	2.0	0.0
M36x120 Bolts /Secondary Lid	211.4	147.4	0.8	0.0

2.13.2.4.4 Side Drop Evaluations

As shown in Sections 2.13.2.1.1 and 2.13.2.1.2, the gap between the cask body and the primary and second lids is smaller than the gap between the bolts and the bolt clearance holes. Therefore, no shear load is imparted to the bolts from the cask body. Since the side impact drop primarily generates shear loads with respect to the bolts, the primary and secondary closure lid bolts do not receive any significant loading from the side impact drop and are acceptable with respect to the end and corner impact drop.

2.13.2.5 Puncture Loads

This section evaluates the results of the various puncture loads.

2.13.2.5.1 End Puncture

Puncture loads in the primary and secondary closure lid bolts due to a puncture are determined using the formulas for evaluating bolt forces/moments in Table 4.7 of NUREG/CR-6007 [Ref. 10].

2.13.2.5.1.1 Primary Lid Bolts

The non-prying tensile bolt force per primary lid bolt F_{tp} is:

$$F_{tp} = \frac{\sin(x_i) \times P_{un}}{N_b}$$

where,

$$\begin{aligned}
 x_i &= \text{End Drop Impact Angle} \\
 &= 90^\circ \\
 P_{un} &= \text{MIN}(P_{un1}, P_{un2}) \\
 N_b &= \text{Number of Bolts} \\
 &= 32
 \end{aligned}$$

The term P_{un} is the maximum impact force that can be generated by puncture pin during a normal impact. It is the smaller of:

$$P_{un1} = 0.75 \times \pi \times D_{pb}^2 \times S_{yl}$$

$$P_{un2} = 0.6 \times \pi \times D_{pb} \times t_l \times S_{ul}$$

where,

$$D_{pb} = \text{Puncture bar diameter}$$

$$= 150 \text{ mm} \quad (10 \text{ CFR } 71.73 \text{ (c)(3) [Ref. 2]})$$

$$t_l = \text{Closure Lid Thickness}$$

$$= 110 \text{ mm}$$

$$\text{(the secondary lid thickness neglecting the lead)}$$

$$S_{yl} = \text{Yield Strength of Closure Lid Material}$$

$$\text{(SA 240 304L)}$$

$$= 172 \text{ MPa at } 20^\circ\text{C} \quad (\text{Table 2.2.1-1})$$

$$S_{ul} = \text{Ultimate Strength of Closure Lid Material}$$

$$\text{(SA 240 304L)}$$

$$= 483 \text{ MPa at } 20^\circ\text{C} \quad (\text{Table 2.2.1-1})$$

thus,

$$P_{un1} = 0.75 \times \pi \times 0.150^2 \times 172000$$

$$= 9,118.5 \text{ kN}$$

$$P_{un2} = 0.6 \times \pi \times 0.150 \times 0.110 \times 483000$$

$$= 15,022 \text{ kN}$$

$$P_{un} = \text{MIN} (9118.5, 15022 \text{ kN})$$

$$= 9,118.5 \text{ kN}$$

and,

$$F_{tp} = \frac{\sin(90) \times 9118.5}{32}$$

$$= 285.0 \text{ kN/bolt.}$$

As shown in Sections 2.13.2.1.1 and 2.13.2.1.2, the design of the primary and secondary lids prevents shear loads from being applied to the bolts. Thus,

$$F_{sp} = 0$$

It is noted that the equation given for F_{sp} in NUREG/CR6007 [Ref. 10] also shows $F_{sp} = 0$.

The fixed edge closure lid force F_f is:

$$F_f = \frac{\sin(x_i) \times P_{un}}{\pi \times D_{lb}}$$

where,

$$\begin{aligned} D_{lb} &= \text{Primary Lid Bolt Circle Diameter} \\ &= 1920 \text{ mm} \end{aligned}$$

The remaining terms are as previously defined. Thus,

$$\begin{aligned} F_f &= \frac{\sin(90) \times 9118.5}{\pi \times 1.920} \\ &= 1,511.7 \text{ kN/m} \end{aligned}$$

The fixed edge closure lid moment M_f is:

$$M_f = \frac{\sin(x_i) \times P_{un}}{4 \times \pi}$$

thus,

$$\begin{aligned} M_f &= \frac{\sin(90) \times 9118.5}{4 \times \pi} \\ &= 725.6 \text{ kN-m/m} \end{aligned}$$

The additional tensile bolt force per bolt F_{tp} caused by the prying action of the primary lid is (NUREG/CR-6007 Table 2.1 [Ref. 10]):

$$\begin{aligned} F_{tp} &= \left(\frac{\pi \times D_{lb}}{N_b} \right) \times \left[\frac{\frac{2 \times M_f}{D_{lo} - D_{lb}} - C1 \times (B - F_f) - C2 \times (B - P)}{C1 + C2} \right] \\ &= 517.3 \text{ kN/bolt} \end{aligned}$$

where,

$$\begin{aligned} P &= \text{Bolt Preload per unit Length of Bolt Circle} \\ &= 692.9 \text{ kN/m (as shown in Section 2.13.2.4.2.1)} \\ B &= \text{Non-prying Tensile Bolt Force} \\ &= \text{MAX}(F_f, P) \\ C1 &= \text{Force Constant} \end{aligned}$$

$$\begin{aligned}
 &= 1.0 \\
 C2 &= \text{Second Force Constant} \\
 &= \left(\frac{8}{3 \times (D_{lo} - D_{lb})^2} \right) \times \left[\frac{E_l \times t_l^3}{1 - N_{ul}} + \frac{(D_{lo} - D_{li}) \times E_{lf} \times t_{lf}^3}{D_{lb}} \right] \\
 &\quad \times \left(\frac{L_b}{N_b \times D_b^2 \times E_b} \right) \\
 &= 3.47 \quad (\text{as shown in Section 2.13.2.4.2.1}) \\
 D_{lo} &= \text{Closure Lid Diameter at Outer Edge} \\
 &= 2016 \text{ mm} \\
 D_{li} &= \text{Closure Lid Diameter at Inner Edge} \\
 &= 1730 \text{ mm} \\
 t_{lf} &= \text{Closure Lid Flange Thickness} \\
 &= 120 \text{ mm} \\
 E_{lf} &= \text{Primary Lid Flange Material Elastic Modulus,} \\
 &\quad ((SA 240 TYPE 304L)) \\
 &= 195 \text{ GPa at } 20^\circ\text{C} \quad (\text{Table 2.2.1-1}) \\
 L_b &= \text{Bolt length between the top and bottom surfaces of the} \\
 &\quad \text{closure lid at the bolt circle} \\
 &= 67 \text{ mm}
 \end{aligned}$$

The total tension force F_a is:

$$\begin{aligned}
 F_a &= F_t + F_{tp} \\
 &= 285.0 + 517.3 \\
 &= 802.3 \text{ kN/bolt}
 \end{aligned}$$

The shear force F_s is 0.

The maximum bending moment generated by the applied loads M_{bb} is:

$$\begin{aligned}
 M_{bb} &= \left(\frac{\pi \times D_{lb}}{N_b} \right) \times \left(\frac{K_b}{K_b + K_l} \right) \times M_f \\
 &= 2.4 \text{ kN-m}
 \end{aligned}$$

where,

$$\begin{aligned}
 K_b &= \left(\frac{N_b}{L_b} \right) \times \left(\frac{E_b}{D_{lb}} \right) \times \left(\frac{D_b^4}{64} \right) \\
 &= 4,167.8 \text{ kN}
 \end{aligned}$$

$$\begin{aligned}
 K1 &= \frac{E_l \times t_l^3}{3 \times \left[(1 - N_{ul}^2) + (1 - N_{ul})^2 \times \left(\frac{D_{lb}}{D_{lo}} \right)^2 \right] \times D_{lb}} \\
 &= 234,719 \text{ kN}
 \end{aligned}$$

2.13.2.5.1.2 Secondary Lid Bolts

The non-prying tensile bolt force per secondary lid bolt F_{ts} is:

$$F_{ts} = \frac{\sin(x_i) \times P_{un}}{N_b}$$

where,

$$\begin{aligned}
 x_i &= \text{End Drop Impact Angle} \\
 &= 90^\circ \\
 P_{un} &= \text{MIN}(P_{un1}, P_{un2}) \\
 N_b &= \text{Number of Bolts} \\
 &= 18
 \end{aligned}$$

P_{un} was evaluated in Section 2.13.2.5.1.1:

$$P_{un'} = 9,118.5 \text{ kN}$$

As shown in Figure 2.7.3-2, the primary and secondary lids act together under the pin puncture load. Therefore, the secondary lid receives only a portion of the impact load from the pin; P_{un} is reduced by the ratio of the secondary lid volume to the total lid volume.

$$\begin{aligned}
 V_s &= \text{Secondary Lid Volume} \\
 &= \frac{\pi}{4} \times D_{lb}^2 \times t_l \\
 V_t &= \text{Total Lid Volume} \\
 &= \frac{\pi}{4} \times D_{lbp}^2 \times t_{la}
 \end{aligned}$$

where,

$$\begin{aligned}
 D_{lbp} &= \text{Closure Lid Bolt Diameter at Primary Lid Bolts} \\
 &= 1920 \text{ mm} \\
 t_{lp} &= \text{Closure Lid Thickness at Primary Lid Bolts} \\
 &= 210 \text{ mm}
 \end{aligned}$$

$$\begin{aligned}
 t_{la} &= \text{Average Lid Thickness} \\
 &= \frac{t_l + t_{lp}}{2}
 \end{aligned}$$

thus,

$$\begin{aligned}
 t_{la} &= \frac{110 + 210}{2} \\
 &= 160 \text{ mm} \\
 V_s &= \frac{\pi}{4} \times 0.926^2 \times 0.110 \\
 &= 0.067 \text{ m}^3 \\
 V_t &= \frac{\pi}{4} \times 1.920^2 \times 0.160 \\
 &= 0.463 \text{ m}^3 \\
 P_{un} &= P'_{un} \times \frac{V_s}{V_t} \\
 P_{un} &= 9118.5 \times \frac{0.067}{0.463} \\
 &= 1325.6 \text{ kN}
 \end{aligned}$$

and

$$\begin{aligned}
 F_{ts} &= \frac{\sin(90) \times 1325.6}{18} \\
 &= 73.6 \text{ kN/bolt.}
 \end{aligned}$$

As shown in Sections 2.13.2.1.1 and 2.13.2.1.2, the design of the primary and secondary lids prevents shear loads being applied to the bolts. Thus,

$$F_{ss} = 0$$

It is noted that the equation given for F_{ss} in NUREG/CR6007 [Ref. 10] also shows $F_{ss} = 0$.

The fixed edge closure lid force F_f is:

$$\begin{aligned}
 F_f &= \frac{\sin(x_i) \times P_{un}}{\pi \times D_{lb}} \\
 &= 455.7 \text{ kN/m}
 \end{aligned}$$

where,

$$\begin{aligned}
 D_{lb} &= \text{Secondary Lid Bolt Circle Diameter} \\
 &= 926 \text{ mm}
 \end{aligned}$$

The fixed edge closure lid moment M_f is:

$$M_f = \frac{\sin(x_i) \times P_{un}}{4 \times \pi}$$

thus,

$$\begin{aligned} M_f &= \frac{\sin(90) \times 1325.6}{4 \times \pi} \\ &= 105.5 \text{ kN-m/m} \end{aligned}$$

The additional tensile bolt force per bolt F_{ts} caused by the prying action of the secondary lid is (NUREG/CR-6007 Table 2.1 [Ref. 10]):

$$\begin{aligned} F_{ts} &= \left(\frac{\pi \times D_{lb}}{N_b} \right) \times \left[\frac{2 \times M_f}{D_{lo} - D_{lb}} - C1 \times (B - F_f) - C2 \times (B - P) \right] \\ &= 164 \text{ kN/bolt} \end{aligned}$$

where,

P = Bolt Preload per unit Length of Bolt Circle
= 446.7 kN/m (as shown in Section 2.13.2.4.2.2)

B = Non-prying Tensile Bolt Force
= MAX(F_f , P)

C1 = Force Constant
= 1.0

C2 = Second Force Constant

$$\begin{aligned} &\left(\frac{8}{3 \times (D_{lo} - D_{lb})^2} \right) \times \left[\frac{E_l \times t_l^3}{1 - N_{ul}} + \frac{(D_{lo} - D_{li}) \times E_{lf} \times t_{lf}^3}{D_{lb}} \right] \\ &= \left(\frac{L_b}{N_b \times D_b^2 \times E_b} \right) \\ &= 1.79 \quad (\text{as shown in Section 2.13.2.4.2.2}) \end{aligned}$$

D_{lo} = Closure Lid Diameter at Outer Edge
= 1000 mm

D_{li} = Closure Lid Diameter at Inner Edge
= 745 mm

t_{lf} = Closure Lid Flange Thickness
= 80 mm

E_{lf} = Secondary Lid Flange Material Elastic Modulus,
(SA 240 TYPE 304L)
= 195 GPa at 20°C (Table 2.2.1-1)

$$\begin{aligned}
 L_b &= \text{Bolt length between the top and bottom surfaces of the} \\
 &\quad \text{closure lid at the bolt circle} \\
 &= 43 \text{ mm}
 \end{aligned}$$

The total tension force F_a is:

$$\begin{aligned}
 F_a &= F_t + F_{ts} \\
 &= 73.6 + 164 \\
 &= 237.6 \text{ kN/bolt}
 \end{aligned}$$

The shear force F_s is 0.

The maximum bending moment generated by the applied loads M_{bb} is:

$$\begin{aligned}
 M_{bb} &= \left(\frac{\pi \times D_{lb}}{N_b} \right) \times \left(\frac{K_b}{K_b + K_1} \right) \times M_f \\
 &= 0.6 \text{ kN/m}
 \end{aligned}$$

where,

$$\begin{aligned}
 K_b &= \left(\frac{N_b}{L_b} \right) \times \left(\frac{E_b}{D_{lb}} \right) \times \left(\frac{D_b^4}{64} \right) \\
 &= 2,396.5 \text{ kN} \quad (\text{as shown in Section 2.13.2.4.2.2})
 \end{aligned}$$

$$\begin{aligned}
 K_1 &= \frac{E_l \times t_l^3}{3 \times \left[(1 - N_{ul}^2) + (1 - N_{ul})^2 \times \left(\frac{D_{lb}}{D_{lo}} \right)^2 \right] \times D_{lb}} \\
 &= 71,203 \text{ kN} \quad (\text{as shown in Section 2.13.2.4.2.2})
 \end{aligned}$$

2.13.2.5.2 Side Puncture

In Section 2.13.2.1.1, the gap between the cask body and the primary lid is shown to be smaller than the gap between the M48 bolts and the bolt clearance holes. Therefore, no shear load is imparted to the bolts from the cask body. Further, there are no other loads resulting from side puncture at the bolts. Thus, no significant loads are imparted to the primary and secondary closure lid bolts during a side puncture event.

2.13.2.6 External Pressure

Loads in the primary and secondary closure lid bolts due to external pressure are evaluated using the formulas for evaluating bolt forces/moments in Table 4.3 of NUREG/CR-6007 [Ref. 10].

2.13.2.6.1 Primary Lid Bolts

The pressure outside the cask P_{lo} in the case of immersion is assumed to be 350 kPa (Calculation Package RTL-001-CALC-TH-0102, Rev. 6 [Ref. 42]). The pressure inside the cask P_{li} is conservatively taken to be 0 kPa.

The axial force per bolt due to external pressure is:

$$F_a = \frac{\pi \times D_{lg}^2 \times (P_{li} - P_{lo})}{4 \times N_b} \quad (\text{Table 4.3 of NUREG/CR-6007 [Ref. 10]})$$

where,

$$\begin{aligned} D_{lg} &= \text{Outside Seal Diameter} \\ &= 1835 \text{ mm} \\ N_b &= \text{Number of Bolts} \\ &= 32 \end{aligned}$$

Since this force is negative (inward acting), the actual resulting bolt force is $F_a = 0$ since the applied load is supported by the cask wall and not by the bolts.

The fixed edge closure lid force is:

$$F_f = \frac{D_{lb} \times (P_{li} - P_{lo})}{4} \quad (\text{Table of 4.3 NUREG/CR-6007 [Ref. 10]})$$

where,

$$\begin{aligned} D_{lb} &= \text{Bolt Circle Diameter} \\ &= 1920 \text{ mm} \end{aligned}$$

thus,

$$\begin{aligned} F_f &= \frac{1.920 \times (0 - 350)}{4} \\ &= -168.0 \text{ kN/m} \end{aligned}$$

The fixed edge closure lid moment is:

$$\begin{aligned} M_f &= \frac{(P_{li} - P_{lo}) \times D_{lb}^2}{32} \quad (\text{Table of 4.3 NUREG/CR-6007 [Ref. 10]}) \\ &= \frac{(0 - 350) \times 1.920^2}{32} \\ &= -40.32 \text{ kN-m/m} \end{aligned}$$

The shear bolt force per bolt is:

$$\begin{aligned}
 F_s &= \frac{\pi \times E_l \times t_l \times (P_{li} - P_{lo}) \times D_{lb}^2}{2 \times N_b \times E_c \times t_c \times (1 - N_{ul})} \text{ (NUREG/CR-6007 [Ref.10])} \\
 &= -296.5 \text{ kN/bolt}
 \end{aligned}$$

The *maximum* gap between the lid and cask body is less than the *minimum* gap between the bolt clearance holes and bolt shank (see Section 2.13.2.1.1). Thus, the RT-100 primary lid bolts are not subjected to any shear loads. Therefore,

$$F_s = 0.0 \text{ kN/bolt.}$$

2.13.2.6.2 Secondary Lid Bolts

The pressure outside the cask P_{lo} in the case of immersion is assumed to be 350 kPa (Calculation Package RTL-001-CALC-TH-0102 Rev. 6 [Ref. 42]). The pressure inside the cask P_{li} is conservatively taken to be 0 kPa.

The axial force per bolt due to external pressure is:

$$\begin{aligned}
 F_a &= \frac{\pi \times D_{lg}^2 \times (P_{li} - P_{lo})}{4 \times N_b} \\
 &= -11.0 \text{ kN/bolt}
 \end{aligned}$$

Thus,

$$\begin{aligned}
 D_{lg} &= \text{Outside Seal Diameter} \\
 &= 850 \text{ mm} \\
 N_b &= \text{Number of Bolts} \\
 &= 18
 \end{aligned}$$

Since this force is negative (inward acting), the actual resulting bolt force is $F_a = 0$ (the load is supported by the cask wall and not by the bolts).

The fixed edge closure lid force is:

$$\begin{aligned}
 F_f &= \frac{D_{lb} \times (P_{li} - P_{lo})}{4} \\
 &= -81.0 \text{ kN/m}
 \end{aligned}$$

where,

$$\begin{aligned}
 D_{lb} &= \text{Bolt Circle Diameter} \\
 &= 926 \text{ mm}
 \end{aligned}$$

The fixed edge closure lid moment is:

$$\begin{aligned}
 M_f &= \frac{(P_{li} - P_{lo}) \times D_{lb}^2}{32} \\
 &= \frac{(0 - 350) \times 0.926^2}{32} \\
 &= -9.4 \text{ kN-m/m}
 \end{aligned}$$

The shear bolt force per bolt is:

$$\begin{aligned}
 F_s &= \frac{\pi \times E_l \times t_l \times (P_{li} - P_{lo}) \times D_{lb}^2}{2 \times N_b \times E_c \times t_c \times (1 - N_{ul})} \\
 &= -64.2
 \end{aligned}$$

The *maximum* gap between the lid and cask body is less than the *minimum* gap between the bolt clearance holes and bolt shank (see Section 2.13.2.1.2). Thus, the RT-100 secondary lid bolts are not subjected to any shear loads. Therefore,

$$F_s = 0.0 \text{ kN/bolt.}$$

2.13.2.7 Gasket Seating Load

A small closure force is required to maintain a positive seal between the cask lid and the cask body. However, this closure force is much less than the minimum preloads provided for the closure bolts at the primary and secondary lids. Therefore, the gasket seating load is negligible, and $F_s = 0$.

2.13.3 Load Combinations

The loadings in Section 2.13.2 are combined to form load cases for the closure bolt analysis per NUREG/CR-6007 [Ref. 10]. The corresponding bolt stresses are obtained and compared to the criteria defined in Section 2.1.2.2. A summary of the loads on the bolts for the primary and secondary lids under the normal conditions of transport and the hypothetical accident conditions is presented in Table 2.13.3-1 and Table 2.13.3-2, respectively.

Table 2.13.3-1 Primary Lid Bolt Load Summary

Load Case	Applied Load		Non-Prying Tensile Force F_t (kN/bolt)	Torsional Moment M_t (kN-m/bolt)	Prying Force F_f (kN/m)	Prying Moment M_f (kN-m/m)
Preload	Residual Torque	Minimum	52.8	0.2	0.0	0.0
		Maximum	130.6	0.5	0.0	0.0
Gasket	Seating Load		0.0	0.0	0.0	0.0
Internal Pressure	250 kN/m ² (35 psi) pressure		20.7	0.0	120.0	28.8
Thermal	100°C		690.9	0.0	0.0	0.0
Puncture	Drop on 15 cm diameter pin		285.0	2.4	1511.7	725.6
External Pressure	350 kPa pressure		0.0	0.0	-168.0	-40.3
Free Drop	Drop from 9 m height		628.9	2.6	3336.4	800.7

Table 2.13.3-2 Secondary Lid Bolt Load Summary

Load Case	Applied Load		Non-Prying Tensile Force F_t (kN/bolt)	Torsional Moment M_t (kN-m/bolt)	Prying Force F_f (kN/m)	Prying Moment M_f (kN-m/m)
Preload	Residual Torque	Minimum	29.6	0.1	0.0	0.0
		Maximum	72.2	0.2	0.0	0.0
Gasket	Seating Load		0.0	0.0	0.0	0.0
Internal Pressure	250 kN/m ² (35 psi) pressure		7.9	0.0	57.9	6.7
Thermal	100°C		388.6	0.0	0.0	0.0
Puncture	Drop on 15 cm diameter pin		237.7	0.6	455.7	105.5
External Pressure	350 kPa pressure		0.0	0.0	-81.0	-9.4
Free Drop	Drop from 9 m height		266.0	1.0	1646.1	190.5

2.13.3.1 Primary Lid Closure Bolt Evaluation under Normal Conditions of Transport

The maximum tension, shear and bolt bearing loads in the primary lid bolts due to the combined NCT loads are evaluated in accordance with NUREG/CR-6007 [Ref. 10], with due consideration given to the prying effects on the fixed lid. Since the prying forces act inward, normal to the cask lid, an additional prying force is generated (NUREG/C-6007 [Ref. 10]). For the NCT condition, the controlling load case is the summation of the bolt preload, the internal pressure

load and the thermal expansion load. The maximum bolt tension load F_t , shear load F_s , and torsional moment M_t for the primary lid bolts are (see Table 2.13.3-1):

$$\begin{aligned}
 F_t &= F_p + F_{ap} + F_{atp} \\
 &= 130.6 + 20.7 + 690.9 \\
 &= 842.1 \text{ kN/bolt} \\
 F_s &= F_{sp} + F_{st} \\
 &= 0.0 + 0.0 \\
 &= 0.0 \text{ kN/bolt} \\
 M_t &= M_{pt} + M_{at} + M_{st} \\
 &= 0.5 + 0.0 + 0.0 \\
 &= 0.5 \text{ kN-m/bolt}
 \end{aligned}$$

Conservatively, the fixed-edge closure lid prying is taken from the external pressure load case. This accident load case bounds all normal conditions and provides a conservative result. The additional tensile bolt force per bolt F_{tp} caused by the prying action of the primary lid is (Table 2.1 of NUREG/CR-6007 [Ref.10]):

$$\begin{aligned}
 F_{tp} &= \left(\frac{\pi \times D_{lb}}{N_b} \right) \times \left[\frac{\frac{2 \times M_f}{D_{li} - D_{lb}} - C1 \times (B - F_f) - C2 \times (B - P)}{C1 + C2} \right] \\
 &= -18.4 \text{ kN/m-m}
 \end{aligned}$$

where,

$$\begin{aligned}
 F_f &= \text{Fixed Edge Closure Force} \\
 &= -168.0 \text{ kN/m} && \text{(Table 2.13.3-1)} \\
 M_f &= \text{Fixed Edge Closure Moment} \\
 &= -40.32 \text{ kN-m/m} && \text{(Table 2.13.3-1)}
 \end{aligned}$$

Since this bolt load is less than the load generated by the minimum bolt preload ($130.6 \text{ kN} > -18.3 \text{ kN}$) the prying force generated by the external pressure is not critical with respect to bolt stress and does not result in the loss of lid seal.

The total tension force F_a is:

$$\begin{aligned}
 F_a &= F_t + F_{tp} \\
 &= 842.1 + (-18.4) \\
 &= 823.7 \text{ kN/bolt}
 \end{aligned}$$

The maximum bending moment generated by the applied loads M_{bb} is:

$$\begin{aligned} M_{bb} &= \left(\frac{\pi \times D_{lb}}{N_b} \right) \times \left(\frac{K_b}{K_b + K_l} \right) \times M_f \\ &= -0.13 \text{ kN-m} \end{aligned}$$

The average bolt stresses from the combined NCT loads are determined in accordance with Table 5.1 of NUREG/CR-6007 [Ref. 10]. The bolt stress diameter D is:

$$\begin{aligned} D &= D_b - 0.9382 \times p \\ &= 0.043 \text{ m} \end{aligned}$$

where,

$$\begin{aligned} p &= \text{Bolt Pitch} \\ &= 5.0 \text{ mm} \quad (\text{Machinery Handbook [Ref.27]}) \end{aligned}$$

The average tensile stress S_{ba} , average shear stress S_{bs} , maximum bending stress S_{bb} , and maximum torsional stress S_{bt} (Table 5.1 of NUREG/CR-6007 [Ref. 10]) are:

$$\begin{aligned} S_{ba} &= \frac{1.2732 \times F_a}{D^2} \\ &= 559.1 \text{ MPa} \\ S_{bs} &= \frac{1.2732 \times F_s}{D^2} \\ &= 0.0 \text{ MPa} \\ S_{bb} &= \frac{10.186 \times M_{bb}}{D_b^3} \\ &= -12.2 \text{ MPa} \\ S_{bt} &= \frac{5.093 \times M_t}{D_b^3} \\ &= 21.6 \text{ MPa} \end{aligned}$$

The allowable stresses for the bolts are:

$$\begin{aligned} \sigma_{ta} &= \text{Allowable Tensile Stress} \\ &= 0.7 \times S_u \\ &= 721 \text{ MPa} \\ \sigma_{sa} &= \text{Allowable Shear Stress} \\ &= 0.42 \times S_u \\ &= 432.6 \text{ MPa} \\ \sigma_{ba} &= \text{Allowable Bending Stress} \end{aligned}$$

$$\begin{aligned}
 &= 1.5 \times S_{mn} \\
 &= 514.5 \text{ MPa}
 \end{aligned}$$

where,

$$\begin{aligned}
 S_u &= \text{Primary Bolt Ultimate Stress (SA 354 Grade BD)} \\
 &= 1034.2 \text{ MPa at } 20^\circ \text{ C} \quad (\text{Table 2.2.1-1}) \\
 S_{mn} &= \text{Primary Bolt Membrane Stress (SA 354 Grade BD)} \\
 &= 434.4 \text{ MPa at } 20^\circ \text{ C} \quad (\text{Table 2.2.1-1})
 \end{aligned}$$

Therefore, the maximum interaction ratio for the combined shear and tension loads is:

$$\begin{aligned}
 \text{I.R.} &= \left(\frac{S_{ba}}{\sigma_{ta}} \right)^2 + \left(\frac{S_{bs}}{\sigma_{sa}} \right)^2 \\
 &= 0.601
 \end{aligned}$$

The minimum factor of safety is:

$$\begin{aligned}
 \text{FS} &= \frac{1}{\text{I.R.}} \\
 &= 1.66 > 1.0
 \end{aligned}$$

thus, the maximum interaction ratio for the bending load is:

$$\begin{aligned}
 \text{I.R.} &= \left(\frac{S_{bb}}{\sigma_{ba}} \right)^2 \\
 &= 0.00056
 \end{aligned}$$

The minimum factor of safety is:

$$\begin{aligned}
 \text{FS} &= \frac{1}{\text{I.R.}} \\
 &= 1774.7 > 1.0
 \end{aligned}$$

The maximum stress intensity in the primary lid bolts under the combined loads S_{bi} is:

$$\begin{aligned}
 S_{bi} &= \sqrt{(S_{ba} + S_{bb})^2 + 4 \times (S_{bs} + S_{bt})^2} \\
 &= 548.6 \text{ MPa}
 \end{aligned}$$

The primary lid closure bolts utilize a custom washer for the bolts with an outer diameter d_{ow} of 130 mm and a hole diameter d_{oh} of 52 mm. Therefore, the bearing stress under the bolt head S_{brg} is:

$$S_{brg} = \frac{F_a}{A_{brg}}$$

$$= 73.9 \text{ MPa}$$

where,

$$A_{brg} = \text{Bolt Bearing Area}$$

$$= \frac{\pi}{4} \times (d_{ow}^2 - d_{oh}^2)$$

$$= \frac{\pi}{4} \times (0.130^2 - 0.052^2)$$

$$= 0.0111 \text{ m}^2$$

The allowable normal condition bearing stress on the lid is taken to be the yield stress of the lid material at 250 °C. The maximum interaction ratio for the bearing load is therefore:

$$I.R. = \frac{S_{brg}}{S_{yl}}$$

$$= 0.65$$

where,

$$S_{yl} = \text{Primary Lid Material Yield Stress,}$$

$$(\text{SA 240 TYPE 304L})$$

$$= 114 \text{ MPa at } 250 \text{ }^\circ\text{C} \quad (\text{Table 2.2.1-1})$$

The minimum factor of safety is:

$$FS = \frac{1}{I.R.}$$

$$= 1.54 > 1.0$$

Because the cask material is weaker than the bolting material, failure occurs at the root of the cask material threads. The minimum required thread engagement length to prevent cask material failure is determined in accordance with the Machinery's Handbook [Ref. 27]. Since the constants in the equation assume customary units, the metric units used for the cask design are converted into English Units for determination of the required engagement length. Thus, the minimum engagement length L_e for the cask is:

$$L_e = \frac{S_{ub} \times 2 \times A_b}{S_{ul} \times \pi \times n \times D_{s,min} \times \left[\frac{1}{2 \times n} + 0.57735 \times (D_{s,min} - E_{n,max}) \right]}$$

$$= 43.5 \text{ mm} < L_{ep} = 72.0 \text{ mm}$$

where,

$$S_{ub} = \text{Primary Bolt External Thread Tensile Strength}$$

$$\begin{aligned}
 & \text{(SA 354 Grade BD)} \\
 & = 149,389 \text{ psi (1,030 MPa) at } 20^\circ \text{C} \quad (\text{Table 2.2.1-1}) \\
 & \approx 150,000 \text{ psi} \\
 S_{ul} & = \text{Cask Internal Thread Tensile Strength} \\
 & \text{(SA 240 TYPE 304L)} \\
 & = 70,000 \text{ psi (482.6 MPa) at } 20^\circ \text{C} \quad (\text{Table 2.2.1-1}) \\
 A_b & = \text{Stress Area of Primary Bolt External Threads} \\
 & = 2.28 \text{ in}^2 (1470 \text{ mm}^2) \quad (\text{Machinery's Handbook [Ref. 27]}) \\
 p & = \text{Bolt Pitch} \\
 & = 0.197 \text{ in (5.0 mm)} \quad (\text{Machinery's Handbook [Ref. 27]}) \\
 n & = \text{Number of Threads per Inch} \\
 & = \frac{1}{p} = 5.08 \text{ threads/in} \\
 D_{s,min} & = \text{Minimum Major Bolt Diameter} \\
 & = 1.866 \text{ in (47.399 mm)} \quad (\text{ASME [Ref. 44]}) \\
 E_{n,max} & = \text{Maximum Pitch Diameter of Internal Thread} \\
 & = 1.705 \text{ in (43.297 mm)} \quad (\text{ASME [Ref. 44]}) \\
 L_{ep} & = \text{Provided Engagement Length} \\
 & = 72.0 \text{ mm}
 \end{aligned}$$

Therefore, the primary closure lid bolts are acceptable for the normal conditions of transport.

2.13.3.2 Secondary Lid Closure Bolt Evaluation under Normal Conditions of Transport

The maximum tension, shear and bolt bearing loads in the secondary lid bolts due to the combined NCT loads are evaluated in accordance with NUREG/CR-6007 [Ref. 10], with due consideration given to the prying effects on the fixed lid. An additional prying force is generated (NUREG/CR-6007 [Ref. 10]) due to the prying forces acting inward and normal to the cask lid. For the NCT, the controlling load case is the summation of the bolt preload, the internal pressure load, and the thermal expansion load. The maximum bolt tension load F_t , shear load F_s , and torsional moment M_t for the primary lid bolts are (see Table 2.13.3-2):

$$\begin{aligned}
 F_t & = F_p + F_{ap} + F_{atp} \\
 & = 72.2 + 7.9 + 388.6 \\
 & = 468.7 \text{ kN/bolt} \\
 F_s & = F_{sp} + F_{st} \\
 & = 0.0 + 0.0 \\
 & = 0.0 \text{ kN/bolt} \\
 M_t & = M_{pt} + M_{at} + M_{st} \\
 & = 0.2 + 0.0 + 0.0 \\
 & = 0.2 \text{ kN-m/bolt}
 \end{aligned}$$

Conservatively, the fixed-edge closure lid prying is taken from the external pressure load case. This accident load case bounds all normal conditions and provides a conservative result. The additional tensile bolt force per bolt F_{tp} caused by the prying action of the secondary lid is (Table 2.1 NUREG/CR-6007 [Ref. 10]):

$$F_{tp} = \left(\frac{\pi \times D_{lb}}{N_b} \right) \times \left[\frac{\frac{2 \times M_f}{D_{li} - D_{lb}} - C1 \times (B - F_f) - C2 \times (B - P)}{C1 + C2} \right]$$

$$= -24.5 \text{ kN-m/m}$$

where,

$$\begin{aligned} F_f &= \text{Fixed Edge Closure Force} \\ &= -81.0 \text{ kN/m} \quad (\text{Table 2.13.3-2}) \\ M_f &= \text{Fixed Edge Closure Moment} \\ &= -9.4 \text{ kN-m/m} \quad (\text{Table 2.13.3-2}) \end{aligned}$$

Since this bolt load is less than the load generated by the minimum bolt preload ($69.5 \text{ kN} > -24.5 \text{ kN}$), the prying force generated by the external pressure is not critical with respect to bolt stress and does not result in the loss of lid closure seal.

The total tension force F_a is:

$$\begin{aligned} F_a &= F_t + F_{tp} \\ &= 468.7 + (-24.5) \\ &= 444.1 \text{ kN/bolt} \end{aligned}$$

The maximum bending moment generated by the applied loads M_{bb} is:

$$\begin{aligned} M_{bb} &= \left(\frac{\pi \times D_{lb}}{N_b} \right) \times \left(\frac{K_b}{K_b + K_l} \right) \times M_f \\ &= -0.05 \text{ kN-m} \end{aligned}$$

The average bolt stresses from the combined NCT loads are determined in accordance with Table 5.1 of NUREG/CR-6007 [Ref. 10]. The bolt stress diameter D is:

$$\begin{aligned} D &= D_b - 0.9382 \times p \\ &= 0.032 \text{ m} \end{aligned}$$

where,

$$\begin{aligned} p &= \text{Bolt Pitch} \\ &= 4.0 \text{ mm} \quad [\text{Ref. 27}] \end{aligned}$$

The average tensile stress S_{ba} , average shear stress S_{bs} , maximum bending stress S_{bb} , and

maximum torsional stress Sbt are:

$$\begin{aligned} S_{ba} &= \frac{1.2732 \times F_a}{D^2} \\ &= 543.8 \text{ MPa} \end{aligned}$$

$$\begin{aligned} S_{bs} &= \frac{1.2732 \times F_s}{D^2} \\ &= 0.0 \text{ MPa} \end{aligned}$$

$$\begin{aligned} S_{bb} &= \frac{10.186 \times M_{bb}}{D_b^3} \\ &= -10.8 \text{ MPa} \end{aligned}$$

$$\begin{aligned} S_{bt} &= \frac{5.093 \times M_t}{D_b^3} \\ &= 21.3 \text{ MPa} \end{aligned}$$

The allowable stresses for the bolts are as previously defined. The maximum interaction ratio for the combined shear and tension loads is therefore:

$$\begin{aligned} I.R. &= \left(\frac{S_{ba}}{\sigma_{ta}} \right)^2 + \left(\frac{S_{bs}}{\sigma_{sa}} \right)^2 \\ &= 0.569 \end{aligned}$$

The minimum factor of safety is:

$$\begin{aligned} FS &= \frac{1}{I.R.} \\ &= 1.8 > 1.0 \end{aligned}$$

The maximum interaction ratio for the bending load is therefore:

$$\begin{aligned} I.R. &= \left(\frac{S_{bb}}{\sigma_{ba}} \right)^2 \\ &= 0.00044 \end{aligned}$$

The minimum factor of safety is:

$$\begin{aligned} FS &= \frac{1}{I.R.} \\ &= 2279.9 > 1.0 \end{aligned}$$

The maximum stress intensity in the primary lid bolts under the combined loads S_{bi} is:

$$\begin{aligned} S_{bi} &= \sqrt{(S_{ba} + S_{bb})^2 + 4 \times (S_{bs} + S_{bt})^2} \\ &= 534.7 \text{ MPa} \end{aligned}$$

The primary lid closure bolts utilize a custom washer for the bolts with an outer diameter d_{ow} of 90 mm and a hole diameter d_{oh} of 40 mm. Therefore, the bearing stress under the bolt head S_{brg} is:

$$\begin{aligned} S_{brg} &= \frac{F_a}{A_{brg}} \\ &= 87.0 \text{ MPa} \end{aligned}$$

where,

$$\begin{aligned} A_{brg} &= \text{Bolt Bearing Area} \\ &= \frac{\pi}{4} \times (d_{ow}^2 - d_{oh}^2) \\ &= 0.0051 \text{ m}^2 \end{aligned}$$

The allowable normal condition bearing stress on the lid is taken to be the yield stress of the lid material at 250 °C. Thus, the maximum interaction ratio for the bearing load is:

$$\begin{aligned} I.R. &= \frac{S_{brg}}{S_{yl}} \\ &= 0.76 \end{aligned}$$

The minimum factor safety is:

$$\begin{aligned} FS &= \frac{1}{I.R.} \\ &= 1.31 > 1.0 \end{aligned}$$

Because the cask material is weaker than the bolting material, failure occurs at the root of the cask material threads. The minimum required thread engagement length to prevent cask material failure is determined in accordance with the “Machinery’s Handbook” [Ref. 27]. Since the constants in the equation assume customary units, the metric units used for the RT-100 design are converted to English Units for determination of the required engagement length. Thus, the minimum engagement length L_e for the RT-100 is:

$$L_e = \frac{S_{ub} \times 2 \times A_b}{S_{ul} \times \pi \times n \times D_{s,min} \times \left[\frac{1}{2 \times n} + 0.57735 \times (D_{s,min} - E_{n,max}) \right]}$$

$$= 32.7 \text{ mm} < L_{ep} = 54.0 \text{ mm}$$

where,

$$\begin{aligned} A_b &= \text{Stress Area of Primary Bolt External Threads} \\ &= 1.27 \text{ in}^2 (817 \text{ mm}^2) \quad [\text{Ref. 27}] \\ P &= \text{Bolt Pitch} \\ &= 0.157 \text{ in (4.0 mm)} \quad [\text{Ref. 27}] \\ n &= \text{Number of Threads per Inch} \\ &= \frac{1}{p} = 6.35 \text{ threads/in} \\ D_{s,min} &= \text{Minimum Major Bolt Diameter} \\ &= 1.396 \text{ in (35.465 mm)} \quad [\text{Ref. 44}] \\ E_{n,max} &= \text{Maximum Pitch Diameter of Internal Thread} \\ &= 1.270 \text{ in (32.270 mm)} \quad [\text{Ref. 44}] \\ L_{ep} &= \text{Provided Engagement Length} \\ &= 54.0 \text{ mm} \end{aligned}$$

Therefore, the secondary closure lid bolts are acceptable for the normal conditions of transport.

2.13.3.3 Primary Lid Closure Bolt Evaluation under Hypothetical Accident Conditions

The maximum tension, shear and bolt bearing loads in the primary lid bolts due to the combined HAC loads are evaluated in accordance with NUREG/CR-6007 [Ref. 10], with due consideration given to the prying effects on the fixed lid. An additional prying force is generated (NUREG/CR-6007 [Ref. 10]) due to the prying forces acting inward and normal to the cask lid. For HAC, the controlling load case is the summation of the bolt preload, the internal pressure load, and the end drop load. Since the internal pressure load acts counter to the drop load, the internal pressure load is considered as negative for determination of the maximum bolt tension load. The maximum bolt tension load F_t , shear load F_s , and torsional moment (M_t) for the primary lid bolts are (see Table 2.13.3-2):

$$\begin{aligned} F_t &= F_p - F_{ap} + F_{atp} \\ &= 130.6 - 20.7 + 628.9 \\ &= 738.8 \text{ kN/bolt} \\ F_s &= F_{sp} + F_{st} \\ &= 0.0 + 0.0 \\ &= 0.0 \text{ kN/bolt} \\ M_t &= M_{pt} + M_{at} + M_{st} \\ &= 0.5 + 0.0 + 0.0 \\ &= 0.5 \text{ kN-m/bolt} \end{aligned}$$

Conservatively, the fixed-edge closure lid prying is taken from the end drop load case. The additional tensile bolt force per bolt F_{tp} caused by the prying action of the primary lid is (Table 2.1 of NUREG/CR-6007 [Ref. 10]):

$$F_{tp} = \left(\frac{\pi \times D_{lb}}{N_b} \right) \times \left[\frac{\frac{2 \times M_f}{D_{li} - D_{lb}} - C1 \times (B - F_f) - C2 \times (B - P)}{C1 + C2} \right]$$

$$= 316.2 \text{ kN-m/m}$$

where,

$$\begin{aligned} F_f &= \text{Fixed Edge Closure Force} \\ &= 3336.4 \text{ kN/m} \quad (\text{Table 2.13.3-1}) \\ M_f &= \text{Fixed Edge closure Moment} \\ &= 800.7 \text{ kN-m/m} \quad (\text{Table 2.13.3-1}) \end{aligned}$$

This bolt load is greater than the load generated by the minimum bolt preload ($130.6 \text{ kN} < 313.7 \text{ kN}$). However, the drop load is an inward load which presses the closure lid against the sealing gasket. Therefore, the prying force generated by the drop load does not result in the loss of lid closure seal. The outward load of the internal pressure has already been evaluated in Section 2.13.3.1 and found to be acceptable. All other accident loads are acceptable by comparison.

The total tension force F_a is:

$$\begin{aligned} F_a &= F_t + F_{tp} \\ &= 738.8 + 316.2 \\ &= 1055.1 \text{ kN/bolt} \end{aligned}$$

The maximum bending moment generated by the applied loads M_{bb} is:

$$\begin{aligned} M_{bb} &= \left(\frac{\pi \times D_{lb}}{N_b} \right) \times \left(\frac{K_b}{K_b + K_1} \right) \times M_f \\ &= 2.6 \text{ kN-m} \end{aligned}$$

The average bolt stresses from the combined HAC loads are determined in accordance with Table 5.1 of NUREG/CR-6007 [Ref. 10]. The bolt stress diameter is as defined previously. The average tensile stress S_{ba} , average shear stress S_{bs} , maximum bending stress S_{bb} , and maximum torsional stress S_{bt} are:

$$S_{ba} = \frac{1.2732 \times F_a}{D^2}$$

$$= 716.2 \text{ MPa}$$

$$S_{bs} = \frac{1.2732 \times F_s}{D^2}$$

$$= 0.0 \text{ MPa}$$

$$S_{bb} = \frac{10.186 \times M_{bb}}{D_b^3}$$

$$= 242.5 \text{ MPa}$$

$$S_{bt} = \frac{5.093 \times M_t}{D_b^3}$$

$$= 21.6 \text{ MPa}$$

The allowable stresses for the bolts are as previously defined. Thus, the maximum interaction ratio for the combined shear and tension loads is:

$$I.R. = \left(\frac{S_{ba}}{\sigma_{ta}} \right)^2 + \left(\frac{S_{bs}}{\sigma_{sa}} \right)^2$$

$$= 0.987$$

The minimum factor of safety is:

$$FS = \frac{1}{I.R.}$$

$$= 1.01 > 1.0$$

Therefore, the maximum interaction ratio for the bending load is:

$$I.R. = \left(\frac{S_{bb}}{\sigma_{ba}} \right)^2$$

$$= 0.222$$

The minimum factor of safety is:

$$\begin{aligned} FS &= \frac{1}{I.R.} \\ &= 4.50 > 1.0 \end{aligned}$$

The primary lid closure bolts utilize a custom washer for the bolts with an outer diameter d_{ow} of 130 mm and a hole diameter d_{oh} of 52 mm. Therefore, the bearing stress under the bolt head S_{brg} is:

$$\begin{aligned} S_{brg} &= \frac{F_a}{A_{brg}} \\ &= 94.6 \text{ MPa} \end{aligned}$$

The allowable normal condition bearing stress on the lid is taken to be the yield stress of the lid material at 250 °C. Thus, the maximum interaction ratio for the bearing load is:

$$\begin{aligned} I.R. &= \frac{S_{brg}}{S_{yl}} \\ &= 0.83 \end{aligned}$$

The minimum factor of safety is:

$$\begin{aligned} FS &= \frac{1}{I.R.} \\ &= 1.21 > 1.0 \end{aligned}$$

Because the cask material is weaker than the bolting material, failure occurs at the root of the cask material threads. The minimum required thread engagement length to prevent cask material failure is determined in accordance with the “Machinery’s Handbook” [Ref. 27]. Since the constants in the equation assume customary units, the metric units used for the cask design are converted to English Units for determination of the required engagement length. Thus, the minimum engagement length L_e for the cask is:

$$\begin{aligned} L_e &= \frac{S_{ub} \times 2 \times A_b}{S_{ul} \times \pi \times n \times D_{s,min} \times \left[\frac{1}{2 \times n} + 0.57735 \times (D_{s,min} - E_{n,max}) \right]} \\ &= 43.5 \text{ mm} < L_{ep} = 72.0 \text{ mm} \end{aligned}$$

Where,

$$\begin{aligned}
 S_{ub} &= \text{Primary Bolt External Thread Tensile Strength} \\
 &\quad (\text{SA 354 Grade BD}) \\
 &= 149,389 \text{ psi (1,030 MPa) at } 20^{\circ}\text{C (Table 2.2.1-1)} \\
 S_{ul} &= \text{Cask Internal Thread Tensile Strength} \\
 &\quad (\text{SA 240 TYPE 304L}) \\
 &= 70,000 \text{ psi (483 MPa) at } 20^{\circ}\text{C (Table 2.2.1-1)} \\
 A_b &= \text{Stress Area of Primary Bolt External Threads} \\
 &= 2.28 \text{ in}^2 (1470 \text{ mm}^2) \quad [\text{Ref. 27}] \\
 p &= \text{Bolt Pitch} \\
 &= 0.197 \text{ in (5.0 mm)} \quad [\text{Ref. 27}] \\
 n &= \text{Number of Threads per Inch} \\
 &= \frac{1}{p} = 5.08 \text{ threads/in} \\
 D_{s,min} &= \text{Minimum Major Bolt Diameter} \\
 &= 1.866 \text{ in (47.399 mm)} \quad [\text{Ref. 44}] \\
 L_{ep} &= \text{Provided Engagement Length} \\
 &= 72.0 \text{ mm}
 \end{aligned}$$

Therefore, the primary closure lid bolts are acceptable for the hypothetical accident conditions.

2.13.3.4 Secondary Lid Closure Bolt Evaluation under Hypothetical Accident Conditions

The maximum tension, shear and bolt bearing loads in the secondary lid bolts due to the combined HAC loads are evaluated in accordance with NUREG/CR-6007 [Ref. 10], with due consideration given to the prying effects on the fixed lid. An additional prying force is generated (NUREG/CR-6007 [Ref. 10]) due to the prying forces acting inward and normal to the cask lid. For HAC, the controlling load case is the summation of the bolt preload, the internal pressure load, and the end drop load. Since the internal pressure load acts counter to the drop load, the internal pressure load is considered as negative for determination of the maximum bolt tension load. The maximum bolt tension load F_t , shear load F_s , and torsional moment M_t for the primary lid bolts are (see Table 2.13.3-2):

$$\begin{aligned}
 F_t &= F_p - F_{ap} + F_{atp} \\
 &= 72.2 - 7.9 + 266.0 \\
 &= 330.4 \text{ kN/bolt} \\
 F_s &= F_{sp} + F_{st} \\
 &= 0.0 + 0.0 \\
 &= 0.0 \text{ kN/bolt}
 \end{aligned}$$

$$\begin{aligned}
 M_t &= M_{pt} + M_{at} + M_{st} \\
 &= 0.2 + 0.0 + 0.0 \\
 &= 0.2 \text{ kN-m/bolt}
 \end{aligned}$$

Conservatively, the fixed-edge closure lid prying is taken from the end drop load case. The additional tensile bolt force per bolt F_{tp} caused by the prying action of the primary lid is (Table 2.1 of NUREG/CR-6007 [Ref. 10]):

$$\begin{aligned}
 F_{tp} &= \left(\frac{\pi \times D_{lb}}{N_b} \right) \times \left[\frac{\frac{2 \times M_f}{D_{li} - D_{lb}} - C1 \times (B - F_f) - C2 \times (B - P)}{C1 + C2} \right] \\
 &= 173.5 \text{ kN-m/m}
 \end{aligned}$$

where,

$$\begin{aligned}
 F_f &= \text{Fixed Edge Closure Force} \\
 &= 1646.1 \text{ kN/m} \quad (\text{Table 2.13.3-2}) \\
 M_f &= \text{Fixed Edge Closure Moment} \\
 &= 190.5 \text{ kN-m/m} \quad (\text{Table 2.13.3-2})
 \end{aligned}$$

This bolt load is greater than the load generated by the minimum bolt preload ($130.6 \text{ kN} < 178.0 \text{ kN}$). However, the drop load is an inward load which presses the closure lid against the sealing gasket. Thus, the prying force generated by the drop load does not result in the loss of lid closure seal. The outward load of the internal pressure has already been evaluated in Section 2.13.3.2 and found to be acceptable. All other accident loads are acceptable by comparison.

The total tension force, F_a , is:

$$\begin{aligned}
 F_a &= F_t + F_{tp} \\
 &= 330.4 + 173.5 \\
 &= 503.8 \text{ kN/bolt}
 \end{aligned}$$

The maximum bending moment generated by the applied loads M_{bb} is:

$$\begin{aligned}
 M_{bb} &= \left(\frac{\pi \times D_{lb}}{N_b} \right) \times \left(\frac{Kb}{Kb + K1} \right) \times M_f \\
 &= 1.0 \text{ kN-m}
 \end{aligned}$$

The average bolt stresses from the combined HAC loads are determined in accordance with Table 5.1 of NUREG/CR-6007 [Ref. 10]. The bolt stress diameter is as defined previously. The average tensile stress S_{ba} , average shear stress S_{bs} , maximum bending stress S_{bb} , and maximum

torsional stress S_b , are:

$$\begin{aligned} S_{ba} &= \frac{1.2732 \times F_a}{D^2} \\ &= 616.8 \text{ MPa} \end{aligned}$$

$$\begin{aligned} S_{bs} &= \frac{1.2732 \times F_s}{D^2} \\ &= 0.0 \text{ MPa} \end{aligned}$$

$$\begin{aligned} S_{bb} &= \frac{10.186 \times M_{bb}}{D_b^3} \\ &= 218.9 \text{ MPa} \end{aligned}$$

$$\begin{aligned} S_{bt} &= \frac{5.093 \times M_t}{D_b^3} \\ &= 21.3 \text{ MPa} \end{aligned}$$

The allowable stresses for the bolts are as previously defined. Therefore, the maximum interaction ratio for the combined shear and tension loads is:

$$\begin{aligned} \text{I.R.} &= \left(\frac{S_{ba}}{\sigma_{ta}} \right)^2 + \left(\frac{S_{bs}}{\sigma_{sa}} \right)^2 \\ &= 0.732 \end{aligned}$$

The minimum factor of safety is:

$$\begin{aligned} \text{FS} &= \frac{1}{\text{I.R.}} \\ &= 1.37 > 1.0 \end{aligned}$$

The maximum interaction ratio for the bending load is:

$$\begin{aligned} \text{I.R.} &= \left(\frac{S_{bb}}{\sigma_{ba}} \right)^2 \\ &= 0.113 \end{aligned}$$

The minimum factor of safety is:

$$\begin{aligned}
 FS &= \frac{1}{I.R.} \\
 &= 8.86 > 1.0
 \end{aligned}$$

The primary lid closure bolts utilize a custom washer for the bolts with an outer diameter d_{ow} of 90 mm and a hole diameter d_{oh} of 40 mm. Therefore, the bearing stress under the bolt head S_{brg} is:

$$\begin{aligned}
 S_{brg} &= \frac{F_a}{A_{brg}} \\
 &= 98.7 \text{ MPa}
 \end{aligned}$$

The allowable normal condition bearing stress on the lid is taken to be the yield stress of the lid material at 250 °C. The maximum interaction ratio for the bearing load is:

$$\begin{aligned}
 I.R. &= \frac{S_{brg}}{S_{yl}} \\
 &= 0.86
 \end{aligned}$$

The minimum factor of safety is:

$$\begin{aligned}
 FS &= \frac{1}{I.R.} \\
 &= 1.16 > 1.0
 \end{aligned}$$

Because the cask material is weaker than the bolting material, failure occurs at the root of the cask material threads. The minimum required thread engagement length to prevent cask material failure is determined in accordance with the “Machinery’s Handbook” [Ref. 27]. Since the constants in the equation assume customary units, the metric units used for the cask design are converted to English Units for determination of the required engagement length. Thus, the minimum engagement length L_e for the cask is:

$$\begin{aligned}
 L_e &= \frac{S_{ub} \times 2 \times A_b}{S_{ul} \times \pi \times n \times D_{s,min} \times \left[\frac{1}{2 \times n} + 0.57735 \times (D_{s,min} - E_{n,max}) \right]} \\
 &= 32.7 \text{ mm} < L_{ep} = 54.0 \text{ mm}
 \end{aligned}$$

Therefore, the secondary closure lid bolts are acceptable for the hypothetical accident conditions.

2.13.4 Seal Integrity

The maximum stress analyses in the previous sections are based on criteria for the accident conditions intended to prevent failures by excessive plastic deformation or by the rupture of the bolt. Using the yield stress as the stress limit for average tensile bolt stress, as per NUREG/CR-6007 [Ref. 10], implies that a small amount (0.02%) of plastic deformation is permitted. The following calculations show that the O-rings will continue to provide positive sealing of the closure lids even with this small plastic deformation.

2.13.4.1 Primary Lid Seals

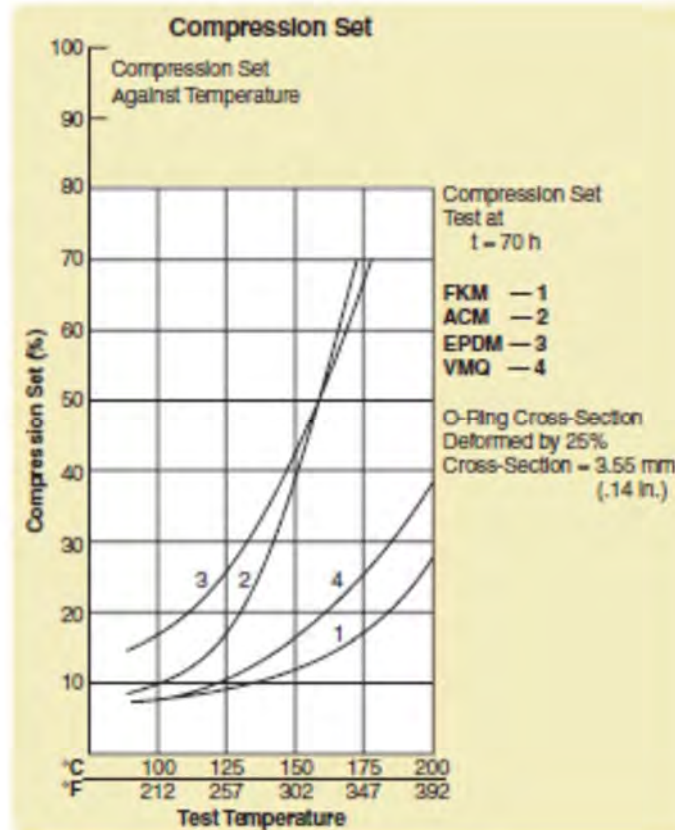
The 0.02% bolt plastic deformation permitted in NUREG/CR-6007 [Ref. 10] is distributed over the 67 mm bolt shank dimension shown in Detail 1 of Drawing RT-100 PE 1001-1 Rev. G (Chapter 1, Appendix 1.4, Attachment 1.4-2). This may result in a separation between the primary lid and cask flange mating surfaces of 0.0134 mm ($= 67\text{mm} \times 0.0002$). However, the primary lid seals are 12 +/-0.3 mm diameter EPDM rubber and the grooves for these seals are 9.4 +/- 0.15 mm deep (Drawing RT-100 PE 1001-1, Rev. G Appendix 1.4). Thus, the seal is minimally compressed 2.15 mm ($= (12 - 0.3) - (9.4 + 0.15)$). Considering that EPDM O-rings have a compression set of up to 45% at 150 °C (Figure 2.13.4-1), the minimum compression in the seal is 1.18 mm ($= 2.15 - 0.45 \times 2.15$). Since the minimum seal compression greatly exceeds the separation due to possible plastic deformation, the primary lid/cask flange containment boundary will remain sealed following an HAC drop event.

2.13.4.2 Secondary Lid Seals

The 0.02% bolt plastic deformation permitted in NUREG/CR-6007 [Ref.10] is distributed over the 43 mm bolt shank dimension shown in Detail 2 of Drawing RT-100 PE 1001-1 Rev G, (Chapter 1, Appendix 1.4, Attachment 1.4-2). This may result in a separation between the secondary and primary lid mating surfaces of 0.0086 mm ($= 43\text{mm} \times 0.0002$). However, the secondary seals are 12 +/-0.3 mm diameter EPDM rubber and the grooves for these seals are 9.4 +/- 0.15 mm deep (Drawing RT-100 PE 1001-1 Rev G (Chapter 1, Appendix 1.4, Attachment 1.4-2). Thus, the seal is minimally compressed 2.15 mm ($= (12 - 0.3) - (9.4 + 0.15)$). Considering that EPDM O-rings have a compression set of up to 45% (Figure 2.13.4-1) at 150 °C, the minimum compression in the seal is 1.18 mm ($= 2.15 - 0.45 \times 2.15$). Since the minimum seal compression greatly exceeds the separation due to possible plastic deformation, the primary to secondary lid containment boundary will remain sealed following an HAC drop event.

Figure 2.13.4-1 Compression Set vs. Temperature

(Figure 2-13 from Parker O-ring Handbook [Ref. 50])

**2.13.5 Vent Port Cover Plate O-Ring and Bolt Evaluation**

The RT-100 cask port cover utilizes a double polymer (EPDM) O-ring configuration face seal to protect the leak test port. For this evaluation the diameter of the outer O-ring is considered to maximize the seating force (Calculation Package RTL-001-CALC-ST-0203, Rev. 6 [Ref.60]). The port cover is sealed with six DIN912 M10 x 30-A4-70 bolts.

2.13.5.1 Vent Port Cover Plate O-Ring Evaluation

This section evaluates the vent port cover sealing force and calculates the preload to maintain a tight seal (Calculation Package RTL-001-CALC-ST-0203, Rev. 6 [Ref 60]).

2.13.5.1.1 O-ring Sealing Force

The O-ring requires a minimum 3.7 N/mm sealing force (Trelleborg, Appendix 1 [Ref. 58]). The force required to seat the polymer O-ring seal is:

$$F_s = Y_f \times C = 3.7 \times (\pi \times 136.6) = 1,587.8 \text{ N}$$

Where,

$$\begin{aligned} Y_f &= \text{Sealing force} \\ C &= \text{O-ring circumference} \end{aligned}$$

2.13.5.1.2 Vent Port Cover Plate Preload

The preload force available to maintain a tight seal that accounts for reduction in preload during HAC is:

$$P_L = F_c - P_{HAC} = 50,522 \text{ N}$$

Where,

$$\begin{aligned} F_c &= \text{Available closure force} \\ &= P_{\min} \times N_b \\ P_{\min} &= \text{Minimum preload per bolt} \\ &= T_{\min} / k / d \\ T_{\min} &= \text{Minimum torque } (-10\%, \text{ Chapter 7, Table 7.4.5-1}) \\ &= 24,300 \text{ N-mm} \\ k &= \text{Nut factor – non-lubricated condition} \\ &= 0.3 \\ d &= \text{Nominal bolt diameter} \\ &= 10 \text{ mm} \\ N_b &= \text{Number of bolts} \\ &= 6 \\ P_{HAC} &= \text{Loss of preload during HAC} \quad [\text{Ref. 10}] \\ &= 0.0002 \times E \times A_T \\ &= 8,910 \text{ N} \\ E &= \text{Modulus of elasticity} \\ &= 1.89 \times 10^{11} \text{ Pa @ } 100^\circ\text{C} \\ A_t &= \text{Tensile area of the bolt} \quad [\text{Ref. 27}] \\ &= 0.7854 \left(d - \frac{0.97431}{n} \right)^2 \\ &= 77.6386 \text{ mm}^2 \\ n &= \text{Number of threads per inch} \\ &= 16.93 \end{aligned}$$

2.13.5.1.3 Factor of Safety to Maintain a Tight Seal

Comparing the available preload force to the load required to maintain a tight seal, the factor of safety is:

$$FS = \frac{50,522}{1587.8} = 31.8$$

2.13.5.2 Bolt Evaluation

This section evaluates the vent port cover thread engagement and associate stress.

2.13.5.2.1 Thread Engagement

For the port cover, the mating internal and external threads are manufactured of materials of equal tensile strengths. To prevent stripping of the external threads, the minimum engagement length, L_e , is:

$$L_e = \frac{2 \times A_t}{\pi \times K_{n,max} \left[\frac{1}{2} + 0.57735 \times n \times (E_{s,min} - K_{n,max}) \right]}$$

$$= 2.46 \text{ mm}$$

Where,

$$K_{n,max} = 8.676 \text{ mm} \quad (\text{Machinery's Handbook [Ref. 27]})$$

$$E_{s,min} = 8.862 \text{ mm} \quad (\text{Machinery's Handbook [Ref. 27]})$$

The available thread length based on the drawings (RT-100 PE 1001-2 Rev G, Chapter 1, Appendix 1.4, Attachment 1.4-3) is 15.5 mm. Since 15.5 mm > 2.46 mm, there are sufficient threads to prevent stripping of the bolts.

2.13.5.2.2 Thread Shear Evaluation

The load necessary to shear the external threads due to the tensile force is:

$$P_s = 0.6 \times A_s \times S_y$$

$$= 121,044 \text{ N}$$

where,

$$A_s = \pi \times n \times L_e \times K_{n,max} \left[\frac{1}{2n} + 0.57735 (E_{s,min} - K_{n,max}) \right]$$

$$L_e = 15.5 \text{ mm}$$

$$S_y = 2.06 \times 10^8 \text{ Pa @ } 100^\circ\text{C}$$

The tensile force generated in the bolt is:

$$P_B = \frac{T}{\left(\frac{l}{2\pi} + \frac{d_2\mu}{2\cos\alpha} + \frac{(d+b)\mu}{4} \right)}$$

$$= 16,791 \text{ N}$$

where,

$$T = \text{Torque}$$

$$= 29700 \text{ N-mm}$$

$$d_2 = \text{Min major diameter} \quad [\text{Ref. 27}]$$

$$= d - 3/4H + EI$$

$$\begin{aligned}
 D &= 10 \text{ mm} \\
 H &= \text{Thread height ignoring flats} \\
 &= \frac{\sqrt{3}}{2} \times P = 1.299 \text{ mm} \\
 EI &= \text{Fundamental deviation} \quad [\text{Ref.27}] \\
 &= 0.032 \\
 P &= \text{Thread pitch} \\
 &= 1.5 \text{ mm} \\
 \alpha &= \text{Half thread angle} \\
 &= 30^\circ \\
 \mu &= \text{Coefficient of friction} \quad [\text{Ref. 27}] \\
 &= 0.15
 \end{aligned}$$

Comparing the load required to shear the external threads with the tensile force generated in the bolt, the factor of safety is:

$$\begin{aligned}
 \text{FS} &= \frac{121,044}{16,791} \\
 &= 7.2
 \end{aligned}$$

2.13.5.2.3 Load to Break Bolt

The load necessary to break the bolt is:

$$\begin{aligned}
 P &= S_u \times A_t \\
 &= 48,058 \text{ N}
 \end{aligned}$$

where,

$$S_u = 6.19 \times 10^8 \text{ Pa @ } 100^\circ\text{C}$$

Since the load required to break the bolt is less than the applied force ($48,058 \text{ N} > 16,791 \text{ N}$), the bolts will not fail.

2.14 Appendix – Fabrication Stress Evaluation

Manufacturing the RT-100 can introduce thermal stresses in the inner shell during the lead pouring process. These thermal stresses are evaluated in this section to provide assurance that the manufacturing process does not adversely affect the normal operation of the cask, or its ability to survive an accident.

According to Regulatory Position 7 of Regulatory Guide 7.6 [Ref. 4], any residual stresses in the containment vessel shell resulting from inelastic strain associated with the secondary local bending stresses (which are due to the lead pour thermal gradient) must be considered in the total stress range for normal and accident load conditions. Residual stresses in the containment vessel (inner shell) induced by shrinkage of the lead shielding after the lead pouring operation are relieved early in the life of the cask because of the low creep strength of lead.

The lead pour process is accomplished by first welding the inner and outer shells to the flange,

which forms an annular region between the shells. Prior to the lead pour process; the initial temperature of the inner and outer shells is pre-heated to approximately 350°C. The lead is heated until the molten temperature is between 390°C and 440°C. Molten lead is then poured continuously through the open end of the cask until the entire annular region is filled. Solidification is allowed only when the entire cavity is completely filled. Water is then used to cool the cask below 327°C, where solidification occurs. Following the pouring process, the cask is allowed to cool to ambient conditions.

2.14.1 Lead Pour

This section evaluates the stresses generated during the lead pouring process.

2.14.1.1 Cask Shell Geometry

At 21°C, the cask inner and outer shell geometry dimensions are:

Inner Shell

Inside Diameter (d_{i-21})	= 1.730 m
Outside Diameter (d_{o-21})	= 1.790 m
Shell Thickness (t_i)	= 0.030 m

Outer Shell

Inside Diameter (D_{i-21})	= 1.970 m
Outside Diameter (D_{o-21})	= 2.040 m
Shell Thickness (T_o)	= 0.035 m

2.14.1.2 Stresses Resulting from Lead Pour

The hydrostatic pressure, Q, produced by the column of lead is:

$$Q = \rho \times h \times g = 224.8 \text{ kPa}$$

Where:

$$\rho = 11340 \text{ kg/m}^3 \text{ (lead density)}$$

$$h = 2.021 \text{ m (maximum height of lead column)}$$

$$g = 9.81 \text{ m/s}^2$$

For this analysis, it is assumed that the lead reaches a maximum temperature of 440°C, and the shells, initially at 21°C, reach an equilibrium temperature of 440°C. At 440°C, key shell geometric dimensions are:

$$d_{o-400} = d_{o-21}(1 + \alpha\Delta T) = 1.80 \text{ m}$$

$$D_{i-400} = D_{i-21}(1 + \alpha\Delta T) = 1.99 \text{ m}$$

$$t_{i-400} = t_{i-21}(1 + \alpha\Delta T) = 0.0302 \text{ m}$$

Where:

$$\alpha = 1.824 \times 10^{-5} \text{ m/m/}^{\circ}\text{C at } 440^{\circ}\text{C (stainless steel)}$$

$$\Delta T = 400 - 21 = 419^{\circ}\text{C}.$$

The hydrostatic pressure of the molten lead subjects the inner shell to an external hydrostatic pressure. The hydrostatic pressure varies from a maximum of 224.8 kPa at the bottom of the inner shell to 0 psi at the top of the lead cylinder. Using Table 29, Case 6 of “Roark’s Formula for Stress and Strain” [Ref. 29], the deformation at the bottom of the inner shell y_B is found to be $-3.567 \times 10^{-5} \text{ m}$. The maximum circumferential membrane stress in the inner shell is:

$$S_{\theta_{\max}} = \frac{y_B E}{R} = -6.67 \text{ MPa}$$

Where:

$$E = 168.5 \text{ GPa at } 399^{\circ}\text{C}$$

$$R = 1.80/2 = 0.90 \text{ m}$$

This stress exists only as long as the lead is molten and produces no plastic deformation of the inner shell. When the lead solidifies and begins to cool, it shrinks and exerts a uniform external pressure on the inner shell due to the lead coefficient of expansion being larger than that of stainless steel.

2.14.2 Cool-down

This section evaluates the stresses that occur during the cool-down process.

Proprietary Information Content Withheld Under 10 CFR 2.390(b)

Proprietary Information Content Withheld Under 10 CFR 2.390(b)

 Proprietary Information Content Withheld Under 10 CFR 2.390(b)

2.14.2.2 Axial Stress

Axial stresses develop in the lead shell and inner shell during fabrication as a result of the unequal shrinkage of the lead and steel shells. Assuming that the lead bonds to the inner shell during the cool-down process after completion of lead pouring, the stress in the lead when cooled to 21°C is:

$$S_{\text{lead}} = \epsilon E = 3.44 \times 10^{-3} \times 16.7 \times 10^9 = 57.4 \text{ MPa}$$

Where:

$$\epsilon_{\text{lead}} = (\alpha_{\text{lead}} - \alpha_{\text{shell}}) \Delta T = 3.44 \times 10^{-3} \text{ m/m}$$

$$\alpha_{\text{lead}} = 2.90 \times 10^{-5} \text{ m/m/}^\circ\text{C}$$

$$\alpha_{\text{shell}} = 1.78 \times 10^{-5} \text{ m/m/}^\circ\text{C}$$

$$\Delta T = 327 - 21 = 327^\circ\text{C}$$

$$E = E_{\text{lead70}} = 16.7 \text{ GPa}$$

The calculated stress is above the yield point of lead (ranging between 5 and 19 MPa at 21°C). The axial load placed on the steel inner shell by shrinkage of the lead is therefore limited by the yield strength of lead. The maximum load imposed by the lead is:

$$P_{\text{lead}} = 19 \times \pi (0.985^2 - 0.895^2) = 1.010 \times 10^7 \text{ N}$$

The corresponding compression stress in the inner shell to maintain equilibrium is:

$$S_{\text{shell}} = \frac{P}{A} = \frac{-1.010 \times 10^7}{\pi((0.985)^2 - (0.895)^2)} = -60.9 \text{ MPa}$$

This value is conservative because the yield strength of lead is very low at elevated temperatures (approximately 3 MPa) and therefore, the creep rate is high. Also, complete bonding of the lead to the stainless steel inner shell is not expected to occur. This case bounds others axial loading configurations since the calculation is based on the yield strength of lead at 21°C.

2.14.2.3 Effects of Temperature Differential during Cool-down

The preceding analyses assume that the inner shell and lead are always at the same temperature at any time during the cool-down process. This assumption may not be true under actual conditions. Because of the high thermal conductivity of the stainless steel and the lead, the temperature differential between the lead and steel inner shell is kept to a minimum. If the inner shell is cooler than the lead, the interference and the corresponding interface pressure and resulting hoop stresses are less than the equal temperatures case. Hence, the preceding analysis is conservative. An analysis is required if the inner shell is hotter than the lead shield. Assuming the temperature of the inner shell is 59°C and the lead is 21°C, the inner radius of the stress-free lead shell at 21°C is 0.892 m; the outer radius of the inner shell at 59°C is:

$$r_o = 0.892 [1 + (1.53 \times 10^{-5})(38)] = 0.893 \text{ m}$$

The interference between the inner shell and the lead is $0.893 - 0.892 = 0.001 \text{ m}$. To accommodate this interference, the lead must deform 0.001 m. For $\delta = 0.001 \text{ m}$, the maximum circumferential stress $S_{\theta\max}$ in the inner shell is:

$$S_{\theta\max} = \frac{\delta(E)}{R} = 9.7 \text{ MPa}$$

where

$$R = 1.784/2 = 0.892 \text{ m}$$

$$E = E_{\text{lead70}} = 16.7 \text{ GPa}$$

2.14.3 Lead Creep

As discussed previously, cooling of the lead shell and inner shell introduces acceptably low hoop and axial stresses in the inner shell. These stresses are relieved early in the life of the cask since lead demonstrates a significant creep rate at both room and elevated temperatures.

2.15 Appendix – Seal Region Stress Evaluation

To provide assurance that the primary and secondary cask seals meet the linear elastic requirements of Regulatory Guide 7.6 [Ref. 4] the contact stresses that represent the maximum nodal stresses on the sealing surfaces and the linearized nodal stresses in the solid elements that comprise the seal regions are evaluated and compared to the yield strength of the material at the maximum NCT temperature. The evaluation shows that the RT-100 seal region does not undergo inelastic deformation.

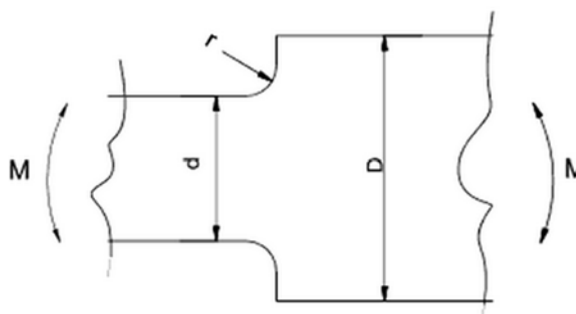
2.15.1 Seal Region Post-Processing Methodology

The cask body calculation reports the primary membrane and membrane plus bending stress

intensities averages across linearized sections. To evaluate the stresses in the lid gasket region, the lid component is first selected as shown in Figure 2.15.4-1. As shown in Figure 2.15.4-2, the elements comprising the lid gasket region are then selected to evaluate the stresses specific to the primary gasket location. Visual inspection of the model shows the location of the peak stress in the gasket region and the nodes are identified to calculate the average stress. The ANSYS finite element program [Ref. 28] calculates the average stress across a section by identifying the nodal points using the ANSYS APDL commands PATH, PDEF and PPATH. Figure 2.15.4-2 provides an example of where 2 points are defined across the gasket region. Once the points and path are defined, the ANSYS APDL command PRSECT reports the average stresses.

2.15.2 Stress Concentration Factors

Trapezoidal grooves are cut into the primary and secondary lids to allow the gaskets to properly seat during the closure process. Figure 2.15.4-3 shows the lid/gasket geometry. Under load, the grooves can cause a stress riser at the radius, r , where the groove transitions from horizontal to vertical ("Standard Handbook for Mechanical Engineers" [Ref. 55]). For this evaluation, the load is in the form of a bending moment. Using the dimensions provided in Figure 2.15.4-3 and Table 2.15.4-1, the resulting stress concentration factors are calculated in terms of the ratios of D/d and r/d . For the primary and secondary lids, the stress concentration factors are 2.6 and 2.2, respectively.



2.15.3 Seal Region Stress Results

The contact stresses that represent the maximum nodal stresses on the sealing surfaces are summarized in Table 2.15.4-2. The resulting membrane plus bending stresses are compared to the yield stress of the material at the maximum NCT temperature for each HAC case.

For the lid gasket grooves, the linearized stress is calculated for each peak stress location as described in Section 2.15.1 and multiplied by the stress concentration factor calculated in Section 2.15.2. Table 2.15.4-3 provides a summary of the resulting factored stress values. As the table shows the minimum factor of safety is 1.2 in accordance with Regulatory Guide 7.6 [Ref.4], the RT-100 seal region experiences no inelastic deformation during all HAC events.

2.15.4 Displacement Results

To determine whether the seal remains tight during HAC, the relative displacement of each sealing surface is determined. Table 2.15.4-4 calculates the relative displacement for each sealing surface and Figure 2.15.4-4 through Figure 2.15.4-9 provide graphical representations of the displacement for each case. From the containment evaluation, the permanent plastic deformation for the EPDM O-ring is approximately 25%. Therefore, based on the seal dimensions, the maximum permissible gap is 1.61mm. Reviewing the relative displacements from Table 2.15.4-4, the maximum separation that occurs is 0.07706mm. Since this maximum separation is less than the permissible gap, the seals are predicted to remain tight during all HAC events.

Table 2.15.4-1 Stress Concentration Factors

D/d	r/d							
	0.01	0.02	0.04	0.06	0.1	0.15	0.2	0.3
1.01	1.76	1.53	1.37	1.32	1.28	1.25	1.22	1.19
1.02	2.05	1.74	1.52	1.42	1.35	1.28	1.25	1.22
1.05	2.58	2.11	1.77	1.62	1.47	1.40	1.34	1.29
1.10	3.09	2.45	2.00	1.80	1.59	1.49	1.40	1.31
1.20	3.62	2.81	2.23	1.97	1.70	1.55	1.44	1.34
1.50	3.80	2.98	2.38	2.15	1.83	1.63	1.52	1.38
2.00		3.14	2.59	2.23	1.88	1.66	1.54	1.40
3.00		3.30	2.68	2.34	1.93	1.67	1.53	1.38

Table 2.15.4-2 Sealing Surface Stress Summary

Accident Condition	Yield Strength at Max. NCT Seal Temp (MPa)	Primary Sealing Surface Contact Stress (MPa)	FS	Primary Seal Linearized Stress Intensity $P_m + P_b$ (MPa)	FS	Secondary Sealing Surface Contact Stress (MPa)	FS	Secondary Seal Linearized Stress Intensity $P_m + P_b$ (MPa)	FS
Side Drop	184.2	40.1	4.6	15.6	11.8	5.7	32.3	33.7	5.5
End Drop	184.2	22.8	8.1	14.3	12.9	0.0	N/A	62.7	2.9
Puncture	184.2	93.2	2.0	77.0	2.4	83.4	2.2	89.7	2.1

Table 2.15.4-3 Lid Seal Groove Region Stresses

Accident Condition	Yield Strength at Max NCT Seal Temp (MPa)	Stress Concentration	Linearized Stress in Primary Lid Primary Seal (MPa)	Maximum Stress (MPa)	FS	Stress Concentration	Linearized Stress in Secondary Lid Primary Seal (MPa)	Maximum Stress (MPa)	FS
Side Drop	184.2	2.6	15.0	38.9	4.7	2.2	66.1	145.3	1.3
End Drop	184.2	2.6	45.1	115.9	1.6	2.2	47.7	102.6	1.8
Puncture	184.2	2.6	59.1	153.6	1.2	2.2	71.8	158.0	1.2

Table 2.15.4-4 HAC Seal Region Displacement

Location	Minimum Displacement (mm)	Maximum Displacement (mm)
HAC Side Drop		
Primary Lid Sealing Surface	-0.047281	-0.33065
Primary Seal Flange Surface	-0.043598	-0.40771
Relative Displacement	↓ -0.003683	↑ 0.07706
Secondary Lid Sealing Surface	-0.12481	-0.31864
Secondary Lid Sealing Surface on Primary Lid	-0.12238	-0.34072
Relative Displacement	↓ -0.00243	↑ 0.02208
HAC End Drop		
Primary Lid Sealing Surface	-0.27689	-0.43679
Primary Seal Flange Surface	-0.27867	-0.43227
Relative Displacement	↑ 0.00178	↓ -0.00452
Secondary Lid Sealing Surface	-0.93881	-1.08
Secondary Lid Sealing Surface on Primary Lid	-0.93328	-1.1009
Relative Displacement	↓ -0.00553	↑ 0.0209
Puncture		
Primary Lid Sealing Surface	0.044821	-0.12329
Primary Seal Flange Surface	0.046104	-0.1212
Relative Displacement	↑ -0.001283	↓ -0.00209
Secondary Lid Sealing Surface	-0.85594	-1.1537
Secondary Lid Sealing Surface on Primary Lid	-0.84898	-1.1475
Relative Displacement	↓ -0.00696	↑ -0.0062

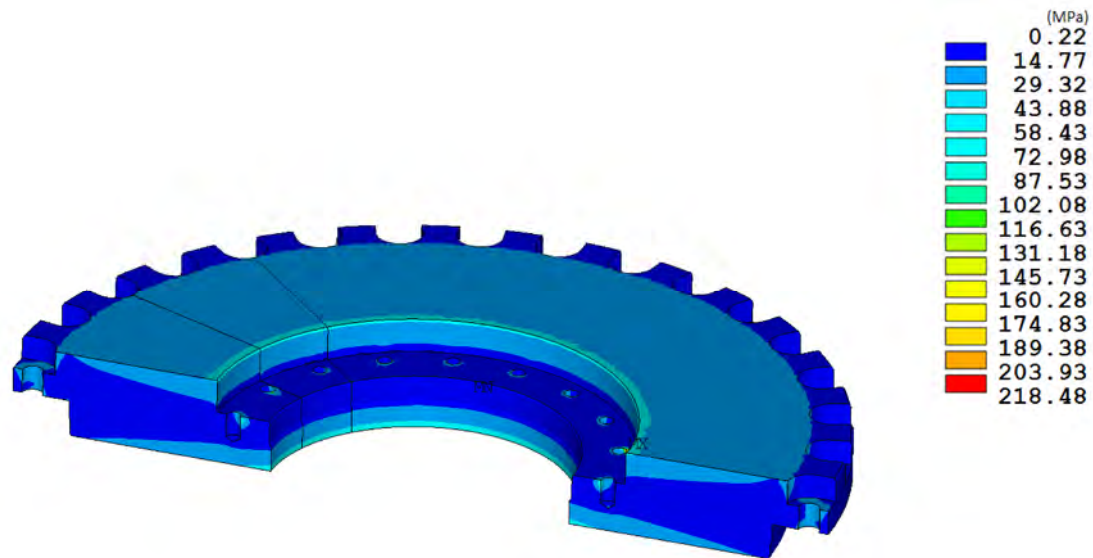


Figure 2.15.4-1 Stress Intensity Contour Plot of Primary Lid Following End Drop.

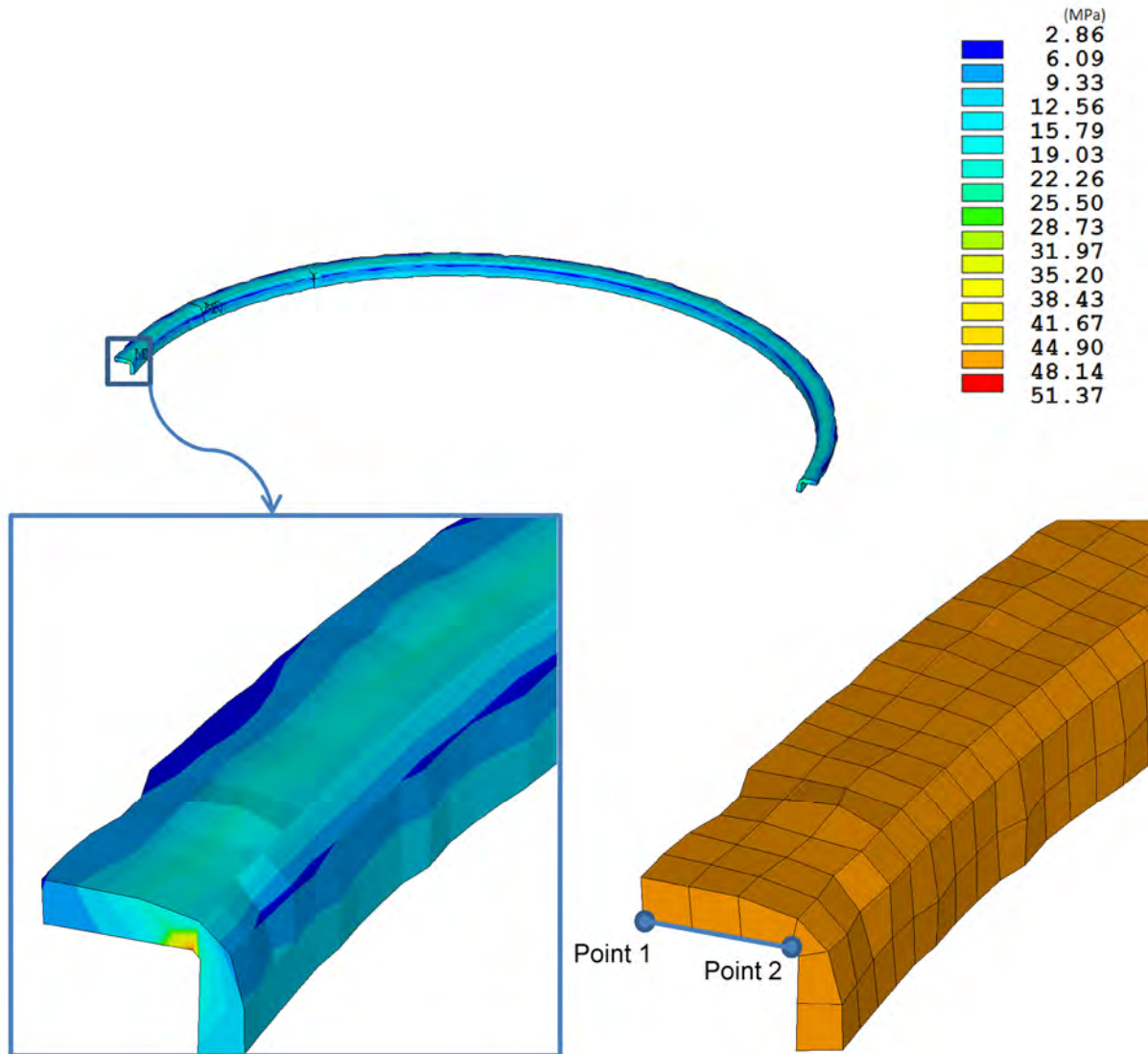


Figure 2.15.4-2 Stress Intensity Contour Plot of the Primary Seal Region

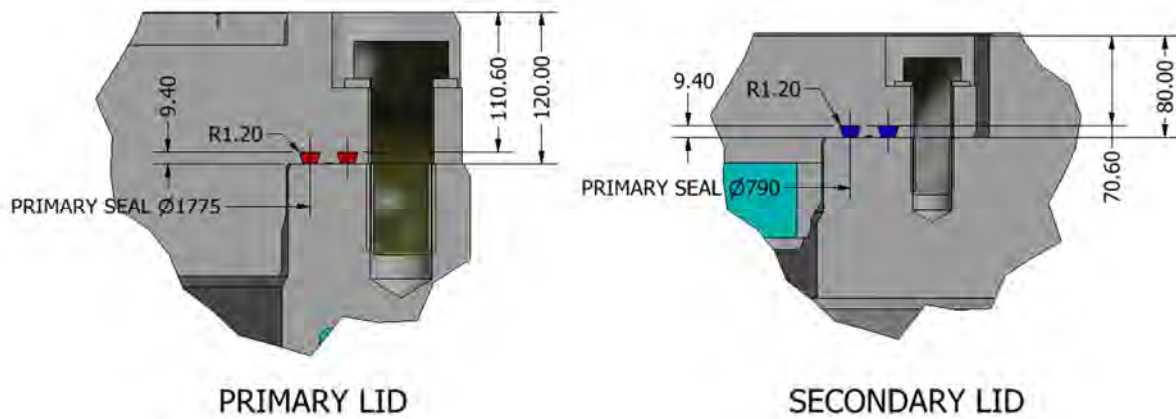


Figure 2.15.4-3 Lid Seal Geometry

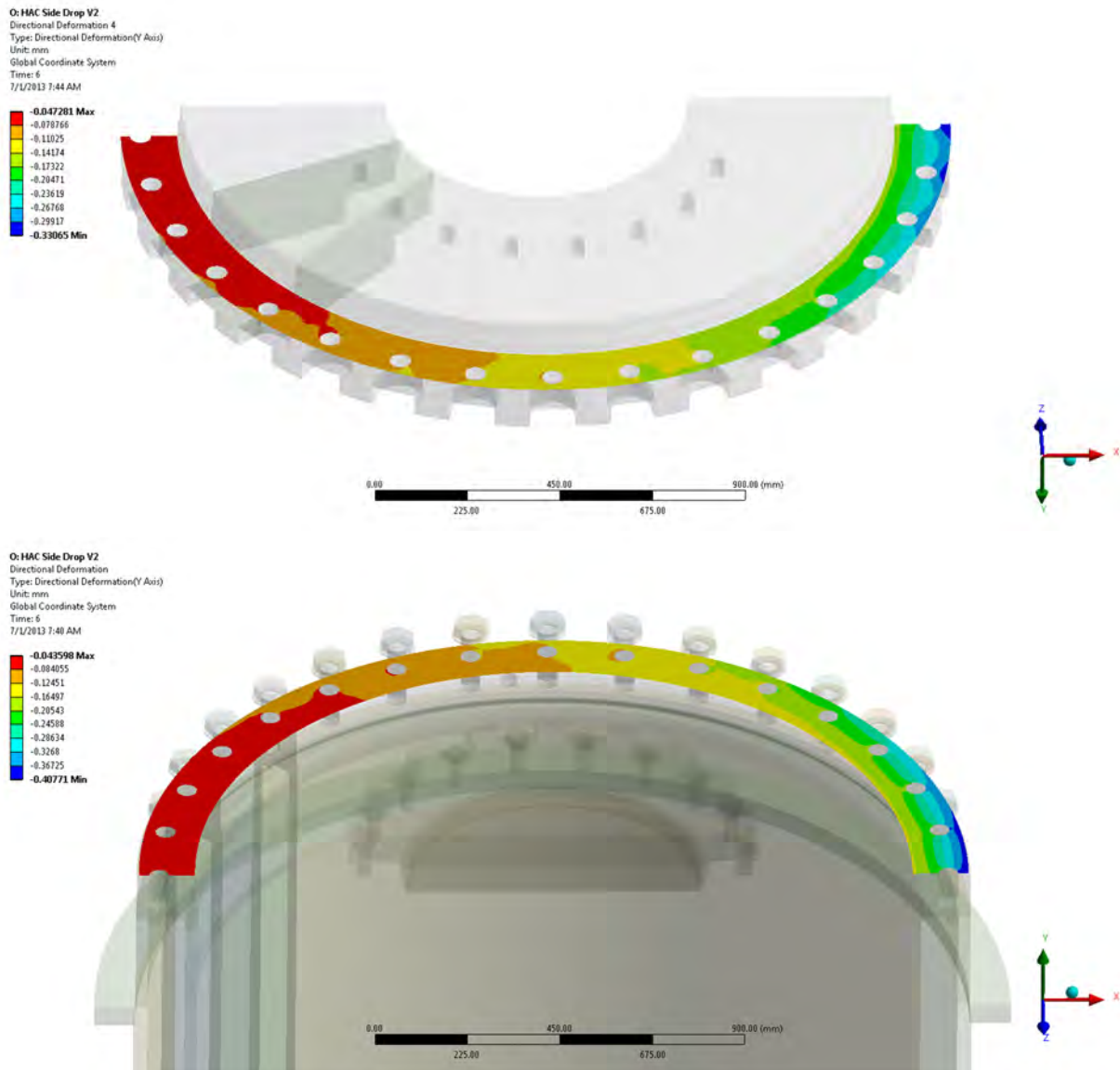


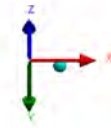
Figure 2.15.4-4 Primary Lid Sealing Surface Displacement during Side drop

O: HAC Side Drop V2
Directional Deformation 6
Type: Directional Deformation(Y Axis)
Unit: mm
Global Coordinate System
Time: 6
7/1/2013 7:47 AM

-0.12481 Max
-0.14635
-0.16788
-0.18942
-0.21096
-0.23249
-0.25403
-0.27557
-0.29711
-0.31864 Min

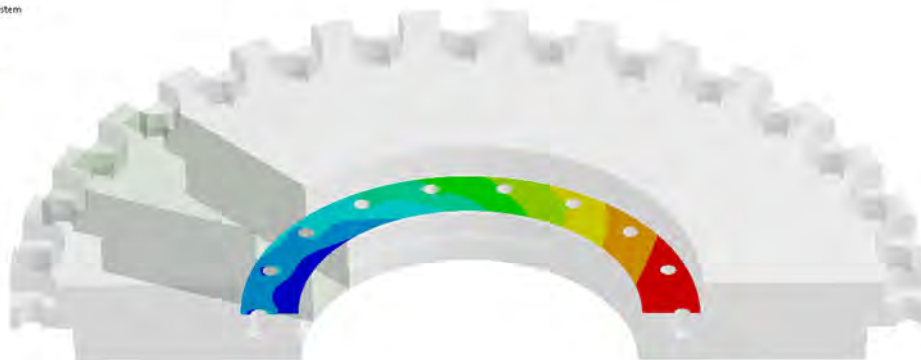


0.00 150.00 300.00 450.00 600.00 (mm)



O: HAC Side Drop V2
Directional Deformation 5
Type: Directional Deformation(Y Axis)
Unit: mm
Global Coordinate System
Time: 5
7/1/2013 7:45 AM

-0.12238 Max
-0.14664
-0.1709
-0.19516
-0.21942
-0.24368
-0.26794
-0.2922
-0.31646
-0.34072 Min



0.00 200.00 400.00 600.00 800.00 (mm)

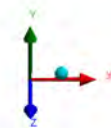


Figure 2.15.4-5 Secondary Lid Sealing Surface Displacement during Side drop

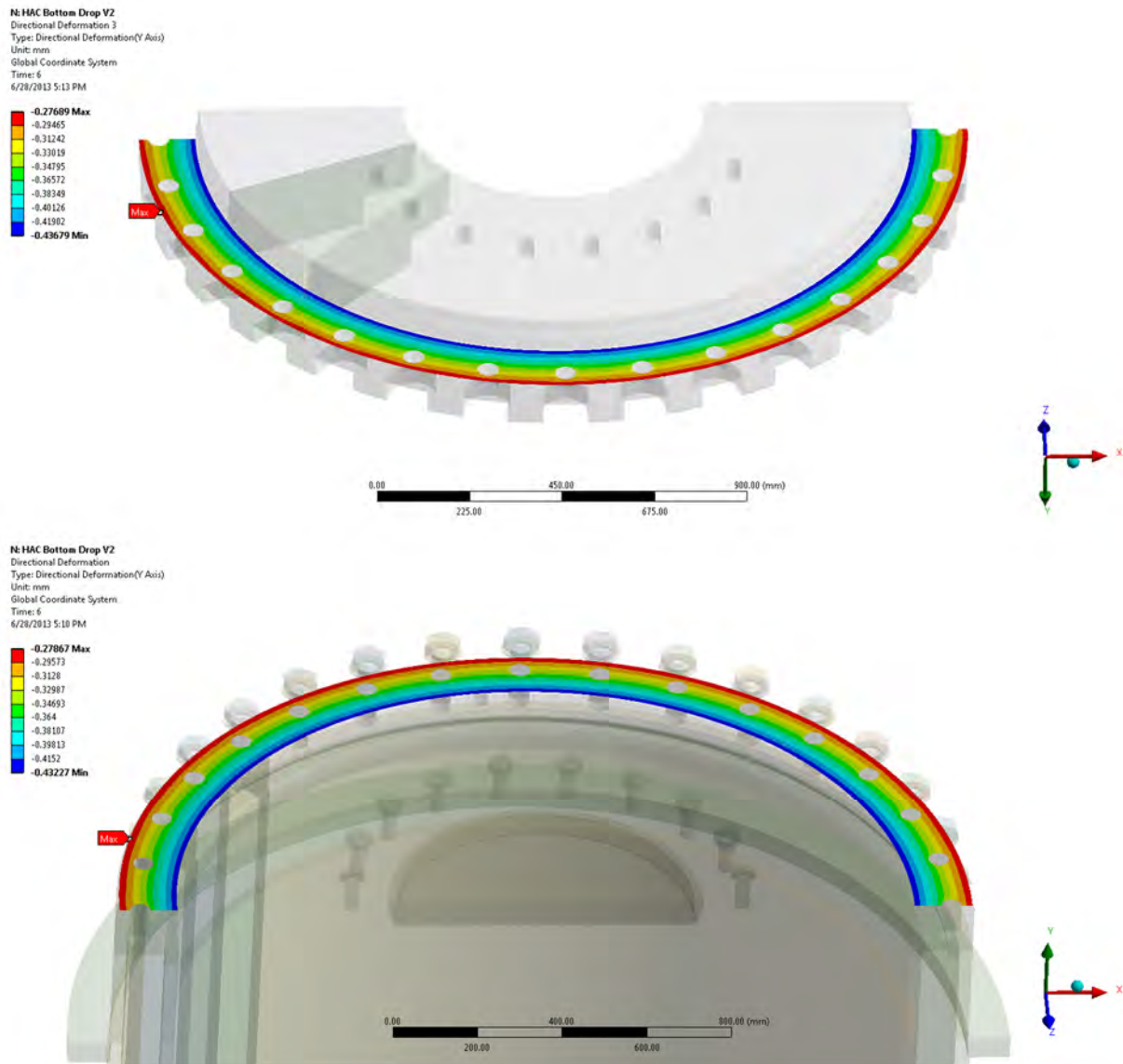


Figure 2.15.4-6 Primary Lid Sealing Surface Displacement during End drop

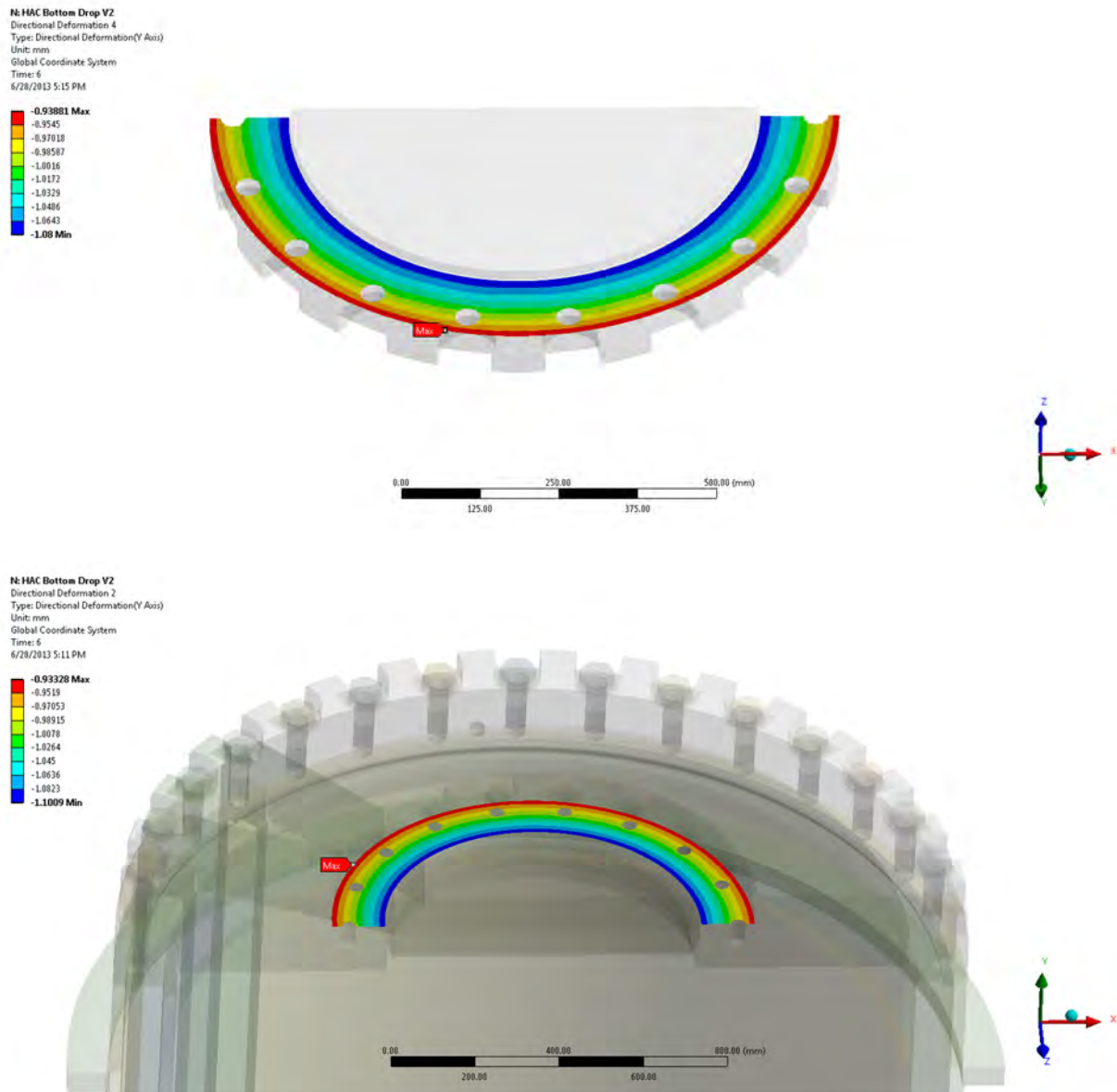


Figure 2.15.4-7 Secondary Lid Sealing Surface Displacement during End drop

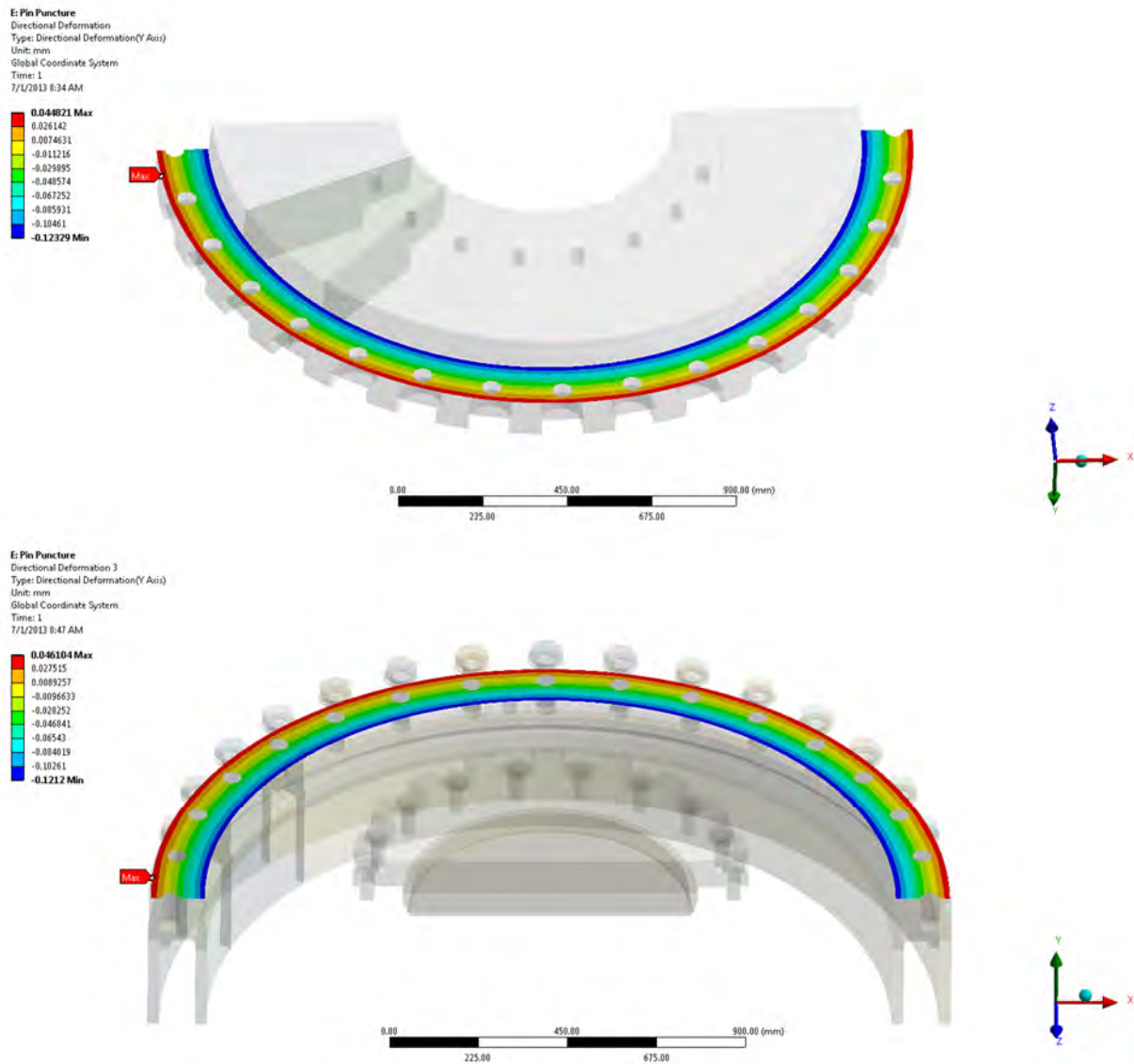


Figure 2.15.4-8 Primary Lid Sealing Surface Displacement during Puncture

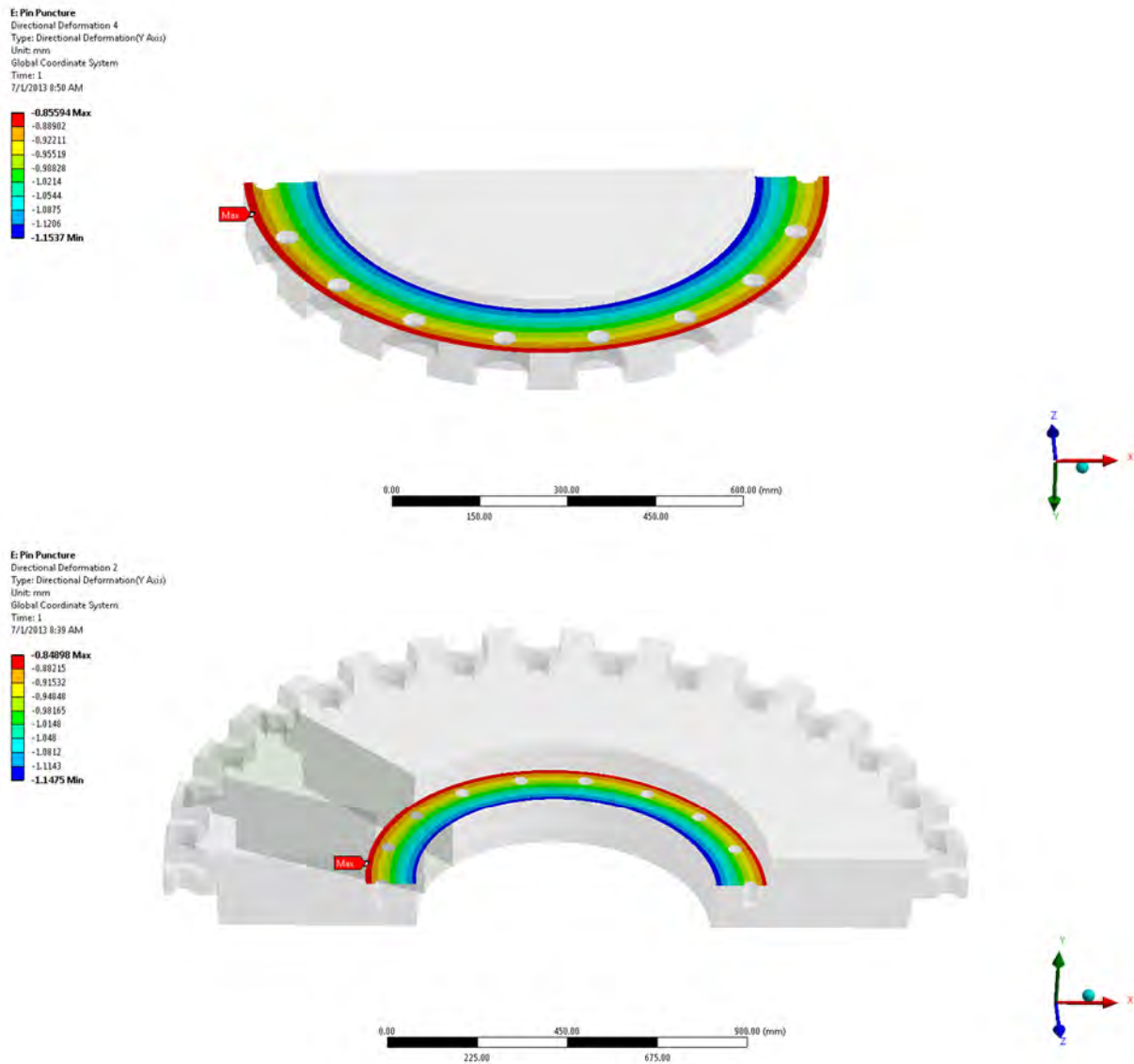


Figure 2.15.4-9 Secondary Lid Sealing Surface Displacement during Puncture

2.16 References

1. Robatel Technologies, LLC, Quality Assurance Program for Packaging and Transportation of Radioactive Material, 10 CFR 71 Subpart H, Rev. 2, Dated November 10, 2017 and NRC Approved on March 21, 2012
2. U.S. Nuclear Regulatory Commission, 10 CFR Part 71--PACKAGING AND TRANSPORTATION OF RADIOACTIVE MATERIAL, dated March 7, 2012 and the following specific Sections:

71.31(a)(1)	71.31(a)(2)	71.33	71.35(a)
71.71	71.73	71.41(a)	71.45
71.85(b)	71.4	71.73(c)(1)	71.73(c)(3)
71.85	71.43	71.45(a)	71.45(b)
7.51	71.73(b)	71.71(c)	71.55(e)
71.59(a)(2)	71.85(b)	71.55	71.61
71.74	71.55(f)	71.75	

3. U.S. Nuclear Regulatory Commission, "Load Combinations for the Structural Analysis of Shipping Casks for Radioactive Material," Regulatory Guide 7.8.
4. U.S. Nuclear Regulatory Commission, "Design Criteria for the Structural Analysis of Shipping Cask Containment Vessels," Regulatory Guide 7.6.
5. U.S. Nuclear Regulatory Commission, "Fracture Toughness Criteria of Base Material for Ferritic Steel Shipping Cask Containment Vessels with a Maximum Wall Thickness of 4 Inches (0.1m)," Regulatory Guide 7.11.
6. U.S. Nuclear Regulatory Commission, "Fabrication Criteria for Shipping Containers," NUREG/CR-3854, March 1985.
7. ASME Boiler & Pressure Vessel Code 2007 Edition, Section III – Division 1 – Subsection ND, "Class 3 Components", The American Society of Mechanical Engineers, Three Park Avenue, New York, NY, www.asme.org.
8. ASME Boiler & Pressure Vessel Code 2007 Edition, Section III – Division 1 – Subsection NF, "Supports", The American Society of Mechanical Engineers, Three Park Avenue, New York, NY, www.asme.org.
9. U.S. Nuclear Regulatory Commission, "SCANS (Shipping Cask Analysis System): A Microcomputer Based Analysis System for Shipping Cask Design Review," NUREG/CR-4554, Volumes 3, 6 and 7, February 1990.
10. U.S. Nuclear Regulatory Commission, "Stress Analysis of Closure Bolts for Shipping Casks," NUREG/CR-6007, January 1993.
11. NUREG/CR-0481, "An Assessment of Stress-Strain Data Suitable for Finite-Element Elastic-Plastic Analysis of Shipping Containers," Rack, H. & Knorovsky, G., Sandia Laboratories, Albuquerque, NM, September 1978, Retrieved on August 28, 2013, Retrieved from http://rampac.energy.gov/docs/nrcinfo/NUREG_0481.pdf.

12. U.S. Nuclear Regulatory Commission, Standard Review Plan for Transportation Packages for Radioactive Material, NUREG-1609, March 31, 1999
13. U.S. Government Code of Federal Regulations, Request for Withholding Information Contained in License Application, 10 CFR 2.790
14. U.S. Nuclear Regulatory Commission, "Dynamic Analysis to Establish Normal Shock and Vibration of Radioactive Material Shipping Packages, Volume 3: Final Summary Report," NUREG/CR-2146, Vol. 3, October 1983.
15. U.S. Nuclear Regulatory Commission, "Engineering Drawings for 10 CFR Part 71 Package Approvals," NUREG/CR-5502, May 1998.
16. U.S. Nuclear Regulatory Commission, "Fracture Toughness Criteria of Base Material for Ferritic Steel Shipping Cask Containment Vessels with a Wall Thickness Greater than 4 Inches (0.1m)," Regulatory Guide 7.12.
17. U.S. Nuclear Regulatory Commission, "Methods for Impact Analysis of Shipping Containers," NUREG/CR-3966, November 1987.
18. U.S. Nuclear Regulatory Commission, "Puncture Testing of Shipping Packages under 10 CFR Part 71," Bulletin 97-02, September 23, 1997.
19. U.S. Nuclear Regulatory Commission, "Recommended Welding Criteria for Use in the Fabrication of Shipping Containers for Radioactive Materials," NUREG/CR-3019, March 1985.
20. U.S. Nuclear Regulatory Commission Bulletin, 97-02.
21. U.S. Nuclear Regulatory Commission, "Shock and Vibration Environments for a Large Shipping Container During Truck Transport (Part II)," NUREG/CR-0128, August 1978.
22. U.S. Nuclear Regulatory Commission, Dynamic Analysis to Establish Normal Shock and Vibration of Radioactive Material Shipping Packages, NUREG-2146, Volumes 1, 2 and 3, dated January 1, 1981-March 31, 1981; April 1, 1981-June 30, 1981; and October 1993, respectively.
23. U.S. Nuclear Regulatory Commission, International Agreement Report, International Code Assessment and Applications Program: Summary of Code Assessment Studies Concerning RELAP5/MOD2, RELAP5/MOD3, and TRAC-B, December 1993.
24. Bickford, J. & Looram, M., "Good Bolting Practices – A Reference Manual for Nuclear Power Plant Maintenance Personnel, Volume 1: Large Bolt Manual," Yalesville, CT: Electric Power Research Institute, 1987.
25. Blodgett, O. W., "Design of Welded Structures", The James F. Lincoln Arc Welding Foundation, Cleveland, Ohio.
26. AISC, "Guide to Design Criteria for Bolted and Riveted Joints", 2nd Edition, 2007.
27. Oberg, Erik, "Machinery's Handbook", 26th Edition.
28. ANSYS, Release 14.0, ANSYS, Inc., Canonsburg, PA, October, 2011
29. Young, Warren C., "Roark's Formulas for Stress and Strain", 6th Edition.

30. U.S. Nuclear Regulatory Commission, "Shock and Vibration Environments for a Large Shipping Container During Truck Transport" NUREG-0128.
31. ASME Boiler & Pressure Vessel Code 2010 Edition, Section II – Part D, "Materials", The American Society of Mechanical Engineers, Three Park Avenue, New York, NY, www.asme.org.
32. ASME Boiler & Pressure Vessel Code 2007 Edition, Section III – Division 1 – Subsection NB, "Class 1 Components", The American Society of Mechanical Engineers, Three Park Avenue, New York, NY, www.asme.org.
33. RTL-001-CALC-ST-0201, Rev. 5, "Lifting Structural Evaluation" (PROPRIETARY)
34. RTL-001-CALC-ST-0202, Rev. 4, "Tie-Down Evaluation" (PROPRIETARY)
35. RTL-001-CALC-ST-0402, Rev. 4, "Cask Body Structural Evaluation" (PROPRIETARY)
36. RTL-001-CALC-ST-0403, Rev. 4, "Pin Puncture Evaluation" (PROPRIETARY)
37. WM2001 Conference paper, "Benchmarking of LS-DYNA for Use with Impact Limiters," Joseph C. Nichols III, Michael E. Cohen, Robert A. Johnson, 2001.
38. RTL-001-CALC-TH-0102, Rev. 6, "RT-100 Cask Maximum Normal Operating Pressure Calculation" (PROPRIETARY)
39. Bickford, J. & Looram, M., "Good Bolting Practices – A Reference Manual for Nuclear Power Plant Maintenance Personnel, Volume 1: Large Bolt Manual," Yalesville, CT: Electric Power Research Institute, 1987.
40. RTL-001-CALC-ST-0401, Rev. 6, "RT-100 Cask Impact Limiter Drop Evaluation" (PROPRIETARY)
41. U.S. Nuclear Regulatory Commission, "Methods for Impact Analysis of Shipping Containers", NUREG/CR-3966.
42. RTL-001-CALC-TH-0102, Rev. 6, "RT-100 Cask Maximum Normal Operating Pressure Calculation" (PROPRIETARY)
43. RTL-001-CALC-TH-0202, Rev. 6, "RT-100 Cask Hypothetical Accident Condition Maximum Pressure Calculation" (PROPRIETARY)
44. ASME B1.13M-2005, METRIC SCREW THREADS: M PROFILE.
45. PAP 008, Specification D'approvisionnement - Mousse Polyurethane - Emballage de TRANSPORT RT-100 (Procurement Specification - Polyurethane Foam - Packaging of TRANSPORT RT-100), Rev. D, ROBATEL Industries (PROPRIETARY)
46. RES 001, Safety Analysis Robatel Package Model RT-100 Drop Test Report, Rev. E, ROBATEL Industries (PROPRIETARY)
47. Drawing 102885 MD 2021-06 Rev. D, "Robatel Transport Package RT100" (PROPRIETARY)
48. Certificate of Conformance for Purchase Order #117039 (Certificate for RT100 Scaled Foam Model) dated 09-07-2012 (PROPRIETARY)
49. U.S. Nuclear Regulatory Commission, "Standard Format and Content of Part 71 Applications for Approval of Packages for Radioactive Material," Regulatory Guide 7.9.

-
50. Parker O-Ring Handbook ORD 5700, Retrieved on August 28, 2013, Retrieved from http://www.parker.com/literature/ORD%205700%20Parker_O-Ring_Handbook.pdf.
 51. Baumeister T. and Marks, L.S. "Standard Handbook for Mechanical Engineers, 7th Edition". New York: McGraw-Hill Book Co., 1967.
 52. U.S. Nuclear Regulatory Commission Bulletin, 96-04.
 53. U.S. Nuclear Regulatory Commission Interim Staff Guidance, "Use of Computational Modeling Software", ISG-21.
 54. Glenn Lee, Radiation Resistance of Elastomers, IEEE Transactions on Nuclear Science, Vol. NS-32, No. 5, October 1985.
 55. Baumeister T. and Marks, L.S. "Standard Handbook for Mechanical Engineers, 9th Edition". New York : McGraw-Hill Book Co., 1987.
 56. ANSI N14.6-1978, "American National Standard for Special Lifting Devices for Shipping Containers Weighing 10000 pounds (4500 kg) or More for Nuclear Materials," American National Standards Institute, Inc., 11 West 42nd Street, New York, NY, www.ansi.org.
 57. KTA 3905, "Load Attaching Points on Loads in Nuclear Power Plants," Safety Standards of the (German) Nuclear Safety Standards Commission, June 1999 Edition including rectification of July 2000.
 58. TRELLEBORG Sealing Solutions O-Ring and Backup Rings Catalog, August 2011 Edition
 59. Shappert, L.B. "The Radioactive Materials Packaging Handbook". Oak Ridge, Tennessee: Oak Ridge National Laboratory, 1988. ORNL/M-5003.
 60. RTL-001-CALC-ST-0203, Rev. 6, "RT-100 Bolting Calculation" (PROPRIETARY)
 61. GENERAL PLASTICS Design Guide for LAST-A-FOAM FR-3700 Crash & Fire Protection of Radioactive Material Shipping Containers, Rev. 02.20.12
 62. J. F. Harvey, Theory and Design of Pressure Vessels, New York: Van Nostrand Reinhold, 1991.
 63. CN-13039-203, Rev. 0, "RT-100 Cask Lead Shrinkage Evaluation" (PROPRIETARY)

This page is intentionally left blank.

3. THERMAL EVALUATION

Robatel has performed a thermal evaluation of the RT-100 using the Nuclear Industry standards and under the RT Company Quality Assurance Program [Ref. 1]. This thermal evaluation shows that the RT-100 meets or exceeds all the 10 CFR 71 regulatory requirements [Ref. 2]. The thermal review is based in part on the descriptions and evaluations presented in the General Information Chapter 1 and Structural Evaluation Chapter 2 of the application. Similarly, results of the thermal review are considered in the review of several other sections of the application. An example of information flow for the thermal review is shown in Figure 3-1.

RT identified, described, discussed, and analyzed the principal thermal engineering design of the RT-100, components, and systems that are important to safety. Section 3 describes how the package complies with the performance requirements of 10 CFR 71 [Ref. 2]. Results of the thermal evaluation verified that the thermal performance of the RT-100 design (for both NCT and HAC) meets the thermal regulatory requirements as follows:

- The RT-100 design is evaluated to demonstrate that it satisfies the thermal requirements of 10 CFR 71.31(a)(1) ; 10 CFR 71.31(a)(2); 10 CFR 71.33, and 10 CFR 71.35(a) [all Ref. 2].
- The application identifies the established codes and standards used for the thermal design according to 10 CFR 71.31(c) [Ref. 2].
- The performance of the RT-100 is evaluated under the tests specified in 10 CFR Part 71.71 [Ref. 2] for NCT and 10 CFR Part 71.73 [Ref. 2] for HAC and also referenced 10 CFR 71.41(a) [Ref. 2].
- The RT-100 is designed, constructed, and prepared for transport so that there is no significant decrease in packaging effectiveness under the tests specified in 10 CFR 71.71 (NCT) and references in 10 CFR 71.43(f) and 71.51(a)(1) [all Ref. 2].
- The RT-100 is designed, constructed, and prepared for transport so that the accessible surface temperature does not exceed the regulatory limits specified in 10 CFR 71.43(g) [Ref. 2].
- The RT-100 design does not rely on mechanical cooling systems to meet containment requirements in reference to 10 CFR 71.51(c) [Ref. 2].
- The RT-100 has adequate thermal performance to meet the containment, shielding, sub-criticality, and temperature requirements of 10 CFR 71 [Ref. 2] for (NCT/HAC).

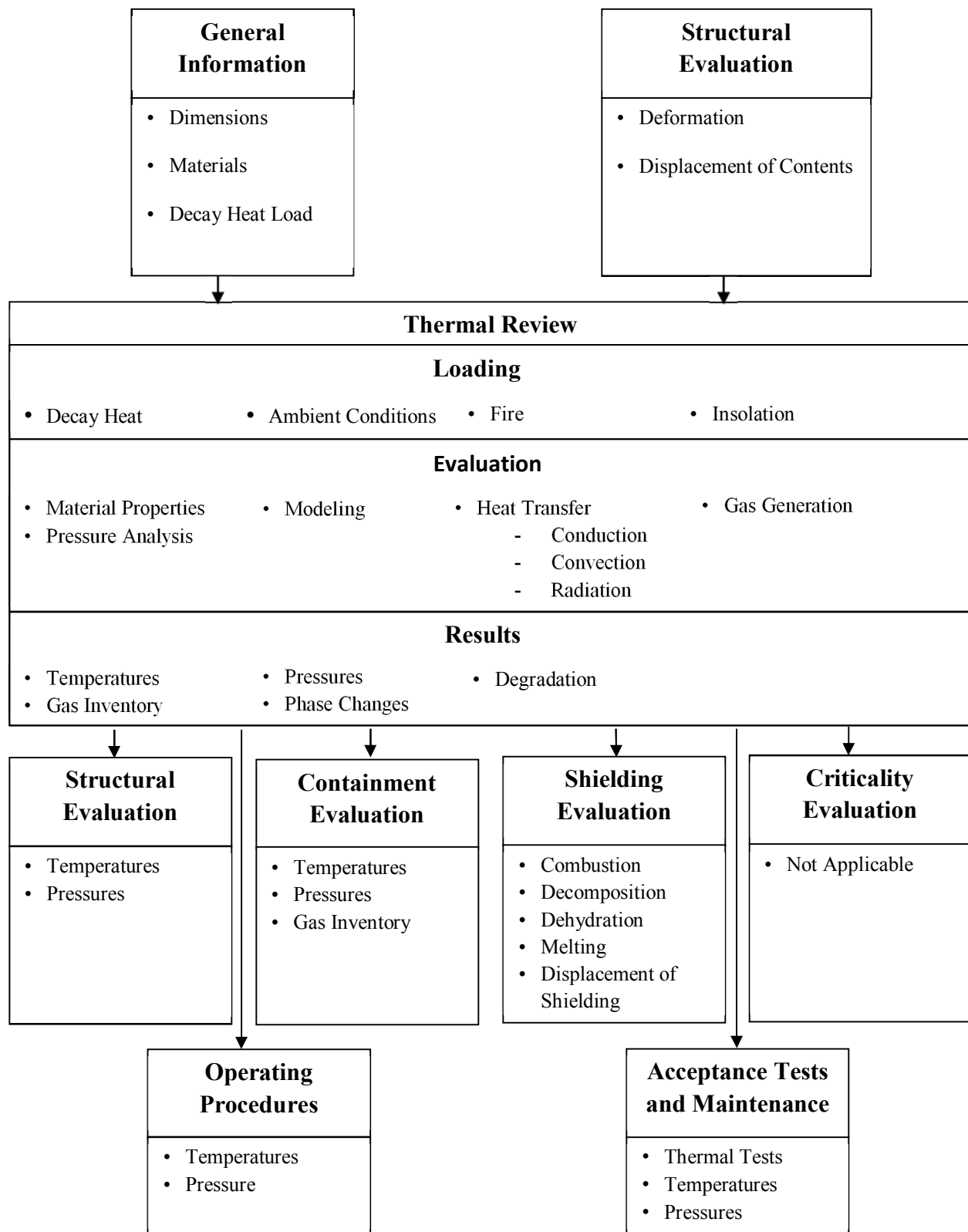


Figure 3-1 Information Flow for the Thermal Review

3.1 Description of Thermal Design

The thermal design aspects of the RT-100 are related primarily to protecting the sensitive components of the cask and the contents from the elevated temperatures produced by the hypothetical fire accident. The primary thermal criteria that are applied to the thermal evaluation are maintaining the lead shielding in the cask body and secondary lid below the melting temperature of lead, and the maximum temperature of the O-ring seals below their maximum operating temperature. The components primarily responsible for maintaining the temperatures of these components below their acceptance criteria are the impact limiters covering the top and bottom of the cask, and the thermal shield on the radial cask surface.

The impact limiters are made from a polyurethane foam material that has a low thermal conductivity. The impact limiters cover the top and bottom ends of the cask. They protect the lead in the bottom of the cask body and the O-rings in the primary lid, secondary lid, and the vent port cover plate. The impact limiters are designed to remain attached to the cask during normal operations and hypothetical accident conditions, and to insulate the lead and O-rings from the high temperatures of the hypothetical fire accident. The thermal shield covering the radial cask surface is made of a ceramic fiber material with a very low thermal conductivity. The ceramic fiber is covered by a thin, stainless steel cover that protects it from damage during normal handling. The ceramic fiber material is designed for use in insulating refractory furnaces, and providing an excellent thermal barrier for the fire accident, thus preventing the radial lead from exceeding its melting point.

The RT-100 is designed to accommodate contents with a maximum decay heat of 200 watts. This low decay heat value does not produce a significant temperature gradient through the cask body, and as a result, no specific design features are required to facilitate removing the heat from the cavity.

3.1.1 Design Features

As briefly described in Section 3.1, the RT-100 design has two primary thermal design features: the impact limiters and the radial thermal shield. These features are identified in Chapter 1, Figure 1.2.1-1 which highlights the primary components of the cask.

3.1.1.1 RT-100 Description

The RT-100 cask body consists of inner and outer shells constructed of 304/304L stainless steel. Lead shielding is provided between these radial shells, as well as between the 304/304L stainless steel bottom forging and bottom plate. The upper end of the cask comprises the upper 304/304L stainless steel forging that is attached to the inner and outer shells, and contains the mating surface for the primary lid. The primary and secondary lids are constructed of 304L stainless steel, as is the cover plate. The primary lid is attached using thirty-two (32) M48 hex head bolts and the secondary lid is secured using eighteen (18) M36 hex head bolts. The upper and lower impact limiter cover each end of the cask, and are constructed of 304L stainless steel shells containing polyurethane foam blocks. The impact limiters are secured to the body via twelve (12) M24 threaded studs. The RT-100 is described in greater detail in Chapter 1, Section 1.2.1.

Most of the outer shell of the cask is covered by a ceramic fiber thermal shield that is secured by a thin 304L stainless steel cover. Other portions of the radial cask surface are covered by the 318

stainless steel tie-down arms and tie-down arm baseplate, and by the 304L stainless steel lifting blocks. The exposed surfaces of the tie-down arm baseplate are covered by the ceramic fiber thermal shield and 304L stainless steel cover.

3.1.1.2 RT-100 Dimensions

The RT-100 thermal analysis is performed using the basic cask dimensions as presented in Appendix 1.4. The inner and outer shell thicknesses at the side of the cask are reduced to account for minimum thickness due to manufacturing tolerances. Specifically, the following material thicknesses are reduced by 2mm:

- Thicknesses of the cask body inner and outer stainless steel shells
- Bottom end of the cask body
- Stainless steel bottom forging welded to the inner shell
- Stainless steel bottom plate welded to the outer shell.

To represent the condition of undersized shells with a poured lead fill, lead thickness in both the sidewalls and the cask bottom end are simultaneously increased by 4 mm. This approach is conservative as it reduces the amount of stainless steel material protecting the lead from the HAC fire temperatures and thus, maximizes temperatures in the lead.

In order to maximize the amount of heat that can enter the cask body during the fire, no gaps are assumed between the lead and the outer shell. The lead and stainless steel outer shell are assumed to be in perfect contact. No other gaps are assumed in the thermal evaluation between the various components of the cask.

3.1.2 Content's Decay Heat

The RT-100 is designed for a maximum decay heat of 200 watts. This value is selected as the design basis, and is conservative for the contaminated resin and filter contents that are transported in the cask.

The analysis of the cask for normal condition of transport (NCT) and hypothetical accident conditions (HAC) is performed using the ANSYS finite element computer code [Ref. 3]. In this analysis, the decay heat of the contents is modeled as a uniform heat flux on the internal surfaces of the cask cavity.

To calculate this uniform heat flux over the inside surface of the cask, the inside diameter and the height of the cask cavity is used.

$$A_{in} = \pi dL + 2(\pi d^2/4)$$

where

$$\begin{aligned} A_{in} &= \text{inside surface area of the cask (m}^2\text{)} \\ d &= \text{inside diameter of the cask (m)} \end{aligned}$$

L = height of the cavity (m)

Based on the RT-100 drawing provided in Appendix 1.4, the cask inside diameter is 1.730 m and the height of the cavity is 1.956 m. The area is then

$$A_{in} = \pi \times 1.730 \times 1.956 + 2(\pi \times 1.730^2 / 4) = 15.332 \text{ m}^2$$

The uniform internal heat flux, q_{int} , is then

$$q_{int} = 200 \text{ W} / 15.332 \text{ m}^2 = 13.04 \text{ W/m}^2$$

3.1.3 Summary Tables of Temperatures

Section 3.1.3 presents summary tables of maximum temperatures occurring in the RT-100 as a result of the NCT and HAC evaluations described in detail in Sections 3.3 and 3.4. Limiting temperatures for consideration in the structural and containment evaluations are the maximum temperatures. Therefore, the following tables present maximum temperatures that occur in the various cask components under NCT and HAC. Table 3.1.3-1 presents the NCT maximum temperatures while Table 3.1.3-2 and Table 3.1.3-3 present the maximum temperatures HAC. For the fire accident evaluation, the time at which the component reaches its maximum temperature is listed along with the temperature. In some cases, temperatures are after cessation of the fire transient.

The tables also present the maximum averaged surface temperature of the inner shell at the cavity side. These averaged surface temperatures are used to predict the cavity pressure under normal and hypothetical conditions, respectively.

Table 3.1.3-1 RT-100 Maximum Normal Condition Temperature Summary

Component	Hot Case 1 (°C)	Hot Case 2 (°C)	Cold Case 1 (°C)	Cold Case 2 (°C)	Allowable Temperature (°C)	Reference
Primary Seal	68.7	42.1	-35.5	-24.5	150	Ref. 8
Secondary Seal	70.3	42.9	-34.7	-23.8	150	Ref. 8
Quick Disc. Valve Cover Seal	72.5 ^(a)	— ^(a)	— ^(a)	— ^(a)	150	Ref. 8
Lead Shield	73.2	43.1	-34.5	-23.6	328	Ref. 5 (p. 907)
Closure Bolts	70.0	42.8	-34.9	-23.9	—	—
Outer Surface	93.0	41.3	-36.3	-25.4	50/85 ^(b)	10 CFR 71.43(g)
Inner Shell Maximum	73.1	42.6	-35.1	-24.1	—	—
Inner Shell Average	71.0	41.7	-36.0	-25.0	—	—
Total Impact Limiter Average	67.4	39.5	-38.3	-27.3	—	—
Top Impact Limiter Average	72.5	39.5	-38.3	-27.4	—	—

- a. The NCT maximum temperature of the components surrounding the cover plate is the upper impact limiter average temperature (reported in Table 3.1.3-1) where the temperatures are higher on the external surfaces of the impact limiter. Thus the maximum temperature of the cover plate containment O-ring is considered to be 72.5°C with no further analysis. Since Hot Case 1 is the bounding upper temperature of this O-ring, the other NCT cases are not considered.
- b. 10 CFR 71.43(g)—A package must be designed, constructed, and prepared for transport so that in still air at 38°C (100°F) and in the shade, no accessible surface of a package would have a temperature exceeding 50°C (122°F) in a nonexclusive use shipment, or 85°C (185°F) in an exclusive use shipment.

Table 3.1.3-2 RT-100 Maximum Calculated Temperature of Cask under HAC with Pin Puncture Damage on Top Impact Limiter

Component	Temperature (°C)	Time After Start of Fire (Minutes)	Allowable Temperature (°C)	Reference
Primary Seal Maximum	110.8	291.6	150	Ref. 8
Secondary Seal Maximum	131.1	33.4	150	Ref. 8
Quick Disc. Valve Cover Seal	133.1 ^(c)	33.4 ^(c)	150	Ref. 8
Lead Shield Maximum	304.8	34.5	328	Ref. 5 (p. 907)
Closure Bolts Maximum	133.1	33.4	—	—
Cask Body Maximum	799.1	30.0	—	—
Inner Shell Average	136.3	—	—	—

- c. The port cover plate location is on the primary lid, close to the primary lid closure bolts. The cover plate is thermally insulated by the upper impact limiter. The highest temperature reported on the primary and secondary lid are the closure bolts (where the puncture bar penetrates the impact limiter) with a maximum temperature of 133.1°C (reported in Table 3.1.3-2). This temperature of 133.1°C being bonding to all the lids and cover plate recorded temperatures, the maximum temperature of the cover plate containment O-ring during HAC is considered to be 133.1°C with no further analysis.

Table 3.1.3-3 RT-100 Maximum Calculated Temperature of Cask under HAC with Pin Puncture Damage at the Side of the Cask Body

Component	Temperature (°C)	Time After Start of Fire (minutes)	Allowable Temperature (°C)	Reference
Primary Seal Maximum	110.3	285.1	150	Ref. 8
Secondary Seal Maximum	91.3	1624.4	150	Ref. 8
Quick Disc. Valve Cover Seal	— ^(d)	— ^(d)	150	Ref. 8
Lead Shield Maximum	304.7	34.5	328	Ref. 5 (p. 907)
Closure Bolts Maximum	91.9	1302.5	—	—
Cask Body Maximum	799.1	30.0	—	—
Inner Shell Average	137.0	—	—	—

- d. The Quick-Disconnect Valve Cover Plate Seal maximum temperature is considered bounded by the result of the top impact limiter pin puncture HAC. Thus, the side puncture result is not reported.

3.1.4 Summary Tables of Maximum Pressures

The maximum internal pressures in the RT-100 are determined using the maximum temperatures presented in Table 3.1.3-1, Table 3.1.3-2, and Table 3.1.3-3 above. Details of these pressure calculations are presented in Section 3.3.2 for NCT and in Section 3.4.3 for HAC. Table 3.1.4-1 presents a summary of the maximum pressure calculations for normal and accident conditions. These pressures are utilized in the structural evaluation presented for the cask body in Sections 2.6 and 2.7.

Table 3.1.4-1 RT-100 Summary of Maximum Normal and Hypothetical Accident Condition Pressures

Condition	Maximum Pressure
Normal Conditions of Transport (MNOP)	342.7 kPa (49.7 psia)
Hypothetical Accident Conditions	689.4 kPa (100 psia)

3.2 Material Properties and Component Specifications

The material properties and specifications for the RT-100 materials of construction are presented in this section. The determination of material properties are carefully evaluated to ensure that for each thermal analysis:

- The appropriate thermal properties for the package materials are correctly incorporated into the thermal evaluations.
- Appropriate expressions are used for conductive, convective, and radiative heat transfer among package components, and from the surfaces of the package to the environment.

3.2.1 Material Properties

The thermal evaluation of the RT-100 is performed using material properties taken from standard industry references or manufacturer provided data in Tables 3.2.1-1 through 3.2.1-4. The thermal absorptivities and emissivities are appropriate for the package surface conditions and each thermal condition. When reporting a property as a single value, the evaluation shows that this value bounds the equivalent temperature-dependent property. This section includes references for the data provided.

Only room temperature values of conductivity, density, and specific heat are available for General Plastics FR-3700 series LAST-A-FOAM [Ref. 10, 11, and 12]. Quantitative temperature dependent material properties are not provided. However, most of the foam remains at temperatures close to ambient due to the dimensions of the RT-100 impact limiters which result in long heat conduction paths (see Figure 3.3.1-3). Thus, reduction in the foam thermal properties due to elevated temperatures will not be significant. Therefore, the use of temperature-independent thermal properties is justified.

Information on the EPDM O-ring material is provided in TRELLEBORG, Aug. 2011 Edition [Ref. 8] and PARKER O-RING Handbook [Ref. 16] for two different suppliers. The temperature range specified in Table 3.2.1-1 is conservative from the values specified in those two references. Additional information on the O-rings is presented in Appendices Attachment 3.5-1 and Attachment 3.5-2.

Table 3.2.1-1 Temperature-Independent Material Properties

Material	Properties	Reference Page Number	Value
Stainless Steel 304	Density	Ref.24: Page 744	8030 kg/m ³
	Emissivity (fire)	Ref. 2	0.9
	Emissivity (cool-down)	Ref. 2	0.8
	Emissivity (normal condition)	Ref. 5: Page 750 and 929	0.2
Lead	Density	Ref. 5: Page 907	11340 kg/m ³
	Melting Point	Ref. 5: Page 907	328°C (601 K)

Proprietary Information Content Withheld Under 10 CFR 2.390(b)

Table 3.2.1-2 Temperature-Dependent Material Properties—Stainless Steel 304

[Ref. 13, page 765]

Temperature (°C)	Specific Heat (J/kg-K)	Thermal Conductivity (W/m-K)
20	472.6	14.8
50	483.6	15.3
75	493.1	15.8
100	499.4	16.2
125	506.7	16.6
150	511.4	17.0
175	520.1	17.5
200	525.7	17.9
225	530.0	18.3
250	532.5	18.6
275	536.5	19.0
300	541.7	19.4
325	545.5	19.8
350	547.7	20.1
375	551.4	20.5
400	552.3	20.8
425	557.0	21.2
450	557.8	21.5
475	562.3	21.9
500	563.1	22.2
525	566.3	22.6
550	568.1	22.9
575	571.2	23.3
600	572.9	23.6
625	575.9	24.0
650	577.5	24.3
675	580.4	24.7
700	581.9	25.0
725	585.8	25.4
750	587.2	25.7

Table 3.2.1-3 Temperature-dependent Material Properties—Lead

[Ref. 5, page 907]

Temperature (°C)	Specific Heat (J/kg- K)	Thermal Conductivity (W/m- K)
-173.15	118	3.97E+01
-73.15	125	3.67E+01
26.85	129	3.53E+01
126.8	132	3.40E+01
326.8	142	3.14E+01

Table 3.2.1-4 Temperature-dependent Material Properties—Ceramic Paper

[Ref. 9]

Temperature (°C)	Thermal Conductivity (W/m-K)
93.3	4.759E-02
204.4	5.206E-02
315.6	5.912E-02
426.7	6.907E-02
537.8	8.219E-02
648.9	9.834E-02
760.0	1.174E-01
871.1	1.396E-01

3.2.2 Component Specifications

This section includes the technical specifications of RT-100 components that are important to the thermal performance, as illustrated by the following examples:

- In the case of seals, the operation temperature limits
- Maximum allowable service temperatures for package components
- Minimum allowable service temperature of all components, which are less than or equal to -40 °C (-40 °F).

Table 3.2.2-1 lists the maximum and/or minimum allowable temperatures for the critical cask components.

Table 3.2.2-1 Component Specifications – Minimum and Maximum Temperatures

Material	Min. Temp.	Max. Temp.	Reference
304/ 304L SS	-	>1400°C (Melting Temp.)	Ref. 14
Lead	-	328°C (Melting Temp.)	Ref. 5
Polyurethane Foam	-	1093°C (2000°F of Foam Char Temp.)	Ref. 15
Seal (EPDM)	-45°C	150°C	Ref. 8 & 16

3.2.3 Content Properties

As described in Chapter 1, Section 1.2.2.3 (Physical and Chemical Form – Density, Moisture Content and Moderators), the RT-100 is designed to transport contents that include contaminated resins and filters. The contents include secondary containers and may also include shoring. Resins are made of thermoplastics such as polystyrene, or material such as inorganic carbon or zeolite. Filters may be constructed from thermoplastics such as nylon, polyester, or polypropylene, or paper. Secondary containers are constructed of either coated/painted carbon steel or stainless steel, or a thermoplastic such as polyethylene or polypropylene. The filter media may be held within a stainless steel cartridge. Shoring can be made of wood or one or several of the materials comprising the secondary containers.

Based on the ASME code, Section II-D [Ref. 13], the acceptable temperature of the carbon steel and stainless steel material is approximately 525°C (977°F) for the range of loads and stresses occurring under NCT and HAC.

The melting temperatures of thermoplastics range from 100°C (212°F) up to 250°C (482°F) SFPE Handbook of Fire Protection Engineering, [Ref. 21], which typically soften at these temperatures and do not produce volatiles that could react with any of the contents. The auto-ignition temperature of thermoplastics is above 300°C (572°F) [Ref. 21].

The auto-ignition temperatures of paper and wood vary widely and are a function of their specific composition and moisture content. A commonly accepted value for the auto-ignition point for paper is 232°C (450°F) “Fundamentals of Combustion Processes,” [Ref. 22]. The auto-ignition point for wood has been shown to be at least 300°C (572°F) An Experimental Study of Autoignition of Wood, T. Poespowati, World Academy of Science, Engineering and Technology 23, 2008. [Ref. 23].

A summary of the maximum temperature specifications for the RT-100 contents is provided in Table 3.2.3-1.

Table 3.2.3-1 Maximum Temperature Limits for RT-100 Content Materials

Material	Maximum Temperature	Reference
Carbon/Stainless Steel	525°C	Ref. 13
Thermoplastics	300°C	Ref. 21
Paper	232°C	Ref. 22
Wood	300°C	Ref. 23

3.3 Thermal Evaluation under Normal Conditions of Transport

This section describes the thermal evaluations performed for the RT-100 for the NCT specified in 10 CFR 71.71 [Ref. 2]. The evaluation considers the response of the RT-100 to a range of temperature and environmental conditions as described in Section 3.3.1. The results are compared with allowable limits of temperature, pressure, etc., for the package components. The information is presented in summary tables, along with statements and appropriate comments. Information that is to be used in other sections of the review is identified. The margins of safety for package temperatures, pressures, and thermal stresses, including the effects of uncertainties in thermal properties, test conditions and diagnostics, and analytical methods are addressed.

The analyses are shown to be reliable and repeatable.

The following general information is considered and included in addressing the sections below, as appropriate:

- Assumptions that are used in the analysis are clearly described and justified.
- For computer analyses, including finite element analyses, the computer program is described and shown to be well benchmarked, widely used for thermal analyses, and applicable to the evaluation.
- Models and modeling details are clearly described.
- The methods used are properly referenced or developed in the application.
- These methods are correctly applied.
- The evaluation considers changes in package geometry and material properties resulting from structural and thermal tests under NCT and HAC.
- The required temperature and thermal boundary conditions for normal conditions of transport and hypothetical accident conditions are correctly applied.
- The time interval after the fire test is adequate to assure that maximum component temperatures and post-fire steady-state temperatures are achieved.

- The maximum temperatures and pressures of the components do not exceed their allowable values.
- Combustion of package components are considered, including the heat produced.
- Temperature data is reported at gaskets, valves, and other containment boundaries, particularly for temperature-sensitive materials as well as, for the overall package.
- Appropriate corrections and evaluations that account for differences in the thermal test are included for conditions like ambient temperature, decay heat of the contents, or package emissivity or absorptivity.
- Both interior and exterior temperatures are included.
- The damage caused by the tests and the results of any measurements made is reported in detail, including photographs of the testing and the test specimen.

3.3.1 Heat and Cold

Section 3.3.1 demonstrates that the tests for NCT do not result in a significant reduction in the RT-100 effectiveness. The following items are considered and addressed:

- Degradation of the heat-transfer capability of the packaging (such as creation of new gaps between components)
- Changes in material conditions or properties (e.g., expansion, contraction, gas generation, and thermal stresses) affecting structural performance
- Changes in the packaging affecting containment, shielding, or criticality (such as thermal decomposition or melting of materials)
- Ability of the packaging to withstand the tests under HAC

The component temperatures and pressures are compared to their allowable values and do not exceed them. This section explicitly shows that the package meets the maximum temperature of the accessible package surface is less than 50 °C (122 °F) for non-exclusive-use shipment or 85 °C (185 °F) for exclusive use shipment when the package is subjected to the heat conditions of 10 CFR 71.43(g) [Ref. 2].

3.3.1.1 Load Cases

Four load cases are analyzed in order to evaluate the RT-100 for the range of temperature and solar insolation conditions specified in 10 CFR 71.71 [Ref. 2] for normal conditions:

- Hot Case 1
- Hot Case 2
- Cold Case 1

- Cold Case 2

Hot case 1 is based on the requirements of 10 CFR 71.71(c)(1) [Ref. 2], which is one of the extreme initial conditions for normal conditions and a precursor for the hypothetical fire accident evaluation. It has the following conditions:

- Ambient temperature, 38°C (100°F)
- Initial temperature, 38°C (100°F)
- Heat transfer to ambient by natural convection, still air
- Heat transfer to ambient by radiation
- Steady-state solar insolation, 776 W/m² for flat surface and 388 W/m² for curved surface
- Internal heat load as a uniform heat flux, 13.04 W/m²

Hot case 2 is based on the requirements of 10 CFR 71.43(g) [Ref. 2] and has the following conditions:

- Ambient temperature, 38°C (100°F)
- Initial temperature, 38°C (100°F)
- Heat transfer to ambient by natural convection, still air
- Heat transfer to ambient by radiation
- No solar insolation, in shade
- Internal heat load as a uniform heat flux, 13.04 W/m²

Cold case 1 is based on the requirements of 10 CFR 71.71(c)(2) [Ref. 2], which is another extreme initial condition for the NCT test evaluation. It has the following conditions:

- Ambient temperature, -40°C (-40°F)
- Initial temperature, -40°C (-40°F)
- Heat transfer to ambient by natural convection, still air
- Heat transfer to ambient by radiation
- No solar insolation, in shade
- Internal heat load as a uniform heat flux, 13.04 W/m²

Cold case 2 is based on requirements of 10 CFR 71.71(b) [Ref. 2] and has the following conditions:

- Ambient temperature, -29°C (-20°F)
- Initial temperature, -29°C (-20°F)
- Heat transfer to ambient by natural convection, still air
- Heat transfer to ambient by radiation
- No solar insolation
- Internal heat load as a uniform heat flux, 13.04 W/m²

Among them, Hot case 1 and Cold case 1 are two extreme conditions for the analyses. Hot case 1

is also referred to as the “normal hot” condition on which conservative boundary conditions are applied. This case provides the highest temperature distributions within the cask, and is used as initial conditions for evaluation of the hypothetical fire accident event as described in Section 3.4.

3.3.1.2 Analytical Model

The thermal evaluation of the RT-100 is performed using the ANSYS finite element computer software [Ref. 3]. The cask model is made of 3D thermal solid elements (SOLID90) that represent the major components of the cask. Contact between the lead and the inner and outer shells are modeled as bonded surfaces for thermal analyses in order to maximize heat input to the lead. The contact between the upper flange and the primary lid is modeled by a pair of 3D thermal contact elements (CONTA174) and 3D target elements (TARGE170), as are the other contacts between the primary lid and the secondary lid, the bolts with the primary lid, and the bolts with the secondary lid.

For conservatism, the top impact limiter is modeled as without the stainless steel plate covering the central hollow portion of the limiter. Thus, the concave area on the top impact limiter is exposed to solar insolation and/or fire. This approach leads to a conservatively high temperature over the top impact limiter. The contacts between the impact limiters and the cask body are also modeled by pairs of 3D thermal contact elements (CONTA174) and 3D target elements (TARGE170) between the relative surfaces.

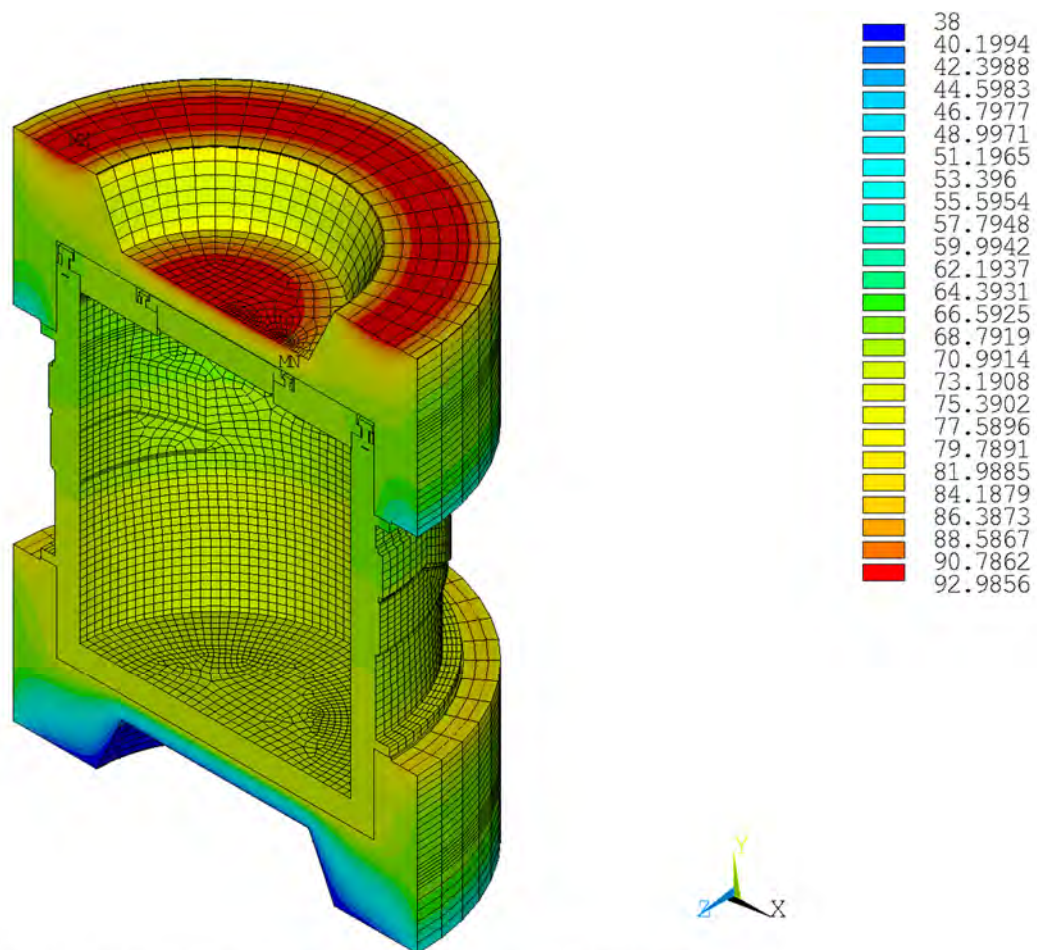
A depiction of the ANSYS thermal model of the RT-100 is provided in Figure 3.3.1-1 and Figure 3.3.1-2. Additional details regarding the modeling and analysis of the RT-100 are presented in Calculation Package RTL-001-CALC-TH-0201, Rev. 6 [Ref. 4].

Proprietary Information Content Withheld Under 10 CFR 2.390(b)

Proprietary Information Content Withheld Under 10 CFR 2.390(b)

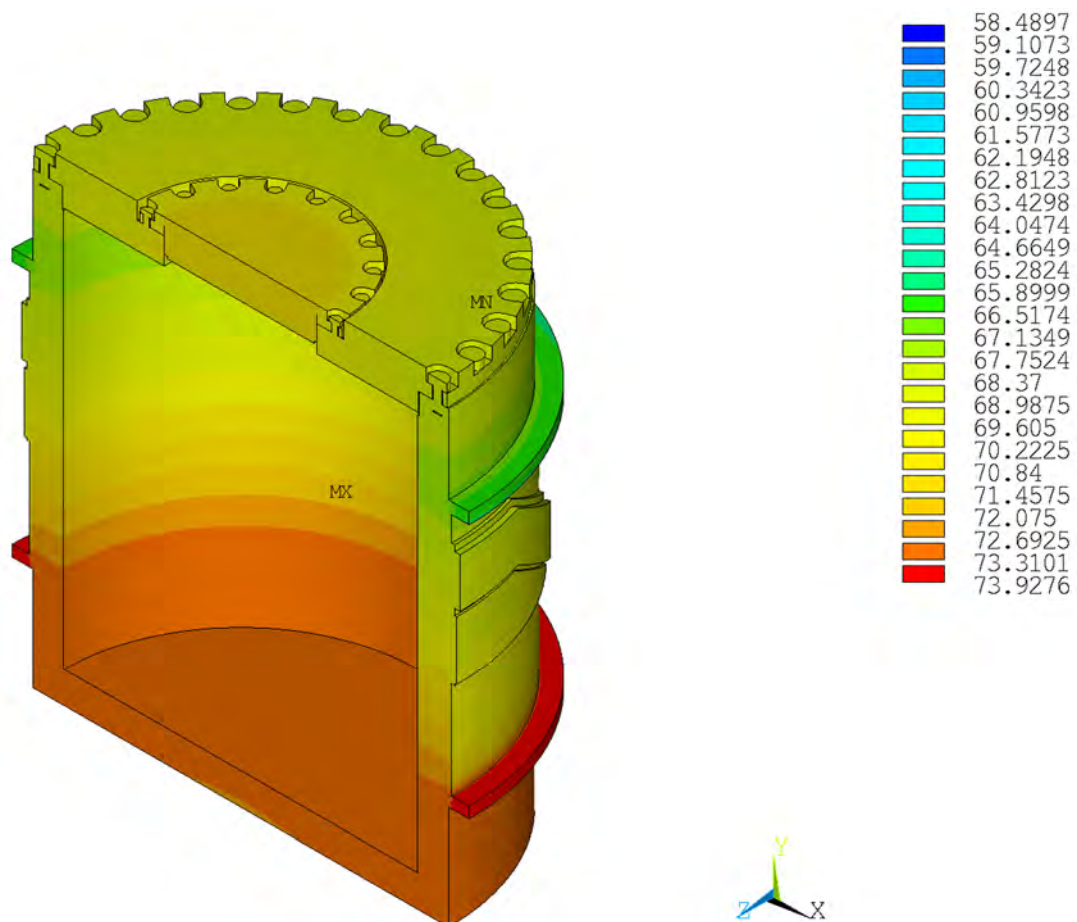
3.3.1.3 Analysis Results

The results of the steady state analyses of the cask model with impact limiters are presented in the form of temperature contour plots. Figure 3.3.1-3 through Figure 3.3.1-6 show the temperature contour plots for Hot case 1. Hot case 1 predicts the maximum temperatures experienced during NCT. The figures show the package, cask body, inner shell surface and lead shielding material, respectively. Figure 3.3.1-7 and Figure 3.3.1-8 provide the results for Hot case 2. Figure 3.3.1-9 and Figure 3.3.1-10 provide the results for Cold case 1. Cold case 1 represents the temperatures experienced by the package during extreme cold conditions. Figure 3.3.1-11 and Figure 3.3.1-12 provide the results for Cold case 2. Maximum temperature results are obtained by selecting the FE model component or material of interest and sorting the nodal results. Table 3.1.3-1 shows the maximum temperatures of the cask under NCT based on the steady state solution.



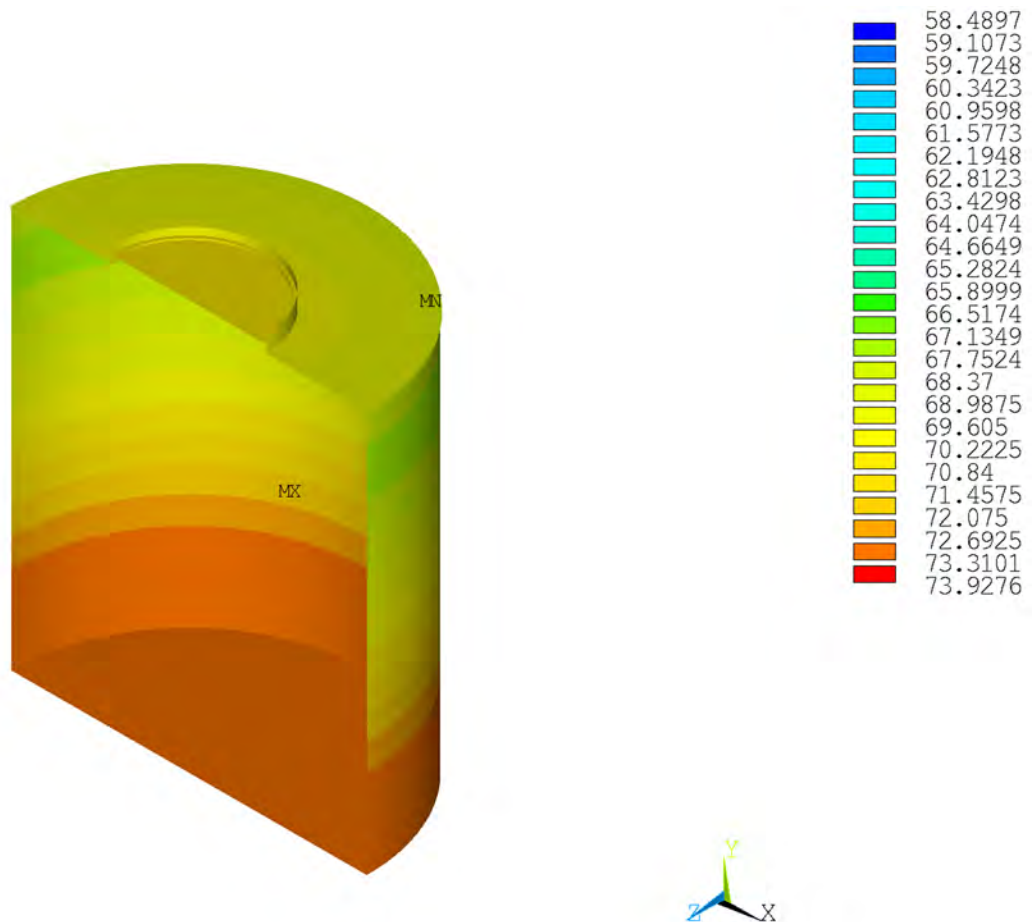
NCT—Case 1, Steady-State Boundary Conditions (Degrees Celsius)

Figure 3.3.1-3 Temperature Contour Plot of Package—Hot Case 1



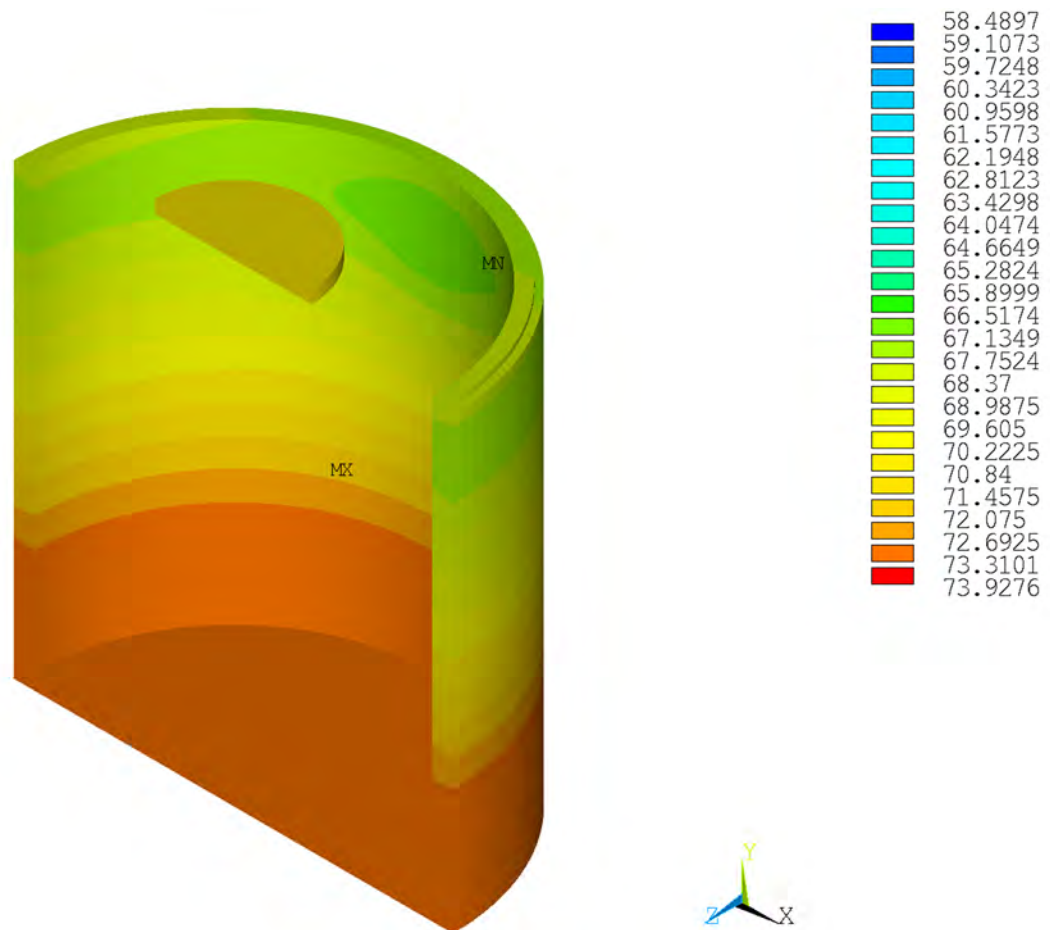
NCT—Case 1, Steady-State Boundary Conditions (Degrees Celsius)

Figure 3.3.1-4 Temperature Contour Plot of Cask Body—Hot Case 1



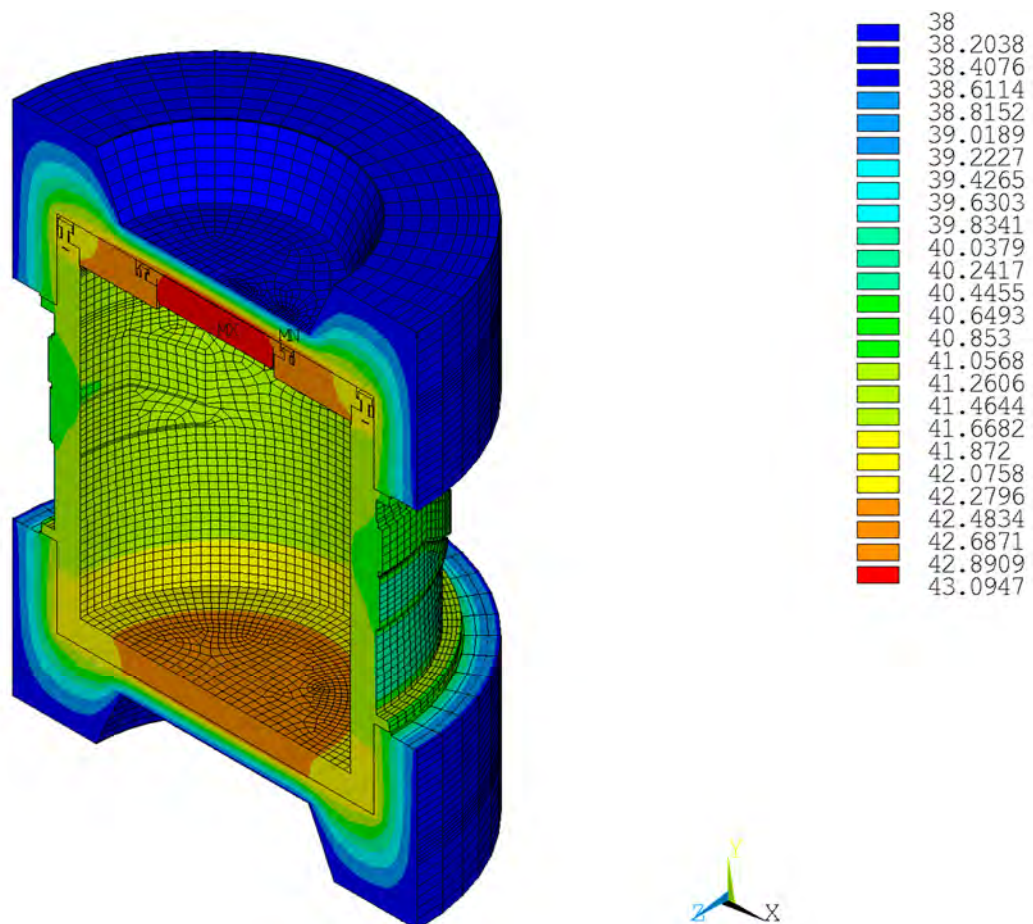
NCT—Case 1, Steady-State Boundary Conditions (Degrees Celsius)

Figure 3.3.1-5 Temperature Contour Plot of Inner Shell Surface—Hot Case 1



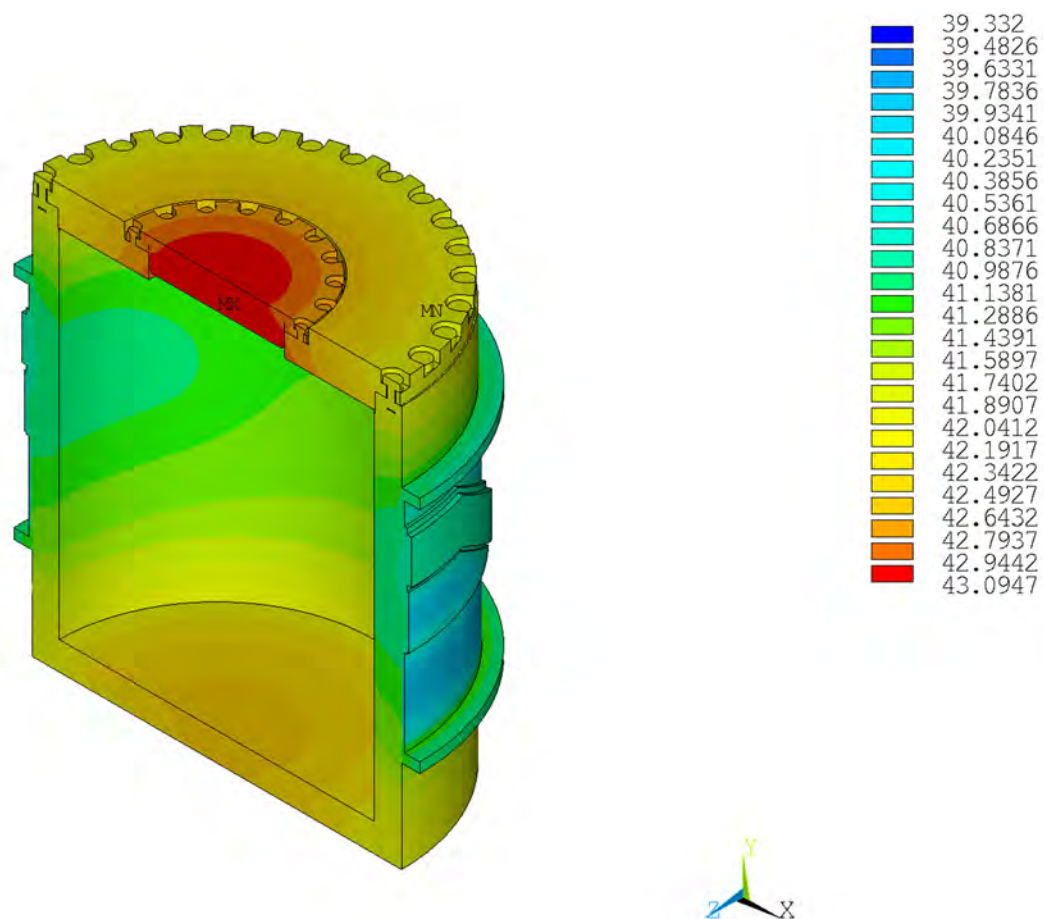
NCT—Case 1, Steady-State Boundary Conditions (Degrees Celsius)

Figure 3.3.1-6 Temperature Contour Plot of Lead Shielding—Hot Case 1



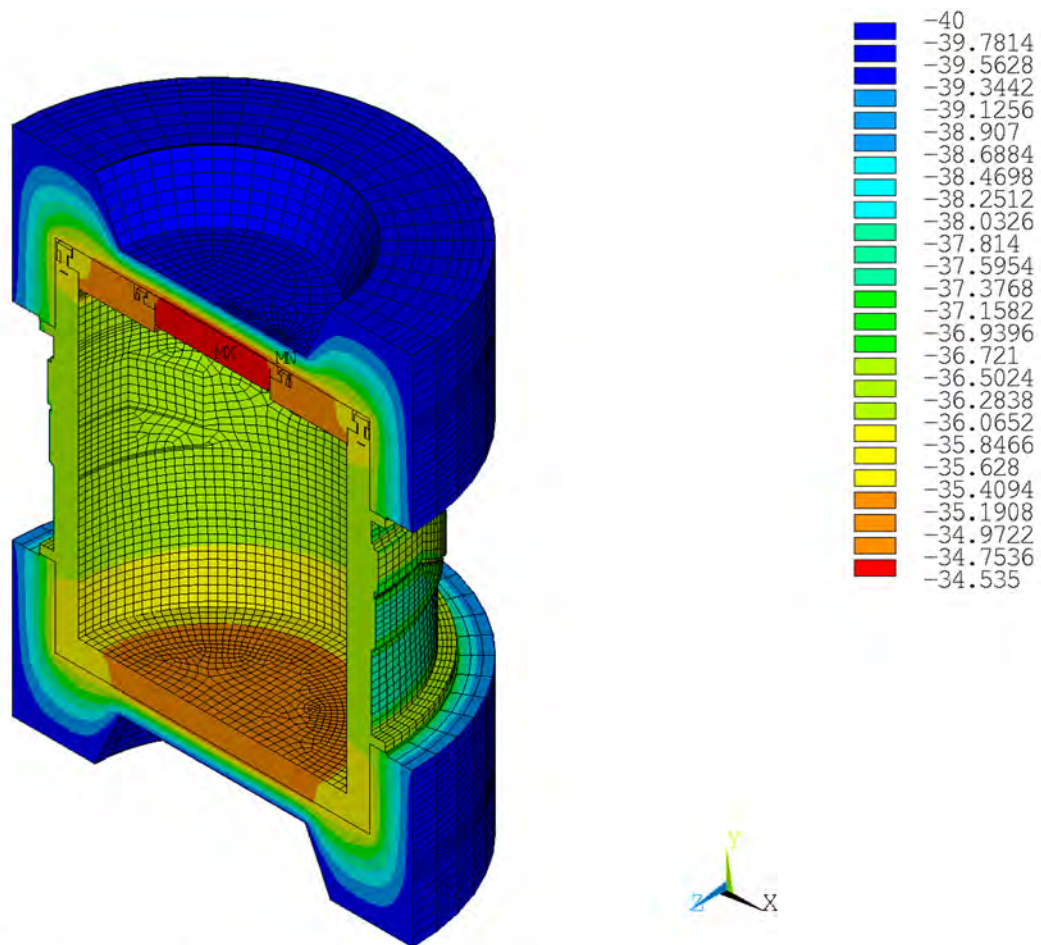
NCT—Case 2, Steady-State Boundary Conditions (Degrees Celsius)

Figure 3.3.1-7 Temperature Contour Plot of Package—Hot Case 2



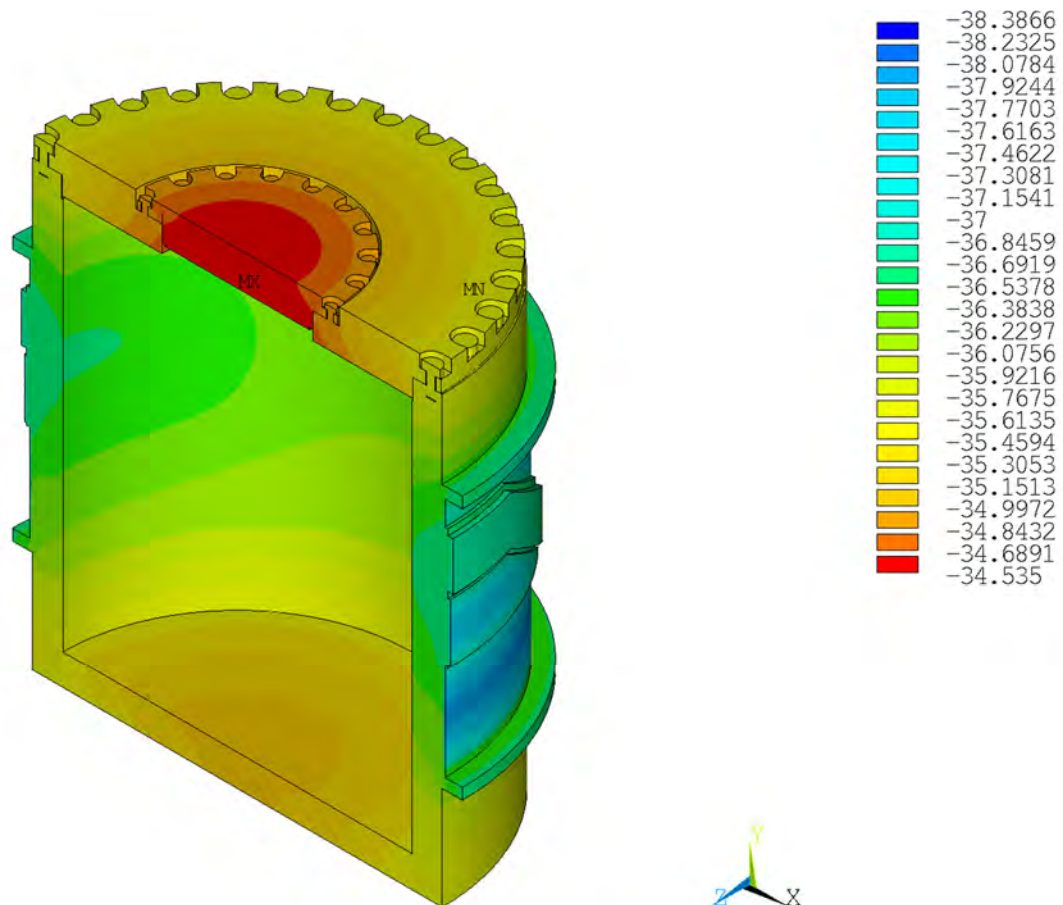
NCT—Case 2, Steady-State Boundary Conditions (Degrees Celsius)

Figure 3.3.1-8 Temperature Contour Plot of Cask Body—Hot Case 2



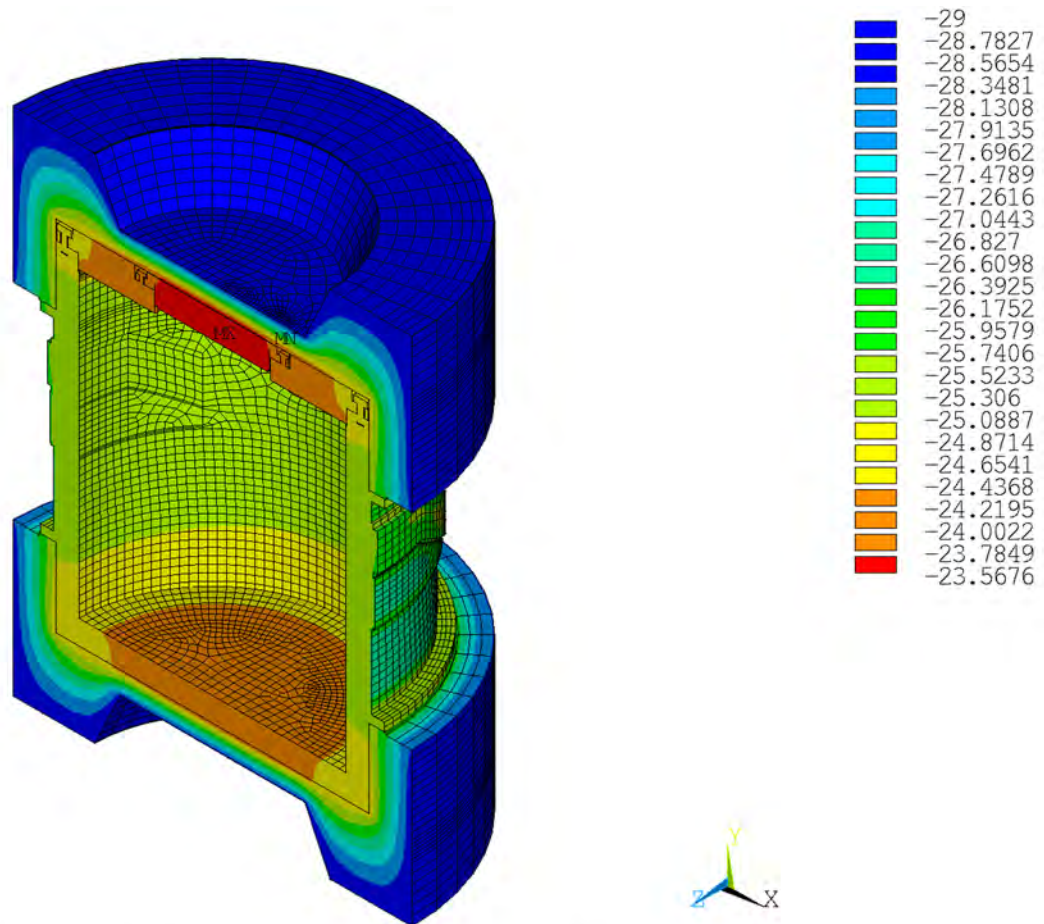
NCT—Case 3, Steady-State Boundary Conditions (Degrees Celsius)

Figure 3.3.1-9 Temperature Contour Plot of Package—Cold Case 1



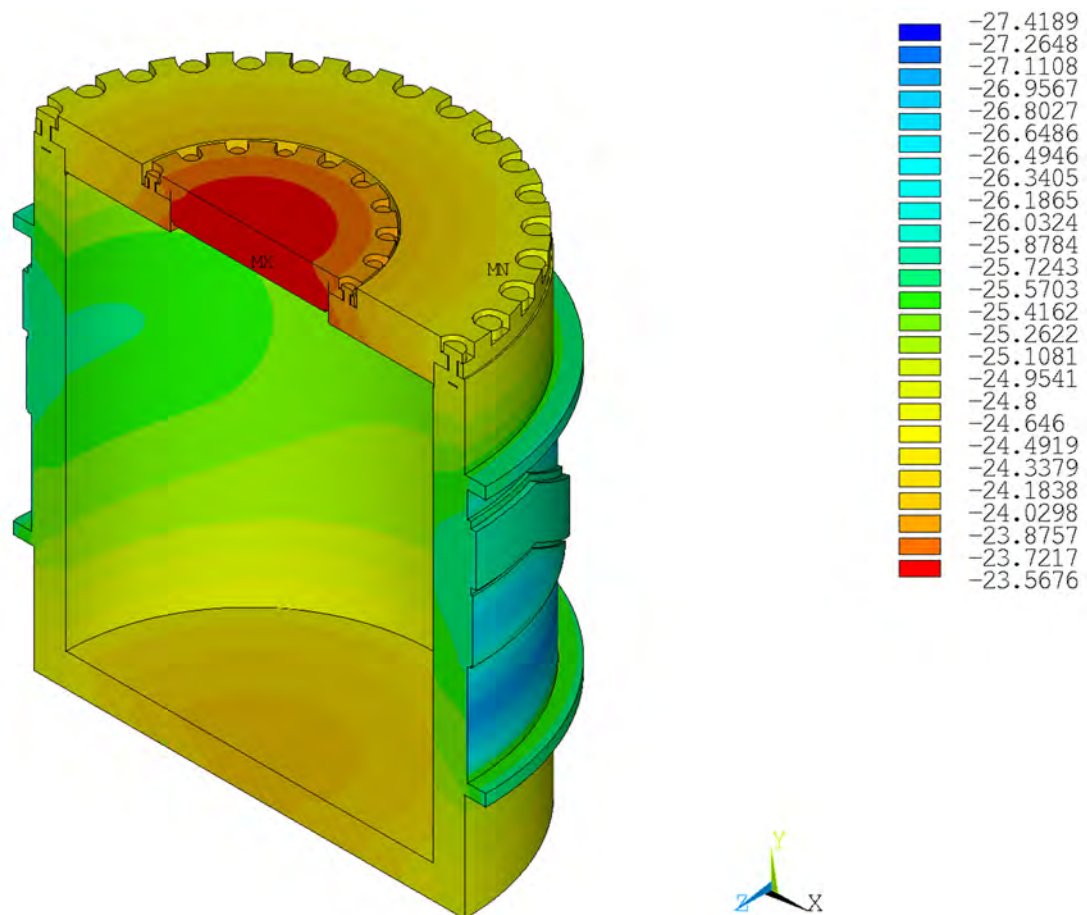
NCT—Case 3, Steady-State Boundary Conditions (Degrees Celsius)

Figure 3.3.1-10 Temperature Contour Plot of Cask Body—Cold Case 1



NCT—Case 4, Steady-State Boundary Conditions (Degrees Celsius)

Figure 3.3.1-11 Temperature Contour Plot of Package—Cold Case 2



NCT—Case 4, Steady-State Boundary Conditions (Degrees Celsius)

Figure 3.3.1-12 Temperature Contour Plot of Cask Body Cold Case 2

3.3.2 Maximum Normal Operating Pressure

The maximum pressure in the RT-100 for NCT is calculated using the maximum temperatures determined for the range of normal condition load cases. The calculation considers possible sources of gases including the following:

- Gases initially present in the package
- Saturated vapor, including water vapor from the contents or packaging
- Hydrogen or other gases resulting from thermal- or radiation-induced decomposition of materials such as water or plastics

Summary of the pressure calculation is provided in the following sections. Additional details are provided in Calculation Package RTL-001-CALC-TH-0102, Rev. 6 [Ref. 6].

3.3.2.1 Calculation Method

To determine the maximum normal operating pressure, the temperature of gas mixture within the cask is evaluated. Maximum temperature of the cask cavity under normal condition is bounded by the upper and lower temperature range of 80 °C (176°F) to -29 °C (-20°F). The total pressure in the cavity is represented by the sum of the primary contributors to the pressure. These are the pressure due to the increased temperature of the cavity gas (ideal gas law), the pressure due to the presence of water vapor, and the pressure due to the generation of gas via radiolysis.

The restriction of the contents to inorganic materials eliminates the potential for gas generation due to thermal degradation or biological activity. Thus, these gas sources are not considered in the evaluation. However, water vapor is present in trace quantities. Therefore, the analysis considers the contribution from the radiolytic decomposition of residual water in the cask cavity.

Per the ideal gas law, air pressure and water vapor pressure are directly proportional to the temperature, and with increase in temperature the pressure also increases. The upper bound temperature results in a higher maximum normal operating pressure for the cask compared to the lower bound. The gas mixture in the cavity is conservatively assumed to be at 80 °C (176°F).

3.3.2.2 Pressure Due to the Initially Sealed Air in the Cavity

Per the ideal gas law, the partial pressure of the air (P_{air}) initially sealed in the fixed volume of the cask at the ambient temperature as it is heated to 80 °C (176 °F) is:

$$P_1 \times T_2 = P_2 \times T_1$$

$$P_{\text{air}} = 101.35 \text{ kPa}[(353.15 \text{ K}) / (294.25 \text{ K})] = 121.64 \text{ kPa (17.64 psia)}$$

3.3.2.3 Pressure Due to the Water Vapor in the Cask

The cask cavity is assumed to contain a small amount of water. By conservatively assuming a condensing surface temperature of 80 °C (176 °F), the water vapor pressure, P_{wv} , at this temperature is:

47.34 kPa [6.87 psia], Fundamentals of Fluid Mechanics, Table B.2, pg. 831 [Ref. 17], Attachment 3.5-3.

Adding the water vapor pressure at 80 °C (176 °F) to the partial pressure of the air in the sealed cask at this temperature gives:

$$P_2 = P_{\text{air}} + P_{\text{wv}} = 121.64 + 47.34 = 169.0 \text{ kPa}$$

$$= 169.0 \text{ kPa} \times 0.145 \text{ psi/kPa} = [24.51 \text{ psia}]$$

3.3.2.4 Pressure Due to Generation of Gas

Solidified or dewatered material may contain some water. Therefore, radiolytic generation of gases from this water could occur. Hydrogen and oxygen may be produced in the cask by radiolytic decomposition of residual water in the cask contents. As described in Chapter 1, Section 1.2.2.6, the maximum quantity of hydrogen must be limited to less than 5% to ensure that an explosive quantity does not accumulate.

The cask atmosphere can be assumed to contain 5% of hydrogen (H₂) gas due to radiolysis of the water. By stoichiometry of the water molecule (H₂O), the cask atmosphere will also contain 2.5% oxygen (O₂) gas generated by radiolysis. Partial pressures in an ideal gas mixture are additive and behave the same as ideal gas volume fraction or mole fractions. Therefore, the partial pressure of hydrogen is described by the following equation:

$$P_{\text{H}_2} = 0.05 P_{\text{pt}}$$

$$\text{Where, } P_{\text{pt}} = P_{\text{air}} + P_{\text{wv}} + P_{\text{H}_2} + P_{\text{O}_2}$$

$$\text{Combining } P_{\text{air}} + P_{\text{wv}} = P_2 \text{ and noting that } P_{\text{O}_2} = 0.5 \times P_{\text{H}_2}.$$

$$P_{\text{H}_2} = 0.05 \times (P_2 + 1.5 P_{\text{H}_2})$$

Solving the equation explicitly for P_{H₂} give:

$$P_{\text{H}_2} = [0.05 P_2] / [1 - 0.05 (1.5)]$$

$$= [0.05 * 169.0 \text{ kPa}] / [1 - 0.05 (1.5)]$$

$$= 9.14 \text{ kPa} [1.32 \text{ psia}]$$

3.3.2.5 Total Pressure

Based on the stoichiometric relationship between hydrogen and oxygen liberated by radiolysis of water, and again combining the pressure of the initially sealed air and water vapor as P₂, the total pressure in the cask at 80°C (176°F) is:

$$P_{\text{Total}} = P_2 + 1.5 P_{\text{H}_2}$$

$$= 169.0 \text{ kPa} + 1.5 * 9.14 \text{ kPa}$$

$$= 182.71 \text{ kPa} [26.5 \text{ psia}] \text{ (actual calculated MNOP)}$$

The design basis maximum normal operating pressure (MNOP) value is conservatively set at 342.7 kPa (49.7 psia or 35 psig) for use in the cask structural analyses for NCT.

3.4 Thermal Evaluation under Hypothetical Accident Conditions

This section describes the thermal evaluation of the RT-100 under hypothetical accident conditions. The RT-100 is evaluated by finite element computer analysis rather than physical testing to demonstrate the performance of the cask in response to the fire test conditions specified in 10 CFR 71.73(c) [Ref. 2]. The HAC defined in 10 CFR 71.73(c) [Ref. 2] are applied sequentially, considering the damaged condition of the packaging following the 30-foot free drop and pin puncture accident events prior to the fire transient. For the accident condition thermal evaluation, the general comments in Section 3.3 are considered and addressed, as appropriate.

As described in Chapter 2, Section 2.7.3 (Puncture), different pin puncture configurations are considered in order to determine the worst case for the accident event. For the structural evaluation, the orientations considered are directly in the middle of the secondary lid to maximize the bending loads in the primary and secondary lids and prying forces in the bolts. The second configuration considers the pin impact directly into the side of the RT-100 to ensure that the outer shell is not punctured by the pin. For the thermal analysis, these two events are also considered to be limiting. The differences are in the location of the pin at impact.

3.4.1 HAC Fire Analysis—Pin Puncture Damage to Top Impact Limiter

The analytical model described in Section 3.3.1.2 is used to evaluate the RT-100 package with damage on the top impact limiter. For this case, the limiting configuration for the thermal analysis considers a pin puncture through the top impact limiter directly into the secondary lid at the location of the O-rings. The model placed a 150 mm (6 in) diameter hole through the upper impact limiter, directly exposing the secondary lid to the thermal environment of the hypothetical accident fire. The following section evaluates both pin puncture orientations to determine the effect to critical components such as the seal locations and lead shielding.

3.4.1.1 Initial Conditions—Pin Puncture Damage to Top Impact Limiter

Per Regulatory Position 1.1 in Regulatory Guide 7.8 [Ref. 20], the initial cask temperature distribution is considered to be at steady state with an ambient temperature of 38°C (100°F) and solar insolation prior to the HAC fire accident. To meet this requirement, the steady-state solution for NCT hot case 1 is used, obtained to the initial temperatures of the cask prior to the fire. The steady-state temperatures are applied as the first load step of the transient solutions. To account for damage to the package that results during the sequential drop accidents, damage due to pin puncture is considered during the top and side puncture. For the top impact limiter 150 mm diameter volume of material including the steel shell and FR3740 foam is removed at the point closest to the elastomer O-ring. This is a conservative approach since the puncture probe will not penetrate through the top skin of the impact limiter and compressed foam will remain beneath the point of impact. Figure 3.4.1-1 shows the temperature contour of the package prior to the fire accident and localized higher temperatures in the region of the damaged impact limiter. Figure 3.4.1-2 and Figure 3.4.1-3 show the cask body and inner shell cavity temperature distribution prior to the fire accident.

3.4.1.2 HAC Fire and Cool-down Analysis—Pin Puncture Damage to Top Impact Limiter

The thermal analysis for HAC includes a 30 minute transient fire followed by the prescribed post-fire cool-down period. The FE model described in Section 3.3.1.2 is analyzed by applying

the following boundary conditions. Following the initial load step in which the steady-state temperatures are applied, the analysis proceeds with the HAC fire transient for 30 minutes (1,800 seconds) followed by a cool-down period with the boundary conditions associated with NCT Hot case 1. The NCT Hot case 1 boundary conditions are applied as constants ignoring the day/night cool-down cycle. The following is a summary of the fire transient boundary conditions:

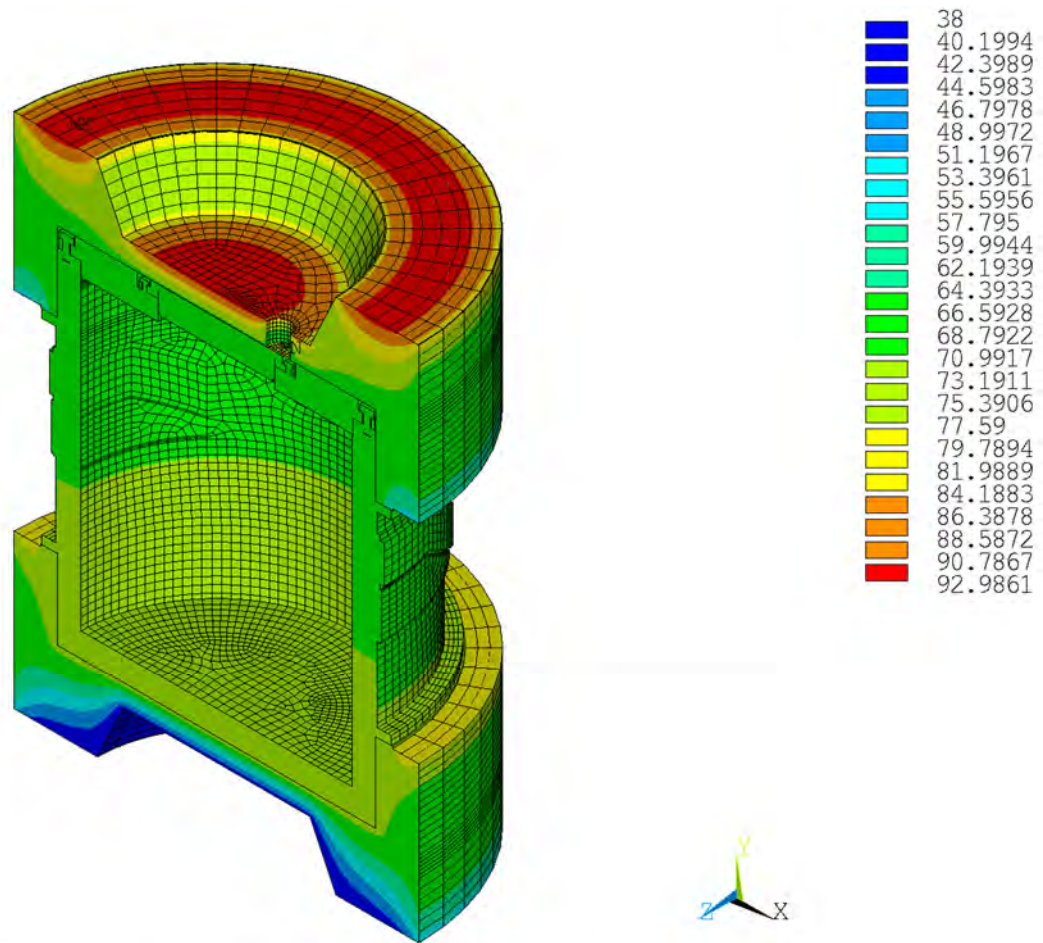
- Environment temperature, 800°C (1472°F)
- No solar insolation, 0 W/m²
- Forced convection, heat transfer coefficient = 10 W/m²·°C
- Radiation from the environment to package surface, flame emissivity = 0.9
- Internal heat load as a uniform heat flux, 13.04 W/m²

The cool-down analysis is performed for 216,000 seconds (2.5 days) with the following boundary conditions:

- Environment temperature, 38°C (100°F)
- Solar insolation applied as constant, 776 W/m² for flat surfaces and 388 W/m² for curved surfaces.
- Natural convection, heat transfer coefficient = 5 W/m²·°C
- Radiation from package surface to the environment, package emissivity = 0.8
- Internal heat load as a uniform heat flux, 13.04 W/m²

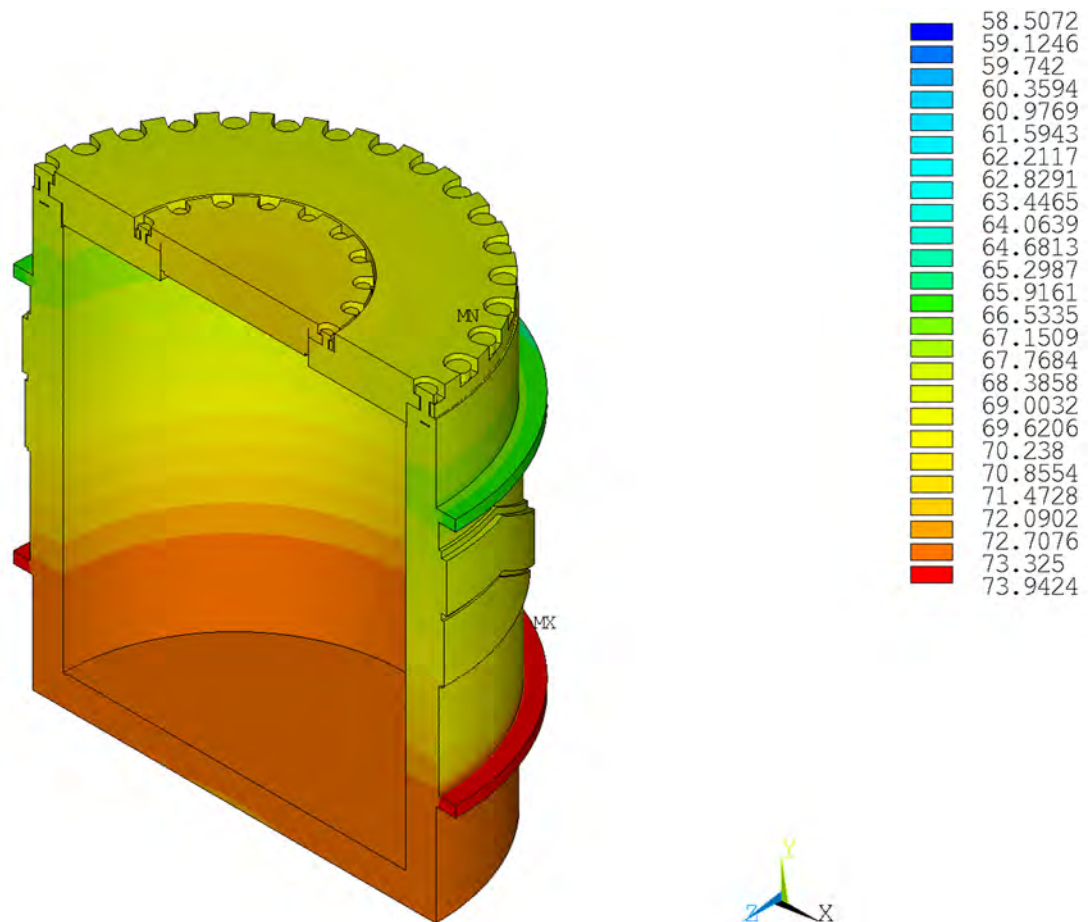
Proprietary Information Content Withheld Under 10 CFR 2.390(b)

Table 3.1.3-2 summarizes the maximum temperatures of the cask under HAC fire with pin puncture damage at the side of the cask body.



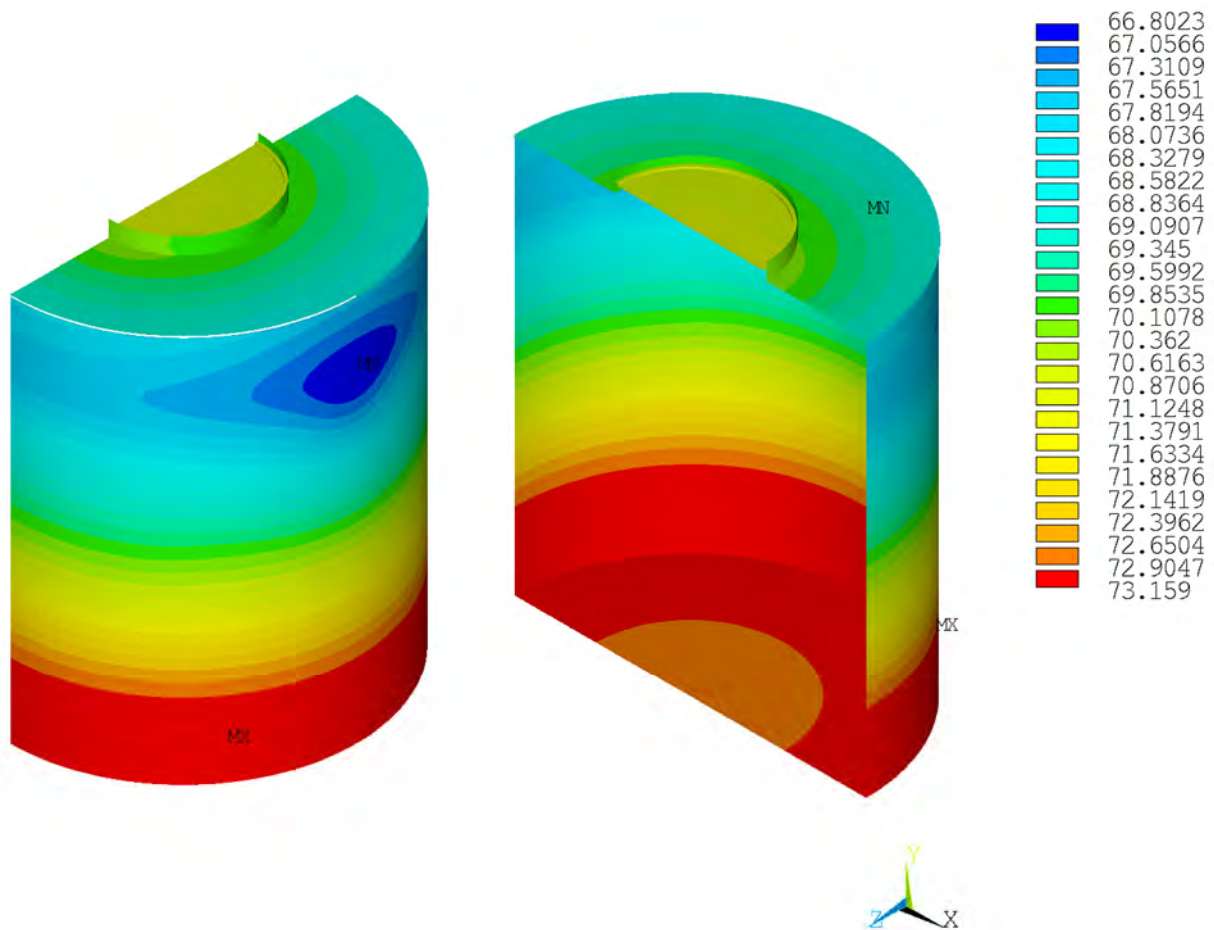
HAC—Fire Top Puncture, Steady-State Initial Conditions (Degrees Celsius)

Figure 3.4.1-1 **Temperature Contour Plot of Package Pre-Fire Fire Condition—
HAC Pin Damage on Top Impact Limiter**



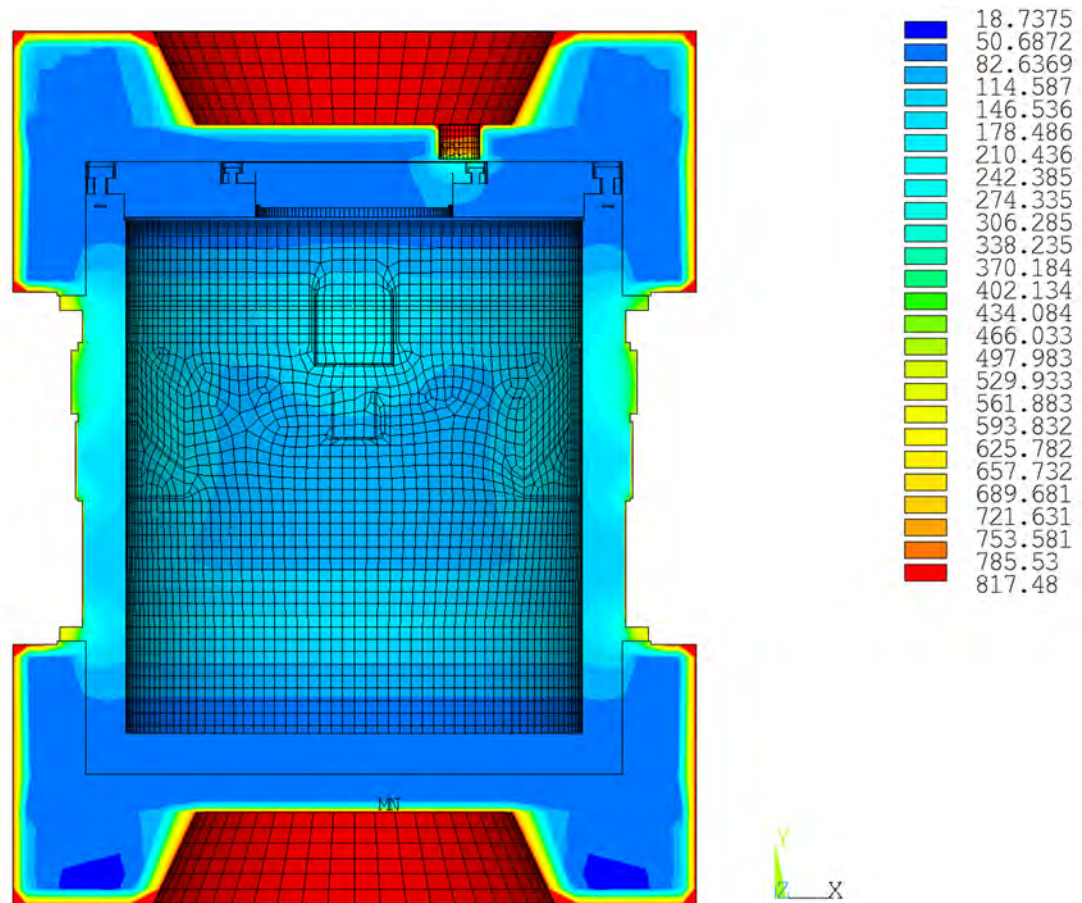
HAC—Fire Top Puncture, Steady-State Initial Conditions (Degrees Celsius)

Figure 3.4.1-2 **Temperature Contour Plot of Cask Body Pre-Fire Condition—HAC**
Pin Damage on Top Impact Limiter



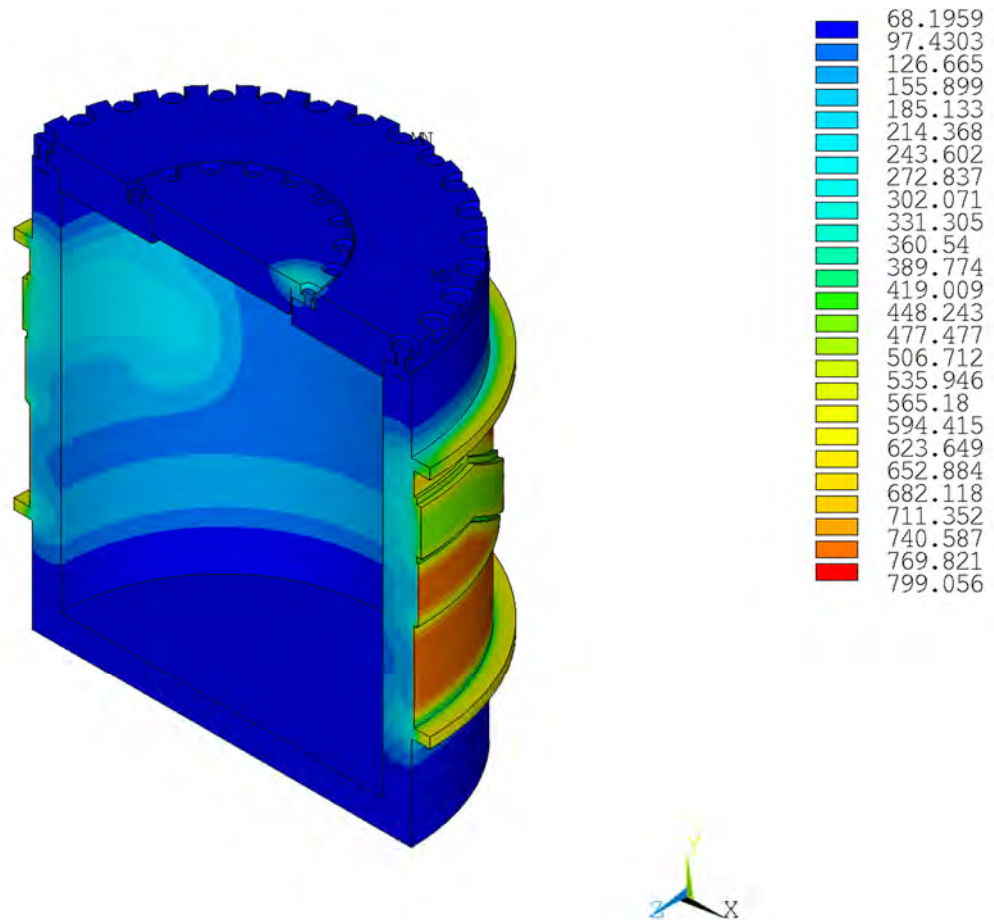
HAC—Fire Top Puncture, Steady-State Initial Conditions (Degrees Celsius)

Figure 3.4.1-3 **Temperature Contour Plot of Inner Shell Pre-Fire Condition—HAC**
Pin Damage on Top Impact Limiter



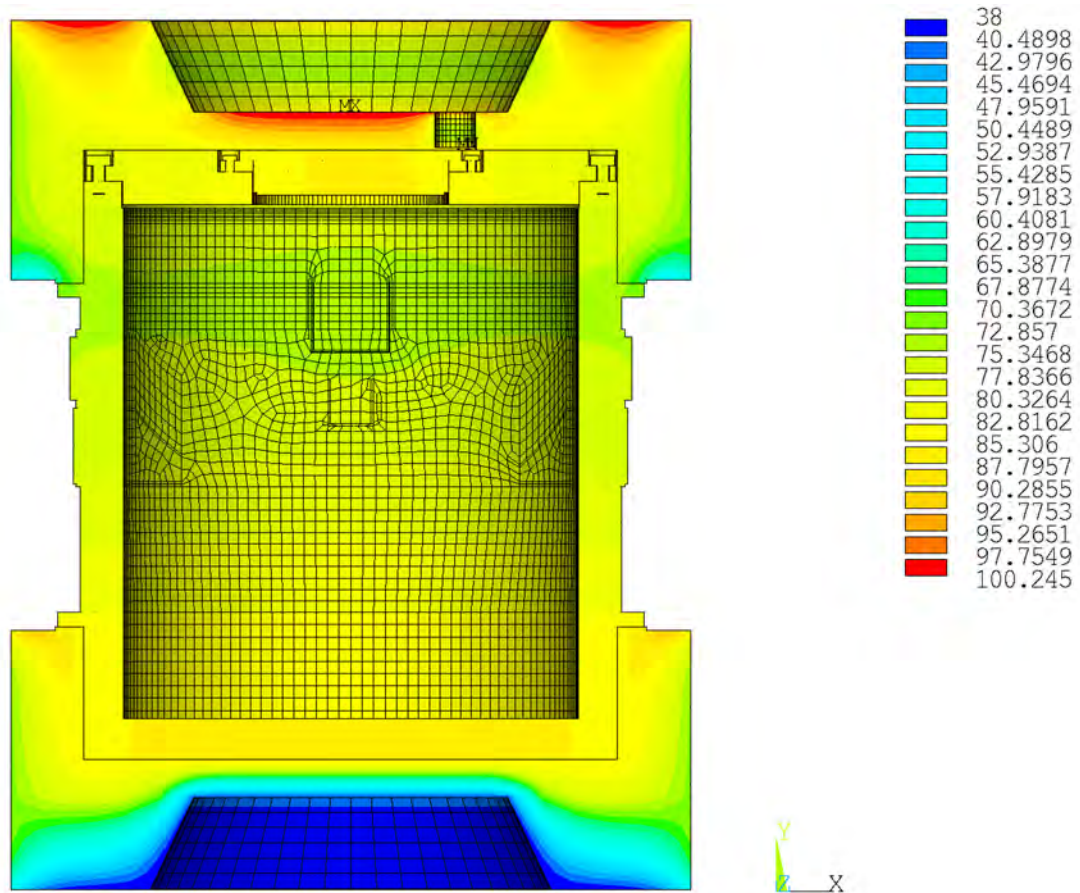
HAC—Fire Top Puncture, Steady-State Initial Conditions (Degrees Celsius)

Figure 3.4.1-4 **Temperature Contour Plot of Package at the End of Fire—HAC Pin Damage on Top Impact Limiter**



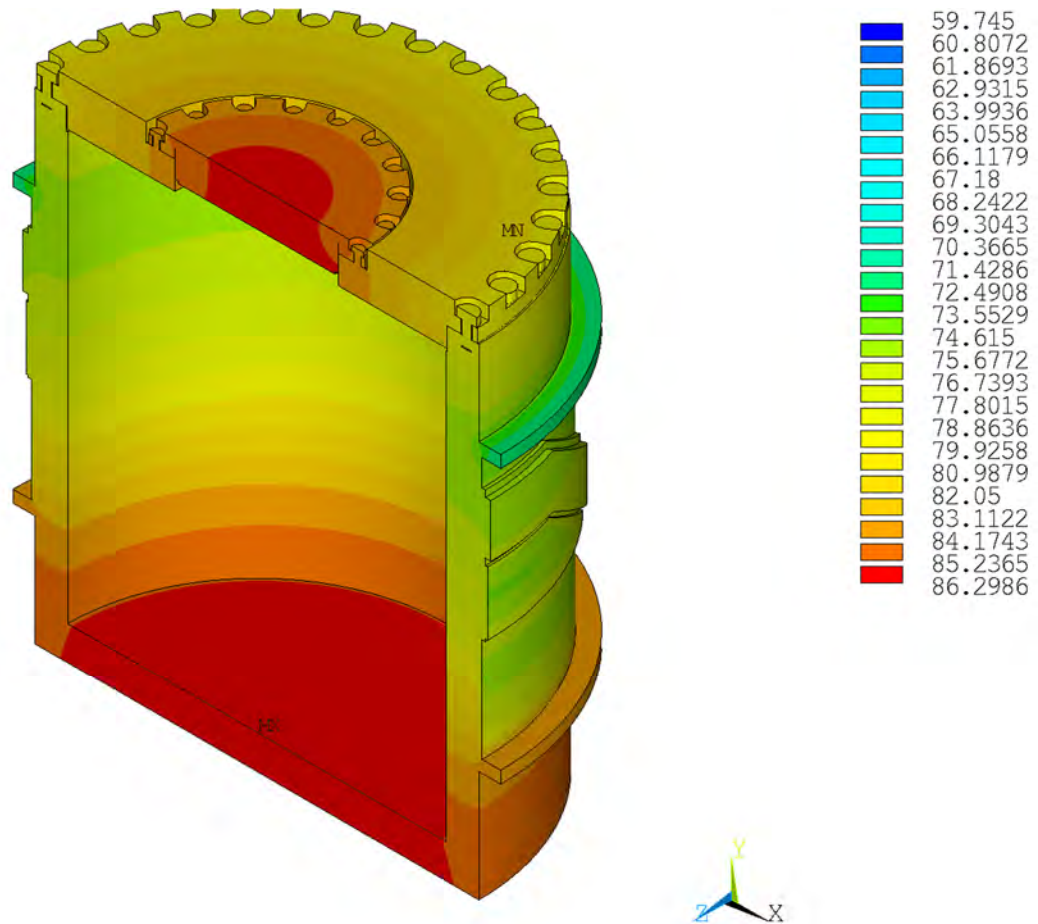
HAC—Fire Top Puncture, Steady-State Initial Conditions (Degrees Celsius)

Figure 3.4.1-5 **Temperature Contour Plot of Cask Body at the End of Fire—HAC
Pin Damage on Top Impact Limiter**



HAC—Fire Top Puncture, Steady-State Initial Conditions (Degrees Celsius)

Figure 3.4.1-6 **Temperature Contour Plot of Package after Cool-Down—HAC Pin Damage on Top Impact Limiter**



HAC—Fire Top Puncture, Steady-State Initial Conditions (Degrees Celsius)

Figure 3.4.1-7 **Temperature Contour Plot of Cask Body after Cool-Down—HAC Pin Damage on Top Impact Limiter**

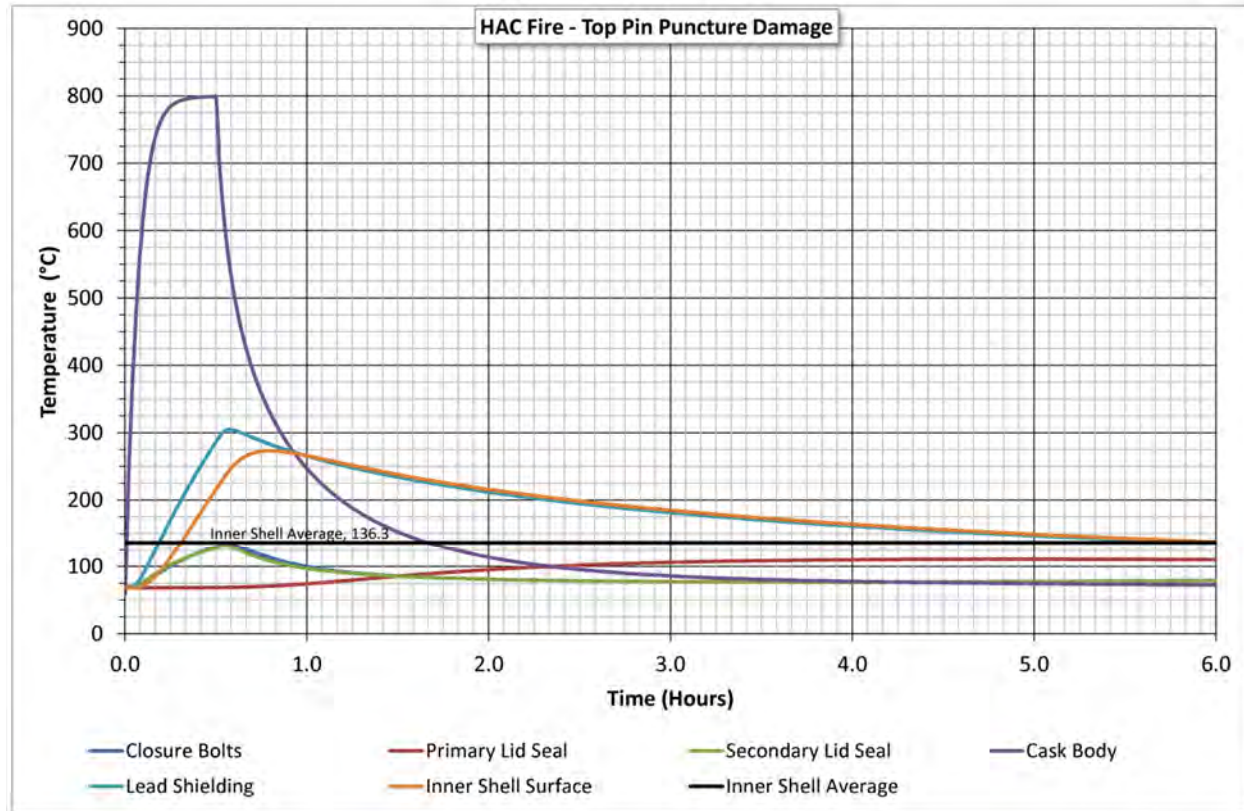


Figure 3.4.1-8 Time-History Plot of Critical Package Components—HAC Pin Damage on Top Impact Limiter

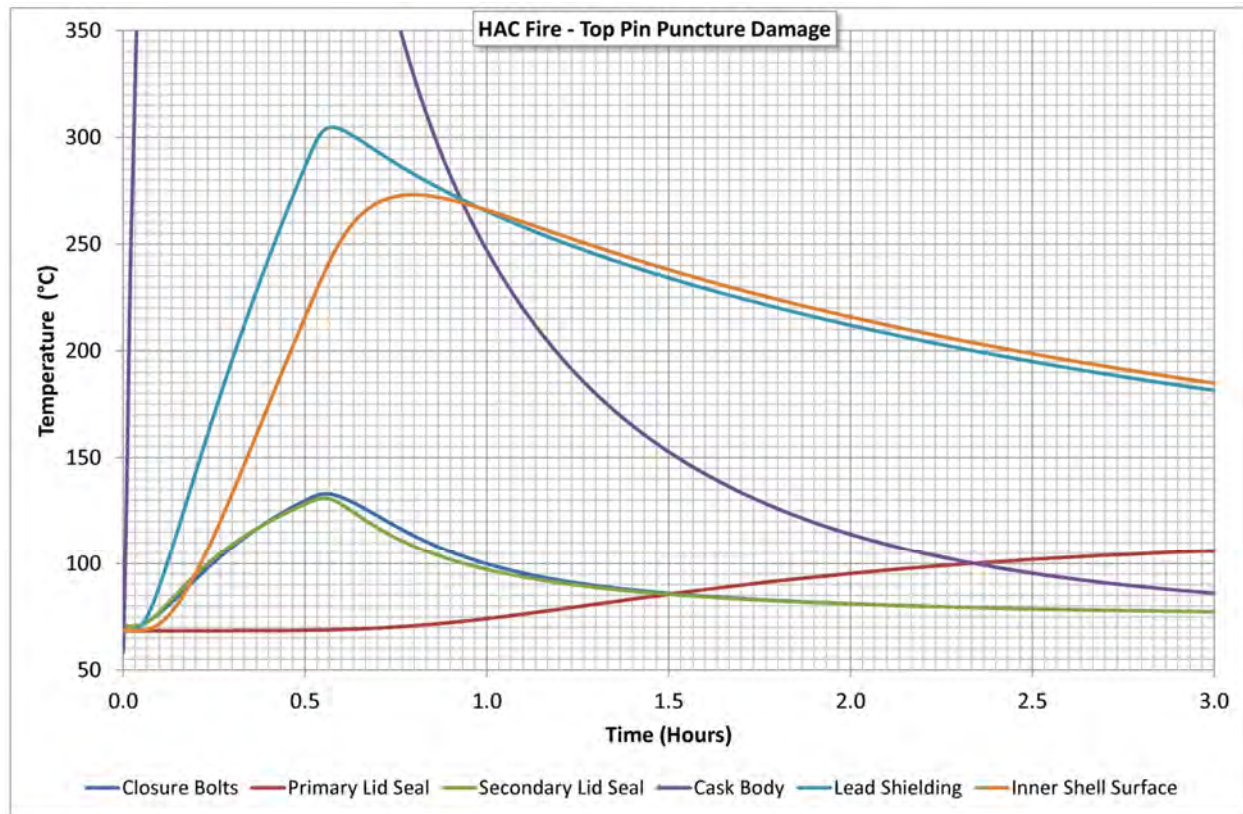
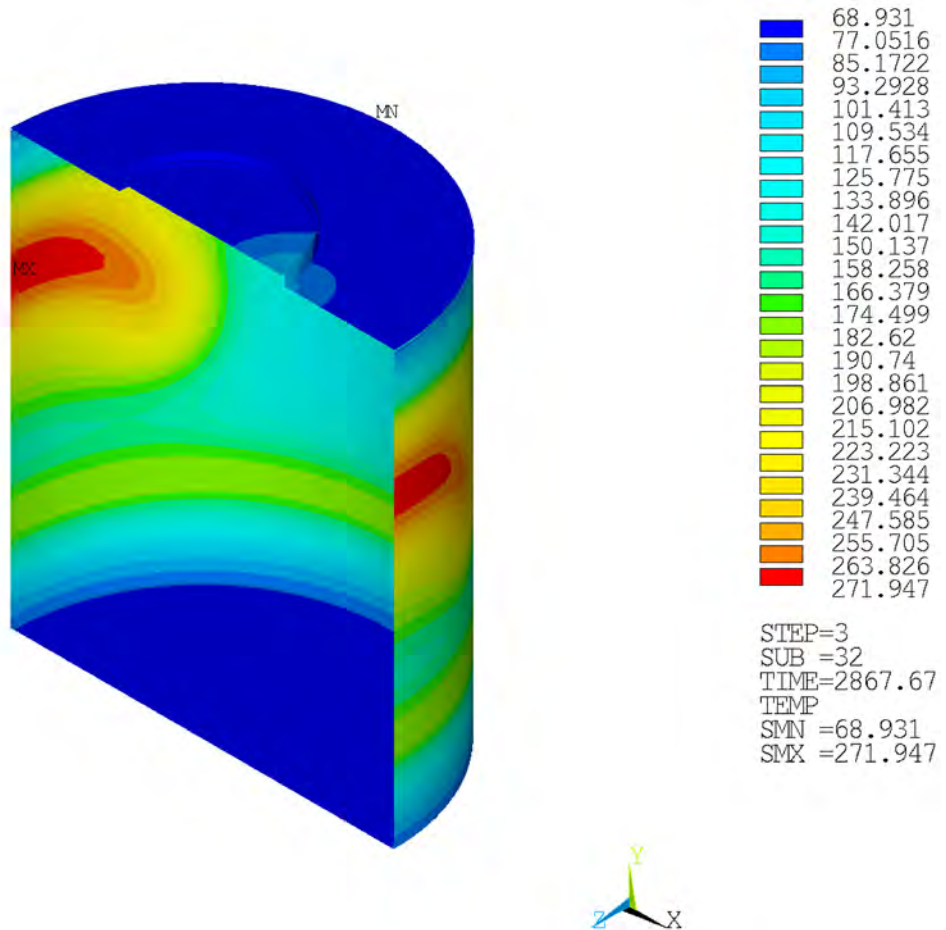
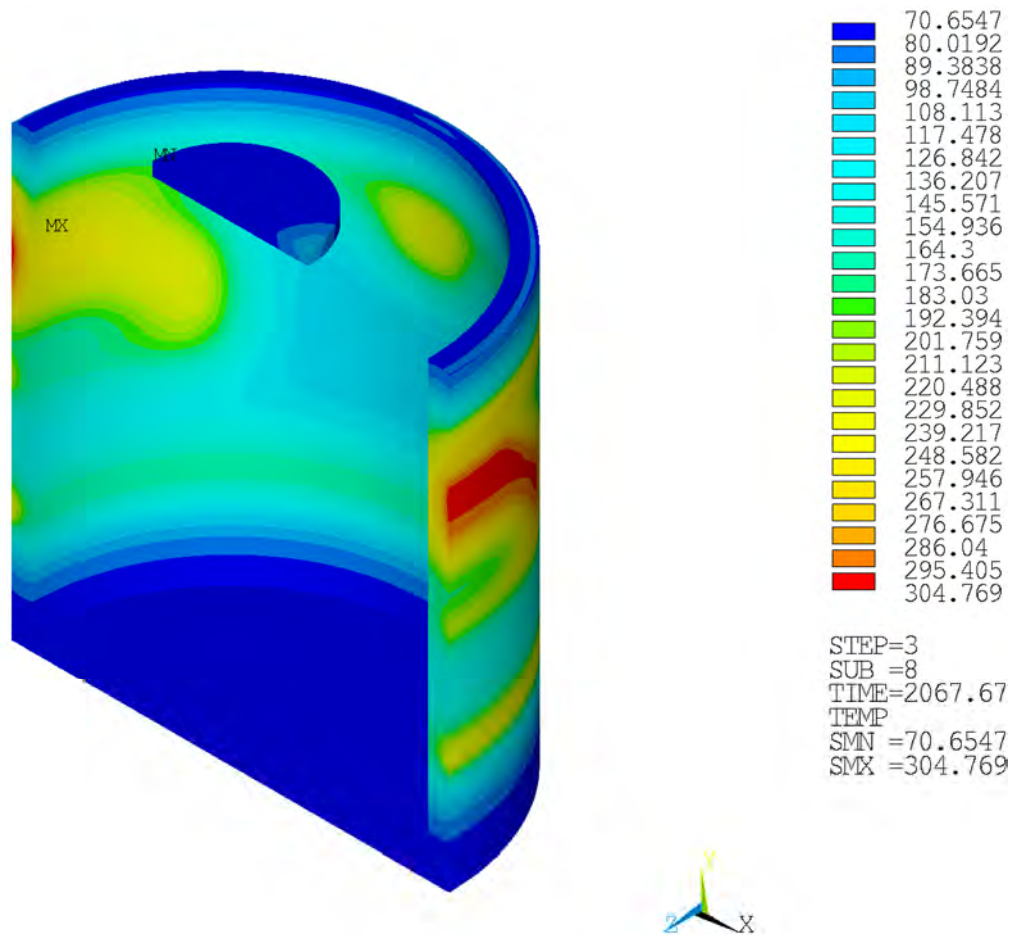


Figure 3.4.1-9 Time-History Enhanced View Plot of Critical Package Components—HAC Pin Damage on Top Impact Limiter



HAC--Fire Top Puncture, Steady-State Initial Conditions (Degrees Celsius)

Figure 3.4.1-10 Maximum Temperature of the Inner Shell—HAC Pin Damage on Top Impact Limiter



HAC—Fire Top Puncture, Steady-State Initial Conditions (Degrees Celsius)

Figure 3.4.1-11 Maximum Temperature of Lead Shielding—HAC Pin Damage on Top Impact Limiter

3.4.2 HAC Fire Evaluation—Pin Puncture Damage to the Side of the Cask Body

The analytical model described in Section 3.3.1.2 is used to evaluate the RT-100 with damage on the cask side wall. For this case, the limiting configuration considers the pin puncturing the thermal shield directly below the lifting block. This configuration increases the area of the outer shell of the cask that is not protected by the thermal shield and maximizes the heat input into the lead. The following section evaluates both pin puncture orientations to determine the effect to critical components such as the seal locations and lead shielding.

3.4.2.1 Initial Condition—Pin Puncture Damage to the Side of the Cask Body

Figure 3.4.2-1 shows the FE model of the cask body due to pin puncture damage on the side. The location of the damage is chosen below the lifting pocket in a region where no thermal insulation exists. Therefore, the heat flow is maximized into the package. The removed elements at this area cover a surface area greater than the area of the pin. As with the pin puncture on the top impact limiter case, NCT Hot case 1 steady state solution is used as the initial condition for the fire cases. The steady-state temperatures are applied as a boundary condition during the first

load step of the transient solution, prior to initiating the HAC fire transient. Figure 3.4.2-2 shows the package temperature distribution prior to the fire. The cask body and inner shell pre-fire temperatures are shown in Figure 3.4.2-3 and Figure 3.4.2-4.

3.4.2.2 HAC Fire Analysis—Pin Puncture Damage to the Side of the Cask Body

The thermal analysis for HAC includes a 30 minute transient fire followed by the prescribed post-fire cool-down period. The FE model described in Section 3.3.1.2 is analyzed by applying the following boundary conditions. Following the initial load step in which the steady-state temperatures are applied, the analysis proceeds with the HAC fire transient for 30 minutes (1,800 seconds) followed by a cool-down period with the boundary conditions associated with NCT hot case 1. The NCT hot case 1 boundary conditions are applied as constants, ignoring the day/night cool-down cycle. The following is a summary of the fire transient boundary conditions:

- Environment temperature, 800°C (1472°F)
- No solar insolation, 0 W/m²
- Forced convection, heat transfer coefficient = 10 W/m²·°C
- Radiation from the environment to package surface, flame emissivity = 0.9
- Internal heat load as a uniform heat flux, 13.04 W/m²

The cool-down analysis is performed for 216,000 seconds (2.5 days) with the following boundary conditions:

- Environment temperature, 38°C (100°F)
- Solar insolation applied as constant, 776 W/m² for flat surfaces and 388 W/m² for curved surfaces.
- Natural convection, heat transfer coefficient = 5 W/m²·°C
- Radiation from package surface to the environment, package emissivity = 0.8
- Internal heat load as a uniform heat flux, 13.04 W/m²

Proprietary Information Content Withheld Under 10 CFR 2.390(b)

Proprietary Information Content Withheld Under 10 CFR 2.390(b)

Table 3.1.3-3 summarizes the maximum temperatures of the cask under HAC fire with pin puncture damage at the side of the cask body.

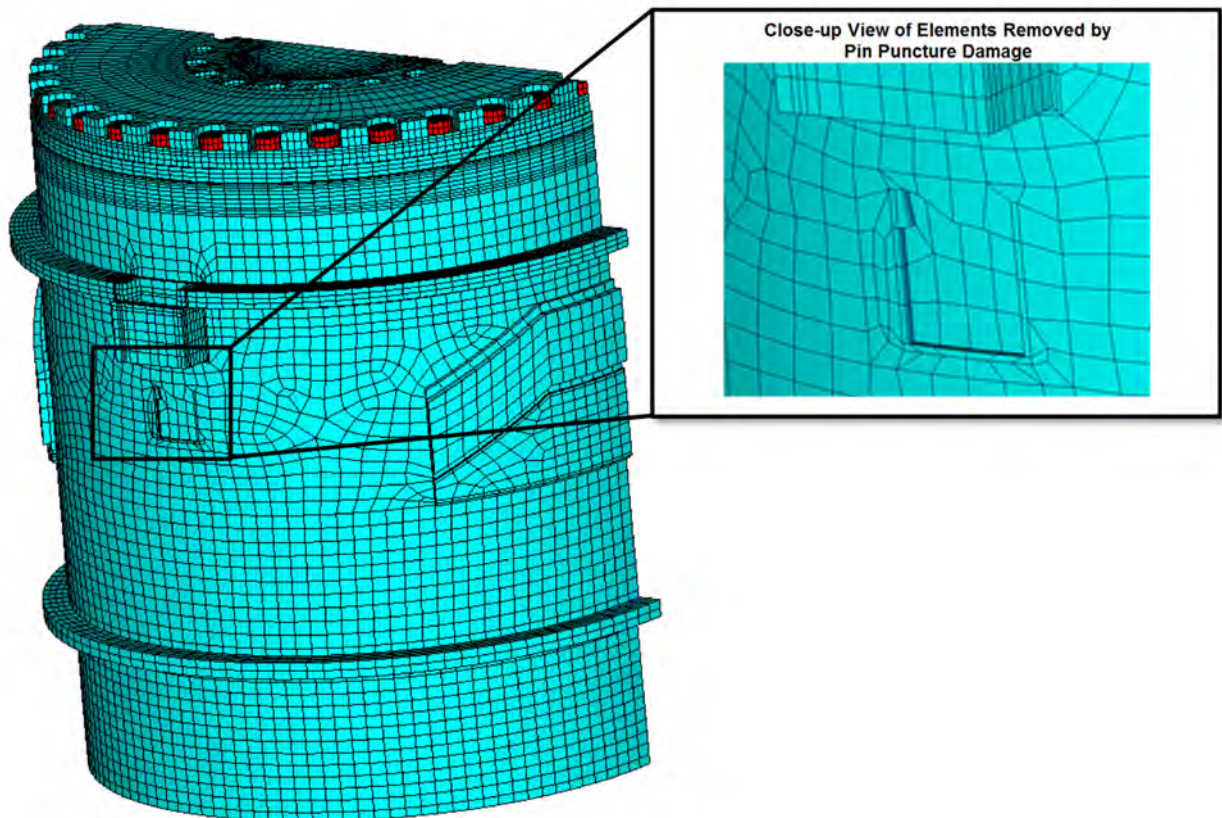
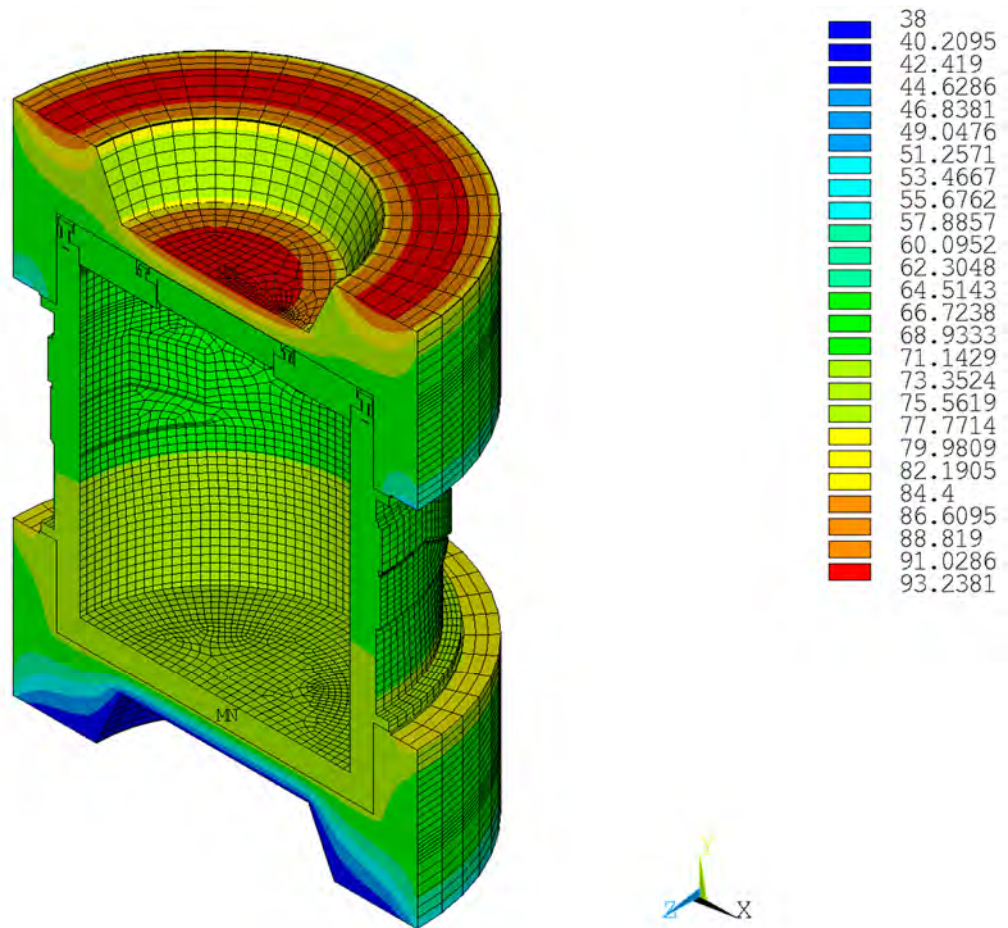
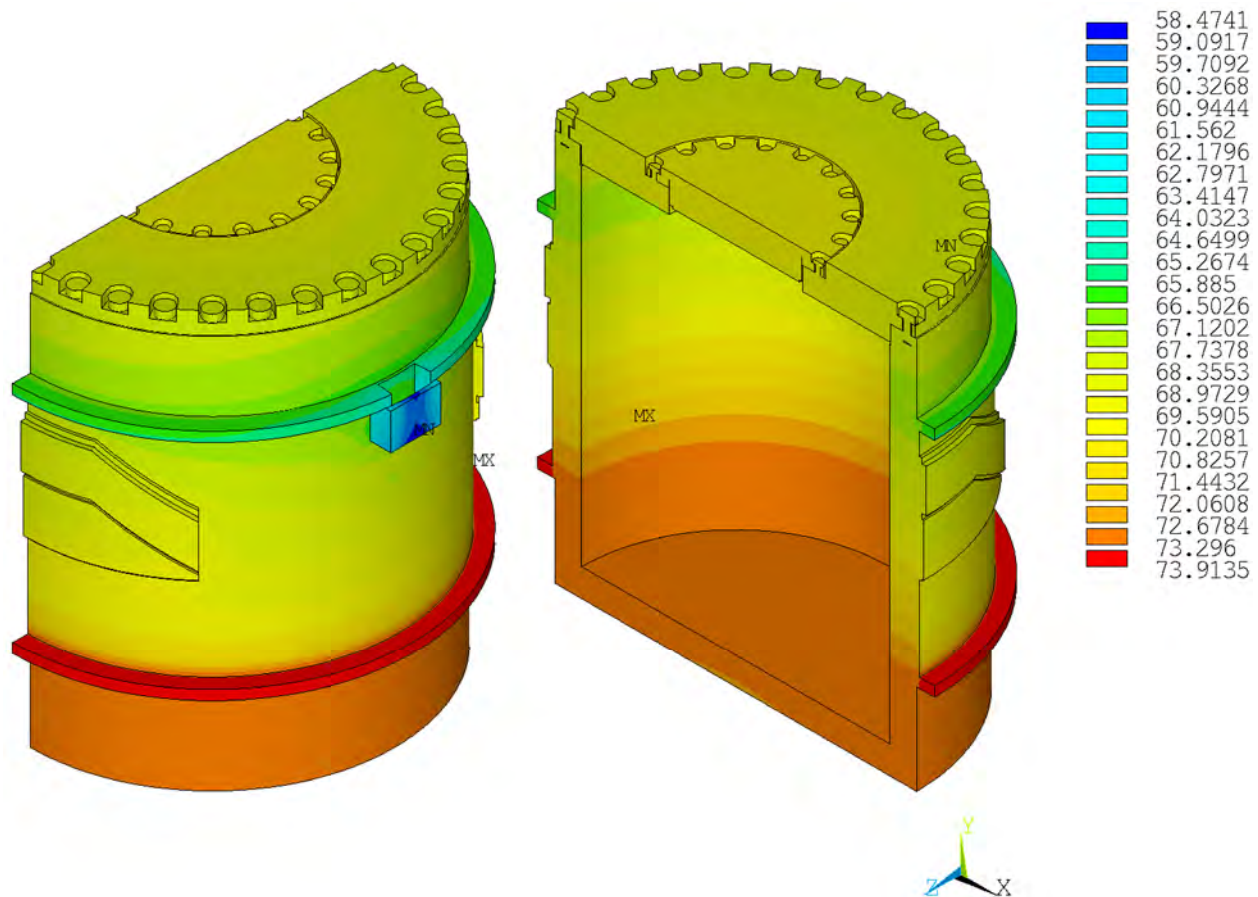


Figure 3.4.2-1 Cask Model-HAC Pin Damage on Cask Body Side



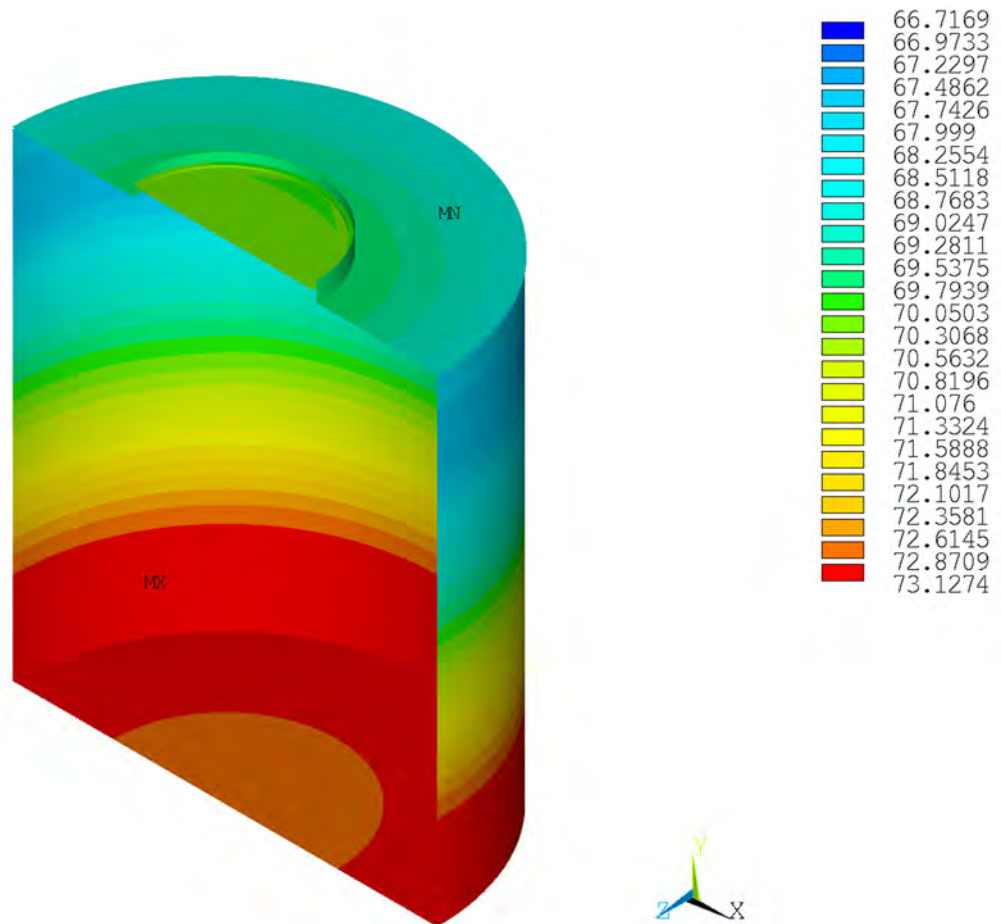
HAC—Fire Side Puncture, Steady-State Initial Conditions (Degrees Celsius)

Figure 3.4.2-2 **Temperature Contour Plot of Package Pre-Fire Condition—HAC Pin Damage on Cask Body Side**



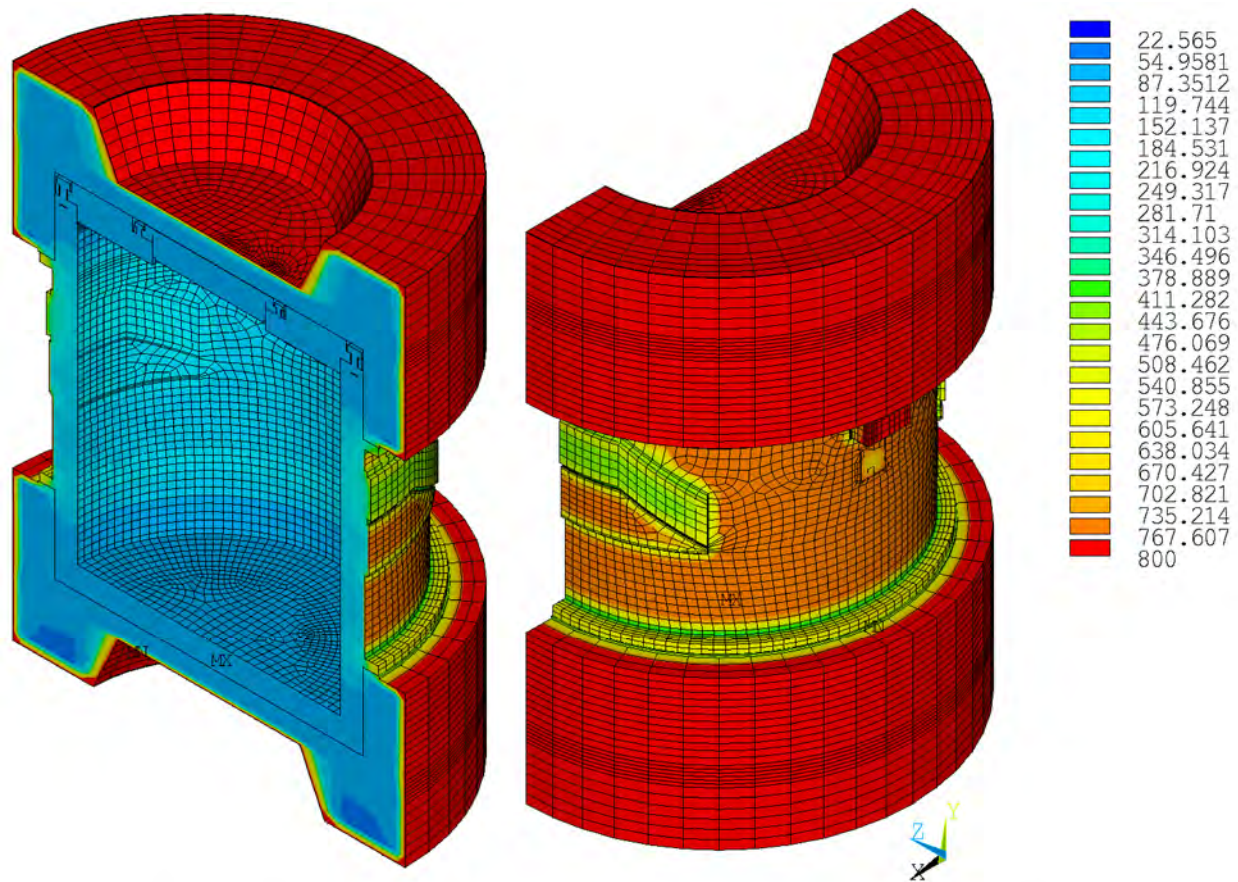
HAC—Fire Side Puncture, Steady-State Initial Conditions (Degrees Celsius)

Figure 3.4.2-3 **Temperature Contour Plot of Cask Body Pre-Fire Condition—HAC**
Pin Damage on Cask Body Side



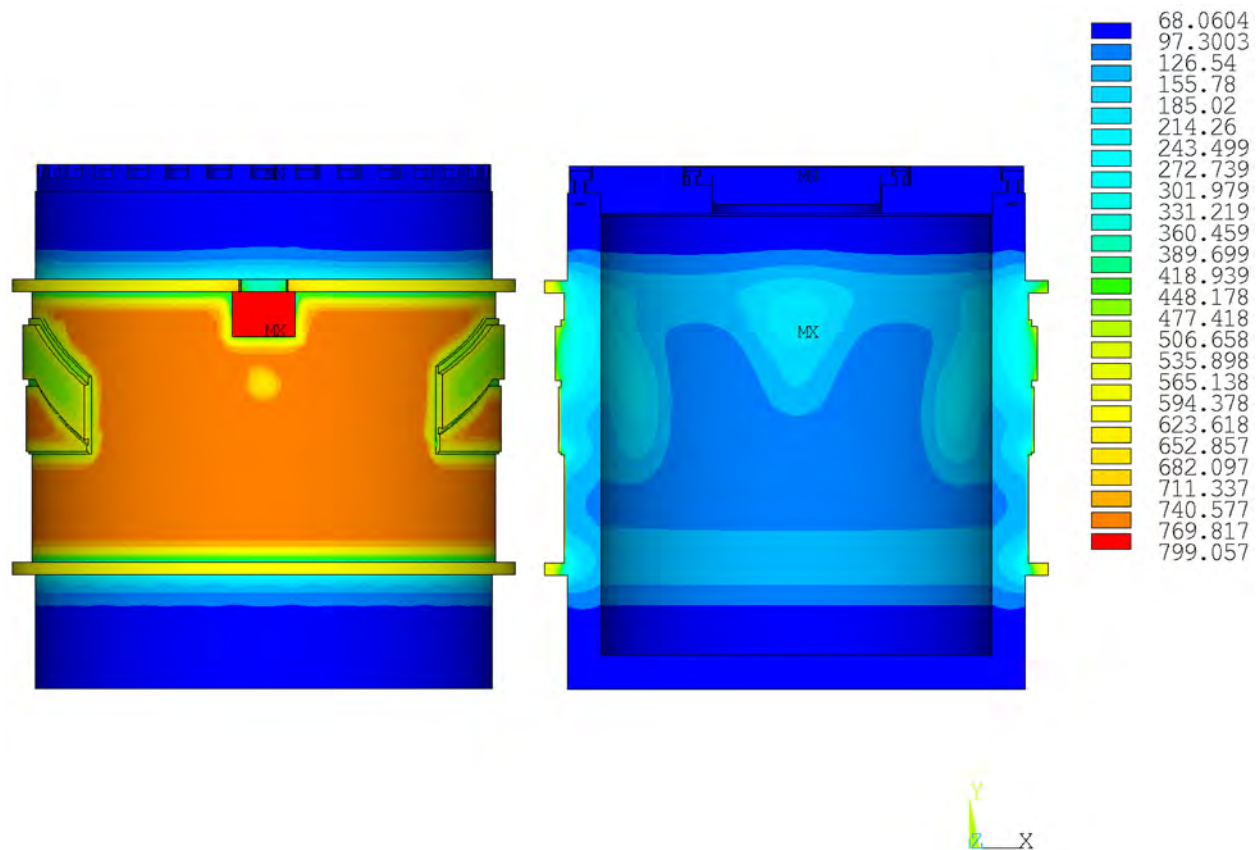
HAC—Fire Side Puncture, Steady-State Initial Conditions (Degrees Celsius)

Figure 3.4.2-4 **Temperature Contour Plot of Inner Shell Pre-Fire Condition—HAC**
Pin Damage on Cask Body Side



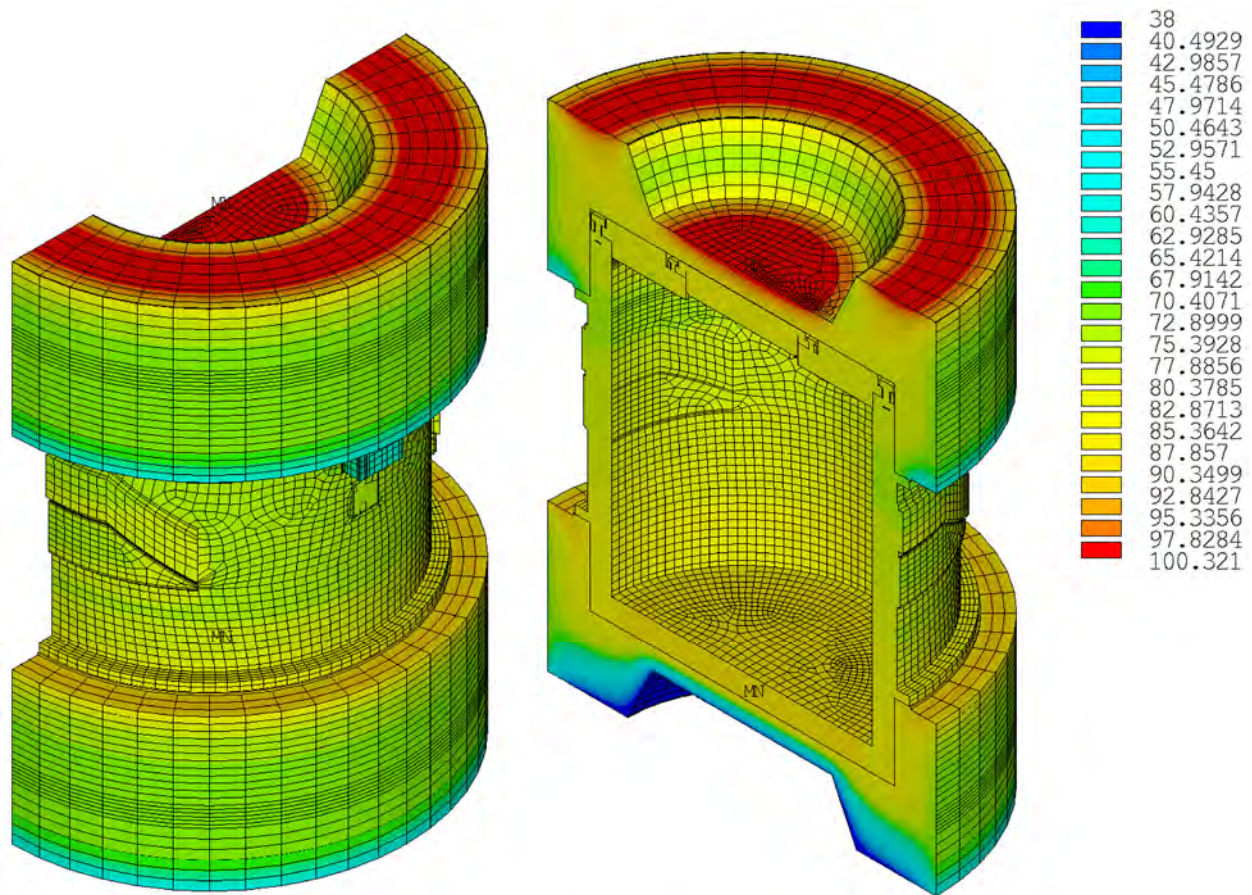
HAC—Fire Side Puncture, Steady-State Initial Conditions (Degrees Celsius)

Figure 3.4.2-5 **Temperature Contour Plot of Package at the End of Fire—HAC Pin Damage on Cask Body Side**



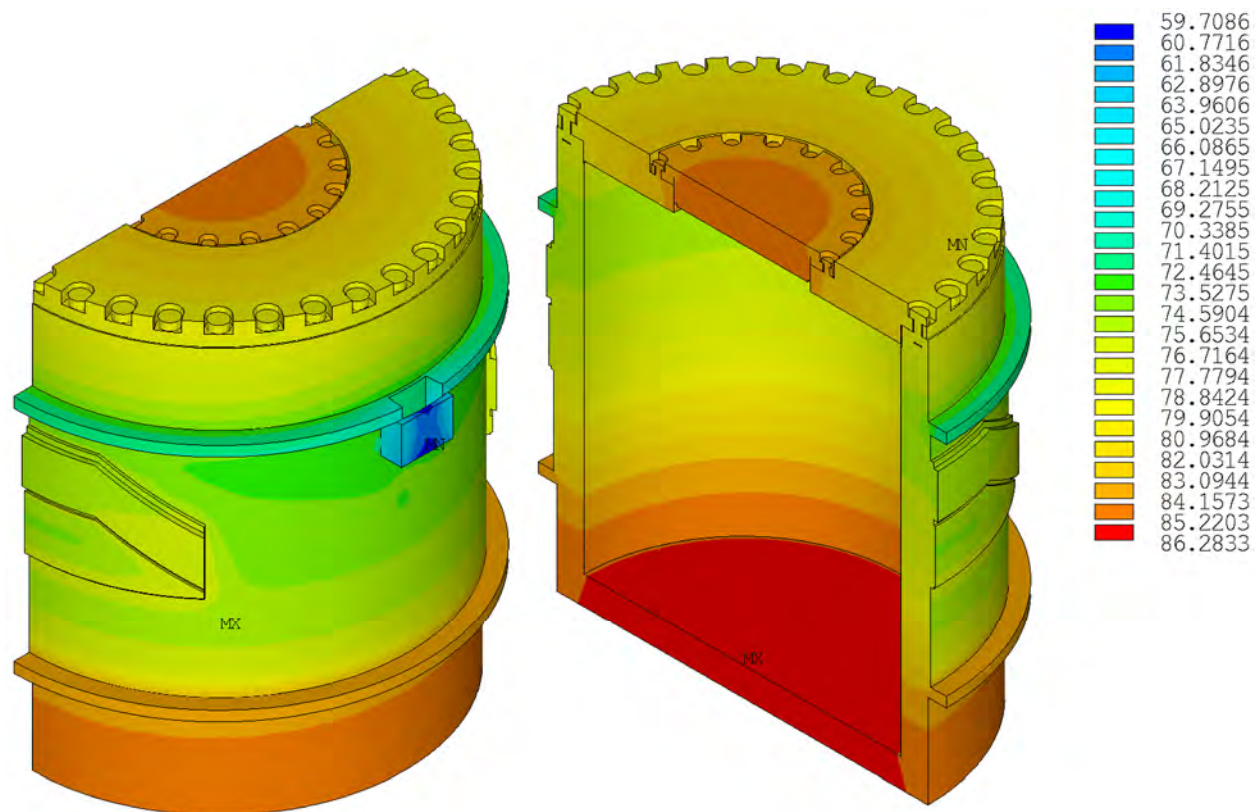
HAC—Fire Side Puncture, Steady-State Initial Conditions (Degrees Celsius)

Figure 3.4.2-6 Temperature Contour Plot of Cask Body at the End of Fire—HAC Pin Damage on Cask Body Side



HAC—Fire Side Puncture, Steady-State Initial Conditions (Degrees Celsius)

Figure 3.4.2-7 **Temperature Contour Plot of Package after Cool-Down—HAC Pin Damage on Cask Body Side**



HAC—Fire Side Puncture, Steady-State Initial Conditions (Degrees Celsius)

Figure 3.4.2-8 Temperature Contour Plot of Cask Body After Cool-Down—HAC Pin Damage on Cask Body Side

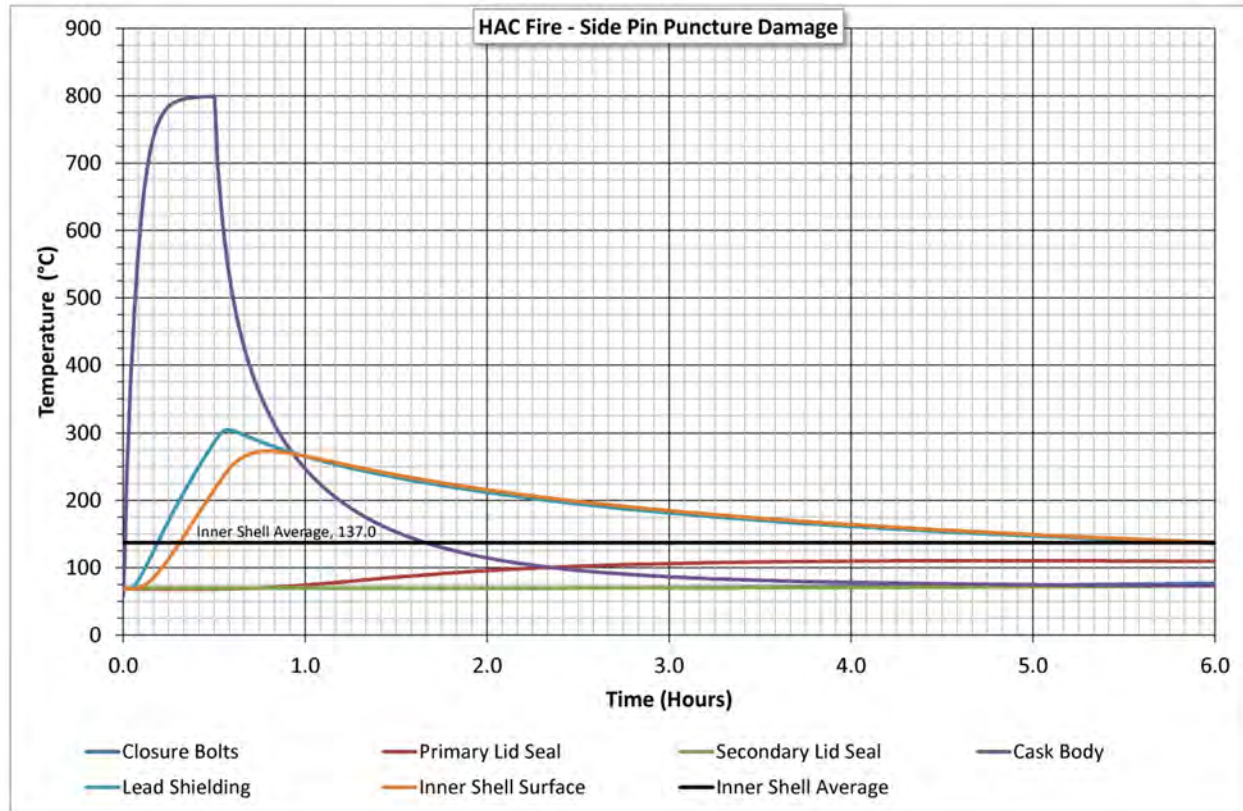


Figure 3.4.2-9 Time-History Plot of Critical Package Components—HAC Pin Damage on Cask Body Side

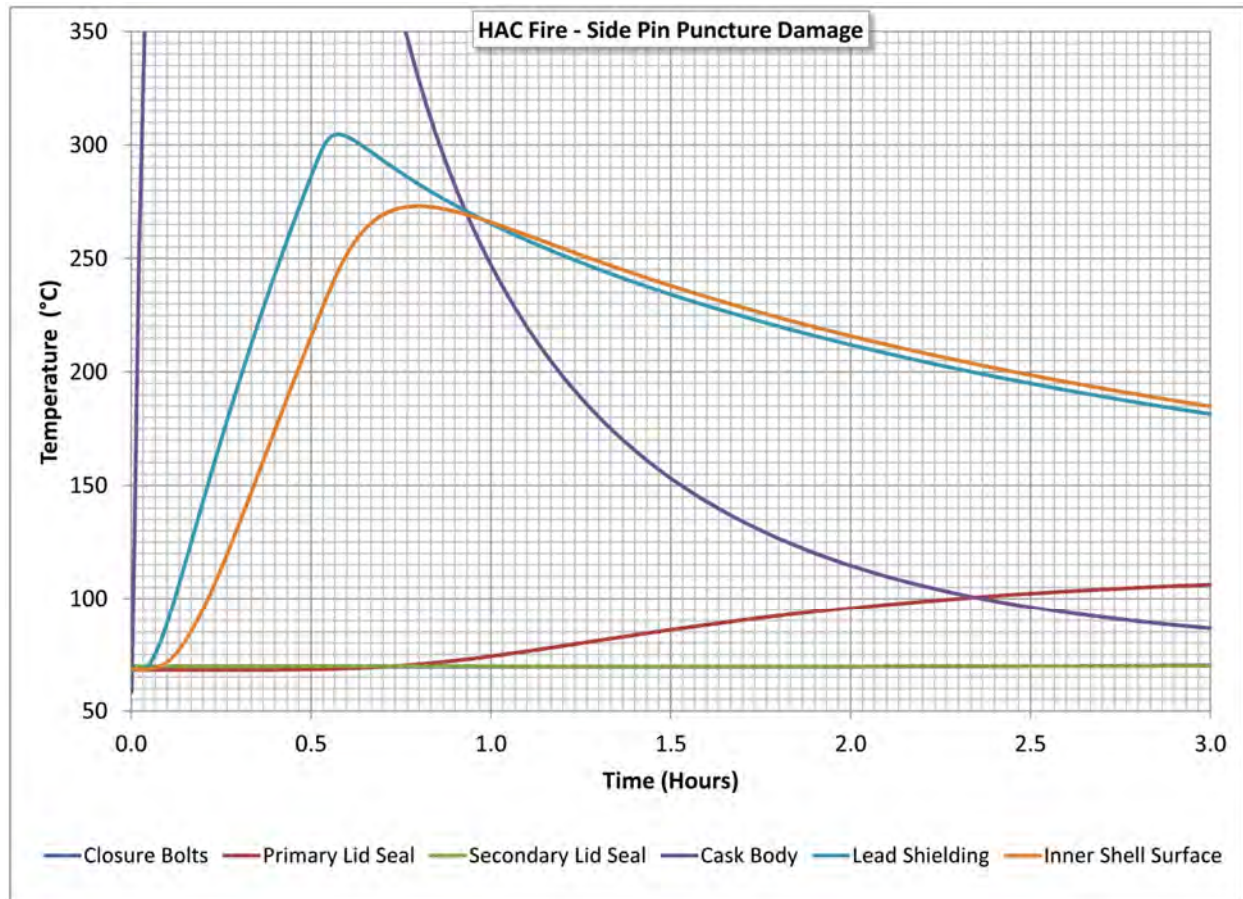
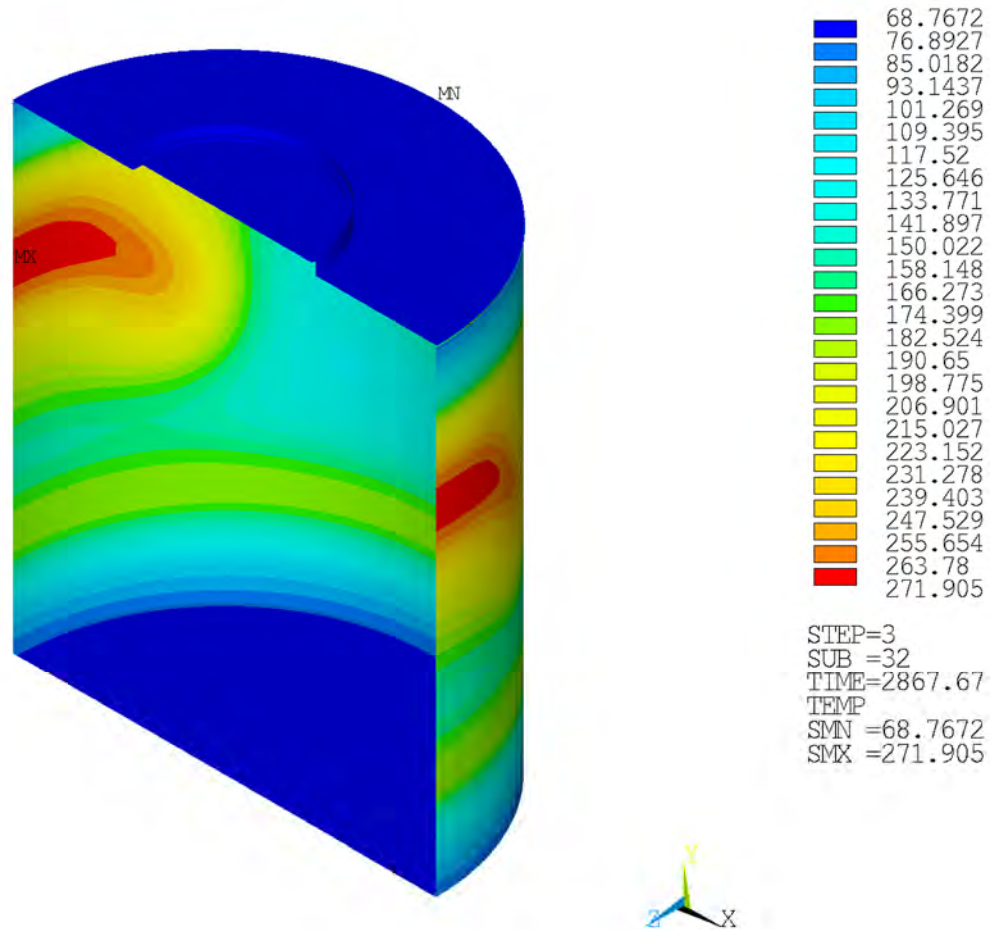
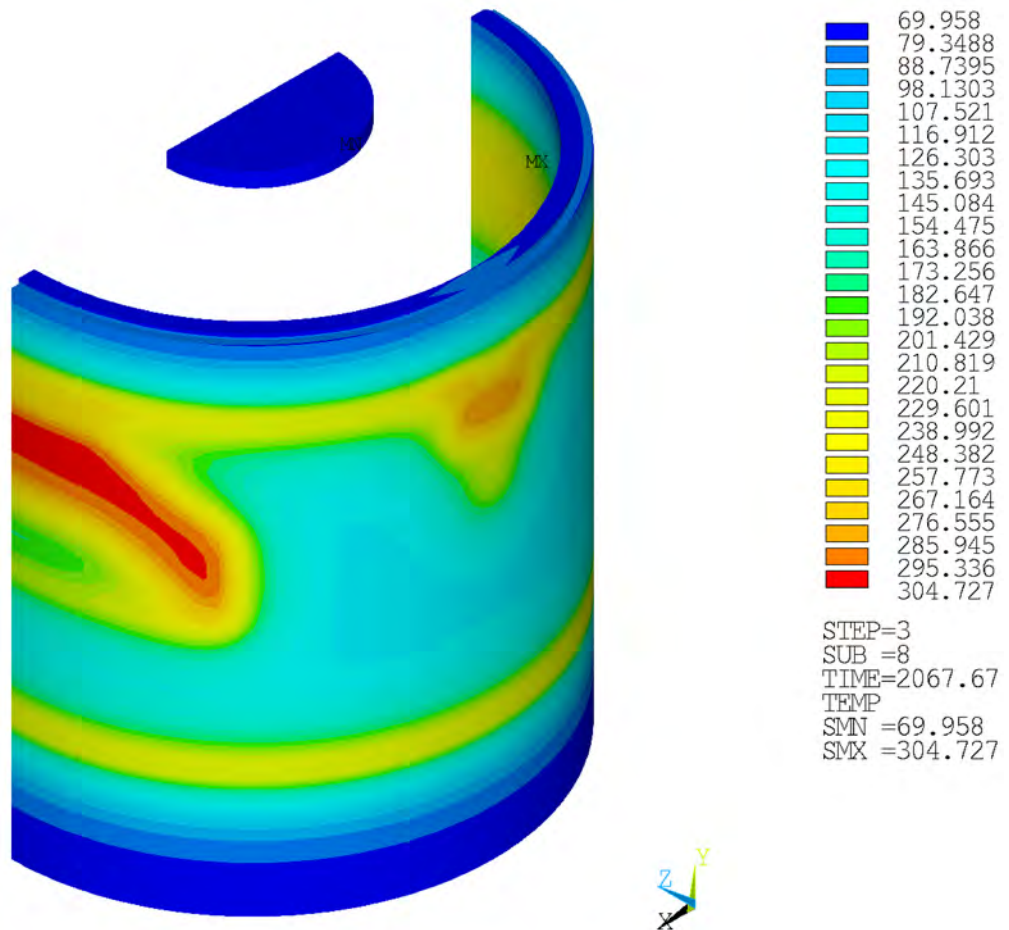


Figure 3.4.2-10 Time-History Enhanced View Plot of Critical Package Components—HAC Pin Damage on Cask Body Side



HAC—Fire Side Puncture, Steady-State Initial Conditions (Degrees Celsius)

Figure 3.4.2-11 Maximum Temperature of the Inner Shell—HAC Pin Damage on Cask Body Side



HAC—Fire Side Puncture, Steady-State Initial Conditions (Degrees Celsius)

Figure 3.4.2-12 Maximum Temperature of Lead Shielding—HAC Pin Damage on Cask Body Side

3.4.3 Maximum Temperatures and Pressure

This section summarizes the peak accident condition temperatures of RT-100 components as a function of time both during and after the fire, as well as the maximum temperatures from the post-fire, steady-state condition. This section includes those temperatures at locations in the package that are significant to the safety analysis and review. The calculations of transient temperatures trace the temperature-time history up to and past the time at which maximum temperatures are achieved and begin to fall. The calculations confirm that these temperatures do not exceed their maximum allowable values. It also confirms that lead shielding does not reach melting temperature.

The RT-100 is evaluated structurally for the maximum HAC temperatures and pressures in Chapter 2, Section 2.7.4 (Thermal).

3.4.3.1 Maximum Temperatures

Section 3.4.1 and 3.4.2 present a summary of the evaluation of the RT-100 for the hypothetical accident condition fire transient. Provided in the summary are figures depicting temperature distributions and time histories as a function of time during and after the fire transient. Maximum temperatures for various cask components as a result of the HAC are presented in Table 3.1.3-2 and Table 3.1.3-3.

Of interest in this section is the determination of the maximum internal pressure in the cask cavity as a result of the fire test. As shown in Table 3.1.3-3, the maximum average inner shell temperature during the fire transient is 137°C. The temperature of the cask body components is increased due to the fire transient, with a maximum normal condition inner shell temperature of 73.1°C as reported in Table 3.1.3-1. Because the temperature of the inner shell of the cask is raised by 64°C as a result of the fire transient and because the maximum internal decay heat of the contents is only 200 watts, it is conservative to assume that the cavity temperatures are bounded by the average inner shell temperatures. For conservatism, the inner shell can be assumed to be at 150°C for the pressure calculations presented in Section 3.4.3.2.

As previously discussed, the primary components of interest during the fire transient from a temperature standpoint are the lead gamma shielding and the O-ring seals in the primary and secondary lids. As described in detail in Section 3.4.2, the lead and O-ring materials do not exceed their allowable, and in fact have safety margins of more than 23°C below their maximum allowable temperatures. The temperature distributions within the cask, as a result of the hypothetical accident condition fire transient, are fully considered in the structural evaluation of the cask presented in Chapter 2, Section 2.7.4 (Thermal).

3.4.3.2 Maximum Accident Condition Pressure

The evaluation of the maximum pressure in the RT-100 is based on the maximum normal operating pressure, and considers fire-induced increases in package temperatures, thermal combustion or decomposition processes, phase changes, etc. (Fuel rod failure is not applicable). The value of this maximum pressure is consistent with the values used in the Structural Evaluation and Containment sections.

Similar to the calculation of the maximum normal operating pressure in Section 3.3.2, the maximum accident condition pressure is calculated using bounding assumptions for the temperatures in the cask as a result of the hypothetical accident condition fire transient. The maximum pressure is the sum of four components:

1. The pressure due to the initially sealed air in the cavity
2. The pressure due to water vapor in the cask
3. The pressure due to the hydrogen and oxygen gases generated by radiolysis
4. The pressure due to the thermal decomposition of the contents

The following sections present a summary of the maximum accident condition pressure calculation. Details of the calculation are provided in Calculation Package RTL-001-CALC- TH-0202, Rev. 6 [Ref. 7], and RTL-001-CALC-TH-0301, Rev. 1 [Ref. 25].

3.4.3.2.1 Calculation Method

The internal cavity pressure due to accident condition temperatures is determined using the same method used to calculate the maximum normal condition pressure in Section 3.3.2. The method presented below is equal to that used previously, with the maximum normal operating pressure and internal temperatures used along with the maximum internal temperature determined in Section 3.4.3.1 to calculate the maximum accident condition pressure.

3.4.3.2.2 Pressure Due to the Initially Sealed Air in the Cavity

Per the ideal gas law, the partial pressure of the air (P_{air}) initially sealed in the fixed volume of the cask at the ambient temperature as it is heated to 150 °C is:

$$P_1 \times T_2 = P_2 \times T_1$$

$$P_{\text{air}} = 101.35 \text{ kPa}[(423.15 \text{ K}) / (294.25 \text{ K})] = 145.8 \text{ kPa (21.15 psia)}$$

3.4.3.2.3 Pressure Due to the Water Vapor in the Cask

The RT-100 cavity is assumed to contain a small amount of water. By conservatively assuming a condensing surface temperature of 150 °C, the water vapor pressure, P_{wv} , at this temperature is 475.8 kPa [69 psia] Fundamentals of Engineering Thermodynamics, 5th Edition, Table A-2 on pg. 761 [Ref. 18], also see Attachment 3.5-4. Adding the water vapor pressure at 150 °C to the partial pressure of the air in the sealed cask at this temperature gives:

$$P_2 = P_{\text{air}} + P_{\text{wv}} = 145.8 + 475.8 = 621.6 \text{ kPa [90.16 psia]}$$

3.4.3.2.4 Pressure Due to Generation of Gas

Solidified or dewatered material may contain some water. Therefore, radiolytic generation of gases from this water could occur. Hydrogen and oxygen may be produced in the cask by radiolytic decomposition of residual water in the cask contents. As described in Section 1.2.2.6, the maximum quantity of hydrogen must be limited to less than 5% to ensure that an explosive quantity does not accumulate.

The cask atmosphere can be assumed to contain 5% of hydrogen (H_2) gas due to radiolysis of the water. By stoichiometry of the water molecule (H_2O), the cask atmosphere will also contain 2.5% oxygen (O_2) gas generated by radiolysis. Partial pressures in an ideal gas mixture are additive and behave the same as ideal gas volume fraction or mole fractions. Therefore, the partial pressure of hydrogen is described by the following equation:

$$P_{H_2} = 0.05 P_{pt}$$

$$\text{Where, } P_{pt} = P_{air} + P_{wv} + P_{H_2} + P_{O_2}$$

$$\text{Combining } P_{air} + P_{wv} = P_2 \text{ and noting that } P_{O_2} = 0.5 \times P_{H_2}.$$

$$P_{H_2} = 0.05 \times (P_2 + 1.5 P_{H_2})$$

Solving the equation explicitly for P_{H_2} gives:

$$\begin{aligned} P_{H_2} &= [0.05 P_2] / [1 - 0.05 (1.5)] \\ &= [0.05 * 621.6 \text{ kPa}] / [1 - 0.05 (1.5)] \\ &= 33.6 \text{ kPa [4.87 psia]} \end{aligned}$$

3.4.3.2.5 Total Pressure

Based on the stoichiometric relationship between hydrogen and oxygen liberated by radiolysis of water, and again combining the pressure of the initially sealed air and water vapor as P_2 , the total pressure in the cask at 150 °C is:

$$\begin{aligned} P_{Total} &= P_2 + 1.5 P_{H_2} \\ &= 621.6 \text{ kPa} + 1.5 * 33.6 \text{ kPa} \\ &= 672 \text{ kPa [97.47 psia]} \end{aligned}$$

The maximum pressure is 672 kPa [97.47 psia] under HAC. For conservatism, the maximum accident pressure is assumed to be 689.4 kPa [100 psia] for the structural analyses presented in Chapter 2, Section 2.7.4 (Thermal).

3.4.3.2.6 Total Pressure Accounting for Combustion of Contents

In addition to the natural effect of temperature increases on pressure buildup in the package, other thermally driven phenomena can contribute to the pressure buildup within the containment boundary of a package. As discussed previously, these include phase transformation of materials in the package and radiolysis of the contents by radioactive decay. Additionally, the pressure increases due to the contribution of the partial pressure that results from the thermal decomposition of the package contents [Ref 25].

Solid polymeric materials, including cellulose such as wood and paper, undergo both physical and chemical changes when heat is applied. Thermal decomposition is a process of extensive

chemical species change caused by heat, generating gaseous fuel vapors which can burn above the solid material. The process is self-sustaining when the burning gases feed back sufficient heat to the material to continue the production of gaseous fuel vapors or volatiles. These volatiles react with the oxygen in the air to generate heat, and part of this heat is transferred back to the polymer to continue the process.

The Robatel RT-100 contents include filters that may be constructed from thermoplastics (nylon, polyester, polypropylene) or paper and shoring made of wood may be contained in the package. Although it is unlikely that temperatures under HAC will approach the auto-ignition temperatures of the contents, the following analysis is performed to evaluate the effect of combustion on the package pressure.

Combustion in a sealed container is limited by the amount of air present to support the chemical reaction for the thermal decomposition of the fuel. Heats from the exothermic combustion reaction will increase the temperature of the contents and packaging. The maximum temperature in a sealed container will determine the maximum pressure, along with some additional pressure from emitted gases. The sealed inner containment of the RT-100 cask contains only enough air (5.75 kg) for complete combustion of approximately 1.127 kg of cellulosic material, paper or wood; or 0.390 kg of polyethylene.

Gibbs-Dalton Law defines total pressure, P_T , equal to the sum of the partial pressures of the individual gases present. The total pressure P_T , in the package containment is the sum of pressures due to phase transformation of materials in the package P_v (Ref. 25, p. 25, where $P_v = P_{sat}$), radiolysis of the contents by radioactive decay P_r ($1.5 P_{H2}$ from Section 3.4.3.2.5), and thermal decomposition of the package contents P_f (Ref. 25, p. 25, where $P_f = P_{fwood}$). The vapor pressure from the phase transformation of water and the partial pressures of hydrogen and oxygen gases generated from the radiolysis of water in the contents are considered in the total pressure calculation.

$$P_T = P_v + P_r + P_f$$

$$P_T = 463.2 \text{ kPa} + 50.4 \text{ kPa} + 171.0 \text{ kPa} = 684.6 \text{ kPa} [99.3 \text{ psia}]$$

where the total pressure of the inner cavity is based on the complete combustion of wood, which has the highest heat of combustion. Since the temperature required to ignite wood are not sustainable, complete combustion is not considered a credible event, therefore, the maximum pressure is taken as 97.47 psia as demonstrated in Section 3.4.3.2.5.

3.4.4 Maximum Thermal Stress

The RT-100 cask is evaluated for the stresses produced by the temperature gradients in the cask body that result from exposure of the cask to the HAC fire transient. This evaluation, which utilizes the temperature distributions resulting from the fire accident as described in Section 3.4.3, is presented in detail in Chapter 2, Section 2.7.4 (Thermal).

3.4.5 Accident Conditions for Fissile Material Packages for Air Transport

This Section is NOT APPLICABLE. The RT-100 is not be used for fissile material air transport.

3.5 Appendix

Attachment 3.5-1 EPDM Temperature Specifications

[Ref. 16]

Basic O-Ring Elastomers

Parker O-Ring Handbook

Not compatible with:

- Fuels of high aromatic content (for flex fuels a special compound must be used).
- Aromatic hydrocarbons (benzene).
- Chlorinated hydrocarbons (trichloroethylene).
- Polar solvents (ketone, acetone, acetic acid, ethylene-ester).
- Strong acids.
- Brake fluid with glycol base.
- Ozone, weather and atmospheric aging.

2.2.2 Carboxylated Nitrile (XNBR)

Carboxylated Nitrile (XNBR) is a special type of nitrile polymer that exhibits enhanced tear and abrasion resistance. For this reason, XNBR based materials are often specified for dynamic applications such as rod seals and rod wipers.

Heat resistance

- Up to 100°C (212°F) with shorter life @ 121°C (250°F).

Cold flexibility

- Depending on individual compound, between -18°C and -48°C (0°F and -55°F).

Chemical resistance

- Aliphatic hydrocarbons (propane, butane, petroleum oil, mineral oil and grease, diesel fuel, fuel oils) vegetable and mineral oils and greases.
- HFA, HFB and HFC hydraulic fluids.
- Many diluted acids, alkali and salt solutions at low temperatures.

Not compatible with:

- Fuels of high aromatic content (for flex fuels a special compound must be used).
- Aromatic hydrocarbons (benzene).
- Chlorinated hydrocarbons (trichloroethylene).
- Polar solvents (ketone, acetone, acetic acid, ethylene-ester).
- Strong acids.
- Brake fluid with glycol base.
- Ozone, weather and atmospheric aging.

2.2.3 Ethylene Acrylate (AEM, Vamac)

Ethylene acrylate is a terpolymer of ethylene and methyl acrylate with the addition of a small amount of carboxylated curing monomer. Ethylene acrylate rubber is not to be confused with polyacrylate rubber (ACM).

Heat resistance

- Up to 149°C (300°F) with shorter life up to 163°C (325°F).

Cold flexibility

- Between -29°C and -40°C (-20°F and -40°F).

Chemical resistance

- Ozone.
- Oxidizing media.
- Moderate resistance to mineral oils.

Not compatible with:

- Ketones.
- Fuels.
- Brake fluids.

2.2.4 Ethylene Propylene Rubber (EPR, EPDM)

EPR copolymer ethylene propylene and ethylene-propylene-diene rubber (EPDM) terpolymer are particularly useful when sealing phosphate-ester hydraulic fluids and in brake systems that use fluids having a glycol base.

Heat resistance

- Up to 150°C (302°F) (max. 204°C (400°F)) in water and/or steam).

Cold flexibility

- Down to approximately -57°C (-70°F).

Chemical resistance

- Hot water and steam up to 149°C (300°F) with special compounds up to 260°C (500°F).
- Glycol based brake fluids (Dot 3 & 4) and silicone-based brake fluids (Dot 5) up to 149°C (300°F).
- Many organic and inorganic acids.
- Cleaning agents, sodium and potassium alkalis.
- Phosphate-ester based hydraulic fluids (HFD-R).
- Silicone oil and grease.
- Many polar solvents (alcohols, ketones, esters).
- Ozone, aging and weather resistant.

Not compatible with:

- Mineral oil products (oils, greases and fuels).

2.2.5 Butyl Rubber (IIR)

Butyl (isobutylene, isoprene rubber, IIR) has a very low permeability rate and good electrical properties.

Heat resistance

- Up to approximately 121°C (250°F).

Cold flexibility

- Down to approximately -59°C (-75°F).


Chemical resistance

- Hot water and steam up to 121°C (250°F).
- Brake fluids with glycol base (Dot 3 & 4).
- Many acids (see Fluid Compatibility Tables in Section VII).
- Salt solutions.
- Polar solvents, (e.g. alcohols, ketones and esters).
- Poly-glycol based hydraulic fluids (HFC fluids) and phosphate-ester bases (HFD-R fluids).
- Silicone oil and grease.
- Ozone, aging and weather resistant.

Not compatible with:

- Mineral oil and grease.
- Fuels.
- Chlorinated hydrocarbons.

2-4

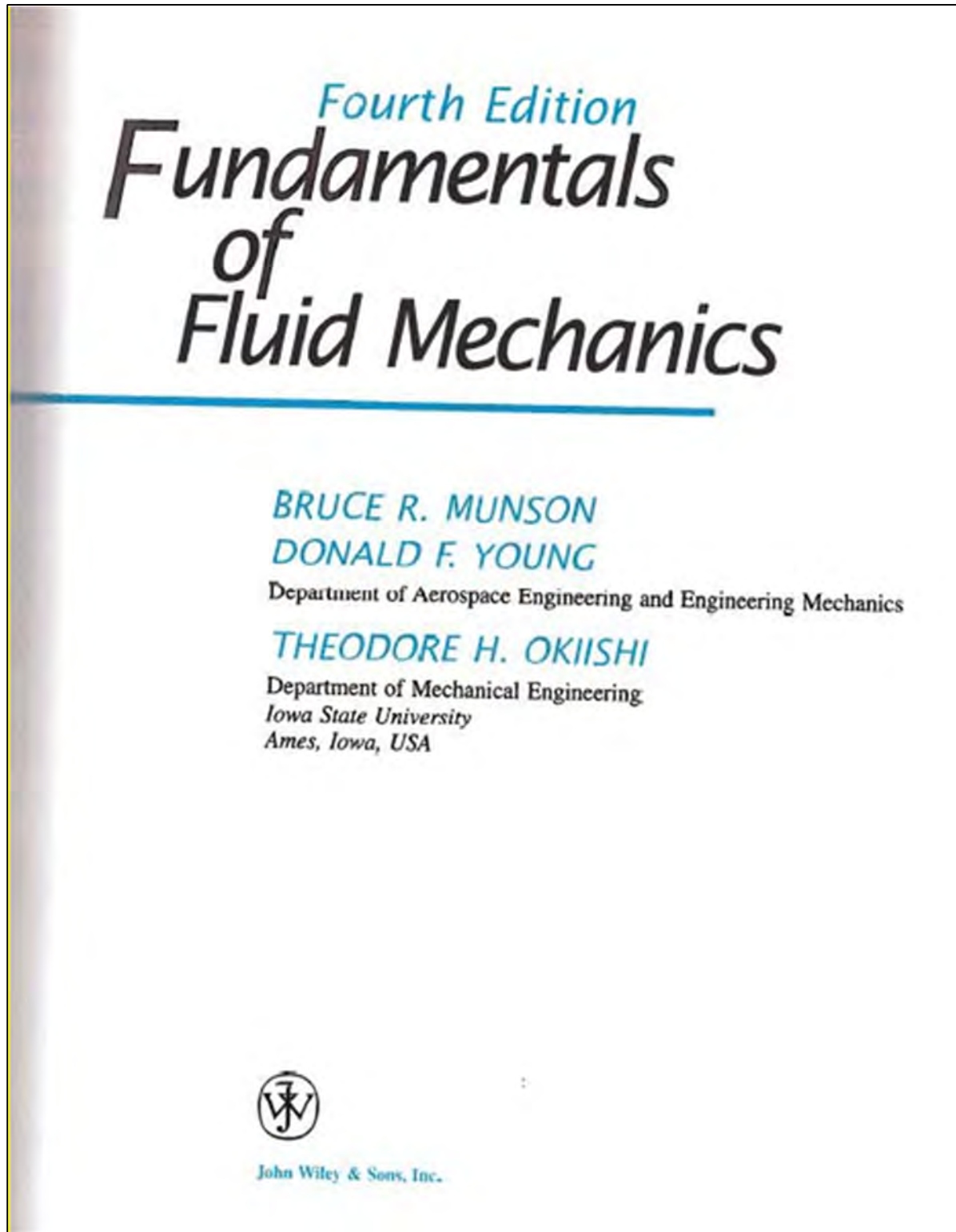


Parker Hannifin Corporation • O-Ring Division
2360 Palumbo Drive, Lexington, KY 40509
Phone: (859) 269-2351 • Fax: (859) 335-5128
www.parkerorings.com

Robatel Technologies, LLC

Page 3-61

Attachment 3.5-3 Water Vapor Pressure Reference (80°C)
[Ref. 17]



Attachment 3.5-3 Water Vapor Pressure Reference (80°C) (Continued)
[Ref. 17]

ACQUISITIONS EDITOR: Wayne Anderson
ASSITANT EDITOR: Jennifer Welter
MARKETING MANAGER: Katherine Hepburn
SENIOR PRODUCTION EDITOR: Valerie A. Vargas
PRODUCTION SERVICES MANAGER: Jeanine Furino
COVER DESIGNER: Madelyn Lesare
ELECTRONIC ILLUSTRATIONS: Radiant Illustration and Design
PRODUCTION MANAGEMENT SERVICES: Ingram Associates

This book was set in 10/12 by TechBooks and printed and bound by R. R. Donnelley & Sons.
The cover was printed by Phoenix Color.

This book is printed on acid-free paper. Ⓢ

Copyright 2002© John Wiley & Sons, Inc. All rights reserved.

No part of this publication may be reproduced, stored in a retrieval system or transmitted in any form by any means, electronic, mechanical, photocopying, recording, scanning or otherwise, except as permitted by Sections 107 or 108 of the 1976 United States Copyright Act, without either the prior written permission of the Publisher, or authorization through payment of the appropriate per-copy fee to the Copyright Clearance Center, 222 Rosewood Drive, Danvers, MA 01923, (978) 750-8400, fax (978) 750-4470. Requests to the Publisher for permission should be addressed to the Permissions Department, John Wiley & Sons, Inc., 111 River Street, Hoboken, NJ 07030, (201) 748-6011, fax (201) 748-6008, E-Mail: PERMREQ @ WILEY.COM.
To order books please call 1(800)-225-5945.

ISBN: 0-471-44250-X

Printed in the United States of America

10 9 8 7 6 5

Attachment 3.5-3 Water Vapor Pressure Reference (80°C) (Continued)

[Ref. 17]

Appendix B / Physical Properties of Fluids ■ 831

TABLE B.1
Physical Properties of Water (BG Units)*

Temperature (°F)	Density, ρ (slugs/ft ³)	Specific Weight ^b , γ (lb/ft ³)	Dynamic Viscosity, μ (lb·s/ft ²)	Kinematic Viscosity, ν (ft ² /s)	Surface Tension ^c , σ (lb/ft)	Vapor Pressure, p_v [lb/in ² (abs)]	Speed of Sound ^d , c (ft/s)
32	1.940	62.42	3.732 E - 5	1.924 E - 5	5.18 E - 3	8.854 E - 2	4603
40	1.940	62.43	3.228 E - 5	1.664 E - 5	5.13 E - 3	1.217 E - 1	4672
50	1.940	62.41	2.730 E - 5	1.407 E - 5	5.09 E - 3	1.781 E - 1	4748
60	1.938	62.37	2.344 E - 5	1.210 E - 5	5.03 E - 3	2.563 E - 1	4814
70	1.936	62.30	2.037 E - 5	1.052 E - 5	4.97 E - 3	3.631 E - 1	4871
80	1.934	62.22	1.791 E - 5	9.262 E - 6	4.91 E - 3	5.069 E - 1	4819
90	1.931	62.11	1.500 E - 5	8.233 E - 6	4.86 E - 3	6.979 E - 1	4960
100	1.927	62.00	1.423 E - 5	7.383 E - 6	4.79 E - 3	9.493 E - 1	4995
120	1.918	61.71	1.164 E - 5	6.067 E - 6	4.67 E - 3	1.692 E + 0	5049
140	1.908	61.38	9.743 E - 6	5.106 E - 6	4.53 E - 3	2.888 E + 0	5091
160	1.896	61.00	8.315 E - 6	4.385 E - 6	4.40 E - 3	4.736 E + 0	5101
180	1.883	60.58	7.207 E - 6	3.827 E - 6	4.26 E - 3	7.507 E + 0	5195
200	1.869	60.12	6.342 E - 6	3.393 E - 6	4.12 E - 3	1.152 E + 1	5089
212	1.860	59.83	5.886 E - 6	3.165 E - 6	4.04 E - 3	1.469 E + 1	5062

*Based on data from *Handbook of Chemistry and Physics*, 69th Ed., CRC Press, 1988. Where necessary, values obtained by interpolation.

^bDensity and specific weight are related through the equation $\gamma = \rho g$. For this table, $g = 32.174$ ft/s².

^cIn contact with air.

^dFrom R. D. Blevins, *Applied Fluid Dynamics Handbook*, Van Nostrand Reinhold Co., Inc., New York, 1984.

TABLE B.2
Physical Properties of Water (SI Units)*

Temperature (°C)	Density, ρ (kg/m ³)	Specific Weight ^b , γ (kN/m ³)	Dynamic Viscosity, μ (N·s/m ²)	Kinematic Viscosity, ν (m ² /s)	Surface Tension ^c , σ (N/m)	Vapor Pressure, p_v [N/m ² (abs)]	Speed of Sound ^d , c (m/s)
0	999.9	9.806	1.787 E - 3	1.787 E - 6	7.56 E - 2	6.105 E + 2	1403
5	1000.0	9.807	1.519 E - 3	1.519 E - 6	7.49 E - 2	8.722 E + 2	1427
10	999.7	9.804	1.307 E - 3	1.307 E - 6	7.42 E - 2	1.228 E + 3	1447
20	998.2	9.789	1.002 E - 3	1.004 E - 6	7.28 E - 2	2.338 E + 3	1481
30	995.7	9.765	7.975 E - 4	8.009 E - 7	7.12 E - 2	4.243 E + 3	1507
40	992.2	9.731	6.529 E - 4	6.580 E - 7	6.96 E - 2	7.376 E + 3	1526
50	988.1	9.690	5.468 E - 4	5.534 E - 7	6.79 E - 2	1.233 E + 4	1541
60	983.2	9.642	4.665 E - 4	4.745 E - 7	6.62 E - 2	1.992 E + 4	1552
70	977.8	9.589	4.042 E - 4	4.134 E - 7	6.44 E - 2	3.116 E + 4	1555
80	971.8	9.530	3.547 E - 4	3.650 E - 7	6.26 E - 2	4.734 E + 4	1555
90	965.3	9.467	3.147 E - 4	3.260 E - 7	6.08 E - 2	7.010 E + 4	1550
100	958.4	9.399	2.818 E - 4	2.940 E - 7	5.89 E - 2	1.013 E + 5	1543

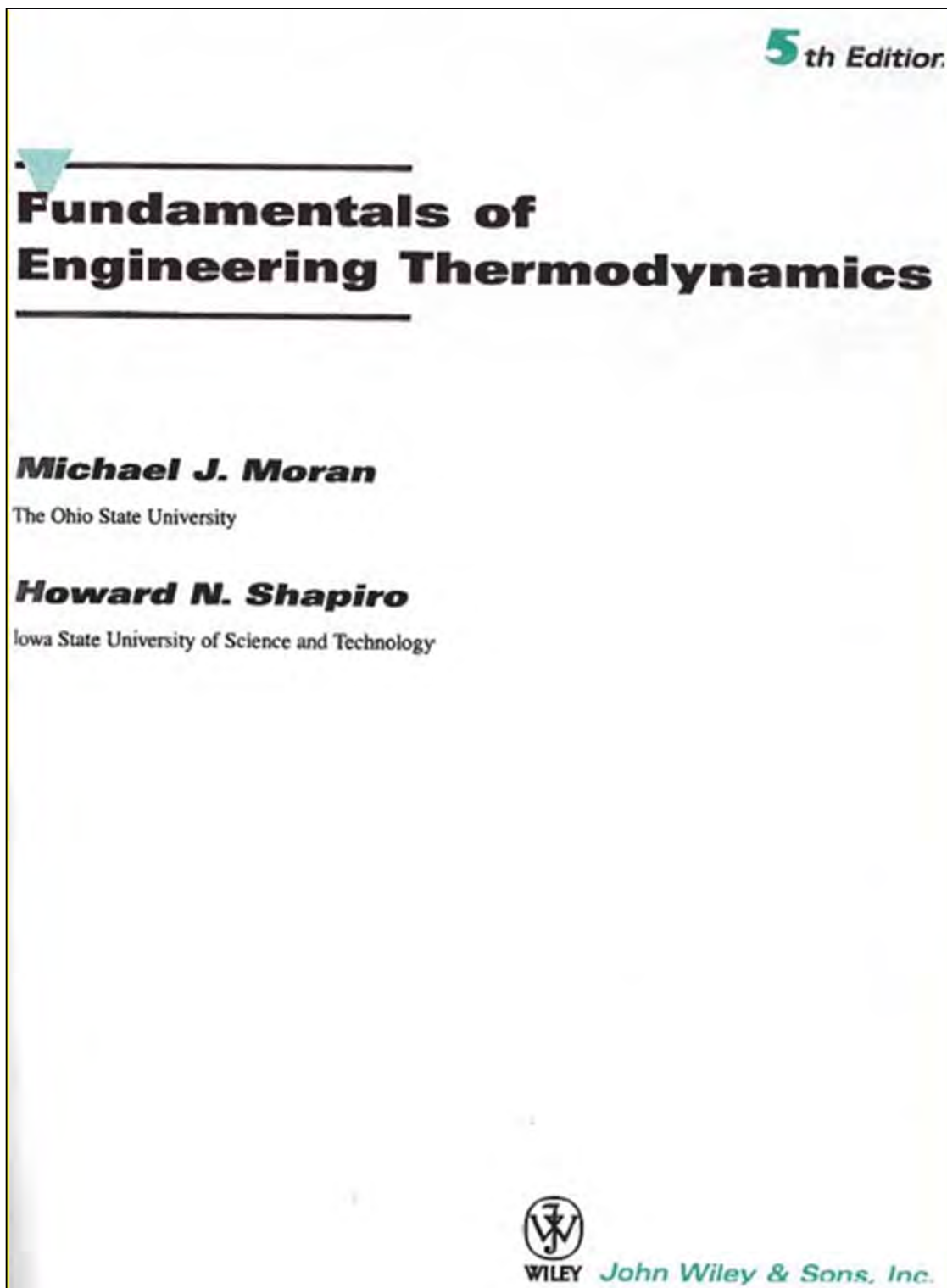
*Based on data from *Handbook of Chemistry and Physics*, 69th Ed., CRC Press, 1988.

^bDensity and specific weight are related through the equation $\gamma = \rho g$. For this table, $g = 9.807$ m/s².

^cIn contact with air.

^dFrom R. D. Blevins, *Applied Fluid Dynamics Handbook*, Van Nostrand Reinhold Co., Inc., New York, 1984.

Attachment 3.5-4 Water Vapor Pressure Reference (150°C)
[Ref. 18]



Attachment 3.5-4 Water Vapor Pressure Reference (150°C) (Continued)

[Ref. 18]

Acquisitions Editor	<i>Joseph Hayton</i>
Senior Marketing Manager	<i>Katherine E. Hepburn</i>
Production Editor	<i>Sandra Dumas</i>
Text and Cover Designer	<i>Madelyn Lesure</i>
Cover Illustration	<i>Roy Wiemann</i>
Production Management Services	<i>Ingrao Associates</i>
Illustrations	<i>Precision Graphics</i>

This book was typeset in 10/12 Times by TechBooks and printed and bound by Von Hoffmann Corporation. The cover was printed by Von Hoffmann Corporation.

The paper in this book was manufactured by a mill whose forest management programs include sustained yield harvesting of its timberlands. Sustained yield harvesting principles ensure that the number of trees cut each year does not exceed the amount of new growth.

This book is printed on acid-free paper. ©

Copyright © 2004 by John Wiley & Sons, Inc. All rights reserved.

No part of this publication may be reproduced, stored in a retrieval system or transmitted in any form or by any means, electronic, mechanical, photocopying, recording, scanning or otherwise, except as permitted under Sections 107 or 108 of the 1976 United States Copyright Act, without either the prior written permission of the Publisher or authorization through payment of the appropriate per-copy fee to the Copyright Clearance Center, 222 Rosewood Drive, Danvers, MA 01923, (978) 750-8400, fax (978) 750-4470. Requests to the Publisher for permission should be addressed to the Permissions Department, John Wiley & Sons, Inc., 111 River Street, Hoboken, NJ 07030, (201) 748-6011, fax (201) 748-6008, E-mail: PERMREQ@WILEY.COM. To order books or for customer service call 1-800-CALL-WILEY (225.5945).

Moran, Michael J.

Fundamentals of Engineering Thermodynamics/Michael J. Moran, Howard N. Shapiro.—5th Edition.

ISBN 0-471-27471-2

WILEY ISBN 0-471-45241-6

Printed in the United States of America.

10 9 8 7 6 5 4 3 2

Attachment 3.5-4 Water Vapor Pressure Reference (150°C) (Continued)

[Ref. 18]

760 Tables in SI Units

Divide by 1000

TABLE A-2 Properties of Saturated Water (Liquid-Vapor): Temperature Table

Temp. °C	Sat. Press. bar	Specific Volume m ³ /kg		Internal Energy kJ/kg		Enthalpy kJ/kg			Entropy kJ/kg · K		Temp. °C
		Sat. Liquid $v_f \times 10^3$	Sat. Vapor v_g	Sat. Liquid u_f	Sat. Vapor u_g	Sat. Liquid h_f	Evap. h_{fg}	Sat. Vapor h_g	Sat. Liquid s_f	Sat. Vapor s_g	
01	0.00611	1.0002	206.136	0.00	2375.3	0.01	2501.3	2501.4	0.0000	9.1562	01
4	0.00813	1.0001	157.232	16.77	2380.9	16.78	2491.9	2508.7	0.0610	9.0514	4
5	0.00872	1.0001	147.120	20.97	2382.3	20.98	2489.6	2510.6	0.0761	9.0257	5
6	0.00935	1.0001	137.734	25.19	2383.6	25.20	2487.2	2512.4	0.0912	9.0003	6
8	0.01072	1.0002	120.917	33.59	2386.4	33.60	2482.5	2516.1	0.1212	8.9501	8
10	0.01228	1.0004	106.379	42.00	2389.2	42.01	2477.7	2519.8	0.1510	8.9008	10
11	0.01312	1.0004	99.857	46.20	2390.5	46.20	2475.4	2521.6	0.1658	8.8765	11
12	0.01402	1.0005	93.784	50.41	2391.9	50.41	2473.0	2523.4	0.1806	8.8524	12
13	0.01497	1.0007	88.124	54.60	2393.3	54.60	2470.7	2525.3	0.1953	8.8285	13
14	0.01598	1.0008	82.848	58.79	2394.7	58.80	2468.3	2527.1	0.2099	8.8048	14
15	0.01705	1.0009	77.926	62.99	2396.1	62.99	2465.9	2528.9	0.2245	8.7814	15
16	0.01818	1.0011	73.333	67.18	2397.4	67.19	2463.6	2530.8	0.2390	8.7582	16
17	0.01938	1.0012	69.044	71.38	2398.8	71.38	2461.2	2532.6	0.2535	8.7351	17
18	0.02064	1.0014	65.038	75.57	2400.2	75.58	2458.8	2534.4	0.2679	8.7123	18
19	0.02198	1.0016	61.293	79.76	2401.6	79.77	2456.5	2536.2	0.2823	8.6897	19
20	0.02339	1.0018	57.791	83.95	2402.9	83.96	2454.1	2538.1	0.2966	8.6672	20
21	0.02487	1.0020	54.514	88.14	2404.3	88.14	2451.8	2539.9	0.3109	8.6450	21
22	0.02645	1.0022	51.447	92.32	2405.7	92.33	2449.4	2541.7	0.3251	8.6229	22
23	0.02810	1.0024	48.574	96.51	2407.0	96.52	2447.0	2543.5	0.3393	8.6011	23
24	0.02985	1.0027	45.883	100.70	2408.4	100.70	2444.7	2545.4	0.3534	8.5794	24
25	0.03160	1.0029	43.360	104.88	2409.8	104.89	2442.3	2547.2	0.3674	8.5580	25
26	0.03363	1.0032	40.994	109.06	2411.1	109.07	2439.9	2549.0	0.3814	8.5367	26
27	0.03567	1.0035	38.774	113.25	2412.5	113.25	2437.6	2550.8	0.3954	8.5156	27
28	0.03782	1.0037	36.690	117.42	2413.9	117.43	2435.2	2552.6	0.4093	8.4946	28
29	0.04008	1.0040	34.733	121.60	2415.2	121.61	2432.8	2554.5	0.4231	8.4739	29
30	0.04246	1.0043	32.894	125.78	2416.6	125.79	2430.5	2556.3	0.4369	8.4533	30
31	0.04496	1.0046	31.165	129.96	2418.0	129.97	2428.1	2558.1	0.4507	8.4329	31
32	0.04759	1.0050	29.540	134.14	2419.3	134.15	2425.7	2559.9	0.4644	8.4127	32
33	0.05034	1.0053	28.011	138.32	2420.7	138.33	2423.4	2561.7	0.4781	8.3927	33
34	0.05324	1.0056	26.571	142.50	2422.0	142.50	2421.0	2563.5	0.4917	8.3728	34
35	0.05628	1.0060	25.216	146.67	2423.4	146.68	2418.6	2565.3	0.5053	8.3531	35
36	0.05947	1.0063	23.940	150.85	2424.7	150.86	2416.2	2567.1	0.5188	8.3336	36
38	0.06632	1.0071	21.602	159.20	2427.4	159.21	2411.5	2570.7	0.5458	8.2950	38
40	0.07384	1.0078	19.523	167.56	2430.1	167.57	2406.7	2574.3	0.5725	8.2570	40
45	0.09593	1.0099	15.258	188.44	2436.8	188.45	2394.8	2583.2	0.6387	8.1648	45

Attachment 3.5-4 Water Vapor Pressure Reference (150°C) (Continued)

[Ref. 18]

Tables in SI Units 761

TABLE A-2 (Continued)

Temp. °C	Press. bar	Specific Volume m ³ /kg		Internal Energy kJ/kg		Enthalpy kJ/kg			Entropy kJ/kg · K		Temp. °C
		Sat. Liquid $v_f \times 10^3$	Sat. Vapor v_g	Sat. Liquid u_f	Sat. Vapor u_g	Sat. Liquid h_f	Evap. h_{fg}	Sat. Vapor h_g	Sat. Liquid s_f	Sat. Vapor s_g	
50	1.235	1.0121	12.032	209.32	2443.5	209.33	2382.7	2592.1	.7038	8.0763	50
55	1.1576	1.0146	9.568	230.21	2450.1	230.23	2370.7	2600.9	.7679	7.9913	55
60	1.0994	1.0172	7.671	251.11	2456.6	251.13	2358.5	2609.6	.8312	7.9096	60
65	1.0503	1.0199	6.197	272.02	2463.1	272.06	2346.2	2618.3	.8955	7.8310	65
70	1.0119	1.0228	5.042	292.95	2469.6	292.98	2333.8	2626.8	.9549	7.7553	70
75	0.9858	1.0259	4.131	313.90	2475.9	313.93	2321.4	2635.3	1.0155	7.6824	75
80	0.9739	1.0291	3.407	334.86	2482.2	334.91	2308.8	2643.7	1.0753	7.6122	80
85	0.9783	1.0325	2.828	355.84	2488.4	355.90	2296.0	2651.9	1.1343	7.5445	85
90	0.9914	1.0360	2.361	376.85	2494.5	376.92	2283.2	2660.1	1.1925	7.4791	90
95	1.0155	1.0397	1.982	397.88	2500.6	397.96	2270.2	2668.1	1.2500	7.4159	95
100	1.0414	1.0435	1.673	418.94	2506.5	419.04	2257.0	2676.1	1.3069	7.3549	100
110	1.1433	1.0516	1.210	461.14	2518.1	461.30	2230.2	2691.5	1.4185	7.2387	110
120	1.3985	1.0603	0.8919	503.50	2529.3	503.71	2202.6	2706.3	1.5276	7.1296	120
130	1.701	1.0697	0.6685	546.02	2539.9	546.31	2174.2	2720.5	1.6344	7.0269	130
140	2.1613	1.0797	0.5089	588.74	2550.0	589.13	2144.7	2733.9	1.7391	6.9299	140
150	2.758	1.0905	0.3928	631.68	2559.5	632.20	2114.3	2746.5	1.8418	6.8379	150
160	3.478	1.1020	0.3071	674.86	2568.4	675.55	2082.6	2758.1	1.9427	6.7502	160
170	4.317	1.1143	0.2428	718.33	2576.5	719.21	2049.5	2768.7	2.0419	6.6663	170
180	5.202	1.1274	0.1941	762.09	2583.7	763.22	2015.0	2778.2	2.1396	6.5857	180
190	6.254	1.1414	0.1565	806.19	2590.0	807.62	1978.8	2786.4	2.2359	6.5079	190
200	7.514	1.1565	0.1274	850.65	2595.3	852.45	1940.7	2793.2	2.3309	6.4323	200
210	8.906	1.1726	0.1044	895.53	2599.5	897.76	1900.7	2798.5	2.4248	6.3585	210
220	10.438	1.1900	0.08619	940.87	2602.4	943.62	1858.5	2802.1	2.5178	6.2861	220
230	12.119	1.2088	0.07158	986.74	2603.9	990.12	1813.8	2804.0	2.6099	6.2146	230
240	13.964	1.2291	0.05976	1033.2	2604.0	1037.3	1766.5	2803.8	2.7015	6.1437	240
250	15.973	1.2512	0.05013	1080.4	2602.4	1085.4	1716.2	2801.5	2.7927	6.0730	250
260	18.158	1.2755	0.04221	1128.4	2599.0	1134.4	1662.5	2796.6	2.8838	6.0019	260
270	20.529	1.3023	0.03564	1177.4	2593.7	1184.5	1605.2	2789.7	2.9751	5.9301	270
280	23.094	1.3321	0.03017	1227.5	2586.1	1236.0	1543.6	2779.6	3.0668	5.8571	280
290	25.863	1.3656	0.02557	1278.9	2576.0	1289.1	1477.1	2766.2	3.1594	5.7821	290
300	28.851	1.4036	0.02167	1332.0	2563.0	1344.0	1404.9	2749.0	3.2534	5.7045	300
320	35.127	1.4988	0.01549	1444.6	2525.5	1461.5	1238.6	2700.1	3.4480	5.5362	320
340	44.59	1.6379	0.01080	1570.3	2464.6	1594.2	1027.9	2622.0	3.6594	5.3357	340
360	58.65	1.8925	0.006945	1725.2	2351.5	1760.5	720.5	2481.0	3.9147	5.0526	360
374.14	220.9	3.155	0.003155	2029.6	2029.6	2099.3	0	2099.3	4.4298	4.4298	374.14

Source: Tables A-2 through A-5 are extracted from J. H. Keenan, F. G. Keyes, P. G. Hill, and J. G. Moore, *Steam Tables*, Wiley, New York, 1969.

3.6 References

1. Robatel Technologies, LLC, Quality Assurance Program for Packaging and Transportation of Radioactive Material, 10 CFR 71 Subpart H, Rev. 2, Dated November 10, 2017 and NRC Approved on March 21, 2012
2. U.S. Nuclear Regulatory Commission, 10 CFR Part 71--PACKAGING AND TRANSPORTATION OF RADIOACTIVE MATERIAL, dated March 7, 2012
3. ANSYS, Release 14.0, ANSYS, Inc., Canonsburg, PA, October, 2011
4. RTL-001-CALC-TH-0201, Rev. 6, "RT-100 Cask Thermal Analyses" (PROPRIETARY)
5. Fundamentals of Heat and Mass Transfer, Frank P. Incropera, David P. DeWitt, 2002, 5th ed., John Wiley & Sons, Inc.
6. RTL-001-CALC-TH-0102, Rev. 6, "RT-100 Cask Maximum Normal Operating Pressure Calculation" (PROPRIETARY)
7. RTL-001-CALC-TH-0202, Rev. 6, "RT-100 Cask Hypothetical Accident Condition Maximum Pressure Calculation" (PROPRIETARY)
8. TRELLEBORG Sealing Solutions O-Ring and Backup Rings Catalog, August 2011 Edition
9. UNIFRAX Fiberfrax 970 Ceramic Paper Data Sheet
Proprietary Information Content Withheld Under 10 CFR 2.390(b)
13. ASME Boiler & Pressure Vessel Code 2007 Edition, Section II – Part D, "Materials", The American Society of Mechanical Engineers, Three Park Avenue, New York, NY, www.asme.org.
14. Sanghavi Bothra Engineering Co. Pvt. Ltd.(SBE) 304/304L Stainless Steel Product Mechanical and Physical Properties
15. GENERAL PLASTICS Design Guide for LAST-A-FOAM FR-3700 Crash & Fire Protection of Radioactive Material Shipping Containers, Rev. 02.20.12
16. Parker O-Ring Handbook ORD 5700, Retrieved on August 28, 2013, Retrieved from http://www.parker.com/literature/ORD%205700%20Parker_O-Ring_Handbook.pdf.
17. Fundamentals of Fluid Mechanics, B. Munson, D. Young and T. Okiishi, 4th ed., John Wiley & Sons, Inc.
18. Fundamentals of Engineering Thermodynamics, M. Moran and H. Shapiro, 5th ed., John Wiley & Sons, Inc.
19. Glenn Lee, Radiation Resistance of Elastomers, IEEE Transactions on Nuclear Science, Vol. NS-32, No. 5, October 1985
20. U.S. Nuclear Regulatory Commission, "Load Combinations for the Structural Analysis of

- Shipping Casks for Radioactive Material,” Regulatory Guide 7.8.
21. SFPE Handbook of Fire Protection Engineering, "Thermal Decomposition of Polymers," C.L. Hirschler, M. Marvelo, Chapter 7 of 3rd Edition, NFPA, 1 Batterymarch Park, Quincy, MA, 2001, www.nfpa.org.
 22. “Fundamentals of Combustion Processes,” A. McAllister, J. Chen, A. Fernandez-Pello, Springer, 2011.
 23. An Experimental Study of Autoignition of Wood, T. Poespowati, World Academy of Science, Engineering and Technology, Vol. 23, 2008., Retrieved on August 28, 2013, Retrieved from <http://www.waset.org/journals/waset/v23/v23-13.pdf>.
 24. ASME Boiler & Pressure Vessel Code, 2010, Section II, Part D, Materials, The American Society of Mechanical Engineers, New York, NY 2010
 25. RTL-001-CALC-TH-0301, Rev. 1, “RT-100 Cask Hypothetical Accident Condition Combustion Analysis” (PROPRIETARY)

This page is intentionally left blank.

4. CONTAINMENT

Chapter 4 describes the RT-100 containment under the RT Quality Assurance Program [Ref. 1] and summarizes the results to demonstrate compliance with the structural requirements of 10 CFR 71 [Ref. 2]. This Chapter demonstrates the RT-100 containment boundary compliance with the permitted activity release limits specified in 10 CFR 71.51(a)(1) [Ref. 2] and 10 CFR 71.51(a)(2) [Ref. 2] for both normal conditions of transport (NCT) and hypothetical accident conditions (HAC) of transport. The reference leakage rates for various cask conditions are normally calculated, and the most bounding value is chosen as the maximum allowable leakage rate for the cask in order to ensure compliance with regulatory limits.

Due to the variety of inventories, diversity in both isotopic composition and in total activity concentration, the RT-100 has been established as a leaktight container. Leaktight is a degree of package containment that in a practical sense precludes any significant release of radioactive materials. This degree of containment is achieved by demonstration of a leakage rate less than or equal to 1×10^{-7} ref·cm³/s, of air at an upstream pressure of 1 atmosphere absolute and a downstream pressure of 0.01 atmosphere absolute or less (ANSI N14.5-2014 [Ref. 3]).

The containment review is based in part on the descriptions and evaluations presented in the General Information, Structural Evaluation and Thermal Evaluation sections of the application. Similarly, results of the containment review are considered in the review of Operating Procedures and Acceptance Tests and Maintenance Program. An example of the information flow for the containment review is shown in Figure 4-1 on the following page.

4.1 Description of Containment System

Section 4.1 provides a detailed description of the containment system. This description includes the containment vessel, welds, seals, lids, cover plates, and other closure devices relevant to the containment boundary of the cask. Materials of construction and applicable codes and standards are presented in the RT100 NM 1000-F - Bill of Material (Chapter 1, Appendix 1.4, Attachment 1.4-1).

4.1.1 Containment Vessel

The package containment system is defined as the inner shell of the shielded transport cask, together with the associated lid, O-ring seals, and lid closure bolts. The inner shell of the RT-100, or containment vessel, consists of a right circular cylinder of 1730 mm inner diameter and 1956 mm inside height. The shell is fabricated of stainless steel. At the base, the cylindrical shell is attached to a circular forged bottom with full penetration weld. At the top, the inner shell is attached to a circular forged flange with a full penetration weld. The primary lid is attached to the cask body with thirty-two (32) equally spaced M48 hex head bolts. A secondary lid covers an opening in the primary lid and is attached to the primary lid using eighteen (18) equally spaced M36 hex head bolts. Refer to Chapter 4, Section 4.1.4 for closure details. The inner shell is shown

to maintain stresses within allowable limits in Chapter 2, Section 2.6.7 for NCT and in Chapter 2, Section 2.7 for HAC. These evaluations demonstrate that the inner shell maintains its integrity and provides containment along with the closure system as described in Section 4.1.4.

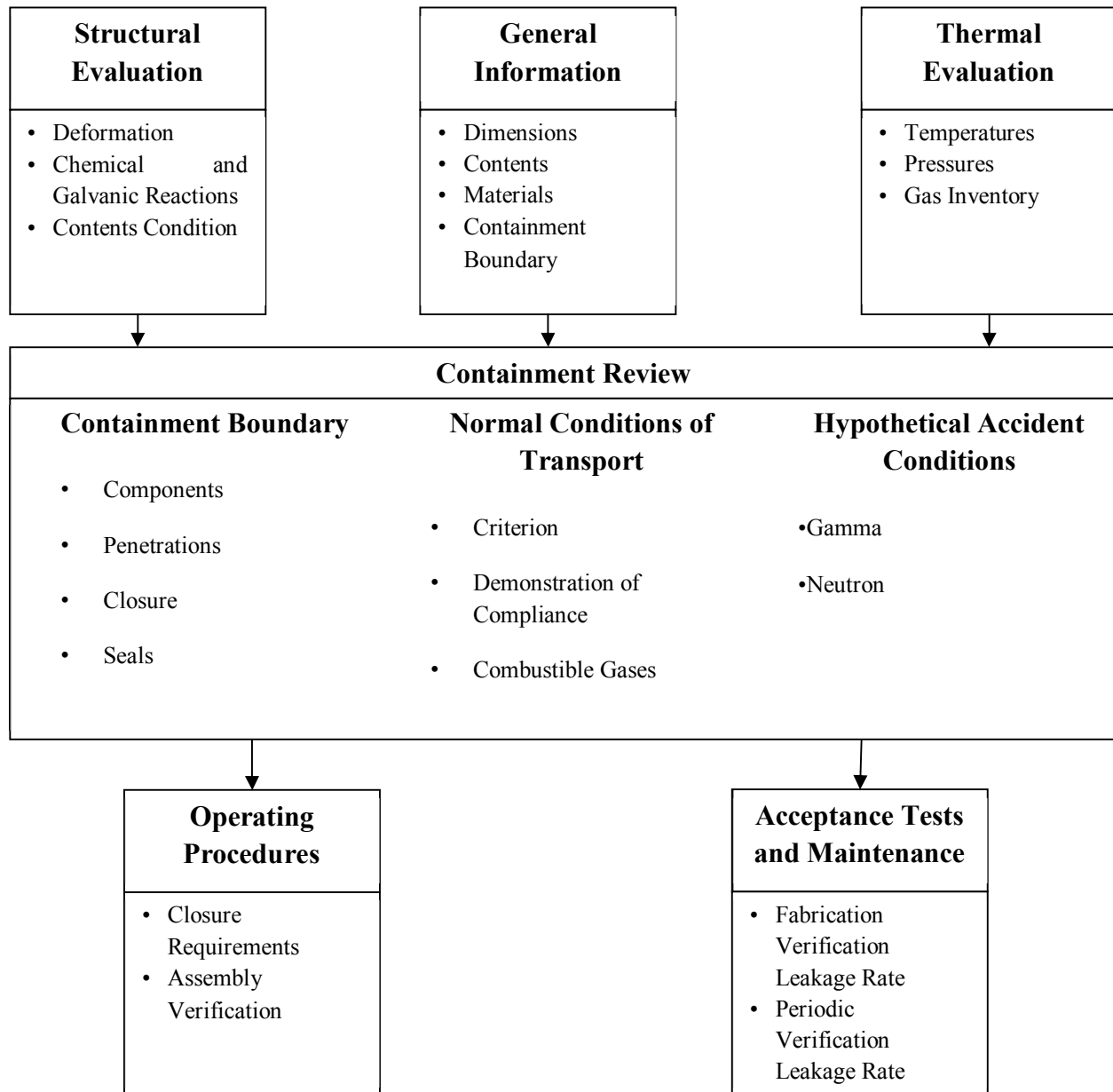


Figure 4-1 Information Flow for the Containment Review

4.1.2 Containment Penetration

There are three locations where the containment vessel may be penetrated. For each location, an inner O-ring seals the containment boundary.

- Primary lid
- Secondary lid
- Cask vent port cover plate

A vent port penetrates the primary lid into the main cask cavity. The vent penetration contains a quick disconnect valve and is sealed with the vent port cover plate. The primary lid, secondary lid and the cover plate are sealed with EPDM O-rings. Figure 4.1.2-1 illustrates the containment boundaries of the RT-100 (in red). The RT-100 does not rely on any valve or pressure relief device to meet the containment requirements. The quick disconnect valve is protected by the vent port cover plate which protects the valve from unauthorized operation and provides a sealed enclosure to retain any leakage from the device.

Proprietary Information Content Withheld Under 10 CFR 2.390(b)

4.1.3 Welds and Seals

The containment vessel is fabricated using full penetration welds. Lid seals are EPDM O-rings and are further addressed in Section 4.1.4. O-rings may be supplied by manufacturers such as those in Parker O-Ring Handbook ORD 5700 [Ref. 10] and Trelleborg Sealing Solutions O-Ring and Backup Rings Catalog, August 2011 [Ref. 11]. Additional information on the O-rings taken from these references is provided in Attachment 4.5-1 through Attachment 4.5-5.

Parker O-Ring Handbook ORD 5700 [Ref. 10] and Trelleborg Sealing Solutions O-Ring and Backup Rings Catalog, August 2011 [Ref. 11] contain information regarding the operating temperature range, gap permeability, and compression set for the material. The temperature performance of the EPDM O-rings is presented in Chapter 3, Section 3.2.1 and the application of the O-rings in the primary and secondary lid seals is addressed in Chapter 2, Appendix 2.13. EPDM radiation resistance is addressed in Radiation Resistance of Elastomers, IEEE Transactions on Nuclear Science, Vol. NS-32, No.5, October 1985 [Ref. 12], indicating that the material is radiation resistant up to 5×10^8 rads while retaining reasonable flexibility and strength, hardness, and very good compression set resistance. A copy of Reference 12 is provided in Attachment 4.5-5.

4.1.4 Closure

The primary lid closure consists of a partially recessed, 210 mm-thick stainless steel plate. The lid is supported at the perimeter of the cylindrical body by a thick flange (upper forging) which is welded to the top of the inner and outer cylindrical shells. The Primary Lid is attached to the cask body by thirty-two (32) equally spaced M48 hex head bolts. Two (2) EPDM O-rings are retained in machined grooves at the lid perimeter. Groove dimensions prevent over-compression of the O-rings by the closure bolt pre-load forces and hypothetical accident impact forces.

The cask is fitted with a recessed secondary lid which consists of 100 mm thick plate, a 60 mm thick lead gamma shield, and 10 mm thick closure plate. The Secondary Lid is attached to the Primary Lid with eighteen (18) equally spaced M36 hex head bolts. Two (2) EPDM O-rings are retained in machined grooves at the lid perimeter.

The quick-disconnect valve is housed under a 10mm thick stainless steel cover plate. The Quick-Disconnect Valve Cover Plate is attached to the primary lid with six (6) equally spaced M10 hex head bolts. Two (2) EPDM O-rings are retained in machined grooves at the lid perimeter.

The torque requirements for these bolts may be seen below in Table 4.1.4-1. Due to this closure setup, continuous venting from the RT-100 is precluded.

As stated above, the containment system is sealed by multiple bolted closures. These closures contain numerous bolts that are required to be tightened to specified torques using approved

procedures during the cask loading process. Secure closure is assured by the torque values specified and the assembly verification leak test performed prior to transport. The torques are specified in order to ensure that sufficient pre-load is applied to the bolts so that they will withstand loads from the maximum normal and accident condition pressures within the cavity.

The closure system is evaluated for NCT and HAC in Chapter 2, Appendix 2.13. Closure bolts are shown to maintain adequate design margin and allow the O-rings to maintain a positive seal at all times.

Table 4.1.4-1 Bolt Torque Requirements

Location	Size	Torque Values (N-m) ± 10% Lubricated
Primary Lid	M48	850
Secondary Lid	M36	350
Quick-Disconnect Valve Cover Plate	M10	27

4.1.5 Cavity Volume, Conditions, and Contents

The cavity dimensions are displayed in Table 4.1.5-1.

Table 4.1.5-1 Cask Cavity Dimensions

	Inches	Centimeters
L_{cavity}	77.2	196
D_{cavity}	68.1	173

Thus, the volume of the cylindrical cavity is

$$V_{\text{cavity}} = (\pi \cdot D_{\text{cavity}}^2 \cdot L_{\text{cavity}}) / 4$$

Table 4.1.5-2 Cask Cavity Volume

Total Cavity Volume [cm³]	4.60E+06
---	----------

The temperature under normal and accident conditions are determined based on the maximum internal cavity temperatures for normal and accident situations. Pressures and temperatures are provided by Calculation Package RTL-001-CALC-TH-0102, Rev. 6 [Ref. 8] and Calculation Package RTL-001-CALC-TH-0202, Rev. 6 [Ref. 9] for normal and accident situations, respectively. The standard leakage rate is the leakage rate of dry air when it is leaking from 1 atm (upstream pressure) to 0.01 atm (downstream pressure) at 298 K (ANSI N14.5-2014 [Ref. 3]). Dynamic viscosity values were generated based on the Sutherland equation

("Fundamentals of Fluid Mechanics", 5th edition [Ref. 14]), Introduction to Nuclear Engineering, 3rd edition [Ref.13] Table IV.4, ANSI N14.5-2014 [Ref. 3] Table B-1, Fundamentals of Fluid Mechanics Table B.4 [Ref. 14] Table B.4, and viscosity of gaseous helium table in Brookhaven National Laboratory, "Selected Cryogenic Data Notebook", Aug. 1980 [Ref. 15].

Table 4.1.5-3 Parameters for Normal Transport and Accident Conditions

Parameter	Normal Conditions ⁸	Accident Conditions ⁹	Standard Conditions
P _u [atm]	3.38	6.8	1
P _d [atm]	1	1	0.01
P _a [atm]	2.19	3.9	0.505
T [°F]	176 (353 K, 80 °C)	302 (423 K, 150 °C)	76.7 (298 K, 25 °C)
M [g/mol]	29 (air), 4 (He)	29 (air), 4 (He)	29 (air), 4 (He)
μ [cP]	0.0207 (air), 0.0224 (He)	0.0236 (air), 0.0254 (He)	0.0185 (air), 0.0198 (He)
a [cm]	0.49	0.49	0.49

4.2 Allowable Leakage Rates at Test Conditions

Un-choked flow correlations are used as they better approximate the true measured flow rate for the leakage rates associated with transportation packages. Using the equations for molecular and continuum flow provided in NUREG/CR-6487 [Ref. 7], the corresponding leak hole diameter is calculated for the RT-100 for standard test conditions by solving Equation 4.1 for D, the leak hole diameter. The capillary length required for Equation 4.1 for the containment system is conservatively chosen as the O-ring groove width in the vent port cover plate lid, which is 0.49 cm.

Equation 4.1

$$L_{@P_a} = \left[\frac{2.49 \times 10^6 D^4}{a \cdot \mu} + \frac{3.81 \times 10^3 D^3 \sqrt{\frac{T}{M}}}{a \cdot P_a} \right] \times [P_u - P_d]$$

where:

- L_{@P_a} is the allowable leakage rate at the average pressure for standard conditions [cm³/s],
- a is the capillary length [0.49 cm],
- T is the temperature for standard conditions [K],
- M is the gas molecular weight [g/mol] = 29.0 for air, 4.0 for He from ANSI N14.5-2014, Table B1,

μ is the dynamic viscosity for helium or air [cP],
 P_u is the upstream pressure [atm],
 P_d is the downstream pressure [atm],
 P_a is the average pressure; $P_a = (P_u + P_d)/2$ for standard conditions [atm], and
 D is the capillary diameter [cm].

The leak hole diameter is determined using the parameters for standard conditions presented in Table 4.1.5-3.

The allowable leakage rate for leaktight conditions is at the upstream pressure, the ratio presented in Equation 4.2 is used to convert Equation 4.1 to upstream leakage rate so that the capillary diameter can be determined.

Equation 4.2

$$L_{@P_a} = L_{@P_u} \frac{P_u}{P_a}$$

where:

$L_{@P_a}$ is the allowable leakage rate at the average pressure [cm³/s] for standard conditions,
 $L_{@P_u}$ is the allowable leakage rate at the upstream pressure [cm³/s] for standard conditions,
 P_u is the upstream pressure [atm],
 P_d is the downstream pressure [atm], and
 P_a is the average pressure; $P_a = (P_u + P_d)/2$ [atm].

The sensitivity for the leakage test procedures is established by ANSI N14.5-2014 [Ref. 3] as shown in Equation 4.3.

Equation 4.3

$$S = \frac{1}{2} \cdot \text{Leakage Rate}^1$$

4.3 Leakage Rate Test for Type B Packages

This section describes the leakage tests used to show that the RT-100 meets the containment requirements of 10 CFR 71.51 [Ref. 2]. Leak test requirements are further specified in Chapter 8, Section 8.1.4.

The following leakage tests are conducted on the RT-100 as required by ANSI N14.5-2014 [Ref. 3]:

¹ Leakage rate in this case is the upstream pressure leakage rate at standard conditions.

Table 4.3-1 Leakage Tests of the RT-100 Package

Test	Frequency	Test Gas	Acceptance Criteria
Maintenance	After maintenance, repair (such as weld repair), or replacement of components of the containment system	Helium	$\leq L_{He}$
Fabrication	Prior to the first use of the RT-100		
Periodic	Within 12 months prior to next shipment		
Pre-Shipment	Before each shipment of Type B waste	Nitrogen or air (optional)	No Leakage at a Sensitivity $\leq 10^{-3}$ ref-cm ³ /sec

*Adjusted for the individual properties of the test gas (calculated below); sensitivity is $\leq L_{He}/2$. As shown in Table 4.3-1, the Maintenance, Fabrication, and Periodic leakage tests may be performed using helium as the test gas. The acceptance criterion for these tests is the equivalent reference leakage rate for helium gas, L_{He} , which is calculated below.

4.3.1 Determination of Equivalent Reference Leakage Rate for Helium Gas

Section 4.3.1 determines the allowable leakage rate using the Helium gas which may be used to perform the annual verification leakage tests summarized in Table 4.3-1 above. This calculation uses formulas presented in ANSI N14.5-2014 [Ref. 3].

It is known that the reference air leakage rate, L_R , is 1.00×10^{-7} ref-cm³/s based on leaktight criteria.

Using Equation 4.1 and Equation 4.2, the maximum capillary diameter, D_{max} , was determined:

$$L_{@P_u} = \left(\frac{2.49 \times 10^6 D_{max}^4}{(0.49 \text{ cm})(0.0185 \text{ cP})} + \frac{3.81 \times 10^3 D_{max}^3 \sqrt{\frac{298 \text{ K}}{29 \text{ g/mole}}}}{(0.49 \text{ cm})(0.505 \text{ atm})} \right) (1 \text{ atm} - 0.01 \text{ atm}) \left(\frac{0.505 \text{ atm}}{1 \text{ atm}} \right)$$

$$= 1 \times 10^{-7} \text{ cm}^3/\text{s}$$

Diameter values are inputted until the result of the above calculation is roughly equivalent to 1×10^{-7} ref-cm³/s. Solving for D_{max} iteratively yields:

$$D_{\max} = 1.3261\text{E-}04 \text{ [cm]}$$

The equivalent air/helium mixture that would leak from D_{\max} during a leak test, as described in Table 4.1.5-3, is determined. The leakage tests are performed with an air/helium mixture. The helium partial pressures can vary from 0.25 atm to 1.0 atm. An example with a helium partial pressure of 0.7 atm has been provided to illustrate the process used to determine the value of the variables used to determine the acceptable test leakage rates.

Assume the cask void is evacuated to 0.3 atm and then pressurized to 1.0 atm with an air/helium mixture.

$$P_{\text{void}} = P_{\text{air}} = 0.3 \text{ atm}$$

$$P_{\text{mix}} = 1.0 \text{ atm}$$

$$P_{\text{He}} = P_{\text{mix}} - P_{\text{air}} = 0.7 \text{ atm}$$

The downstream pressure, P_d , under standard conditions is 0.01 atm.

$$P_a = 0.5 \times (P_{\text{mix}} + P_d) \rightarrow P_a = 0.505 \text{ atm}$$

From ANSI N14.5-2014 [Ref. 3]:

$$M_{\text{He}} = 4.0 \text{ g/mol} \quad M_{\text{air}} = 29.0 \text{ g/mol}$$

$$\mu_{\text{He}} = 0.0198 \text{ cP} \quad \mu_{\text{air}} = 0.0185 \text{ cP}$$

The mass of the mixture of air/helium gases is then determined:

$$M_{\text{mix}} = \frac{M_{\text{He}}P_{\text{He}} + M_{\text{air}}P_{\text{air}}}{P_{\text{mix}}} \rightarrow M_{\text{mix}} = 11.5 \text{ g/mol} \quad \text{Eqn. B.7 from ANSI N14.5-2014 [Ref. 3]}$$

$$\mu_{\text{mix}} = \frac{\mu_{\text{He}}P_{\text{He}} + \mu_{\text{air}}P_{\text{air}}}{P_{\text{mix}}} \rightarrow \mu_{\text{mix}} = 0.0194 \text{ cP} \quad \text{Eqn B.8 from ANSI N14.5-2014 [Ref. 3]}$$

Change in viscosity as a function of temperature was taken into consideration by using the values listed in Table 4.3.1-1, and performing linear interpolation. Mixture viscosity was determined for each temperature using the same methodology described above.

Table 4.3.1-1 Helium and Air Viscosity

Temperature (Kelvin)	Helium Viscosity (cP)	Temperature (Kelvin)	Air Viscosity (cP)
250	0.0178 ²	273.15	0.0171 ⁴
275	0.0191 ²	278.15	0.0173 ⁴
300	0.0201 ³	283.15	0.0176 ⁴
350	0.0223 ³	288.15	0.0180 ⁴
		293.15	0.0182 ⁴
		298.15	0.0185 ⁴
		303.15	0.0186 ⁴
		313.15	0.0187 ⁴
		323.15	0.0195 ⁴
		333.15	0.0197 ⁴

Determine L_{mix} as a function of temperature

Temperature range for test = $T = 273$ to 328 K, or equivalently 31.73 °F to 130.73 °F

$$F_c(D_{max}) = \frac{2.49 \cdot 10^6 \cdot (D_{max})^4}{a \cdot \mu_{mix}} \quad \text{Equation B.3 from ANSI N14.5-2014 [Ref. 3]}$$

$$F_m(T) = \frac{3.81 \cdot 10^3 \cdot (D_{max})^3 \sqrt{\frac{T}{M_{mix}}}}{a \cdot P_a} \quad \text{Equation B.4 from ANSI N14.5-2014 [Ref. 3]}$$

$$L_{mix}(T) = (F_c + F_m(T)) (P_{mix} - P_d) \frac{P_a}{P_{mix}} \quad \text{Equation B.5 from ANSI N14.5-2014 [Ref. 3]}$$

Convert the test temperature to Fahrenheit: $T_F(T) = [(9/5)T_K - 459.67] \text{ °F}$

Figure 4.3.1-1 illustrates the air and helium mixture test leakage rates, L_{mix} , as a function of temperature in degrees Fahrenheit for helium partial pressures of 0.25, 0.35, 0.45, 0.55, 0.65, 0.75, 0.85, and 0.95 atm.

² Viscosity based on Reference 15

³ Viscosity based on Reference 13.

⁴ Viscosity based on Reference 14.

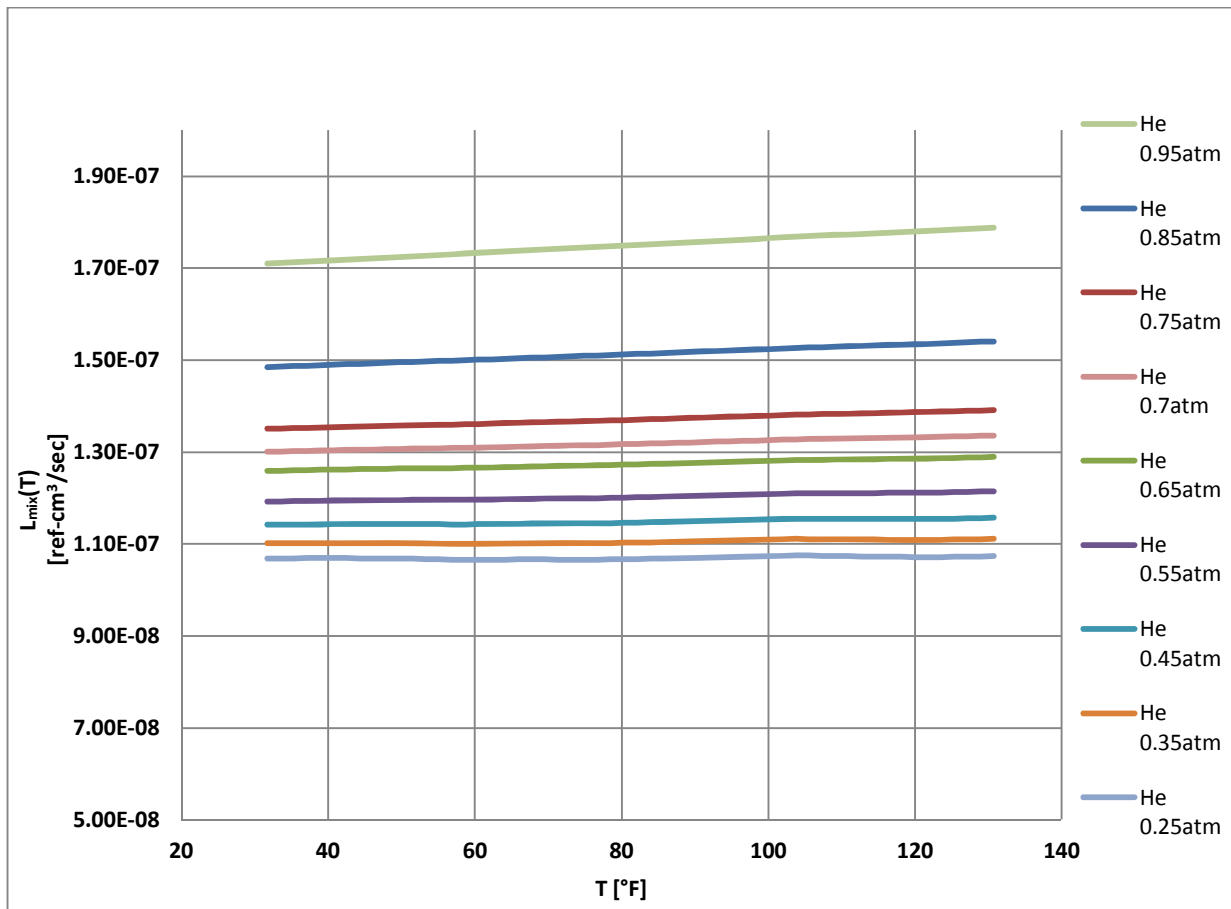


Figure 4.3.1-1 Allowable Air/Helium Mixture Test Leakage Rates

The helium component of this leak rate is determined by multiplying the leak rate of the mixture by the ratio of the helium partial pressure to the total mix pressure.

$$L_{\text{He}}(T) = L_{\text{mix}}(T) \cdot \frac{P_{\text{He}}}{P_{\text{mix}}}$$

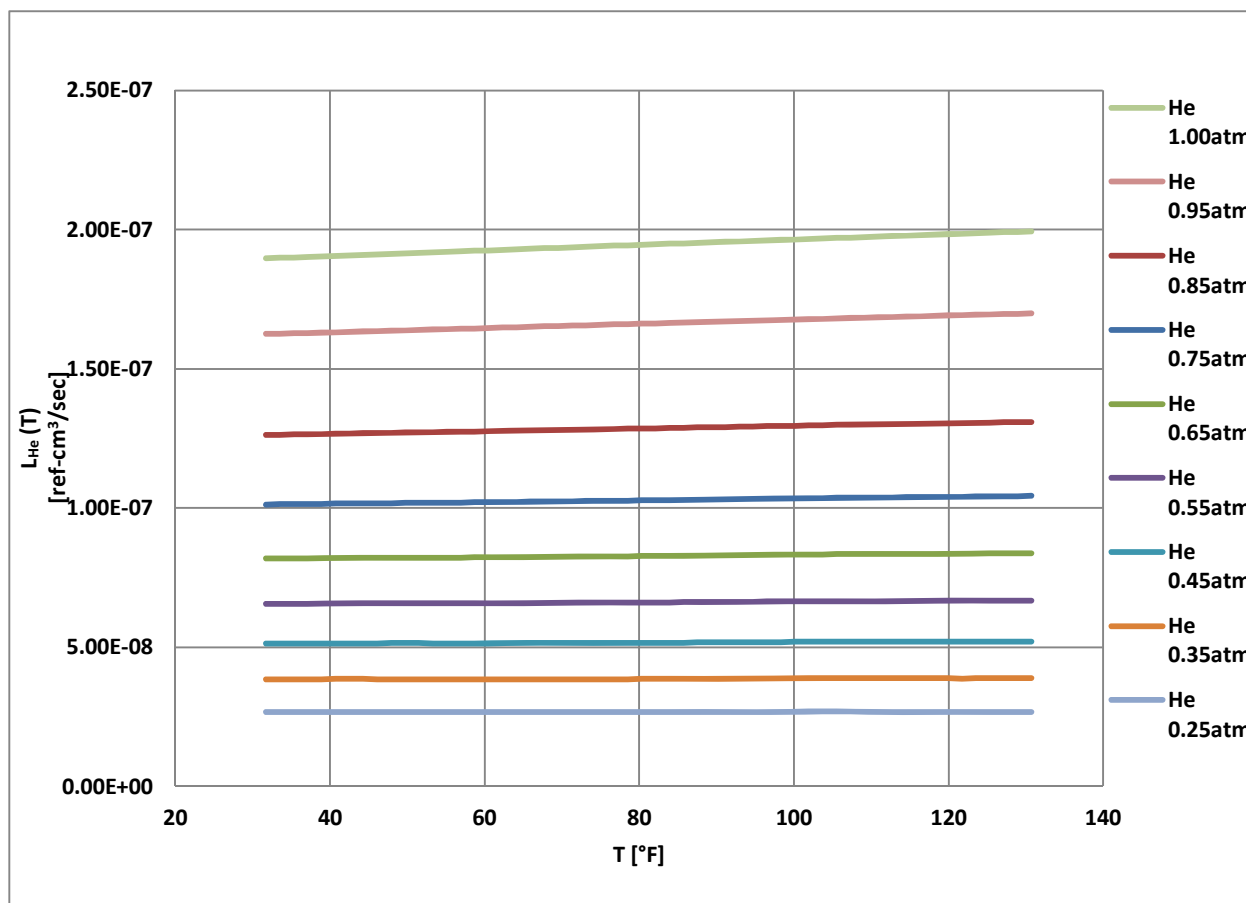


Figure 4.3.1-2 Allowable Helium Test Leakage Rates

Table 4.3.1-2 Allowable Helium Test Leakage Rates, cm³/sec

Temperature (°F)	Temperature (Kelvin)	Helium Leakage Rate P _{He} -1.0atm	Helium Leakage Rate P _{He} -0.85atm	Helium Leakage Rate P _{He} -0.65atm	Helium Leakage Rate P _{He} -0.45atm	Helium Leakage Rate P _{He} -0.25atm
31.73	273	1.897E-07	1.263E-07	8.185E-08	5.137E-08	2.672E-08
33.53	274	1.898E-07	1.263E-07	8.188E-08	5.138E-08	2.673E-08
35.33	275	1.900E-07	1.264E-07	8.191E-08	5.139E-08	2.673E-08
37.13	276	1.902E-07	1.265E-07	8.194E-08	5.141E-08	2.673E-08
38.93	277	1.903E-07	1.266E-07	8.198E-08	5.142E-08	2.673E-08
40.73	278	1.905E-07	1.267E-07	8.202E-08	5.144E-08	2.674E-08
42.53	279	1.907E-07	1.267E-07	8.205E-08	5.144E-08	2.673E-08
44.33	280	1.909E-07	1.268E-07	8.208E-08	5.144E-08	2.673E-08
46.13	281	1.911E-07	1.269E-07	8.211E-08	5.145E-08	2.672E-08
47.93	282	1.913E-07	1.270E-07	8.214E-08	5.145E-08	2.672E-08
49.73	283	1.914E-07	1.271E-07	8.217E-08	5.146E-08	2.671E-08
51.53	284	1.916E-07	1.272E-07	8.219E-08	5.145E-08	2.670E-08
53.33	285	1.918E-07	1.272E-07	8.221E-08	5.144E-08	2.668E-08
55.13	286	1.920E-07	1.273E-07	8.222E-08	5.144E-08	2.667E-08
56.93	287	1.922E-07	1.274E-07	8.224E-08	5.143E-08	2.666E-08
58.73	288	1.924E-07	1.275E-07	8.226E-08	5.142E-08	2.664E-08
60.53	289	1.925E-07	1.276E-07	8.230E-08	5.144E-08	2.665E-08
62.33	290	1.927E-07	1.277E-07	8.234E-08	5.145E-08	2.665E-08
64.13	291	1.929E-07	1.278E-07	8.238E-08	5.147E-08	2.666E-08
65.93	292	1.931E-07	1.278E-07	8.242E-08	5.148E-08	2.666E-08
67.73	293	1.933E-07	1.279E-07	8.246E-08	5.150E-08	2.667E-08
69.53	294	1.935E-07	1.280E-07	8.249E-08	5.151E-08	2.666E-08
71.33	295	1.936E-07	1.281E-07	8.253E-08	5.151E-08	2.666E-08
73.13	296	1.938E-07	1.282E-07	8.256E-08	5.152E-08	2.666E-08
74.93	297	1.940E-07	1.283E-07	8.259E-08	5.153E-08	2.665E-08
76.73	298	1.942E-07	1.284E-07	8.262E-08	5.153E-08	2.665E-08
78.53	299	1.944E-07	1.285E-07	8.267E-08	5.156E-08	2.666E-08
80.33	300	1.945E-07	1.286E-07	8.272E-08	5.159E-08	2.667E-08
82.13	301	1.947E-07	1.286E-07	8.276E-08	5.161E-08	2.669E-08
83.93	302	1.949E-07	1.287E-07	8.281E-08	5.164E-08	2.670E-08
85.73	303	1.951E-07	1.288E-07	8.286E-08	5.166E-08	2.671E-08
87.53	304	1.952E-07	1.289E-07	8.291E-08	5.169E-08	2.673E-08
89.33	305	1.954E-07	1.290E-07	8.296E-08	5.172E-08	2.675E-08
91.13	306	1.956E-07	1.291E-07	8.301E-08	5.176E-08	2.676E-08
92.93	307	1.958E-07	1.292E-07	8.306E-08	5.179E-08	2.678E-08
94.73	308	1.959E-07	1.293E-07	8.311E-08	5.182E-08	2.680E-08
96.53	309	1.961E-07	1.294E-07	8.317E-08	5.185E-08	2.681E-08

Table 4.3.1-2 Allowable Helium Test Leakage Rates, cm³/sec (Continued)

Temperature (°F)	Temperature (Kelvin)	Helium Leakage Rate P _{He} -1.0atm	Helium Leakage Rate P _{He} -0.85atm	Helium Leakage Rate P _{He} -0.65atm	Helium Leakage Rate P _{He} -0.45atm	Helium Leakage Rate P _{He} -0.25atm
98.33	310	1.963E-07	1.295E-07	8.322E-08	5.188E-08	2.683E-08
100.13	311	1.965E-07	1.296E-07	8.327E-08	5.191E-08	2.685E-08
101.93	312	1.966E-07	1.297E-07	8.332E-08	5.194E-08	2.686E-08
103.73	313	1.968E-07	1.297E-07	8.337E-08	5.197E-08	2.688E-08
105.53	314	1.970E-07	1.298E-07	8.340E-08	5.197E-08	2.687E-08
107.33	315	1.971E-07	1.299E-07	8.342E-08	5.197E-08	2.686E-08
109.13	316	1.973E-07	1.300E-07	8.344E-08	5.196E-08	2.685E-08
110.93	317	1.975E-07	1.300E-07	8.346E-08	5.196E-08	2.684E-08
112.73	318	1.977E-07	1.301E-07	8.348E-08	5.196E-08	2.683E-08
114.53	319	1.978E-07	1.302E-07	8.350E-08	5.195E-08	2.682E-08
116.33	320	1.980E-07	1.303E-07	8.352E-08	5.195E-08	2.681E-08
118.13	321	1.982E-07	1.304E-07	8.354E-08	5.195E-08	2.680E-08
119.93	322	1.984E-07	1.304E-07	8.356E-08	5.195E-08	2.679E-08
121.73	323	1.985E-07	1.305E-07	8.359E-08	5.195E-08	2.678E-08
123.53	324	1.987E-07	1.306E-07	8.363E-08	5.197E-08	2.679E-08
125.33	325	1.989E-07	1.307E-07	8.368E-08	5.199E-08	2.681E-08
127.13	326	1.990E-07	1.308E-07	8.373E-08	5.202E-08	2.682E-08
128.93	327	1.992E-07	1.309E-07	8.377E-08	5.205E-08	2.683E-08
130.73	328	1.994E-07	1.310E-07	8.382E-08	5.207E-08	2.685E-08

Figure 4.3.1-2 provides acceptable helium leakage rates at partial helium pressures of 0.25, 0.35, 0.45, 0.55, 0.65, 0.75, 0.85, 0.95, and 1.00 atm. Table 4.3.1-2 provides acceptable helium leakage rates for several helium partial pressures at temperatures ranging from 31.73 °F (273 K) to 130.73 °F (328 K). Figure 4.3.1-2 and Table 4.3.1-2 are to be used to determine the allowable leak rate L_{He} for the maintenance, fabrication, and periodic leak tests of the RT-100 based on partial pressure of helium and ambient temperatures used in the test. If the measured leakage rate is below the value shown in Figure 4.3.1-2, then the leaktight criteria has been met.

4.3.2 Determination of Equivalent Reference Leakage Rate for Air

For the pre-shipment leakage test described in Table 4.3-1, the acceptance criteria is based on standard leakage test conditions. NUREG/CR-6487 Section 2.2.6 defines the standard leak rate as corresponding to the upstream volumetric flow rate of dry air with an upstream pressure of 1.0 atmosphere, a downstream pressure of 0.01 atmospheres, and a temperature of 298 K. Tests may be performed at other conditions, provided the acceptance criterion at the testing conditions correspond to the calculated standard leakage rate acceptance criterion [Ref. 4]. The method for determining the corresponding leak rate is described in ANSI N14.5-2014 Section B.4.4 [Ref. 3].

Two pre-shipment leak test procedures are described in Chapter 8 of this SAR; a gas-pressure rise method (Section 8.2.2.2), and a gas-pressure drop method (Section 8.2.2.3). The gas-pressure drop method requires a set of conditions different than the standard leak rate conditions. In order to simplify this leak test, a pressure differential was selected that corresponds to a sensitivity of $1 \times 10^{-3} \text{ cm}^3/\text{sec}$. Given atmospheric air pressure conditions of 1 atm and a temperature of 298K, the upstream air pressure should be 1.67 atm, as described in Calculation Package 2014-020-CALC-LT-001, Rev. 0 [Ref. 25].

4.4 Hydrogen Gas Generation

Hydrogen gas buildup in loads containing waste material typically occurs due to radiolysis of hydrogenous material in the contents. As hydrogen is generated, it could potentially accumulate within the cask cavity in flammable concentrations. Based on USNRC guidance, the flammability limit of 0.05 volume fraction (mole fraction and volume fraction is interchangeable when discussing ideal gas buildup) hydrogen in air was measured in accordance with NUREG/CR-6673 “*Hydrogen Generation in TRU Waste Transportation Packages*” [Ref. 16], and supplemented with data from EPRI NP-5977 “*Radwaste Radiolytic Gas Generation Literature Review*” [Ref. 21].

Materials that make up the contents that can undergo radiolysis include primarily ion exchange resins, with lesser quantities of polystyrene and polyamides (nylon). Materials that make up the secondary container and shoring that can undergo radiolysis include polyethylene, wood, and polypropylene. Free water in the contents and moisture in the resin beads are also included in the analysis. In order to provide a bounding analysis, it is assumed that all of the decay energy in the contents produces gas generation in the waste or secondary container.

The rate of gas generation by radiolysis in these materials is dependent upon the type of incident radiation. Alpha emitters tend to generate more hydrogen per unit of energy deposited than gamma/beta emitters. Typical resin and filter waste produced at commercial nuclear power reactor facilities contains a high percentage of gamma in relation to alpha emitters. Typical examples of historical shipment data are provided with RT100-REF-01-01 “*Historical Cask Summaries by Waste Category*” [Ref. 22]. Because NUREG/CR-6673 is primarily focused on the alpha radiation predominant in TRU waste, EPRI NP-5977 is utilized to obtain gamma radiation G Values for these primary waste materials.

The typical shipment data referenced above indicates that the decay energy is approximately 90~100% from gamma radiation. In order to bound these shipments and to facilitate the utilization of a loading curve as a function of decay heat and waste volume in the cask, a decay energy distribution of 80% gamma and 20% alpha decay energy is assumed. The evaluation presented in Sections 4.4.1, 4.4.2, and 4.4.3 utilize this distribution as a way of illustrating the calculational method. Section 4.4.4 provides the user with a simplified model used to develop the

loading curve (Figure 4.4.4-1) in order to determine the maximum allowable decay heat as a function of waste volume. Section 4.4.5 provides the user with an analytical model along with a set of G Values for the bounding waste material as a function of the gamma and alpha decay energy distribution for cases that do not fit the loading curve.

Package material and content that can generate flammable gas shall be appropriately assigned as part of the ionic resin bead waste or polyethylene container when using the Loading Curve (Figure 4.4.4-1) or detailed analysis (Section 4.4.5) to determine acceptable hydrogen gas generation-related parameters of shipping time and decay heat. For example, waste filters (made of material other than polypropylene or polyethylene) shall be grouped as ionic bead waste and wood shoring would be grouped as part of the polyethylene container. If filters are made of polyethylene or polypropylene, they are to be included in the secondary container volume for the hydrogen gas generation detailed analysis.

4.4.1 Determination of Bounding G Values

The first step in performing a gas generation calculation is to determine the G Values. As such, the following sections describe the steps in this process.

4.4.1.1 G Values for Waste and Secondary Container Materials

A list of G Values is provided in Table 4.4-1 and are taken from NUREG/CR-6673 [Ref. 16], EPRI NP-5977 [Ref. 21], and RH-TRU 72-B SAR [Ref. 23]. These materials represent all potential cask contents as indicated in Section 1.2.2.3, *Physical and Chemical Form – Density, Moisture Content and Moderators*. Potential materials in the waste that can undergo radiolysis are polystyrene, nylon, polyamides, ion exchange resins, and any residual water. Secondary container and shoring materials include polyethylene, wood and polypropylene.

Table 4.4-1 G Values (Molecules/100eV) for Potential Content Materials

Material	G_H G (H ₂)	G_{FG} G (flammable gas)	G_T G (net gas)
Waste Materials			
Polystyrene (Alpha Radiation)	0.20	0.20	0.20
Polyamides/Nylon ⁵	1.10	1.20	1.50
Ion Exchange Resins (Alpha Radiation)	1.70	1.70	2.10
Ion Exchange Resins (Gamma/Beta Radiation) ⁶	0.62	0.62	0.62
Water (Liquid Phase, Gamma Radiation) ⁷	0.45	0.45	0.45 ⁽⁸⁾
Water (Liquid Phase, Alpha Radiation)	1.60	1.60	1.60 ⁽⁸⁾
Paper	0.90	0.90	1.50
Polyethylene Filter	4.00	4.10	4.10
Polypropylene Filter	3.30	3.40	3.40
Secondary Container / Shoring			
Polyethylene	4.00	4.10	4.10
Wood (Cellulose)	3.20	3.20	10.20
Polypropylene	3.30	3.40	3.40

The ion exchange resin has the highest flammable gas G Value due to alpha radiation when compared to the other hydrogenous materials that could be contained within the waste. The G Value of ionic resin for gamma radiation is taken from EPRI NP-5977, which indicates that fully swollen ionic exchange resins have flammable gas G Values of up to 0.62.

Ionic resins are dewatered before transport, meaning most of the free water is removed. Even in a fully “dewatered” state, ion exchange resin beads can contain from 50% to 66% moisture, per NUREG/CR-6673 and EPRI NP-5977. The term “dewatered” should not be confused with the term “dry” for ionic resins. Based on Section 4 of EPRI NP-5977, the G Values for fully dried resins are a factor of 10 less than swollen resin beads (from 0.001 to 0.067 in recorded experiments). As such, it can be concluded that the G values for ionic resins are primarily driven by moisture content and the values utilized in Table 4.4-1 already take into consideration the moisture content in the resin.

⁵ Based on NUREG/CR-6673, Section D.7.22 [Ref. 16], nylon is a polyamide. Polyamides are bounded by these values.

⁶ The G_{FG} value for ionic resin is used for G_T because no value is provided in EPRI NP-5977 [Ref. 21]. Less non-flammable gas production will decrease the amount of time required to achieve a flammable mixture, making this a bounding assumption.

⁷ Based on NUREG/CR-6673 Table D.1 [Ref. 16], the largest $G(H_2)$ for liquid water subjected to gamma radiation is 0.45 molecules/100eV.

⁸ For water, The G_T value is set to the G_{FG} value, as explained later in Section 4.4.1.1.

Only hydrogen gas was considered as a byproduct of the radiolysis of water. This results in the fraction of flammable gas to the total gas generated (α) of 1.0 in Equation 4.8 of NUREG/CR-6673 [Ref. 16]. Including oxygen in the total gas generation from the radiolysis of water would decrease the mole fraction of hydrogen (X_H) in the free gas volume. This is because the alpha term would be less than 1.0. Thus, using the value of 1.0 would yield the most bounding result.

4.4.1.2 Calculation of Effective G Values

Table 4.4-1 lists the G Values for the material that could be transported in the cask. Both alpha and gamma G Values are provided for the most predominant waste contents of resin and water. For other materials, the more conservative alpha radiation values are utilized. As noted in Section 4.4, hydrogen gas generation calculations for typical resin waste contents are performed assuming that the decay energy of the waste is 80% gamma and 20% alpha. The effective G Values for these materials is calculated using these fractions applied to the corresponding G Value. Materials without a gamma G Value are taken as the alpha G Value. The effective G Values are provided in Table 4.4-2.

Table 4.4-2 Effective G Values (Molecules/100eV) for Potential Content Materials

Material	Effective G_H G (H ₂)	Effective G_{FG} G (flam. gas)	Effective G_T G (net gas)
Waste Materials			
Polystyrene	0.20	0.20	0.20
Polyamides/Nylon	1.10	1.20	1.50
Ion Exchange Resins	0.84	0.84	0.92
Water	0.68	0.68	0.68
Paper	0.90	0.90	1.50
Polyethylene Filter	4.00	4.10	4.10
Polypropylene Filter	3.30	3.40	3.40
Secondary Container / Shoring			
Polyethylene	4.00	4.10	4.10
Wood (Cellulose)	3.20	3.20	10.20
Polypropylene	3.30	3.40	3.40

4.4.1.3 Operating Temperature G Value Adjustment

As described in Section 2.4.2 of NUREG/CR-6673 [Ref. 16], the hydrogen gas generation rate of some materials is noticeably affected by the temperature in the container during transport. This is contingent upon the activation energy of the material being shipped in the cask. The activation energies for the materials used in the hydrogen generation calculations are shown in Table 4.4-3, and are based on Table 3.11 of NUREG/CR-6673 and RH-TRU 72-B Appendices [Ref. 23]. The activation energy for ionic resin is not specifically listed in NUREG/CR-6673, but RH-TRU 72-B SAR specifies that organic resins have an activation energy of 2.1 kcal/mole.

Table 4.4-3 Activation Energy

Material	Activation Energy (kcal/mole)
Waste Materials	
Polystyrene	0.8
Polyamides/Nylon	0.8
Resins	2.1
Water	0.0
Paper	1.3
Polyethylene Filter	0.8
Polypropylene Filter	0.8
Secondary Container / Shoring	
Polyethylene	0.8
Wood	2.1
Polypropylene	0.8

The G value at NCT temperatures is determined using Equation 2.2 of NUREG/CR-6673.

$$G_{T_2} = G_{T_1} \exp \left[\left(\frac{E_a}{R} \right) \left(\frac{T_2 - T_1}{T_2 T_1} \right) \right]$$

where: G_{T1} = radiolytic G value at 298 K [molecules/100eV]
 G_{T2} = radiolytic G value at transport temperature [molecules/100eV],
 E_a = activation energy for radiolytic gas generation [kcal/gmol],
 R = gas law constant [1.987×10^{-3} kcal/gmol-K],
 T_1 = 298 K
 T_2 = temperature of contents during transport [K]

Based on Table 3.1.3-1, the maximum inner shell temperature during NCT is 73.1 °C. Therefore, a bounding value of 80 °C (353.15 K) is utilized for the contents in this analysis. For example, the resultant G_{FG} value (and G_T value because they are the same for polyethylene) for

polyethylene at 353.15 K is equivalent to:

$$G_{FG} = (4.1 \text{ molecules}/100\text{eV}) \exp \left[\left(\frac{0.8 \text{ kcal/gmol}}{1.987 \times 10^{-3} \text{ kcal/gmolK}} \right) \left(\frac{353.15\text{K} - 298\text{K}}{(353.15\text{K})(298\text{K})} \right) \right]$$

$$= 5.06 \text{ molecules}/100\text{eV}$$

The final G values used in the hydrogen generation calculations are shown in Table 4.4-4.

Table 4.4-4 Bounding G Values for Contents at Maximum NCT Temperature

Material	G (H ₂), G _H	G (flammable gas), G _{FG}	G (net gas), G _T
Waste Materials			
Polystyrene	0.25	0.25	0.25
Polyamides	1.36	1.48	1.85
Ion Exchange Resins	1.45	1.45	1.59
Water	0.68	0.68	0.68
Paper	1.27	1.27	2.11
Polyethylene Filter	4.94	5.06	5.06
Polypropylene Filter	4.08	4.20	4.20
Secondary Container / Shoring			
Polyethylene	4.94	5.06	5.06
Wood	5.57	5.57	17.75
Polypropylene	4.08	4.20	4.20

Of the materials that could comprise the waste, resin and water are present in the greatest quantities. While polyamides have a slightly higher G(flammable gas) value than the resins, resins were chosen as the bounding contents because resins have a much higher density when loaded than the polyamides which form a small part of filters. In addition, hydrolysis of polyamides produces nonflammable gas which would tend to dilute hydrogen concentration. If polyethylene or polypropylene filters are loaded into the cask, their volumes shall be accounted for as a polyethylene secondary container in the calculation. Therefore, resin and water are selected for utilization in the gas generation calculations.

The secondary container and shoring materials are assumed to be polyethylene. Like polyamides in the waste, wood has a slightly higher G Value than polyethylene. However, wood has a significantly higher total gas G Value, which offsets the impact of flammable gas generation by generating more than 2 moles of non-flammable gas for every mole of flammable gas. Additionally, the wood would be present only in limited quantities as shoring material on the outside of the secondary container.

As described in Section 4.4, the gas generation analysis is performed assuming that all decay energy is absorbed in either the waste or the secondary container, maximizing the amount of gas generated through radiolysis. In fact, much of the gamma radiation emitted from the waste escapes the cavity and is absorbed in the cask's lead shielding material.

These G values are then utilized to calculate the hydrogen gas generation rates as described in Section 4.4.3.

4.4.2 Hydrogen Gas Generation by Radiolysis

For the hydrogen generation evaluation, the RT-100 is treated as a single rigid non-leaking enclosure. Using Equation 4.8 on page 31 of NUREG/CR-6673 [Ref. 16], an equation characterizing the mole fraction of hydrogen (or flammable gas) in the RT-100 over time for a single material generating hydrogen is shown below.

Equation 4.4

$$X_H = \frac{n_H}{n_0 + n_{net}} = \frac{\frac{D_H}{100} \frac{\alpha G_T t}{A_N}}{\frac{P_0 V}{R_g T_0} + \frac{D_H}{100} \frac{G_T t}{A_N}}$$

where:

- X_H = mole fraction of hydrogen,
- n_H = number of moles of hydrogen [gmol],
- n_0 = initial number of gas moles in the container when the vessel was closed [gmol],
- n_{net} = number of moles of gas generated [gmol],
- G_T = total radiolytic G value [molecules/100eV],
- D_H = decay heat that is absorbed by the radiolytic materials [eV/s],
- α = fraction of G_T that is equivalent to G_{FG} , flammable gas released,
- A_N = Avogadro's constant [6.022×10^{23} molecules/gmol],
- P_0 = pressure when the container is sealed [atm],
- T_0 = temperature when the container is sealed [K],
- V = is the container void volume [cm^3],
- R_g = gas law constant [$82.05 \text{ cm}^3 \text{ atm/gmolK}$],
- t = time [seconds]

Based on Section 5 of NUREG/CR-6673 [Ref. 16], shipping periods other than one year need to be defined as one half the time it takes for hydrogen to accumulate in the package to a concentration equivalent to the lower flammability limit. To ensure that this is taken into consideration in the calculations, the equation above has been adjusted to incorporate a multiple of 2 times the shipping period required. Equation 4.4 is also limited to providing hydrogen mole fraction over time for one hydrogenous material. In this analysis there are three hydrogenous materials that are taken into consideration, water in the waste material, the resin, and the

polyethylene container. The resultant equation generated once these parameters are taken into consideration (the increase in shipping time and the number of hydrogenous materials) is shown below in Equation 4.5.

Equation 4.5

$$X_H = \frac{\frac{D_i}{100} \frac{\alpha_i G_{Ti}(2t)}{A_N} + \frac{D_C}{100} \frac{\alpha_C G_{TC}(2t)}{A_N} + \frac{D_W}{100} \frac{\alpha_W G_{TW}(2t)}{A_N}}{\frac{P_0 V}{R_g T_0} + \frac{D_i}{100} \frac{G_{Ti}(2t)}{A_N} + \frac{D_C}{100} \frac{G_{TC}(2t)}{A_N} + \frac{D_W}{100} \frac{G_{TW}(2t)}{A_N}}$$

$$X_H = \frac{\frac{D_H}{100} \frac{\alpha_i G_{Ti}(2t) F_i}{A_N} + \frac{D_H}{100} \frac{\alpha_C G_{TC}(2t) F_C}{A_N} + \frac{D_H}{100} \frac{\alpha_W G_{TW}(2t) F_W}{A_N}}{\frac{P_0 V}{R_g T_0} + \frac{D_H}{100} \frac{G_{Ti}(2t) F_i}{A_N} + \frac{D_H}{100} \frac{G_{TC}(2t) F_C}{A_N} + \frac{D_H}{100} \frac{G_{TW}(2t) F_W}{A_N}}$$

where: X_H = mole fraction of hydrogen,
 G_{Ti} = total radiolytic G value for ionic resin and stainless steel filters [molecules/100eV],
 G_{TC} = total radiolytic G value for polyethylene container, shoring, and polyethylene or polypropylene filters [molecules/100eV],
 G_{TW} = total radiolytic G value for water in waste [molecules/100eV],
 D_H = decay heat that is absorbed by the radiolytic materials [eV/s],
 D_i = decay heat that is absorbed by the ionic resin and stainless steel filters [eV/s],
 D_C = decay heat that is absorbed by the polyethylene container, shoring, and polyethylene or polypropylene filters [eV/s],
 D_W = decay heat that is absorbed by the water [eV/s],
 α_i = fraction of G_{Ti} that is equivalent to G_{FGi} , flammable gas released, for the ionic resin and stainless steel filters,
 α_C = fraction of G_{TC} that is equivalent to G_{FGC} , flammable gas released, for the secondary container, shoring, and polyethylene or polypropylene filters in the waste,
 α_W = fraction of G_{TW} that is equivalent to G_{FGW} , flammable gas released, for the water in waste,
 F_W = fraction of decay heat energy absorbed by the water in the waste material,
 F_i = fraction of decay heat energy absorbed by the ionic resin and stainless steel filters in the waste material,
 F_C = fraction of decay heat energy absorbed by the polyethylene container, shoring, and polyethylene or polypropylene filters,
 A_N = Avogadro's constant [6.022×10^{23} molecules/gmol],
 P_0 = pressure when the container is sealed [atm],
 T_0 = temperature when the container is sealed [K],
 V = is the container void volume [cm^3],
 R_g = gas law constant [$82.05 \text{ cm}^3 \text{ atm/gmol-K}$],
 t = time [seconds]

4.4.3 Hydrogen Generation – Radiolysis in Waste, Water and Polyethylene Container

In order to determine the time available to transport the RT-100, Equation 4.5 must be manipulated to provide time limit versus waste volume and decay heat of inventory. Given the decay heat and other cask content parameters, the time to reach 5% by volume of combustible gases is determined as follows.

Solve for t,

$$X_H = \frac{\frac{D_H}{100} \frac{\alpha_i G_{Ti}(2t) F_i}{A_N} + \frac{D_H}{100} \frac{\alpha_C G_{TC}(2t) F_C}{A_N} + \frac{D_H}{100} \frac{\alpha_W G_{TW}(2t) F_W}{A_N}}{\frac{P_0 V}{R_g T_0} + \frac{D_H}{100} \frac{G_{Ti}(2t) F_i}{A_N} + \frac{D_H}{100} \frac{G_{TC}(2t) F_C}{A_N} + \frac{D_H}{100} \frac{G_{TW}(2t) F_W}{A_N}}$$

$$X_H \left(\frac{P_0 V}{R_g T_0} + \frac{D_H}{100} \frac{G_{Ti}(2t) F_i}{A_N} + \frac{D_H}{100} \frac{G_{TC}(2t) F_C}{A_N} + \frac{D_H}{100} \frac{G_{TW}(2t) F_W}{A_N} \right) =$$

$$\frac{D_H}{100} \frac{\alpha_i G_{Ti}(2t) F_i}{A_N} + \frac{D_H}{100} \frac{\alpha_C G_{TC}(2t) F_C}{A_N} + \frac{D_H}{100} \frac{\alpha_W G_{TW}(2t) F_W}{A_N}$$

$$t = \frac{50 A_N X_H \frac{P_0 V}{R_g T_0}}{F_i G_{Ti} D_H [\alpha_i - X_H] + F_C G_{TC} D_H [\alpha_C - X_H] + F_W G_{TW} D_H [\alpha_W - X_H]}$$

Alternatively, given the limiting transport time and other cask parameters, the Equation 4.5 must be manipulated to provide decay heat limit versus the waste volume and the shipping period. The decay heat limit versus the free gas volume and shipping period (all decay heat energy deposited into the waste material and the polyethylene container) is determined as follows.

Solve for D_H ,

$$X_H = \frac{\frac{D_H}{100} \frac{\alpha_i G_{Ti}(2t) F_i}{A_N} + \frac{D_H}{100} \frac{\alpha_C G_{TC}(2t) F_C}{A_N} + \frac{D_H}{100} \frac{\alpha_W G_{TW}(2t) F_W}{A_N}}{\frac{P_0 V}{R_g T_0} + \frac{D_H}{100} \frac{G_{Ti}(2t) F_i}{A_N} + \frac{D_H}{100} \frac{G_{TC}(2t) F_C}{A_N} + \frac{D_H}{100} \frac{G_{TW}(2t) F_W}{A_N}}$$

$$X_H \left(\frac{P_0 V}{R_g T_0} + \frac{D_H}{100} \frac{G_{Ti}(2t) F_i}{A_N} + \frac{D_H}{100} \frac{G_{TC}(2t) F_C}{A_N} + \frac{D_H}{100} \frac{G_{TW}(2t) F_W}{A_N} \right) =$$

$$\frac{D_H}{100} \frac{\alpha_i G_{Ti}(2t) F_i}{A_N} + \frac{D_H}{100} \frac{\alpha_C G_{TC}(2t) F_C}{A_N} + \frac{D_H}{100} \frac{\alpha_W G_{TW}(2t) F_W}{A_N}$$

$$D_H = \frac{50 A_N X_H \frac{P_0 V}{R_g T_0}}{F_i G_{Ti} t [\alpha_i - X_H] + F_C G_{TC} t [\alpha_C - X_H] + F_W G_{TW} t [\alpha_W - X_H]}$$

where:	X_H	=	mole fraction of hydrogen,
	G_{Ti}	=	total radiolytic G value for ionic resin and stainless steel filters [molecules/100eV],
	G_{TC}	=	total radiolytic G value for polyethylene container, shoring, and polyethylene or polypropylene filters [molecules/100eV],
	G_{TW}	=	total radiolytic G value for water in waste [molecules/100eV],
	D_H	=	decay heat that is absorbed by the radiolytic materials [eV/s],
	D_i	=	decay heat that is absorbed by the ionic resin and stainless steel filters [eV/s],
	D_C	=	decay heat that is absorbed by the polyethylene container, shoring, and polyethylene or polypropylene filters [eV/s],
	D_W	=	decay heat that is absorbed by the water [eV/s],
	α_i	=	fraction of G_{Ti} that is equivalent to G_{FGi} , flammable gas released, for the ionic resin and stainless steel filters,
	α_C	=	fraction of G_{TC} that is equivalent to G_{FGC} , flammable gas released, for the secondary container, shoring, and polyethylene or polypropylene filters in the waste,
	α_W	=	fraction of G_{TW} that is equivalent to G_{FGW} , flammable gas released, for the water in waste,
	F_W	=	fraction of decay heat energy absorbed by the water in the waste material,
	F_i	=	fraction of decay heat energy absorbed by the ionic resin and stainless steel filters in the waste material,
	F_C	=	fraction of decay heat energy absorbed by the polyethylene container, shoring, and polyethylene or polypropylene filters,
	A_N	=	Avogadro's constant [6.022×10^{23} molecules/gmol],
	P_0	=	pressure when the container is sealed [atm],
	T_0	=	temperature when the container is sealed [K],
	V	=	is the container void volume [cm^3],
	R_g	=	gas law constant [$82.05 \text{ cm}^3 \text{ atm/gmolK}$],
	t	=	time [seconds]

The next step is to determine the values of the variables in this equation. Avogadro's constant and the gas law constant are known values set at 6.022×10^{23} molecules/gmol and $82.05 \text{ cm}^3 \text{ atm/gmolK}$, respectively, in this analysis. Initial gas temperature and pressure have been set at maximum NCT conditions (311 K and 1 atm). Based on USNRC guidance, the flammability limit of 0.05 volume fraction hydrogen in air was measured NUREG/CR-6673 [Ref. 16]. The radiolytic G values and α values utilized are as provided in Table 4.4-5. The time required has been arbitrarily set at 10 days (864,000 seconds) in this analysis (reminder that equations automatically double the time entered into the equation based on guidance suggested in NUREG/CR-6673 [Ref. 16]).

Table 4.4-5 Effective G Values and Corresponding α Values for Contents

Gamma Frac.	Alpha Frac.	Material	G (flam gas), G_{FG}	G (net gas), G_T	α
80%	20%	Polyethylene	5.06	5.06	1.00
80%	20%	Resin	1.45	1.59	0.91
80%	20%	Water	0.68	0.68	1.00 ⁽⁹⁾

Determining the fraction of decay heat energy absorbed by the free water in the waste material (F_W), ionic resin and stainless steel filters in the waste material (F_i), and by the polyethylene container, shoring, and polyethylene or polypropylene filters in the waste material (F_C) is approximated by assuming that the energy absorbed is proportional to the volume of the material in question divided by the total volume of hydrogenous material being shipped in the cask. Thus, the fractions can be described as follows:

$$F_W = \frac{V_W}{V_W + V_i + V_C}$$

$$F_i = \frac{V_i}{V_W + V_i + V_C}$$

$$F_C = \frac{V_C}{V_W + V_i + V_C}$$

where: V_W = volume of free water in the waste
 V_i = volume of dewatered¹⁰, ionic resin in the waste, including absorbed moisture, and stainless steel filters in the waste material
 V_C = volume occupied by the secondary container, shoring, and polyethylene or polypropylene filters in the waste material

Water is present in resin bead shipments in two distinct forms; one is “absorbed moisture” within the resin bead itself; the other is “free water” that is present between the resin beads. The absorbed moisture within the resin bead is considered in the hydrogen generation analysis as it is incorporated into G Value of the resins.

The volume occupied by the waste (V_{waste}) is assumed to be 99% ionic resin and 1% free water.

⁹ For water, The G_T value is set to the G_{FG} value to obtain an α value of 1.0.

¹⁰ The term “dewatered resin” refers to resins in which free water has been removed from between the resin beads at the time of preparation for storage or transportation. The amount of free water in “dewatered” resins is typically around 1% after mechanical draining (EPRI NP-5977 “Radwaste Radiolytic Gas Generation Literature Review”, page 10 [Ref. 21]). The term “dewatered” should not be confused with “dry”. Dewatered resin beads shipped in the RT-100 could have a moisture content up to 50~66% based on NUREG/CR-4062 “Extended Storage of Low-Level Radioactive Waste, Potential Problem Areas” [Ref. 20], and EPRI NP-5977.

The ionic resin beads are assumed to be uniform spheres. Since the random packing fraction for uniform spheres is 0.64 [Ref. 5], the remaining free space (0.36) of the waste volume is assumed to be 0.11 air and 0.25 water to account for grossly dewatered material content. Thus, the volumes of ionic resin and water in the waste can be described as follows:

$$V_W = (0.99)(0.25)V_{waste} + (0.01)V_{waste} = (0.2575)V_{waste}$$

$$V_i = (0.99)(0.64)V_{waste} = (0.6336)V_{waste}$$

As noted, the assumed content is either dewatered resin or grossly dewatered resin. The amount of free water in “dewatered resins”¹⁰ is typically around 1% after mechanical draining, by regulation no more than 1% to meet disposal requirements. Grossly dewatered resins have a higher free water amount that shall be limited to 20% of the ionic resin volume (20.75% of the waste volume). Therefore, the amount of “free water” assumed (25.75% of waste volume) thus represents a free water volume that bounds the dewatered resin state by an order of magnitude, and bounds the grossly dewatered resin state by around 25%, and was chosen to represent a bounding condition for hydrogen generation.

Therefore, the fraction of decay heat energy absorbed by the water in the waste volume (F_W), ionic resin and stainless steel filters the waste volume (F_i), and by the polyethylene container, shoring, and polyethylene or polypropylene filter (F_C) are equivalent to:

$$F_W = \frac{0.2575V_{waste}}{(0.2575V_{waste} + 0.6336V_{waste} + V_C)}$$

$$F_i = \frac{0.6336V_{waste}}{(0.2575V_{waste} + 0.6336V_{waste} + V_C)}$$

$$F_C = \frac{V_C}{(0.2575V_{waste} + 0.6336V_{waste} + V_C)}$$

The remaining 0.11 fraction of ionic resin volume is air. The remaining fraction of air volume in the ionic resin is taken into consideration in the total free gas volume (V). Where the free gas volume (V) is equivalent to the total cavity volume ($4.60 \times 10^6 \text{ cm}^3$) minus the sum of the container, shoring, and polyethylene or polypropylene filter volume (V_C), water volume (V_W), and the ionic resin and stainless steel filter volume (V_i).

$$V = (4.60 \times 10^6 \text{ cm}^3) - (V_C + V_W + V_i)$$

$$V = (4.60 \times 10^6 \text{ cm}^3) - (V_C + 0.2575V_{waste} + 0.6336V_{waste})$$

$$V = (4.60 \times 10^6 \text{ cm}^3) - V_C - 0.8911V_{waste}$$

Incorporating the equations for fraction of decay heat energy absorbed by the water in the waste volume, ionic resin in the waste volume and by the polyethylene container into the derivation of time limit and decay heat limit results in the following equations.

Equation 4.6

$$t = \frac{50A_N X_H \frac{P_0 V}{R_g T_0} (0.2575V_{waste} + 0.6336V_{waste} + V_C)}{(0.6336V_{waste})G_{Ti}D_H[\alpha_i - X_H] + (V_C)G_{TC}D_H[\alpha_C - X_H] + (0.2575V_{waste})G_{TW}D_H[\alpha_W - X_H]}$$

Equation 4.7

$$D_H = \frac{50A_N X_H \frac{P_0 V}{R_g T_0} (0.2575V_{waste} + 0.6336V_{waste} + V_C)}{(0.6336V_{waste})G_{Ti}t[\alpha_i - X_H] + V_C G_{TC}t[\alpha_C - X_H] + (0.2575V_{waste})G_{TW}t[\alpha_W - X_H]}$$

The final step to solving the equation is determining the free gas volume which will vary based on the inventory in the RT-100. The maximum cavity volume is known to be $4.60 \times 10^6 \text{ cm}^3$ (162.37 ft^3) based on Table 4.1.5-2. In order to determine the free gas volume an approximation of the volume occupied by the polyethylene liner needs to be made. The guiding technical issue in determining the free gas volume is to maximize the hydrogen gas mole fraction buildup rate that then results in a conservative shipping time (limiting the allowable shipping time). A greater hydrogen mole fraction buildup rate in the cavity is produced by minimizing the free gas volume of the cavity. Minimizing the available free gas volume is accomplished by using the polyethylene container with the largest container volume. “Exhibit A of Cask Procurement Agreement dated April 10, 2012” [Ref. 17], provides the burial volume, maximum internal volume, and empty weight of various containers, and is shown in Table 4.4.3-6.

The container volume may be calculated from the empty weight and material density. In order to calculate the largest container volume, a minimum material density is used. The material density of high density polyethylene is 0.959 g/cm^3 , while the material density of plain carbon steel is 7.85 g/cm^3 [Ref. 24]. For a bounding assumption, and to take into account empty liner weight tolerances, the densities were reduced by 10%, resulting in a density of 0.863 g/cm^3 (53.88 lb/ft^3) for polyethylene and 7.065 g/cm^3 (441.05 lb/ft^3) for steel. The result is that the EL-142 container has the largest container volume of 27.02 ft^3 . A volume of 30.1 ft^3 was used in the analysis to represent the volume occupied by the secondary container and any shoring. Therefore, the maximum free gas volume (no waste volume) is 132.27 ft^3 . If a different container is used in the RT-100 transport cask, the equations generated in this section of the SAR can be adjusted.

The analysis assumes use of a polyethylene container. As described in Section 4.4.1.3 this is considered a bounding assumption based on material G Values. Use of a steel liner listed in Table 4.4.3-6 is considered acceptable because steel does not contribute to hydrogen gas generation.

Given the 10 day limiting transport time, the concern is how much waste volume and decay heat is acceptable for the individual shipments. The waste volume is then equal to the maximum cavity volume subtracted by the free gas volume and the polyethylene container volume.

A loading curve of allowable decay heat as a function of waste volume is provided in Section 4.4.4 for a specific set of waste parameters, including G-Values based on a bounding decay heat distribution of 80% gamma and 20% alpha. Additionally, in case a detailed analysis is performed, a procedure is given in Section 4.4.5, and a list of effective G Values for other distributions of gamma and alpha radiation is provided in Table 4.4.5-2.

Table 4.4.3-6 Secondary Container Volumes and Allowable Shoring Volume

Container	Material Type	Empty Weight ¹¹ (lbs)	Density ¹² (lb/ft ³)	Volume Occupied by Container ¹³ (ft ³)	Allowable Shoring Volume (ft ³)
PL 6-80 MT	Polyethylene	500	53.88	9.28	20.82
PL 6-80 MTIF	Polyethylene	525	53.88	9.74	20.36
PL 6-80 FR	Polyethylene	550	53.88	10.21	19.89
PL 6-80 FP/FEDX	Polyethylene	625	53.88	11.60	18.50
PL 8-120 MT	Polyethylene	600	53.88	11.14	18.96
PL 8-120 MTIF	Polyethylene	625	53.88	11.60	18.50
PL 8-120 FR	Polyethylene	650	53.88	12.06	18.04
PL 8-120 FP/FEDX	Polyethylene	725	53.88	13.46	16.64
PL 8-120 CMT	Polyethylene	720	53.88	13.36	16.74
PL 14-150	Polyethylene	800	53.88	14.85	15.25
PL 10-160 MT	Polyethylene	700	53.88	12.99	17.11
PL 10-160 MTIF	Polyethylene	735	53.88	13.64	16.46
PL 10-160 FR	Polyethylene	750	53.88	13.92	16.18
PL 10-160 FP/FEDX	Polyethylene	825	53.88	15.31	14.79
NUHIC-55	Polyethylene	150	53.88	2.78	27.32
NUHIC-136	Polyethylene	600	53.88	11.14	18.96
Radlok 500	Polyethylene	680	53.88	12.62	17.48
EL-50	Polyethylene	909	53.88	16.87	13.23
EL-142	Polyethylene	1456	53.88	27.02	3.08
L 6-80 MT	Steel	1000	441.05	2.27	27.83
L 6-80 CMT	Steel	1150	441.05	2.61	27.49
L 6-80 IN-SITU	Steel	3500	441.05	7.94	22.16
L 6-80 FP	Steel	1050	441.05	2.38	27.72
L 6-80 FP/FEDX	Steel	1225	441.05	2.78	27.32
L 8-120 MT	Steel	1200	441.05	2.72	27.38
L 8-120 CMT	Steel	1350	441.05	3.06	27.04
L 8-120 IN-SITU	Steel	4200	441.05	9.52	20.58
L 8-120 FR	Steel	1250	441.05	2.83	27.27
L 8-120 FP/FEDX	Steel	1325	441.05	3.00	27.10
ES-50	Steel	250	441.05	0.57	29.53
ES-142	Steel	1100	441.05	2.49	27.61

¹¹ From Exhibit A of Cask Procurement Agreement dated April 10, 2012 by and between Waste Control Specialists LLC and Robatel Technologies, LLC et al [Ref. 17].

¹² The bounding calculation assumes a maximum container volume. Therefore, lower density values of 0.863 g/cm³ and 7.065 g/cm³ were chosen for polyethylene and steel.

¹³ Calculated as the Empty Weight divided by the Density, neglecting void space.

4.4.4 Hydrogen Gas Generation – Simplified Model used to develop Loading Curve

Using Equation 4.7, the decay heat limit versus waste volume can be determined for a limit of 5% in the cavity free volume. Figure 4.4.4-1 provides a curve illustrating the waste volume to decay heat value that would result in the generation of a flammable gas mixture within 10 days assuming that all decay heat is absorbed by the waste material and the polyethylene container. The calculation assumes that the hydrogen generation occurs over a period of time that is twice the allowable shipping time.

For most shipments, this simplified graphical model (Loading Curve) can be used to determine the maximum heat load. However, use of the Loading Curve is limited to the restrictions noted in Table 4.4.4-1. One restriction of using the Loading Curve is that the secondary container is listed in Table 4.4.3-6, or is a container of equivalent material volume.

If the waste volume and decay heat values for the contents fall below the Loading Curve illustrated in Figure 4.4.4-1, and the restrictions listed in Table 4.4.4-1 are met, the load would not generate a flammable gas mixture during shipment. Otherwise, the user must perform a more detailed calculation of hydrogen generation for their specific contents and expected shipping time using the information provided in Section 4.4.5. The use of this calculation ensures that the requirements of NUREG/CR-6673 [Ref. 16] are met.

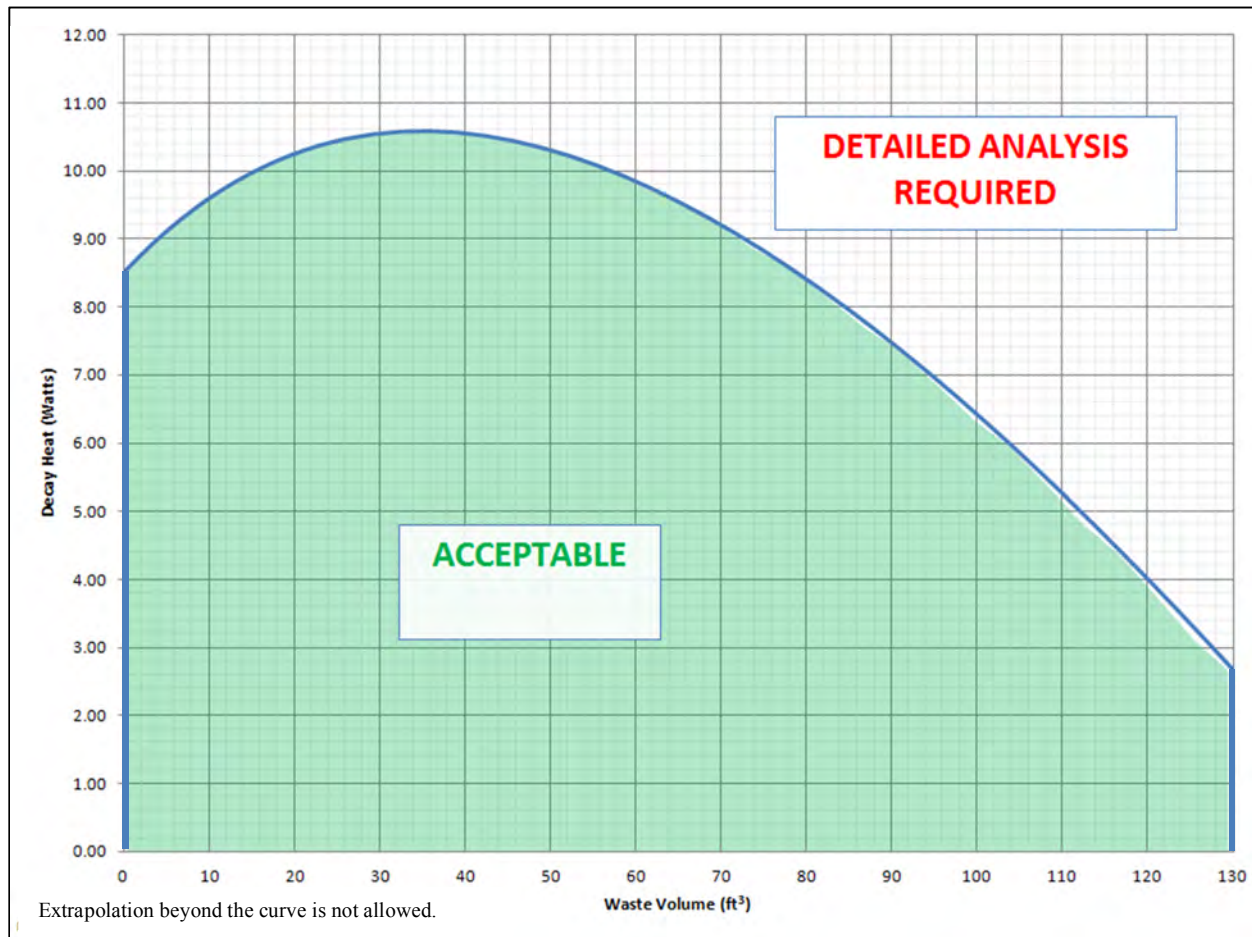


Figure 4.4.4-1 Package Loading Curve for Hydrogen Generation – Decay Heat Limit Versus Waste Volume

**Table 4.4.4-1 Conditions and Justifications for using Package Loading Curve
(Figure 4.4.4-1)**

Condition for Shipper to use Loading Curve	Justification
Waste consisting of resins and filters from commercial power plants	Historically shipments of commercial resins and filters have consisted of approximately 90-100% gamma radiation [Ref. 22]. To bound these shipments, the calculation assumes a decay energy distribution of 80% gamma and 20% alpha radiation. This results in effective G-Values for resin beads of 0.836 and for water of 0.68 molecules/100eV at 298K. These values are adjusted for maximum NCT temperature of 80 °C, and bound the expected G-Values for resins and filters from commercial reactors.
Waste has been dewatered or grossly dewatered	The loading curve assumes a free water volume of 25.75%. The main effect of free water is to limit the void volume in the cavity, thereby increasing the hydrogen mole fraction. Since the loading curve assumes 25.75% free water for a hydrogen concentration of 5% or less, shippers must ensure that the limit is not exceeded.
No limit on moisture content of resin	The G-values for resins, as noted in Table 5.3 of EPRI NP-5977, are for resins with high moisture contents (i.e., swollen resin).
Use of a liner (or equivalent) listed in Table 4.4.3-6 with maximum shoring volume as specified	The calculation determines the free volume for waste by subtracting the maximum liner and shoring volume from the cask cavity volume. Equivalent liners may be used provided the volume occupied by the liner and shoring material does not exceed 30.1 ft ³ .
Shipment time not greater than 10 days	Shipment time calculated for 20 days (allowing a shipment within 10 days following regulation).
Loading at temperature not to exceed 38 °C and standard pressure (1 atm)	The maximum ambient NCT temperature is 38 °C per 10 CFR 71.
Secondary containers are passively vented within the cask cavity during shipment.	Secondary containers are required to be passively vented within the cask cavity. The loading curve assumes the gases generated are free to occupy the cask cavity volume inside and outside the secondary container.
Filters are not made of polyethylene or polypropylene	Polyethylene or polypropylene filters have higher G Values than resins, therefore, they require performing the detailed analysis and addition of their volume to the secondary container volume (V_C).
Waste volume not greater than 130 ft ³	Extrapolation beyond the curve is not allowed.

4.4.5 Hydrogen Gas Generation – Analytical Model used for Detailed Analysis

If Figure 4.4.4-1 is not applicable to a shipment, or if further analysis is required, the equations derived in Section 4.4.3 can be used. With substitution and further simplification of Equation 4.6 and Equation 4.7, the maximum allowable shipping time (t_{max}) or the maximum allowable decay heat ($D_{H,max}$) can be described as:

Equation 4.8

$$t_{max} = \frac{(2.5A_N P_0)(4.6E6 - V_C - 0.8911V_{WASTE})(0.8911V_{WASTE} + V_C)}{(R_g T_0 D_H)[0.6336V_{WASTE} G_{Ti}(\alpha_i - 0.05) + V_C G_{TC}(\alpha_C - 0.05) + 0.2575V_{WASTE} G_{TW}(\alpha_W - 0.05)]}$$

Equation 4.9

$$D_{H,max} = \frac{(2.5A_N P_0)(4.6E6 - V_C - 0.8911V_{WASTE})(0.8911V_{WASTE} + V_C)}{(R_g T_0 t)[0.6336V_{WASTE} G_{Ti}(\alpha_i - 0.05) + V_C G_{TC}(\alpha_C - 0.05) + 0.2575V_{WASTE} G_{TW}(\alpha_W - 0.05)]}$$

where:

- A_N = Avogadro's constant [6.022×10^{23} molecules/gmol]
- R_g = gas law constant [$82.05 \text{ cm}^3 \cdot \text{atm} / \text{gmol} \cdot \text{K}$]
- P_0 = pressure when the container is sealed [atm]
- T_0 = temperature when the container is sealed [K]
- D_H = decay heat of cask contents [eV/s]
- t = shipment time [s]
- V_C = volume occupied by the secondary container, shoring, and polyethylene or polypropylene filters in the waste [cm^3]
- V_{WASTE} = volume occupied by the ionic resin and stainless steel filters in the waste material [cm^3]
- G_{Ti} = total radiolytic G value for the ionic resin and stainless steel filters [molecules/100eV]
- G_{TC} = total radiolytic G value for the secondary container, shoring, and polyethylene or polypropylene filters in the waste [molecules/100eV]
- G_{TW} = total radiolytic G value for water in waste [molecules/100eV]
- α_i = fraction of G_{Ti} that is equivalent to G_{FGi} , flammable gas released, for the ionic resin and stainless steel filters
- α_C = fraction of G_{TC} that is equivalent to G_{FGC} , flammable gas released, for the secondary container, shoring, and polyethylene or polypropylene filters in the waste
- α_W = fraction of G_{TW} that is equivalent to G_{FGW} , flammable gas released, for water in the waste

NOTE: Use of Equation 4.8 and Equation 4.9 are valid only when the conditions listed in Table 4.4.5-1 are met. Shipments are allowed only if the conditions in Table 4.4.5-1 are met.

Table 4.4.5-1 Conditions for Shipper to use the Detailed Analysis

1	Waste consists of resins and filters from commercial power plants.
2	Waste has been grossly dewatered.
3	Secondary containers are passively vented within the cask cavity during shipment.

The user may measure the decay heat of the cask contents (D_H) in order to calculate the maximum allowable shipping time (t_{max}) using Equation 4.8.

Alternately, the user may know the shipment time (t) and calculate the maximum allowable decay heat of the cask contents ($D_{H,max}$) using Equation 4.9.

Initial pressure (P_0) and initial temperature (T_0) may be measured by the user at the time of loading. The volume occupied by the secondary container, shoring, and polyethylene or polypropylene filters in the waste (V_C) and the volume occupied by the ionic resin and stainless steel filters in the waste material (V_{WASTE}) are known.

The use of different G-values (G_{Ti} , G_{TC} , G_{TW}) and α fractions (α_i , α_C , α_W) must be justified by the user based on waste characterization. These variables must be adjusted for the transport temperature of 80 °C as described in Section 4.4.1.3, in order to meet the requirements of NUREG/CR-6673 [Ref. 16].

The values must also be adjusted for the appropriate alpha/gamma radiation distribution. One example of this adjustment is provided in Table 4.4.5-2 for the same G-values in the bounding case loading curve for the 80% gamma/20% alpha decay heat distribution.

Table 4.4.5-2 G-values and α -Fractions for a Range of Alpha/Gamma Decay Heat Distributions

Gamma Frac	Alpha Frac	Material	G (H ₂), G _H	G (flam gas), G _{FG}	G (net gas), G _T	α
0.0	1.0	Polyethylene	4.94	5.06	5.06	1.00
		Resin	2.96	2.96	3.65	0.81
		Water	1.60	1.60	1.60	1.00 ⁽¹⁴⁾
0.1	0.9	Polyethylene	4.94	5.06	5.06	1.00
		Resin	2.77	2.77	3.40	0.82
		Water	1.49	1.49	1.49	1.00 ⁽¹⁴⁾
0.2	0.8	Polyethylene	4.94	5.06	5.06	1.00
		Resin	2.58	2.58	3.14	0.82
		Water	1.37	1.37	1.37	1.00 ⁽¹⁴⁾
0.3	0.7	Polyethylene	4.94	5.06	5.06	1.00
		Resin	2.39	2.39	2.88	0.83
		Water	1.26	1.26	1.26	1.00 ⁽¹⁴⁾
0.4	0.6	Polyethylene	4.94	5.06	5.06	1.00
		Resin	2.21	2.21	2.62	0.84
		Water	1.14	1.14	1.14	1.00 ⁽¹⁴⁾
0.5	0.5	Polyethylene	4.94	5.06	5.06	1.00
		Resin	2.02	2.02	2.37	0.85
		Water	1.03	1.03	1.03	1.00 ⁽¹⁴⁾
0.6	0.4	Polyethylene	4.94	5.06	5.06	1.00
		Resin	1.83	1.83	2.11	0.87
		Water	0.91	0.91	0.91	1.00 ⁽¹⁴⁾
0.7	0.3	Polyethylene	4.94	5.06	5.06	1.00
		Resin	1.64	1.64	1.85	0.89
		Water	0.80	0.80	0.80	1.00 ⁽¹⁴⁾
0.8	0.2	Polyethylene	4.94	5.06	5.06	1.00
		Resin	1.45	1.45	1.59	0.91
		Water	0.68	0.68	0.68	1.00 ⁽¹⁴⁾
0.9	0.1	Polyethylene	4.94	5.06	5.06	1.00
		Resin	1.27	1.27	1.34	0.95
		Water	0.57	0.57	0.57	1.00 ⁽¹⁴⁾
0.95	0.05	Polyethylene	4.94	5.06	5.06	1.00
		Resin	1.17	1.17	1.21	0.97
		Water	0.51	0.51	0.51	1.00 ⁽¹⁴⁾
1.0	0.0	Polyethylene	4.94	5.06	5.06	1.00
		Resin	1.08	1.08	1.08	1.00
		Water	0.45	0.45	0.45	1.00 ⁽¹⁴⁾

¹⁴ For water, the α value is set to 1.0.

4.5 Appendix

Attachment 4.5-1 EPDM Temperature Specifications

[Ref. 10]

Parker O-Ring Handbook	
Basic O-Ring Elastomers	<p>Not compatible with:</p> <ul style="list-style-type: none"> Fuels of high aromatic content (for flex fuels a special compound must be used). Aromatic hydrocarbons (benzene). Chlorinated hydrocarbons (trichloroethylene). Polar solvents (ketone, acetone, acetic acid, ethylene-ester). Strong acids. Brake fluid with glycol base. Ozone, weather and atmospheric aging.
	<p>2.2.2 Carboxylated Nitrile (XNBR)</p> <p>Carboxylated Nitrile (XNBR) is a special type of nitrile polymer that exhibits enhanced tear and abrasion resistance. For this reason, XNBR based materials are often specified for dynamic applications such as rod seals and rod wipers.</p> <p>Heat resistance</p> <ul style="list-style-type: none"> Up to 100°C (212°F) with shorter life @ 121°C (250°F). <p>Cold flexibility</p> <ul style="list-style-type: none"> Depending on individual compound, between -18°C and -48°C (0°F and -55°F). <p>Chemical resistance</p> <ul style="list-style-type: none"> Aliphatic hydrocarbons (propane, butane, petroleum oil, mineral oil and grease, diesel fuel, fuel oils) vegetable and mineral oils and greases. HFA, HFB and HFC hydraulic fluids. Many diluted acids, alkali and salt solutions at low temperatures. <p>Not compatible with:</p> <ul style="list-style-type: none"> Fuels of high aromatic content (for flex fuels a special compound must be used). Aromatic hydrocarbons (benzene). Chlorinated hydrocarbons (trichloroethylene). Polar solvents (ketone, acetone, acetic acid, ethylene-ester). Strong acids. Brake fluid with glycol base. Ozone, weather and atmospheric aging.
	<p>2.2.4 Ethylene Propylene Rubber (EPR, EPDM)</p> <p>EPR copolymer ethylene propylene and ethylene-propylene-diene rubber (EPDM) terpolymer are particularly useful when sealing phosphate-ester hydraulic fluids and in brake systems that use fluids having a glycol base.</p> <p>Heat resistance</p> <ul style="list-style-type: none"> Up to 150°C (302°F) (max. 204°C (400°F)) in water and/or steam). <p>Cold flexibility</p> <ul style="list-style-type: none"> Down to approximately -57°C (-70°F). <p>Chemical resistance</p> <ul style="list-style-type: none"> Hot water and steam up to 149°C (300°F) with special compounds up to 260°C (500°F). Glycol based brake fluids (Dot 3 & 4) and silicone-based brake fluids (Dot 5) up to 149°C (300°F). Many organic and inorganic acids. Cleaning agents, sodium and potassium alkalis. Phosphate-ester based hydraulic fluids (HFD-R). Silicone oil and grease. Many polar solvents (alcohols, ketones, esters). Ozone, aging and weather resistant. <p>Not compatible with:</p> <ul style="list-style-type: none"> Mineral oil products (oils, greases and fuels).
	<p>2.2.5 Butyl Rubber (IIR)</p> <p>Butyl (isobutylene, isoprene rubber, IIR) has a very low permeability rate and good electrical properties.</p> <p>Heat resistance</p> <ul style="list-style-type: none"> Up to approximately 121°C (250°F). <p>Cold flexibility</p> <ul style="list-style-type: none"> Down to approximately -59°C (-75°F). <p>Chemical resistance</p> <ul style="list-style-type: none"> Hot water and steam up to 121°C (250°F). Brake fluids with glycol base (Dot 3 & 4). Many acids (see Fluid Compatibility Tables in Section VII). Salt solutions. Polar solvents, (e.g. alcohols, ketones and esters). Poly-glycol based hydraulic fluids (HFC fluids) and phosphate-ester bases (HFD-R fluids). Silicone oil and grease. Ozone, aging and weather resistant. <p>Not compatible with:</p> <ul style="list-style-type: none"> Mineral oil and grease. Fuels. Chlorinated hydrocarbons.
	<p>2.2.3 Ethylene Acrylate (AEM, Vamac)</p> <p>Ethylene acrylate is a terpolymer of ethylene and methyl acrylate with the addition of a small amount of carboxylated curing monomer. Ethylene acrylate rubber is not to be confused with polyacrylate rubber (ACM).</p> <p>Heat resistance</p> <ul style="list-style-type: none"> Up to 149°C (300°F) with shorter life up to 163°C (325°F). <p>Cold flexibility</p> <ul style="list-style-type: none"> Between -29°C and -40°C (-20°F and -40°F). <p>Chemical resistance</p> <ul style="list-style-type: none"> Ozone. Oxidizing media. Moderate resistance to mineral oils.

Attachment 4.5-2 Seal Material EPDM Working Temperature

[Ref. 11]

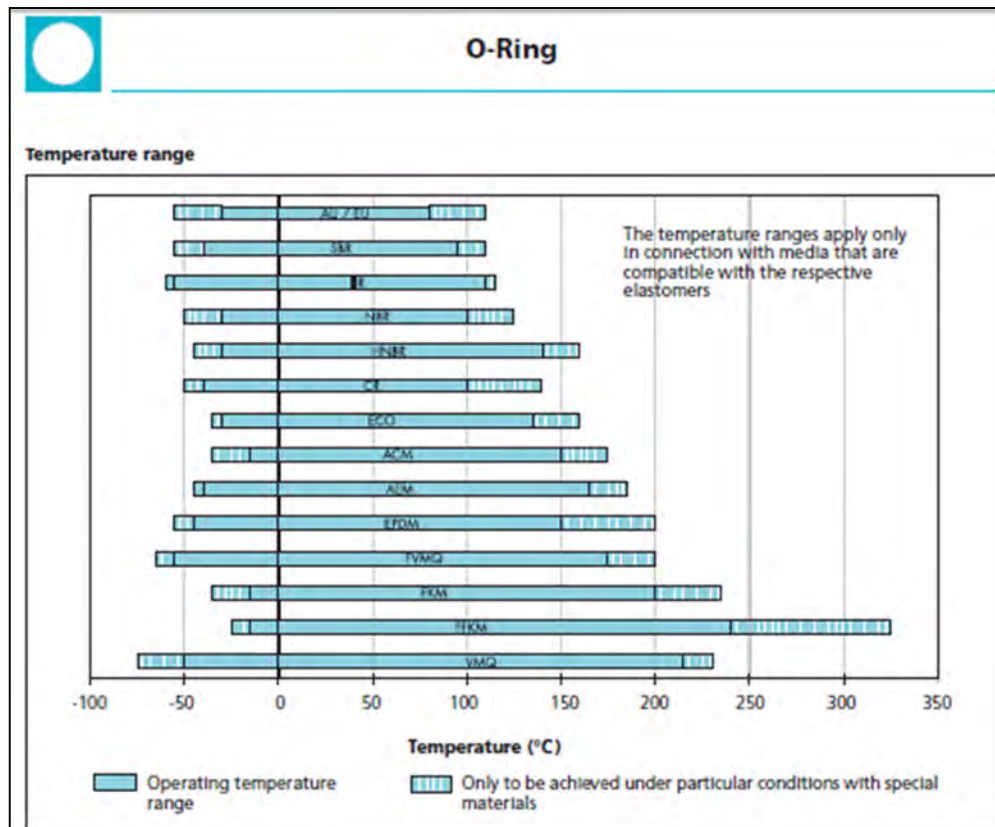


Figure 4 Temperature range of various elastomers

General field of application

Elastomer materials are used to cover a large number of fields of application. The various elastomers can be characterised as follows:

ACM (Polyacrylate Rubber)

ACM shows excellent resistance to ozone, weathering and hot air, although it shows only a medium physical strength, low elasticity and a relatively limited low temperature capability. The operating temperatures range from -20 °C and +150 °C (for a short period of time up to +175 °C). Special types can be used down to -35 °C. ACM-materials are mainly used in automotive applications which require special resistance to lubricants containing many additives (incl. sulphur) at high temperatures.

CR (Chloroprene Rubber)

In general the CR materials show relatively good resistances to ozone, weathering, chemicals and aging. Also they show good non-flammability, good mechanical properties and cold flexibility. The operating temperatures range between -35 °C and +90 °C (for a short period of time up to +120 °C). Special types can be used down to

-55 °C. CR materials are found in sealing applications such as refrigerants, for outdoor applications and in the glue industry.


EPDM (Ethylene Propylene Diene Rubber)

EPDM shows good heat, ozone and aging resistance. In addition they also exhibit high levels of elasticity, good low temperature behaviour as well as good insulating properties. The operating temperatures of applications for EPDM range between -45 °C and +150 °C (for a short period of time up to +175 °C). With sulphur cured types the range is reduced to -45 °C and +130 °C (for short period of time up to +150 °C). EPDM can often be found in applications with brake fluids (based on glycol) and hot water.

FFKM (Perfluoro Rubber)

Perfluoroelastomers show broad chemical resistance similar to PTFE as well as good heat resistance. They show low swelling with almost all media. Depending on the material the operating temperatures range between -25 °C and +240 °C. Special types can be used up to +325 °C. Applications for FFKM can be mostly found in the chemical and process industries and in all applications with either aggressive environments or high temperatures.

Attachment 4.5-3 Seal Material EPDM Helium gas permeation rate [Ref. 11]



O-Ring

Materials

FEP sheath

FEP is the abbreviated designation for Tetrafluoroethylene-hexafluoropropylene. This material has similar properties to those of Polytetrafluoroethylene (PTFE). It also has a very high chemical resistance and exhibits a good resistance to abrasion.

In contrast to PTFE, however, FEP is thermoplastically moldable. This allows the material to be processed to form flexible semifinished products, such as thin-walled hoses.

PFA sheath

PFA is the abbreviation for Perfluoralkoxy. This material is a type of Fluoropolymer with properties similar to Polytetrafluoroethylene (PTFE). Differing from PTFE, like FEP, PFA it is melt-processable but shares PTFE's useful properties of low coefficient of friction and non-reactivity.

PFA is preferable to FEP in high temperature situations. PFA is more affected by water absorption and weathering than FEP, but is superior in terms of salt spray resistance.

Inner ring

A choice of three materials is available for the elastomer inner rings with FEP encapsulation and two materials for the inner ring with PFA encapsulation. The choice of the material also determines the service temperature range.

- Fluorocarbon rubber (FKM),
temperature range: -20 °C up to +200 °C
material code with FEP sheath: VZ00R
material code with PFA sheath: VZ01R
- Silicone Rubber (VMQ),
temperature range: -50 °C up to +175 °C
material code with FEP sheath: SZ00R
material code with PFA sheath: SZ01R
- Ethylene Propylene Dien Rubber,
temperature range: -45 °C up to +150 °C
material code with FEP sheath: EZ00R

The specified temperature ranges are limits which must always be considered in conjunction with the medium to be sealed and the working pressure. The permissible continuous operating temperatures are always lower than the given upper limits.

Design recommendations

FEP encapsulated O-Rings are fully interchangeable with standard O-Ring seals. There is no need to modify the groove dimensions. The FEP sheath is relatively thin-walled.

All the specifications given in this catalogue therefore refer to the installation dimensions of elastomer O-Rings.

As a result of the FEP sheath, the O-Rings are less flexible than elastomer O-Rings. They have limited stretch and higher permanent deformation.

Split grooves are recommended, especially for outside sealing FEP encapsulated O-Rings, in order to avoid overstretching during installation.

The general information on the construction, design and surfaces given for the elastomer O-Rings applies also to FEP encapsulated O-Rings.

At higher pressures, additional concave Back-up Rings should be used.

Application in gases

Where the O-Ring is used to seal gases, the permeation rate must be taken into consideration. In this case the material of the inner ring must also have a good resistance to the medium to be sealed. The permeation rate depends on the exposed surface area, the temperature, the working pressure and the thickness of the FEP sheath.

The thickness of the FEP sheath can be found in Table 32.

Compliances and approvals

The FEP-sheath of material VZ00R, SZ00R and EZ00R is in compliance with the following regulations governing plastic materials for food contact applications:

- Commission Directive 2002/72/EC and amendments 2004/1/EC, 2004/19/EC 2005/79/EC, 2007/19/EC, 2008/39/EC, Reg. (EC) 975/2009
- Requirement of the German Food and Feed Code, LFGB and regulation (EC) 1935/2004, article 5

OML (Overall Migration Limits):
Migration testing was done according to 82/711/EEC and 85/572/EEC and amendments. The OML was below the required limit of 10 mg/dm² in aqueous, acidic and fatty food in repeated contact.


Sensory Tests:
The material meets the requirements of the LFGB and Regulation (EC) 1935/2004 for aqueous, acidic and fatty food in repeated contact. Test condition: 30 min at 95 °C. Surface volume ratio: 30 cm²/1000 ml.

Both the FEP and the PFA sheath are also in compliance with the FDA Regulation 21 CFR Part 177.1550.

Table 32 Thickness of the FEP and PFA sheath

O-Ring		Thickness of the FEP/PFA Sheath
Cross section d ₂	Tolerance ±	
1.78 1.80	0.10	0.20
2.62 2.65	0.10	0.30
3.53 3.55	0.12	0.38
5.34 5.30	0.25	0.50
7.00	0.38	0.50

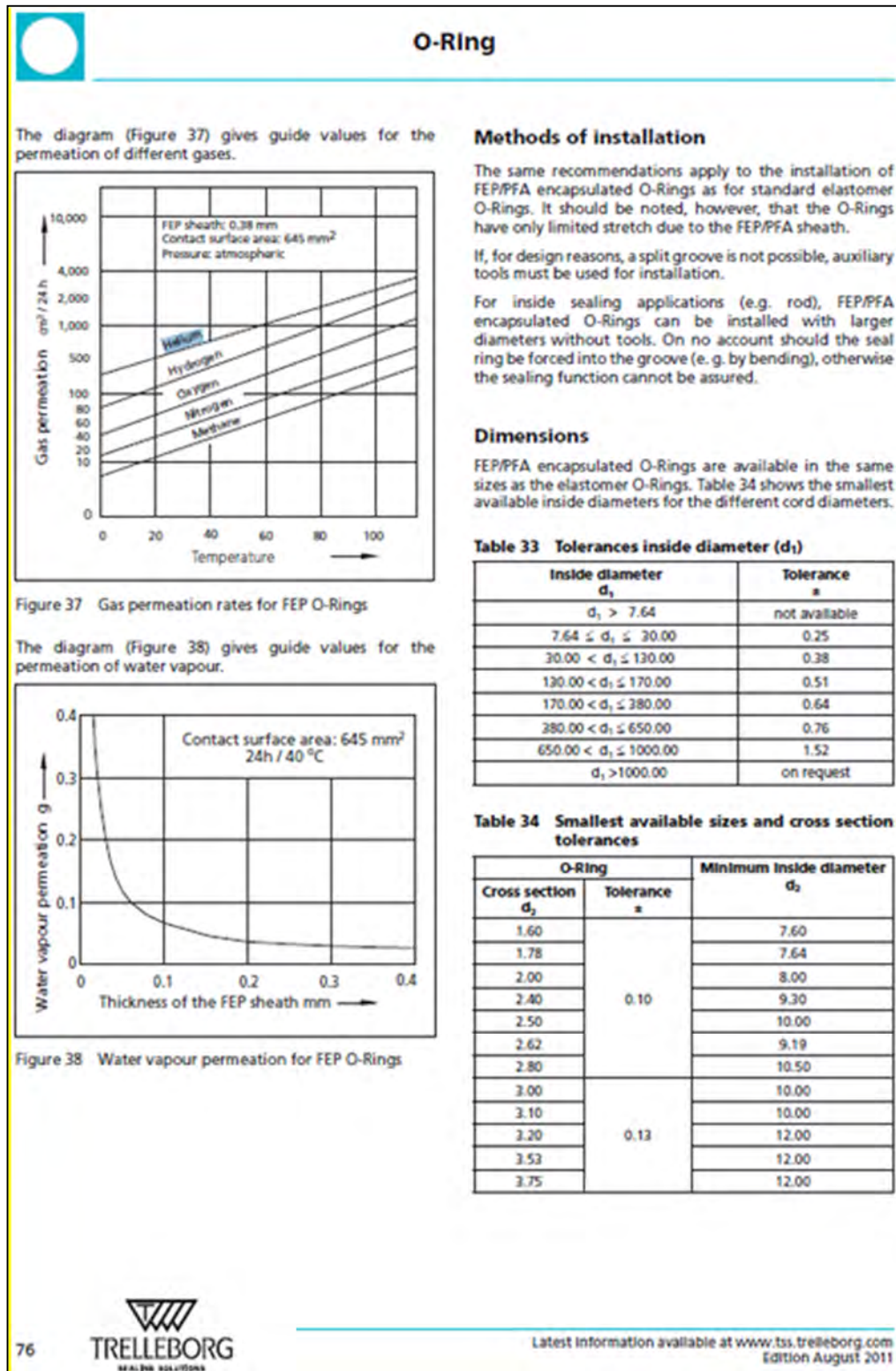
Latest information available at www.tss.trelleborg.com
Edition August 2011



75

Attachment 4.5-3 Seal Material EPDM Helium gas permeation rate (Continued)

[Ref. 11]



Attachment 4.5-4 Seal Material EPDM Characteristics With Respect to Damage by Radiation and Hardness Concerns

[Ref. 11]

A General quality criteria

The cost-effective use of seals and bearings is highly influenced by the quality criteria applied in production. Seals and bearings from Trelleborg Sealing Solutions are continuously monitored according to strict quality standards from material acquisition through to delivery.

Certification of our production plants in accordance with international standards QS 9000/ISO 9000 meets the specific requirements for quality control and management of purchasing, production and marketing functions.

Our quality policy is consistently controlled by strict procedures and guidelines which are implemented within all strategic areas of the company.

All testing of materials and products is performed in accordance with accepted test standards and specifications, e.g. random sample testing in accordance with ISO 2859-1:2004-01 AQL 1,0 general inspection level II, normal inspection.

Inspection specifications correspond to standards applicable to individual product groups (e.g. for O-Rings: ISO 3601).

Our sealing materials are produced free of chlorofluorinated hydrocarbons and carcinogenic elements.

B Guidelines for the storage of polymer products based on ISO 2230

Many polymer products and components are stored for long periods of time before being put into service, so it is important they are stored in conditions that minimize unwanted changes in properties. Such changes may result from degradation, in which case they may include excessive hardening, softening, cracking, crazing and other surface effects. Other changes may be caused by deformation, contamination or mechanical damage.

Packaging

Unless otherwise specified in the appropriate product specification, rubber products should be enclosed in individual sealed envelopes. The packaging should be carried out in an atmosphere in which the relative humidity is less than 70 %, or if polyurethanes are being packed, less than 65 %. Where there is serious risk of ingress of moisture (e.g. rubber-metal bonded parts), aluminum foil/paper/polyethylene laminate or other similar means of protection should be used to ensure protection from ingress of moisture.

Temperature

The storage temperature should be below 25 °C and the products should be stored away from direct sources of heat such as boilers, radiators and direct sunlight. If the storage temperature is below 15 °C, care should be

exercised during handling of stored products, as they may have stiffened and have become susceptible to distortion if not handled carefully.

Humidity

The relative humidity should be such that, given in the variations of temperature in storage, condensation does not occur. In all cases, the relative humidity of the atmosphere in storage should be less than 70 %, or if polyurethanes are being stored, less than 65 %.

Light

Rubber should be protected from light sources, in particular direct sunlight or intense light having a high ultraviolet content. It is advisable that any windows of storage rooms be covered with a red or orange coating or screen.

Radiation

Precautions should be taken to protect stored products from all sources of ionizing radiation likely to cause damage to the products.

Ozone

Ozone has a particularly harmful effect on rubber. Storage rooms should not contain any equipment that is capable of generating ozone, such as mercury vapor lamps or high-voltage electrical equipment giving rise to electric sparks or electrical discharges. Combustion gases and organic vapors should also be excluded, as they may give rise to ozone via photo-chemical processes. When equipment such as a fork-lift truck is used to handle large rubber products, care needs to be taken to ensure this equipment is not a source of pollution that may affect the rubber. Combustion gases should be considered separately. While they are responsible for generating ground-level ozone, they may also contain unburned fuel which, by condensing on rubber products, can cause additional deterioration.

Deformation

Rubber should be stored free from tension, compressive stresses or other causes of deformation. Where products are packaged in a strain-free condition, they should be stored in their original packaging. In case of doubt, the manufacturer's advice should be sought. It is advisable that rings of large internal diameter are formed into three equal loops so as to avoid creasing or twisting. It is not possible to achieve this condition by forming just two loops.

Contact with liquids and semi-liquid materials

Rubber should not be allowed to come into contact with liquid or semi-liquid materials (for example, petrol, greases, acids, disinfectants, cleaning fluids) or their vapors at any time during storage, unless these materials are by design an integral part of the product or the manufacturer's packaging. When rubber products are received coated with their operational media, they should be stored in this condition.

Attachment 4.5-4 Seal Material EPDM Characteristics With Respect to Damage by Radiation and Hardness Concerns (Continued)

[Ref. 11]

B.1.3 Characteristics and inspection of elastomers

Hardness

One of the most often named properties regarding Polymer materials is hardness. Even so the values can be quite misleading.

Hardness is the resistance of a body against penetration of an even harder body - of a standard shape defined pressure.

There are two procedures for hardness tests regarding test samples and finished parts made out of elastomer material:

1. Shore A / D according to ISO 868 / ISO 7619 / DIN 53505 / ASTM D 2240
Measurement for test samples
2. Durometer IRHD (International Rubber Hardness Degree) according to ISO 48 / ASTM 1414 and 1415
Measurement of test samples and finished parts

The hardness scale has a range of 0 (softest) to 100 (hardest). The measured values depend on the elastic qualities of the elastomers, especially on the tensile strength.

The test should be carried out at temperatures of 23 ± 2 °C - not earlier than 16 hours after the last vulcanisation process (manufacturing stage). If other temperatures are being used this should be mentioned in the test report.

Tests should only be carried out with samples which have not been previously stressed mechanically.

Hardness tests according to Shore A / D

The hardness test device Shore A (indenter with pyramid base) is a sensible application in the hardness range 10 to 90. Samples with a larger hardness should be tested with the device Shore D (indenter with spike).

Test specimen:

Diameter min. 1.181 inches (30 mm)

Thickness min. .240 inches (6 mm)

Upper and lower sides smooth and flat

When thin material is being tested it can be layered providing minimal sample thickness is achieved by a maximum of 3 layers. All layers must be at minimum .080 inches (2 mm) thick.

The measurement is done at three different places at a defined distance and time.

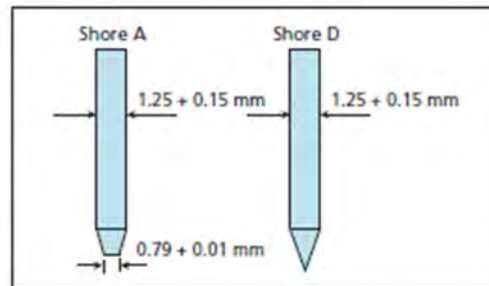


Figure 5 Indentor according to Shore A / D

Hardness test according to IRHD

The test of the Durometer according to IRHD is used with test samples as well as with finished goods.

The thickness of the test material has to be adjusted according to the range of hardness. According to ISO 48 there are two hardness ranges:

- Soft: 10 to 35 IRHD ⇒ Sample thickness
.394 to .591 inches
(10 to 15 mm) / procedure "L"
- Normal: over 35 IRHD ⇒ Sample thickness
.315 to .394 inches
(8 to 10 mm) / procedure "N"
- Sample thickness
.059 to .098 inches
(1.5 to 2.5 mm) / procedure "M"

The hardness determined with finished parts or samples usually vary in hardness determined from specimen samples, especially those with a curved surface.

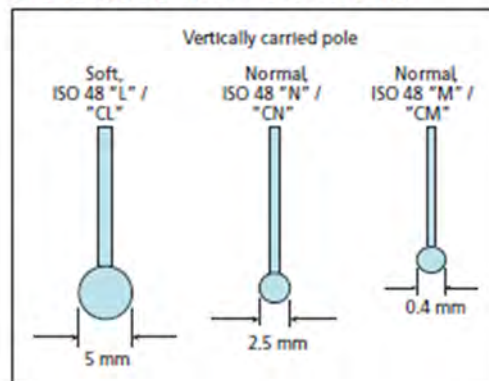


Figure 6 Indentor according to IRHD

Attachment 4.5-4 Seal Material EPDM Characteristics With Respect to Damage by Radiation and Hardness Concerns (Continued)

[Ref. 11]

Influencing parameters on the hardness test for polymer materials

Various sample thicknesses and geometries as well as various tests can show different hardness values even though the same materials have been used.

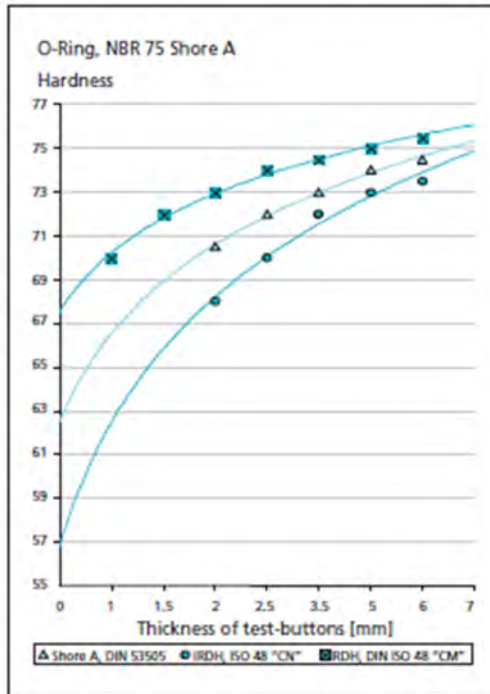


Figure 7 Ranges of hardness depending on sample thickness and test method

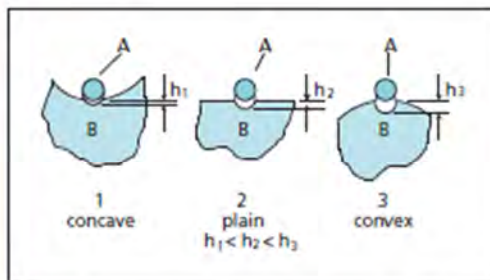


Figure 8 Range of hardness depending on surface geometry for the equivalent material characteristics

With equivalent material characteristics of the elastomer sample B, the indenter penetrates the deepest at the surface 3 (convex) and therefore establishes the softest area.

As the convex geometry (3) has a stronger effect on smaller width O-Rings, the tolerances on hardness for widths under 2.0 mm should be increased up to +5/-8 IRHD based on the valid IRHD nominal value.

Compression set

An important parameter regarding the sealing capability is the compression set (CS) of the O-Ring material. Elastomers when under compression show aside from an elastic element also a permanent plastic deformation (Figure 9).

The compression set is determined in accordance with ISO 815 as follows:

Standard test piece: Cylindrical disc, diameter .512 and height .236 inches (13 mm and height 6 mm)
Deformation: 25 %
Tension release time: 30 minutes

$$CS = \frac{h_0 - h_2}{h_0 - h_1} \cdot 100(\%)$$

Where h_0 = Original height (cross section d_2)
 h_1 = Height in the compressed state
 h_2 = Height after tension release

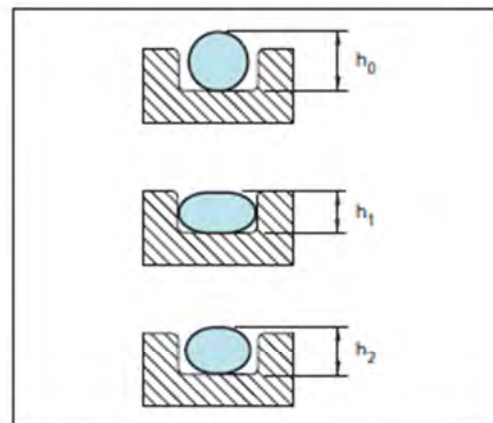


Figure 9 Illustration of the compression set

Attachment 4.5-4 Seal Material EPDM Characteristics With Respect to Damage by Radiation and Hardness Concerns (Continued)

[Ref. 11]

The accuracy of the measured value depends on:

- Test sample thickness
- Deformation
- Measurement deviations

Therefore the values which have been identified with the test sample cannot be transferred onto the finished part. The result of the measured finished parts are strongly influenced by geometrics and measurements as well as the measuring accuracy of the test equipment.

The following illustration shows the influence of various measuring deviations (in mm) in respect to the established compression set CS depending on the cross section of the measured O-Rings.

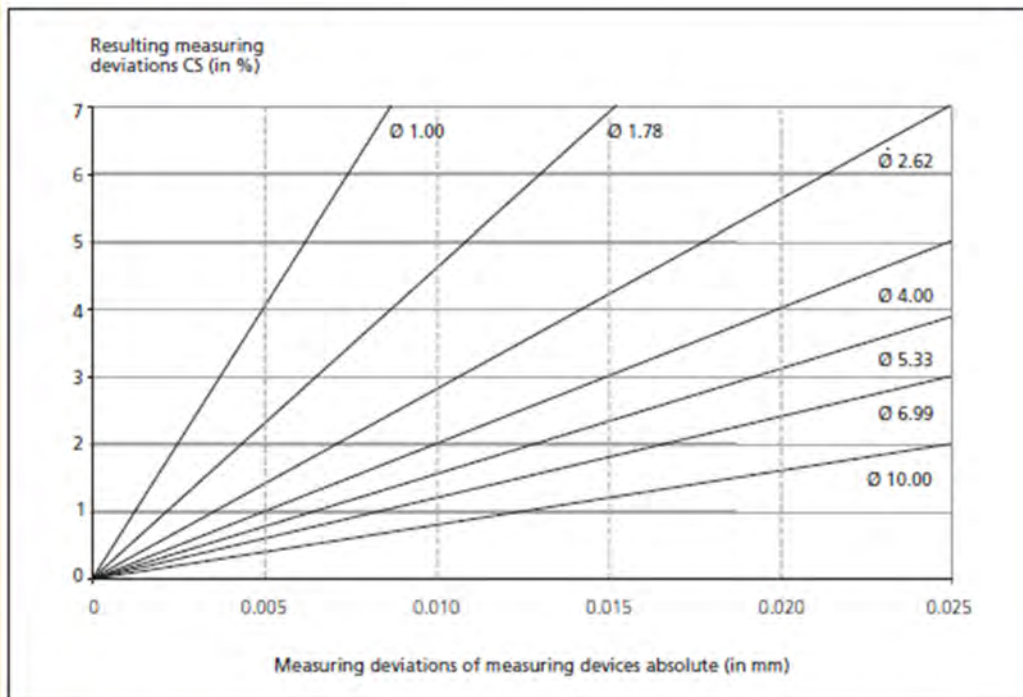


Figure 10 Measuring deviations CS depending on O-Ring cross section and measuring accuracy of the test equipment (schematic illustration)

Attachment 4.5-5 Additional Support Information about EPDM Resistance to Radiation Up to 5×10^8 Rads While Retaining Reasonable Flexibility and Strength, Hardness and Very Good Compression Set Resistance

[Ref. 12]

© 1985 IEEE. Personal use of this material is permitted. However, permission to reprint/republish this material for advertising or promotional purposes or for creating new collective works for resale or redistribution to servers or lists, or to reuse any copyrighted component of this work in other works must be obtained from the IEEE.

IEEE Transactions on Nuclear Science, Vol. NS-32, No. 3, October 1985

3806

RADIATION RESISTANCE OF ELASTOMERS

Glenn Lee
Fermi National Accelerator Laboratory*
P.O. Box 500
Batavia, Illinois 60510

Abstract

Various data has indicated that some elastomers have much higher radiation resistance than Viton. Nine samples of elastomers were irradiated with gamma rays. Two Ethylene Propylene Diene compounds, EPDM's, were found to exhibit acceptable properties for o-rings after radiation levels of 5×10^8 rads, while Viton failed at 1×10^8 rads. Vacuum tests also were favorable so EPDM o-rings were chosen as seals in the Energy Saver cryostat vacuum system.

Introduction

Viton is commonly used for o-ring seals in high vacuum systems, and failures have occurred in radiation areas such as particle beam transport lines due to radiation from beam loss. In a search for radiation resistant seals suitable for vacuum systems, nine elastomer samples were obtained from Minnesota Rubber Company and irradiated with gamma rays.

Materials Tested

The samples tested were:

Compound #	Material
559N	EPDM (Ethylene Propylene Diene)
559CQ	EPDM (Ethylene Propylene Diene)
365T	NBR (Nitrile)
514AB	Viton
71417	Silicone
512AJ	Sulfur Cured Urethane
482BJ	Neoprene
560ND	EPDM (tightly cured)
564FP	Peroxide Cured Urethane
564PS	Sulfur Cured Urethane

Affect of Radiation

Minnesota Rubber Company tested the elastomers after irradiation. There are some variances of data due to the size of the samples tested and the results are as follows.

The compound, 512AJ, sulfur cured Urethane, appears to have the best radiation resistance. Even after 10^8 rads 512AJ has some elongation and tensile and little change in hardness. However, the compression set of 512AJ, even originally, is poor which is typical of sulfur cured Urethanes. In a seal application, compression set is a critical property and such extremely poor set resistance will cause part failure.

The EPDM compounds 559N and 559CQ show the best all around properties with radiation levels up to 5.0×10^8 rads. They exhibit good tensile and are still elastomeric though elongation is low and hardness is high. Compression set is excellent even at 5.0×10^8 rads. The EPDM's are not good at levels of 10^8 rads since in the compression set test both samples disintegrated.

The other compounds were brittle at or before 3.0×10^8 rads. Compound 365T, a NBR, retains good properties at 10^8 rads. Compound 482BJ, a Neoprene, was brittle at 3×10^8 rads though it had good properties at 10^8 rads. Both 71417, silicone, and 514AB, Viton, were significantly affected by the radiation, becoming hard even at 3×10^8 rads and brittle at 3×10^8 rads.

For all radiation applications up to 5.0×10^8 rads the best compounds are 559N or 559CQ, the EPDM's. If radiation levels are higher than 5.0×10^8 rads, then compound 512AJ could be used, but difficulty would be encountered in designing a functional part because of the high set it exhibits.

The test results confirmed that EPDM compounds have the best all around properties with radiation levels up to 5×10^8 rads. They retain reasonable flexibility and strength, hardness, and very good compression set resistance.

A Urethane that is sulfur cured has the best flexibility, strength and hardness even up to 2×10^8 rads. However, they have very poor compression set qualities even before treatment of radiation. The sulfur cured Urethane fail completely by $.85 \times 10^8$ rads in compression set.

The peroxide cured Urethanes have an initial change of properties but seem to stabilize through to 2.0×10^8 rads and is very brittle at 3×10^8 rads. The initial compression set characteristics is much better than the sulfur cured Urethanes but again failure is seen at $.85 \times 10^8$ rads.

There are many new compounds now that have not been tested. Quite possibly elastomers with properties superior to the EPDM's could be found.

Vacuum Tests at Fermilab

Urethane o-rings have been used for a few vacuum applications in high radiation areas, but extreme outgassing eliminated their use in high vacuum apparatus. Samples of compounds 560ND, 564PS, 564FP, Viton, and polyurethane cord purchased from Eagle Belting Company were tested for outgassing in a very simple vacuum chamber. The chamber consisted of a spare Fermilab main ring ion pump with a short tube extension and a roughing valve. Equal weights of elastomer samples were placed in the tube extension and the chamber was then roughed down and the ion pump started. The ion pump power supply frequency was used as the pressure indicator since an ion gauge was not available. A frequency of 10 kHz indicated a pressure of approximately 1×10^{-8} Torr. A table of test results indicates the extreme outgassing of the Urethane materials as compared to Viton, while the ethylene propylene compound wasn't so bad. No data was obtained as to actual outgassing rates due to lack of personnel, time, and equipment.

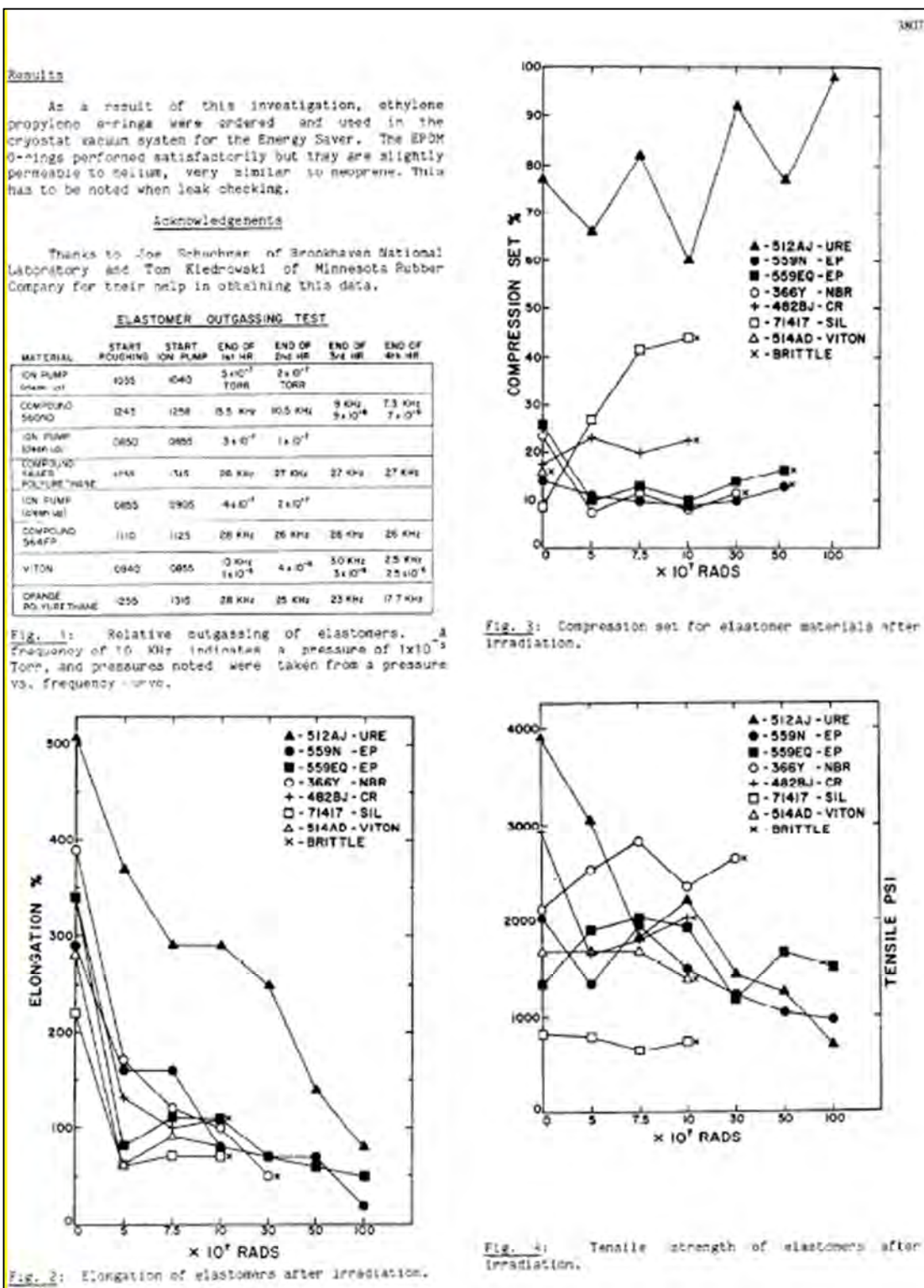
Figure 1 shows the pump-down data for six of the compounds tested. Figures 2, 3, 4, and 5 show respectively, the elongation, compression set, tensile, and hardness properties.

*Operated by Universities Research Association, Inc. under contract with the U.S. Department of Energy.

0018-9499/85/1000-3806\$01.00 © 1985 IEEE

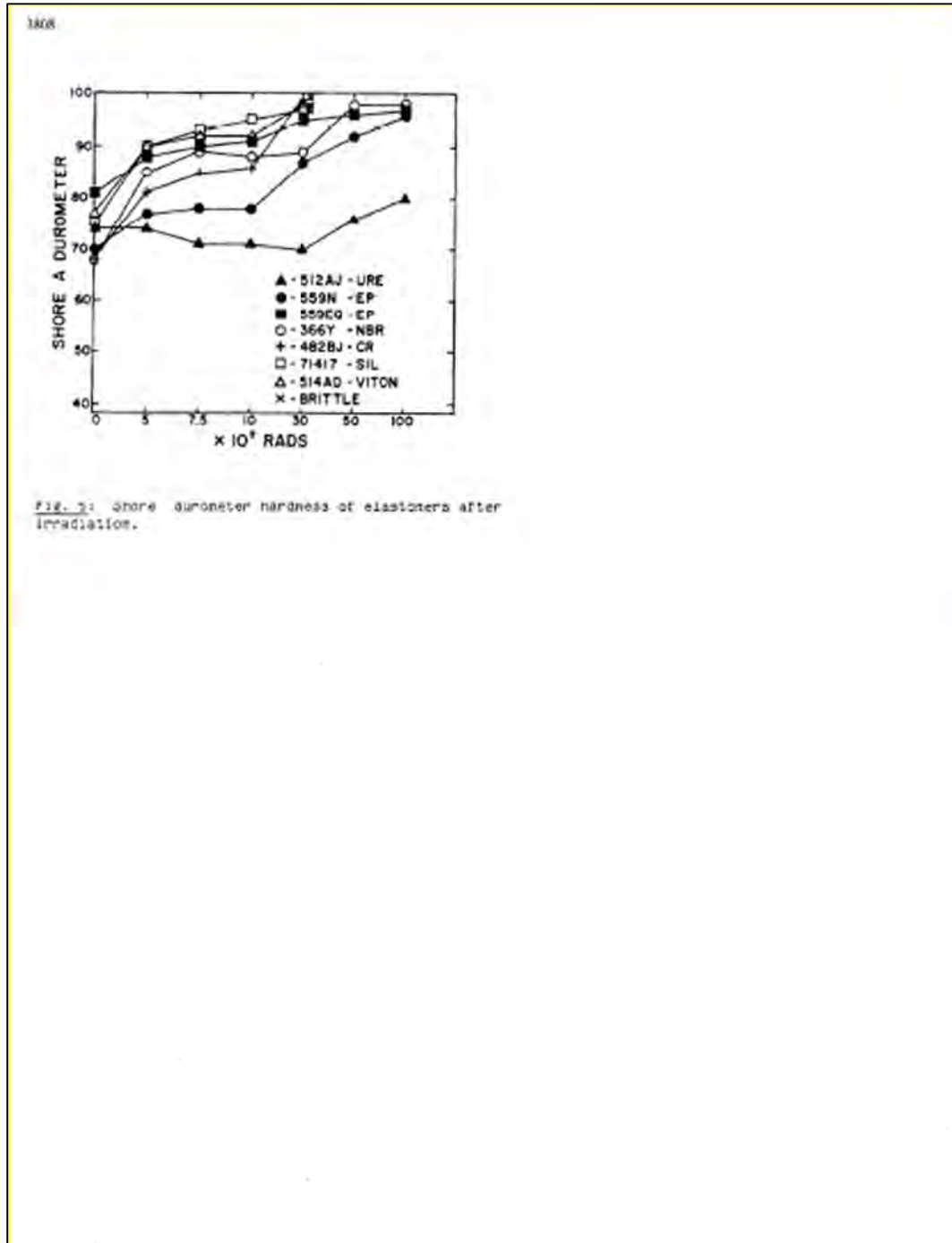
Attachment 4.5-5 Additional Support Information about EPDM Resistance to Radiation Up to 5x10⁸ Rads While Retaining Reasonable Flexibility and Strength, Hardness and Very Good Compression Set Resistance (Continued)

[Ref. 12]



**Attachment 4.5-5 Additional Support Information about EPDM Resistance to Radiation
Up to 5×10^8 Rads While Retaining Reasonable Flexibility and Strength, Hardness and
Very Good Compression Set Resistance (Continued)**

[Ref. 12]



4.6 References

1. Robatel Technologies, LLC, Quality Assurance Program for Packaging and Transportation of Radioactive Material, 10 CFR 71 Subpart H, Rev. 2, Dated November 10, 2017 and NRC Approved on March 21, 2012
2. U.S. Nuclear Regulatory Commission, 10 CFR Part 71--PACKAGING AND TRANSPORTATION OF RADIOACTIVE MATERIAL, dated March 7, 2012 and the following specific Sections:

71.31(a)(1)	71.31(a)(2)	71.33	71.35(a)
71.31(c)	71.43(c)	71.73(d)	71.4(e)
71.71	71.43(f)	71.51(a)(1)	71.43(h)
71.51(a)(2)	71.51	71.63	71.63(b)
71.51(a)(1)	71.51(a)(2)	71.73	

3. ANSI N14.5-2014, "American National Standard for Radioactive Materials – Leakage Tests on Packages for Shipment," American National Standards Institute, Inc., 11 West 42nd Street, New York, NY, www.ansi.org.
4. U.S. Nuclear Regulatory Commission, "Containment Analysis for Type B Packages Used to Transport Various Contents," NUREG/CR-6487, November 1996.
5. "Particle-size distribution and packing fraction of geometric random packings." H. J. H. Brouwers, Physical Review E 74, 031309, 2006.
6. DOE Handbook, *Airborne Release Fractions/Rates and Respirable Fractions for Nonreactor Nuclear Facilities*, "Volume I - Analysis of Experimental Data," U.S. Department of Energy, Washington, D.C., 1994.
7. NUREG/CR-6487, "Containment Analysis for Type B Packages Used to Transport Various Contents," Anderson, B., Carlson, R., & Fischer, L., Lawrence Livermore National Laboratory, Livermore, CA, November 1996, Retrieved on August 28, 2013, Retrieved from http://rampac.energy.gov/docs/nrcinfo/NUREG_6487.pdf.
8. RTL-001-CALC-TH-0102, Rev. 6, "RT-100 Cask Maximum Normal Operating Pressure Calculation" (PROPRIETARY)
9. RTL-001-CALC-TH-0202, Rev. 6, "RT-100 Cask Hypothetical Accident Condition Maximum Pressure Calculation" (PROPRIETARY)
10. Parker O-Ring Handbook ORD 5700, Retrieved on August 28, 2013, Retrieved from http://www.parker.com/literature/ORD%205700%20Parker_O-Ring_Handbook.pdf.
11. TRELLEBORG Sealing Solutions O-Ring and Backup Rings Catalog, August 2011 Edition
12. Glenn Lee, Radiation Resistance of Elastomers, IEEE Transactions on Nuclear Science, Vol. NS-32, No. 5, October 1985.

13. Lamarsh, J. & Baratta, A., "Introduction to Nuclear Engineering", 3rd Edition, 2001.
14. Fundamentals of Fluid Mechanics, B. Munson, D. Young and T. Okiishi, 5th ed., John Wiley & Sons, Inc., 2006.
15. Brookhaven National Laboratory, "Selected Cryogenic Data Notebook", August 1980.
16. NUREG/CR-6673, "Hydrogen Generation in TRU Waste Transportation Packages," Anderson, B., Sheaffer, M., & Fischer, L., Lawrence Livermore National Laboratory, Livermore, CA, May 2000.
17. "Exhibit A of Cask Procurement Agreement dated April 10, 2012 by and between Waste Control Specialists LLC and Robatel Technologies, LLC et al."
18. [Withdrawn]
19. RTL-001-CALC-CN-0101, Rev 6, "Containment Evaluation for the RT-100" (PROPRIETARY)
20. NUREG/CR-4062 "Extended Storage of Low-Level Radioactive Waste: Potential Problem Areas", B. Siskind D.R. Dougherty, D. R. MacKenzie.
21. EPRI NP-5977, "Radwaste Radiolytic Gas Generation Literature Review", Electric Power Research Institute, September 1988.
22. RT100-REF-01-01, Rev. 0, "*Historical Cask Summaries by Waste Category*" (PROPRIETARY)
23. "RH-TRU 72-B SAR Payload Appendices", Rev. 0, June 2006.
24. "Materials Science and Engineering", W. Callister, Jr., 6th Edition, John Wiley & Sons, Inc., 2003.
25. 2014-020-CALC-LT-001, Rev. 0, "Calculation of RT-100 Pressure Drop Leak Test Conditions" (PROPRIETARY)

This page is intentionally left blank.

5. SHIELDING EVALUATION

This Chapter describes the RT-100 shielding evaluation under the RT Quality Assurance Program [Ref. 1] and summarizes the results to demonstrate compliance with the shielding requirements of 10 CFR 71 [Ref. 2]. The RT-100 cask package is designed to transport contaminated resin and filter media from nuclear power plant operation. The RT-100 has a robust gamma shielding design comprised of a steel/lead/steel body with a steel primary lid and a steel/lead/steel secondary lid. The primary lid is bolted onto the body, and the secondary lid is bolted into the primary lid. Both lids, along with their O-ring seals provide secure containment of the radioactive material contents. Analyses presented in this chapter demonstrate that the shielding design produces dose rates below the external radiation requirements of 10 CFR 71 [Ref. 2] under Normal Conditions of Transport (NCT) and Hypothetical Accident Conditions (HAC). The package and vehicle radiation limits are for exclusive use of an open (flat-bed) transport vehicle. Operating limits are established for the specific activities of individual radionuclides (Ci/g) allowed in the contents of the package.

The RT-100 is designed in compliance with the external radiation standards that are specified in 10 CFR Part 71 [Ref. 2] as:

- The RT-100 is designed, constructed, and prepared for shipment so that the external radiation levels will not significantly increase under the tests specified in 10 CFR 71.71 (Normal Conditions of Transport) in accordance with 10 CFR 71.43(f) and 10 CFR 71.51(a)(1).
- Under NCT tests specified in 10 CFR 71.71, the external radiation levels meet the requirements of 10 CFR 71.47(b) for exclusive-use shipments.
- Under HAC tests specified in 10 CFR 71.73, the external radiation level does not exceed 10 mSv/hr (1 rem/hr) at one meter from the surface of the package in accordance with 10 CFR 71.51(a)(2).

The shielding evaluation is based on the descriptions and evaluations presented in the General Information, Structural Evaluation and Thermal Evaluation sections of the application. Results of the shielding evaluation are considered in the preparation of Operating Procedures and the Acceptance Tests and Maintenance Program. An example of information flow for the shielding evaluation is shown in Figure 5-1 .

The approach used to calculate the maximum allowable limits is intended to assure that the maximum activity of each radionuclide includes sufficient margin to ensure that the maximum dose rates of a loaded RT-100 cask will comply with regulatory dose rate limits. The process used to calculate the radionuclide-specific source strength densities (Ci/g) is summarized as:

1. Shielding Model package geometry, materials, source definition, tallies

An MCNP6 shielding model is constructed using the minimum shielding material thicknesses, and assumes that the maximum activity concentration of a specific radionuclide completely fills the cask cavity with no credit given for attenuation provided by secondary containers. Separate tallies are defined in the shielding model to determine the peak external dose rate at all locations required by the regulations (i.e. package surface, 1m, 2m). The input file for MCNP6 is a shielding model that represents the package geometry, materials, source definition, and tallies as described in Section 5.3 and 5.4.1.1.

2. External dose rates for package transport conditions

The shielding analysis, to determine external dose rates for the RT-100 package, is performed with MCNP6 [Ref. 3]. The output from MCNP6 is a dose rate response in mrem/hr/Ci for each of the generic source energies that has been modified by fluence-to-dose conversion factors and is normalized per 1 Curie of activity. A detailed description of the shielding analysis method is provided in Section 5.4.1.2.

The actual dose rate associated with a particular radionuclide in the cask contents is a function of the package shielding configuration, the interaction of emitted radiation with the cask contents, and the spectrum of radiation emitted from decay of the radionuclides. Since there are numerous potential radionuclides in the cask contents (as discussed in Section 5.2) with each radionuclide having an emission spectrum containing multiple energy levels, it is impractical to explicitly analyze each energy level for each potential radionuclide separately. Rather, a finite number of energy levels are selected that are representative of the expected range of radiation energies from all radionuclides. The shielding analysis is performed for each of these representative energy levels, referred to in this evaluation as *generic energies*. The generic energy source term used for the calculation assumes the probability of particle emission is 100 percent per disintegration, and the actual emission probability (i.e. intensity) is accounted for in the dose rate response calculation for individual nuclides.

3. Dose rate response for individual radionuclides

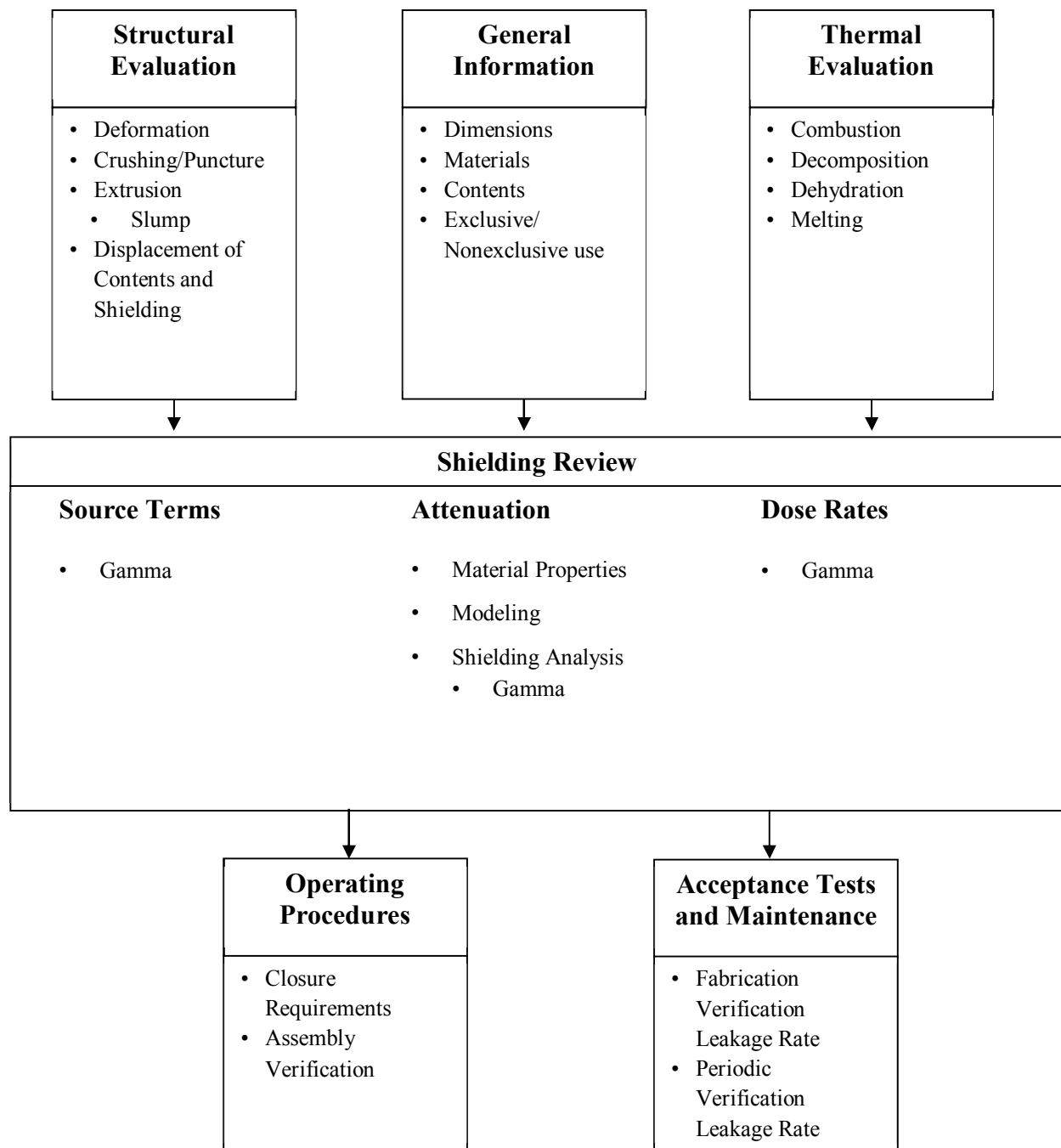
The MCNP6 shielding evaluation calculates the dose rate responses for a finite set of generic source energies, independent of the radionuclide responsible for the particle emission. In this evaluation, 26 discrete generic energies were analyzed. The generic energy dose rate responses from MCNP6 are processed and used as input to calculate the dose rate response for individual radionuclides. The method utilized to determine the dose rates from 1 Curie of a specific radionuclide uses the calculated responses of the generic energy lines to determine the response at each energy line of the respective radionuclide. A radionuclide dose rate response in mrem/hr/Ci is calculated by summing the determined dose rate responses for all energy lines of the respective radionuclide.

The dose rates for the most significant radionuclides are calculated separately from the generic energy line response method, with individual MCNP6 inputs modeling the actual source spectrum of each radionuclide. The radionuclides considered individually in this analysis are: Co-60, Zn-65, Fe-59, Mn-54, Co-58, Ag-110m, Cs-134, and Cs-137. A detailed description of the method used to calculate radionuclide dose rate responses is provided in Section 5.4.1.2.

4. Calculate the maximum allowable source strength density

Based on the maximum possible mass of resin material in the RT-100, the regulatory dose rate at a given location, and the calculated radionuclide dose rate response at the respective regulatory location, a maximum quantity of each radionuclide allowed to be transported in the cask is specified in the form of specific activities (Ci/g), also referred to as the *source strength density*. The radionuclide-specific source strength densities are used to verify that the actual contents being shipped will comply with the regulatory requirements for external radiation levels. The maximum allowed source strength densities calculated in the shielding evaluation are used in an operating procedure, referred to as the *loading table*, which is used for mixtures of radionuclides. A detailed description of the method used to calculate the maximum allowable source strength is provided in Section 5.4.1.3.

The actual contents can vary significantly for shipments; therefore, it is not practical to explicitly evaluate the actual contents that are shipped. This methodology is used to imply a dose rate associated with a particular mixture of radionuclides in the contents by calculating an effective source strength density that is a sum of the fraction of the maximum allowable source strength densities for the individual radionuclides. A sum of the fractions for radionuclide-specific maximum allowable source strength densities that is less than or equal to 1.0 implies that the external radiation levels meet the regulatory limits. Further description of the loading table operating procedure is provided in Chapter 7, Section 7.6.1 of this SAR.

Figure 5-1 Information Flow for the Shielding Evaluation

5.1 Description of Shielding Design

A description of the shielding design, as well as a summary of the results of the analysis for this design is provided below.

5.1.1 Design Features

The RT-100 body is a right circular cylinder 2060 mm in diameter and 2324 mm in height without the impact limiters attached. The cavity of the RT-100 is 1730 mm in diameter and 1956 mm in height. Surrounding the cavity are the cask radial wall, cask bottom wall, primary lid and a secondary lid embedded in the primary lid. The cask radial wall comprises 30 mm of steel, 90 mm of lead and 35 mm of steel for gamma shielding. The cask bottom wall comprises 50 mm of steel, 75 mm of lead and 30 mm of steel for gamma shielding. The primary lid comprises 210 mm of steel for gamma shielding. Embedded in the primary lid is a secondary lid that comprises 100 mm of steel, 60 mm of lead and 10 mm of steel for gamma shielding. The primary lid is 2016 mm in diameter and the secondary lid is 1000 mm in diameter. Under transport conditions, the top and bottom impact limiters provide additional gamma shielding from the 10 mm inner steel shell, polyurethane foam and 4 mm outer steel shell.

Dimensional tolerances and material densities used in the shielding evaluations are given in Section 5.3.1 and Section 5.3.2, respectively.

During normal conditions of transport, shielding evaluations assume that the RT-100 is transported on a truck trailer that is 2438.4 mm wide and 12801.6 mm long with the cask tied down in the center. Thus, the 2 meter radial surface is 3219.2 mm from the cask centerline and the distance to the cab, taking into account the trailer hookup and the distance to back of cab, is 8915.4 mm from the cask centerline. This is a conservative assumption since the actual occupied position is at least 1828.8 mm forward from the back of the cab. A visual representation of the dose locations is provided in Figure 5.4.4-4.

5.1.2 Summary Table of Maximum Radiation Levels

The transport regulations provide dose limits in 10 CFR 71.47 and 71.51 at locations external to the package for rates for both Normal Conditions of Transport (NCT) and Hypothetical Accident Conditions (HAC). A full discussion of the methods employed to analyze the RT-100 cask design and results of applying these methods that demonstrate compliance with the regulatory limits are presented in the sections that follow. Table 5.1.2-1 shown below summarizes the calculated results for the maximum radiation levels allowed for exclusive use shipment using an open (flat-bed) transport vehicle under NCT and HAC for the worst-case loading of radionuclides. These results represent the maximum dose rates for the worst-case allowable contents as presented in Section 5.4.4.

Table 5.1.2-1 Summary Table of External Radiation Levels (Exclusive Use)

Normal Conditions of Transport (NCT)	Package Surface ¹ mSv/hr (mrem/hr)			2 Meter from Edge of Vehicle mSv/hr (mrem/hr)	Vehicle Occupied Position mSv/hr (mrem/hr)
Radiation ²	Side	Bottom	Top	Side	Cab
Gamma	1.13 (113.2)	0.47 (47.2)	0.87 (86.7)	0.095 (9.5)	0.01 (1.3)
10 CFR 71.47 (b) Limit	2.0 (200.0)	2.0 (200.0)	2.0 (200.0)	0.1 (10.0)	0.02 (2.0)

Hypothetical Accident Conditions (HAC)	1 Meter from Package Surface ¹ mSv/hr (mrem/hr)		
Radiation ²	Side	Bottom	Top
Gamma	9.5 (950)	1.16 (115.9)	2.36 (235.7)
10 CFR 71.51 (a)(2) Limit	10 (1000)	10 (1000)	10 (1000)

Note 1: The gamma dose rates are each calculated for a contents limit corresponding to a limiting regulatory dose rate. These values are the maximum of all the radionuclides that were evaluated in Section 5.4.4.5.

Note 2: Typical contents will not contain a significant neutron source term.

5.2 Source Specification

The RT-100 is designed to transport nuclear plant radioactive resins and filters. This content is described in Chapter 1, Section 1.2.2. The radionuclides in these resins and filters produce primarily gamma emissions and trace neutron emissions from actinide spontaneous fission and alpha-n reactions in the media.

The shielding evaluation for the RT-100 calculates a dose rate response that is normalized to one Curie (mrem/hr/Ci) for each radionuclide with a half-life greater than 1 day. Thus, the gamma dose rate responses are specified on a per Curie basis. The total dose rate will be based on the loaded activity, in Curies, of the resin or filter media. In general, the gamma source terms decrease over time.

5.2.1 Gamma Source

Gamma spectra, i.e. the photon lines, are explicitly evaluated in the RT-100 shielding evaluation for radionuclides with greater than 1 day half-life. The radionuclide gamma spectra and intensities are taken from the SCALE 6.0 ORIGEN-S data libraries: *origen.rev02.mpdkgam.dat* [Ref. 4]. This data file was reformatted into an excel file for use in the generic energy dependent response approach to compute radionuclide dose rates from a one Curie source for each radionuclide.

The ORIGEN-S radionuclide data library *origen.rev04.endfdec.data* [Ref. 5] was read to determine all radionuclides with greater than 1 day half-life for use in the generic approach to compute radionuclide specific gamma dose rates. The list of 281 radionuclides with greater than

1 day half-life is given in Table 5.5.1-1. The selection details and associated spectra data file are provided in the “ORIGEN-S: Data Libraries” [Ref. 4]. Due to the magnitude of the data, all gamma source terms cannot be provided in the SAR, but the gamma spectra for 1 Curie Co-60 is shown in Table 5.2.1-1. Co-60 is the dominant gamma emitter and dose rate contributor from resins and filter media.

Table 5.2.1-1 One Curie Co-60 Gamma Source Term

Photon Energy ¹ (MeV)	Intensity Photon/dis	1 Curie	
		Photon/s	MeV/s
1.17E+00	1.00E+00	3.70E+10	4.34E+10
1.33E+00	1.00E+00	3.70E+10	4.93E+10
	Total	7.40E+10	9.27E+10

Note 1: Only the prominent photon lines are considered for Co-60 in the individual analysis.

Beta Emitter/ Bremsstrahlung source

Another source of gamma radiation is from radionuclide beta emission Bremsstrahlung (braking radiation). Contributions from Bremsstrahlung gamma radiation have been evaluated by explicit mode e-p (electron-photon) transport calculation. The following radionuclides with beta $E_{\max} > 2$ MeV were evaluated, as well as Cs-137, due to its typical high activity in resins and filters:

Y-90	$E_{\max} = 2.281$ MeV
Sb-124	$E_{\max} = 2.302$ MeV
Cs-137	$E_{\max} = 1.175$ MeV
La-140	$E_{\max} = 2.165$ MeV
Ce-144	$E_{\max} = 2.996$ MeV

Binned radionuclide beta source spectra are compiled in Calculation Package RTL-001-CALC-SH-0101, Rev. 1 [Ref. 6]. As discussed in Section 5.4.4.3, an assessment of the contribution to exterior dose rates from Bremsstrahlung due to these fission product beta emitting radionuclides is evaluated for the RT-100 NCT configuration and found to contribute less than 1.0 percent of the total dose due to gamma radiation. Therefore, gamma radiation from Bremsstrahlung is not included in the determination of maximum allowed source strength densities.

5.2.2 Neutron Source

The RT-100 cask is not designed for shielding neutrons, thus neutron emitters in the contents are limited to trace amounts that may be present in the activated resin and filter media. For this packaging, any neutron source is limited to 3.5E-06 Ci/g, based on Class C burial limits.

5.3 Shielding Model

MCNP6 [Ref. 3] is used to perform the shielding evaluation of the RT-100. Two sets of MCNP6 shielding models are created for the evaluations of the RT-100 for NCT and HAC. In both cases, the model geometry was developed from the drawings provided in Appendix 1.4. For evaluation purposes, the thicknesses of shielding materials that comprise the package (steel shells, lead shielding, and lids) are reduced by subtracting the manufacturing tolerance from the nominal dimensions. Using minimum thicknesses of shielding materials in the model bounds any effect that a variation in thickness due to fabrication tolerances may have on external dose rates. A summary of the nominal and minimum shield thicknesses is given in Table 5.3-1. For the NCT

Proprietary Information Content Withheld Under 10 CFR 2.390(b)

rate responses. The shielding from the high integrity container (HIC) used to store and transfer resin into the RT-100 cavity is neglected in the shielding evaluations. The effects of resin and filter density changes and redistribution of the content media due to NCT and HAC are modeled by decreasing the volume occupied by the source term.

Table 5.3-1 Model Shielding Thicknesses

Component	Nominal (mm)	Model (mm)
Interior Barrel	30	29.7
Lead	90	85
Exterior Barrel	35	34.7
Bottom Forging	50	49.7
Bottom Lead	75	70
Bottom Wall	30	29.7
Primary Lid	210	209.5
Secondary Lid	170	169.5
Secondary Lid Lead	60	58

5.3.1 Configuration of Source and Shielding

The RT-100 is designed to transport resins and filters that are contaminated with radioactive material. Due to the physical form of these contents, the resins and filters are packaged within a secondary container placed in the cask cavity. Except for close fitting contents, the secondary container is positioned within the cavity using shoring. Additional details regarding physical form of the contents, including the secondary container and shoring, are provided in Chapter 1, Section 1.2.2.3. The volume of the radioactive source term within the RT-100, as modeled in the analyses that follow, does not take credit for the reduction in available volume associated with a secondary container or any shoring. As described below, the source term is assumed to uniformly fill the

entire cavity (i.e., fill-volume) and no credit is taken for radiation attenuation provided by a secondary container or shoring materials.

5.3.1.1 Source Term

The NCT and HAC shielding models consider the photon source uniformly distributed throughout the geometry cell representing the resin/filter media. With this approach the source strength density limit is based on the maximum specific activity evenly distributed throughout the entire cask cavity. In the actual operation of the cask, the contents will not be homogeneously distributed. However, the contents of a liner are characterized by the shipper prior to cask loading. The maximum specific activity determined in the characterization for a given nuclide is used in the loading table, and thus is considered as the source strength density throughout the entire contents. This ensures that while the source distribution will be inhomogeneous, the source strength density used in the loading tables to show compliance with regulatory limits will be bounding of the contents for that shipment.

5.3.1.2 NCT Model

For the shielding analysis, there is one NCT shielding model. In the NCT model, for the dose rate response calculation for all generic energies, the resin material filling the RT-100 cavity is considered as void, neglecting all photon attenuation in the resin and filter media of the contents. For the dose rate response calculation for the eight radionuclides that are considered individually, the RT-100 cask cavity is filled with carbon at 1 g/cm³. This case takes credit for some photon attenuation in the resin material, but with the most restrictive condition. It is established in CN-13039-502 [Ref. 8] that Carbon at 1 g/cm³, produces the most restrictive Ci/g limits for all radionuclides (also discussed in Section 5.3.2). The NCT models are shown in Figure 5.3.1-1.

The tally surfaces for dose rate response estimation in accordance with 10 CFR 71.47(b) [Ref. 2], are shown in Figure 5.3.1-2, where the 2 meter surface is the vertical plane projected from the outer side edge of an open (flat-bed) transport vehicle. The radial tally surfaces are segmented into 10 cm increments by planes perpendicular to the z axis. The maximum segment dose rate response is determined by post processing the MCNP6 output files.

5.3.1.3 HAC Model

The HAC configuration assumes the following damage from the 9 meter drop, 1 meter puncture drop, and fire:

1. Loss of impact limiters
2. One inch puncture depth in the lead
3. Lead slump

For the shielding analysis, two HAC shielding models are developed. Both HAC models include an annular void at the top from the postulated end drop and a 1 inch x 6 inch diameter indentation from the postulated pin puncture. The annular void is a 5 mm lead slump at the top of the lead column. This value is based on the lead slump calculation provided in Section 2.7.1.1.2. The two different HAC models differ in how the resin and filter material and source are modeled inside the cavity of each. As is the case with the NCT model, for the first HAC model, used for the dose rate response calculation for all generic energies, the RT-100 cavity is considered full, with the resin material considered as void for the generic energy dose calculations and as carbon at 1 g/cm³ for the individual radionuclides considered. This first HAC model is only used for the bottom 1 meter dose rate response calculations. For the second HAC model, used for the side and top 1 meter dose rate calculations, the resin material is compacted to the top of the RT-100 cavity providing a more restrictive source geometry for these cases. Once again, the resin material in the RT-100 cavity is considered void for the generic energy line dose rate response calculations and as carbon at 1 g/cm³ for the individual nuclide calculations. The location of the pin puncture is moved between the two models such that it remains at the axial midplane of the resin material. The HAC models are shown in Figure 5.3.1-3 and Figure 5.3.1-4.

The tally surfaces and for dose rate response estimation in accordance with 10 CFR 71.51(a)(2) [Ref. 2] are shown in Figure 5.3.1-5 and Figure 5.3.1-6, respectively. Note that the arrangement of tallies shown in these two figures is used for both HAC models. Figure 5.3.1-5 shows the general tally surfaces that are segmented with axial planes for the side and cylinders for the top and bottom tallies. A set spacing of 10 cm between axial planes and concentric cylinders is utilized in order to determine the maximum dose rate response as a function of elevation and radius, respectively. A comparison with 5 cm segmentation provided in Calculation Package RTL-001-CALC-SH-0201, Rev. 5 [Ref. 7] shows nearly identical results for the maximum dose rate response and location, particularly for the limiting NCT 2 meter dose rate response and the limiting HAC 1 meter response. Figure 5.3.1-5 shows a three-dimensional view of a RT-100 HAC model and the tally segments used to calculate the dose rate response 1 meter from the side surface at the lead slump and pin puncture locations. These tallies are formed by segmenting the 1 meter cylindrical tally surface. The lead slump segment is formed by two segmenting planes that are 1 cm apart, centered around the lead slump. The pin puncture segment is formed by a segmenting cylinder with a diameter equal to the pin puncture (6 inches) at the axial location of the puncture.

Proprietary Information Content Withheld Under 10 CFR 2.390(b)

Proprietary Information Content Withheld Under 10 CFR 2.390(b)

Proprietary Information Content Withheld Under 10 CFR 2.390(b)

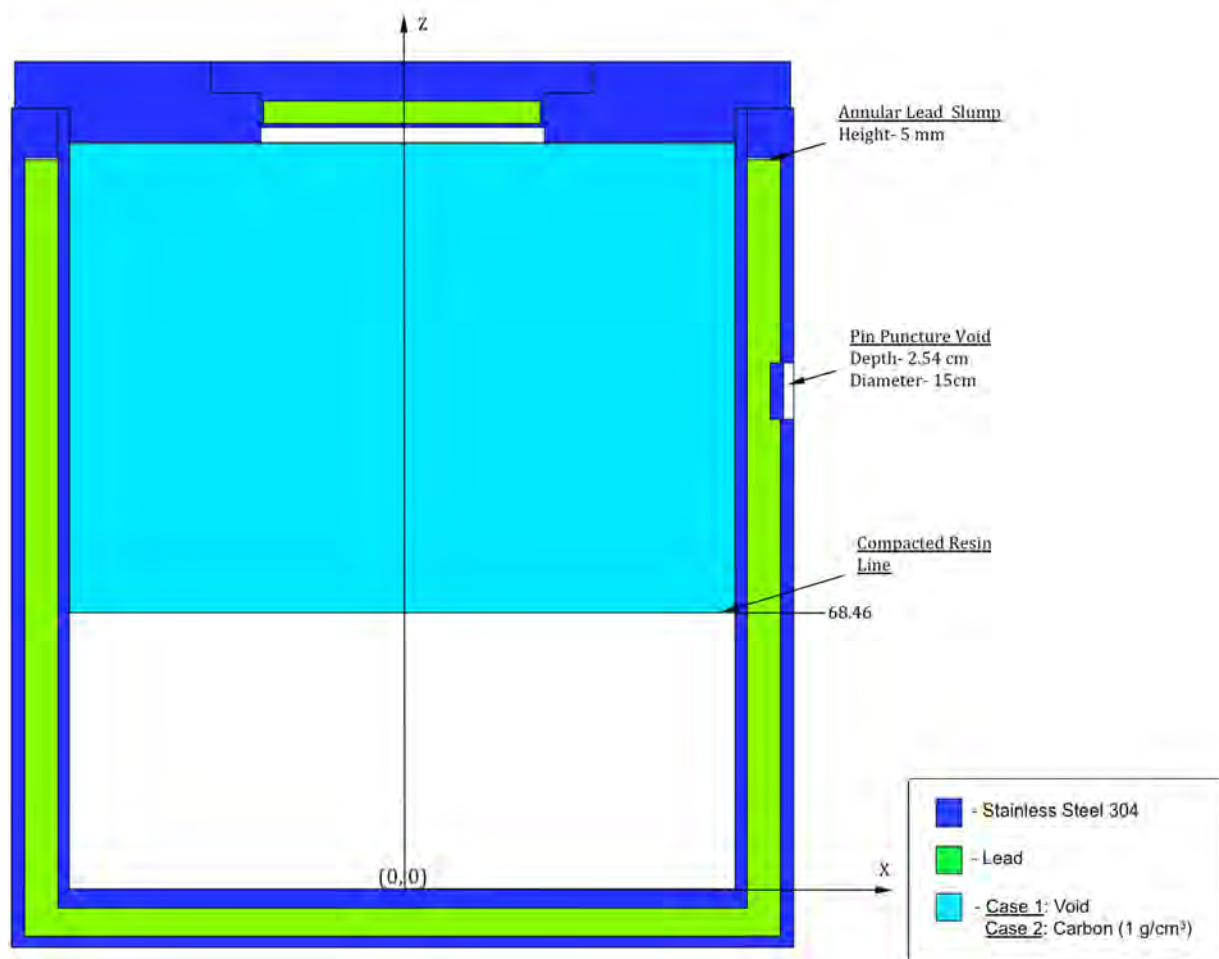


Figure 5.3.1-4 HAC Model 2

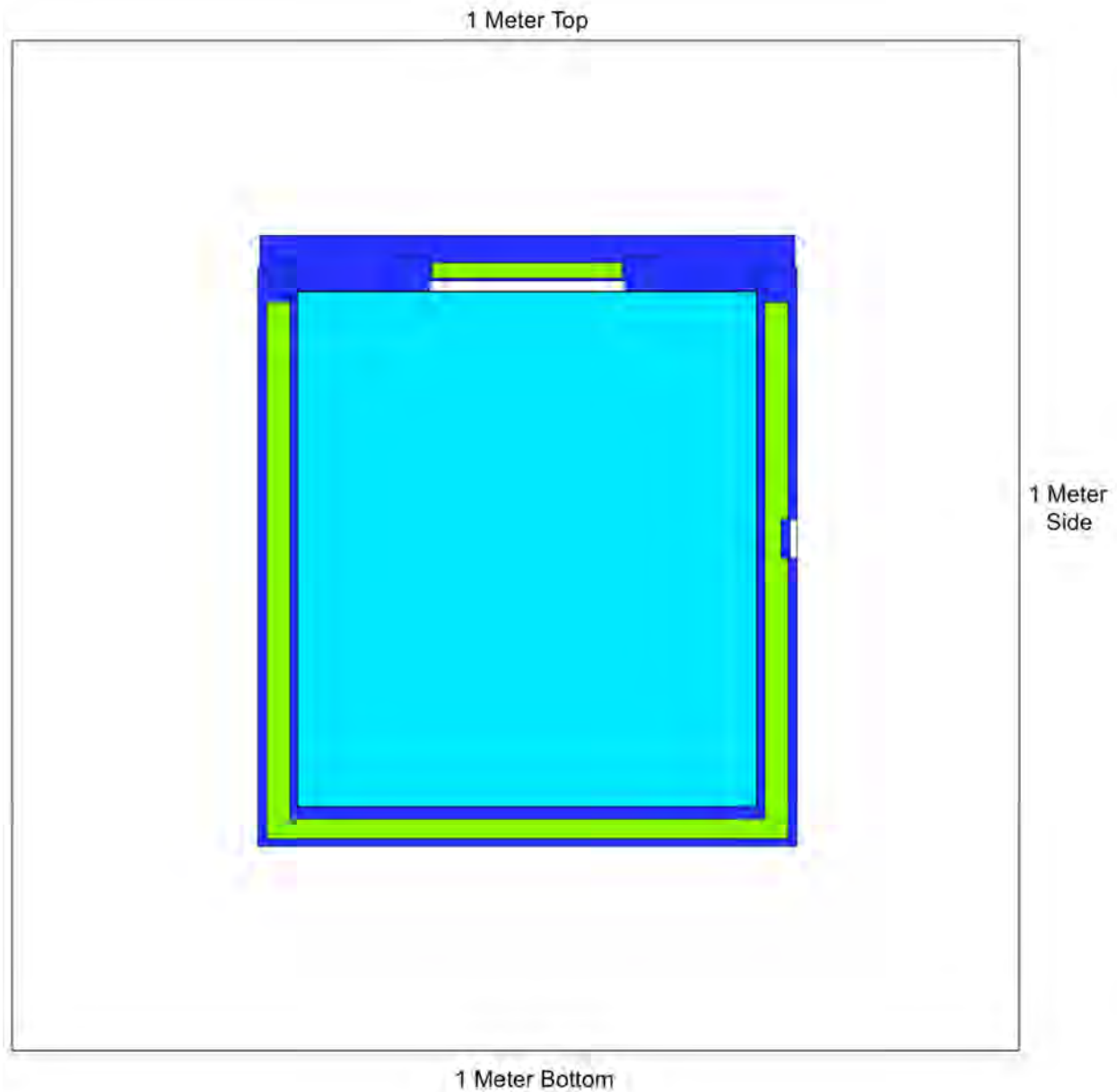


Figure 5.3.1-5 HAC Model General Tally Surfaces

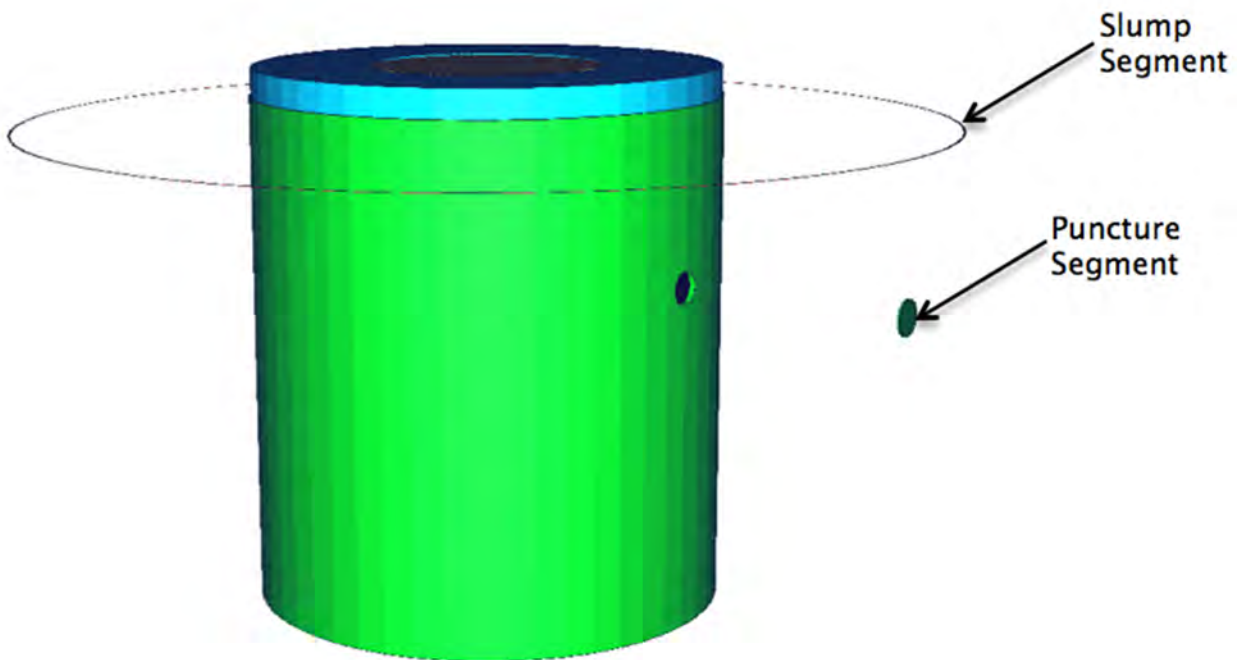


Figure 5.3.1-6 HAC Model Surface Tally

5.3.2 Material Properties

Materials used for the fabrication of the RT-100 are stainless steel and lead in the body, and for the fabrication of the impact limiters the materials used are polyurethane and stainless steel. The material properties used in the shielding evaluations are shown in Table 5.3.2-1. No changes in material properties are expected under Normal Conditions of Transport or Hypothetical Accident Conditions. Melting of the lead will not occur based on the thermal evaluation in Chapter 3. Also, the shielding properties of these materials will not degrade during the service life of the RT-100.

Contents transported in the RT-100 are resins and filter media. The following four materials, typical of resins and filter media, are considered as the cask contents:

- Polystyrene based resins such as Duralite
- Activated Charcoal
- Nylon filter media
- Zeolite - hydrated aluminosilicates such as Faujasite

In the case of nylon filter media, any steel cartridge structure is neglected and the cavity is assumed to be completely filled with nylon material at a reduced density. It is established in CN-13039-502 [Ref. 8] that carbon (activated charcoal) is the least effective shielding material between the four materials considered, and thus calculates the most restrictive specific activity (Ci/g) limits for all radionuclides, so in the shielding analysis the contents are modeled as carbon for both NCT and HAC.

The densities for resin and filter materials can vary quite a lot depending on the size of the particles, configuration of the filter media (i.e. tubes or fiber sheets) and the theoretical density of the material. The theoretical densities of polystyrene, carbon, Faujasite and nylon are 1.04, 2.2, 1.93 and 1.08 g/cm³, respectively, but resin media bulk densities for all the typical material compositions can vary from 0.3 to 1.0 g/cm³. It is established in CN-13039-502 [Ref. 8] that a contents density of 1 g/cm³ calculates the most restrictive specific activity (Ci/g) limits for all radionuclides, so the shielding analysis uses this density for the modeled contents media for both NCT and HAC.

For all bottom dose rate response calculations, a 10% compaction of the resin is considered, and the results from the shielding analysis are adjusted to consider this variation, though the bottom dose rate locations are never the limiting case.

Table 5.3.2-1 RT-100 Material Composition Summary

Material	Density (g/cm³)	Element	Nuclide ID	Weight Fraction
Stainless Steel 304 [Ref. 9]	7.94	Fe	26000	0.68375
		Ni	28000	0.09500
		Cr	24000	0.19000
		Mn	25055	0.02000
		Si	14000	0.01000
		C	6000	0.00080
		P	15000	0.00045
Lead [Ref. 9]	11.35	Pb	82000	1.0000

Proprietary Information Content Withheld Under 10 CFR 2.390(b)

Polystyrene [Ref. 10]	0.3 – 1.0	H	1001	0.0774
		C	6000	0.9226
Activated Carbon [Ref. 9]	0.3 – 1.0	C	6000	1.0000
Nylon [Ref. 10]	0.3 – 1.0	H	1001	0.0980
		C	6000	0.6369
		N	7014	0.1238
		O	8016	0.1414
Zeolite (Faujasite-Na) [Ref. 11]	0.3 – 1.0	O	8016	0.6067
		Si	14000	0.2263
		Al	13027	0.0895
		H	1001	0.0306
		Na	11023	0.0229
		Ca	20000	0.0199
		Mg	12000	0.0040

Proprietary Information Content Withheld Under 10 CFR 2.390(b)

5.4 Shielding Evaluation

Section 5.4 describes the shielding evaluation for the RT-100 using industry accepted methods.

5.4.1 Methods

5.4.1.1 MCNP6 Analysis

MCNP6 [Ref. 3] is used to perform the shielding evaluation of the RT-100. The ENDF/B-VI Release 8 Photo-atomic Data gamma cross section library, and MCPLIB84 [Ref. 12], are utilized in the transport computations.

MCNP6 is a Monte Carlo transport code that offers a full three-dimensional combinatorial geometry modeling capability. This type of modeling means that no gross approximations are required to represent the RT-100 Cask in the shielding analysis. However as stated in Section 5.3, bounding shielding material thicknesses are used in the MCNP6 models. The mesh based weight windows approach was utilized as the primary variance reduction technique in the shielding evaluation of the RT 100 and is further described in Section 5.4.1.4.

5.4.1.2 Dose Rate Response Calculation

The dose rate response calculations between the Generic Energy Line Method and those for the individual nuclides of interest differ slightly as described below.

Generic Energy Line Calculation

For the generic energy line outputs, the dose rate responses reported by each tally are binned by the emission energies, so a dose rate response is reported for each generic energy line separately. The MCNP6 calculated dose rate response (R) is calculated for the gamma flux at a distance (r) originating as source particles at a generic energy (E_s). Interactions in the contents and packaging media result in particles at a continuous spectrum of energies (E_i). The dose rate response from the flux $\Phi(r, E_i)$ of particles is binned using MCNP6 special tally treatment, which bins the response based on the source energy (E_s). The dose rate response (R) is obtained by multiplying the tally flux for each energy (E_i) in the segment by the source emission rate (S), a flux-to-dose conversion factor for each energy $\mathcal{R}(E_i)$ and a source term normalization constant (N). The response function is defined by the flux-to-dose conversion factors provided in ANSI 6.1.1-1977 [Ref. 13], and the source emission rate (S) equivalent to 1 Curie ($3.7E+10$ disintegrations/second), such that the modified tally normalized per 1 Curie, and the source term normalization constant (N) is equal to the number of energy lines in the MCNP6 source term in the respective input,

$$\begin{aligned}
 R(r, E_s) & \left[\frac{\frac{mrem}{hr}}{Ci} \cdot \frac{disintegration}{emitted\ photons} \right] \\
 &= \sum_i \Phi(r, E_i) \left[\frac{\frac{photons}{cm^2}}{emitted\ photon} \right] \cdot S \left[\frac{\frac{disintegration}{sec}}{Ci} \right] \cdot \mathcal{R}(E_i) \left[\frac{\frac{mrem}{hr}}{\frac{photons}{cm^2 \cdot sec}} \right] \cdot N
 \end{aligned}$$

For gamma emitting radionuclides, the dose rate responses (mrem/hr/Ci) are computed for each tally segment or detector at the following 26 discrete emission energies (E_s) in a range from 0.5 MeV to 8.0 MeV that are grouped into MCNP6 files as follows:

Low Energies (N=2)

0.5, 0.6

Middle Energies (N=4)

0.7, 0.8, 0.9, 1.0

High Energies (N=18)

1.1, 1.2, 1.3, 1.4, 1.5, 1.6, 1.7, 1.8, 1.9, 2.0, 2.5, 3.0, 3.5, 4.0, 4.5, 5.0, 5.5, 6.0

Additional Energy Lines (N=2)

7.0, 8.0

The energy lines for any given radionuclide that are above 0.1 MeV are rounded up to the next generic energy line and summed to create a grouped spectrum for each radionuclide, where photon emission energies are binned by the generic energy lines. All energy lines below 0.1 MeV are considered insignificant and are neglected. An example of the energy grouping is shown for Fe-59 in Figure 5.4.1-1, as the 12 radionuclide specific energy lines are grouped into 4 generic energy bins (0.5, 1.1, 1.3, and 1.5 MeV).

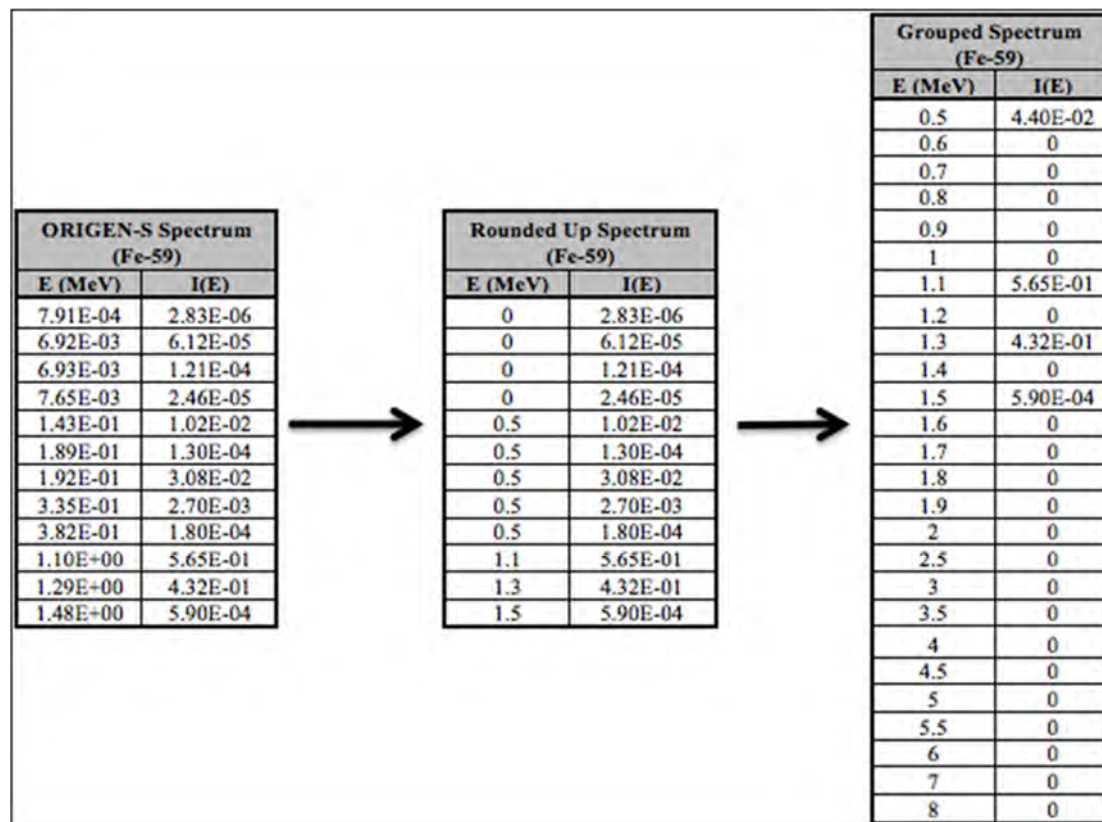


Figure 5.4.1-1 Fe-59 Spectrum Grouped into Generic Energy Lines

The photon emission intensities $I_X(E_s)$ of the grouped energy spectrum for a given radionuclide X are used, along with the radionuclide branching ratio BR and the MCNP6 calculated responses, to calculate the contribution to the total dose rate from generic energy line Es for the respective nuclide ($D_X(r, E_s)$). Note that the only nuclides with dose rates calculated incorporating branching ratios are listed in Table 5.5.1-1, labeled with a 'br' in the 'Branch' column of the table. For nuclides with dose rates calculated using the Generic Energy Line this includes the long lived beta emitters Mo-99, Sr-90, and Ru-106 that have the short lived gamma emitting daughters Tc-99m (BR=0.88), Y-90 (BR=1.0), and Rh-106 (BR=1.0), respectively.

$$D_X(r, E_s) \left[\frac{mrem}{hr} \right] = BR_X \cdot I_X(E_s) \left[\frac{\text{emitted photons}}{\text{disintegration}} \right] \cdot R(r, E_s) \left[\frac{mrem}{Ci} \cdot \frac{\text{disintegration}}{\text{emitted photons}} \right]$$

The uncertainty from the MCNP6 calculated response $\sigma_R(r, E)$ translates to an uncertainty in the dose rate contribution from the generic energy line $\sigma_{D_X}(r, E)$ as:

$$\sigma_{D_X}(r, E_s)^2 = (BR_X \cdot I_X(E_s))^2 \cdot \sigma_R(r, E_s)^2$$

The total dose rate, in mrem/hr/Ci, from nuclide X at regulatory dose rate location r can then be calculated by summing the contributions (plus 2 sigma) from each of the 26 generic energies:

$$D_X(r) \left[\frac{\text{mrem}}{\text{hr}} \right] \frac{1}{\text{Ci}} = \sum_{s=1}^{26} D_X(r, E_s) + 2 \cdot \sqrt{\sum_{s=1}^{26} \sigma_{D_X}(r, E_s)^2}$$

Individual Radionuclides

For the 8 radionuclides that are calculated individually all nuclide specific energy lines above 0.1 MeV are included in the MCNP6 model source, so the calculated dose rate response at location r for radionuclide X is calculated as,

$$R_X(r) \left[\frac{\text{mrem}}{\text{hr}} \cdot \frac{\text{disintegration}}{\text{Ci}} \cdot \frac{1}{\text{emitted photons}} \right] = \sum_i \Phi(r) \left[\frac{\text{photons}}{\text{cm}^2} \cdot \frac{1}{\text{emitted photon}} \right] \cdot S \left[\frac{\text{disintegration}}{\text{Ci}} \right] \cdot \mathcal{R}(E_i) \left[\frac{\text{mrem}}{\text{h}} \cdot \frac{1}{\text{photons}} \cdot \frac{1}{\text{cm}^2 \cdot \text{sec}} \right]$$

With the dose rate from radionuclide X at dose rate location r determined, the total dose rate for the given nuclide is calculated by incorporating the MCNP6 calculated statistical uncertainty (plus 2 sigma), the total number of emitted photons per disintegration, and the branching ratio. Note that the only nuclide with dose rates calculated individually, that incorporates a branching ratio is the long lived beta emitters Cs-137 that has the short lived gamma emitting daughter Ba-137m (BR=0.95).

$$D_X(r) \left[\frac{\text{mrem}}{\text{hr}} \right] \frac{1}{\text{Ci}} = \left(R_X(r) + 2 \cdot \sigma_{R_X}(r) \right) \left[\frac{\text{mrem}}{\text{hr}} \cdot \frac{\text{disintegration}}{\text{Ci}} \cdot \frac{1}{\text{emitted photons}} \right] \cdot \sum_{s=1}^n I_X(E_s) \left[\frac{\text{emitted photons}}{\text{disintegration}} \right] \cdot BR_X$$

Beta Emitter Dose Rate Contribution

NCT beta/Bremsstrahlung dose rate responses are computed on a radionuclide basis for a set of limiting radionuclides as defined in RTL-001-CALC-SH-0101, Rev. 1 [Ref. 6]. Based on major beta emitting radionuclides ($E_{\text{max}} > 2\text{MeV}$) ORIGEN-S: Data Libraries [Ref. 4], shielding calculations provided in Calculation Package RTL-001-CALC-SH-0201 [Ref. 7] show negligible Bremsstrahlung contribution to exterior dose rate for the current resin/filter contents to be shipped in the RT-100.

5.4.1.3 Maximum allowed source strength density

The radionuclide-specific activity limit $A_X(r)$ is calculated as,

$$A_X(r)[Ci] = \frac{\dot{D}(r) \left[\frac{mrem}{hr} \right]}{D_X(r) \left[\frac{mrem/hr}{Ci} \right]}$$

Where, the regulatory dose rate limit for a given location $\dot{D}(r)$ that is specified in 10 CFR 71 is reduced by 5% to account for uncertainty representing the actual packaging and characterization of the contents.

More specifically, the regulatory NCT limit for the package surface is reduced from 200 mrem/hr to 190 mrem/hr, the limit at 2 meters from the transport vehicle is reduced from 10 mrem/hr to 9.5 mrem/hr, and the cab limit is reduced from 2 mrem/hr to 1.9 mrem/hr. Similarly, the HAC limit at 1 meter is reduced from 1000 mrem/hr to 950 mrem/hr.

For example, the activity limit of Co-60 for NCT as a function of the dose rate limit at 2 meters is calculated as,

$$A_{Co60}(2m) = \frac{9.5}{D_{Co60}(2m)}$$

The radionuclide-specific maximum allowable source strength density a_X is calculated by dividing the minimum activity limit from all regulatory dose rate locations of the given nuclide by the maximum resin and filter mass m allowed in the RT-100 packaging (at 1 g/cm³ $m=4597809.127$ g).

$$a_X \left[\frac{Ci}{g} \right] = \frac{A_X(r)_{min}[Ci]}{m[g]}$$

For example, because the minimum activity limit calculated for Co-60 is based on the 2 meter dose rate location, the maximum allowable source strength density is calculated as,

$$a_{Co60} = \frac{A_{Co60}(2m)}{4597809.127}$$

For a mixture of radionuclides, the source strength density for each radionuclide (Ci/g) is divided by the source strength density limit from the shielding evaluations, and the results summed for all radionuclides must be less than 100% to be acceptable for shipment. Further details of the

loading table construction are given in Section 7.6.1.

5.4.1.4 Variance Reduction

The primary variance reduction technique used is the mesh based weight windows approach. The cards used in the MCNP6 input file to implement the weight windows include: WWG and MESH for generating mesh based weight window files, and WWP for calling in the generated weight window mesh file. Pages 3-43 through 3-50 of the MCNP6 manual provide additional details on weight window card development [Ref. 3].

A cylindrical spatial mesh is superimposed over the geometry with the MESH card. This mesh defines a cylindrical grid of cells independent of the MCNP6 geometry that extends slightly beyond the boundaries of the model geometry. Multiple iterations are performed in order to generate an effective importance map. The term iteration in this case means that a run has been performed and a mesh importance map is generated and then the mesh importance map is used in a subsequent MCNP6 run on the same model. The importance map generated in the previous run is fed back into the model and run again with the intent of generating a new importance map with the old map improving the performance and results of the subsequent run. The weight windows estimated by the MCNP6 WWG card are subject to statistical fluctuations, thus some manual refining of the generated weight window mesh may be necessary.

Once a reasonable weight window mesh is obtained through this iterative process, production runs are executed with sufficient histories, such that the statistical errors for most tallies meet the 0.10 fractional standard deviation (fsd) criterion, and all statistical tests are passed for every tally in every MCNP6 output. Using an effective set of weight windows is the key to achieving statistical convergence for all tallies in a reasonable runtime.

5.4.2 Input and Output Data

All relevant inputs and outputs for the gamma shielding analysis are provided with calculation package CN-13039-502. Post processing of the energy dependent responses into detailed dose rate responses (mrem/hr/Ci) is performed for all radionuclides and is shown in Tables 5.5.2-1 and 5.5.2-2. Using these responses and the content activity loading, the total dose rate in mrem/hr can be computed for NCT and HAC conditions. This is demonstrated in Section 5.4.4.5 for the maximum source strength density of Co-60. A guide is provided in Appendix 5.5.4 that relates the process steps to the input and output files used for the shielding evaluation.

5.4.3 Flux-to-Dose Rate Conversion

MCNP6 [Ref. 3] calculates a photon flux (particles/s-cm²) at a particular tally or detector location given the source magnitude. These values are converted into dose by use of flux-to-dose response functions. This conversion is done internally in MCNP6 [Ref. 3] by

associating dose response functions to each tally in the input file. Gamma flux-to-dose response functions used in these calculations are listed in Table 5.4.3-1.

Table 5.4.3-1 ANSI/ANS 6.1.1-1977 – Gamma Flux-to-Dose Conversion Factors

Gamma Energy (MeV)	(rem/hr)/ (photon/cm ² -s)
0.01	3.96E-06
0.03	5.82E-07
0.05	2.90E-07
0.07	2.58E-07
0.10	2.83E-07
0.15	3.79E-07
0.20	5.01E-07
0.25	6.31E-07
0.30	7.59E-07
0.35	8.78E-07
0.40	9.85E-07
0.45	1.08E-06
0.50	1.17E-06
0.55	1.27E-06
0.60	1.36E-06
0.65	1.44E-06
0.70	1.52E-06
0.80	1.68E-06
1.00	1.98E-06
1.40	2.51E-06
1.80	2.99E-06
2.20	3.42E-06
2.60	3.82E-06
2.80	4.01E-06
3.25	4.41E-06
3.75	4.83E-06
4.25	5.23E-06
4.75	5.60E-06
5.00	5.80E-06
5.25	6.01E-06
5.75	6.37E-06
6.25	6.74E-06
6.75	7.11E-06
7.50	7.66E-06
9.00	8.77E-06
11.0	1.03E-05
13.0	1.18E-05
15.0	1.33E-05

5.4.4 External Radiation Levels

The maximum external radiation levels are determined by the quantity of each radionuclide in the resin and filter media that is to be shipped. This limiting quantity of each radionuclide is determined by the respective source strength density limit of each. For the radionuclides considered, the source strength density is always limited by either the NCT 2 meter or the HAC side 1 meter regulatory limits. Thus, the maximum dose rate that can be measured at any regulatory location can only be equal to the regulatory limit at the NCT 2 meter or the HAC side 1 meter locations. For example, for radionuclides whose source strength density is limited by the NCT 2 meter location, the maximum dose rate at 2 meters from the edge of the vehicle is 9.5 mrem/hr and the dose rate at all other regulatory locations will be some amount less than the regulatory limit for that location because the source strength density is based on the NCT 2 meter location. Likewise, for radionuclides whose source strength density is limited by the HAC side 1 meter location, the maximum dose rate at 1 meter from the package surface is 950 mrem/hr and the dose rate at all other regulatory locations will be some amount less than the regulatory limit at that location.

Table 5.5.2-1 and Table 5.5.2-2 give the complete list of gamma radionuclide responses. Using these responses and the respective source strength density limits in Table 5.5.3-1, the total dose rate in mrem/hr at each regulatory location can be computed for any radionuclide as described in Section 5.4.4.5. The maximum dose rates under NCT and HAC from each radionuclide individually are shown in Table 5.4.4-5 and Table 5.4.4-6. Table 5.4.4-1 provides a summary of the maximum calculated dose rate at each regulatory location, and the radionuclide responsible for each maximum dose rate. Combining contributions from multiple radionuclides, as is done in the loading table, can only result in a dose rate at each regulatory location that is equal to or less than the maximum values reported below in Table 5.4.4-1.

Table 5.4.4-1 Maximum Dose Rates and Responsible Radionuclides

Normal Conditions of Transport	Package Surface (mrem/hr)			2 Meters from Edge of Vehicle (mrem/hr)	Vehicle Occupied Position (mrem/hr)	
	Source	Side	Bottom			Top
Gamma		113.2 Pm-144	47.2 Cs-144	86.7 Pm-144	9.50 MULTIPLE	1.21 MULTIPLE

Hypothetical Accident Conditions	1 Meter from Package Surface (mrem/hr)			
	Source	Side	Bottom	Top
Gamma	950.0 MULTIPLE	115.93 Mn-54	235.7 Mn-54	

5.4.4.1 MCNP6 Statistics Evaluation

5.4.4.1.1 Tally Statistics Diagnostics

MCNP6 produces information about a simulation to allow the user to assess the precision (not the accuracy) of the result. MCNP6 provides 10 statistical tests performed on the tally for assessing the reliability of results. If any of the 10 tests are not met, they are recorded as “NO”. MCNP6 automatically produces additional output to aid the user in interpreting the cause of the failed tests. The 10 tests are summarized as,

Tally Mean, \bar{x}

1. The mean must exhibit, for the last half of the problem, only random fluctuations as N increases. No up or down trends must be exhibited.

Relative Error, R

2. R must be less than 0.1 (0.05 for point/ring detectors).
3. R must decrease monotonically with N for the last half of the problem.
4. R must decrease as $1/\sqrt{N}$ for the last half of the problem.

Variance of the Variance, VOV:

5. The magnitude of the VOV must be less than 0.1 for all types of tallies.
6. VOV must decrease monotonically for the last half of the problem.
7. VOV must decrease as $1/N$ for the last half of the problem.

Figure of Merit, FOM:

8. FOM must remain statistically constant for the last half of the problem.
9. FOM must exhibit no monotonic up or down trends in the last half of the problem.

Tally PDF, $f(x)$

10. The SLOPE determined from the 201 largest scoring events must be greater than 3.

The MCNP Manual states that “A tally is considered to be converged with high confidence only when it passes all ten statistical checks” [Ref. 3]. Every tally in all MCNP6 outputs in the shielding analysis passes all 10 statistical tests, indicating that the reported results are reliable.

5.4.4.1.2 Fractional Standard Deviation of Individual Tally Segments

Of all tally bins included in the 72 MCNP outputs for the gamma shielding analysis, there are a total of 17 bins with reported fractional standard deviations larger than the MCNP6 requirement for reliable results ($fsd < 0.10$). These tally segment bins with a fractional standard deviation greater than 0.1 are far from the maximum segment, with a calculated dose rate that is orders of magnitude less than the value reported at the maximum segment. This is shown for Cs-137 in Figure 5.4.1-1, where it can be noted that the tally segments that don’t meet the fsd requirement are on the bottom impact limiter, with reported dose rates that are multiple orders of magnitude less than the segments at the axial location of the streaming peak. All maximum dose rate segments have an fsd of 0.05 or less, most being significantly lower.

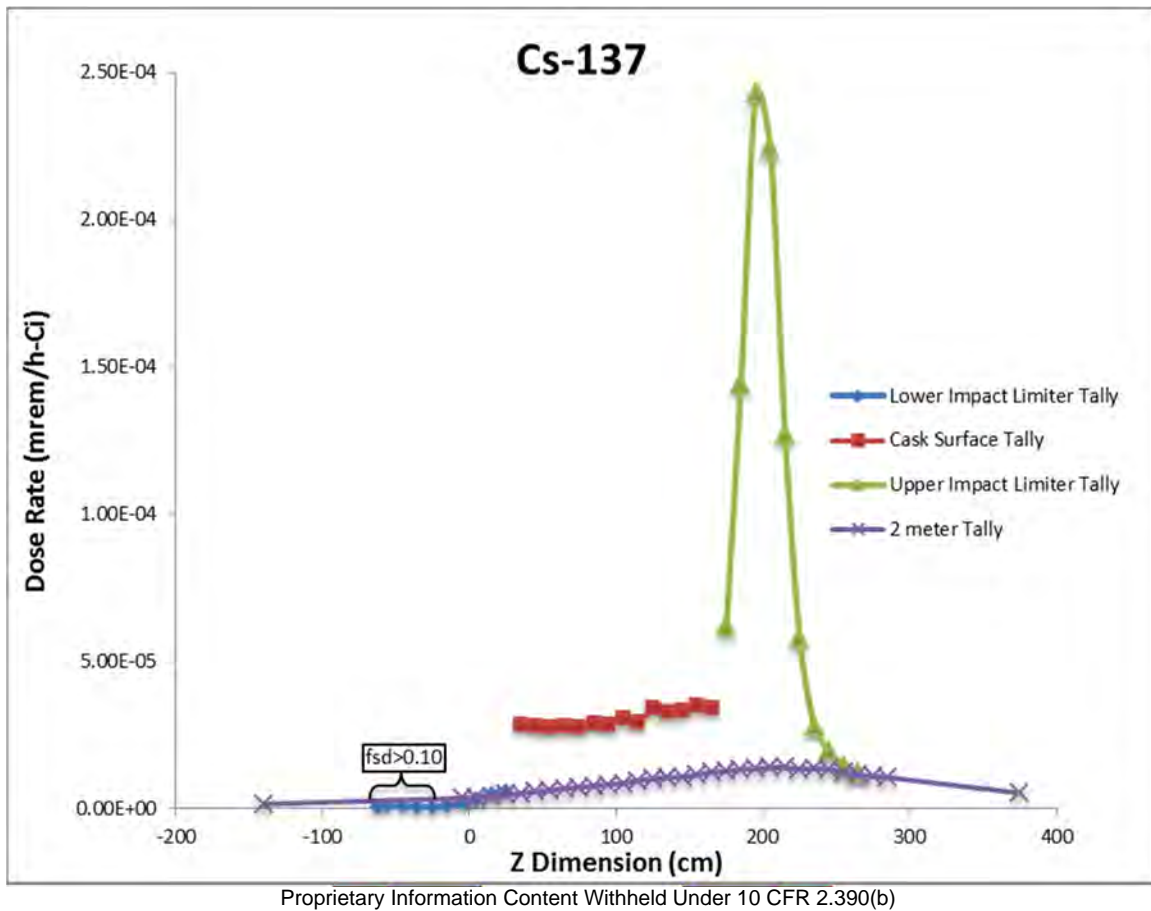


Figure 5.4.4-1 Fluctuation in Radial Dose Rates (Cs-137)

5.4.4.2 Media Composition and Density

The effect of the media composition is addressed in calculation RTL-001-CALC-SH-0201 Section 7.7.2 “*Content Density and Material Variation*” [Ref. 7]. The MCNP calculations for the final dose rate response functions of the 8 radionuclides considered individually are performed using carbon at a density of 1.00 g/cm³ as the material composition and density. Parametric studies were performed to evaluate the effect of other media compositions (polystyrene, nylon, and zeolite) and media densities in the range from 0.65 to 1.0 g/cm³ on the dose rate response. The maximum allowable source strength density (Ci/g) decreases slightly with increasing material density and carbon material composition results in the most limiting source strength density. The final dose rate responses used to calculate the maximum source strength densities are calculated modeling the resin media as carbon at 1 g/cm³, instead of adjusting the calculated dose rate responses for polystyrene at 0.65 g/cm³ using correction factors as originally discussed in Section 7.7.2 of the calculation RTL-001-CALC-SH-0201 [Ref. 7].

5.4.4.2.1 Effect of Media Composition

The effect of media composition was evaluated by calculating the dose rate response for the generic energies using the typical resin and filter material compositions at a fixed material density, 0.65 g/cc. The ratio $\mathfrak{R}_X(r, \chi)$ between the dose rate calculated for each media composition χ and the base case (polystyrene) is determined for each radionuclide X at each regulatory dose rate limit location r . A comparison of the average of the calculated ratios is presented in Table 5.4.4-2, where it is shown that modeling activated carbon as the attenuating media results in the highest calculated dose rates.

$$\mathfrak{R}_X(r, \chi) = \frac{D_X(r, \chi) \left[\frac{\text{mrem/hr}}{\text{Ci}} \right]}{D_X(r, \chi = \text{Polystyrene}) \left[\frac{\text{mrem/hr}}{\text{Ci}} \right]}$$

$$\mathfrak{R}(\chi) = \text{avg}\{\mathfrak{R}_X(r, \chi)\}$$

Table 5.4.4-2 Media Composition Comparison

χ	$\mathfrak{R}(\chi)$		
	Side	Bottom	Top
Polystyrene	1.00	1.00	1.00
Activated Carbon	1.07	1.10	1.09
Nylon	0.98	1.02	1.05
Zeolite [10]	1.04	1.03	1.06

5.4.4.2.2 Effect of Media Density

The effect of media density was evaluated by calculating the specific activity limit a_X for the generic energies using the material compositions for a range of material densities for one material composition, polystyrene. The ratio $\mathfrak{R}_X(r, \rho)$ between the specific activity limit calculated for each density ρ and the base case (0.65 g/cm³) is determined for each radionuclide X at each regulatory dose rate limit location r . A comparison of the maximum calculated ratios is presented in Table 5.4.4-3, where it shown that modeling the content media at 1 g/cm³ results in the most restrictive calculated specific activity limits.

$$\mathfrak{R}_X(r, \rho) = \frac{a_X(r, \rho) [Ci/g]}{a_X(r, \rho = 1.00) [Ci/g]}$$

$$\mathfrak{R}(\rho) = \max\{\mathfrak{R}_X(r, \rho)\}$$

Table 5.4.4-3 Media Density Comparison

ρ [g/cm ³]	$\mathfrak{R}(\rho)$
0.65	1.053
0.75	1.041
0.85	1.035
1.00	1.000

5.4.4.3 Shielding Evaluation Uncertainty

Accurate results from the shielding analysis of transport casks are important to ensure that loading limits yield doses that do not exceed the regulatory limits for external radiation levels. Content loading limits (i.e. specific source strength densities) for the RT-100 are determined using regulatory dose rate limits. These regulatory limits are reduced by 5 percent to account for any uncertainty in representing the packaging and the characterization of the contents. The uncertainties and margins are summarized in Figure 5.4.4-2.

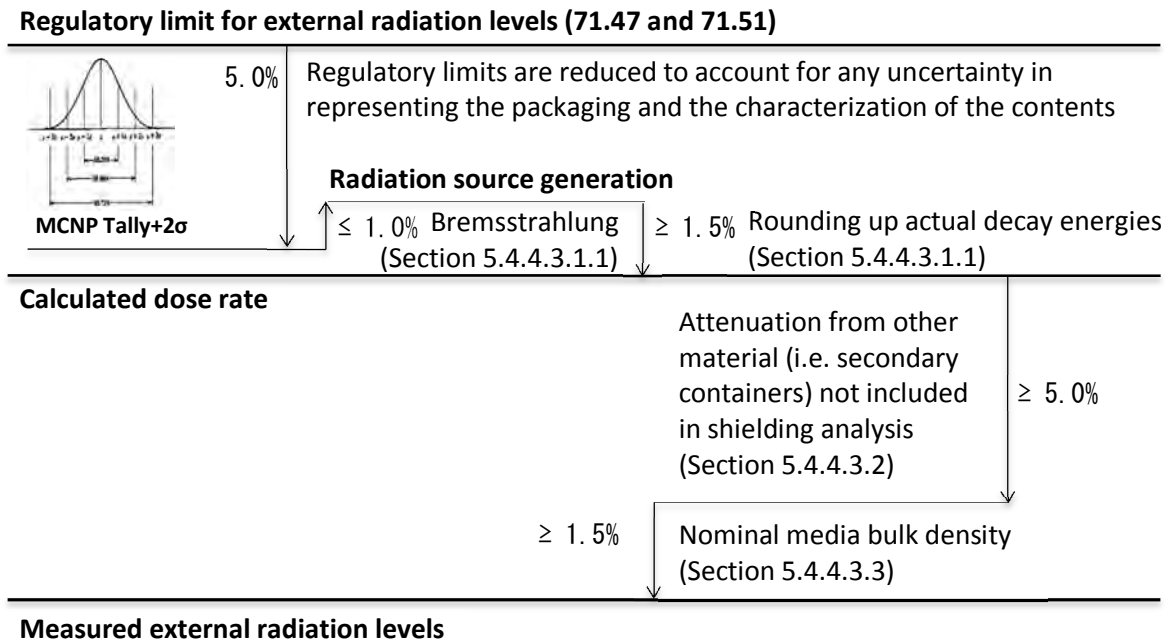


Figure 5.4.4-2 Summary of Calculated Dose Rate Margins

5.4.4.3.1 Calculation of Dose Rates

Uncertainty in calculated dose rates arises from three major analysis areas: radiation source generation, use of cross-section data, and the radiation transport codes used to evaluate doses.

5.4.4.3.1.1 Radiation Source Generation

Generation of the source specification is discussed in detail in Section 5.2.

Bremsstrahlung

The dose rate from Bremsstrahlung is not included, as this source term accounts for less than 1% of the regulatory dose rate limit, and there is no significant uncertainty associated with the radiation source definition for gammas.

An evaluation of the contribution of Beta/Bremsstrahlung radiation to external dose rates was performed in the calculation report RTL-001-CALC-SH-0201. The NCT results for this analysis

are presented for Y-90, Sb-124, Cs-137, La-140 and Ce-144 in Table 5.4.4-4. Based on this assessment, the contribution of Beta/Bremsstrahlung to exterior doses on the RT-100 can be neglected as long as the beta activity is well below 60,000 Curies (the Curie content of Ce-144 that would produce 1% of the chosen dose rate limit for two meters, or 0.095 mrem/hr). The 3000 A₂ limit precludes the shipment of sufficient Curies of the beta/bremsstrahlung emitting isotopes to exceed the 1% of the total dose rate limit at two meters, and the bremsstrahlung gamma response functions are therefore omitted from the loading tables.

Table 5.4.4-4 NCT Dose Rate Responses Due to Bremsstrahlung

Maximum Response + 2σ (mrem/hr/Ci) for Side Dose Locations					
Radionuclide	Top Surface	Side Surface	Bottom Surface	2 Meter	Cab
Y-90	2.80E-06	6.00E-06	3.78E-06	6.60E-07	1.88E-07
SB-124	2.00E-06	1.43E-06	4.49E-07	1.59E-07	4.38E-08
CS-137	0.00E+00	3.37E-11	0.00E+00	1.45E-11	5.89E-12
LA-140	6.13E-08	4.46E-07	3.94E-07	3.88E-08	1.25E-08
CE-144	4.76E-06	1.23E-05	1.80E-05	1.95E-06	5.49E-07
CE-144-void	1.16E-04	2.75E-04	2.43E-04	3.64E-05	1.04E-05
CE-144-4	1.16E-05	2.37E-05	1.25E-05	3.12E-06	8.18E-07

Rounding up actual decay energies

The use of a generic energy spectrum method as described in Section 5.4.1 overestimates the dose rate from specific radionuclides. Rounding up the gamma energies of the specific radionuclides to the nearest generic energy line may result in a 1.5% to 40% increase in dose rates depending on the radionuclide.

5.4.4.3.1.2 Cross Section Data

The use of continuous pointwise energy cross section data libraries in MCNP6 eliminates any uncertainty due to the choice of energy-collapsing spectrum and parent fine-group data.

5.4.4.3.1.3 Radiation Transport Codes

The use of MCNP6 to calculate the dose rate responses is discussed in detail in Section 5.4.1.2. The mean tally value plus two standard deviations as calculated by MCNP6 is used to calculate the limiting dose rate responses. Adding two standard deviations to the calculated average value means that there is at least a 95% confidence that the calculated dose rate response will be less than the limiting dose rate response.

5.4.4.3.2 Attenuation from other material (i.e. secondary containers) not included in shielding analysis

The secondary container is fabricated using approximately 1.27 cm thickness polyethylene. The half-value layer (HVL) for polyethylene for 1 MeV for gammas is approximately 15 cm. The

secondary container provides a reduction in external dose levels of approximately 6%.

5.4.4.3 Nominal Media Bulk Density

The bulk density of dewatered resins is typically less than 1 g/cm^3 . Compliance with the regulatory dose rate limits is demonstrated using the limiting source strength density values for a bulk density of 1 g/cm^3 . When the maximum allowed source strength density (i.e. the value at 1 g/cm^3) is used to estimate the expected dose rate for media densities less than 1 g/cm^3 , the calculated dose rate is greater than the estimated dose rate using the source strength density (Ci/g) for 1 g/cm^3 , and the actual media density (g/cm^3) and associated dose rate response (mrem/hr/Ci). An example of this conservatism is shown in Figure 5.4.4-3.

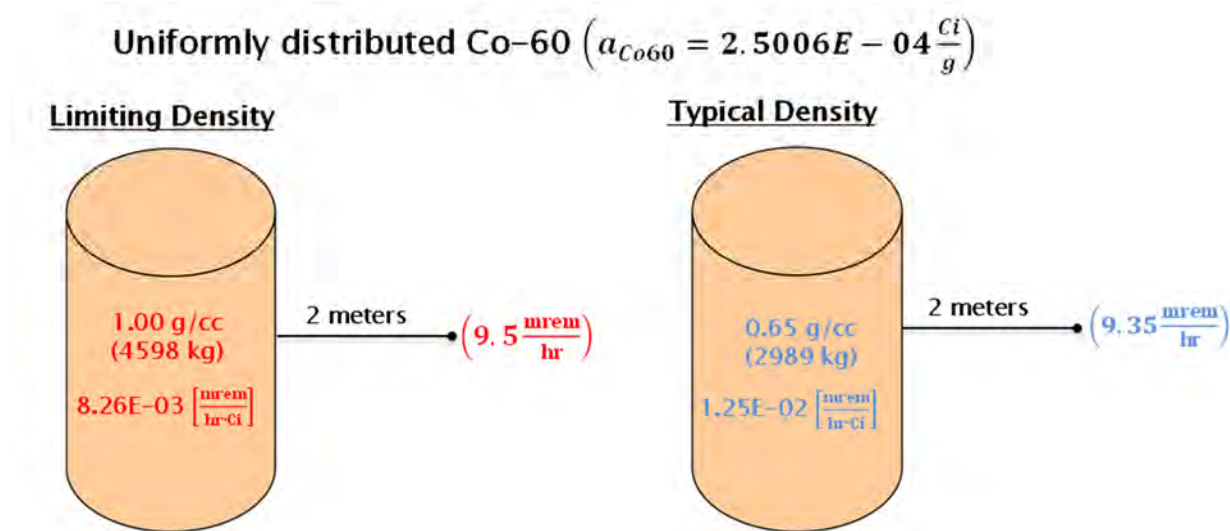


Figure 5.4.4-3 Example of Media Density Effect

5.4.4.4 Loading Table

Ultimately, a loading table specifying the maximum Curies per gram of each radionuclide is developed. The maximum Curies per gram are defined as the minimum specific activity at which the regulatory dose rate limit for either NCT or HAC is met. For conservatism 5% lower than the regulatory limits is assumed, thus the NCT limit at the package surface is taken as 190 mrem/hr, at 2 meters from the transport vehicle as 9.5 mrem/hr and the cab limit is taken as 1.9 mrem/hr. Similarly, the HAC limit at 1 meter is evaluated at 950 mrem/hr.

For NCT, the maximum source strength density (Ci/g) is computed as the minimum of the following:

$$a_X(\text{Package Surface}) \left[\frac{\text{Ci}}{\text{g}} \right] = \frac{190 \left[\frac{\text{mrem}}{\text{hr}} \right]}{D_X(\text{Package surface}) \left[\frac{\text{mrem}/\text{hr}}{\text{Ci}} \right] \cdot m \left(1.00 \frac{\text{g}}{\text{cm}^3} \right) [\text{g}]}$$

$$a_X(2 \text{ meter}) \left[\frac{\text{Ci}}{\text{g}} \right] = \frac{9.5 \left[\frac{\text{mrem}}{\text{hr}} \right]}{D_X(2 \text{ meter}) \left[\frac{\text{mrem}/\text{hr}}{\text{Ci}} \right] \cdot m \left(1.00 \frac{\text{g}}{\text{cm}^3} \right) [\text{g}]}$$

$$a_X(\text{Cab}) \left[\frac{\text{Ci}}{\text{g}} \right] = \frac{1.9 \left[\frac{\text{mrem}}{\text{hr}} \right]}{D_X(\text{Cab}) \left[\frac{\text{mrem}/\text{hr}}{\text{Ci}} \right] \cdot m \left(1.00 \frac{\text{g}}{\text{cm}^3} \right) [\text{g}]}$$

For HAC, the maximum source strength density (Ci/g) is computed as the minimum of the following:

$$a_X(1 \text{ meter}) \left[\frac{\text{Ci}}{\text{g}} \right] = \frac{950 \left[\frac{\text{mrem}}{\text{hr}} \right]}{D_X(1 \text{ meter}) \left[\frac{\text{mrem}/\text{hr}}{\text{Ci}} \right] \cdot m \left(1.00 \frac{\text{g}}{\text{cm}^3} \right) [\text{g}]}$$

Whichever condition is more limiting, either NCT or HAC determines the maximum Curies per gram of a particular radionuclide **X**. Section 5.5, Appendix 5.5.3 gives the complete list of the maximum allowable source strength density (Ci/g) limits for each of the gamma emitting radionuclides and for each of the predominant neutron emitting radionuclides. These limits are based on resin or filter material at a density of 1.0 g/cm³ filling the entire cavity of the RT-100 (4597809 total grams).

In the loading table, the actual source strength density for each radionuclide is divided by the maximum allowable source strength density from the shielding evaluations, and the results summed for all radionuclides must be less than 1.0 to be acceptable for shipment.

5.4.4.5 Dose Rates for Maximum Radionuclide Loading

External radiation levels at a given dose rate location **D_X(r)** are computed for the maximum radionuclide loadings in the RT-100 by using the calculated nuclide-specific dose rate per Curie responses **D_X(r)** along with the source strength density limit set for the respective radionuclide **a_X** to demonstrate the dose rates produced for a given content isotopic loading as follows:

$$D_X(r) \left[\frac{\text{mrem}}{\text{hr}} \right] = a_X \left[\frac{\text{Ci}}{\text{g}} \right] \cdot D_X(r) \left[\frac{\text{mrem}/\text{hr}}{\text{Ci}} \right] \cdot m [\text{g}]$$

An example of the maximum dose rates and their corresponding measurement locations are

shown in Figure 5.4.4-4 for Co-60 (assuming the maximum mass of 4597809 grams).

Dose rates for other radionuclides with a greater than one (1) day half-life can also be computed in the same manner using radionuclide gamma dose rate per Ci responses in Table 5.5.2-1 for NCT and Table 5.5.2-2 for HAC, and the source strength densities in Table 5.5.3-1. The estimated dose rates due to the maximum allowed loading of each radionuclide considered individually is shown in Table 5.4.4-5 and Table 5.4.4-6. Any mixture of radionuclides can be evaluated with a characterization of the actual source strength density (Ci/g) of each radionuclide, using the loading table.

The RT-100 loading table procedure as outlined in Chapter 7, Section 7.6.1 provides the guidance on the acceptability of a mixture of radionuclides in resin and filter material based on the maximum Ci/g for each radionuclide in the mixture. This loading table procedure, based on sum of the fractions of contributions, determines whether the radionuclide mixture meets or exceeds 10 CFR 71.47(b) or 10 CFR 71.51(a) (2) [*both* Ref. 2] radiation limits. In addition, the loading table determines whether the combined A_2 and mixture heat load meets or exceeds licensed limits.

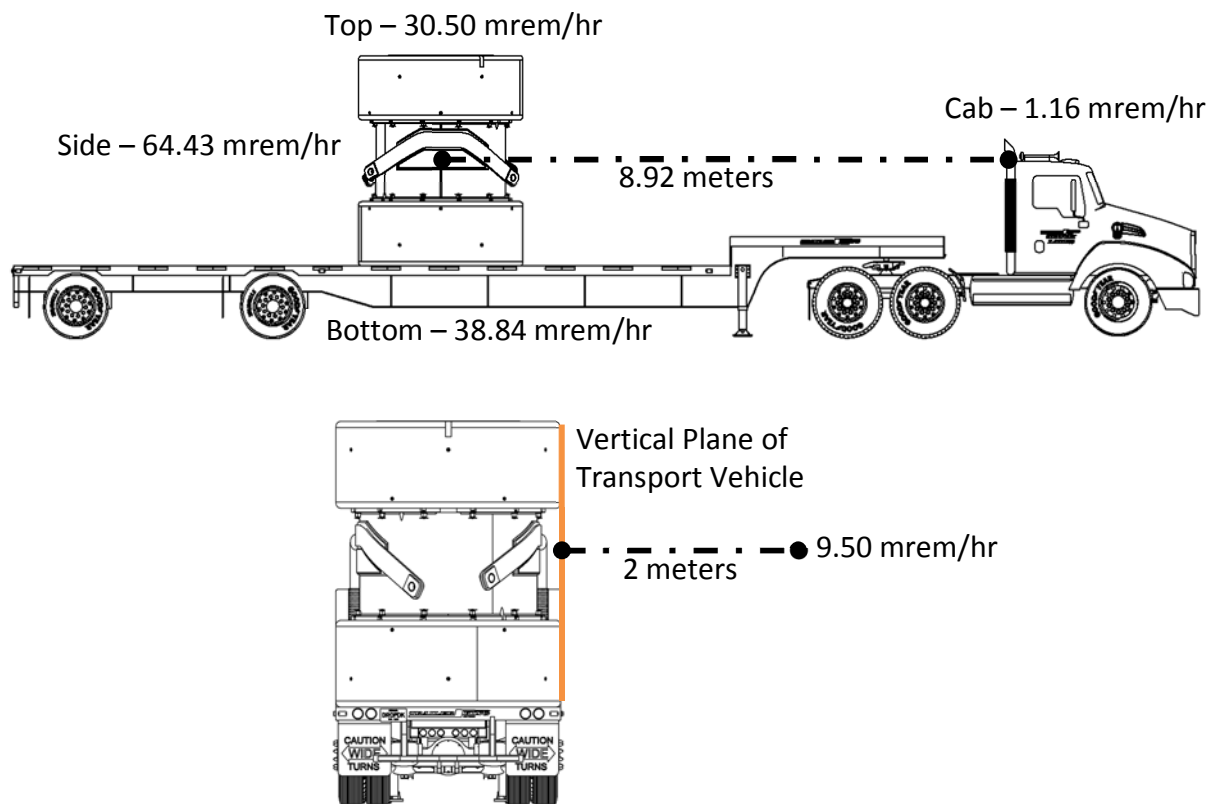


Figure 5.4.4-4 NCT Maximum Gamma Dose Rates for Co-60 Content at 1.00 g/cc

Table 5.4.4-5 NCT Gamma Dose Rates for the Maximum Radionuclide Loading

Radionuclide	Source Strength Density (Ci/g)	Package Surface (mrem/hr)			2 Meter from Edge of Vehicle (mrem/hr)	Vehicle Occupied Position (mrem/hr)
X	a_X	Side	Bottom	Top	Side	Cab
na24	3.38E-06	65.9	46.7	33.6	9.5	1.2
bi208	3.76E-06	65.9	47.1	34.2	9.5	1.2
cs144	5.27E-06	65.2	47.2	35.1	9.5	1.2
y88	1.02E-05	67.0	44.3	29.1	9.5	1.2
la140	1.63E-05	66.5	43.5	29.6	9.5	1.2
sb124	2.19E-05	66.9	43.5	29.9	9.5	1.2
eu156	2.26E-05	65.8	45.1	30.9	9.5	1.2
sc48	2.67E-05	66.2	43.4	30.8	9.5	1.2
la138	3.87E-05	67.0	42.7	29.6	9.5	1.2
tb156	4.10E-05	67.1	43.7	30.4	9.5	1.2
ag106m	4.45E-05	67.2	43.3	30.9	9.5	1.2
lu169	4.55E-05	66.5	43.6	30.1	9.5	1.2
na22	5.38E-05	68.3	43.9	31.7	9.5	1.2
sb120m	5.51E-05	66.6	43.9	33.4	9.5	1.2
i124	5.54E-05	66.9	44.0	30.5	9.5	1.2
br82	5.93E-05	67.4	43.0	31.5	9.5	1.2
lu172	6.68E-05	66.4	44.2	32.9	9.5	1.2
ta182	6.93E-05	67.3	43.6	31.5	9.5	1.2
ca47	7.23E-05	67.8	44.0	31.5	9.5	1.2
sc46	7.66E-05	66.3	43.6	33.9	9.5	1.2
te131m	7.96E-05	66.7	44.6	32.4	9.5	1.2
eu152	8.35E-05	67.0	43.1	31.0	9.5	1.2
as72	8.49E-05	66.1	46.0	35.0	9.5	1.2
tm172	9.32E-05	66.7	42.9	29.1	9.5	1.2
eu154	9.69E-05	67.5	44.0	32.5	9.5	1.2
cs136	1.09E-04	66.5	44.9	36.3	9.5	1.2
pm148	1.10E-04	66.9	42.8	29.9	9.5	1.2
ge69	1.25E-04	66.8	43.5	31.4	9.5	1.2
tb160	1.56E-04	66.4	44.0	34.3	9.5	1.2
sn125	1.82E-04	65.7	45.5	32.3	9.5	1.2
rh102m	1.88E-04	69.2	43.7	36.8	9.5	1.2
gd147	1.93E-04	67.4	43.8	33.9	9.5	1.2
tc96	2.23E-04	66.4	45.2	46.3	9.5	1.2
sr83	2.25E-04	67.4	43.8	31.9	9.5	1.2
k40	2.42E-04	66.9	42.7	29.3	9.5	1.2
co60	2.50E-04	64.4	38.8	30.5	9.5	1.2
as76	2.84E-04	67.2	44.6	31.5	9.5	1.2
nb92	3.41E-04	66.3	45.6	42.5	9.5	1.2
np238	3.49E-04	65.7	45.6	38.4	9.5	1.2
am240	4.09E-04	64.7	46.1	43.0	9.5	1.2
tb158	4.32E-04	65.4	45.5	40.2	9.5	1.2
pm148m	4.79E-04	74.0	43.8	46.2	9.5	1.2
ag110m	4.84E-04	64.5	38.7	30.6	9.5	1.2
ho166m	5.45E-04	69.8	44.7	49.8	9.5	1.2
pa232	5.96E-04	65.0	46.0	44.8	9.5	1.2
sb126	6.14E-04	83.0	42.1	56.4	9.5	1.2

Table 5.4.4-5 NCT Gamma Dose Rates for the Maximum Radionuclide Loading (Cont.)

Radionuclide	Source Strength Density (Ci/g)	Package Surface (mrem/hr)			2 Meter from Edge of Vehicle (mrem/hr)	Vehicle Occupied Position (mrem/hr)
X	a_X	Side	Bottom	Top	Side	Cab
nb94	6.40E-04	68.4	46.6	60.1	9.5	1.2
rb84	6.41E-04	66.0	45.2	42.9	9.5	1.2
tm168	6.65E-04	67.8	45.2	49.0	9.5	1.2
pr144	6.75E-04	65.7	45.5	31.1	9.5	1.2
fe59	7.11E-04	64.5	39.0	31.7	9.5	1.2
rh99	7.83E-04	69.1	42.7	32.1	9.5	1.2
tm165	8.21E-04	68.0	43.0	34.4	9.5	1.2
zr89	1.18E-03	69.6	42.5	30.4	9.5	1.2
rh102	1.23E-03	69.8	42.5	33.5	9.5	1.2
as71	1.37E-03	72.7	42.5	37.6	9.5	1.2
ru106	1.57E-03	69.1	43.9	34.2	9.5	1.2
tc95m	1.59E-03	69.2	44.8	51.4	9.5	1.2
rb86	1.82E-03	66.3	45.4	36.7	9.5	1.2
tc98	1.97E-03	99.9	42.0	86.1	9.5	1.2
ag108m	2.12E-03	102.2	40.9	86.4	9.5	1.2
ho166	2.17E-03	66.5	42.8	28.5	9.5	1.2
ir194m	2.25E-03	109.2	34.4	71.0	9.5	1.2
zn65	2.34E-03	64.3	39.2	35.1	9.5	1.2
cs132	2.34E-03	87.1	39.7	51.4	9.5	1.2
lu171	2.56E-03	80.4	44.7	65.0	9.5	1.2
nb95	2.59E-03	87.3	45.3	79.1	9.5	1.3
zr95	2.62E-03	87.3	45.3	79.1	9.5	1.3
tb153	2.83E-03	70.3	43.5	41.2	9.5	1.2
te121m	3.15E-03	71.1	41.9	34.3	9.5	1.2
ag105	3.32E-03	76.6	42.6	45.3	9.5	1.2
sb127	3.61E-03	89.3	40.5	60.3	9.5	1.2
sb122	3.62E-03	80.2	40.0	41.3	9.5	1.2
pm144	3.14E-03	113.2	25.8	86.7	7.8	1.0
cd115m	4.17E-03	67.0	44.4	33.7	9.5	1.2
kr79	4.27E-03	74.5	41.2	38.7	9.5	1.2
pm146	4.35E-03	92.1	43.4	80.2	9.5	1.3
gd149	4.88E-03	83.2	41.9	59.0	9.5	1.2
i126	5.10E-03	88.0	39.3	53.7	9.5	1.2
cs134	6.03E-03	62.4	37.2	44.7	9.5	1.2
os185	6.57E-03	64.9	46.8	56.3	9.5	1.2
cu64	6.61E-03	77.3	39.5	37.1	9.5	1.2
pm143	6.71E-03	87.3	45.3	79.1	9.5	1.3
co58	6.96E-03	64.3	37.8	43.3	9.5	1.2
as74	7.27E-03	106.9	32.1	61.5	9.5	1.1
ba131	7.28E-03	82.8	39.8	46.8	9.5	1.2
br77	9.13E-03	86.3	39.3	55.7	9.5	1.2
ce143	9.23E-03	82.9	40.8	53.2	9.5	1.2
pm151	1.27E-02	95.0	38.8	70.3	9.5	1.2
mn54	1.65E-02	79.8	38.6	73.6	9.5	1.3
y91	1.80E-02	67.8	44.0	31.3	9.5	1.2
sb125	1.29E-02	96.2	17.8	69.8	6.2	0.8

Table 5.4.4-5 NCT Gamma Dose Rates for the Maximum Radionuclide Loading (Cont.)

Radionuclide	Source Strength Density (Ci/g)	Package Surface (mrem/hr)			2 Meter from Edge of Vehicle (mrem/hr)	Vehicle Occupied Position (mrem/hr)
X	a_X	Side	Bottom	Top	Side	Cab
sr85	1.15E-02	85.0	4.8	54.9	4.5	0.5
rb83	1.23E-02	86.8	6.6	57.0	4.8	0.6
te121	1.15E-02	84.6	4.7	54.6	4.5	0.5
sn123	2.46E-02	66.3	45.4	36.7	9.5	1.2
i131	1.71E-02	72.2	10.5	46.8	4.6	0.5
ag110	3.68E-02	81.2	41.4	46.1	9.5	1.2
cm241	1.16E-02	55.4	1.3	29.6	2.8	0.3
lu176	1.12E-02	52.6	0.2	26.9	2.6	0.3
au198	2.01E-02	66.5	10.1	35.3	4.6	0.5
se75	1.14E-02	52.7	0.3	27.0	2.6	0.3
y87	1.16E-02	52.8	0.3	27.0	2.6	0.3
rh101	1.30E-02	52.6	0.2	26.9	2.6	0.3
in114m	4.87E-02	106.1	37.7	84.3	9.5	1.2
hf181	1.36E-02	53.0	0.4	27.3	2.6	0.3
ru103	1.83E-02	63.4	4.3	37.3	3.5	0.4
cs129	2.97E-02	71.4	13.0	40.2	5.2	0.6
xe127	1.73E-02	52.7	0.3	27.0	2.6	0.3
bi210m	2.20E-02	61.0	3.5	35.1	3.3	0.4
ru97	2.01E-02	54.7	1.5	29.0	2.9	0.3
yb169	1.97E-02	52.6	0.3	26.9	2.6	0.3
co57	1.99E-02	52.9	0.4	27.2	2.6	0.3
ta183	2.04E-02	52.6	0.2	26.9	2.6	0.3
np239	2.04E-02	52.6	0.2	26.9	2.6	0.3
ba133	2.04E-02	52.6	0.2	26.9	2.6	0.3
zr88	2.05E-02	52.6	0.2	26.9	2.6	0.3
zn72	2.06E-02	52.6	0.2	26.9	2.6	0.3
rh101m	2.23E-02	55.4	0.6	29.3	2.8	0.3
cd115	3.40E-02	79.4	4.0	50.0	4.2	0.5
pt191	3.21E-02	71.7	4.6	43.7	3.9	0.4
te132	2.17E-02	52.6	0.2	26.9	2.6	0.3
cf249	2.18E-02	52.7	0.3	27.0	2.6	0.3
ba140	3.43E-02	76.6	3.5	47.6	4.0	0.4
hf182	2.22E-02	52.6	0.2	26.9	2.6	0.3
tc99m	2.24E-02	52.6	0.2	26.9	2.6	0.3
sn117m	2.25E-02	52.6	0.2	26.9	2.6	0.3
te129m	8.36E-02	94.3	40.6	70.6	9.5	1.2
hf175	2.30E-02	52.6	0.2	26.9	2.6	0.3
u235	2.32E-02	52.6	0.3	26.9	2.6	0.3
te123m	2.37E-02	52.6	0.2	26.9	2.6	0.3
hg203	2.45E-02	52.6	0.2	26.9	2.6	0.3
cm247	2.45E-02	52.6	0.2	26.9	2.6	0.3
cf251	2.48E-02	52.6	0.2	26.9	2.6	0.3
ce139	2.50E-02	52.6	0.2	26.9	2.6	0.3
pu246	2.54E-02	52.6	0.2	26.9	2.6	0.3
mo99	9.03E-03	100.0	38.4	76.0	9.5	1.2
ar37	4.49E-02	70.4	7.1	43.9	4.1	0.5

Table 5.4.4-5 NCT Gamma Dose Rates for the Maximum Radionuclide Loading (Cont.)

Radionuclide	Source Strength Density (Ci/g)	Package Surface (mrem/hr)			2 Meter from Edge of Vehicle (mrem/hr)	Vehicle Occupied Position (mrem/hr)
X	a_X	Side	Bottom	Top	Side	Cab
sc47	2.93E-02	52.6	0.2	26.9	2.6	0.3
in113m	3.11E-02	52.6	0.2	26.9	2.6	0.3
u237	3.13E-02	52.6	0.2	26.9	2.6	0.3
cm243	3.16E-02	52.6	0.2	26.9	2.6	0.3
pa233	3.22E-02	52.6	0.2	26.9	2.6	0.3
ga67	4.31E-02	57.0	4.3	31.2	3.4	0.4
tb155	3.46E-02	53.0	0.3	27.3	2.6	0.3
er172	3.72E-02	53.1	0.4	27.4	2.6	0.3
nd147	6.37E-02	82.2	5.6	52.9	4.5	0.5
lu177m	3.73E-02	52.6	0.2	26.9	2.6	0.3
cm245	3.76E-02	52.6	0.2	26.9	2.6	0.3
np236	3.88E-02	52.6	0.2	26.9	2.6	0.3
cs137	7.95E-02	94.2	9.4	65.9	5.3	0.6
cu67	4.00E-02	52.6	0.2	26.9	2.6	0.3
au199	4.09E-02	52.6	0.2	26.9	2.6	0.3
ce141	4.14E-02	52.6	0.2	26.9	2.6	0.3
tm167	4.47E-02	54.7	0.5	28.7	2.7	0.3
th227	5.64E-02	53.3	0.8	27.5	2.7	0.3
ra223	5.77E-02	53.4	0.5	27.6	2.6	0.3
pu237	6.27E-02	52.6	0.2	26.9	2.6	0.3
sm153	6.61E-02	53.1	0.3	27.3	2.6	0.3
sn126	6.59E-02	52.6	0.2	26.9	2.6	0.3
os191	6.88E-02	52.6	0.2	26.9	2.6	0.3
nb95m	7.52E-02	53.0	0.5	27.3	2.6	0.3
rh105	8.17E-02	52.6	0.2	26.9	2.6	0.3
os193	1.08E-01	61.0	3.1	34.4	3.3	0.4
re189	9.10E-02	55.6	0.6	29.5	2.8	0.3
pm149	3.21E-01	83.1	39.9	61.4	9.5	1.2
eu155	9.11E-02	52.6	0.2	26.9	2.6	0.3
gd153	9.29E-02	52.6	0.2	26.9	2.6	0.3
th229	9.61E-02	52.6	0.2	26.9	2.6	0.3
lu177	1.12E-01	52.6	0.2	26.9	2.6	0.3
hf172	1.20E-01	52.6	0.2	26.9	2.6	0.3
ba135m	1.28E-01	52.6	0.2	26.9	2.6	0.3
eu149	1.91E-01	58.6	1.0	32.0	2.9	0.3
yb175	1.69E-01	52.6	0.2	26.9	2.6	0.3
ce144	1.80E-01	52.6	0.2	26.9	2.6	0.3
be7	1.93E-01	52.6	0.2	26.9	2.6	0.3
re186	2.10E-01	54.4	1.4	28.8	2.8	0.3
cr51	1.98E-01	52.6	0.2	26.9	2.6	0.3
xe133m	1.99E-01	52.6	0.2	26.9	2.6	0.3
pa231	2.09E-01	52.7	0.3	27.0	2.6	0.3
ag111	2.47E-01	54.7	1.8	29.0	2.9	0.3
ir192	2.36E-01	52.9	0.5	27.3	2.6	0.3
xe129m	4.35E-01	52.6	0.2	26.9	2.6	0.3
ra224	4.99E-01	52.9	0.3	27.2	2.6	0.3

Table 5.4.4-5 NCT Gamma Dose Rates for the Maximum Radionuclide Loading (Cont.)

Radionuclide	Source Strength Density (Ci/g)	Package Surface (mrem/hr)			2 Meter from Edge of Vehicle (mrem/hr)	Vehicle Occupied Position (mrem/hr)
X	a_X	Side	Bottom	Top	Side	Cab
ac225	5.06E-01	52.9	0.3	27.2	2.6	0.3
kr81	5.11E-01	52.6	0.2	26.9	2.6	0.3
ra226	5.69E-01	52.7	0.3	27.0	2.6	0.3
np237	5.86E-01	52.6	0.2	26.9	2.6	0.3
as77	7.12E-01	61.5	1.4	34.5	3.1	0.3
pt195m	6.57E-01	52.6	0.2	26.9	2.6	0.3
ni59	3.30E+00	78.1	43.3	58.6	9.5	1.2
xe131m	1.02E+00	52.6	0.2	26.9	2.6	0.3
sn113	1.09E+00	52.7	0.3	27.0	2.6	0.3
kr85	2.62E+00	84.9	4.7	54.8	4.5	0.5
th231	1.60E+00	52.6	0.2	26.9	2.6	0.3
dy166	1.70E+00	52.6	0.2	26.9	2.6	0.3
nb91	3.47E+00	84.9	4.7	54.8	4.5	0.5
am243	2.81E+00	53.0	0.4	27.3	2.6	0.3
w188	3.13E+00	52.6	0.2	26.9	2.6	0.3
th228	3.85E+00	52.7	0.3	27.0	2.6	0.3
tb161	4.57E+00	58.6	1.0	32.0	2.9	0.3
es254	4.48E+00	52.6	0.2	26.9	2.6	0.3
u230	6.10E+00	52.7	0.3	27.0	2.6	0.3
la137	1.73E+01	106.0	21.8	79.6	7.1	0.9
te125m	7.07E+00	52.6	0.2	26.9	2.6	0.3
th234	7.08E+00	52.6	0.2	26.9	2.6	0.3
rn222	1.50E+01	84.9	4.7	54.8	4.5	0.5
am242m	1.20E+01	52.6	0.2	26.9	2.6	0.3
te127m	3.73E+01	101.1	18.7	74.2	6.5	0.8
es253	1.90E+01	55.8	2.5	29.0	3.1	0.3
w181	1.72E+01	52.6	0.2	26.9	2.6	0.3
pt193m	1.78E+01	52.6	0.2	26.9	2.6	0.3
po210	7.99E+01	62.2	47.0	53.8	9.5	1.2
u233	2.67E+01	55.1	2.0	28.2	3.0	0.3
u232	2.54E+01	52.7	0.3	27.0	2.6	0.3
xe133	2.72E+01	52.6	0.2	26.9	2.6	0.3
th230	2.84E+01	52.6	0.3	26.9	2.6	0.3
am241	6.02E+01	59.3	4.2	33.7	3.3	0.4
ac227	4.82E+01	52.6	0.2	26.9	2.6	0.3
u234	5.50E+01	52.7	0.3	27.0	2.6	0.3
pd103	6.91E+01	52.6	0.2	26.9	2.6	0.3
th232	7.27E+01	52.6	0.2	26.9	2.6	0.3
cd113m	8.69E+01	52.6	0.2	26.9	2.6	0.3
sr90	3.64E+02	65.5	45.8	31.2	9.5	1.2
u236	9.99E+01	52.6	0.2	26.9	2.6	0.3
v49	1.07E+02	53.8	0.4	27.9	2.7	0.3
pu239	1.14E+02	54.1	1.1	28.4	2.8	0.3
w185	1.07E+02	52.6	0.2	26.9	2.6	0.3
pu236	1.44E+02	57.2	1.7	31.2	2.9	0.3
cf252	1.34E+02	52.6	0.2	26.9	2.6	0.3

Table 5.4.4-5 NCT Gamma Dose Rates for the Maximum Radionuclide Loading (Cont.)

Radionuclide	Source Strength Density (Ci/g)	Package Surface (mrem/hr)			2 Meter from Edge of Vehicle (mrem/hr)	Vehicle Occupied Position (mrem/hr)
X	a_X	Side	Bottom	Top	Side	Cab
cm242	4.05E+02	79.1	18.2	46.2	6.3	0.7
u238	1.86E+02	52.6	0.2	26.9	2.6	0.3
cl36	3.35E+02	84.9	4.7	54.8	4.5	0.5
cm244	8.69E+02	88.5	38.3	64.5	9.5	1.2
pu240	2.60E+02	53.1	0.5	27.4	2.6	0.3
ca41	4.10E+02	52.6	0.2	26.9	2.6	0.3
pu238	1.62E+03	89.9	29.4	59.0	8.1	1.0
sm145	5.73E+02	52.6	0.2	26.9	2.6	0.3
pu242	6.96E+02	52.6	0.2	26.9	2.6	0.3
pm147	7.00E+02	52.6	0.2	26.9	2.6	0.3
er169	1.53E+03	52.6	0.2	26.9	2.6	0.3
fe55	1.63E+03	52.6	0.2	26.9	2.6	0.3
pu241	3.67E+03	52.6	0.2	26.9	2.6	0.3
bi210	1.96E+04	52.6	0.2	26.9	2.6	0.3
bk249	5.28E+04	52.6	0.2	26.9	2.6	0.3
pr143	2.15E+05	87.3	45.3	79.1	9.5	1.3
tc97	5.81E+05	52.6	0.2	26.9	2.6	0.3
ca45	5.83E+05	52.6	0.2	26.9	2.6	0.3
ge71	5.83E+05	52.6	0.2	26.9	2.6	0.3
nb93m	5.83E+05	52.6	0.2	26.9	2.6	0.3
mo93	5.83E+05	52.6	0.2	26.9	2.6	0.3
tc97m	5.83E+05	52.6	0.2	26.9	2.6	0.3
cd109	5.83E+05	52.6	0.2	26.9	2.6	0.3
sn113m	5.83E+05	52.6	0.2	26.9	2.6	0.3
sn119m	5.83E+05	52.6	0.2	26.9	2.6	0.3
sn121m	5.83E+05	52.6	0.2	26.9	2.6	0.3
te123	5.83E+05	52.6	0.2	26.9	2.6	0.3
i125	5.83E+05	52.6	0.2	26.9	2.6	0.3
i129	5.83E+05	52.6	0.2	26.9	2.6	0.3
cs131	5.83E+05	52.6	0.2	26.9	2.6	0.3
pm145	5.83E+05	52.6	0.2	26.9	2.6	0.3
sm151	5.83E+05	52.6	0.2	26.9	2.6	0.3
tb157	5.83E+05	52.6	0.2	26.9	2.6	0.3
dy159	5.83E+05	52.6	0.2	26.9	2.6	0.3
tm170	5.83E+05	52.6	0.2	26.9	2.6	0.3
tm171	5.83E+05	52.6	0.2	26.9	2.6	0.3
os194	5.83E+05	52.6	0.2	26.9	2.6	0.3
pt193	5.83E+05	52.6	0.2	26.9	2.6	0.3
tl204	5.83E+05	52.6	0.2	26.9	2.6	0.3
pb205	5.83E+05	52.6	0.2	26.9	2.6	0.3
pb210	5.83E+05	52.6	0.2	26.9	2.6	0.3
ra225	5.83E+05	52.6	0.2	26.9	2.6	0.3
ra228	5.83E+05	52.6	0.2	26.9	2.6	0.3
np235	5.83E+05	52.6	0.2	26.9	2.6	0.3
cm246	5.83E+05	52.6	0.2	26.9	2.6	0.3
cm248	5.83E+05	52.6	0.2	26.9	2.6	0.3

Table 5.4.4-5 NCT Gamma Dose Rates for the Maximum Radionuclide Loading (Cont.)

Radionuclide	Source Strength Density (Ci/g)	Package Surface (mrem/hr)			2 Meter from Edge of Vehicle (mrem/hr)	Vehicle Occupied Position (mrem/hr)
X	a_X	Side	Bottom	Top	Side	Cab
cf250	5.83E+05	52.6	0.2	26.9	2.6	0.3
se72	5.83E+05	52.6	0.2	26.9	2.6	0.3
as73	5.83E+05	52.6	0.2	26.9	2.6	0.3
te118	5.83E+05	52.6	0.2	26.9	2.6	0.3
sb119	5.83E+05	52.6	0.2	26.9	2.6	0.3
nd140	5.83E+05	52.6	0.2	26.9	2.6	0.3
yb166	5.83E+05	52.6	0.2	26.9	2.6	0.3
h3	5.83E+05	52.6	0.2	26.9	2.6	0.3
ni63	5.83E+05	52.6	0.2	26.9	2.6	0.3
sr89	5.83E+05	52.6	0.2	26.9	2.6	0.3
tc99	5.83E+05	52.6	0.2	26.9	2.6	0.3
am242	5.83E+05	52.6	0.2	26.9	2.6	0.3
c14	5.83E+05	52.6	0.2	26.9	2.6	0.3

Table 5.4.4-6 HAC Gamma Dose Rates for the Maximum Radionuclide Loading

Radionuclide	Source Strength Density (Ci/g)	1 Meter from Package Surface (mrem/hr)		
		Side	Bottom	Top
na24	3.38E-06	34.7	53.9	53.0
bi208	3.76E-06	33.4	53.7	53.1
cs144	5.27E-06	34.5	53.2	55.0
y88	1.02E-05	39.6	54.7	48.3
la140	1.63E-05	42.1	53.8	49.5
sb124	2.19E-05	42.4	54.5	48.3
eu156	2.26E-05	39.2	53.7	50.5
sc48	2.67E-05	60.2	58.7	58.9
la138	3.87E-05	48.2	57.0	51.4
tb156	4.10E-05	53.0	56.9	53.4
ag106m	4.45E-05	63.2	56.2	55.8
lu169	4.55E-05	48.4	56.0	52.3
na22	5.38E-05	62.5	59.8	57.2
sb120m	5.51E-05	76.6	60.8	64.9
i124	5.54E-05	45.6	54.0	49.9
br82	5.93E-05	71.3	57.8	59.0
lu172	6.68E-05	69.0	59.2	60.6
ta182	6.93E-05	62.0	59.4	58.7
ca47	7.23E-05	56.1	60.1	56.6
sc46	7.66E-05	82.3	60.2	67.2
te131m	7.96E-05	61.5	56.0	57.3
eu152	8.35E-05	60.6	58.2	56.3
as72	8.49E-05	63.9	54.5	59.4
tm172	9.32E-05	45.6	55.9	50.2
eu154	9.69E-05	68.0	60.0	60.0
cs136	1.09E-04	93.7	63.3	71.1
pm148	1.10E-04	51.2	57.2	52.5
ge69	1.25E-04	65.2	57.1	58.4
tb160	1.56E-04	86.0	61.1	68.3
sn125	1.82E-04	48.3	55.2	54.8
rh102m	1.88E-04	121.6	61.1	74.0
gd147	1.93E-04	93.3	59.0	65.5
tc96	2.23E-04	185.0	66.3	101.6
sr83	2.25E-04	69.2	55.0	56.2
k40	2.42E-04	46.0	56.9	50.7
co60	2.50E-04	70.0	97.6	81.7
as76	2.84E-04	54.5	54.9	53.4
nb92	3.41E-04	159.4	67.6	94.4
np238	3.49E-04	102.6	65.8	77.8
am240	4.09E-04	152.4	68.5	95.5
tb158	4.32E-04	128.3	66.4	87.1
pm148m	4.79E-04	229.9	64.0	98.9
ag110m	4.84E-04	84.9	93.4	80.5
ho166m	5.45E-04	250.0	66.0	110.6
pa232	5.96E-04	173.8	68.6	100.2
sb126	6.14E-04	372.3	62.5	127.2

Table 5.4.4-6 HAC Gamma Dose Rates for the Maximum Radionuclide Loading (Cont.)

Radionuclide	Source Strength Density (Ci/g)	1 Meter from Package Surface (mrem/hr)		
		Side	Bottom	Top
nb94	6.40E-04	304.1	72.3	140.0
rb84	6.41E-04	167.5	63.1	90.3
tm168	6.65E-04	231.9	67.1	108.8
pr144	6.75E-04	36.0	52.6	49.7
fe59	7.11E-04	82.1	100.4	88.5
rh99	7.83E-04	100.7	55.2	58.5
tm165	8.21E-04	118.2	58.9	68.0
zr89	1.18E-03	80.2	53.6	53.0
rh102	1.23E-03	123.5	56.3	64.9
as71	1.37E-03	194.4	58.7	75.4
ru106	1.57E-03	96.4	55.1	61.7
tc95m	1.59E-03	281.8	67.1	115.2
rb86	1.82E-03	88.0	64.7	70.9
tc98	1.97E-03	663.3	68.0	208.2
ag108m	2.12E-03	733.4	66.3	209.9
ho166	2.17E-03	44.3	55.6	50.5
ir194m	2.25E-03	855.9	52.2	168.6
zn65	2.34E-03	104.8	103.1	102.3
cs132	2.34E-03	359.9	55.3	112.9
lu171	2.56E-03	390.4	68.8	151.2
nb95	2.59E-03	526.8	72.8	190.2
zr95	2.62E-03	526.8	72.8	190.2
tb153	2.83E-03	220.5	62.5	88.5
te121m	3.15E-03	186.3	57.2	69.7
ag105	3.32E-03	311.8	61.6	96.4
sb127	3.61E-03	469.1	60.1	138.4
sb122	3.62E-03	277.3	54.9	86.2
pm144	3.14E-03	950.0	43.6	213.8
cd115m	4.17E-03	73.8	61.8	64.6
kr79	4.27E-03	228.3	56.6	81.3
pm146	4.35E-03	644.9	69.8	194.6
gd149	4.88E-03	524.1	64.0	139.7
i126	5.10E-03	428.5	55.8	118.3
cs134	6.03E-03	263.9	104.3	138.8
os185	6.57E-03	266.8	72.1	130.4
cu64	6.61E-03	238.9	52.8	77.0
pm143	6.71E-03	526.8	72.8	190.2
co58	6.96E-03	218.0	100.1	128.3
as74	7.27E-03	747.3	43.2	141.1
ba131	7.28E-03	529.7	57.6	104.4
br77	9.13E-03	538.8	58.1	127.3
ce143	9.23E-03	458.4	59.6	121.5
pm151	1.27E-02	814.1	60.7	171.7
mn54	1.65E-02	483.9	115.9	235.7
y91	1.80E-02	54.9	60.0	56.3
sb125	1.29E-02	950.0	30.4	175.2

Table 5.4.4-6 HAC Gamma Dose Rates for the Maximum Radionuclide Loading (Cont.)

Radionuclide	Source Strength Density (Ci/g)	1 Meter from Package Surface (mrem/hr)		
		Side	Bottom	Top
sr85	1.15E-02	950.0	8.6	140.9
rb83	1.23E-02	950.0	11.5	145.8
te121	1.15E-02	950.0	8.4	140.3
sn123	2.46E-02	87.8	64.6	70.8
i131	1.71E-02	950.0	17.6	121.7
ag110	3.68E-02	268.4	54.5	94.6
cm241	1.16E-02	950.0	2.6	82.0
lu176	1.12E-02	950.0	0.9	75.7
au198	2.01E-02	950.0	15.0	92.1
se75	1.14E-02	950.0	0.9	75.7
y87	1.16E-02	950.0	0.9	76.0
rh101	1.30E-02	950.0	0.9	75.7
in114m	4.87E-02	945.3	60.9	208.4
hf181	1.36E-02	950.0	1.1	76.5
ru103	1.83E-02	950.0	7.8	99.8
cs129	2.97E-02	950.0	20.0	104.8
xe127	1.73E-02	950.0	0.9	75.8
bi210m	2.20E-02	950.0	6.3	94.6
ru97	2.01E-02	950.0	2.9	80.4
yb169	1.97E-02	950.0	0.9	75.7
co57	1.99E-02	950.0	1.1	76.4
ta183	2.04E-02	950.0	0.9	75.7
np239	2.04E-02	950.0	0.9	75.7
ba133	2.04E-02	950.0	0.9	75.7
zr88	2.05E-02	950.0	0.9	75.7
zn72	2.06E-02	950.0	0.9	75.7
rh101m	2.23E-02	950.0	1.5	81.3
cd115	3.40E-02	950.0	7.2	129.6
pt191	3.21E-02	950.0	8.1	114.7
te132	2.17E-02	950.0	0.9	75.7
cf249	2.18E-02	950.0	1.0	75.9
ba140	3.43E-02	950.0	6.5	124.0
hf182	2.22E-02	950.0	0.9	75.7
tc99m	2.24E-02	950.0	0.9	75.7
sn117m	2.25E-02	950.0	0.9	75.7
te129m	8.36E-02	540.0	62.5	165.0
hf175	2.30E-02	950.0	0.9	75.7
u235	2.32E-02	950.0	0.9	75.7
te123m	2.37E-02	950.0	0.9	75.7
hg203	2.45E-02	950.0	0.9	75.7
cm247	2.45E-02	950.0	0.9	75.7
cf251	2.48E-02	950.0	0.9	75.7
ce139	2.50E-02	950.0	0.9	75.7
pu246	2.54E-02	950.0	0.9	75.7
mo99	9.03E-03	885.2	60.8	186.6
ar37	4.49E-02	950.0	12.2	115.2

Table 5.4.4-6 HAC Gamma Dose Rates for the Maximum Radionuclide Loading (Cont.)

Radionuclide	Source Strength Density (Ci/g)	1 Meter from Package Surface (mrem/hr)		
		Side	Bottom	Top
sc47	2.93E-02	950.0	0.9	75.7
in113m	3.11E-02	950.0	0.9	75.7
u237	3.13E-02	950.0	0.9	75.7
cm243	3.16E-02	950.0	0.9	75.7
pa233	3.22E-02	950.0	0.9	75.7
ga67	4.31E-02	950.0	7.1	85.3
tb155	3.46E-02	950.0	1.1	76.5
er172	3.72E-02	950.0	1.1	76.7
nd147	6.37E-02	950.0	9.9	136.4
lu177m	3.73E-02	950.0	0.9	75.7
cm245	3.76E-02	950.0	0.9	75.7
np236	3.88E-02	950.0	0.9	75.7
cs137	7.95E-02	950.0	31.3	214.4
cu67	4.00E-02	950.0	0.9	75.7
au199	4.09E-02	950.0	0.9	75.7
ce141	4.14E-02	950.0	0.9	75.7
tm167	4.47E-02	950.0	1.4	79.9
th227	5.64E-02	950.0	1.7	76.9
ra223	5.77E-02	950.0	1.3	77.3
pu237	6.27E-02	950.0	0.9	75.7
sm153	6.61E-02	950.0	1.1	76.7
sn126	6.59E-02	950.0	0.9	75.7
os191	6.88E-02	950.0	0.9	75.7
nb95m	7.52E-02	950.0	1.3	76.7
rh105	8.17E-02	950.0	0.9	75.7
os193	1.08E-01	950.0	5.4	93.0
re189	9.10E-02	950.0	1.6	81.7
pm149	3.21E-01	716.4	61.5	149.1
eu155	9.11E-02	950.0	0.9	75.7
gd153	9.29E-02	950.0	0.9	75.7
th229	9.61E-02	950.0	0.9	75.7
lu177	1.12E-01	950.0	0.9	75.7
hf172	1.20E-01	950.0	0.9	75.7
ba135m	1.28E-01	950.0	0.9	75.7
eu149	1.91E-01	950.0	2.3	87.7
yb175	1.69E-01	950.0	0.9	75.7
ce144	1.80E-01	950.0	0.9	75.7
be7	1.93E-01	950.0	0.9	75.7
re186	2.10E-01	950.0	2.8	80.0
cr51	1.98E-01	950.0	0.9	75.7
xe133m	1.99E-01	950.0	0.9	75.7
pa231	2.09E-01	950.0	0.9	75.8
ag111	2.47E-01	950.0	3.3	80.3
ir192	2.36E-01	950.0	1.3	76.4
xe129m	4.35E-01	950.0	0.9	75.7
ra224	4.99E-01	950.0	1.1	76.3

Table 5.4.4-6 HAC Gamma Dose Rates for the Maximum Radionuclide Loading (Cont.)

Radionuclide	Source Strength Density (Ci/g)	1 Meter from Package Surface (mrem/hr)		
		Side	Bottom	Top
ac225	5.06E-01	950.0	1.0	76.3
kr81	5.11E-01	950.0	0.9	75.7
ra226	5.69E-01	950.0	0.9	75.8
np237	5.86E-01	950.0	0.9	75.7
as77	7.12E-01	950.0	2.9	93.5
pt195m	6.57E-01	950.0	0.9	75.7
ni59	3.30E+00	408.4	66.1	136.6
xe131m	1.02E+00	950.0	0.9	75.7
sn113	1.09E+00	950.0	1.0	75.9
kr85	2.62E+00	950.0	8.5	140.8
th231	1.60E+00	950.0	0.9	75.7
dy166	1.70E+00	950.0	0.9	75.7
nb91	3.47E+00	950.0	8.5	140.8
am243	2.81E+00	950.0	1.2	76.6
w188	3.13E+00	950.0	0.9	75.7
th228	3.85E+00	950.0	1.0	75.8
tb161	4.57E+00	950.0	2.3	87.7
es254	4.48E+00	950.0	0.9	75.7
u230	6.10E+00	950.0	0.9	75.8
la137	1.73E+01	950.0	37.2	197.8
te125m	7.07E+00	950.0	0.9	75.7
th234	7.08E+00	950.0	0.9	75.7
rn222	1.50E+01	950.0	8.5	140.8
am242m	1.20E+01	950.0	0.9	75.7
te127m	3.73E+01	950.0	32.0	185.3
es253	1.90E+01	950.0	4.2	80.2
w181	1.72E+01	950.0	0.9	75.7
pt193m	1.78E+01	950.0	0.9	75.7
po210	7.99E+01	237.9	72.2	124.1
u233	2.67E+01	950.0	3.4	78.1
u232	2.54E+01	950.0	1.0	75.8
xe133	2.72E+01	950.0	0.9	75.7
th230	2.84E+01	950.0	0.9	75.7
am241	6.02E+01	950.0	7.3	91.3
ac227	4.82E+01	950.0	0.9	75.7
u234	5.50E+01	950.0	0.9	75.8
pd103	6.91E+01	950.0	0.9	75.7
th232	7.27E+01	950.0	0.9	75.7
cd113m	8.69E+01	950.0	0.9	75.7
sr90	3.64E+02	34.1	52.4	49.4
u236	9.99E+01	950.0	0.9	75.7
v49	1.07E+02	950.0	1.2	78.1
pu239	1.14E+02	950.0	2.3	79.0
w185	1.07E+02	950.0	0.9	75.7
pu236	1.44E+02	950.0	3.4	85.6
cf252	1.34E+02	950.0	0.9	75.7

Table 5.4.4-6 HAC Gamma Dose Rates for the Maximum Radionuclide Loading (Cont.)

Radionuclide	Source Strength Density (Ci/g)	1 Meter from Package Surface (mrem/hr)		
		Side	Bottom	Top
cm242	4.05E+02	950.0	27.5	116.7
u238	1.86E+02	950.0	0.9	75.7
cl36	3.35E+02	950.0	8.5	140.8
cm244	8.69E+02	797.4	59.4	157.5
pu240	2.60E+02	950.0	1.3	76.8
ca41	4.10E+02	950.0	0.9	75.7
pu238	1.62E+03	950.0	45.3	146.1
sm145	5.73E+02	950.0	0.9	75.7
pu242	6.96E+02	950.0	0.9	75.7
pm147	7.00E+02	950.0	0.9	75.7
er169	1.53E+03	950.0	0.9	75.7
fe55	1.63E+03	950.0	0.9	75.7
pu241	3.67E+03	950.0	0.9	75.7
bi210	1.96E+04	950.0	0.9	75.7
bk249	5.28E+04	950.0	0.9	75.7
pr143	2.15E+05	526.8	72.8	190.2
tc97	5.81E+05	950.0	0.9	75.7
ca45	5.83E+05	950.0	0.9	75.7
ge71	5.83E+05	950.0	0.9	75.7
nb93m	5.83E+05	950.0	0.9	75.7
mo93	5.83E+05	950.0	0.9	75.7
tc97m	5.83E+05	950.0	0.9	75.7
cd109	5.83E+05	950.0	0.9	75.7
sn113m	5.83E+05	950.0	0.9	75.7
sn119m	5.83E+05	950.0	0.9	75.7
sn121m	5.83E+05	950.0	0.9	75.7
te123	5.83E+05	950.0	0.9	75.7
i125	5.83E+05	950.0	0.9	75.7
i129	5.83E+05	950.0	0.9	75.7
cs131	5.83E+05	950.0	0.9	75.7
pm145	5.83E+05	950.0	0.9	75.7
sm151	5.83E+05	950.0	0.9	75.7
tb157	5.83E+05	950.0	0.9	75.7
dy159	5.83E+05	950.0	0.9	75.7
tm170	5.83E+05	950.0	0.9	75.7
tm171	5.83E+05	950.0	0.9	75.7
os194	5.83E+05	950.0	0.9	75.7
pt193	5.83E+05	950.0	0.9	75.7
tl204	5.83E+05	950.0	0.9	75.7
pb205	5.83E+05	950.0	0.9	75.7
pb210	5.83E+05	950.0	0.9	75.7
ra225	5.83E+05	950.0	0.9	75.7
ra228	5.83E+05	950.0	0.9	75.7
np235	5.83E+05	950.0	0.9	75.7
cm246	5.83E+05	950.0	0.9	75.7
cm248	5.83E+05	950.0	0.9	75.7

Table 5.4.4-6 HAC Gamma Dose Rates for the Maximum Radionuclide Loading (Cont.)

Radionuclide	Source Strength Density (Ci/g)	1 Meter from Package Surface (mrem/hr)		
X	a_X	Side	Bottom	Top
cf250	5.83E+05	950.0	0.9	75.7
se72	5.83E+05	950.0	0.9	75.7
as73	5.83E+05	950.0	0.9	75.7
te118	5.83E+05	950.0	0.9	75.7
sb119	5.83E+05	950.0	0.9	75.7
nd140	5.83E+05	950.0	0.9	75.7
yb166	5.83E+05	950.0	0.9	75.7
h3	5.83E+05	950.0	0.9	75.7
ni63	5.83E+05	950.0	0.9	75.7
sr89	5.83E+05	950.0	0.9	75.7
tc99	5.83E+05	950.0	0.9	75.7
am242	5.83E+05	950.0	0.9	75.7
c14	5.83E+05	950.0	0.9	75.7

5.5 Appendix

5.5.1 List of Gamma Radionuclides with Greater than 1 Day Half Life

Table 5.5.1-1 List of Gamma Radionuclides with Greater Than 1 Day Half Life

Nuclide	ID	Branch	Daughter	Yield	Nuclide	ID	Branch	Daughter	Yield	Nuclide	ID	Branch	Daughter	Yield
na22	110220				cs134	551340				pa232	912320			
na24	110240				cs136	551360				pa233	912330			
cl36	170360				ba131	561310				u230	922300			
ar37	180370				ba133	561330				u232	922320			
k40	190400				ba135m	561351				u233	922330			
ca41	200410				cs137	561371	br	ba137m	0.95	u234	922340			
ca45	200450				ba140	561400				u235	922350			
ca47	200470				la137	571370				u236	922360			
sc46	210460				la138	571380				u237	922370			
sc47	210470				la140	571400				u238	922380			
sc48	210480				ce139	581390				np235	932350			
v49	230490				ce141	581410				np236	932360			
cr51	240510				ce143	581430				np237	932370			
mn54	250540				ce144	581440				np238	932380			
fe55	260550				pr143	591430				np239	932390			
fe59	260590				pr144	591440				pu236	942360			
co57	270570				nd147	601470				pu237	942370			
co58	270580				pm145	611450				pu238	942380			
co60	270600				pm147	611470				pu239	942390			
ni59	280590				pm148	611480				pu240	942400			
cu64	290640				pm148m	611481				pu241	942410			
cu67	290670				pm149	611490				pu242	942420			
zn65	300650				pm151	611510				pu246	942460			
ge71	320710				sm145	621450				am240	952400			
as76	330760				sm151	621510				am241	952410			
as77	330770				sm153	621530				am242m	952421			
se75	340750				eu152	631520				am243	952430			
br82	350820				eu154	631540				cm241	962410			
kr79	360790				eu155	631550				cm242	962420			
kr81	360810				eu156	631560				cm243	962430			
kr85	360850				gd153	641530				cm244	962440			
rb86	370860				tb157	651570				cm245	962450			
sr85	380850				tb160	651600				cm246	962460			
sr90	390900	br	y90	1	tb161	651610				cm247	962470			
y91	390910				dy159	661590				cm248	962480			
zr89	400890				dy166	661660				bk249	972490			
zr95	400950				ho166	671660				cf249	982490			
nb91	410910				ho166m	671661				cf250	982500			
nb92	410920				er169	681690				cf251	982510			
nb93m	410931				er172	681720				cf252	982520			
nb94	410940				tm170	691700				es253	992530			
nb95	410950				tm171	691710				es254	992540			
nb95m	410951				tm172	691720				be7	40070			
mo93	420930				yb169	701690				ga67	310670			
tc97	430970				yb175	701750				ge69	320690			
tc97m	430971				lu176	711760				as71	330710			
tc98	430980				lu177	711770				zn72	300720			
mo99	430991	br	tc99m	0.88	lu177m	711771				as72	330720			
ru97	440970				hf175	721750				se72	340720			
ru103	441030				hf181	721810				as73	330730			

Table 5.5.1-1 (continued)

Nuclide	ID	Branch	Daughter	Yield
rh102	451020			
rh105	451050			
ru106	451060	br	rh106	1
pd103	461030			
ag108m	471081			
ag110	471100			
ag110m	471101			
ag111	471110			
cd109	481090			
cd113m	481131			
cd115	481150			
cd115m	481151			
in113m	491131			
in114m	491141			
sn113	501130			
sn113m	501131			
sn117m	501171			
sn119m	501191			
sn121m	501211			
sn123	501230			
sn125	501250			
sb122	511220			
sb124	511240			
sb125	511250			
sb126	511260			
te121	521210			
te121m	521211			
te123	521230			
te123m	521231			
te125m	521251			
te127m	521271			
te129m	521291			
te131m	521311			
i125	531250			
i126	531260			
i129	531290			
i131	531310			
xe127	541270			
xe129m	541291			
xe131m	541311			
xe133	541330			
xe133m	541331			
cs131	551310			
cs132	551320			

Nuclide	ID	Branch	Daughter	Yield
hf182	721820			
ta182	731820			
ta183	731830			
w181	741810			
w185	741850			
w188	741880			
re186	751860			
re189	751890			
os185	761850			
os191	761910			
os193	761930			
os194	761940			
ir192	771920			
ir194m	771941			
pt191	781910			
pt193	781930			
pt193m	781931			
pt195m	781951			
au198	791980			
au199	791990			
hg203	802030			
tl204	812040			
pb205	822050			
bi208	832080			
bi210	832100			
bi210m	832101			
po210	842100			
pb210	822100			
rn222	862220			
ra223	882230			
ra224	882240			
ra225	882250			
ra226	882260			
ra228	882280			
ac225	892250			
ac227	892270			
th227	902270			
th228	902280			
th229	902290			
th230	902300			
th231	902310			
th232	902320			
th234	902340			
pa231	912310			

Nuclide	ID	Branch	Daughter	Yield
as74	330740			
br77	350770			
rb83	370830			
sr83	380830			
rb84	370840			
y87	390870			
y88	390880			
zr88	400880			
tc95m	430951			
tc96	430960			
rh99	450990			
rh101	451010			
rh101m	451011			
rh102m	451021			
ag105	471050			
ag106m	471061			
te118	521180			
sb119	511190			
sb120m	511201			
i124	531240			
sn126	501260			
sb127	511270			
cs129	551290			
te132	521320			
nd140	601400			
pm143	611430			
cs144	551440			
pm144	611440			
pm146	611460			
gd147	641470			
eu149	631490			
gd149	641490			
tb153	651530			
tb155	651550			
tb156	651560			
tb158	651580			
tm165	691650			
yb166	701660			
tm167	691670			
tm168	691680			
lu169	711690			
lu171	711710			
lu172	711720			
hf172	721720			

5.5.2 Gamma Radionuclide Responses

Table 5.5.2-1 NCT Gamma Dose Rate Responses (mrem/hr/Ci)

Radionuclide	NCT Surface 71.47(b)(1) or (2)			NCT 2 Meter 71.47(b)(3)	Normally occupied space 71.47(b)(4)
	Side	Bottom	Top		
na24	4.24E+00	3.01E+00	2.16E+00	6.11E-01	1.51E-01
bi208	3.81E+00	2.73E+00	1.98E+00	5.50E-01	1.36E-01
cs144	2.69E+00	1.95E+00	1.45E+00	3.92E-01	9.64E-02
y88	1.43E+00	9.45E-01	6.21E-01	2.03E-01	4.99E-02
la140	8.89E-01	5.82E-01	3.96E-01	1.27E-01	3.11E-02
sb124	6.64E-01	4.32E-01	2.96E-01	9.43E-02	2.29E-02
eu156	6.34E-01	4.34E-01	2.97E-01	9.15E-02	2.22E-02
sc48	5.39E-01	3.54E-01	2.51E-01	7.74E-02	1.88E-02
la138	3.76E-01	2.40E-01	1.66E-01	5.34E-02	1.30E-02
tb156	3.56E-01	2.32E-01	1.61E-01	5.04E-02	1.23E-02
ag106m	3.28E-01	2.11E-01	1.51E-01	4.65E-02	1.14E-02
lu169	3.18E-01	2.08E-01	1.44E-01	4.54E-02	1.10E-02
na22	2.76E-01	1.78E-01	1.28E-01	3.84E-02	9.44E-03
sb120m	2.63E-01	1.73E-01	1.32E-01	3.75E-02	9.17E-03
i124	2.63E-01	1.73E-01	1.20E-01	3.73E-02	9.05E-03
br82	2.47E-01	1.58E-01	1.16E-01	3.48E-02	8.48E-03
lu172	2.16E-01	1.44E-01	1.07E-01	3.09E-02	7.59E-03
ta182	2.11E-01	1.37E-01	9.87E-02	2.98E-02	7.26E-03
ca47	2.04E-01	1.32E-01	9.46E-02	2.86E-02	7.02E-03
sc46	1.88E-01	1.24E-01	9.61E-02	2.70E-02	6.57E-03
te131m	1.82E-01	1.22E-01	8.86E-02	2.60E-02	6.31E-03
eu152	1.74E-01	1.12E-01	8.06E-02	2.47E-02	6.03E-03
as72	1.69E-01	1.18E-01	8.96E-02	2.43E-02	5.97E-03
tm172	1.56E-01	1.00E-01	6.79E-02	2.22E-02	5.38E-03
eu154	1.52E-01	9.87E-02	7.29E-02	2.13E-02	5.23E-03
pm148	1.33E-01	8.48E-02	5.94E-02	1.88E-02	4.60E-03
cs136	1.32E-01	8.93E-02	7.23E-02	1.89E-02	4.69E-03
ge69	1.16E-01	7.55E-02	5.44E-02	1.65E-02	4.00E-03
tb160	9.28E-02	6.15E-02	4.79E-02	1.33E-02	3.23E-03
rh102m	8.02E-02	5.06E-02	4.27E-02	1.10E-02	2.70E-03
sn125	7.86E-02	5.44E-02	3.87E-02	1.14E-02	2.77E-03
gd147	7.59E-02	4.93E-02	3.82E-02	1.07E-02	2.61E-03
sr83	6.53E-02	4.24E-02	3.09E-02	9.20E-03	2.24E-03
tc96	6.48E-02	4.41E-02	4.52E-02	9.27E-03	2.30E-03
k40	6.02E-02	3.84E-02	2.64E-02	8.55E-03	2.09E-03
co60 ¹	5.60E-02	3.38E-02	2.65E-02	8.26E-03	1.01E-03

Table 5.5.2-1 (Continued)

Radionuclide	NCT Surface 71.47(b)(1) or (2)			NCT 2 Meter 71.47(b)(3)	Normally occupied space 71.47(b)(4)
	Side	Bottom	Top		
as76	5.15E-02	3.42E-02	2.42E-02	7.28E-03	1.77E-03
nb92	4.23E-02	2.91E-02	2.71E-02	6.06E-03	1.48E-03
np238	4.09E-02	2.84E-02	2.39E-02	5.92E-03	1.47E-03
am240	3.44E-02	2.45E-02	2.29E-02	5.05E-03	1.24E-03
tb158	3.30E-02	2.29E-02	2.03E-02	4.79E-03	1.17E-03
sb126	2.94E-02	1.49E-02	2.00E-02	3.37E-03	8.33E-04
ag110m ¹	2.90E-02	1.74E-02	1.38E-02	4.27E-03	5.24E-04
ho166m	2.79E-02	1.78E-02	1.99E-02	3.79E-03	9.43E-04
pa232	2.37E-02	1.68E-02	1.64E-02	3.47E-03	8.54E-04
pm148m	3.36E-02	1.99E-02	2.10E-02	4.31E-03	1.07E-03
nb94	2.32E-02	1.58E-02	2.04E-02	3.23E-03	8.18E-04
rb84	2.24E-02	1.53E-02	1.46E-02	3.22E-03	8.00E-04
tm168	2.21E-02	1.48E-02	1.60E-02	3.11E-03	7.73E-04
pr144	2.12E-02	1.47E-02	1.00E-02	3.06E-03	7.43E-04
fe59 ¹	1.97E-02	1.19E-02	9.70E-03	2.91E-03	3.57E-04
rh99	1.92E-02	1.19E-02	8.93E-03	2.64E-03	6.42E-04
tm165	1.80E-02	1.14E-02	9.10E-03	2.52E-03	6.11E-04
zr89	1.29E-02	7.86E-03	5.62E-03	1.76E-03	4.33E-04
rh102	1.24E-02	7.53E-03	5.93E-03	1.68E-03	4.07E-04
as71	1.16E-02	6.76E-03	5.99E-03	1.51E-03	3.70E-04
tc98	1.10E-02	4.62E-03	9.49E-03	1.05E-03	2.69E-04
ag108m	1.05E-02	4.21E-03	8.88E-03	9.77E-04	2.49E-04
ru106	9.55E-03	6.08E-03	4.73E-03	1.31E-03	3.21E-04
tc95m	9.44E-03	6.12E-03	7.01E-03	1.30E-03	3.24E-04
ir194m	1.06E-02	3.32E-03	6.86E-03	9.18E-04	2.23E-04
cs132	8.10E-03	3.69E-03	4.78E-03	8.84E-04	2.15E-04
rb86	7.93E-03	5.43E-03	4.39E-03	1.14E-03	2.85E-04
pm144	7.84E-03	1.79E-03	6.00E-03	5.43E-04	1.34E-04
nb95	7.33E-03	3.81E-03	6.64E-03	7.98E-04	2.07E-04
zr95	7.25E-03	3.76E-03	6.57E-03	7.88E-04	2.05E-04
lu171	6.84E-03	3.80E-03	5.52E-03	8.08E-04	2.05E-04
ho166	6.68E-03	4.30E-03	2.86E-03	9.54E-04	2.31E-04
zn65 ¹	5.98E-03	3.65E-03	3.27E-03	8.84E-04	1.09E-04
sb127	5.38E-03	2.44E-03	3.63E-03	5.73E-04	1.41E-04
tb153	5.40E-03	3.35E-03	3.17E-03	7.30E-04	1.78E-04
ag105	5.01E-03	2.79E-03	2.97E-03	6.22E-04	1.55E-04
te121m	4.92E-03	2.89E-03	2.37E-03	6.56E-04	1.59E-04
sb122	4.82E-03	2.40E-03	2.49E-03	5.71E-04	1.38E-04

Table 5.5.2-1 (Continued)

Radionuclide	NCT Surface 71.47(b)(1) or (2)			NCT 2 Meter 71.47(b)(3)	Normally occupied space 71.47(b)(4)
	Side	Bottom	Top		
pm146	4.61E-03	2.17E-03	4.01E-03	4.75E-04	1.22E-04
kr79	3.80E-03	2.10E-03	1.97E-03	4.84E-04	1.17E-04
i126	3.75E-03	1.68E-03	2.29E-03	4.05E-04	9.91E-05
gd149	3.71E-03	1.87E-03	2.63E-03	4.24E-04	1.05E-04
cd115m	3.49E-03	2.32E-03	1.76E-03	4.96E-04	1.21E-04
as74	3.20E-03	9.61E-04	1.84E-03	2.84E-04	6.68E-05
pm143	2.83E-03	1.47E-03	2.56E-03	3.08E-04	7.99E-05
cu64	2.54E-03	1.30E-03	1.22E-03	3.12E-04	7.49E-05
ba131	2.47E-03	1.19E-03	1.40E-03	2.84E-04	6.94E-05
cs134 ¹	2.25E-03	1.34E-03	1.61E-03	3.43E-04	4.36E-05
os185	2.15E-03	1.55E-03	1.86E-03	3.14E-04	7.92E-05
co58 ¹	2.01E-03	1.18E-03	1.35E-03	2.97E-04	3.83E-05
ce143	1.95E-03	9.61E-04	1.25E-03	2.24E-04	5.49E-05
sb125	1.62E-03	3.00E-04	1.18E-03	1.05E-04	2.54E-05
pm151	1.62E-03	6.63E-04	1.20E-03	1.62E-04	4.00E-05
sr85	1.61E-03	9.07E-05	1.04E-03	8.62E-05	1.89E-05
te121	1.60E-03	8.81E-05	1.03E-03	8.52E-05	1.86E-05
br77	2.06E-03	9.35E-04	1.33E-03	2.26E-04	5.55E-05
rb83	1.53E-03	1.16E-04	1.01E-03	8.54E-05	1.90E-05
mn54 ¹	1.05E-03	5.09E-04	9.71E-04	1.25E-04	1.65E-05
cm241	1.04E-03	2.41E-05	5.56E-04	5.29E-05	1.13E-05
lu176	1.02E-03	4.84E-06	5.22E-04	5.03E-05	1.05E-05
se75	1.00E-03	4.83E-06	5.14E-04	4.95E-05	1.03E-05
tc99m	5.12E-04	2.42E-06	2.62E-04	2.52E-05	5.27E-06
y87	9.93E-04	5.00E-06	5.09E-04	4.89E-05	1.02E-05
i131	9.19E-04	1.33E-04	5.96E-04	5.84E-05	1.36E-05
rh101	8.83E-04	4.18E-06	4.52E-04	4.35E-05	9.09E-06
mo99	2.41E-03	9.25E-04	1.83E-03	2.29E-04	5.70E-05
hf181	8.50E-04	6.10E-06	4.37E-04	4.20E-05	8.81E-06
y91	8.21E-04	5.33E-04	3.79E-04	1.15E-04	2.82E-05
ru103	7.53E-04	5.15E-05	4.44E-04	4.12E-05	9.16E-06
au198	7.21E-04	1.09E-04	3.83E-04	4.98E-05	1.13E-05
xe127	6.63E-04	3.25E-06	3.39E-04	3.26E-05	6.83E-06
bi210m	6.05E-04	3.45E-05	3.47E-04	3.25E-05	7.15E-06
ru97	5.93E-04	1.67E-05	3.14E-04	3.09E-05	6.59E-06
sn123	5.85E-04	4.01E-04	3.24E-04	8.39E-05	2.11E-05
yb169	5.81E-04	2.79E-06	2.97E-04	2.86E-05	5.98E-06
co57	5.78E-04	4.02E-06	2.97E-04	2.86E-05	5.99E-06

Table 5.5.2-1 (Continued)

Radionuclide	NCT Surface 71.47(b)(1) or (2)			NCT 2 Meter 71.47(b)(3)	Normally occupied space 71.47(b)(4)
	Side	Bottom	Top		
ta183	5.61E-04	2.66E-06	2.87E-04	2.76E-05	5.78E-06
np239	5.60E-04	2.65E-06	2.87E-04	2.76E-05	5.77E-06
ba133	5.60E-04	2.65E-06	2.87E-04	2.76E-05	5.77E-06
zr88	5.58E-04	2.64E-06	2.86E-04	2.75E-05	5.75E-06
zn72	5.55E-04	2.63E-06	2.84E-04	2.73E-05	5.71E-06
rh101m	5.41E-04	6.06E-06	2.86E-04	2.70E-05	5.67E-06
te132	5.28E-04	2.50E-06	2.70E-04	2.60E-05	5.44E-06
cf249	5.25E-04	2.91E-06	2.69E-04	2.59E-05	5.42E-06
cs129	5.24E-04	9.56E-05	2.95E-04	3.84E-05	8.74E-06
hf182	5.15E-04	2.44E-06	2.64E-04	2.54E-05	5.31E-06
sn117m	5.08E-04	2.41E-06	2.60E-04	2.50E-05	5.23E-06
cd115	5.08E-04	2.53E-05	3.19E-04	2.69E-05	5.85E-06
hf175	4.98E-04	2.36E-06	2.55E-04	2.45E-05	5.13E-06
u235	4.93E-04	2.37E-06	2.52E-04	2.43E-05	5.08E-06
ba140	4.86E-04	2.24E-05	3.02E-04	2.56E-05	5.55E-06
pt191	4.85E-04	3.11E-05	2.95E-04	2.65E-05	5.84E-06
te123m	4.82E-04	2.29E-06	2.47E-04	2.38E-05	4.97E-06
ag110	4.79E-04	2.45E-04	2.72E-04	5.61E-05	1.37E-05
in114m	4.73E-04	1.68E-04	3.76E-04	4.24E-05	1.06E-05
hg203	4.68E-04	2.22E-06	2.39E-04	2.30E-05	4.81E-06
cm247	4.67E-04	2.21E-06	2.39E-04	2.30E-05	4.80E-06
cf251	4.61E-04	2.18E-06	2.36E-04	2.27E-05	4.75E-06
ce139	4.59E-04	2.17E-06	2.35E-04	2.26E-05	4.72E-06
pu246	4.51E-04	2.14E-06	2.31E-04	2.22E-05	4.64E-06
sc47	3.90E-04	1.85E-06	2.00E-04	1.92E-05	4.02E-06
in113m	3.69E-04	1.75E-06	1.89E-04	1.81E-05	3.79E-06
u237	3.66E-04	1.73E-06	1.87E-04	1.80E-05	3.77E-06
cm243	3.62E-04	1.71E-06	1.85E-04	1.78E-05	3.73E-06
pa233	3.55E-04	1.68E-06	1.82E-04	1.75E-05	3.66E-06
ar37	3.41E-04	3.44E-05	2.13E-04	2.00E-05	4.54E-06
tb155	3.33E-04	2.13E-06	1.71E-04	1.65E-05	3.45E-06
er172	3.10E-04	2.32E-06	1.60E-04	1.54E-05	3.22E-06
lu177m	3.07E-04	1.45E-06	1.57E-04	1.51E-05	3.16E-06
cm245	3.04E-04	1.44E-06	1.56E-04	1.50E-05	3.13E-06
np236	2.95E-04	1.40E-06	1.51E-04	1.45E-05	3.04E-06
ga67	2.87E-04	2.16E-05	1.57E-04	1.69E-05	3.71E-06
cu67	2.86E-04	1.36E-06	1.46E-04	1.41E-05	2.95E-06
nd147	2.81E-04	1.90E-05	1.81E-04	1.53E-05	3.38E-06

Table 5.5.2-1 (Continued)

Radionuclide	NCT Surface 71.47(b)(1) or (2)			NCT 2 Meter 71.47(b)(3)	Normally occupied space 71.47(b)(4)
	Side	Bottom	Top		
au199	2.80E-04	1.32E-06	1.43E-04	1.38E-05	2.88E-06
ce141	2.77E-04	1.31E-06	1.42E-04	1.36E-05	2.85E-06
tm167	2.67E-04	2.58E-06	1.40E-04	1.32E-05	2.78E-06
cs137 ¹	2.58E-04	2.58E-05	1.80E-04	1.45E-05	1.76E-06
te129m	2.45E-04	1.06E-04	1.84E-04	2.47E-05	6.18E-06
th227	2.05E-04	2.99E-06	1.06E-04	1.04E-05	2.19E-06
ra223	2.01E-04	1.79E-06	1.04E-04	9.98E-06	2.10E-06
pu237	1.83E-04	8.65E-07	9.35E-05	9.00E-06	1.88E-06
sm153	1.75E-04	1.14E-06	8.99E-05	8.63E-06	1.81E-06
sn126	1.74E-04	8.23E-07	8.89E-05	8.56E-06	1.79E-06
os191	1.66E-04	7.89E-07	8.52E-05	8.20E-06	1.71E-06
nb95m	1.53E-04	1.40E-06	7.91E-05	7.63E-06	1.60E-06
rh105	1.40E-04	6.64E-07	7.17E-05	6.90E-06	1.44E-06
re189	1.33E-04	1.54E-06	7.05E-05	6.62E-06	1.39E-06
eu155	1.26E-04	5.96E-07	6.43E-05	6.19E-06	1.29E-06
gd153	1.23E-04	5.84E-07	6.31E-05	6.07E-06	1.27E-06
os193	1.23E-04	6.19E-06	6.92E-05	6.71E-06	1.45E-06
th229	1.19E-04	5.64E-07	6.09E-05	5.86E-06	1.23E-06
lu177	1.03E-04	4.86E-07	5.25E-05	5.05E-06	1.06E-06
hf172	9.56E-05	4.53E-07	4.89E-05	4.71E-06	9.85E-07
ba135m	8.95E-05	4.24E-07	4.58E-05	4.41E-06	9.22E-07
yb175	6.78E-05	3.21E-07	3.47E-05	3.34E-06	6.98E-07
eu149	6.68E-05	1.19E-06	3.65E-05	3.36E-06	7.12E-07
ce144	6.37E-05	3.02E-07	3.26E-05	3.14E-06	6.55E-07
be7	5.94E-05	2.81E-07	3.04E-05	2.92E-06	6.11E-07
cr51	5.79E-05	2.74E-07	2.96E-05	2.85E-06	5.96E-07
xe133m	5.74E-05	2.72E-07	2.94E-05	2.83E-06	5.91E-07
re186	5.64E-05	1.47E-06	2.99E-05	2.91E-06	6.22E-07
pm149	5.62E-05	2.70E-05	4.16E-05	6.43E-06	1.57E-06
pa231	5.47E-05	2.67E-07	2.80E-05	2.70E-06	5.64E-07
ir192	4.88E-05	4.30E-07	2.51E-05	2.43E-06	5.09E-07
ag111	4.81E-05	1.58E-06	2.55E-05	2.54E-06	5.44E-07
xe129m	2.63E-05	1.25E-07	1.35E-05	1.30E-06	2.71E-07
ra224	2.30E-05	1.51E-07	1.18E-05	1.14E-06	2.38E-07
ac225	2.28E-05	1.24E-07	1.17E-05	1.12E-06	2.35E-07
kr81	2.24E-05	1.06E-07	1.15E-05	1.10E-06	2.30E-07
ra226	2.01E-05	9.93E-08	1.03E-05	9.92E-07	2.07E-07
np237	1.95E-05	9.26E-08	1.00E-05	9.63E-07	2.01E-07

Table 5.5.2-1 (Continued)

Radionuclide	NCT Surface 71.47(b)(1) or (2)			NCT 2 Meter 71.47(b)(3)	Normally occupied space 71.47(b)(4)
	Side	Bottom	Top		
as77	1.88E-05	4.38E-07	1.05E-05	9.53E-07	2.03E-07
pt195m	1.74E-05	8.25E-08	8.91E-06	8.58E-07	1.79E-07
xe131m	1.13E-05	5.33E-08	5.76E-06	5.54E-07	1.16E-07
sn113	1.05E-05	5.74E-08	5.39E-06	5.18E-07	1.08E-07
th231	7.14E-06	3.38E-08	3.65E-06	3.51E-07	7.35E-08
kr85	7.04E-06	3.90E-07	4.54E-06	3.76E-07	8.21E-08
dy166	6.73E-06	3.19E-08	3.45E-06	3.32E-07	6.93E-08
nb91	5.32E-06	2.95E-07	3.43E-06	2.84E-07	6.21E-08
ni59	5.15E-06	2.86E-06	3.87E-06	6.27E-07	1.56E-07
am243	4.11E-06	3.15E-08	2.12E-06	2.04E-07	4.27E-08
w188	3.66E-06	1.73E-08	1.87E-06	1.80E-07	3.77E-08
th228	2.98E-06	1.70E-08	1.53E-06	1.47E-07	3.08E-08
tb161	2.79E-06	4.99E-08	1.53E-06	1.40E-07	2.97E-08
es254	2.56E-06	1.21E-08	1.31E-06	1.26E-07	2.63E-08
u230	1.88E-06	9.22E-09	9.62E-07	9.26E-08	1.94E-08
te125m	1.62E-06	7.67E-09	8.28E-07	7.97E-08	1.67E-08
th234	1.62E-06	7.66E-09	8.28E-07	7.97E-08	1.67E-08
la137	1.33E-06	2.74E-07	9.99E-07	8.85E-08	2.16E-08
rn222	1.23E-06	6.83E-08	7.96E-07	6.58E-08	1.44E-08
am242m	9.57E-07	4.53E-09	4.90E-07	4.71E-08	9.85E-09
w181	6.67E-07	3.16E-09	3.41E-07	3.29E-08	6.87E-09
pt193m	6.44E-07	3.05E-09	3.30E-07	3.17E-08	6.63E-09
es253	6.40E-07	2.88E-08	3.33E-07	3.50E-08	7.52E-09
te127m	5.89E-07	1.09E-07	4.32E-07	3.81E-08	9.22E-09
u232	4.51E-07	2.46E-09	2.31E-07	2.22E-08	4.65E-09
u233	4.50E-07	1.66E-08	2.30E-07	2.42E-08	5.16E-09
xe133	4.21E-07	1.99E-09	2.15E-07	2.07E-08	4.33E-09
th230	4.03E-07	1.92E-09	2.06E-07	1.99E-08	4.15E-09
ac227	2.38E-07	1.13E-09	1.22E-07	1.17E-08	2.45E-09
am241	2.14E-07	1.52E-08	1.22E-07	1.21E-08	2.68E-09
u234	2.08E-07	1.02E-09	1.07E-07	1.03E-08	2.14E-09
po210	1.69E-07	1.28E-07	1.46E-07	2.59E-08	6.50E-09
pd103	1.66E-07	7.85E-10	8.48E-08	8.16E-09	1.71E-09
th232	1.57E-07	7.46E-10	8.05E-08	7.75E-09	1.62E-09
cd113m	1.32E-07	6.24E-10	6.74E-08	6.49E-09	1.36E-09
u236	1.15E-07	5.43E-10	5.87E-08	5.65E-09	1.18E-09
v49	1.09E-07	8.22E-10	5.66E-08	5.39E-09	1.13E-09
w185	1.07E-07	5.06E-10	5.46E-08	5.26E-09	1.10E-09

Table 5.5.2-1 (Continued)

Radionuclide	NCT Surface 71.47(b)(1) or (2)			NCT 2 Meter 71.47(b)(3)	Normally occupied space 71.47(b)(4)
	Side	Bottom	Top		
pu239	1.03E-07	2.08E-09	5.42E-08	5.26E-09	1.12E-09
pu236	8.60E-08	2.57E-09	4.69E-08	4.42E-09	9.48E-10
cf252	8.54E-08	4.04E-10	4.37E-08	4.20E-09	8.79E-10
u238	6.15E-08	2.92E-10	3.15E-08	3.03E-09	6.34E-10
cl36	5.51E-08	3.06E-09	3.56E-08	2.94E-09	6.43E-10
pu240	4.44E-08	4.12E-10	2.29E-08	2.21E-09	4.64E-10
cm242	4.25E-08	9.80E-09	2.48E-08	3.37E-09	7.87E-10
sr90	3.91E-08	2.73E-08	1.86E-08	5.67E-09	1.38E-09
ca41	2.79E-08	1.32E-10	1.43E-08	1.37E-09	2.87E-10
cm244	2.22E-08	9.60E-09	1.61E-08	2.38E-09	5.80E-10
sm145	2.00E-08	9.46E-11	1.02E-08	9.84E-10	2.06E-10
pu242	1.64E-08	7.79E-11	8.41E-09	8.10E-10	1.69E-10
pm147	1.64E-08	7.75E-11	8.37E-09	8.06E-10	1.68E-10
pu238	1.21E-08	3.95E-09	7.93E-09	1.09E-09	2.65E-10
er169	7.46E-09	3.54E-11	3.82E-09	3.68E-10	7.68E-11
fe55	7.02E-09	3.33E-11	3.59E-09	3.46E-10	7.23E-11
pu241	3.12E-09	1.48E-11	1.60E-09	1.54E-10	3.21E-11
bi210	5.83E-10	2.76E-12	2.99E-10	2.87E-11	6.01E-12
bk249	2.17E-10	1.03E-12	1.11E-10	1.07E-11	2.23E-12
pr143	8.82E-11	4.58E-11	7.99E-11	9.59E-12	2.49E-12
tc97	1.97E-11	9.34E-14	1.01E-11	9.71E-13	2.03E-13
ca45	1.96E-11	9.30E-14	1.00E-11	9.67E-13	2.02E-13
ge71	1.96E-11	9.30E-14	1.00E-11	9.67E-13	2.02E-13
nb93m	1.96E-11	9.30E-14	1.00E-11	9.67E-13	2.02E-13
mo93	1.96E-11	9.30E-14	1.00E-11	9.67E-13	2.02E-13
tc97m	1.96E-11	9.30E-14	1.00E-11	9.67E-13	2.02E-13
cd109	1.96E-11	9.30E-14	1.00E-11	9.67E-13	2.02E-13
sn113m	1.96E-11	9.30E-14	1.00E-11	9.67E-13	2.02E-13
sn119m	1.96E-11	9.30E-14	1.00E-11	9.67E-13	2.02E-13
sn121m	1.96E-11	9.30E-14	1.00E-11	9.67E-13	2.02E-13
te123	1.96E-11	9.30E-14	1.00E-11	9.67E-13	2.02E-13
i125	1.96E-11	9.30E-14	1.00E-11	9.67E-13	2.02E-13
i129	1.96E-11	9.30E-14	1.00E-11	9.67E-13	2.02E-13
cs131	1.96E-11	9.30E-14	1.00E-11	9.67E-13	2.02E-13
pm145	1.96E-11	9.30E-14	1.00E-11	9.67E-13	2.02E-13
sm151	1.96E-11	9.30E-14	1.00E-11	9.67E-13	2.02E-13
tb157	1.96E-11	9.30E-14	1.00E-11	9.67E-13	2.02E-13
dy159	1.96E-11	9.30E-14	1.00E-11	9.67E-13	2.02E-13

Table 5.5.2-1 (Continued)

Radionuclide	NCT Surface 71.47(b)(1) or (2)			NCT 2 Meter 71.47(b)(3)	Normally occupied space 71.47(b)(4)
	Side	Bottom	Top		
tm170	1.96E-11	9.30E-14	1.00E-11	9.67E-13	2.02E-13
tm171	1.96E-11	9.30E-14	1.00E-11	9.67E-13	2.02E-13
os194	1.96E-11	9.30E-14	1.00E-11	9.67E-13	2.02E-13
pt193	1.96E-11	9.30E-14	1.00E-11	9.67E-13	2.02E-13
tl204	1.96E-11	9.30E-14	1.00E-11	9.67E-13	2.02E-13
pb205	1.96E-11	9.30E-14	1.00E-11	9.67E-13	2.02E-13
pb210	1.96E-11	9.30E-14	1.00E-11	9.67E-13	2.02E-13
ra225	1.96E-11	9.30E-14	1.00E-11	9.67E-13	2.02E-13
ra228	1.96E-11	9.30E-14	1.00E-11	9.67E-13	2.02E-13
np235	1.96E-11	9.30E-14	1.00E-11	9.67E-13	2.02E-13
cm246	1.96E-11	9.30E-14	1.00E-11	9.67E-13	2.02E-13
cm248	1.96E-11	9.30E-14	1.00E-11	9.67E-13	2.02E-13
cf250	1.96E-11	9.30E-14	1.00E-11	9.67E-13	2.02E-13
se72	1.96E-11	9.30E-14	1.00E-11	9.67E-13	2.02E-13
as73	1.96E-11	9.30E-14	1.00E-11	9.67E-13	2.02E-13
te118	1.96E-11	9.30E-14	1.00E-11	9.67E-13	2.02E-13
sb119	1.96E-11	9.30E-14	1.00E-11	9.67E-13	2.02E-13
nd140	1.96E-11	9.30E-14	1.00E-11	9.67E-13	2.02E-13
yb166	1.96E-11	9.30E-14	1.00E-11	9.67E-13	2.02E-13
h3	1.96E-11	9.30E-14	1.00E-11	9.67E-13	2.02E-13
ni63	1.96E-11	9.30E-14	1.00E-11	9.67E-13	2.02E-13
sr89	1.96E-11	9.30E-14	1.00E-11	9.67E-13	2.02E-13
tc99	1.96E-11	9.30E-14	1.00E-11	9.67E-13	2.02E-13
am242	1.96E-11	9.30E-14	1.00E-11	9.67E-13	2.02E-13
c14	1.96E-11	9.30E-14	1.00E-11	9.67E-13	2.02E-13

Note 1: Marked nuclides are analyzed individually.

Table 5.5.2-2 HAC Gamma Dose Rate Responses (mrem/hr/Ci)

Radionuclide	HAC 1 Meter 71.51(a)(2)		
	Side	Bottom	Top
na24	2.23E+00	3.47E+00	3.41E+00
bi208	1.93E+00	3.11E+00	3.07E+00
cs144	1.43E+00	2.20E+00	2.27E+00
y88	8.44E-01	1.17E+00	1.03E+00
la140	5.64E-01	7.20E-01	6.62E-01
sb124	4.20E-01	5.41E-01	4.79E-01
eu156	3.77E-01	5.17E-01	4.86E-01
sc48	4.91E-01	4.79E-01	4.80E-01
la138	2.71E-01	3.20E-01	2.89E-01
tb156	2.81E-01	3.02E-01	2.83E-01
ag106m	3.09E-01	2.75E-01	2.73E-01
lu169	2.32E-01	2.68E-01	2.50E-01
na22	2.53E-01	2.42E-01	2.32E-01
sb120m	3.02E-01	2.40E-01	2.56E-01
i124	1.79E-01	2.12E-01	1.96E-01
br82	2.61E-01	2.12E-01	2.16E-01
lu172	2.25E-01	1.93E-01	1.97E-01
ta182	1.94E-01	1.86E-01	1.84E-01
ca47	1.69E-01	1.81E-01	1.70E-01
sc46	2.34E-01	1.71E-01	1.91E-01
te131m	1.68E-01	1.53E-01	1.56E-01
eu152	1.58E-01	1.52E-01	1.47E-01
as72	1.64E-01	1.40E-01	1.52E-01
tm172	1.06E-01	1.30E-01	1.17E-01
eu154	1.53E-01	1.35E-01	1.35E-01
pm148	1.01E-01	1.13E-01	1.04E-01
cs136	1.86E-01	1.26E-01	1.41E-01
ge69	1.13E-01	9.91E-02	1.01E-01
tb160	1.20E-01	8.54E-02	9.54E-02
rh102m	1.41E-01	7.07E-02	8.57E-02
sn125	5.79E-02	6.61E-02	6.56E-02
gd147	1.05E-01	6.65E-02	7.37E-02
sr83	6.71E-02	5.33E-02	5.44E-02
tc96	1.81E-01	6.47E-02	9.92E-02
k40	4.14E-02	5.12E-02	4.56E-02
co60 ¹	6.08E-02	8.49E-02	7.11E-02

Table 5.5.2-2 (Continued)

Radionuclide	HAC 1 Meter 71.51(a)(2)		
	Side	Bottom	Top
as76	4.18E-02	4.21E-02	4.10E-02
nb92	1.02E-01	4.31E-02	6.02E-02
np238	6.39E-02	4.10E-02	4.85E-02
am240	8.10E-02	3.64E-02	5.08E-02
tb158	6.46E-02	3.35E-02	4.39E-02
sb126	1.32E-01	2.21E-02	4.51E-02
ag110m ¹	3.82E-02	4.20E-02	3.62E-02
ho166m	9.97E-02	2.63E-02	4.41E-02
pa232	6.34E-02	2.50E-02	3.65E-02
pm148m	1.04E-01	2.90E-02	4.49E-02
nb94	1.03E-01	2.46E-02	4.76E-02
rb84	5.68E-02	2.14E-02	3.06E-02
tm168	7.58E-02	2.19E-02	3.56E-02
pr144	1.16E-02	1.70E-02	1.60E-02
fe59 ¹	2.51E-02	3.07E-02	2.71E-02
rh99	2.80E-02	1.53E-02	1.63E-02
tm165	3.13E-02	1.56E-02	1.80E-02
zr89	1.48E-02	9.89E-03	9.80E-03
rh102	2.19E-02	9.97E-03	1.15E-02
as71	3.09E-02	9.34E-03	1.20E-02
tc98	7.31E-02	7.49E-03	2.30E-02
ag108m	7.54E-02	6.82E-03	2.16E-02
ru106	1.33E-02	7.62E-03	8.54E-03
tc95m	3.84E-02	9.16E-03	1.57E-02
ir194m	8.27E-02	5.04E-03	1.63E-02
cs132	3.35E-02	5.14E-03	1.05E-02
rb86	1.05E-02	7.74E-03	8.49E-03
pm144	6.58E-02	3.02E-03	1.48E-02
nb95	4.42E-02	6.11E-03	1.60E-02
zr95	4.37E-02	6.04E-03	1.58E-02
lu171	3.32E-02	5.86E-03	1.29E-02
ho166	4.45E-03	5.59E-03	5.07E-03
zn65 ¹	9.75E-03	9.59E-03	9.52E-03
sb127	2.83E-02	3.62E-03	8.34E-03
tb153	1.69E-02	4.80E-03	6.80E-03
ag105	2.04E-02	4.03E-03	6.31E-03
te121m	1.29E-02	3.95E-03	4.81E-03
sb122	1.67E-02	3.30E-03	5.18E-03

Table 5.5.2-2 (Continued)

Radionuclide	HAC 1 Meter 71.51(a)(2)		
	Side	Bottom	Top
pm146	3.23E-02	3.49E-03	9.73E-03
kr79	1.16E-02	2.89E-03	4.15E-03
i126	1.83E-02	2.38E-03	5.05E-03
gd149	2.34E-02	2.86E-03	6.23E-03
cd115m	3.85E-03	3.22E-03	3.37E-03
as74	2.24E-02	1.29E-03	4.22E-03
pm143	1.71E-02	2.36E-03	6.16E-03
cu64	7.86E-03	1.74E-03	2.53E-03
ba131	1.58E-02	1.72E-03	3.12E-03
cs134 ¹	9.51E-03	3.76E-03	5.00E-03
os185	8.83E-03	2.38E-03	4.31E-03
co58 ¹	6.81E-03	3.13E-03	4.01E-03
ce143	1.08E-02	1.40E-03	2.86E-03
sb125	1.60E-02	5.12E-04	2.95E-03
pm151	1.39E-02	1.04E-03	2.93E-03
sr85	1.80E-02	1.63E-04	2.67E-03
te121	1.79E-02	1.59E-04	2.65E-03
br77	1.28E-02	1.38E-03	3.03E-03
rb83	1.68E-02	2.02E-04	2.57E-03
mn54 ¹	6.38E-03	1.53E-03	3.11E-03
cm241	1.78E-02	4.96E-05	1.54E-03
lu176	1.84E-02	1.76E-05	1.47E-03
se75	1.81E-02	1.75E-05	1.45E-03
tc99m	9.23E-03	8.84E-06	7.36E-04
y87	1.79E-02	1.76E-05	1.43E-03
i131	1.21E-02	2.24E-04	1.55E-03
rh101	1.59E-02	1.52E-05	1.27E-03
mo99	2.13E-02	1.46E-03	4.49E-03
hf181	1.52E-02	1.81E-05	1.23E-03
y91	6.64E-04	7.26E-04	6.81E-04
ru103	1.13E-02	9.23E-05	1.19E-03
au198	1.03E-02	1.63E-04	9.99E-04
xe127	1.20E-02	1.16E-05	9.53E-04
bi210m	9.41E-03	6.28E-05	9.37E-04
ru97	1.03E-02	3.18E-05	8.71E-04
sn123	7.75E-04	5.71E-04	6.25E-04
yb169	1.05E-02	1.01E-05	8.36E-04
co57	1.04E-02	1.21E-05	8.34E-04

Table 5.5.2-2 (Continued)

Radionuclide	HAC 1 Meter 71.51(a)(2)		
	Side	Bottom	Top
ta183	1.01E-02	9.69E-06	8.07E-04
np239	1.01E-02	9.68E-06	8.06E-04
ba133	1.01E-02	9.68E-06	8.06E-04
zr88	1.01E-02	9.64E-06	8.03E-04
zn72	1.00E-02	9.58E-06	7.98E-04
rh101m	9.28E-03	1.51E-05	7.94E-04
te132	9.53E-03	9.12E-06	7.60E-04
cf249	9.46E-03	9.73E-06	7.56E-04
cs129	6.96E-03	1.46E-04	7.68E-04
hf182	9.30E-03	8.90E-06	7.41E-04
sn117m	9.17E-03	8.78E-06	7.31E-04
cd115	6.07E-03	4.62E-05	8.28E-04
hf175	9.00E-03	8.61E-06	7.17E-04
u235	8.90E-03	8.57E-06	7.09E-04
ba140	6.03E-03	4.12E-05	7.87E-04
pt191	6.43E-03	5.50E-05	7.76E-04
te123m	8.71E-03	8.33E-06	6.94E-04
ag110	1.58E-03	3.22E-04	5.58E-04
in114m	4.22E-03	2.72E-04	9.30E-04
hg203	8.44E-03	8.08E-06	6.73E-04
cm247	8.42E-03	8.06E-06	6.71E-04
cf251	8.32E-03	7.96E-06	6.63E-04
ce139	8.28E-03	7.92E-06	6.60E-04
pu246	8.14E-03	7.79E-06	6.49E-04
sc47	7.04E-03	6.74E-06	5.61E-04
in113m	6.65E-03	6.37E-06	5.30E-04
u237	6.61E-03	6.32E-06	5.26E-04
cm243	6.53E-03	6.25E-06	5.20E-04
pa233	6.41E-03	6.13E-06	5.11E-04
ar37	4.60E-03	5.91E-05	5.58E-04
tb155	5.97E-03	6.66E-06	4.81E-04
er172	5.55E-03	6.71E-06	4.48E-04
lu177m	5.53E-03	5.30E-06	4.41E-04
cm245	5.49E-03	5.26E-06	4.38E-04
np236	5.32E-03	5.09E-06	4.24E-04
ga67	4.79E-03	3.59E-05	4.30E-04
cu67	5.16E-03	4.94E-06	4.11E-04
nd147	3.24E-03	3.40E-05	4.66E-04

Table 5.5.2-2 (Continued)

Radionuclide	HAC 1 Meter 71.51(a)(2)		
	Side	Bottom	Top
au199	5.05E-03	4.83E-06	4.02E-04
ce141	4.99E-03	4.78E-06	3.98E-04
tm167	4.63E-03	6.76E-06	3.89E-04
cs137 ¹	2.60E-03	8.58E-05	5.87E-04
te129m	1.41E-03	1.63E-04	4.29E-04
th227	3.66E-03	6.58E-06	2.97E-04
ra223	3.58E-03	4.84E-06	2.91E-04
pu237	3.30E-03	3.16E-06	2.63E-04
sm153	3.13E-03	3.53E-06	2.52E-04
sn126	3.14E-03	3.00E-06	2.50E-04
os191	3.00E-03	2.88E-06	2.39E-04
nb95m	2.75E-03	3.71E-06	2.22E-04
rh105	2.53E-03	2.42E-06	2.02E-04
re189	2.27E-03	3.79E-06	1.95E-04
eu155	2.27E-03	2.17E-06	1.81E-04
gd153	2.22E-03	2.13E-06	1.77E-04
os193	1.91E-03	1.09E-05	1.87E-04
th229	2.15E-03	2.06E-06	1.71E-04
lu177	1.85E-03	1.77E-06	1.48E-04
hf172	1.73E-03	1.65E-06	1.38E-04
ba135m	1.62E-03	1.55E-06	1.29E-04
yb175	1.22E-03	1.17E-06	9.75E-05
eu149	1.08E-03	2.59E-06	1.00E-04
ce144	1.15E-03	1.10E-06	9.16E-05
be7	1.07E-03	1.03E-06	8.54E-05
cr51	1.04E-03	9.99E-07	8.32E-05
xe133m	1.04E-03	9.92E-07	8.26E-05
re186	9.85E-04	2.89E-06	8.30E-05
pm149	4.85E-04	4.16E-05	1.01E-04
pa231	9.87E-04	9.58E-07	7.87E-05
ir192	8.75E-04	1.16E-06	7.04E-05
ag111	8.35E-04	2.92E-06	7.06E-05
xe129m	4.76E-04	4.55E-07	3.79E-05
ra224	4.14E-04	4.67E-07	3.32E-05
ac225	4.09E-04	4.20E-07	3.28E-05
kr81	4.04E-04	3.87E-07	3.22E-05
ra226	3.63E-04	3.54E-07	2.90E-05
np237	3.53E-04	3.38E-07	2.81E-05

Table 5.5.2-2 (Continued)

Radionuclide	HAC 1 Meter 71.51(a)(2)		
	Side	Bottom	Top
as77	2.90E-04	8.95E-07	2.85E-05
pt195m	3.14E-04	3.01E-07	2.51E-05
xe131m	2.03E-04	1.94E-07	1.62E-05
sn113	1.89E-04	1.94E-07	1.51E-05
th231	1.29E-04	1.23E-07	1.03E-05
kr85	7.87E-05	7.05E-07	1.17E-05
dy166	1.22E-04	1.16E-07	9.69E-06
nb91	5.95E-05	5.33E-07	8.82E-06
ni59	2.69E-05	4.36E-06	9.01E-06
am243	7.36E-05	9.09E-08	5.94E-06
w188	6.60E-05	6.32E-08	5.26E-06
th228	5.37E-05	5.58E-08	4.28E-06
tb161	4.52E-05	1.08E-07	4.18E-06
es254	4.61E-05	4.42E-08	3.68E-06
u230	3.39E-05	3.30E-08	2.70E-06
te125m	2.92E-05	2.80E-08	2.33E-06
th234	2.92E-05	2.79E-08	2.33E-06
la137	1.19E-05	4.67E-07	2.48E-06
rn222	1.38E-05	1.23E-07	2.04E-06
am242m	1.73E-05	1.65E-08	1.38E-06
w181	1.20E-05	1.15E-08	9.60E-07
pt193m	1.16E-05	1.11E-08	9.26E-07
es253	1.09E-05	4.85E-08	9.19E-07
te127m	5.54E-06	1.87E-07	1.08E-06
u232	8.12E-06	8.29E-09	6.49E-07
u233	7.75E-06	2.75E-08	6.37E-07
xe133	7.60E-06	7.27E-09	6.05E-07
th230	7.27E-06	6.98E-09	5.80E-07
ac227	4.29E-06	4.11E-09	3.42E-07
am241	3.43E-06	2.63E-08	3.30E-07
u234	3.75E-06	3.66E-09	3.00E-07
po210	6.48E-07	1.96E-07	3.38E-07
pd103	2.99E-06	2.86E-09	2.38E-07
th232	2.84E-06	2.72E-09	2.26E-07
cd113m	2.38E-06	2.28E-09	1.90E-07
u236	2.07E-06	1.98E-09	1.65E-07
v49	1.92E-06	2.38E-09	1.58E-07
w185	1.93E-06	1.84E-09	1.54E-07

Table 5.5.2-2 (Continued)

Radionuclide	HAC 1 Meter 71.51(a)(2)		
	Side	Bottom	Top
pu239	1.81E-06	4.31E-09	1.51E-07
pu236	1.43E-06	5.06E-09	1.29E-07
cf252	1.54E-06	1.47E-09	1.23E-07
u238	1.11E-06	1.06E-09	8.85E-08
cl36	6.17E-07	5.52E-09	9.15E-08
pu240	7.94E-07	1.09E-09	6.42E-08
cm242	5.11E-07	1.48E-08	6.27E-08
sr90	2.04E-08	3.13E-08	2.95E-08
ca41	5.04E-07	4.82E-10	4.02E-08
cm244	2.00E-07	1.49E-08	3.94E-08
sm145	3.60E-07	3.45E-10	2.87E-08
pu242	2.97E-07	2.84E-10	2.36E-08
pm147	2.95E-07	2.83E-10	2.35E-08
pu238	1.28E-07	6.08E-09	1.96E-08
er169	1.35E-07	1.29E-10	1.07E-08
fe55	1.27E-07	1.21E-10	1.01E-08
pu241	5.63E-08	5.39E-11	4.49E-09
bi210	1.05E-08	1.01E-11	8.39E-10
bk249	3.92E-09	3.75E-12	3.12E-10
pr143	5.32E-10	7.35E-11	1.92E-10
tc97	3.56E-10	3.40E-13	2.83E-11
ca45	3.54E-10	3.39E-13	2.82E-11
ge71	3.54E-10	3.39E-13	2.82E-11
nb93m	3.54E-10	3.39E-13	2.82E-11
mo93	3.54E-10	3.39E-13	2.82E-11
tc97m	3.54E-10	3.39E-13	2.82E-11
cd109	3.54E-10	3.39E-13	2.82E-11
sn113m	3.54E-10	3.39E-13	2.82E-11
sn119m	3.54E-10	3.39E-13	2.82E-11
sn121m	3.54E-10	3.39E-13	2.82E-11
te123	3.54E-10	3.39E-13	2.82E-11
i125	3.54E-10	3.39E-13	2.82E-11
i129	3.54E-10	3.39E-13	2.82E-11
cs131	3.54E-10	3.39E-13	2.82E-11
pm145	3.54E-10	3.39E-13	2.82E-11
sm151	3.54E-10	3.39E-13	2.82E-11
tb157	3.54E-10	3.39E-13	2.82E-11
dy159	3.54E-10	3.39E-13	2.82E-11

Table 5.5.2-2 (Continued)

Radionuclide	HAC 1 Meter 71.51(a)(2)		
	Side	Bottom	Top
tm170	3.54E-10	3.39E-13	2.82E-11
tm171	3.54E-10	3.39E-13	2.82E-11
os194	3.54E-10	3.39E-13	2.82E-11
pt193	3.54E-10	3.39E-13	2.82E-11
tl204	3.54E-10	3.39E-13	2.82E-11
pb205	3.54E-10	3.39E-13	2.82E-11
pb210	3.54E-10	3.39E-13	2.82E-11
ra225	3.54E-10	3.39E-13	2.82E-11
ra228	3.54E-10	3.39E-13	2.82E-11
np235	3.54E-10	3.39E-13	2.82E-11
cm246	3.54E-10	3.39E-13	2.82E-11
cm248	3.54E-10	3.39E-13	2.82E-11
cf250	3.54E-10	3.39E-13	2.82E-11
se72	3.54E-10	3.39E-13	2.82E-11
as73	3.54E-10	3.39E-13	2.82E-11
te118	3.54E-10	3.39E-13	2.82E-11
sb119	3.54E-10	3.39E-13	2.82E-11
nd140	3.54E-10	3.39E-13	2.82E-11
yb166	3.54E-10	3.39E-13	2.82E-11
h3	3.54E-10	3.39E-13	2.82E-11
ni63	3.54E-10	3.39E-13	2.82E-11
sr89	3.54E-10	3.39E-13	2.82E-11
tc99	3.54E-10	3.39E-13	2.82E-11
am242	3.54E-10	3.39E-13	2.82E-11
c14	3.54E-10	3.39E-13	2.82E-11

Note 1: Marked nuclides are analyzed individually.

5.5.3 Radionuclide Maximum Ci/g Loading Limits

Table 5.5.3-1 Radionuclide Maximum Ci/g Loading Limits based on Gamma Response

Ordered by Alphanumeric			Ordered by Atomic Number		
Radionuclide	Max. Ci/g	Condition	Radionuclide	Max. Ci/g	Condition
ac225	5.06E-01	HAC	h3	5.83E+05	HAC
ac227	4.82E+01	HAC	be7	1.93E-01	HAC
ag105	3.32E-03	NCT	c14	5.83E+05	HAC
ag106m	4.45E-05	NCT	na22	5.38E-05	NCT
ag108m	2.12E-03	NCT	na24	3.38E-06	NCT
ag110	3.68E-02	NCT	cl36	3.35E+02	HAC
ag110m¹	4.84E-04	NCT	ar37	4.49E-02	HAC
ag111	2.47E-01	HAC	k40	2.42E-04	NCT
am240	4.09E-04	NCT	ca41	4.10E+02	HAC
am241	6.02E+01	HAC	ca45	5.83E+05	HAC
am242	5.83E+05	HAC	sc46	7.66E-05	NCT
am242m	1.20E+01	HAC	ca47	7.23E-05	NCT
am243	2.81E+00	HAC	sc47	2.93E-02	HAC
ar37	4.49E-02	HAC	sc48	2.67E-05	NCT
as71	1.37E-03	NCT	v49	1.07E+02	HAC
as72	8.49E-05	NCT	cr51	1.98E-01	HAC
as73	5.83E+05	HAC	mn54¹	1.65E-02	NCT
as74	7.27E-03	NCT	fe55	1.63E+03	HAC
as76	2.84E-04	NCT	co57	1.99E-02	HAC
as77	7.12E-01	HAC	co58¹	6.96E-03	NCT
au198	2.01E-02	HAC	fe59¹	7.11E-04	NCT
au199	4.09E-02	HAC	ni59	3.30E+00	NCT
ba131	7.28E-03	NCT	co60¹	2.50E-04	NCT
ba133	2.04E-02	HAC	ni63	5.83E+05	HAC
ba135m	1.28E-01	HAC	cu64	6.61E-03	NCT
ba140	3.43E-02	HAC	zn65¹	2.34E-03	NCT
be7	1.93E-01	HAC	cu67	4.00E-02	HAC
bi208	3.76E-06	NCT	ga67	4.31E-02	HAC
bi210	1.96E+04	HAC	ge69	1.25E-04	NCT
bi210m	2.20E-02	HAC	as71	1.37E-03	NCT
bk249	5.28E+04	HAC	ge71	5.83E+05	HAC
br77	9.13E-03	NCT	as72	8.49E-05	NCT
br82	5.93E-05	NCT	se72	5.83E+05	HAC
c14	5.83E+05	HAC	zn72	2.06E-02	HAC
ca41	4.10E+02	HAC	as73	5.83E+05	HAC
ca45	5.83E+05	HAC	as74	7.27E-03	NCT

Table 5.5.3-1 (Continued)

Ordered by Alphanumeric			Ordered by Atomic Number		
Radionuclide	Max. Ci/g	Condition	Radionuclide	Max. Ci/g	Condition
ca47	7.23E-05	NCT	se75	1.14E-02	HAC
cd109	5.83E+05	HAC	as76	2.84E-04	NCT
cd113m	8.69E+01	HAC	as77	7.12E-01	HAC
cd115	3.40E-02	HAC	br77	9.13E-03	NCT
cd115m	4.17E-03	NCT	kr79	4.27E-03	NCT
ce139	2.50E-02	HAC	kr81	5.11E-01	HAC
ce141	4.14E-02	HAC	br82	5.93E-05	NCT
ce143	9.23E-03	NCT	rb83	1.23E-02	HAC
ce144	1.80E-01	HAC	sr83	2.25E-04	NCT
cf249	2.18E-02	HAC	rb84	6.41E-04	NCT
cf250	5.83E+05	HAC	kr85	2.62E+00	HAC
cf251	2.48E-02	HAC	sr85	1.15E-02	HAC
cf252	1.34E+02	HAC	rb86	1.82E-03	NCT
cl36	3.35E+02	HAC	y87	1.16E-02	HAC
cm241	1.16E-02	HAC	y88	1.02E-05	NCT
cm242	4.05E+02	HAC	zr88	2.05E-02	HAC
cm243	3.16E-02	HAC	sr89	5.83E+05	HAC
cm244	8.69E+02	NCT	zr89	1.18E-03	NCT
cm245	3.76E-02	HAC	sr90	3.64E+02	NCT
cm246	5.83E+05	HAC	nb91	3.47E+00	HAC
cm247	2.45E-02	HAC	y91	1.80E-02	NCT
cm248	5.83E+05	HAC	nb92	3.41E-04	NCT
co57	1.99E-02	HAC	mo93	5.83E+05	HAC
co58¹	6.96E-03	NCT	nb93m	5.83E+05	HAC
co60¹	2.50E-04	NCT	nb94	6.40E-04	NCT
cr51	1.98E-01	HAC	nb95	2.59E-03	NCT
cs129	2.97E-02	HAC	zr95	2.62E-03	NCT
cs131	5.83E+05	HAC	nb95m	7.52E-02	HAC
cs132	2.34E-03	NCT	tc95m	1.59E-03	NCT
cs134¹	6.03E-03	NCT	tc96	2.23E-04	NCT
cs136	1.09E-04	NCT	ru97	2.01E-02	HAC
cs137¹	7.95E-02	HAC	tc97	5.81E+05	HAC
cs144	5.27E-06	NCT	tc97m	5.83E+05	HAC
cu64	6.61E-03	NCT	tc98	1.97E-03	NCT
cu67	4.00E-02	HAC	mo99	9.03E-03	NCT
dy159	5.83E+05	HAC	rh99	7.83E-04	NCT
dy166	1.70E+00	HAC	tc99	5.83E+05	HAC
er169	1.53E+03	HAC	tc99m	2.24E-02	HAC

Table 5.5.3-1 (Continued)

Ordered by Alphanumeric			Ordered by Atomic Number		
Radionuclide	Max. Ci/g	Condition	Radionuclide	Max. Ci/g	Condition
er172	3.72E-02	HAC	rh101	1.30E-02	HAC
es253	1.90E+01	HAC	rh101m	2.23E-02	HAC
es254	4.48E+00	HAC	rh102	1.23E-03	NCT
eu149	1.91E-01	HAC	rh102m	1.88E-04	NCT
eu152	8.35E-05	NCT	pd103	6.91E+01	HAC
eu154	9.69E-05	NCT	ru103	1.83E-02	HAC
eu155	9.11E-02	HAC	ag105	3.32E-03	NCT
eu156	2.26E-05	NCT	rh105	8.17E-02	HAC
fe55	1.63E+03	HAC	ru106	1.57E-03	NCT
fe59¹	7.11E-04	NCT	ag106m	4.45E-05	NCT
ga67	4.31E-02	HAC	ag108m	2.12E-03	NCT
gd147	1.93E-04	NCT	cd109	5.83E+05	HAC
gd149	4.88E-03	NCT	ag110	3.68E-02	NCT
gd153	9.29E-02	HAC	ag110m¹	4.84E-04	NCT
ge69	1.25E-04	NCT	ag111	2.47E-01	HAC
ge71	5.83E+05	HAC	sn113	1.09E+00	HAC
h3	5.83E+05	HAC	cd113m	8.69E+01	HAC
hf172	1.20E-01	HAC	in113m	3.11E-02	HAC
hf175	2.30E-02	HAC	sn113m	5.83E+05	HAC
hf181	1.36E-02	HAC	in114m	4.87E-02	NCT
hf182	2.22E-02	HAC	cd115	3.40E-02	HAC
hg203	2.45E-02	HAC	cd115m	4.17E-03	NCT
ho166	2.17E-03	NCT	sn117m	2.25E-02	HAC
ho166m	5.45E-04	NCT	te118	5.83E+05	HAC
i124	5.54E-05	NCT	sb119	5.83E+05	HAC
i125	5.83E+05	HAC	sn119m	5.83E+05	HAC
i126	5.10E-03	NCT	sb120m	5.51E-05	NCT
i129	5.83E+05	HAC	te121	1.15E-02	HAC
i131	1.71E-02	HAC	sn121m	5.83E+05	HAC
in113m	3.11E-02	HAC	te121m	3.15E-03	NCT
in114m	4.87E-02	NCT	sb122	3.62E-03	NCT
ir192	2.36E-01	HAC	sn123	2.46E-02	NCT
ir194m	2.25E-03	NCT	te123	5.83E+05	HAC
k40	2.42E-04	NCT	te123m	2.37E-02	HAC
kr79	4.27E-03	NCT	i124	5.54E-05	NCT
kr81	5.11E-01	HAC	sb124	2.19E-05	NCT
kr85	2.62E+00	HAC	i125	5.83E+05	HAC
la137	1.73E+01	HAC	sb125	1.29E-02	HAC

Table 5.5.3-1 (Continued)

Ordered by Alphanumeric			Ordered by Atomic Number		
Radionuclide	Max. Ci/g	Condition	Radionuclide	Max. Ci/g	Condition
la138	3.87E-05	NCT	sn125	1.82E-04	NCT
la140	1.63E-05	NCT	te125m	7.07E+00	HAC
lu169	4.55E-05	NCT	i126	5.10E-03	NCT
lu171	2.56E-03	NCT	sb126	6.14E-04	NCT
lu172	6.68E-05	NCT	sn126	6.59E-02	HAC
lu176	1.12E-02	HAC	sb127	3.61E-03	NCT
lu177	1.12E-01	HAC	xe127	1.73E-02	HAC
lu177m	3.73E-02	HAC	te127m	3.73E+01	HAC
mn54¹	1.65E-02	NCT	cs129	2.97E-02	HAC
mo93	5.83E+05	HAC	i129	5.83E+05	HAC
mo99	9.03E-03	NCT	te129m	8.36E-02	NCT
na22	5.38E-05	NCT	xe129m	4.35E-01	HAC
na24	3.38E-06	NCT	ba131	7.28E-03	NCT
nb91	3.47E+00	HAC	cs131	5.83E+05	HAC
nb92	3.41E-04	NCT	i131	1.71E-02	HAC
nb93m	5.83E+05	HAC	te131m	7.96E-05	NCT
nb94	6.40E-04	NCT	xe131m	1.02E+00	HAC
nb95	2.59E-03	NCT	cs132	2.34E-03	NCT
nb95m	7.52E-02	HAC	te132	2.17E-02	HAC
nd140	5.83E+05	HAC	ba133	2.04E-02	HAC
nd147	6.37E-02	HAC	xe133	2.72E+01	HAC
ni59	3.30E+00	NCT	xe133m	1.99E-01	HAC
ni63	5.83E+05	HAC	cs134¹	6.03E-03	NCT
np235	5.83E+05	HAC	ba135m	1.28E-01	HAC
np236	3.88E-02	HAC	cs136	1.09E-04	NCT
np237	5.86E-01	HAC	cs137¹	7.95E-02	HAC
np238	3.49E-04	NCT	la137	1.73E+01	HAC
np239	2.04E-02	HAC	la138	3.87E-05	NCT
os185	6.57E-03	NCT	ce139	2.50E-02	HAC
os191	6.88E-02	HAC	ba140	3.43E-02	HAC
os193	1.08E-01	HAC	la140	1.63E-05	NCT
os194	5.83E+05	HAC	nd140	5.83E+05	HAC
pa231	2.09E-01	HAC	ce141	4.14E-02	HAC
pa232	5.96E-04	NCT	ce143	9.23E-03	NCT
pa233	3.22E-02	HAC	pm143	6.71E-03	NCT
pb205	5.83E+05	HAC	pr143	2.15E+05	NCT
pb210	5.83E+05	HAC	ce144	1.80E-01	HAC
pd103	6.91E+01	HAC	cs144	5.27E-06	NCT

Table 5.5.3-1 (Continued)

Ordered by Alphanumeric			Ordered by Atomic Number		
Radionuclide	Max. Ci/g	Condition	Radionuclide	Max. Ci/g	Condition
pm143	6.71E-03	NCT	pm144	3.14E-03	HAC
pm144	3.14E-03	HAC	pr144	6.75E-04	NCT
pm145	5.83E+05	HAC	pm145	5.83E+05	HAC
pm146	4.35E-03	NCT	sm145	5.73E+02	HAC
pm147	7.00E+02	HAC	pm146	4.35E-03	NCT
pm148	1.10E-04	NCT	gd147	1.93E-04	NCT
pm148m	4.79E-04	NCT	nd147	6.37E-02	HAC
pm149	3.21E-01	NCT	pm147	7.00E+02	HAC
pm151	1.27E-02	NCT	pm148	1.10E-04	NCT
po210	7.99E+01	NCT	pm148m	4.79E-04	NCT
pr143	2.15E+05	NCT	eu149	1.91E-01	HAC
pr144	6.75E-04	NCT	gd149	4.88E-03	NCT
pt191	3.21E-02	HAC	pm149	3.21E-01	NCT
pt193	5.83E+05	HAC	pm151	1.27E-02	NCT
pt193m	1.78E+01	HAC	sm151	5.83E+05	HAC
pt195m	6.57E-01	HAC	eu152	8.35E-05	NCT
pu236	1.44E+02	HAC	gd153	9.29E-02	HAC
pu237	6.27E-02	HAC	sm153	6.61E-02	HAC
pu238	1.62E+03	HAC	tb153	2.83E-03	NCT
pu239	1.14E+02	HAC	eu154	9.69E-05	NCT
pu240	2.60E+02	HAC	eu155	9.11E-02	HAC
pu241	3.67E+03	HAC	tb155	3.46E-02	HAC
pu242	6.96E+02	HAC	eu156	2.26E-05	NCT
pu246	2.54E-02	HAC	tb156	4.10E-05	NCT
ra223	5.77E-02	HAC	tb157	5.83E+05	HAC
ra224	4.99E-01	HAC	tb158	4.32E-04	NCT
ra225	5.83E+05	HAC	dy159	5.83E+05	HAC
ra226	5.69E-01	HAC	tb160	1.56E-04	NCT
ra228	5.83E+05	HAC	tb161	4.57E+00	HAC
rb83	1.23E-02	HAC	tm165	8.21E-04	NCT
rb84	6.41E-04	NCT	dy166	1.70E+00	HAC
rb86	1.82E-03	NCT	ho166	2.17E-03	NCT
re186	2.10E-01	HAC	yb166	5.83E+05	HAC
re189	9.10E-02	HAC	ho166m	5.45E-04	NCT
rh101	1.30E-02	HAC	tm167	4.47E-02	HAC
rh101m	2.23E-02	HAC	tm168	6.65E-04	NCT
rh102	1.23E-03	NCT	er169	1.53E+03	HAC
rh102m	1.88E-04	NCT	lu169	4.55E-05	NCT

Table 5.5.3-1 (Continued)

Ordered by Alphanumeric			Ordered by Atomic Number		
Radionuclide	Max. Ci/g	Condition	Radionuclide	Max. Ci/g	Condition
rh105	8.17E-02	HAC	yb169	1.97E-02	HAC
rh99	7.83E-04	NCT	tm170	5.83E+05	HAC
rn222	1.50E+01	HAC	lu171	2.56E-03	NCT
ru103	1.83E-02	HAC	tm171	5.83E+05	HAC
ru106	1.57E-03	NCT	er172	3.72E-02	HAC
ru97	2.01E-02	HAC	hf172	1.20E-01	HAC
sb119	5.83E+05	HAC	lu172	6.68E-05	NCT
sb120m	5.51E-05	NCT	tm172	9.32E-05	NCT
sb122	3.62E-03	NCT	hf175	2.30E-02	HAC
sb124	2.19E-05	NCT	yb175	1.69E-01	HAC
sb125	1.29E-02	HAC	lu176	1.12E-02	HAC
sb126	6.14E-04	NCT	lu177	1.12E-01	HAC
sb127	3.61E-03	NCT	lu177m	3.73E-02	HAC
sc46	7.66E-05	NCT	hf181	1.36E-02	HAC
sc47	2.93E-02	HAC	w181	1.72E+01	HAC
sc48	2.67E-05	NCT	hf182	2.22E-02	HAC
se72	5.83E+05	HAC	ta182	6.93E-05	NCT
se75	1.14E-02	HAC	ta183	2.04E-02	HAC
sm145	5.73E+02	HAC	os185	6.57E-03	NCT
sm151	5.83E+05	HAC	w185	1.07E+02	HAC
sm153	6.61E-02	HAC	re186	2.10E-01	HAC
sn113	1.09E+00	HAC	w188	3.13E+00	HAC
sn113m	5.83E+05	HAC	re189	9.10E-02	HAC
sn117m	2.25E-02	HAC	os191	6.88E-02	HAC
sn119m	5.83E+05	HAC	pt191	3.21E-02	HAC
sn121m	5.83E+05	HAC	ir192	2.36E-01	HAC
sn123	2.46E-02	NCT	os193	1.08E-01	HAC
sn125	1.82E-04	NCT	pt193	5.83E+05	HAC
sn126	6.59E-02	HAC	pt193m	1.78E+01	HAC
sr83	2.25E-04	NCT	os194	5.83E+05	HAC
sr85	1.15E-02	HAC	ir194m	2.25E-03	NCT
sr89	5.83E+05	HAC	pt195m	6.57E-01	HAC
sr90	3.64E+02	NCT	au198	2.01E-02	HAC
ta182	6.93E-05	NCT	au199	4.09E-02	HAC
ta183	2.04E-02	HAC	hg203	2.45E-02	HAC
tb153	2.83E-03	NCT	tl204	5.83E+05	HAC
tb155	3.46E-02	HAC	pb205	5.83E+05	HAC
tb156	4.10E-05	NCT	bi208	3.76E-06	NCT

Table 5.5.3-1 (Continued)

Ordered by Alphanumeric			Ordered by Atomic Number		
Radionuclide	Max. Ci/g	Condition	Radionuclide	Max. Ci/g	Condition
tb157	5.83E+05	HAC	bi210	1.96E+04	HAC
tb158	4.32E-04	NCT	pb210	5.83E+05	HAC
tb160	1.56E-04	NCT	po210	7.99E+01	NCT
tb161	4.57E+00	HAC	bi210m	2.20E-02	HAC
tc95m	1.59E-03	NCT	rn222	1.50E+01	HAC
tc96	2.23E-04	NCT	ra223	5.77E-02	HAC
tc97	5.81E+05	HAC	ra224	4.99E-01	HAC
tc97m	5.83E+05	HAC	ac225	5.06E-01	HAC
tc98	1.97E-03	NCT	ra225	5.83E+05	HAC
tc99	5.83E+05	HAC	ra226	5.69E-01	HAC
tc99m	2.24E-02	HAC	ac227	4.82E+01	HAC
te118	5.83E+05	HAC	th227	5.64E-02	HAC
te121	1.15E-02	HAC	ra228	5.83E+05	HAC
te121m	3.15E-03	NCT	th228	3.85E+00	HAC
te123	5.83E+05	HAC	th229	9.61E-02	HAC
te123m	2.37E-02	HAC	th230	2.84E+01	HAC
te125m	7.07E+00	HAC	u230	6.10E+00	HAC
te127m	3.73E+01	HAC	pa231	2.09E-01	HAC
te129m	8.36E-02	NCT	th231	1.60E+00	HAC
te131m	7.96E-05	NCT	pa232	5.96E-04	NCT
te132	2.17E-02	HAC	th232	7.27E+01	HAC
th227	5.64E-02	HAC	u232	2.54E+01	HAC
th228	3.85E+00	HAC	pa233	3.22E-02	HAC
th229	9.61E-02	HAC	u233	2.67E+01	HAC
th230	2.84E+01	HAC	th234	7.08E+00	HAC
th231	1.60E+00	HAC	u234	5.50E+01	HAC
th232	7.27E+01	HAC	np235	5.83E+05	HAC
th234	7.08E+00	HAC	u235	2.32E-02	HAC
tl204	5.83E+05	HAC	np236	3.88E-02	HAC
tm165	8.21E-04	NCT	pu236	1.44E+02	HAC
tm167	4.47E-02	HAC	u236	9.99E+01	HAC
tm168	6.65E-04	NCT	np237	5.86E-01	HAC
tm170	5.83E+05	HAC	pu237	6.27E-02	HAC
tm171	5.83E+05	HAC	u237	3.13E-02	HAC
tm172	9.32E-05	NCT	np238	3.49E-04	NCT
u230	6.10E+00	HAC	pu238	1.62E+03	HAC
u232	2.54E+01	HAC	u238	1.86E+02	HAC
u233	2.67E+01	HAC	np239	2.04E-02	HAC

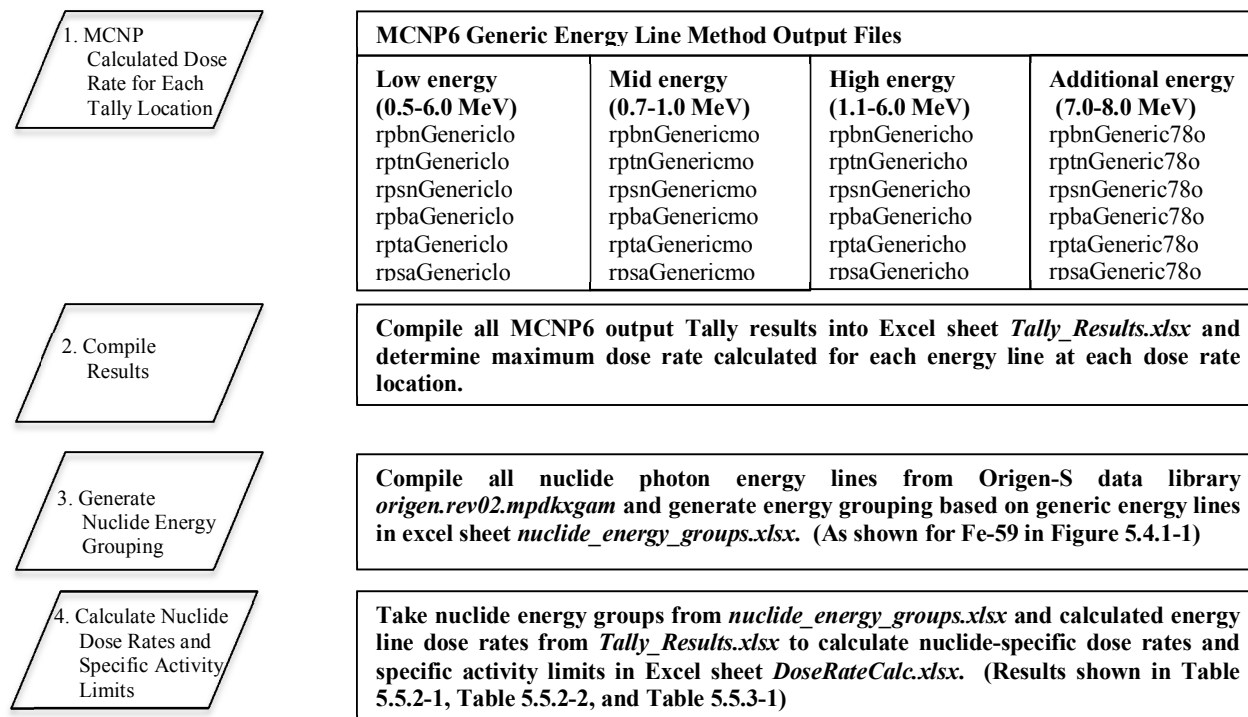
Table 5.5.3-1 (Continued)

Ordered by Alphanumeric			Ordered by Atomic Number		
Radionuclide	Max. Ci/g	Condition	Radionuclide	Max. Ci/g	Condition
u234	5.50E+01	HAC	pu239	1.14E+02	HAC
u235	2.32E-02	HAC	am240	4.09E-04	NCT
u236	9.99E+01	HAC	pu240	2.60E+02	HAC
u237	3.13E-02	HAC	am241	6.02E+01	HAC
u238	1.86E+02	HAC	cm241	1.16E-02	HAC
v49	1.07E+02	HAC	pu241	3.67E+03	HAC
w181	1.72E+01	HAC	am242	5.83E+05	HAC
w185	1.07E+02	HAC	cm242	4.05E+02	HAC
w188	3.13E+00	HAC	pu242	6.96E+02	HAC
xe127	1.73E-02	HAC	am242m	1.20E+01	HAC
xe129m	4.35E-01	HAC	am243	2.81E+00	HAC
xe131m	1.02E+00	HAC	cm243	3.16E-02	HAC
xe133	2.72E+01	HAC	cm244	8.69E+02	NCT
xe133m	1.99E-01	HAC	cm245	3.76E-02	HAC
y87	1.16E-02	HAC	cm246	5.83E+05	HAC
y88	1.02E-05	NCT	pu246	2.54E-02	HAC
y91	1.80E-02	NCT	cm247	2.45E-02	HAC
yb166	5.83E+05	HAC	cm248	5.83E+05	HAC
yb169	1.97E-02	HAC	bk249	5.28E+04	HAC
yb175	1.69E-01	HAC	cf249	2.18E-02	HAC
zn65¹	2.34E-03	NCT	cf250	5.83E+05	HAC
zn72	2.06E-02	HAC	cf251	2.48E-02	HAC
zr88	2.05E-02	HAC	cf252	1.34E+02	HAC
zr89	1.18E-03	NCT	es253	1.90E+01	HAC
zr95	2.62E-03	NCT	es254	4.48E+00	HAC

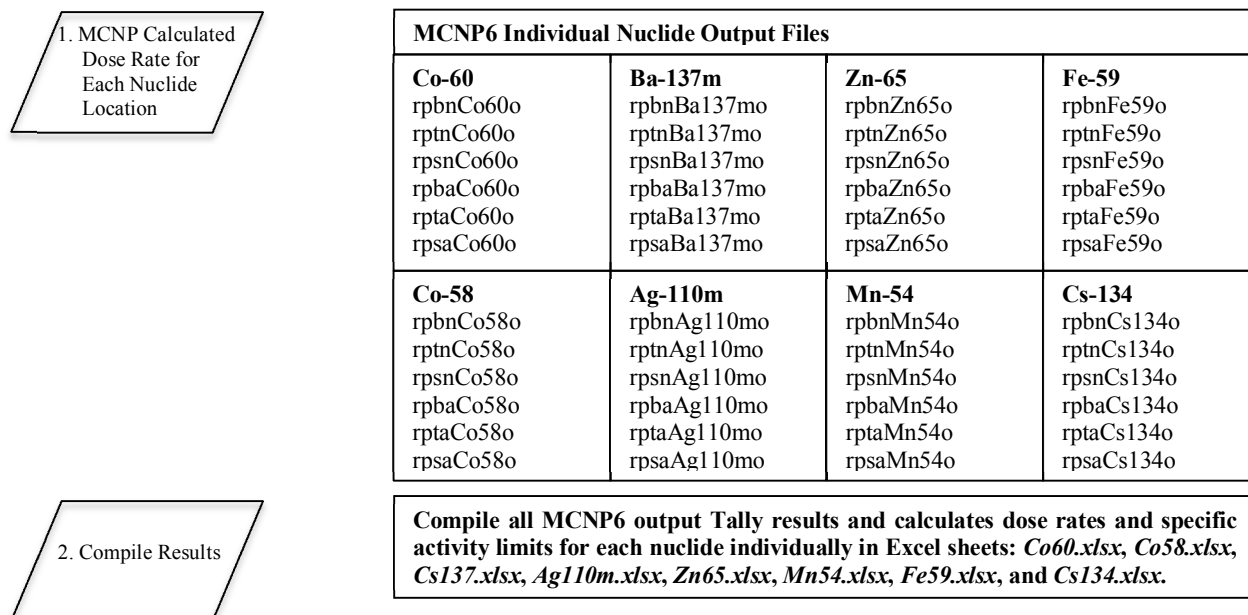
Note 1: Marked nuclides are analyzed individually.

5.5.4 Process Description for Calculating Maximum Allowed Source Strength Density

Generic Energy Line Method:



Individual Nuclides:



5.6 References

1. Robatel Technologies, LLC, Quality Assurance Program for Packaging and Transportation of Radioactive Material, 10 CFR 71 Subpart H, Rev. 2, Dated November 10, 2017 and NRC Approved on March 21, 2012.
2. U.S. Nuclear Regulatory Commission, 10 CFR Part 71--PACKAGING AND TRANSPORTATION OF RADIOACTIVE MATERIAL, dated March 7, 2012 and the following specific Sections:

71.31(a)(1)	71.31(a)(2)	71.33	71.35(a)
71.31(c)	71.71	71.43(f)	71.51(a)(1)
71.47(a)	71.47(b)	71.47	71.31
71.51(a)(2)	71.73		

3. LA-UR-13-22934, "Initial MCNP 6 Release Overview – MCNP6 version 1.0," Los Alamos National Laboratory, T. Goorley, et al., April 2013.
4. "ORIGEN-S Data Libraries," ORNL/TM-2005/39, Volume 3, Section M6, January 2009.
5. LA-UR-13-22934, "Initial MCNP 6 Release Overview – MCNP6 version 1.0," Los Alamos National Laboratory, T. Goorley, et al., April 20 "ORIGEN-S: SCALE System Module To Calculate Fuel Depletion, Actinide Transmutation, Fission Product Buildup And Decay, And Associated Radiation Source Terms," I. C. Gauld, O. W. Herman and R. M. Westfall, ORNL/TM-2005/39, Volume 2, Section F7, January 2009. "ORIGEN-S Data Libraries," ORNL/TM-2005/39, Volume 3, Section M6, January 2009.
6. RTL-001-CALC-SH-0101, Rev. 1, "Source Term Characterization for the RT-100" (PROPRIETARY)
7. RTL-001-CALC-SH-0201, Rev. 5, "Shielding Evaluation of the RT-100 Transport Cask" (PROPRIETARY)
8. CN-13039-502, "Updated Resin/Filter Shielding Evaluation of the RT-100 Transport Cask"
9. ORNL/TM-2005/39, Volume III, Section M8, "Standard Composition Library," L.M. Petrie, P.B. Fox and K. Lucius, January 2009.
10. PNNL-15870, "Compendium of Material Composition Data for Radiation Transport Modeling," R.G. Williams III, C.J. Gesh and R.T. Pagh, April 2006.
11. Faujasite-Na Mineral Data, Retrieved August 27, 2013, Retrieved from <http://webmineral.com/data/Faujasite-Na.shtml>.
12. J. Conlin, et al., "Listing of Available ACE Data Tables," LA-UR-13-21822 Rev-2, Los Alamos National Laboratory, Dec 2013.
13. ANSI/ANS 6.1.1-1997, "American National Standard for Neutron and Gamma Flux-To-Dose Conversion Factors," American Nuclear Society, 555 North Kensington Avenue, La Grange Park, IL, www.ans.org.

This page is intentionally left blank.

6. CRITICALITY EVALUATION

This Section is NOT APPLICABLE. The RT-100 is not designed to transport fissile material subject to the requirements of 10 CFR Part 71 Sections 71.55 or 71.59. Therefore, no criticality evaluation is necessary for the SAR of the RT-100.

This page is intentionally left blank.

7. PACKAGE OPERATIONS

Chapter 7 describes the RT-100 operations during loading and preparation for shipment. These operations delineate the fundamental steps needed to ensure that the RT-100 is properly prepared for transport, and ensure that the operations are consistent with the previous sections of this application.

RT-100 loading and preparation operations are consistent with maintaining occupational radiation exposures as low as reasonably achievable (ALARA), as required by the “Standards for Protection Against Radiation” in 10 CFR 20.1101(b) [Ref. 8]. RT verifies that the operating controls and procedures meet the requirements of 10 CFR Part 71; furthermore, the operating procedures are adequate to ensure the RT-100 is operated in a manner consistent with the procedures and requirements of this Safety Analysis Report. The RT operating controls and procedures ensure the transportation safety with respect to the United States (US) requirements for transportation packages for radioactive material.

A separate operations manual is to be prepared for the RT-100 to describe the operational steps in greater detail. The regulatory requirements for the operating controls and procedures evaluation from 10 CFR Part 71 [Ref. 2] include the following issues:

- Application identifies the established codes and standards used for the operating procedures in accordance to 10 CFR Part 71 Section 71.31(c) [Ref. 2].
- Application for a fissile material is not applicable for the RT-100 since it will not be used for fissile material transport.
- RT-100 shall be transported as a Type B shipment B(U)-96 exclusive use shipment.
- The shipper shall ensure that the routine determination of 10 CFR 71.87 [Ref. 2] is met prior to each shipment. Prior to delivery of a package to a carrier, RT will send to the consignee any special instructions needed to safely open the package and use it in accordance with 10 CFR 20.1906(e) [Ref. 8] and 10 CFR Part 71 Section 71.89 [Ref. 2].
- The operating procedures meet the regulatory requirements listed in the Preparation of Empty Package for Transport Section.
- The operating procedures are adequate to ensure that the package will be operated in accordance with the Safety Analysis Report.

Input from the other sections of this application are used to develop the RT-100 operational controls and procedures. Information flow for the operating procedures evaluation is shown in Figure 7-1.

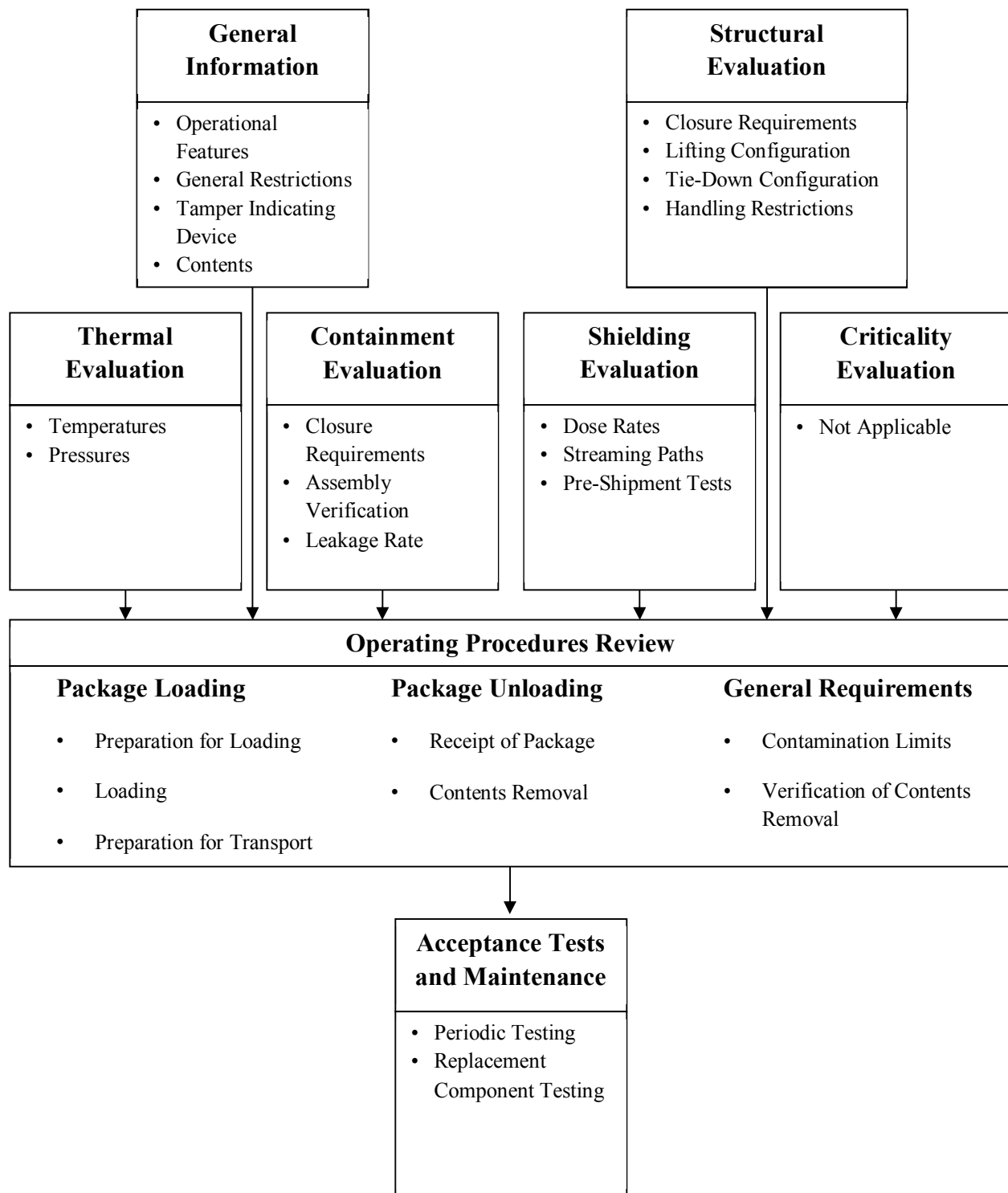


Figure 7-1 Information Flow for the Operating Procedures Review

7.1 Package Loading

Section 7.1 describes loading-related preparations, tests, and inspections of the package. These actions include the inspections made before loading the package to ensure the package is not damaged, and that radiation and surface contamination levels are within allowable limits.

The procedures for loading of the RT-100 are defined as follows:

- 7.1.1 Preparation for Loading
- 7.1.2 Loading of the RT-100
- 7.1.3 Preparation for Transport

7.1.1 Preparation for Loading

The following actions are taken prior to loading operations:

1. RT-100 is surveyed for surface contamination to ensure it is within allowable limits. If the package exceeds contamination limits, the RT-100 must be decontaminated prior to the next step.
2. A visual inspection is performed to determine if any component damage has occurred that would prevent safe performance of the package under NCT and HAC. Any damaged/out-of-specification components are repaired or replaced.
3. A pre-loading briefing is conducted with the loading team with the purpose of reviewing all procedures, and ensuring everyone is cognizant of the loading requirements and the associated safety measures. Pre-loading actions include appropriate ALARA measures and contamination control.
4. The package contents data is reviewed to ensure the contents meet the Certificate of Compliance.
5. The following conditions must be met for safe handling of the RT-100:
 - All operating instructions/procedures outlined in the Safety Analysis Report must be followed.
 - RT-100 shall not be lifted via the lifting rings on the upper impact limiter.
 - RT-100 shall only be lifted in the vertical position.
 - RT-100 shall not be placed in an upside down position at any time.
 - RT-100 shall not be handled while tied down.

Loading of the RT-100 can take place on or off the trailer, and with or without the lower impact limiter attached. Additionally, loading can take place via the primary or secondary lid. Figure 7.1.1-1 illustrates the process flow for these steps. Subsequent sections describe these steps in greater detail. If the RT-100 remains on the trailer, the trailer and lower impact limiter must be protected against contamination during the procedure.

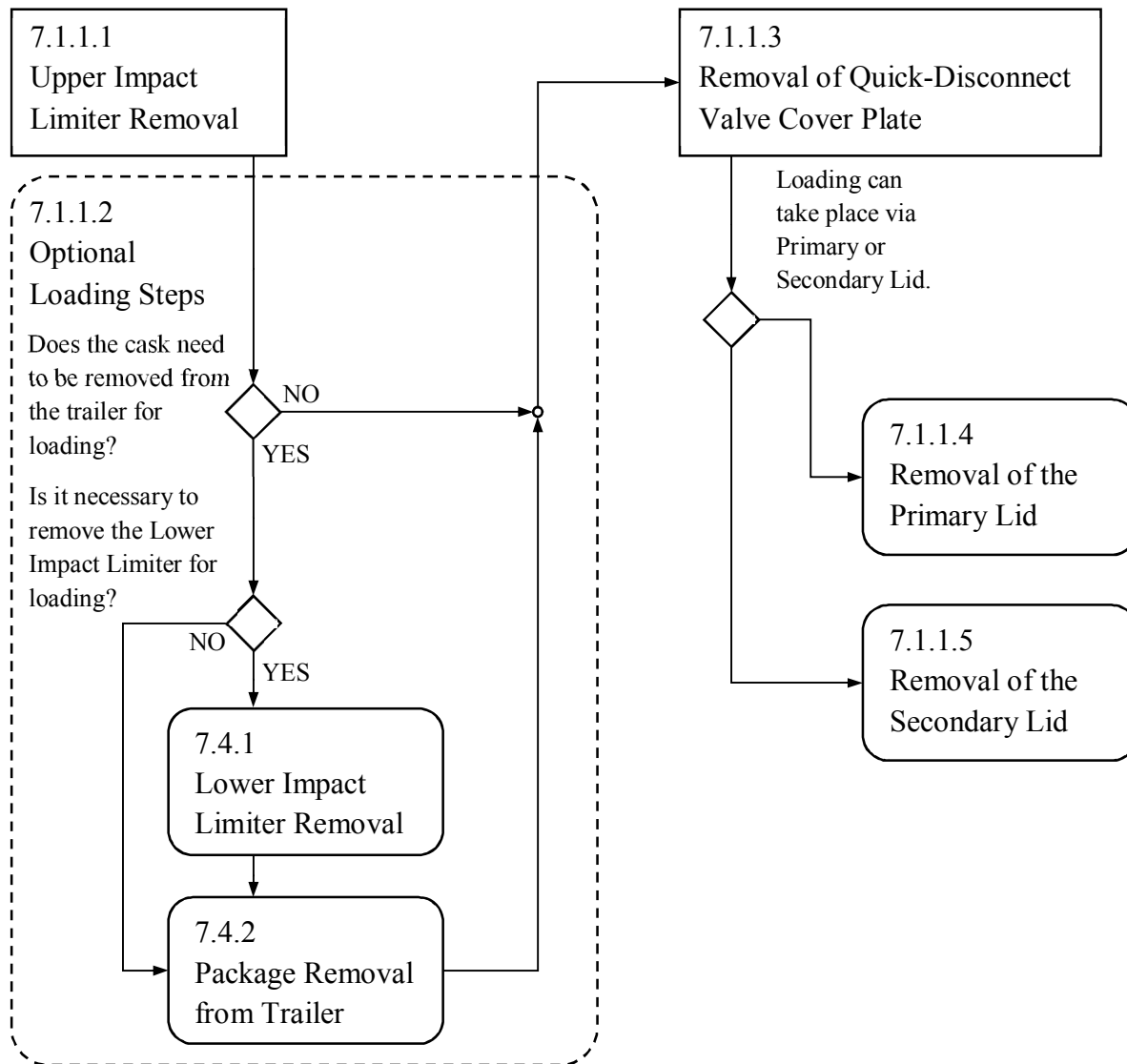


Figure 7.1.1-1 Preparation for Loading Process Flowchart

7.1.1.1 Upper Impact Limiter Removal

Remove the upper impact limiter by following these steps:

1. Remove tamper indicating seal from the upper impact limiter aligning pin.
2. Remove the cotter pin from each upper impact limiter bolt.
3. Using appropriate tools loosen and remove all head nuts (12 Hex Head Nuts, M36) which secure the impact limiter to the cask body.
4. Install three lifting rings to the upper impact limiter. Remove the impact limiter using an appropriate lifting device attached to the three (3) lifting rings.

NOTE: To prevent damage, the impact limiter shall be handled and stored with care. It must be placed on a clean, flat surface in a position so that the studs and aligning pins do not touch the ground.

7.1.1.2 Optional Loading Steps

- Lower Impact Limiter Removal: Refer to the actions described in Section 7.4.1.
- Package Removal from Trailer: Refer to the actions described in Section 7.4.2.

7.1.1.3 Removal of Quick-Disconnect Valve Cover Plate

CAUTION: In the event of failure of the quick disconnect valve, radioactive material may be released when opening the vent port cover plate. Use caution to consider potential release of material consistent with the form of the cask contents.

Before opening the primary or secondary lid, internal and external pressure must be balanced to ensure safety, contamination control and to easily remove the lid(s). This is accomplished following these steps:

1. With appropriate tools, loosen and remove all bolts (6 Socket Head Cap Screws, M10x30) which secure the quick-disconnect valve cover plate to the primary lid.
2. Manually install and hand tighten two (2) of the six (6) bolts previously removed from the quick-disconnect valve cover plate into two (2) threaded holes specially designed for this purpose. Remove the cover plate using the bolts.
3. Vent the cask cavity by connecting the quick-disconnect valve to a leak tight ventilation system.

NOTES:

- Treat the quick-disconnect valve cover plate, its cavity surfaces, bolts and O-rings as potentially contaminated.
- The quick-disconnect valve cover plate must be set down with caution to prevent damage.
- Any defective bolts or O-rings, or those showing signs of deterioration shall be replaced with components meeting the specifications in the RT100 NM 1000-F Bill of Material (Chapter 1, Appendix 1.4, Attachment 1.4-1).

- Maintenance leakage rate testing shall be performed in accordance with Section 8.2.2.1 prior to returning a package to service following maintenance, repair (Such as a weld repair), or replacement of components of a containment boundary.

7.1.1.4 Removal of the Primary Lid

Remove the primary lid by following these steps:

1. Remove all the bolts (32 Hex Head Cap Screws, M48x170) securing the lid to the cask body.
2. Insert the three (3) lid lifting rings in the threaded holes designed for this purpose on the upper side of the primary lid.
3. Remove primary lid using suitable lifting equipment attached to the three lifting rings.
4. Inspect all bolt threads, hole threads, and O-rings for damage.

NOTES:

- Treat the primary lid, cask cavity surfaces, bolts, and O-rings as potentially contaminated.
- The primary lid shall be handled and stored with care in order to prevent damage.
- Any defective bolt or O-ring, or those showing signs of deterioration shall be replaced with components meeting the specifications in the RT100 NM 1000-F Bill of Material (Chapter 1, Appendix 1.4, Attachment 1.4-1).
- Maintenance leakage rate testing shall be performed in accordance with Section 8.2.2.1 prior to returning a package to service following maintenance, repair (Such as a weld repair), or replacement of components of a containment boundary.
- Removal of the secondary lid is not necessary to remove the primary lid.

7.1.1.5 Removal of the Secondary Lid

Remove the secondary lid by following these steps:

1. Remove all the bolts (18 Hex Head Cap Screws, M36x120) securing the secondary lid to the primary lid.
2. Insert the three (3) lid lifting rings in the threaded holes designed for this purpose in the upper side of the secondary lid.
3. Remove secondary lid using suitable lifting equipment attached to the three lifting rings.
4. Inspect all bolt threads, hole threads, and O-rings for damage.

NOTES:

- Treat the secondary lid, cask cavity surfaces, bolts, and O-rings as potentially contaminated.
- The secondary lid shall be handled and stored with care in order to prevent damage.
- Any defective bolt or O-ring, or those showing signs of deterioration shall be replaced with components meeting the specifications in the Bill of Material (Appendix 1.4).
- Maintenance leakage rate testing shall be performed in accordance with Section 8.2.2.1 prior to returning a package to service following maintenance, repair (Such as a weld

repair), or replacement of components of a containment boundary.

7.1.2 Loading of the RT-100

Section 7.1.2 addresses the actions for loading of the RT-100. Figure 7.1.2-1 describes the process flow for these steps. Subsequent sections describe these steps in detail.

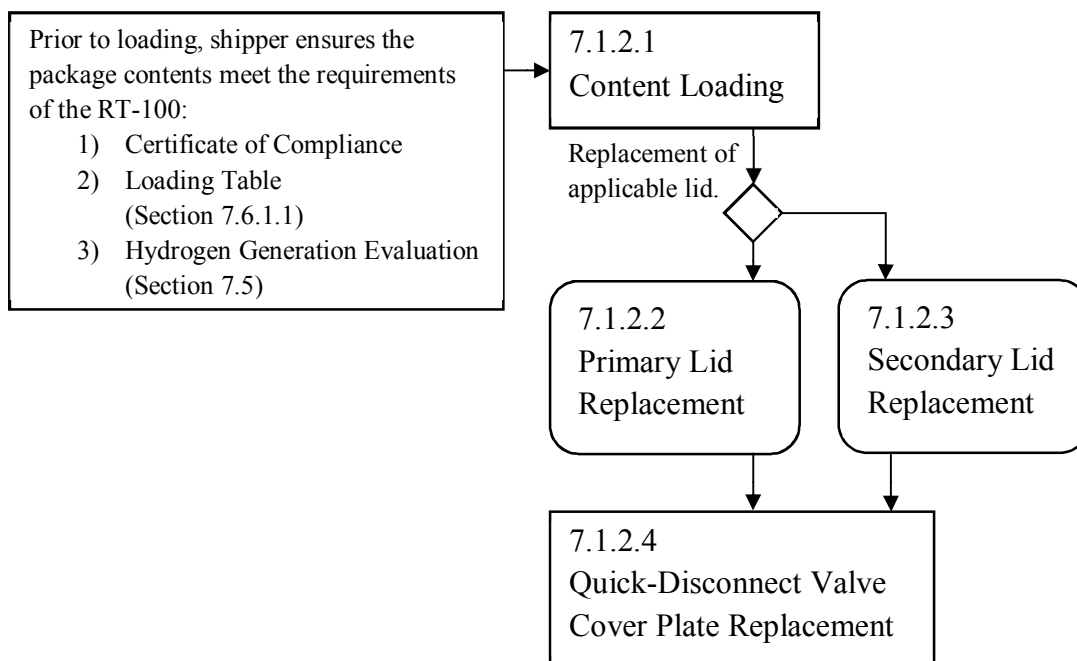


Figure 7.1.2-1 Loading of the RT-100 Process Flowchart

7.1.2.1 Content Loading

Load the cask by following these steps:

1. Prior to loading of the RT-100, the following conditions shall be met:
 - a. Package contents meet the requirements of the RT-100 Certificate of Compliance
 - b. Package contents meet the requirements of Appendix 7.6 and its loading table addressed in Section 7.6.1.1
 - c. Package contents meet the requirements of the hydrogen generation evaluation described in Section 7.5
2. Ensure the contents, secondary container, and packaging are chemically compatible (i.e., will not react to produce flammable gases).
3. Inspect RT-100 interior for any damage, loose material or moisture.
4. Radioactively contaminated liquids may be pumped out or removed using absorbent material.
5. Removal of any material from inside the cask is performed under the supervision of qualified health physics personnel, and in accordance with health & safety requirements.
6. Pre-position any shoring necessary to shore/brace the liner during normal transit.
7. Inspect the applicable sealing surface before loading. Clean if necessary.

Note: Cleanliness of the sealing surface will have a direct effect on leak testing results.

8. Place disposable liner, drums, or other containers into the pre-positioned shoring; install additional shoring or bracing as necessary to restrict movement of contents during normal transport.
9. Process liner as necessary and cap the liner as required.

7.1.2.2 Primary Lid Replacement

The primary lid is attached by following these steps:

1. Clean and inspect the O-rings. Lubricate if necessary. Contact RT if any damage, crack, or condition is noted that can prevent O-rings from sealing properly.
Note: This step may be performed prior to cask loading.
2. If not already present, install the three (3) lifting rings on the primary lid in the threaded holes designed for this purpose.
3. Place the primary lid on the cask. The lid is positioned by an aligning pin to ensure the proper placement of the primary lid on the cask body.
4. Lubricate (if necessary) the thirty-two (32) bolt and hole threads.
5. Install the bolts with washers.
6. Tighten the bolts using the “star pattern” method to ensure evenly distributed pressure on the primary lid and cask body.
 - a. Use an initial torque of $400 \text{ N-m} \pm 10\%$.
 - b. Use a final torque of $850 \text{ N-m} \pm 10\%$.
7. Remove the three (3) lifting rings from the primary lid.
8. Refer to Section 8.2.2.2 or Section 8.2.2.3 for instructions regarding Pre-shipment Leak Testing.

7.1.2.3 Secondary Lid Replacement

The secondary lid is attached by following these steps:

1. Clean and inspect the O-rings. Lubricate if necessary. Contact RT if any damage, crack, or condition is noted that can prevent O-rings from sealing properly.
Note: This step may be performed prior to cask loading.
2. If not already present, install the three (3) lifting rings on the secondary lid in the threaded holes designed for this purpose.
3. Place the secondary lid on the primary lid. The lid is positioned by an aligning pin to ensure the proper placement of the secondary lid on the primary lid.
4. Lubricate (if necessary) the eighteen (18) bolt and hole threads.
5. Install the bolts with washers.
6. Tighten the bolts using the “star pattern” method to ensure evenly distributed pressure on the secondary and primary lids.
 - a. Use an initial torque of $150 \text{ N-m} \pm 10\%$.
 - b. Use a final torque of $350 \text{ N-m} \pm 10\%$.

7. Remove the three (3) lifting rings from the secondary lid.
8. Refer to Section 8.2.2.2 or Section 8.2.2.3 for instructions regarding Pre-shipment Leak Testing.

7.1.2.4 Quick-Disconnect Valve Cover Plate Replacement

The quick-disconnect valve cover plate is replaced in the following manner:

1. Clean and inspect the O-rings. Lubricate if necessary. Contact RT if any damage, crack, or condition is noted that can prevent O-rings from sealing properly.
Note: This step may be performed prior to cask loading.
2. Install two (2) of the previously removed cover plate bolts (Socket Head Cap Screw, M10x30) in the threaded holes on the cover plate. Manually place the cover plate on the primary lid. Subsequently, remove these two (2) bolts.
3. Lubricate (if necessary) the six (6) quick-disconnect valve cover plate bolt and hole threads.
4. Secure the quick-disconnect valve onto the primary lid using plate bolts and washers.
5. Tighten bolts using the “star pattern” method to ensure consistent pressure on the quick-disconnect valve and primary lid.
 - a. Tighten the bolts by hand to compress the O-rings (no specific torque required).
 - b. Use a final torque of $27 \text{ N}\cdot\text{m} \pm 10\%$.
6. Refer to Section 8.2.2.2 or Section 8.2.2.3 for instructions regarding Pre-shipment Leak Testing.

7.1.3 Preparation for Transport

The following general requirements are completed prior to final transport of the RT-100:

1. Contamination survey completed on the external surfaces to confirm that non-fixed (removable) radioactive contamination is as low as reasonably achievable, and is within the limits specified in 49 CFR 173.443 [Ref. 3], as required by 10 CFR 71.87 [Ref. 2]. If contamination is within limits, preparation for transport may be conducted. If contamination exceeds the limits, the RT-100 must be decontaminated until the contamination limits are met.
2. Measure the exterior gamma radiation levels following RIS 13-04 to ensure these do not exceed 200 millirem per hour (2 mSv/h) at any point on the vertical planes projected from the outer edges of the trailer, on surface of the impact limiter at the axial center line of the package, and on the lower external surface of the trailer, 10 millirem per hour (0.1 mSv/h) at any point 2 meters (6.6 feet) from the vertical planes projected by the outer edges of the trailer (excluding the underside of the trailer) and 2 millirem per hour (0.02 mSv/h) in the tractor cab, in accordance with 49 CFR 173.441 and 10 CFR 71.47. Measurements shall be made at the axial mid-plane of the cask and below the cask end on the lower external surface of the trailer. Also measure the neutron radiation to ensure there is not unexpected neutron sources in the content.

- Caution: Ensure calibration is current and address radiation detector uncertainty when measuring pre-shipment dose rates.
- 3. If necessary, install the lower impact limiter and load the package on the trailer:
 - Replacement of Lower Impact Limiter: Refer to Section 7.4.3
 - Reloading the Package onto the Trailer: Refer to Section 7.4.4

Figure 7.1.3-1 describes the process flow for transport preparation. Subsequent sections describe these steps in greater detail.

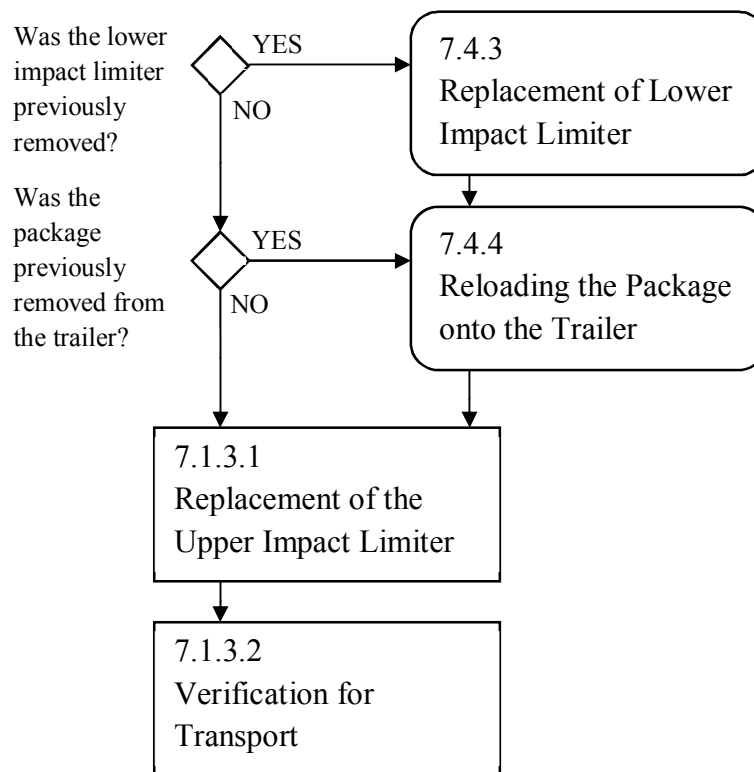


Figure 7.1.3-1 Preparation for Transport Process Flowchart

7.1.3.1 Replacement of Upper Impact Limiter

Install the upper impact limiter using the following steps:

1. Inspect the cask body flange. Inspect each threaded stud for cleanliness, defects, and lubrication – Replace if necessary in accordance with Section 7.4.5.3.
Note: This step may be performed prior to cask loading.
2. Lift the upper impact limiter using an appropriate lifting device fixed to its three (3) lifting rings.
3. Position the upper impact limiter using the two (2) aligning pins.
4. Lower the upper impact limiter slowly and cautiously to prevent any damage to threaded studs and aligning pins.
5. Disconnect the lifting device from the upper impact limiter.

6. Disconnect or render inoperable the 3 lifting rings on the upper impact limiter.
7. Secure the cask to the upper impact limiter by installing twelve (12) head nuts on the threaded studs. The head nuts do not require any specific torque. The nuts must be in contact with the cask attachment ring.
8. Install a cotter pin on each threaded stud.
9. Install a tamper indicating seal on the upper impact limiter aligning pin.

7.1.3.2 Verification for Transport

The following actions are confirmed prior to shipment of a loaded package.

- Licensed consignee who expects to receive the package containing materials in excess of Type A quantities specified in 10 CFR 20.1906(a) [Ref. 8] meets and follows the requirements of 10 CFR 20.1906 [Ref. 8], as applicable.
- Before delivery of a package to a carrier for transport, the shipper shall ensure that any special instructions needed to safely open the package have been sent to, or otherwise made available to, the consignee for the consignee's use in accordance with 10 CFR 20.1906(e) [Ref. 8].
- Trailer placarding and cask labeling meet DOT specifications (49 CFR 172).
- Provisions of 10 CFR 71.87 [Ref. 2] are met.
- Radiation dose rates are in accordance with 10 CFR 71.47 [Ref. 2]
 - ≤ 200 mrem/hr at package surface.
 - ≤ 10 mrem/hr at 2 meters from the vertical side of the trailer.
 - ≤ 2 mrem/hr at the cab of the tractor
- No temperature survey is required. The thermal evaluation demonstrates that the temperature requirement of 10 CFR 71.43(g) [Ref. 2] is met.
- Security seals are properly installed as required by 10 CFR 71.43(b) [Ref. 2]
- Inspect the exterior of the cask for damage prior to shipping a loaded package. Contact RT if damage is present.
- Ensure that the RT-100 is correctly tied-down to the trailer.

7.2 Package Unloading

Section 7.2 addresses the unloading operations for the RT-100.

The procedures for unloading the RT-100 are defined as follows:

- 7.2.1 Receipt of Package from Carrier
- 7.2.2 Removal of Contents

7.2.1 Receipt of Package from Carrier

The following actions are taken upon receipt of the RT-100 from the carrier:

1. User shall follow the applicable requirements of 10 CFR 20.1906 [Ref. 8] "Procedures for Receiving and Opening Packages" when the package contains radioactive material in

excess of Type A quantities. Corresponding packages are identified by review of the shipping papers.

2. Any special instructions provided by the shipper in accordance with 10 CFR 71.89 [Ref. 2] are reviewed and followed.
3. Perform visual examination of the unopened cask. Any damage is reported to the shipper and actions taken to replace or repair any components that would jeopardize the integrity of the RT-100.
4. Inspect the tamper indicating seal at the upper impact limiter aligning pin. Shipper is notified and the shipment may be rejected by the consignee if the tamper seal has been removed or tampered with in any way. At consignee discretion, the consignee may proceed to accept the RT-100 contents if the tamper indicating seal was damaged during shipment.
5. Conduct contamination and radiation dose rate surveys to determine if the levels are compliant with the DOT and NRC. If either of these surveys exceeds the limits, the shipper is notified immediately, and the shipper collaborates with consignee; or the appropriate regulatory authorities and DOT, to resolve the issue.
6. Measure the exterior gamma radiation levels following RIS 13-04 to ensure these do not exceed 200 millirem per hour (2 mSv/h) at any point on the vertical planes projected from the outer edges of the trailer, on surface of the impact limiter at the axial center line if the package, and on the lower external surface of the trailer, 10 millirem per hour (0.1 mSv/h) at any point 2 meters (6.6 feet) from the vertical planes projected by the outer edges of the trailer (excluding the underside of the trailer) and 2 millirem per hour (0.02 mSv/h) in the tractor cab, in accordance with 49 CFR 173.441 and 10 CFR 71.47. Measurements shall be made at the axial mid-plane of the cask and below the cask end on the lower external surface of the trailer. Also measure the neutron radiation to ensure there is not unexpected neutron sources in the content.

7.2.2 Removal of Contents

Unloading is conducted with the RT-100 in a vertical position in an approved licensed radioactive materials facility. If desired, the RT-100 may be removed from the trailer and the lower impact limiter may be removed. Follow the instructions in Section 7.4 for these optional steps.

The following procedures are used to remove the contents from the RT-100:

1. Remove the upper impact limiter in accordance with Section 7.1.1.1.
2. Remove the quick-disconnect valve cover plate and balance the interior and exterior pressures in accordance with Section 7.1.1.3.
 - **Caution:** In the event of failure of the quick disconnect valve, radioactive material may be released when opening the vent port cover plate. Use caution to consider potential release of material consistent with the form of the cask contents.
3. Remove applicable lid (handle as contaminated):
 - Removal of the Primary Lid: Section 7.1.1.4

- Removal of the Secondary Lid: Section 7.1.1.5
- 4. Use appropriate equipment to remove the contents.
- 5. Inspect RT-100 interior for any damage, loose material, or moisture. Clean seal surfaces. Contact RT in case of damaged O-ring.

NOTES:

- Care should be taken not to damage the cask or the sealing surfaces.
- Remove any material from inside the cask under the supervision of qualified health physics personnel, and by following appropriate health & safety protocols.
- Radioactively contaminated liquids may be pumped or removed by absorbent material.

7.3 Preparation of Empty Package for Transport

Section 7.3 describes the operations used to certify that the empty package is safe for transportation in accordance with 49 CFR 173.428, “Empty Class 7 (Radioactive) Material Packaging” [Ref. 4].

These operations must be completed before shipment of the empty RT-100:

1. Confirm the cavity is empty of contents as far as practicable
2. Survey the lid, quick connect cover and interior:
 - Decontaminate if the limits of 49 CFR 173.428(d) [Ref. 4] are exceeded.
3. Replace and secure the applicable lid:
 - Primary Lid Replacement 7.1.2.2
 - Secondary Lid Replacement 7.1.2.3
4. Replace and secure the quick-disconnect valve cover in accordance with Section 7.1.2.4.
5. Decontaminate the exterior surfaces of the cask, as necessary.
6. If previously removed, replace lower impact limiter in accordance with Section 7.4.3.
7. If previously removed, replace RT-100 on the trailer in accordance with Section 7.4.4.
8. Replace upper impact limiter in accordance with Section 7.1.3.1.
9. Inspect the exterior and confirm it is undamaged and unimpaired.

7.4 Other Operations

Section 7.4 describes provisions for any special operational controls.

7.4.1 Lower Impact Limiter Removal

The lower impact limiter may be removed by following these steps:

1. Remove the cotter pin from each lower impact limiter threaded stud.
2. Using appropriate tools loosen and remove all the head nuts which secure the impact limiter to the cask body.
3. Remove the cask from the trailer following the sequence described in Section 7.4.2.
4. Install three lifting rings to the lower impact limiter using three (3) 120° distant studs.
5. Remove the impact limiter using an appropriate lifting device attached to the three (3) lifting

rings.

NOTE: To prevent damage, the impact limiter shall be handled and stored with care. It must be placed on a clean, flat surface in a position so that the studs and aligning pins do not touch the ground.

7.4.2 Package Removal from Trailer

The RT-100 may be removed from the trailer by following these steps:

1. Verify transport trailer is in appropriate area for unloading.
2. Disconnect tie-down system and render the holes inoperable so that they cannot be used for lifting of the packaging.
3. If not already complete, remove upper impact limiter in accordance with Section 7.1.1.1.
4. Inspect condition of the cask lifting pocket welds.
5. Install Lifting Yoke. (RT-100 Lifting Yoke must be handled with its two (2) suitable lifting rings connected to the lifting crane.)
 - a. Engage two (2) lifting yoke arms in the cask lifting pockets (Figure 7.4.2-1).
 - b. Connect arms in the lifting pockets by inserting the pin in each arm (Figure 7.4.2-2).
 - c. Secure lifting yoke arms by inserting lock pin in the pin hole below the cask lifting pockets, and secure the lock pin with a cotter pin (Figure 7.4.2-3).
6. With or without the lower impact limiter attached, lift the RT-100 cask from the transport trailer (Figure 7.4.2-4).
7. Place the RT-100 cask (and lower impact limiter) in an approved storage area. Care should be taken to prevent the cask assembly and the lifting equipment from any damage.
8. Disconnect the lifting yoke from the cask.

**Figure 7.4.2-1 Lifting Yoke Arm
Positioned on Cask**



**Figure 7.4.2-2 Lifting Yoke
Connections**



Figure 7.4.2-3 Lifting Yoke Secured with Locking Pin



**Figure 7.4.2-4 Assembled Cask Ready to Lift
(shown with Lower Impact Limiter installed)**



7.4.3 Replacement of Lower Impact Limiter

Replace the lower impact limiter by following these steps:

1. Verify that the lower impact limiter is correctly positioned and located in an appropriate area for installing the cask. The installation of the lower impact limiter can be conducted with the limiter already positioned on the transport trailer.
2. Inspect and clean the lower impact limiter surface.
3. Inspect each threaded stud for cleanliness, defects and lubrication – replace if necessary in accordance with Section 7.4.5.3.
4. Install the lifting yoke on the cask as written in Section 7.4.2 (upper impact limiter shall not be installed on the cask).
5. Lift cask with appropriate lifting equipment.
6. Inspect and clean (if necessary) bottom surface of cask.
7. Position the cask body using the two (2) lower impact limiter aligning pins.
8. Using caution, slowly lower the cask body to prevent any damage to the lower impact limiter and the cask body.
9. Secure cask on the lower impact limiter by installing the twelve (12) nuts on the threaded studs. The head nuts do not require any specific torque. The nuts must be in contact with the cask attachment ring.
10. Install a cotter pin on each of the 12 threaded studs.

7.4.4 Reloading the Package onto the Trailer

The RT-100 may be reloaded onto the trailer by following these steps:

1. Verify the transport trailer is located in an appropriate area for loading. Figure 7.4.4-1 shows an example trailer illustration.
2. Install the lifting yoke on the cask as written in Section 7.4.2 (upper impact limiter shall not be installed on the cask).
3. Lift the RT-100 cask onto the transport trailer as shown in Figure 7.4.4-2. Position the tie-down arms along the trailer as shown in Figure 7.4.4-2.
4. Disconnect the lifting yoke from the cask as described in Section 7.4.2.
5. The lifting pockets must be rendered inoperable prior to transport. Acceptable options for this step include: inserting the lifting pins in the lifting pockets and securing with the lock pins, or inserting and securing dedicated pins into the lifting pockets.
6. Install the upper impact limiter as described in Section 7.1.3.1.
7. Connect the four (4) tie-down arms to the trailer by the tie-down equipment.
8. Tighten the tie-down equipment to ensure no movement of the RT-100 in any direction.



Figure 7.4.4-1 Example Trailer Illustration



Figure 7.4.4-2 Loading of the RT-100 on Transportation Trailer

7.4.5 Tightening of Components

Section 7.4.5 addresses issues associated with components that require tightening.

7.4.5.1 Tightening Torques

Table 7.4.5-1 provides descriptive information and torque values for lid bolts. Table 7.4.5-2 provides descriptive information and torque values for other parts.

Table 7.4.5-1 Lid Bolt Tightening Torques

Description	Dimensions	Qty.	Tightening Torque [N-m]	Tolerance
Primary lid bolts	HHCS M48x170	32	850	± 10%
Secondary lid bolts	HHCS M36x120	18	350	± 10%
Quick disconnect valve disconnect valve cover plate bolts	SHCS M10x30	6	27	± 10%

Table 7.4.5-2 Tightening Torques - Other Parts

Description	Dimensions	Qty.	Tightening Torque [N-m]	Tolerance
Primary Lid Aligning Pin	M42	1	850	± 10%
Secondary Lid Aligning Pin	M24	1	200	± 10%
Impact Limiter Studs	M36	24	N/A ¹	-
Impact Limiter Nuts	HM36	24	N/A ¹	-
Quick Disconnect Valve Cover Plate Leak Test Port Plug	M10	1	10	± 10%
Quick Disconnect Valve	G 3/8	1	50	± 10%
Primary and Secondary Lid Leak Test Port Plug	M20	2	100	± 10%

¹ The lower and upper impact limiter nuts do not require any specific torque to ensure function. They are hand-torqued when assembled. Thus, no control of the tightening torque on these nuts is necessary.

7.4.5.2 Threaded Bolts – Tightening Methods and Equipment

Threaded bolts and parts must be tightened to the torque limits specified in Table 7.4.5-1 and Table 7.4.5-2, using a wrench that displays the torque applied during tightening.

1. Bolts and bolt holes are cleaned prior to use.
2. If necessary, bolts and nuts are lubricated before tightening.
3. Bolts on the primary and secondary lids are tightened via the “star pattern” in a minimum of two stages:
 - a. Use an initial torque of approximately 50% of required torque.
 - b. Use a final torque of the full required torque.

7.4.5.3 Replacement of the Impact Limiter Threaded Studs

The impact limiter threaded studs may be replaced in the following manner:

1. Remove the spring pin securing the threaded stud.
2. Unscrew the threaded stud and remove it.
3. Install a new threaded stud and tighten it by hand to align the stud and the embossing holes (no specific torque required).
4. Install a new spring pin to secure the threaded stud.

7.5 Hydrogen Buildup in RT-100 Transport Cask

The RT-100 is designed for a maximum decay heat of 200 Watts, as described in Section 1.2.2.8. The rate of hydrogen gas generation must also be considered when evaluating the heat load. The method for calculating the hydrogen gas generation is described in Section 4.4. Two evaluation methods are described in the following sections – a simplified model (Section 7.5.1) which is used for most shipments but is limited to certain restrictions, and an analytical model (Section 7.5.2) used for other cases. An example calculation using the analytical model is detailed in Section 7.5.3.

Package material and content that can generate flammable gas shall be appropriately assigned as part of the ionic resin bead waste or polyethylene container when using the Loading Curve (Figure 7.5-1 and Table 7.5.1-1) or detailed analysis (Section 7.5.2) to determine acceptable hydrogen gas generation-related parameters of shipping time and decay heat. For example, waste filters (made of material other than polypropylene or polyethylene) shall be grouped as ionic bead waste and wood shoring would be grouped as part of the polyethylene container. If filters are made of polyethylene or polypropylene, they are to be included in the secondary container volume for the hydrogen gas generation detailed analysis.

7.5.1 Hydrogen Gas Generation – Simplified Model used to develop Loading Curve

Using the equations derived in Chapter 4, Section 4.4, the decay heat limit versus waste volume can be determined for a limit of 5% in the cavity free volume. Figure 7.5-1 provides a curve illustrating the waste volume to decay heat value that would result in the generation of a flammable gas mixture within 10 days assuming that all decay heat is absorbed by the waste material and the polyethylene container. The calculation assumes that the hydrogen generation occurs over a period of time that is twice the allowable shipping time. For most shipments, this simplified graphical model (Loading Curve) can be used to determine the maximum heat load.

Use the following procedure to confirm the decay heat of the cask contents meet the requirements of NUREG/CR-6673 [Ref. 16]:

1. Confirm all the restrictions listed in Table 7.5.1-1 are met. Confirm the secondary container is listed in Table 7.5.1-2, or is a container of equivalent material volume. Confirm the shoring volume does not exceed the allowable volume. If these restrictions cannot be met, the analytical model described in Section 7.5.2 must be used.
2. Identify the waste volume (V_{WASTE}) in cubic feet.
3. Use the Loading Curve shown in Figure 7.5-1 to find the maximum allowable decay heat ($D_{H,max}$) in Watts.
4. Confirm that the cask contents have a decay heat (D_H) that is less than the maximum allowable decay heat ($D_{H,max}$).

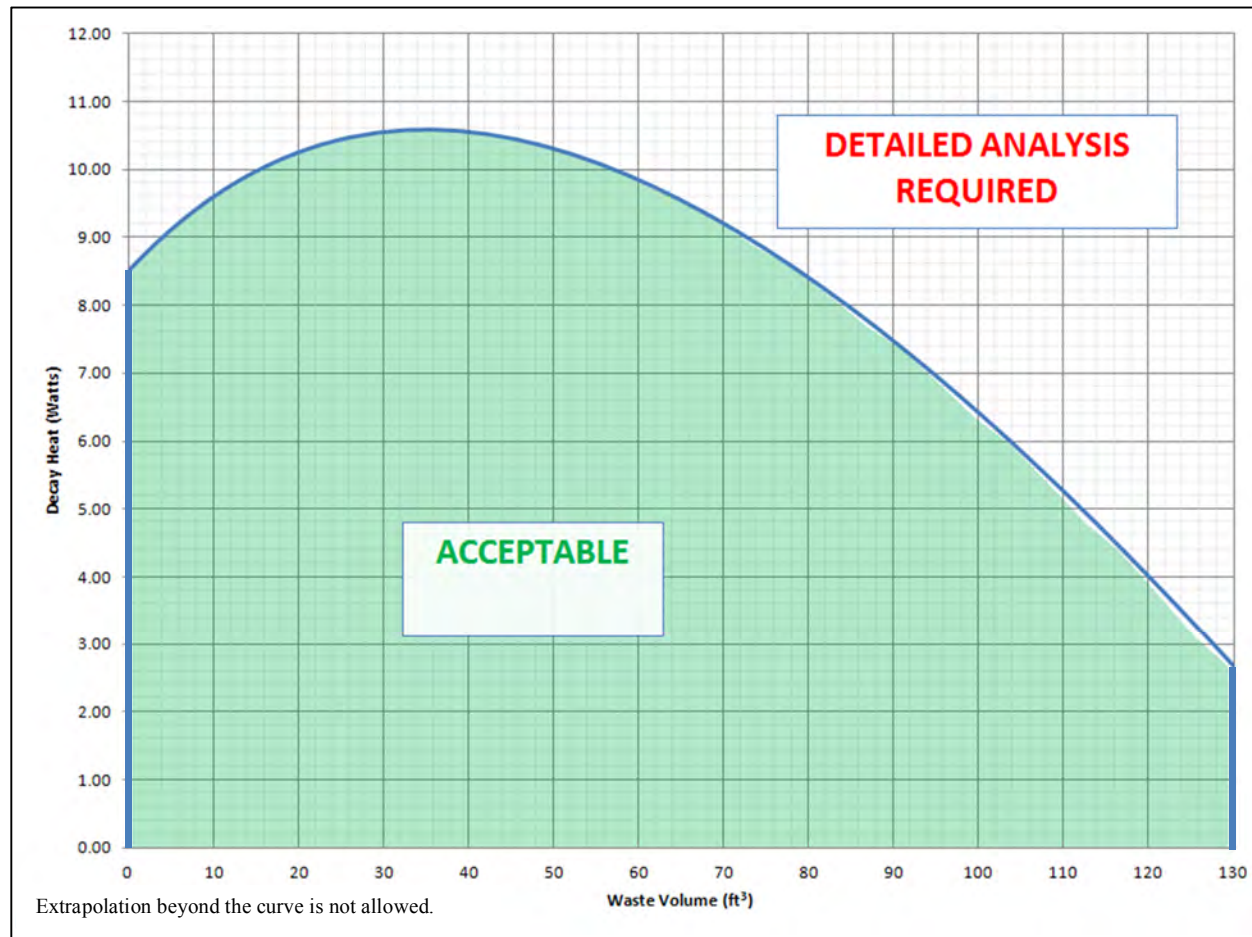


Figure 7.5-1 Package Loading Curve for Hydrogen Generation – Decay Heat Limit Versus Waste Volume

Table 7.5.1-1 Conditions for using Package Loading Curve (Excerpt from Table 4.4.4-1)

Condition for Shipper to use Loading Curve	
1	Waste consisting of resins and filters from commercial power plants
2	Waste has been dewatered or grossly dewatered
3	No limit on moisture content of resin
4	Use of a liner (or equivalent) listed in Table 7.5.1-2 with maximum shoring volume as specified
5	Shipment time not greater than 10 days
6	Loading at temperature not exceeding 38 °C and standard pressure (1 atm)
7	Secondary containers are passively vented within the cask cavity during shipment.
8	Filters in the waste are not made of polyethylene or polypropylene.
9	Waste Volume not greater than 130 ft ³ .

Table 7.5.1-2 Secondary Container and Allowable Shoring Volumes
(Excerpt from Table 4.4.3-6)

Secondary Container	Volume Occupied by Container		Allowable Shoring Volume	
	(ft ³)	(cm ³)	(ft ³)	(cm ³)
PL 6-80 MT	9.28	2.63E+05	20.82	5.90E+05
PL 6-80 MTIF	9.74	2.76E+05	20.36	5.76E+05
PL 6-80 FR	10.21	2.89E+05	19.89	5.63E+05
PL 6-80 FP/FEDX	11.60	3.28E+05	18.50	5.24E+05
PL 8-120 MT	11.14	3.15E+05	18.96	5.37E+05
PL 8-120 MTIF	11.60	3.28E+05	18.50	5.24E+05
PL 8-120 FR	12.06	3.42E+05	18.04	5.11E+05
PL 8-120 FP/FEDX	13.46	3.81E+05	16.64	4.71E+05
PL 8-120 CMT	13.36	3.78E+05	16.74	4.74E+05
PL 14-150	14.85	4.20E+05	15.25	4.32E+05
PL 10-160 MT	12.99	3.68E+05	17.11	4.84E+05
PL 10-160 MTIF	13.64	3.86E+05	16.46	4.66E+05
PL 10-160 FR	13.92	3.94E+05	16.18	4.58E+05
PL 10-160 FP/FEDX	15.31	4.34E+05	14.79	4.19E+05
NUHIC-55	2.78	7.88E+04	27.32	7.74E+05
NUHIC-136	11.14	3.15E+05	18.96	5.37E+05
Radlok 500	12.62	3.57E+05	17.48	4.95E+05
EL-50	16.87	4.78E+05	13.23	3.75E+05
EL-142	27.02	7.65E+05	3.08	8.72E+04
L 6-80 MT	2.27	6.42E+04	27.83	7.88E+05
L 6-80 CMT	2.61	7.38E+04	27.49	7.79E+05
L 6-80 IN-SITU	7.94	2.25E+05	22.16	6.28E+05
L 6-80 FP	2.38	6.74E+04	27.72	7.85E+05
L 6-80 FP/FEDX	2.78	7.86E+04	27.32	7.74E+05
L 8-120 MT	2.72	7.70E+04	27.38	7.75E+05
L 8-120 CMT	3.06	8.67E+04	27.04	7.66E+05
L 8-120 IN-SITU	9.52	2.70E+05	20.58	5.83E+05
L 8-120 FR	2.83	8.03E+04	27.27	7.72E+05
L 8-120 FP/FEDX	3.00	8.51E+04	27.10	7.67E+05
ES-50	0.57	1.61E+04	29.53	8.36E+05
ES-142	2.49	7.06E+04	27.61	7.82E+05

7.5.2 Hydrogen Gas Generation – Analytical Model used for Detailed Analysis

If Figure 7.5-1 is not applicable to a shipment, or if further analysis is required, the equations given in Section 4.4.5 can be used to determine the maximum allowable decay heat. Equation 4.8 and Equation 4.9 are given below for reference:

Equation 4.8

Determination of maximum shipping time based on a known decay heat:

$$t_{max} = \frac{(2.5A_N P_0)(4.6E6 - V_C - 0.8911V_{WASTE})(0.8911V_{WASTE} + V_C)}{(R_g T_0 D_H)[0.6336V_{WASTE} G_{Ti}(\alpha_i - 0.05) + V_C G_{TC}(\alpha_C - 0.05) + 0.2575V_{WASTE} G_{TW}(\alpha_W - 0.05)]}$$

Equation 4.9

Determination of the maximum decay heat based on a known shipment time:

$$D_{H,max} = \frac{(2.5A_N P_0)(4.6E6 - V_C - 0.8911V_{WASTE})(0.8911V_{WASTE} + V_C)}{(R_g T_0 t)[0.6336V_{WASTE} G_{Ti}(\alpha_i - 0.05) + V_C G_{TC}(\alpha_C - 0.05) + 0.2575V_{WASTE} G_{TW}(\alpha_W - 0.05)]}$$

where: t_{max} = maximum allowable shipping time for a given decay heat to ensure the hydrogen generated during shipment does not exceed 5% [s]
 $D_{H,max}$ = maximum allowable decay heat for a given shipping time to ensure the hydrogen generated during shipment does not exceed 5% [eV/s]
 A_N = Avogadro's constant [6.022×10^{23} molecules/gmol]
 R_g = gas law constant [$82.05 \text{ cm}^3 \cdot \text{atm}/\text{gmol} \cdot \text{K}$]
 P_0 = pressure when the container is sealed [atm]
 T_0 = temperature when the container is sealed [K]
 t = shipment time [s]
 D_H = decay heat of cask contents [eV/s]
 V_C = volume occupied by the secondary container, shoring, and polyethylene or polypropylene filters in the waste [cm^3]
 V_{WASTE} = volume occupied by the ionic resin and stainless steel filters in the waste material [cm^3]
 G_{Ti} = total radiolytic G value for the ionic resin and stainless steel filters [molecules/100eV]
 G_{TC} = total radiolytic G value for the secondary container, shoring, and polyethylene or polypropylene filters in the waste [molecules/100eV]
 G_{TW} = total radiolytic G value for water in waste [molecules/100eV]
 α_i = fraction of G_{Ti} that is equivalent to G_{FGi} , flammable gas released, for the ionic resin and stainless steel filters
 α_C = fraction of G_{TC} that is equivalent to G_{FGC} , flammable gas released, for the secondary container, shoring, and polyethylene or polypropylene filters in the waste
 α_W = fraction of G_{TW} that is equivalent to G_{FGW} , flammable gas released, for water in the waste

NOTE: Use of Equation 4.8 and Equation 4.9 are valid only when the conditions listed in Table 7.5.2-1 are met. Shipments are allowed only if the conditions in Table 7.5.2-1 are met.

Table 7.5.2-1 Conditions for Shipper to use the Detailed Analysis (From Table 4.4.5-1)

1	Waste consists of resins and filters from commercial power plants.
2	Waste has been grossly dewatered.
3	Secondary containers are passively vented within the cask cavity during shipment.

Use the following procedure to confirm the decay heat of the cask contents meet the requirements of NUREG/CR-6673 [Ref. 16]:

1. Determine the values of the variables P_0 , T_0 , V_C , and V_{WASTE} . Initial pressure (P_0) and initial temperature (T_0) may be measured by the user at the time of loading. The volume occupied by the secondary container, shoring, and polyethylene or polypropylene filters in the waste (V_C) and the volume occupied by the ionic resin and stainless steel filters in the waste material (V_{WASTE}) are known.
2. Determine the values of the variables G_{Ti} , G_{TC} , G_{TW} , α_i , α_C , and α_W . G-values (G_{Ti} , G_{TC} , G_{TW}) and α fractions (α_i , α_C , α_W) must be justified by the user based on waste characterization. These variables must be adjusted for the transport temperature of 80 °C, as described in Section 4.4.1.3, in order to meet the requirements of NUREG/CR-6673 [Ref. 12]. The values must also be adjusted for the appropriate alpha/gamma radiation distribution. One example of this adjustment is provided in Table 7.5.2-2 for the same G-values in the bounding case loading curve for the 80% gamma/20% alpha decay heat distribution.
3. Use one of the following methods (a *or* b).
 - a. Take the decay heat of the cask contents (D_H) and solve Equation 4.8 for the maximum allowable shipping time (t_{max}). Confirm the shipment time (t) will be less than the maximum allowable shipping time (t_{max}).
 - b. Take the shipment time (t) and solve Equation 4.9 for the maximum allowable decay heat ($D_{H,max}$). Confirm the actual decay heat of the contents (D_H) is less than the maximum allowable decay heat ($D_{H,max}$).

Table 7.5.2-2 G-values and α -Fractions for a Range of Alpha/Gamma Decay Heat Distributions (Excerpt from Table 4.4.5-2)

Gamma Frac	Alpha Frac	Material	G (net gas), G_T		α	
0.0	1.0	Polyethylene	G_{TC}	5.06	α_C	1.00
		Resin	G_{Ti}	3.65	α_i	0.81
		Water	G_{TW}	1.60	α_W	1.00 ⁽¹⁶⁾
0.1	0.9	Polyethylene	G_{TC}	5.06	α_C	1.00
		Resin	G_{Ti}	3.40	α_i	0.82
		Water	G_{TW}	1.49	α_W	1.00 ⁽¹⁶⁾
0.2	0.8	Polyethylene	G_{TC}	5.06	α_C	1.00
		Resin	G_{Ti}	3.14	α_i	0.82
		Water	G_{TW}	1.37	α_W	1.00 ⁽¹⁶⁾
0.3	0.7	Polyethylene	G_{TC}	5.06	α_C	1.00
		Resin	G_{Ti}	2.88	α_i	0.83
		Water	G_{TW}	1.26	α_W	1.00 ⁽¹⁶⁾
0.4	0.6	Polyethylene	G_{TC}	5.06	α_C	1.00
		Resin	G_{Ti}	2.62	α_i	0.84
		Water	G_{TW}	1.14	α_W	1.00 ⁽¹⁶⁾
0.5	0.5	Polyethylene	G_{TC}	5.06	α_C	1.00
		Resin	G_{Ti}	2.37	α_i	0.85
		Water	G_{TW}	1.03	α_W	1.00 ⁽¹⁶⁾
0.6	0.4	Polyethylene	G_{TC}	5.06	α_C	1.00
		Resin	G_{Ti}	2.11	α_i	0.87
		Water	G_{TW}	0.91	α_W	1.00 ⁽¹⁶⁾
0.7	0.3	Polyethylene	G_{TC}	5.06	α_C	1.00
		Resin	G_{Ti}	1.85	α_i	0.89
		Water	G_{TW}	0.80	α_W	1.00 ⁽¹⁶⁾
0.8	0.2	Polyethylene	G_{TC}	5.06	α_C	1.00
		Resin	G_{Ti}	1.59	α_i	0.91
		Water	G_{TW}	0.68	α_W	1.00 ⁽¹⁶⁾
0.9	0.1	Polyethylene	G_{TC}	5.06	α_C	1.00
		Resin	G_{Ti}	1.34	α_i	0.95
		Water	G_{TW}	0.57	α_W	1.00 ⁽¹⁶⁾
0.95	0.05	Polyethylene	G_{TC}	5.06	α_C	1.00
		Resin	G_{Ti}	1.21	α_i	0.97
		Water	G_{TW}	0.51	α_W	1.00 ⁽¹⁶⁾
1.0	0.0	Polyethylene	G_{TC}	5.06	α_C	1.00
		Resin	G_{Ti}	1.08	α_i	1.00
		Water	G_{TW}	0.45	α_W	1.00 ⁽¹⁶⁾

¹⁶ For water, the α value is set to 1.0.

7.5.3 Hydrogen Gas Generation – Analytical Model Example

An example calculation using the analytical model developed in Section 7.5.2 is shown below.

The following two variables are constants are known:

$$A_N = 6.022E23 \text{ molecules/gmol}$$

$$R_g = 82.05 \text{ cm}^3 \cdot \text{atm/gmol} \cdot \text{K}$$

In this example, the user has input the following parameters:

$$P_0 = 1 \text{ atm}$$

$$T_0 = 89^\circ \text{F} = 305 \text{ K}$$

$$t = 8 \text{ days} = 691200 \text{ s}$$

$$V_C = 30.1 \text{ ft}^3 = 8.52E05 \text{ cm}^3$$

$$V_{WASTE} = 70.0 \text{ ft}^3 = 1.98E06 \text{ cm}^3$$

These variables are substituted into the maximum allowable decay heat equation as shown:

$$\begin{aligned}
 D_{H,max} &= \frac{(2.5A_N P_0)(4.6E6 - V_C - 0.8911V_{WASTE})(0.8911V_{WASTE} + V_C)}{(R_g T_0 t)[0.6336V_{WASTE} G_{Ti}(\alpha_i - 0.05) + V_C G_{TC}(\alpha_C - 0.05) + 0.2575V_{WASTE} G_{TW}(\alpha_W - 0.05)]} \\
 &= \frac{[(2.5)(6.022E23)(1)] \times [4.6E6 - 8.52E5 - (0.8911)(1.98E6)] \times [(0.8911)(1.98E6) + 8.52E5]}{[(82.05)(305)(691200)][0.6336(1.98E6)G_{Ti}(\alpha_i - 0.05) + (8.52E5)G_{TC}(\alpha_C - 0.05) + 0.2575(1.98E6)G_{TW}(\alpha_W - 0.05)]} \\
 &= \frac{[1.51E24] \times [1.98E6] \times [2.62E6]}{[1.73E10][(1.25E6)G_{Ti}(\alpha_i - 0.05) + (8.52E5)G_{TC}(\alpha_C - 0.05) + (5.10E5)G_{TW}(\alpha_W - 0.05)]}
 \end{aligned}$$

Additionally, the user knows the decay heat distribution of the waste stream is 95% gamma. Using the information provided in Table 7.5.2-2, the user inputs the following G-values and α fractions. (Note that the values listed in Table 7.5.2-2 have already been adjusted for bounding NCT temperature.)

$$G_{Ti} = 1.21 \text{ molecules/100eV}$$

$$G_{TC} = 5.06 \text{ molecules/100eV}$$

$$G_{TW} = 0.51 \text{ molecules/100eV}$$

$$\alpha_i = 0.97$$

$$\alpha_C = 1.00$$

$$\alpha_W = 1.00$$

With further substitution, the maximum allowable decay heat ($D_{H,max}$), may be calculated:

$$\begin{aligned}
 &= \frac{[1.51E24] \times [1.98E6] \times [2.62E6]}{[1.73E10][(1.25E6)(1.21)(0.97 - 0.05) + (8.52E5)(5.06)(1 - 0.05) + (5.10E5)(0.51)(1 - 0.05)]} \\
 &= \frac{[7.81E36]}{[1.73E10][(1.40E6) + (4.10E6) + (2.47E5)]}
 \end{aligned}$$

$$D_{H,max} = 7.87 \times 10^{19} \frac{\text{eV}}{\text{s}} = 12.61 \text{ Watts}$$

7.6 Appendix

The following appendices are included for Chapter 7 instruction and information. Additional steps and conditions of use for the RT-100 are as follows:

1. The maximum content density is 1.0 g/cm^3 . The weight of free water must be excluded in this determination. The source strength density must be ensured at any point of the content. Average density by dividing the total activity by total weight is not acceptable.
2. No neutron emitting nuclides, except in trace amounts.
3. The weight of water must be excluded when determining the Ci/gram of content limit.
4. The source concentration must not exceed the Curies per gram limit determined using the method and the loading tables as prescribed in Appendix 7.6 of this Chapter and no concentration or shift during normal conditions of transport.
5. The user/shipper must analyze the constituent radioactive nuclides of the content on a per-gram basis.
6. The user/shipper must determine the allowable content based on the loading tables provided in Section 7.6.1.1.
7. The user/shipper must ensure the per gram activities at any point within the content does not exceed the limit that is specified according to the loading table.
8. The allowable content must be determined based on dry resin or filter media. Any potential concentration of sources during loading and transport is not permitted.
9. The radioactive content is not to exceed 1.0 g/cm^3 and the nuclear physical characteristics, i.e., the gamma attenuation coefficient of the content must not be smaller than that of the carbon material resin.
10. A comprehensive dose rate measurement is performed prior to transport of the package as described in Section 7.1.3.
11. A comprehensive dose rate measurement is performed after arrival at the destination as described in Section 7.2.1.
12. Compare pre-shipment dose rate measurements to dose rate measurements at the arrival of the package. Stop any further shipment if the measured dose rates show significant differences from the pre-shipment measurement values.

7.6.1 RT-100 Loading Table Discussion

The dose rate compliance of the RT-100 cask is ensured by: first, determining the percent of each radionuclide activity relative to its maximum allowable value, and then summing up this dose rate percentage for all radionuclides and assuring that the sum does not exceed 100%. In addition, the activity for the package shall be less than 3000 A₂, the total decay heat output shall be less than 200 watts, and the actual content activity concentration of neutron emitters shall be less than 3.5 milliCuries/kg. This compliance is facilitated by employing a loading table that is completed by the shipper of the RT-100. The loading table has ten columns as follows:

- “Actual Content Nuclide” – Radionuclide entered by user into the loading table. Qualification of the content loaded into the RT-100 cask is under the responsibility of the shipper/user.
- “Maximum Allowable Activity Concentration” – The maximum allowed activity for the isotope being entered into the RT-100 transport cask, in milliCuries/kg, that is based on the methodology described in Section 5.4.4 and presented in Table 7.6.1-6.
- “Actual Content Activity Concentration” – The maximum activity concentration of the isotope to be placed in the RT-100 transport entered by the user in units of milliCuries/kg. This value should be the maximum for any waste stream placed in the cask. The user shall ensure that the bulk density of the resin or filter media does not exceed 1 g/cm³.
- “% of Maximum” – The percent of maximum column represents the percentage of the activity concentration entered by the user for the isotope in question versus the maximum allowable activity concentration established by the methodology described in Section 5.4.4.
- “A₂” – The total activity equivalent to 1 A₂ in Curies for isotope entered by the user.
- “Activity(i) / A₂(i)” – The total A₂ quantity for the isotope entered by the user.
- “Q Value” – The amount of heat energy released per unit activity, in Watts/milliCurie, for the isotope entered by the user.
- “Heat Load” – The total heat load contribution, in Watts, for the activity concentration and mass entered by the user for the isotope.
- “Neutron Emitter?” – This column indicates whether the Radionuclide entered by the user is a neutron emitter (²³⁸Pu, ²³⁹Pu, ²⁴⁰Pu, ²⁴²Pu, ²⁴²Cm, ²⁴³Cm, ²⁴⁴Cm, ²⁴⁸Cm, ²⁴¹Am, or ²⁵²Cf).

- “Actual Content Activity Concentration” – For neutron emitters, the previously entered activity concentration is shown in this column.

The total waste inventory volume and mass is entered into the first two rows in cubic feet and kilograms (in the yellow cells in Table 7.6.1-1). The “Actual Content Activity Concentration (milliCuries/kg)” and “Actual Content Nuclide” columns (columns in yellow in Table 7.6.1-1) is where the user inputs the activity concentration and radionuclides in the package.

Once total mass in kilograms, total activity concentration in milliCuries/kg, and radionuclides are input into the table, the rest is automatically updated. The “% of Maximum” column is the ratio of the results in “Actual Content Activity Concentration (milliCuries/kg)” column divided by the values in “Maximum Allowable Activity Concentration (milliCuries/kg)” column.

The “Maximum Allowable Activity Concentration (milliCuries/kg)” column contains the maximum activity per kilogram allowed for each isotope based on the NCT and HAC dose rate limits and the most conservative response functions (mrem/hr/Curie) generated by MCNP calculations. The “% of Maximum” column is summed at the end of the column. If the sum is greater than 100%, then the inventory dose rate would potentially exceed the NCT or HAC dose rate limits, which would make the package not acceptable. If the sum is less than or equal to 100%, the package would generate an acceptable dose rate under NCT and HAC conditions. The “A2 (Curie)” column contains the A₂ activity value in Curies for the isotope. The “Activity (i) / A2(i)” column is the ratio of the activity entered by the user divided by the A₂ value for the isotope. The “Activity (i) / A2(i)” column is summed. If the value is under 3000 A₂, the inventory total activity is below the containment limit.

The third test is determining the total heat load of the inventory. Each radionuclide’s activity is multiplied by the value in the “Q Value (Watts/milliCurie)” column and the result is automatically entered into the “Heat Load (Watts)” column. At the end of the column, the results are summed and compared to the 200 Watt limit. If it is below the limit, the package is acceptable under heat load limitations.

The final test is to ensure the neutron emitter limit of 3.5 milliCuries/kg is not exceeded. If the user-entered radionuclide is a neutron emitter, it is indicated in the “Neutron Emitter?” column. For these radionuclides, the “Actual Content Activity Concentration” is shown. At the end of the column, the results are summed and compared to the limit of 3.5 milliCuries/kg. If the sum is below the limit, the package is considered to contain only trace amounts of neutron-emitting radionuclides.

At the end of each evaluation, a marker indicating if the inventory passes a particular set of

criteria (for example the cell beside “Passed Shielding Criteria”) is provided. If the cell turns green and states “TRUE”, then the inventory passes that particular set of criteria. If the cell turns red and states “FALSE”, then the inventory has failed that particular set of criteria. An inventory must pass all four criteria (shielding, containment, heat load, and neutron limit) in order to be shipped in an RT-100 cask.

Notes for the RT-100 Loading Table:

- Each radionuclide in the resin mixture is listed by row.
- The sum of column 4 (% of max) should be less than 100% for dose rate regulatory compliance and the sum of column 6 (C(i)/A(i)) should be less than 3000 A₂ for containment regulatory compliance.
- The sum of column eight should be less than 200 Watts in order to satisfy the heat load limit.
- A basic procedure has been provided in Section 7.6.1.1.
- Several examples have been provided in Section 7.6.1.2, Section 7.6.1.3, and Section 7.6.1.4.
- Example of RT-100 Loading Table format provided below in Table 7.6.1-1.

Table 7.6.1-1 RT-100 Loading Table Illustration

Waste Vol (ft ³)		Actual Content Loading Evaluation							
Content Mass (kg)									
Gamma Emitting Nuclides		Shielding Evaluation		Containment Evaluation		Heat Load Evaluation		Neutron Emitter† Evaluation	
Actual Content Nuclide	Maximum Allowable Activity Concentration (milliCuries/kg)	Actual Content Activity Concentration (milliCuries/kg)	% of Maximum	A2 (Curie)	Activity(i) / A2(i)	Q Value (Watts/mCi)	Heat Load (Watts)	Neutron Emitter?	Actual Content Activity Concentration (milliCuries/kg)
ac225	5.06E+05	0.00E+00	0.00	0.16	0.00E+00	3.49E-05	0.00E+00	N	
ag108m	2.12E+03	0.00E+00	0.00	19	0.00E+00	9.70E-06	0.00E+00	N	
ag110	3.68E+04	0.00E+00	0.00	0.54	0.00E+00	7.18E-06	0.00E+00	N	
ag110m	4.84E+02	0.00E+00	0.00	11	0.00E+00	1.67E-05	0.00E+00	N	
am241	6.02E+07	0.00E+00	0.00	0.027	0.00E+00	3.34E-05	0.00E+00	Y	0.00E+00
am242	5.83E+11	0.00E+00	0.00	0.54	0.00E+00	1.15E-06	0.00E+00	N	
am243	2.81E+06	0.00E+00	0.00	0.027	0.00E+00	3.47E-05	0.00E+00	N	
au199	4.09E+04	0.00E+00	0.00	16	0.00E+00	1.38E-06	0.00E+00	N	
ba140	3.43E+04	0.00E+00	0.00	8.1	0.00E+00	2.92E-06	0.00E+00	N	
be7	1.93E+05	0.00E+00	0.00	540	0.00E+00	2.00E-06	0.00E+00	N	
c14	5.83E+11	0.00E+00	0.00	81	0.00E+00	2.93E-07	0.00E+00	N	
cd109	5.83E+11	0.00E+00	0.00	54	0.00E+00	1.17E-07	0.00E+00	N	
ce139	2.50E+04	0.00E+00	0.00	54	0.00E+00	1.47E-06	0.00E+00	N	
ce141	4.14E+04	0.00E+00	0.00	16	0.00E+00	1.46E-06	0.00E+00	N	
ce144	1.80E+05	0.00E+00	0.00	5.4	0.00E+00	7.99E-06	0.00E+00	N	
cm241	1.16E+04	0.00E+00	0.00	27	0.00E+00	4.05E-06	0.00E+00	N	
cm242	4.05E+08	0.00E+00	0.00	0.27	0.00E+00	3.65E-05	0.00E+00	Y	0.00E+00
cm243	3.16E+04	0.00E+00	0.00	0.027	0.00E+00	3.66E-05	0.00E+00	Y	0.00E+00
cm244	8.69E+08	0.00E+00	0.00	0.054	0.00E+00	3.50E-05	0.00E+00	Y	0.00E+00
cm245	3.76E+04	0.00E+00	0.00	0.024	0.00E+00	3.33E-05	0.00E+00	N	
cm246	5.83E+11	0.00E+00	0.00	0.024	0.00E+00	3.28E-05	0.00E+00	N	
co57	1.99E+04	0.00E+00	0.00	270	0.00E+00	8.52E-07	0.00E+00	N	
co58	6.96E+03	0.00E+00	0.00	27	0.00E+00	5.99E-06	0.00E+00	N	
co60	2.50E+02	0.00E+00	0.00	11	0.00E+00	1.54E-05	0.00E+00	N	
cr51	1.98E+05	0.00E+00	0.00	810	0.00E+00	2.20E-07	0.00E+00	N	
cs134	6.03E+03	0.00E+00	0.00	19	0.00E+00	1.02E-05	0.00E+00	N	
cs136	1.09E+02	0.00E+00	0.00	14	0.00E+00	1.22E-05	0.00E+00	N	
cs137	7.95E+04	0.00E+00	0.00	16	0.00E+00	5.04E-06	0.00E+00	N	
cs144	5.27E+00	0.00E+00	0.00	0.54	0.00E+00	3.00E-05	0.00E+00	N	
cu64	6.61E+03	0.00E+00	0.00	27	0.00E+00	1.86E-06	0.00E+00	N	
eu154	9.69E+01	0.00E+00	0.00	16	0.00E+00	9.08E-06	0.00E+00	N	
eu155	9.11E+04	0.00E+00	0.00	81	0.00E+00	7.77E-07	0.00E+00	N	
fe55	1.63E+09	0.00E+00	0.00	1100	0.00E+00	3.40E-08	0.00E+00	N	
fe59	7.11E+02	0.00E+00	0.00	24	0.00E+00	7.74E-06	0.00E+00	N	
h3	5.83E+11	0.00E+00	0.00	1100	0.00E+00	3.37E-08	0.00E+00	N	
hf181	1.36E+04	0.00E+00	0.00	14	0.00E+00	4.34E-06	0.00E+00	N	
hg203	2.45E+04	0.00E+00	0.00	27	0.00E+00	1.99E-06	0.00E+00	N	
i124	5.54E+01	0.00E+00	0.00	27	0.00E+00	7.75E-06	0.00E+00	N	
i125	5.83E+11	0.00E+00	0.00	81	0.00E+00	3.49E-07	0.00E+00	N	
i129	5.83E+11	0.00E+00	0.00	Unlimited		4.68E-07	0.00E+00	N	
i131	1.71E+04	0.00E+00	0.00	19	0.00E+00	3.40E-06	0.00E+00	N	
in113m	3.11E+04	0.00E+00	0.00	54	0.00E+00	2.29E-06	0.00E+00	N	
k40	2.42E+02	0.00E+00	0.00	24	0.00E+00	3.76E-06	0.00E+00	N	
kr85	2.62E+06	0.00E+00	0.00	270	0.00E+00	1.50E-06	0.00E+00	N	
la140	1.63E+01	0.00E+00	0.00	11	0.00E+00	1.68E-05	0.00E+00	N	
mn54	1.65E+04	0.00E+00	0.00	27	0.00E+00	4.98E-06	0.00E+00	N	

Table 7.6.1-1 RT-100 Loading Table Illustration (Continued)

mo99	9.03E+03	0.00E+00	0.00	16	0.00E+00	4.01E-06	0.00E+00	N	
na24	3.38E+00	0.00E+00	0.00	5.4	0.00E+00	2.77E-05	0.00E+00	N	
nb94	6.40E+02	0.00E+00	0.00	19	0.00E+00	1.02E-05	0.00E+00	N	
nb95	2.59E+03	0.00E+00	0.00	27	0.00E+00	4.80E-06	0.00E+00	N	
ni59	3.30E+06	0.00E+00	0.00	Unlimited		4.36E-08	0.00E+00	N	
ni63	5.83E+11	0.00E+00	0.00	810	0.00E+00	1.02E-07	0.00E+00	N	
np237	5.86E+05	0.00E+00	0.00	0.054	0.00E+00	2.85E-05	0.00E+00	N	
pa233	3.22E+04	0.00E+00	0.00	19	0.00E+00	2.54E-06	0.00E+00	N	
pm144	3.14E+03	0.00E+00	0.00	19	0.00E+00	9.35E-06	0.00E+00	N	
po210	7.99E+07	0.00E+00	0.00	0.54	0.00E+00	3.21E-05	0.00E+00	N	
pr144	6.75E+02	0.00E+00	0.00	0.54	0.00E+00	7.34E-06	0.00E+00	N	
pu238	1.62E+09	0.00E+00	0.00	0.027	0.00E+00	3.31E-05	0.00E+00	Y	0.00E+00
pu239	1.14E+08	0.00E+00	0.00	0.027	0.00E+00	3.11E-05	0.00E+00	Y	0.00E+00
pu240	2.60E+08	0.00E+00	0.00	0.027	0.00E+00	3.11E-05	0.00E+00	Y	0.00E+00
pu241	3.67E+09	0.00E+00	0.00	1.6	0.00E+00	3.18E-08	0.00E+00	N	
pu242	6.96E+08	0.00E+00	0.00	0.027	0.00E+00	2.95E-05	0.00E+00	Y	0.00E+00
rb86	1.82E+03	0.00E+00	0.00	14	0.00E+00	4.51E-06	0.00E+00	N	
ru103	1.83E+04	0.00E+00	0.00	54	0.00E+00	3.33E-06	0.00E+00	N	
ru106	1.57E+03	0.00E+00	0.00	5.4	0.00E+00	9.65E-06	0.00E+00	N	
sb122	3.62E+03	0.00E+00	0.00	11	0.00E+00	5.94E-06	0.00E+00	N	
sb124	2.19E+01	0.00E+00	0.00	16	0.00E+00	1.33E-05	0.00E+00	N	
sb125	1.29E+04	0.00E+00	0.00	27	0.00E+00	3.16E-06	0.00E+00	N	
sc46	7.66E+01	0.00E+00	0.00	14	0.00E+00	1.26E-05	0.00E+00	N	
se75	1.14E+04	0.00E+00	0.00	81	0.00E+00	2.41E-06	0.00E+00	N	
sn113	1.09E+06	0.00E+00	0.00	54	0.00E+00	1.66E-07	0.00E+00	N	
sn113m	5.83E+11	0.00E+00	0.00	0.54	0.00E+00	3.87E-07	0.00E+00	N	
sn117m	2.25E+04	0.00E+00	0.00	11	0.00E+00	1.86E-06	0.00E+00	N	
sr85	1.15E+04	0.00E+00	0.00	54	0.00E+00	3.12E-06	0.00E+00	N	
sr89	5.83E+11	0.00E+00	0.00	16	0.00E+00	3.46E-06	0.00E+00	N	
sr90	3.64E+08	0.00E+00	0.00	8.1	0.00E+00	6.70E-06	0.00E+00	N	
tc99	5.83E+11	0.00E+00	0.00	24	0.00E+00	5.02E-07	0.00E+00	N	
tc99m	2.24E+04	0.00E+00	0.00	110	0.00E+00	9.35E-07	0.00E+00	N	
te123m	2.37E+04	0.00E+00	0.00	27	0.00E+00	1.46E-06	0.00E+00	N	
te132	2.17E+04	0.00E+00	0.00	11	0.00E+00	1.98E-06	0.00E+00	N	
th228	3.85E+06	0.00E+00	0.00	0.027	0.00E+00	2.07E-04	0.00E+00	N	
u233	2.67E+07	0.00E+00	0.00	0.16	0.00E+00	2.91E-05	0.00E+00	N	
xe131m	1.02E+06	0.00E+00	0.00	1100	0.00E+00	9.61E-07	0.00E+00	N	
xe133	2.72E+07	0.00E+00	0.00	270	0.00E+00	1.09E-06	0.00E+00	N	
y88	1.02E+01	0.00E+00	0.00	11	0.00E+00	1.60E-05	0.00E+00	N	
zn65	2.34E+03	0.00E+00	0.00	54	0.00E+00	3.50E-06	0.00E+00	N	
zr95	2.62E+03	0.00E+00	0.00	22	0.00E+00	5.04E-06	0.00E+00	N	
		Gamma Sum (%)	0.00	Gamma Sum (A2)	0.00	Gamma Sum (Watts)	0.00	Neutron Sum (mCi/kg)	0.00
		Limit (% of 95% of the NCT and HAC dose rate criteria)	100	Limit (A2)	3000	Limit (Watts)	200	Limit† (Neutron Sum, mCi/kg)	3.50
		Passed Shielding Criteria	TRUE	Passed Containment Criteria	TRUE	Passed Heat Load Criteria	TRUE	Passed Neutron Limit Criteria	TRUE

7.6.1.1 RT-100 Loading Table Procedure

Step 1: In top left corner of the Loading Table, input the inventory volume and mass in cubic feet and kilograms (the cells are highlighted in yellow). Verify that the bulk density of the resin or filter media does not exceed 1 g/cm^3 at any point of the content. The weight of water must be excluded when determining the Ci/gram of radioactive content limit. Resin or filter media having a bulk density above 1 g/cm^3 cannot be shipped in the RT-100 cask.

Step 2: Input an isotope in the first column of the loading table. Format is element symbol in lower case letters, followed by mass number with no spaces or dashes (i.e. i129 or eu154). Input radionuclide's activity concentration (in milliCuries/kilogram) in the "Actual Content Activity Concentration (milliCuries/kilogram)" column. The activity concentration input for each isotope should be the maximum for any waste stream placed in the cask.

Step 3: Repeat process until all isotopes and associated activity concentrations are listed. As each new isotope and concentration is entered, a new row is displayed. If "N/A" appears in any of the columns for the isotope entered, the isotope is not applicable to the RT-100 Loading Table or it is incorrectly input into the spreadsheet.¹⁷

Step 4: Once all relevant inventory inputs (inventory mass, radioisotopes, and activity concentration of each radioisotope) are entered into the table, check cells at the end of the evaluation columns, beside "Passed Criteria" cells. If cell beside passed criteria is green and states "TRUE", inventory has passed that particular set of criteria (for example, passed the shielding criteria). If cell beside criteria is red and states "FALSE", inventory has failed that particular set of criteria.

Step 5: An inventory **must pass all** test criteria before it can be shipped in an RT-100 cask.

7.6.1.2 Turkey Point Source Term Example Evaluation

The following is a sample from stored spent resin and used filters in High Integrity Containers (HIC's) from Turkey Point Units 3 & 4 Low Level Waste Facility [Ref. 9]. Sample results were increased by three standard deviations in order to generate a conservative source term, within 99% confidence interval. Based on Reference 9, mass of a particular Turkey Point HIC's contents was on the order of 2060 kg. Sample results were entered into the RT-100 Loading Table and the results are shown in Table 7.6.1-2.

The spent resin and used filter inventory from Turkey Point generates a value of 3.42% in the "%

¹⁷ If "N/A" appears in containment column but the isotope passes the shielding evaluation, the isotope is not in Table A-1 of Appendix A of 10 CFR 71. Look up the radiation type of the isotope. Based on Table A-3 of Appendix A of 10 CFR 71, enter 0.54 Ci for A2 of beta or gamma emitters and 0.0024 Ci for alpha emitters.

of Maximum” column, which is below 100%. The inventory satisfies the dose rate regulatory compliance. The total inventory A_2 value is 8.37 A_2 , which is below the 3000 A_2 limit. The inventory satisfies the containment limit. The total power output is 1.13 Watts, which is below the 200 Watts limit. The actual content activity concentration of neutron emitters is 0.00 milliCuries/kilogram, which is below the limit of 3.5 milliCuries/kilogram. Therefore, this package’s inventory would be considered acceptable.

Table 7.6.1-2 Turkey Point Loading Table Example

Waste Vol (ft ³)		Actual Content Loading Evaluation							
2060.00		Content Mass (kg)							
Gamma Emitting Nuclides		Shielding Evaluation		Containment Evaluation		Heat Load Evaluation		Neutron Emitter† Evaluation	
Actual Content Nuclide	Maximum Allowable Activity Concentration (milliCuries/kg)	Actual Content Activity Concentration (milliCuries/kg)	% of Maximum	A ₂ (Curie)	Activity(i) / A ₂ (i)	Q Value (Watts/mCi)	Heat Load (Watts)	Neutron Emitter?	Actual Content Activity Concentration (milliCuries/kg)
h3	5.83E+11	1.45E-03	0.00	1100	2.72E-06	3.37E-08	1.01E-07	N	
c14	5.83E+11	1.25E-03	0.00	81	3.18E-05	2.93E-07	7.55E-07	N	
fe55	1.63E+09	8.40E+00	0.00	1100	1.57E-02	3.40E-08	5.88E-04	N	
ni63	5.83E+11	4.68E+01	0.00	810	1.19E-01	1.02E-07	9.80E-03	N	
sr89	5.83E+11	1.73E-03	0.00	16	2.23E-04	3.46E-06	1.23E-05	N	
sr90	3.64E+08	1.46E-02	0.00	8.1	3.71E-03	6.70E-06	2.01E-04	N	
tc99	5.83E+11	4.10E-03	0.00	24	3.52E-04	5.02E-07	4.24E-06	N	
pu241	3.67E+09	4.52E-03	0.00	1.6	5.82E-03	3.18E-08	2.96E-07	N	
i129	5.83E+11	4.40E-05	0.00	Unlimited		4.68E-07	4.24E-08	N	
mn54	1.65E+04	9.17E-01	0.01	27	7.00E-02	4.98E-06	9.41E-03	N	
co57	1.99E+04	2.23E-01	0.00	270	1.70E-03	8.52E-07	3.92E-04	N	
co58	6.96E+03	1.00E+00	0.01	27	7.63E-02	5.99E-06	1.23E-02	N	
co60	2.50E+02	7.28E+00	2.91	11	1.36E+00	1.54E-05	2.31E-01	N	
sb125	1.29E+04	5.19E-01	0.00	27	3.96E-02	3.16E-06	3.38E-03	N	
cs134	6.03E+03	2.69E+01	0.45	19	2.92E+00	1.02E-05	5.65E-01	N	
cs137	7.95E+04	2.84E+01	0.04	16	3.66E+00	5.04E-06	2.95E-01	N	
ce144	1.80E+05	1.88E-01	0.00	5.4	7.17E-02	7.99E-06	3.10E-03	N	
cm242	4.05E+08	2.84E-05	0.00	0.27	2.17E-04	3.65E-05	2.13E-06	Y	2.84E-05
pu238	1.62E+09	9.97E-05	0.00	0.027	7.61E-03	3.31E-05	6.81E-06	Y	9.97E-05
pu239	1.14E+08	5.47E-05	0.00	0.027	4.17E-03	3.11E-05	3.50E-06	Y	5.47E-05
am241	6.02E+07	8.45E-05	0.00	0.027	6.45E-03	3.34E-05	5.81E-06	Y	8.45E-05
cm243	3.16E+04	9.16E-05	0.00	0.027	6.99E-03	3.66E-05	6.91E-06	Y	9.16E-05
		Gamma Sum (%)	3.42	Gamma Sum (A ₂)	8.37	Gamma Sum (Watts)	1.13	Neutron Sum (mCi/kg)	0.00
		Limit (% of 95% of the NCT and HAC dose rate criteria)	100	Limit (A ₂)	3000	Limit (Watts)	200	Limit† (Neutron Sum, mCi/kg)	3.50
		Passed Shielding Criteria	TRUE	Passed Containment Criteria	TRUE	Passed Heat Load Criteria	TRUE	Passed Neutron Limit Criteria	TRUE

7.6.1.3 St. Lucie Loading Table

The following is source term information for a typical St. Lucie HIC source term [Ref. 10]. Two sets of sample results were increased by three standard deviations in order to generate a conservative source term, within 99% confidence interval. If multiple samples are taken from a shipment, the maximum activity concentration values for each isotope should be used in the RT-100 Loading Table. Based on Reference 10, mass of a particular St. Lucie HIC's contents was on the order of 1950 kg. The maximum values for each isotope from the two samples were inputted into the RT-100 Loading Table and the results are shown in Table 7.6.1-3.

The spent resin and used filter inventory from St. Lucie generates a value of 9.78% in the “% of Maximum” column, which is below 100%. The inventory satisfies the dose rate regulatory compliance. The total inventory A_2 value is 1.70 A_2 , which is below the 3000 A_2 limit. The heat load is 0.23 Watts, which is below the 200 Watt limit. The actual content activity concentration of neutron emitters is 0.00 milliCuries/kilogram, which is below the limit of 3.5 milliCuries/kilogram. Therefore, this package's inventory would be considered acceptable.

Table 7.6.1-3 St. Lucie Loading Table Example

Waste Vol (ft ³)		Actual Content Loading Evaluation							
1950.00		Content Mass (kg)							
Gamma Emitting Nuclides		Shielding Evaluation		Containment Evaluation		Heat Load Evaluation		Neutron Emitter† Evaluation	
Actual Content Nuclide	Maximum Allowable Activity Concentration (milliCuries/kg)	Actual Content Activity Concentration (milliCuries/kg)	% of Maximum	A2 (Curie)	Activity(i) / A2(i)	Q Value (Watts/mCi)	Heat Load (Watts)	Neutron Emitter?	Actual Content Activity Concentration (milliCuries/kg)
h3	5.83E+11	3.90E-03	0.00	1100	6.91E-06	3.37E-08	2.57E-07	N	
c14	5.83E+11	1.55E-02	0.00	81	3.73E-04	2.93E-07	8.86E-06	N	
fe55	1.63E+09	3.65E+00	0.00	1100	6.47E-03	3.40E-08	2.42E-04	N	
ni63	5.83E+11	3.00E+01	0.00	810	7.22E-02	1.02E-07	5.94E-03	N	
sr89	5.83E+11	9.20E-03	0.00	16	1.12E-03	3.46E-06	6.20E-05	N	
sr90	3.64E+08	2.86E-03	0.00	8.1	6.89E-04	6.70E-06	3.74E-05	N	
tc99	5.83E+11	2.70E-03	0.00	24	2.19E-04	5.02E-07	2.64E-06	N	
pu241	3.67E+09	4.00E-03	0.00	1.6	4.88E-03	3.18E-08	2.48E-07	N	
i129	5.83E+11	2.45E-04	0.00	Unlimited		4.68E-07	2.23E-07	N	
cr51	1.98E+05	1.46E+00	0.00	810	3.51E-03	2.20E-07	6.27E-04	N	
mn54	1.65E+04	8.35E-01	0.01	27	6.03E-02	4.98E-06	8.11E-03	N	
co57	1.99E+04	3.21E-01	0.00	270	2.32E-03	8.52E-07	5.34E-04	N	
co58	6.96E+03	1.59E+00	0.02	27	1.15E-01	5.99E-06	1.86E-02	N	
fe59	7.11E+02	9.00E-02	0.01	24	7.31E-03	7.74E-06	1.36E-03	N	
co60	2.50E+02	3.92E+00	1.57	11	6.95E-01	1.54E-05	1.18E-01	N	
zn65	2.34E+03	1.28E-01	0.01	54	4.62E-03	3.50E-06	8.73E-04	N	
nb94	6.40E+02	4.20E-02	0.01	19	4.31E-03	1.02E-05	8.34E-04	N	
zr95	2.62E+03	1.21E-01	0.00	22	1.07E-02	5.04E-06	1.19E-03	N	
nb95	2.59E+03	2.15E-01	0.01	27	1.55E-02	4.80E-06	2.01E-03	N	
ru103	1.83E+04	1.37E-01	0.00	54	4.95E-03	3.33E-06	8.89E-04	N	
ru106	1.57E+03	2.90E-01	0.02	5.4	1.05E-01	9.65E-06	5.45E-03	N	
ag108m	2.12E+03	5.20E-02	0.00	19	5.34E-03	9.70E-06	9.83E-04	N	
ag110m	4.84E+02	1.30E-01	0.03	11	2.30E-02	1.67E-05	4.23E-03	N	
sb124	2.19E+01	3.60E-02	0.16	16	4.39E-03	1.33E-05	9.31E-04	N	
sb125	1.29E+04	3.32E-01	0.00	27	2.40E-02	3.16E-06	2.05E-03	N	
cs134	6.03E+03	4.20E-02	0.00	19	4.31E-03	1.02E-05	8.35E-04	N	
cs137	7.95E+04	1.72E-01	0.00	16	2.10E-02	5.04E-06	1.69E-03	N	
la140	1.63E+01	1.29E+00	7.93	11	2.29E-01	1.68E-05	4.22E-02	N	
ce141	4.14E+04	2.92E-01	0.00	16	3.56E-02	1.46E-06	8.33E-04	N	
ce144	1.80E+05	5.70E-01	0.00	5.4	2.06E-01	7.99E-06	8.88E-03	N	
am241	6.02E+07	4.10E-05	0.00	0.027	2.96E-03	3.34E-05	2.67E-06	Y	4.10E-05
cm242	4.05E+08	1.56E-05	0.00	0.27	1.13E-04	3.65E-05	1.11E-06	Y	1.56E-05
cm243	3.16E+04	2.44E-04	0.00	0.027	1.76E-02	3.66E-05	1.74E-05	Y	2.44E-04
pu238	1.62E+09	5.70E-05	0.00	0.027	4.12E-03	3.31E-05	3.68E-06	Y	5.70E-05
pu239	1.14E+08	5.90E-05	0.00	0.027	4.26E-03	3.11E-05	3.58E-06	Y	5.90E-05
		Gamma Sum (%)	9.78	Gamma Sum (A2)	1.70	Gamma Sum (Watts)	0.23	Neutron Sum (mCi/kg)	0.00
		Limit (% of 95% of the NCT and HAC dose rate criteria)	100	Limit (A2)	3000	Limit (Watts)	200	Limit† (Neutron Sum, mCi/kg)	3.50
		Passed Shielding Criteria	TRUE	Passed Containment Criteria	TRUE	Passed Heat Load Criteria	TRUE	Passed Neutron Limit Criteria	TRUE

7.6.1.4 Additional Examples

Two additional examples have been generated to show the maximum Co-60 loading for the RT-100 and an arbitrary example showing a load that fails the RT-100 Loading Table. Table 7.6.1-4 shows the maximum Co-60 inventory allowed due to shielding limits. The activity concentration is at 100% under the “% of Maximum” column. Table 7.6.1-5 shows the effect of inputting two radionuclides that individually would pass the compliance tests, but having both radionuclide quantities in the cask would generate a dose rate that would fail either NCT or HAC shielding conditions. This is illustrated by the red “FALSE” cell due to shielding sum is 100.73%, which is above the 100% limit. The inventory in Table 7.6.1-5 would not be acceptable in an RT-100 Transport Cask.

Table 7.6.1-4 Maximum Co-60 Loading Table Example

Waste Vol (ft ³)		Actual Content Loading Evaluation							
2988.58		Content Mass (kg)							
Gamma Emitting Nuclides		Shielding Evaluation		Containment Evaluation		Heat Load Evaluation		Neutron Emitter† Evaluation	
Actual Content Nuclide	Maximum Allowable Activity Concentration (milliCuries/kg)	Actual Content Activity Concentration (milliCuries/kg)	% of Maximum	A2 (Curie)	Activity(i) / A2(i)	Q Value (Watts/mCi)	Heat Load (Watts)	Neutron Emitter?	Actual Content Activity Concentration (milliCuries/kg)
co60	2.50E+02	2.50E+02	100.00	11	6.79E+01	1.54E-05	1.15E+01	N	
		Gamma Sum (%)	100.00	Gamma Sum (A2)	67.94	Gamma Sum (Watts)	11.52	Neutron Sum (mCi/kg)	0.00
		Limit (% of 95% of the NCT and HAC dose rate criteria)	100	Limit (A2)	3000	Limit (Watts)	200	Limit† (Neutron Sum, mCi/kg)	3.50
		Passed Shielding Criteria	TRUE	Passed Containment Criteria	TRUE	Passed Heat Load Criteria	TRUE	Passed Neutron Limit Criteria	TRUE

Table 7.6.1-5 Failed Loading Table Example

Waste Vol (ft ³)		Actual Content Loading Evaluation							
3000.00		Content Mass (kg)							
Gamma Emitting Nuclides		Shielding Evaluation		Containment Evaluation		Heat Load Evaluation		Neutron Emitter† Evaluation	
Actual Content Nuclide	Maximum Allowable Activity Concentration (milliCuries/kg)	Actual Content Activity Concentration (milliCuries/kg)	% of Maximum	A2 (Curie)	Activity(i) / A2(i)	Q Value (Watts/mCi)	Heat Load (Watts)	Neutron Emitter?	Actual Content Activity Concentration (milliCuries/kg)
co60	2.50E+02	2.33E+02	93.18	11	6.35E+01	1.54E-05	1.08E+01	N	
cs137	7.95E+04	6.00E+03	7.55	16	1.13E+03	5.04E-06	9.07E+01	N	
		Gamma Sum (%)	100.73	Gamma Sum (A2)	1188.55	Gamma Sum (Watts)	101.51	Neutron Sum (mCi/kg)	0.00
		Limit (% of 95% of the NCT and HAC dose rate criteria)	100	Limit (A2)	3000	Limit (Watts)	200	Limit† (Neutron Sum, mCi/kg)	3.50
		Passed Shielding Criteria	FALSE	Passed Containment Criteria	TRUE	Passed Heat Load Criteria	TRUE	Passed Neutron Limit Criteria	TRUE

Table 7.6.1-6 Radionuclide Activity Concentration Limits

Project Task		RT-100 Transport Cask Maximum Curies Per Gram Limits
Gamma Emitting Radionuclides		
Radionuclide	Max. Ci/g	Condition
na24	3.38E-06	NCT
bi208	3.76E-06	NCT
cs144	5.27E-06	NCT
y88	1.02E-05	NCT
la140	1.63E-05	NCT
sb124	2.19E-05	NCT
eu156	2.26E-05	NCT
sc48	2.67E-05	NCT
la138	3.87E-05	NCT
tb156	4.10E-05	NCT
ag106m	4.45E-05	NCT
lu169	4.55E-05	NCT
na22	5.38E-05	NCT
sb120m	5.51E-05	NCT
i124	5.54E-05	NCT
br82	5.93E-05	NCT
lu172	6.68E-05	NCT
ta182	6.93E-05	NCT
ca47	7.23E-05	NCT
sc46	7.66E-05	NCT
te131m	7.96E-05	NCT
eu152	8.35E-05	NCT
as72	8.49E-05	NCT
tm172	9.32E-05	NCT
eu154	9.69E-05	NCT
cs136	1.09E-04	NCT
pm148	1.10E-04	NCT
ge69	1.25E-04	NCT
tb160	1.56E-04	NCT
sn125	1.82E-04	NCT
rh102m	1.88E-04	NCT
gd147	1.93E-04	NCT
tc96	2.23E-04	NCT
sr83	2.25E-04	NCT
k40	2.42E-04	NCT
co60	2.50E-04	NCT
as76	2.84E-04	NCT
nb92	3.41E-04	NCT

Project	RT-100 Transport Cask	
Task	Maximum Curies Per Gram Limits	
Gamma Emitting Radionuclides		
Radionuclide	Max. Ci/g	Condition
np238	3.49E-04	NCT
am240	4.09E-04	NCT
tb158	4.32E-04	NCT
pm148m	4.79E-04	NCT
ag110m	4.84E-04	NCT
ho166m	5.45E-04	NCT
pa232	5.96E-04	NCT
sb126	6.14E-04	NCT
nb94	6.40E-04	NCT
rb84	6.41E-04	NCT
tm168	6.65E-04	NCT
pr144	6.75E-04	NCT
fe59	7.11E-04	NCT
rh99	7.83E-04	NCT
tm165	8.21E-04	NCT
zr89	1.18E-03	NCT
rh102	1.23E-03	NCT
as71	1.37E-03	NCT
ru106	1.57E-03	NCT
tc95m	1.59E-03	NCT
rb86	1.82E-03	NCT
tc98	1.97E-03	NCT
ag108m	2.12E-03	NCT
ho166	2.17E-03	NCT
ir194m	2.25E-03	NCT
zn65	2.34E-03	NCT
cs132	2.34E-03	NCT
lu171	2.56E-03	NCT
nb95	2.59E-03	NCT
zr95	2.62E-03	NCT
tb153	2.83E-03	NCT
te121m	3.15E-03	NCT
ag105	3.32E-03	NCT
sb127	3.61E-03	NCT
sb122	3.62E-03	NCT
pm144	3.14E-03	NCT
cd115m	4.17E-03	NCT
kr79	4.27E-03	NCT
pm146	4.35E-03	NCT

Project	RT-100 Transport Cask	
Task	Maximum Curies Per Gram Limits	
Gamma Emitting Radionuclides		
Radionuclide	Max. Ci/g	Condition
gd149	4.88E-03	NCT
i126	5.10E-03	NCT
tc99m	2.24E-02	HAC
cs134	6.03E-03	NCT
os185	6.57E-03	NCT
cu64	6.61E-03	NCT
pm143	6.71E-03	NCT
co58	6.96E-03	NCT
as74	7.27E-03	NCT
ba131	7.28E-03	NCT
br77	9.13E-03	NCT
ce143	9.23E-03	NCT
pm151	1.27E-02	NCT
lu176	1.12E-02	HAC
se75	1.14E-02	HAC
y87	1.16E-02	HAC
cm241	1.16E-02	HAC
sr85	1.15E-02	HAC
te121	1.15E-02	HAC
rb83	1.23E-02	HAC
rh101	1.30E-02	HAC
sb125	1.29E-02	HAC
hf181	1.36E-02	HAC
mn54	1.65E-02	NCT
y91	1.80E-02	NCT
i131	1.71E-02	HAC
xe127	1.73E-02	HAC
ru103	1.83E-02	HAC
yb169	1.97E-02	HAC
co57	1.99E-02	HAC
au198	2.01E-02	HAC
ru97	2.01E-02	HAC
ta183	2.04E-02	HAC
np239	2.04E-02	HAC
ba133	2.04E-02	HAC
sn123	2.46E-02	NCT
zr88	2.05E-02	HAC
zn72	2.06E-02	HAC
te132	2.17E-02	HAC

Project	RT-100 Transport Cask	
Task	Maximum Curies Per Gram Limits	
Gamma Emitting Radionuclides		
Radionuclide	Max. Ci/g	Condition
cf249	2.18E-02	HAC
bi210m	2.20E-02	HAC
hf182	2.22E-02	HAC
rh101m	2.23E-02	HAC
sn117m	2.25E-02	HAC
hf175	2.30E-02	HAC
u235	2.32E-02	HAC
te123m	2.37E-02	HAC
hg203	2.45E-02	HAC
cm247	2.45E-02	HAC
cf251	2.48E-02	HAC
ce139	2.50E-02	HAC
pu246	2.54E-02	HAC
mo99	9.03E-03	NCT
sc47	2.93E-02	HAC
cs129	2.97E-02	HAC
ag110	3.68E-02	NCT
in113m	3.11E-02	HAC
u237	3.13E-02	HAC
cm243	3.16E-02	HAC
pa233	3.22E-02	HAC
pt191	3.21E-02	HAC
tb155	3.46E-02	HAC
cd115	3.40E-02	HAC
ba140	3.43E-02	HAC
er172	3.72E-02	HAC
lu177m	3.73E-02	HAC
cm245	3.76E-02	HAC
np236	3.88E-02	HAC
cu67	4.00E-02	HAC
in114m	4.87E-02	NCT
au199	4.09E-02	HAC
ce141	4.14E-02	HAC
ga67	4.31E-02	HAC
tm167	4.47E-02	HAC
ar37	4.49E-02	HAC
th227	5.64E-02	HAC
ra223	5.77E-02	HAC
pu237	6.27E-02	HAC

Project	RT-100 Transport Cask	
Task	Maximum Curies Per Gram Limits	
Gamma Emitting Radionuclides		
Radionuclide	Max. Ci/g	Condition
nd147	6.37E-02	HAC
sn126	6.59E-02	HAC
cs137	7.95E-02	HAC
sm153	6.61E-02	HAC
os191	6.88E-02	HAC
te129m	8.36E-02	NCT
nb95m	7.52E-02	HAC
rh105	8.17E-02	HAC
eu155	9.11E-02	HAC
re189	9.10E-02	HAC
gd153	9.29E-02	HAC
th229	9.61E-02	HAC
os193	1.08E-01	HAC
lu177	1.12E-01	HAC
hf172	1.20E-01	HAC
ba135m	1.28E-01	HAC
yb175	1.69E-01	HAC
ce144	1.80E-01	HAC
eu149	1.91E-01	HAC
be7	1.93E-01	HAC
cr51	1.98E-01	HAC
xe133m	1.99E-01	HAC
pa231	2.09E-01	HAC
re186	2.10E-01	HAC
ir192	2.36E-01	HAC
ag111	2.47E-01	HAC
pm149	3.21E-01	NCT
xe129m	4.35E-01	HAC
ra224	4.99E-01	HAC
ac225	5.06E-01	HAC
kr81	5.11E-01	HAC
ra226	5.69E-01	HAC
np237	5.86E-01	HAC
pt195m	6.57E-01	HAC
as77	7.12E-01	HAC
xe131m	1.02E+00	HAC
sn113	1.09E+00	HAC
th231	1.60E+00	HAC
dy166	1.70E+00	HAC

Project	RT-100 Transport Cask	
Task	Maximum Curies Per Gram Limits	
Gamma Emitting Radionuclides		
Radionuclide	Max. Ci/g	Condition
kr85	2.62E+00	HAC
ni59	3.30E+00	NCT
am243	2.81E+00	HAC
w188	3.13E+00	HAC
nb91	3.47E+00	HAC
th228	3.85E+00	HAC
es254	4.48E+00	HAC
tb161	4.57E+00	HAC
u230	6.10E+00	HAC
te125m	7.07E+00	HAC
th234	7.08E+00	HAC
am242m	1.20E+01	HAC
rn222	1.50E+01	HAC
w181	1.72E+01	HAC
la137	1.73E+01	HAC
pt193m	1.78E+01	HAC
es253	1.90E+01	HAC
u232	2.54E+01	HAC
u233	2.67E+01	HAC
xe133	2.72E+01	HAC
th230	2.84E+01	HAC
te127m	3.73E+01	HAC
ac227	4.82E+01	HAC
u234	5.50E+01	HAC
am241	6.02E+01	HAC
po210	7.99E+01	NCT
pd103	6.91E+01	HAC
th232	7.27E+01	HAC
cd113m	8.69E+01	HAC
u236	9.99E+01	HAC
w185	1.07E+02	HAC
v49	1.07E+02	HAC
pu239	1.14E+02	HAC
cf252	1.34E+02	HAC
pu236	1.44E+02	HAC
u238	1.86E+02	HAC
pu240	2.60E+02	HAC
sr90	3.64E+02	NCT
cl36	3.35E+02	HAC

Project	RT-100 Transport Cask	
Task	Maximum Curies Per Gram Limits	
Gamma Emitting Radionuclides		
Radionuclide	Max. Ci/g	Condition
cm242	4.05E+02	HAC
ca41	4.10E+02	HAC
sm145	5.73E+02	HAC
pu242	6.96E+02	HAC
pm147	7.00E+02	HAC
cm244	8.69E+02	NCT
er169	1.53E+03	HAC
pu238	1.62E+03	NCT
fe55	1.63E+03	HAC
pu241	3.67E+03	HAC
bi210	1.96E+04	HAC
bk249	5.28E+04	HAC
pr143	2.15E+05	NCT
tc97	5.81E+05	HAC
ca45	5.83E+05	HAC
ge71	5.83E+05	HAC
nb93m	5.83E+05	HAC
mo93	5.83E+05	HAC
tc97m	5.83E+05	HAC
cd109	5.83E+05	HAC
sn119m	5.83E+05	HAC
sn121m	5.83E+05	HAC
te123	5.83E+05	HAC
i125	5.83E+05	HAC
i129	5.83E+05	HAC
cs131	5.83E+05	HAC
pm145	5.83E+05	HAC
sm151	5.83E+05	HAC
tb157	5.83E+05	HAC
dy159	5.83E+05	HAC
tm170	5.83E+05	HAC
tm171	5.83E+05	HAC
os194	5.83E+05	HAC
pt193	5.83E+05	HAC
tl204	5.83E+05	HAC
pb205	5.83E+05	HAC
pb210	5.83E+05	HAC
ra225	5.83E+05	HAC
ra228	5.83E+05	HAC

Project		RT-100 Transport Cask
Task		Maximum Curies Per Gram Limits
Gamma Emitting Radionuclides		
Radionuclide	Max. Ci/g	Condition
np235	5.83E+05	HAC
cm246	5.83E+05	HAC
cm248	5.83E+05	HAC
cf250	5.83E+05	HAC
se72	5.83E+05	HAC
as73	5.83E+05	HAC
te118	5.83E+05	HAC
sb119	5.83E+05	HAC
nd140	5.83E+05	HAC
yb166	5.83E+05	HAC
h3	5.83E+05	HAC
ni63	5.83E+05	HAC
sr89	5.83E+05	HAC
tc99	5.83E+05	HAC
sn113m	5.83E+05	HAC
am242	5.83E+05	HAC
c14	5.83E+05	HAC

7.7 References

1. Robatel Technologies, LLC, Quality Assurance Program for Packaging and Transportation of Radioactive Material, 10 CFR 71 Subpart H, Rev. 2, Dated November 10, 2017 and NRC Approved on March 21, 2012

2. U.S. Nuclear Regulatory Commission, 10 CFR Part 71--PACKAGING AND TRANSPORTATION OF RADIOACTIVE MATERIAL, and the following specific Sections:

71.31(c)	71.45	71.47	71.47(b)(1)	71.89
71.87	71.47(b-d)	71.35(c)	71.43(g)	

3. U.S. Department of Transportation, Hazard Communications for Class 7 (Radioactive) Materials – Package and Vehicle Contamination Limits, 49 CFR 173.443.

4. U.S. Department of Transportation, Empty Class 7 (Radioactive) Materials Packaging, 49 CFR 173.428.

5. ANSI N14.5-2014, "American National Standard for Radioactive Materials – Leakage Tests on Packages for Shipment," American National Standards Institute, Inc., 11 West 42nd Street, New York, NY, www.ansi.org.

6. U.S. Nuclear Regulatory Commission, REGULATORY GUIDE 7.9 – Standard format and content of Part 71 applications for approval of packages for radioactive material, dated March 2005

7. U.S. Nuclear Regulatory Commission, "Guide for Preparing Operating Procedures for Shipping Packages," NUREG/CR-4775, July 1988.

8. U.S. Nuclear Regulatory Commission, 10 CFR Part 20--STANDARDS FOR PROTECTION AGAINST RADIATION, and the following specific Sections:

20.1101(b)	20.1906	20.1906(e), 20.1906(a)
------------	---------	---------------------------

9. LLW-11-026, "Turkey Point Unit 3 & 4 Low Level Waste Facility PTN Source Term Information", P. A. Miktus, September 7, 2011.

10. LLW-09-002, "St. Lucie Unit 1 & 2 Low Level Waste Facility RFI Response", B. Bedford, December 2, 2009.

11. [Withdrawn]

12. NUREG/CR-6673, "Hydrogen Generation in TRU Waste Transportation Packages," Anderson, B., Sheaffer, M., & Fischer, L., Lawrence Livermore National Laboratory, Livermore, CA, May 2000.

8. ACCEPTANCE TESTS AND MAINTENANCE PROGRAM

Initially, RT employs an Assessment Test program to meet the requirements of 10 CFR Part 71 [Ref. 2], Subpart G. The RT Package Maintenance Program ensures the RT- 100 meets its Certificate of Compliance requirements throughout the package service life. Both the acceptance tests and maintenance programs are conducted in accordance with the RT Quality Assurance Program [Ref. 1]. Figure 8-1 shows flow of information for acceptance test and maintenance programs.

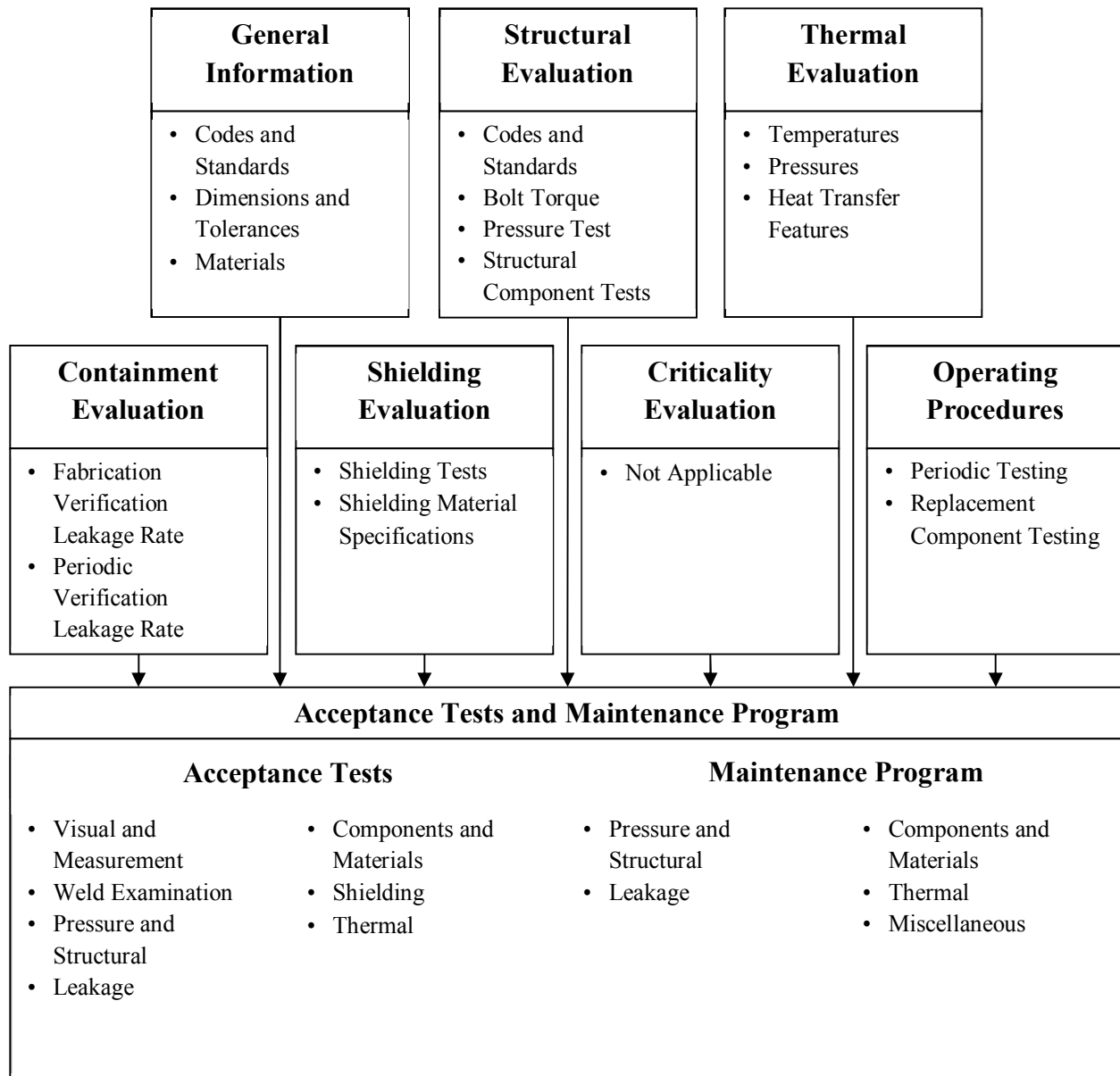


Figure 8-1 Information Flow for the Acceptance Tests and Maintenance Program Review

8.1 Acceptance Tests

Requirements for the acceptance testing include the following criteria:

- The SAR identifies codes, standards, and provisions of the quality assurance program used for the acceptance testing of the packaging in accordance with 10 CFR 71.31(c) and 71.37(b) [Ref. 2]. The SAR is prepared and the RT-100 is fabricated in accordance with the RT Quality Assurance Program [Ref. 1], approved by the USNRC on 21 March 2012.
- The fabrication of the RT-100 is verified to be in accordance with the approved design and in accordance with 10 CFR 71.85(c) [Ref. 2].
- The RT-100 is inspected for cracks, pinholes, uncontrolled voids, or other defects that could significantly reduce its effectiveness; inspection is conducted in accordance with 10 CFR 71.85(a) [Ref. 2].
- Prior to lead pouring, measure the average clearance annular gap between the inner and outer shell of the cask body. Using a gauge, verify that the annular gap is above 86 mm at every point between the two shells. After lead pouring, the maximum annular gap between the lead and the inner and outer shell shall not exceed 0.1 cm.
- Since the RT-100 maximum normal operating pressure exceeds 35 kPa (5 psi) gauge, prior to first use the cask will be tested at an internal pressure at least 150% of the maximum normal operating pressure to verify its ability to maintain structural integrity at that pressure in accordance with 10 CFR 71.85(b) [Ref. 2].
- The RT-100 is conspicuously and durably marked with its model number, serial number, gross weight, and a package identification number assigned by the NRC in accordance with 10 CFR 71.85(c) [Ref. 2].
- Robatel Technologies, LLC performs all tests required by the NRC in accordance with 10 CFR 71.93(b) [Ref. 2].
- RT-100 is fabricated in accordance with drawings provided in Chapter 1, Appendix 1.4.

General Notes

- A pre-shipment leak test is performed before each shipment of Type B waste, per ANSI N14.5-2014 [Ref. 6], as mentioned in Table 4.3-1.
- All disassembled parts will be reassembled in accordance with requirement stated in Chapter 7. In particular, this requirement applies to bolt/nut tightening, and torques applied.
- Cleanliness of sealing surfaces is of highest priority during package disassembly and assembly. This requirement particularly applies to O-rings and seal surfaces.
- O-rings are replaced within a 12 month period of use in accordance with Regulatory Guide 7.9 [Ref. 3] and NUREG-1609 [Ref. 4].
 - The RT-100 has two (2) O-rings associated with each of the primary lid, secondary lid, and quick-disconnect valve.
 - Replaced O-rings are leak tested in accordance with Section 8.1.4.2 or 8.1.4.3.

8.1.1 Visual Inspections and Measurements

Throughout the fabrication process, confirmation by visual inspection and measurement are required to verify that the RT-100 packaging dimensionally conforms to the drawings RT100 PE 1001-1, Rev. H and RT100 PE 1001-2, Rev. H provided in Chapter 1, Appendix 1.4. In addition, the packaging is to be visually inspected for any adverse conditions in materials or fabrication that would prevent the package from being assembled or operated in accordance with requirements outlined in Chapter 7, or tested in accordance with the requirements of Chapter 8. Visual and non-destructive examination shall be performed by ASNT or COFREND certified inspectors.

8.1.2 Weld Examinations

Containment boundary welds are identified in drawing RT100 PRS 1011, Rev. E in Chapter 1, Appendix 1.4. The following welds on this drawing are classified as containment boundary welds: S.1011.01, S.1011.02, and S.1011.03. These welds are required to be inspected and meet the acceptance requirements of ASME Code, Section III, Division I, Subsection ND, Article ND-5000 [Ref. 5].

The weld maps RT100 PRS 1011, Rev. E, RT100 PRS 1013, Rev. C, RT100 PRS 1031, Rev. D and RT100 PRS 1032, Rev. D listed in Chapter 1, Appendix 1.4, provide the examination criteria for each weld. Radiographic testing, dye penetrant testing, and/or visual testing is performed in accordance with applicable ASME standards. The Containment Boundary welds are also inspected by radiographic examination. Non-destructive examination shall be performed by ASNT or COFREND certified inspectors.

8.1.3 Structural and Pressure Tests

A pressure test of the containment system is performed as required by 10 CFR 71.85 [Ref. 2]. As described in Chapter 3, Section 3.3.2.5, Maximum Normal Operating Pressure for the RT-100 cavity is 182.71 kPa. Per 10 CFR 71.85(b) [Ref. 2], the containment system shall be tested at an internal pressure at least 50% higher than the actual maximum normal operating pressure, or 274 kPa. However, for conservatism, the minimum test pressure is set to 300 kPa. The hydrostatic test pressure is held for a minimum of 10 minutes. Afterward, the primary lid and secondary lid closures are examined for leakage.

Except from temporary connections, leaks are remedied, and the test and inspection are repeated. After depressurization and draining, the cask cavity and seal areas are visually inspected for cracks and deformation. Any cracks or deformation are remedied, and the test and inspection repeated.

8.1.4 Leakage Tests

Section 8.1.4 describes the leakage tests to be performed on the RT-100 prior to its initial use. Refer to Section 8.3 and Table 8.3-1 for a summary of the leak test types.

Testing performed on the cask body containment boundaries during fabrication:

8.1.4.1 Cask Containment Boundary

8.1.4.1.1 Cask Body Leak Testing – Prior to Lead Pouring

8.1.4.1.2 Primary Lid Assembly Including Secondary Lid and Cover Plate – Prior to Final Assembly

Verification testing performed on the cask after final assembly:

8.1.4.2 Primary and Secondary Lid Containment O-Rings Helium Leak Testing

8.1.4.3 Quick Disconnect Valve Helium Leak Testing

8.1.4.4 Quick Disconnect Valve Cover Plate Containment O-Rings Helium Leak Testing

Note Regarding Test Personnel Qualifications

Detailed procedures following the instructions below are to be approved by personnel certified in ASNT NDT or COFREND Level III leak testing. The use of COFREND certified personnel instead of ASNT certified personnel is accepted for leakage testing for the RT-100, based on the equivalence note 102885 EQN 001 Rev. C [Ref. 12].

Note Regarding Test Duration

For each helium test, the duration must be calculated by test personnel. The Test Duration is a function of the System Response Time and the Helium Penetration Time.

The System Response Time is defined as the time from admitting helium to a test assembly with a known leak, until the measured leakage rate increases to $2 \times 10^{-7} \text{ cm}^3/\text{s}$ above background. For the Primary Lid O-ring, which has the longest response time, the time has been experimentally determined to be less than 20 seconds.

The Helium Penetration Time is defined as the time from admitting helium to a test assembly, until the measured leakage rate of helium gas permeating through the seal under test increases to a rate of $2 \times 10^{-7} \text{ cm}^3/\text{s}$ above background. For the Vent Port Cover Plate O-ring, which has the shortest penetration time, the time has been experimentally determined to be approximately 5 minutes.

The Test Duration should be such that:

$$2 \times \text{System Response Time} < \text{Test Duration} < 80\% \text{ Helium Penetration Time}$$

$$40 \text{ sec} < \text{Test Duration} < 240 \text{ sec}$$

In order to meet the above criterion, the Test Duration is specified as approximately 2 minutes.

8.1.4.1 Cask Containment Boundary

8.1.4.1.1 Cask Body Leak Testing – Prior to Lead Pouring

Testing of the cask body containment boundary is performed prior to the lead shield pour to allow access to all containment welds and base material. This test is conducted using a helium leak detector in accordance with ANSI N14.5-2014 table A1 test A.5.3 [Ref. 6] to demonstrate compliance with the leaktight criteria. Figure 8.1.4-1 shows a general diagram of the test apparatus. Calibration of the helium detector is performed using an appropriate leak standard, in accordance with Section 10 of ASTM E-499 [Ref. 7] or equivalent.

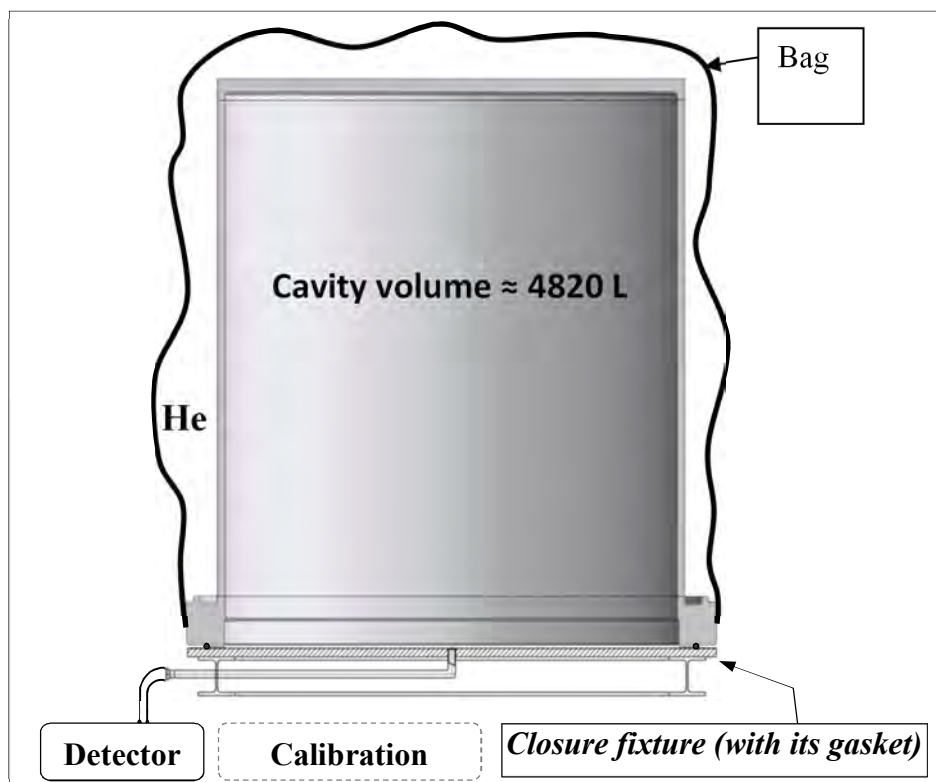


Figure 8.1.4-1 Cask Body Containment Boundary Test Apparatus

- *Test Personnel Qualifications*

Test personnel shall be ASNT NDT or COFREND Level II certified in leakage testing.

- *Frequency*

Cask body containment boundaries are tested only once during fabrication.

- *Components to be tested*

The body containment boundary includes the inner shell, the cask forged bottom, and the upper flange.

- *Testing Procedure*

1. Assemble the cask body with a substitute sealed plate used in place of the cask lid.

Note: The material in contact with the cask must be chemically compatible with the cask body material (stainless steel) and the test gas (helium).

2. Place the entire vessel in a bag taped on the outer surface of the upper flange, as shown in Figure 8.1.4-1.
 3. Create a vacuum in the cask cavity (0.01 atm abs or less).
 4. Fill the bag with helium to a partial pressure of at least 25% of the total gas pressure.
 5. Measure the helium flow signal detected in the interspace. The test duration will be approximately 2 minutes as described in Section 8.1.4.
- *Acceptance Criteria*
Refer to Table 8.3-1 and Table 8.3-2 for test acceptance criteria.
 - *Actions to be taken if test fails*
Any condition which results in leakage in excess of the maximum allowable leak rate is corrected and re-tested.

8.1.4.1.2 Primary Lid Assembly Including Secondary Lid and Cover Plate – Prior to Final Assembly

Testing of the Primary Lid Assembly is performed prior to final assembly of the Cask. This test is conducted using a helium leak detector in accordance with ANSI N14.5-2014 table A1 test A.5.3 [Ref. 6] to demonstrate compliance with the leaktight criteria. Figure 8.1.4-2 shows a general diagram of the test apparatus. Calibration of the helium detector is performed using an appropriate leak standard, in accordance with Section 10 of ASTM E-499 [Ref. 7] or equivalent.

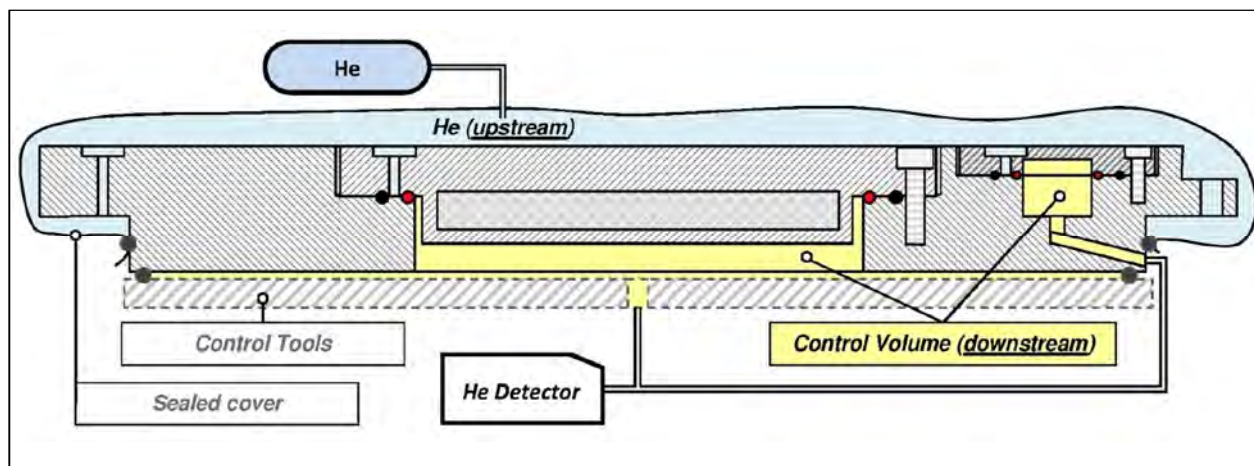


Figure 8.1.4-2 Primary Lid Assembly Containment Boundary Test Apparatus

- *Test Personnel Qualifications*
Test personnel shall be ASNT NDT or COFREND Level II certified in leakage testing.
- *Frequency*
Cask body containment boundaries are tested only once during fabrication.
- *Components to be tested*
The Primary Lid Assembly Containment Boundary includes the Primary Lid, Secondary Lid, and Quick-Disconnect Valve Cover Plate.
- *Testing Procedure*

1. Remove the Quick-Disconnect Valve.
 2. Assemble the Primary Lid per Chapter 7, Section 7.1.2.3, Secondary Lid Replacement, and 7.1.2.4, Quick-Disconnect Valve Cover Plate Replacement. The bolts must be torqued to the specifications listed in Table 7.4.5-1.
 3. Attach to the Primary Lid Assembly a control tool as shown in Figure 8.1.4-2.
Note: The material in contact with the lid assembly must be chemically compatible with the primary lid assembly material (stainless steel) and the test gas (helium).
 4. A sealing cover is arranged above the primary lid assembly as shown in Figure 8.1.4-2, and sealed just below the closure bolt flange.
Note: The sealing cover should not be placed over the opening leading to the Quick-Disconnect Valve Cover Plate.
 5. Create a vacuum in the control volume (0.01 atm abs or less).
 6. Fill the bag with helium to a partial pressure of at least 25% of the total gas pressure.
 7. Measure the helium flow signal detected in the control volume. The test duration will be approximately 2 minutes as described in Section 8.1.4.
- *Acceptance Criteria*
Refer to Table 8.3-1 and Table 8.3-2 for test acceptance criteria.
 - *Actions to be taken if test fails*
Any condition which results in leakage in excess of the maximum allowable leak rate is corrected and re-tested.

8.1.4.2 Primary and Secondary Lid Containment O-Rings Helium Leak Testing

Verification of the primary and secondary lid containment boundaries is performed prior to its initial use, periodically every 12 months, and after maintenance. This test is conducted using a helium leak detector in accordance with ANSI N14.5-2014 table A1 test A.5.3 [Ref. 6] to demonstrate compliance with the leaktight criteria. Calibration of the helium detector is performed using an appropriate leak standard, in accordance with Section 10 of ASTM E-499 [Ref. 7] or equivalent.

- *Test Personnel Qualifications*
Test personnel shall be ASNT NDT or COFREND Level II certified in leakage testing.
- *Frequency*
Maintenance leakage rate testing shall be performed prior to returning a package to service following maintenance, repair (such as a weld repair), or replacement of components of a containment boundary.
- *Components to be tested*
The components tested are the inner O-rings in the primary lid or the secondary lid.
- *Testing Procedure*
 1. Assemble the cask lids per Chapter 7, Section 7.1.2.2, Primary Lid Replacement, and 7.1.2.3, Secondary Lid Replacement. The bolts must be torqued to the specifications listed in Table 7.4.5-1.

2. Remove the quick disconnect valve cover plate, per Chapter 7, Section 7.1.1.3.
 3. Remove the leak test port plug on either the primary or secondary lid, whichever containment boundary is to be tested. Attach the vacuum pump and the leak detection equipment to the port.
 4. Pull a vacuum in the O-ring interspace (0.01 atm abs or less).
 5. Fill the internal cavity with helium through the vent port (min helium partial pressure 25% of total pressure).
 6. Measure the helium flow signal detected in the interspace. The test duration will be approximately 2 minutes as described in Section 8.1.4.
- *Acceptance Criteria*
Refer to Table 8.3-1 and Table 8.3-2 for test acceptance criteria.
 - *Actions to be taken if test fails*
Any condition which results in leakage in excess of the maximum allowable leak rate is corrected and re-tested.

8.1.4.3 Quick Disconnect Valve Helium Leak Testing

As described in Section 4.1.2, the RT-100 does not rely on any valve or pressure relief device to meet the containment requirements. The Quick Disconnect valve is protected by the vent port cover plate, as shown in Figure 4.1.2-1. Therefore, it is not necessary for the Quick Disconnect Valve to meet the ANSI N14.5-2014 leaktight criteria. However, as an additional safety precaution, the Quick Disconnect valve is leak tested as described below.

Verification of the quick disconnect valve is performed prior to its initial use, periodically every 12 months, and after maintenance. This test is conducted using a helium leak detector in accordance with ANSI N14.5-2014 table A1 test A.5.3 [Ref. 6]. Calibration of the helium detector is performed using an appropriate leak standard, in accordance with Section 10 of ASTM E-499 [Ref. 7] or equivalent.

- *Test Personnel Qualifications*
Test personnel shall be ASNT NDT or COFREND Level II certified in leakage testing.
- *Frequency*
Maintenance leakage rate testing shall be performed prior to returning a package to service following maintenance, repair (such as a weld repair), or replacement of components of a containment boundary.
- *Components to be tested*
The component tested is the quick-disconnect valve.
- *Testing Procedure*
 1. The quick-disconnect valve must be assembled and torqued to the specification listed in Table 7.4.5-2.
 2. Install a bag on the vent port hole under the primary lid as shown in Figure 8.1.4-3.
Note: Alternately, the primary lid may be assembled to the cask body without the

- secondary lid, and the cavity filled with helium via the primary lid opening as shown in Figure 8.1.4-4.
3. Remove the quick disconnect valve cover plate, per Chapter 7, Section 7.1.1.3.
 4. Install a vacuum clutch over the vent port. Pull a vacuum of 0.01 atm abs or less.
 5. Fill the bag (or alternatively the containment vessel) with helium (min helium partial pressure 25% of total pressure).
 6. Measure the helium flow signal detected in the interspace. The test duration will be approximately 2 minutes as described in Section 8.1.4.
- *Acceptance Criteria*
Refer to Table 8.3-1 for test acceptance criteria.
 - *Actions to be taken if test fails*
Any condition which results in leakage in excess of the maximum allowable leak rate is corrected and re-tested.

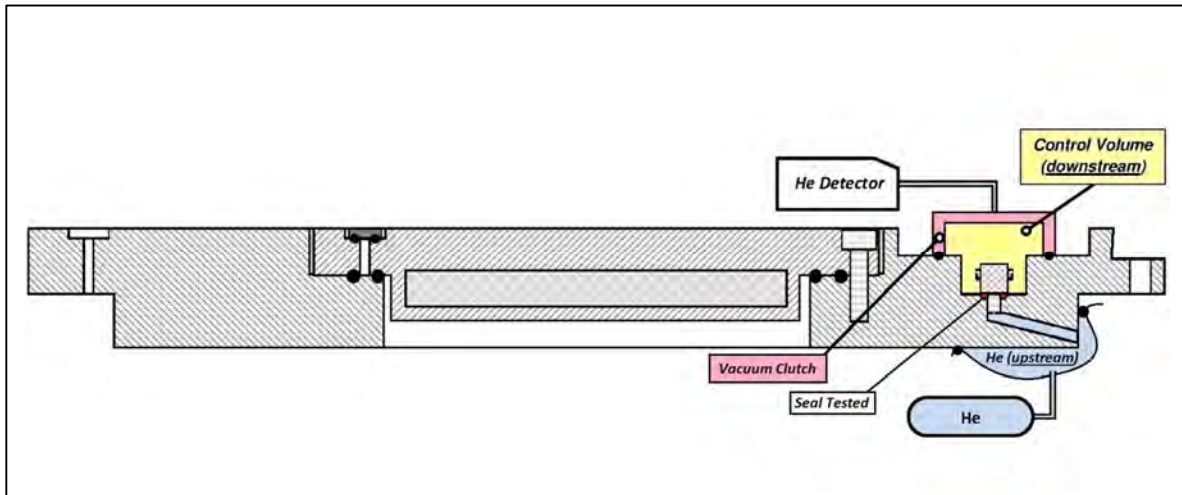


Figure 8.1.4-3 **Test Apparatus for Measuring the Helium Leak Rate through the Quick Disconnect Valve**

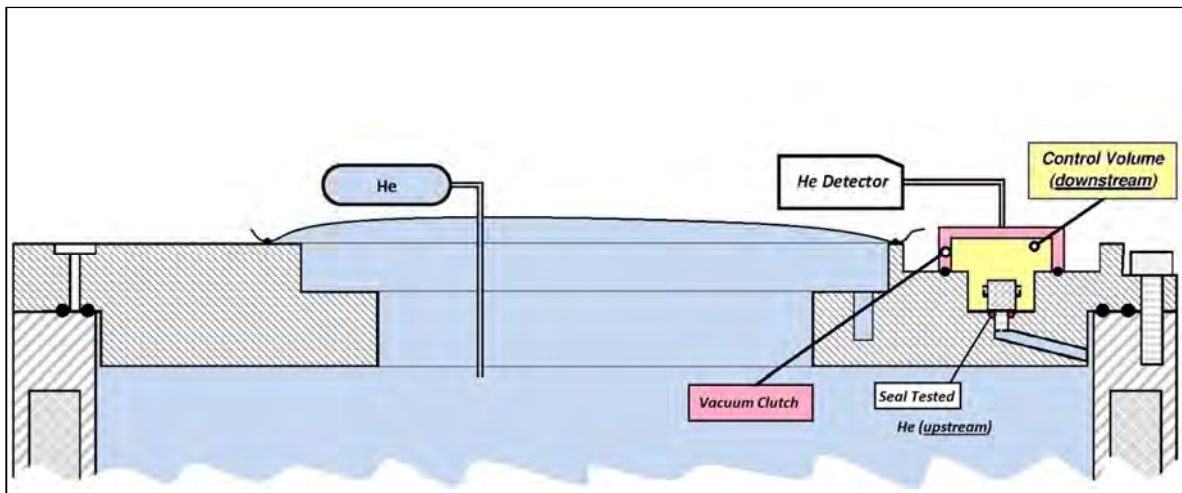


Figure 8.1.4-4 **Alternate Test Apparatus for Measuring the Helium Leak Rate through the Quick Disconnect Valve**

8.1.4.4 Quick Disconnect Valve Cover Plate Containment O-Rings Helium Leak Testing

Verification of the quick disconnect valve cover plate containment boundary is prior to its initial use, periodically every 12 months, and after maintenance. This test is conducted using a helium leak detector in accordance with ANSI N14.5-2014 table A1 test A.5.3 [Ref. 6] to demonstrate compliance with the leaktight criteria. Calibration of the helium detector is performed using an appropriate leak standard, in accordance with Section 10 of ASTM E-499 [Ref. 7] or equivalent.

- *Test Personnel Qualifications*

Test personnel shall be ASNT NDT or COFREND Level II certified in leakage testing.

- *Frequency*

Maintenance leakage rate testing shall be performed prior to returning a package to service following maintenance, repair (such as a weld repair), or replacement of components of a containment boundary.

- *Components to be tested*

The component tested is the inner O-ring seal in the quick disconnect valve cover plate.

- *Testing Procedure*

1. Install a bag on the vent port hole under the primary lid as shown in Figure 8.1.4-5.

Note: Alternately, the primary lid may be assembled to the cask body without the secondary lid, and the cavity filled with helium via the primary lid opening as shown in Figure 8.1.4-6.

2. Remove the quick disconnect valve.

3. Assemble the cover plate per Chapter 7, Section 7.1.2.4 Quick Disconnect Valve Cover Plate Replacement. The bolts must be torqued to the specifications listed in Table 7.4.5-1.

4. Remove the quick disconnect valve cover plate leak test plug. Attach the vacuum pump and the leak detection equipment to the port.

5. Pull a vacuum in the O-ring interspace (0.01 atm abs or less).

6. Fill the bag (or alternatively the containment vessel) with helium (min helium partial pressure 25% of total pressure).

7. Measure the helium flow signal detected in the interspace. The test duration will be approximately 2 minutes as described in Section 8.1.4.

- *Acceptance Criteria*

Refer to Table 8.3-1 and Table 8.3-2 for test acceptance criteria.

- *Actions to be taken if test fails*

Any condition which results in leakage in excess of the maximum allowable leak rate is corrected and re-tested.

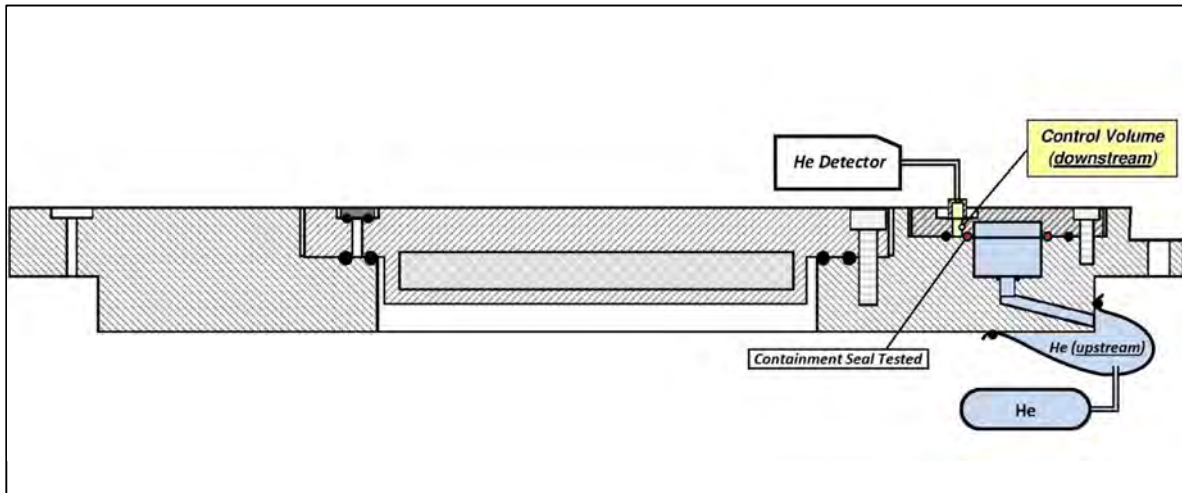


Figure 8.1.4-5 **Test Apparatus for Measuring the Helium Leak Rate through the Quick Disconnect Valve Cover Plate**

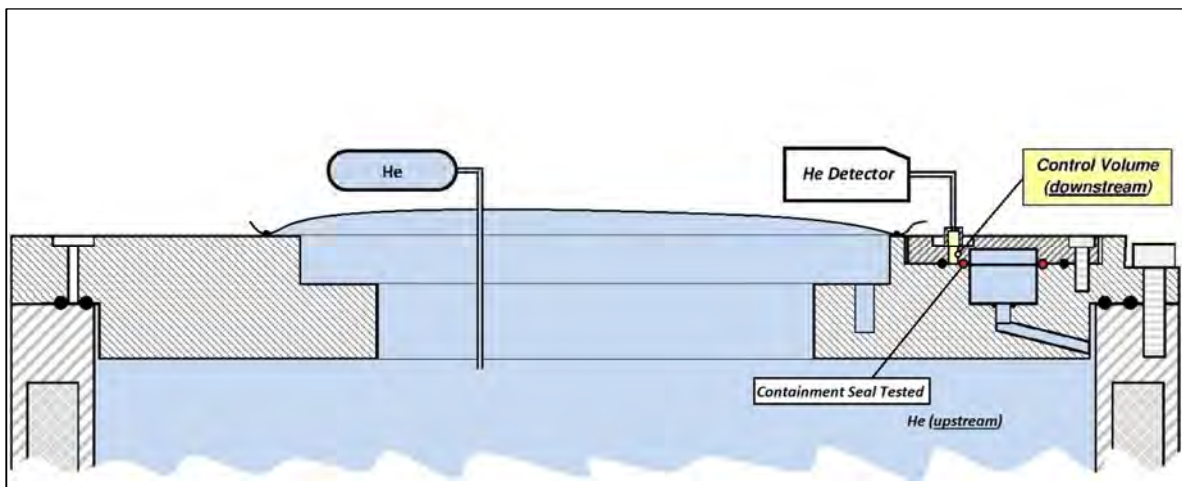


Figure 8.1.4-6 **Alternate Test Apparatus for Measuring the Helium Leak Rate through the Quick Disconnect Valve Cover Plate**

8.1.5 Component and Material Tests

The RT-100 is fabricated using industry wide procurement practices for the materials. All materials undergo extensive testing to meet the ASME standards of the material specifications. These specifications (including ASME standards) are part of the procurement process to ensure component materials meet or exceed nuclear industry practices.

To confirm that acceptance criteria are met, materials used for the fabrication of the RT-100 are procured in accordance with RT Quality Assurance Program [Ref. 1] standards. Materials not meeting these standards are replaced. Any materials replacing the originally purchased component parts are subject to the same testing to ensure conformance with specifications.

Where possible, materials for the RT-100 are procured in accordance with ASME/ASTM standards. In certain cases materials may be procured to other standards, such as DIN or ISO. For these materials, a Commercial Grade Dedication (CGD) Plan is prepared to ensure the material meets all specifications critical to safety; such CGD Plans may include independent analyses to confirm supplier material specifications. The CGD Plan is prepared in accordance with RT Quality Assurance Program [Ref. 1] requirements. The following sections give additional information regarding CGD Plan characteristics:

- 8.1.5.1 Foam
- 8.1.5.2 O-Ring
- 8.1.5.3 Ceramic Paper
- 8.1.5.4 Fusible Plugs
- 8.1.5.5 Carbon Steel and Alloy Steel Fasteners
- 8.1.5.6 Stainless Steel Fasteners
- 8.1.5.7 Thread Inserts
- 8.1.5.8 Quick Disconnect Valve

8.1.5.1 Foam

The impact limiter foam is procured from General Plastics (GP), series FR3700. The density tolerance is specified as $\pm 10\%$. GP provides in its documentation the mechanical characteristics of the foam. As GP is a NQA-1 company, the critical characteristics of the foam are not retested.

Proprietary Information Content Withheld Under 10 CFR 2.390(b)

Proprietary Information Content Withheld Under 10 CFR 2.390(b)

8.1.5.4 Fusible Plugs

The fusible plugs used for the RT-100 are made of polyethylene. The critical characteristic of the fusible plugs is the melting temperature, which shall be less than 160°C. This temperature is based on Robatel Industries' experience with other material plugs.

The melting temperature requirement is based on the ability of the plug to vent the pyrolysis gases produced during decomposition of the polyurethane impact limiter foam in the

hypothetical fire accident. Polyurethanes do not break down below 475 K, or 202°C [Ref. 10]. Since the melting temperature of the fusible plug is less than the decomposition temperature of the impact limiter foam, the gases will be vented.

Another thermoplastic material can be used provided the fusible plugs have a melting temperature below 160°C.

Proprietary Information Content Withheld Under 10 CFR 2.390(b)

Proprietary Information Content Withheld Under 10 CFR 2.390(b)

Proprietary Information Content Withheld Under 10 CFR 2.390(b)

Proprietary Information Content Withheld Under 10 CFR 2.390(b)

Proprietary Information Content Withheld Under 10 CFR 2.390(b)

8.1.5.8 Quick Disconnect Valve

The quick disconnect valve used in the RT-100 is a Staubli HCB 08.1152/IC/JE, made of stainless steel, and supplied with an EPDM O-ring. The critical characteristic of the valve is its leakage rate. As previously described in Section 8.1.4.3, when assembled, the quick disconnect valve is leak tested.

8.1.6 Shielding Tests

The RT-100 is designed to provide sufficient shielding to meet or exceed NRC and DOT requirements for a Type B (U)-96 package. Specifically, the RT-100 design includes gamma radiation shielding to meet 10 CFR Part 71 [Ref. 2] during both NCT and HAC.

Shielding integrity of the RT-100 is tested using nondestructive examination techniques (e.g., gamma scanning method) to ensure there are neither direct radiation streams nor voids greater than the acceptance criteria in the lead shield annulus. The acceptance criterion is defined as follows: measurements indicate that no lead layer is less than the minimum specified on the drawing. Any results not meeting this requirement are remedied, and the test and inspection are repeated.

To ensure that the minimum lead thickness is poured, prior to lead pouring, a gauge of 86 mm is utilized to verify that at any point, the distance between the cask inner and outer shell is at least 86 mm. See Appendix 8.3, Section 8.3.1 for further information regarding the lead pouring process.

8.1.7 Thermal Tests

No thermal acceptance testing is required for the RT-100. Refer to the thermal evaluation of the RT-100 described in Chapter 3, Section 3.3, Thermal Evaluation under Normal Conditions of Transport and 3.4 Thermal Evaluation under HAC of the SAR.

8.1.8 Miscellaneous Tests

No miscellaneous tests are to be performed on the RT-100 package.

8.2 Maintenance Program

The RT-100 is subjected to routine inspection and periodic maintenance to ensure its compliance with this SAR and standards required by the NRC. In addition, requirements of the RT Quality Assurance Program [Ref. 1] are employed to direct required maintenance periods. Defective items are replaced or remedied, and tested as appropriate.

- The SAR identifies codes, standards, and provisions of the quality assurance program used for the maintenance of the RT-100 in accordance with 10 CFR 71.31(c) [Ref. 2], and 71.37(b) [Ref. 2]. The RT Quality Assurance Program [Ref. 1] addresses all criteria of 10 CFR 71 [Ref. 2].
- The RT-100 is maintained in an unimpaired physical condition other than superficial defects in accordance with 10 CFR 71.87(b) [Ref. 2]. Any major changes to the RT-100 result in an evaluation for repair/ replacement of damaged parts.
- The RT-100 is not designed to transport fissile material in accordance with 10 CFR 71.87(g) [Ref. 2] and thus, the presence of any moderator or neutron absorber in a fissile material package is not applicable.
- RT shall perform any and all tests deemed appropriate by the NRC in accordance with 10 CFR 71.93(b) [Ref. 2]. NRC is permitted to perform tests on the RT-100 that it deems necessary.
- A maintenance program is part of the operational procedures to ensure that the package performs as intended throughout its service life.

Any RT-100 that does not comply with the specifications and verifications of the SAR is taken out of service until the corrective action(s) have been completed. All corrective actions are reported to RT, NRC, and approved RT-100 Users.

8.2.1 Structural and Pressure Tests

No routine or periodic structural or periodic testing will be performed on the RT-100 transportation cask.

The RT-100 lifting fixture shall be tested annually in accordance with ANSI N14.6 [Ref.8] requirements to verify continuing compliance.

Each containment weld is inspected from the inner surface using dye penetrant methods to detect cracks. Any results not meeting the ASME Code, Section III, Division I, Subsection ND, Article ND-5000 [Ref. 5] requirement are remedied, and the test and inspection are repeated.

8.2.2 Leakage Tests

Section 8.2.2 describes leakage tests to be performed on the RT-100 during its use. This section is subdivided into testing performed after annual inspection or maintenance, and testing performed prior to each shipment. Refer to Appendix 8.3, Section 8.3.1 and Table 8.3-1 for a summary of the leak test types.

Note: Procedures described below are approved by ASNT NDT or COFREND Level III certified personnel in leakage testing.

8.2.2.1 Periodic and Maintenance Leak Test

Leak testing of the RT-100 must be performed after completion of annual inspection and after maintenance or repair. These tests are identical to those performed on the RT-100 prior to its initial use. Refer to the following applicable subsections of Section 8.1.4 for details:

- 8.1.4.2 Primary and Secondary Lid Containment O-Rings Helium Leak Testing
- 8.1.4.3 Quick Disconnect Valve Helium Leak Testing
- 8.1.4.4 Quick Disconnect Valve Cover Plate Containment O-Rings Helium Leak Testing

8.2.2.2 Pre-Shipment Leak Test – Gas Pressure Rise Option

A pre-shipment leakage test is required before each shipment of Type B material quantities to verify proper integrity of the containment system. The following test method is a gas-pressure rise approach in accordance with ANSI N14.5-2014 table A1 test A.5.2 [Ref. 6]. Test equipment shall be calibrated and traceable to an appropriate standard.

Note: As an alternative to the pressure rise method, the pre-shipment leak test can be performed following the pressure drop method described in Section 8.2.2.3.

- *Test Personnel Qualifications*

Leakage rate testing shall be performed by personnel that are qualified and certified in accordance with the requirements of SNT-TC-1A-2006.

- *Frequency*

Testing is performed prior to each shipment of Type B material.

- *Components to be tested*

The vent port cover plate O-ring seals, and the primary or secondary lid O-ring seals, depending on which lid was removed prior to content loading. In case the contents are

loaded through the primary lid, the secondary lid and vent port cover plate can be leak tested before the contents are loaded, in accordance with ALARA principles.

In case the contents are loaded through the secondary lid, the primary lid and vent port cover plate can be leak tested before the contents are loaded, in accordance with ALARA principles.

Caution: Users of the RT-100 shall be aware that containment boundary components (detailed in Figure 4.1.2-1) could have been opened during a prior shipment of Type A contents, but a pre-shipment leakage rate test might not have been performed. The user must verify that an unopened lid has been previously leak tested in accordance with the Certificate of Compliance. If this verification cannot be made, the appropriate containment boundary seal must be leak tested.

○ *Testing Procedure*

1. Assemble the cask lids per Chapter 7, Section 7.1.2.2, Primary Lid Replacement, 7.1.2.3, Secondary Lid Replacement, and Section 7.1.2.4, Quick-Disconnect Valve Cover Plate Replacement. The bolts must be torqued to the specifications listed in Table 7.4.5-1.
2. Remove the applicable leak test port plug.
3. Ensure that the O-ring on the test manifold is in good condition and lubricated. Connect the vacuum pump test assembly to the appropriate test port. The test assembly should consist of a vacuum pump isolated by a valve, with a gauge indicating the system pressure.
4. Accurately determine and record the control volume. The control volume includes the volume of the interspace between the O-rings as given in Table 8.2.2-1, plus the volume associated with the measuring instrumentation manifold.

Table 8.2.2-1 Volume of the Interspaces between the O-rings

Interspace Location	Volume [cm ³]	Volume [m ³]
Primary Lid	70.0	0.000070
Secondary Lid	35.0	0.000035
Quick-Disconnect Valve Cover Plate	3.5	0.0000035

5. Determine and record the pressure gauge resolution, p .
6. Measure and record the base metal temperature of the cask lid, T_{amb} .
Note: Test should be carried out, where possible, in isothermal conditions. Small temperature variations can lead to large pressure variations.
7. Calculate the minimum required test duration, H_{min} , following the method described in the *Acceptance Criteria* section below.
8. Create a vacuum in the interspace between the O-rings.
Note: Absolute pressure of 30 ~ 90 mbar is recommended. Lower absolute pressure may lead to outgassing of the interspace surfaces requiring longer pumping

time to reach a sensitivity of 10^{-3} ref·cc/sec.

Note: Vacuum conditioning of the O-ring seals may be required.

9. Isolate the pump. Physically disconnect the pump and/or turn the pump off.
10. Wait for the vacuum pressure to stabilize, with an absolute pressure of 30 ~ 90 mbar before starting the test.
11. Record the start time, t_1 , and start pressure, P_1 .
12. After the test duration, H , record the end time, t_2 , and end pressure, P_2 . Ensure that the test duration is greater than the minimum required test duration, H_{min} .
13. Calculate the pressure change during the test, ΔP . Ensure that the pressure change is less than or equal to the pressure gauge resolution, p .

Note: This test procedure confirms functionality of the containment seal and the control seal simultaneously. In the event of test failure, either O-ring may be responsible for the leakage.

14. Replace the applicable leak test port plug.

○ *Acceptance Criteria*

The preshipment leakage rate test need not be more sensitive than 1×10^{-3} ref·cm³/s [Ref. 6], as shown in Table 8.3-1. This corresponds to a minimum sensitivity, S_{min} , under standard conditions of 1.01×10^{-4} Pa·m³/s. The test is carried out by the pressure rise method. Using formula B.14 given in Annex B of ANSI N14.5-2014, the test duration, H , must be greater than the minimum required test duration, H_{min} :

$$H > H_{min} = \frac{V_C \cdot p}{S_{min}} \cdot \frac{T_{std}}{T_{amb}}$$

where: H = actual test duration [s]
 H_{min} = minimum required test duration [s]¹⁸
 S_{min} = minimum required sensitivity [1.01×10^{-4} Pa·m³/s]
 p = minimum measurable pressure [Pa] for the test, or gauge resolution
 V_C = control volume [m³]
 T_{std} = standard temperature [298 K]
 T_{amb} = base metal temperature of the cask lid [K] measured during the test

Over the calculated test duration, there can be no measurable pressure rise. I.e., the minimum measurable pressure rise, ΔP , must be less than or equal to the gauge resolution, p :

$$\Delta P = P_2 - P_1 \leq p$$

where: P_1 = pressure [Pa] at the start of the test, t_1 being the start time [s]
 P_2 = pressure [Pa] at the end of the test, t_2 being the end time [s]
 ΔP = change in pressure [Pa] during the test
 p = minimum measurable pressure [Pa] for the test, or gauge resolution

¹⁸Regardless of gauge resolution, the minimum required test duration shall be at least 10 seconds.

- *Actions to be taken if test fails*

Any condition which results in leakage in excess of the maximum allowable leak rate is corrected and re-tested.

Note: The pre-shipment leak test is not required before a shipment if the contents meet the definition for low specific activity materials or surface contaminated objects as stated in 10 CFR 71.4 [Ref. 2] and also, meet the exemption standard for low specific activity materials or surface contaminated objects as stated in 10 CFR 71.14(b)(3)(i) [Ref. 2].

8.2.2.3 Pre-Shipment Leak Test – Gas Pressure Drop Option

A pre-shipment leakage test is required before each shipment of Type B material quantities to verify proper integrity of the containment system. The following test method is a gas-pressure drop approach in accordance with ANSI N14.5-2014 table A1 test A.5.1 [Ref. 6]. Test equipment shall be calibrated and traceable to an appropriate standard.

Note: As an alternative to the pressure drop option, the pre-shipment leak test can be performed following the pressure rise method described in Section 8.2.2.2.

- *Test Personnel Qualifications*

Leakage rate testing shall be performed by personnel that are qualified and certified in accordance with the requirements of SNT-TC-1A-2006.

- *Frequency*

Testing is performed prior to each shipment of Type B material.

- *Components to be tested*

The vent port cover plate O-ring seals, and the primary or secondary lid O-ring seals, depending on which lid was removed prior to content loading. In case the contents are loaded through the primary lid, the secondary lid and vent port cover plate can be leak tested before the contents are loaded, in accordance with ALARA principles.

In case the contents are loaded through the secondary lid, the primary lid and vent port cover plate can be leak tested before the contents are loaded, in accordance with ALARA principles.

Caution: Users of the RT-100 shall be aware that containment boundary components (detailed in Figure 4.1.2-1) could have been opened during a prior shipment of Type A contents, but a pre-shipment leakage rate test might not have been performed. The user must verify that an unopened lid has been previously leak tested in accordance with the Certificate of Compliance. If this verification cannot be made, the appropriate containment boundary seal must be leak tested.

- *Testing Procedure*

1. Assemble the cask lids per Chapter 7, Section 7.1.2.2, Primary Lid Replacement,

7.1.2.3, Secondary Lid Replacement, and Section 7.1.2.4, Quick-Disconnect Valve Cover Plate Replacement. The bolts must be torqued to the specifications listed in Table 7.4.5-1.

2. Remove the applicable leak test port plug.
3. Ensure that the O-ring on the test manifold is in good condition and lubricated. Connect the pump test assembly to the appropriate test port. The test assembly should consist of a pump isolated by a valve, with a gauge indicating the system pressure.
4. Accurately determine and record the control volume. The control volume includes the volume of the interspace between the O-rings as given in Table 8.2.2-1, plus the volume associated with the measuring instrumentation manifold.
5. Determine and record the pressure gauge resolution, p .
6. Measure and record the base metal temperature of the cask lid, T_{amb} .

Note: Tests should take place at isothermal conditions, if at all possible, as temperature changes lead to corresponding pressure changes.

7. The minimum required test duration, H_{min} , shall be calculated, following the method described in the *Acceptance Criteria* section below.
8. Pressurize the cavity in the interspace between the O-rings.

Note: Minimum absolute pressure of 1.67 atm [24.5 psia] is recommended. Another pressure differential may be used provided the cask user converts the reference leak rate for the new test conditions in accordance with NUREG/CR-6847 Section 2.2.6. Refer to Section 4.3.2 for details regarding the conversion of equivalent air leakage rates.

9. Isolate the pump. Physically disconnect the pump and/or turn the pump off. Wait for the pressure to stabilize, with an absolute pressure of 1.67 ~ 1.75 atm [24.5 ~ 25.7 psia] before starting the test.

Note: Another pressure differential may be used provided the cask user converts the reference leak rate for the new test conditions in accordance with NUREG/CR-6847 Section 2.2.6. Refer to Section 4.3.2 for details regarding the conversion of equivalent air leakage rates.

10. Record the start time, t_1 , and the start pressure, P_1 .
11. After the test duration, H , record the end time, t_2 , and end pressure, P_2 . Ensure that the test duration is greater than the minimum required test duration, H_{min} .
12. Calculate the pressure change during the test, ΔP . Ensure that the pressure change is less than or equal to the pressure gauge resolution, p .

Note: This test procedure confirms functionality of the containment seal and the control seal simultaneously. In the event of test failure, either O-ring may be responsible for the leakage.

13. Replace the applicable leak test port plug.

○ *Acceptance Criteria*

The preshipment leakage rate test need not be more sensitive than 1×10^{-3} ref-cm³/s

[Ref. 6], as shown in Table 8.3-1. This corresponds to a minimum sensitivity, S_{min} , of 1.01×10^{-4} Pa-m³/s, when the pressure in the test cavity is 1.67 atm and atmospheric pressure is 1 atm. The test is carried out by the pressure drop method. Using formula B.14 given in Annex B of ANSI N14.5-2014, the test duration, H , must be greater than the minimum required test duration, H_{min} :

$$H > H_{min} = \frac{V_C \cdot p}{S_{min}} \cdot \frac{T_{std}}{T_{amb}}$$

where: H = actual test duration [s]
 H_{min} = minimum required test duration [s]¹⁹
 S_{min} = minimum required sensitivity [1.01×10^{-4} Pa-m³/s]
 p = minimum measurable pressure [Pa] for the test, or gauge resolution
 V_C = control volume [m³]
 T_{std} = standard temperature [298 K]
 T_{amb} = base metal temperature of the cask lid [K] measured during the test

Over the calculated test duration, there can be no measurable pressure rise. I.e., the minimum measurable pressure rise, ΔP , must be less than or equal to the gauge resolution, p :

$$\Delta P = P_1 - P_2 \leq p$$

where: P_1 = pressure [Pa] at the start of the test, t_1 being the start time [s]
 P_2 = pressure [Pa] at the end of the test, t_2 being the end time [s]
 ΔP = change in pressure [Pa] during the test
 p = minimum measurable pressure [Pa] for the test, or gauge resolution

○ *Actions to be taken if test fails*

Any condition which results in leakage in excess of the maximum allowable leak rate is corrected and re-tested.

Note: The pre-shipment leak test is not required before a shipment if the contents meet the definition for low specific activity materials or surface contaminated objects as stated in 10 CFR 71.4 [Ref. 2] and also, meet the exemption standard for low specific activity materials or surface contaminated objects as stated in 10 CFR 71.14(b)(3)(i) [Ref. 2].

8.2.3 Component and Material Tests

Section 8.2.3 describes periodic tests and replacement schedules for components. This section is subdivided into routine component inspection and annual component inspection.

8.2.3.1 Routine Component Inspection

Maintenance during normal use is performed to ensure that the RT-100 continues to meet design specifications and functions. Each time the RT-100 goes through the cycle of loading and

¹⁹Regardless of gauge resolution, the minimum required test duration shall be at least 10 seconds.

unloading, the following components are visually inspected:

- Fasteners: Inspect threaded studs, bolts, nuts, washers, secure pins, and thread inserts. Clean and lubricate; replace as necessary.
- Subcomponents: Inspect the condition of the primary lid, secondary lid, quick disconnect valve cover plate, upper impact limiter and lower impact limiter.
- Welds: Inspect the condition of cask attachment ring welds and cask lifting pocket welds.
- Seals: Inspect the RT-100 seals and check maintenance records to ensure the seals are within the 12 month replacement period. If replacement is necessary, contact RT and perform a leakage rate test after seal replacement.
- Labels: Inspect and record the readability of the RT-100 labeling. Repair if necessary.

8.2.3.2 Annual Component Inspection

Inspections, tests and maintenance are performed every twelve (12) months of cask service as required in accordance with the SAR and NRC compliance requirements. The following steps are performed to ensure all components are in proper working order:

1. The exterior surfaces of the cask are visually inspected for damage and the results of the survey are documented. The major components and items to be inspected include the following items:
 - Upper and Lower impact limiters
 - RT-100 body
 - Condition of the fusible plugs in the impact limiters
 - Condition and readability of RT-100 markings
2. Following procedures in Chapter 7, the RT-100 is disassembled into its components:

<ul style="list-style-type: none"> ○ Upper and Lower impact limiters ○ Primary and Secondary lids ○ Quick disconnect valve cover plate ○ Quick disconnect valve 	<ul style="list-style-type: none"> ○ Leak test port plugs ○ Cask body ○ Primary lid, secondary lid, and vent port cover plate O-rings
---	--
3. Cask visible exterior surface welds and interior cavity welds are visually inspected for defects.
4. The primary lid, secondary lid and quick-disconnect valve cover plate sealing surfaces are cleaned.
5. New inner and outer containment boundary O-rings are installed according to the recommendation of NUREG-1609 [Ref. 4].

8.2.4 Thermal Tests

No thermal tests are required for the RT-100. At least every four (4) years, testing is performed on the cask body lifting elements (lifting pockets). At the same time, examination of the inner shell visible welds parts on the cask body is performed in addition to the periodic maintenance every twelve (12) months.

8.2.5 Miscellaneous Tests

Threaded inserts may be used to repair threaded bolts holes. At a minimum, each repaired bolt hole will be tested for proper installation by assembling the joint components where the insert is used and ensuring the bolt can be tightened to the required torque. Refer to Tables 7.4.5-1 and 7.4.5-2 for applicable torque requirements.

If a threaded hole for lifting components is repaired, a load test shall be performed. The affected component must be able to withstand a load equal to 150% of the maximum service load. Each threaded insert shall be visually inspected after testing to ensure that there is no visible damage or deformation to the insert.

RT does not envision any other miscellaneous test being required of the RT-100.

8.3 Appendix

8.3.1 Summary of Leak Test Requirements

Table 8.3-1 RT-100 Leakage Test Types

Section	Component(s) to be tested	ANSI N14.5 table A1 test type	Test Frequency	Test Gas	Max. Leak Rate	Min. Sensitivity
8.1.4.1.1	Inner Shell Containment Boundary	A.5.3	Only once during fabrication	Helium	Table 8.3-2	
8.1.4.1.2	Primary Lid Assembly Containment Boundary	A.5.3	Only once during fabrication	Helium	Table 8.3-2	
8.1.4.2	Inner O-ring seals in the primary lid or the secondary lid	A.5.3	Performed prior to initial use, periodically every 12 months, and after maintenance	Helium	Table 8.3-2	
8.1.4.3	Quick-disconnect valve	A.5.3	Performed prior to initial use, periodically every 12 months, and after maintenance	Helium	No Leakage	1×10^{-3} ref-cm ³ /sec
8.1.4.4	Inner O-ring seal in the quick disconnect valve cover plate	A.5.3	Performed prior to initial use, periodically every 12 months, and after maintenance	Helium	Table 8.3-2	
8.2.2.2	Vent port cover plate O-ring seals, and the primary or secondary lid O-ring seals	A.5.2	Prior to each shipment of Type B material	N/A (vacuum)	No Leakage	1×10^{-3} ref-cm ³ /sec
8.2.2.3	Vent port cover plate O-ring seals, and the primary or secondary lid O-ring seals	A.5.1	Prior to each shipment of Type B material	Air	No Leakage	1×10^{-3} ref-cm ³ /sec

Table 8.3-2 Allowable Helium Leakage Rates

Helium Partial Pressure	Max. Leak Rate ¹	Min. Sensitivity
0.25 atm	2.672E-08 cm ³ /sec	1.336 E-08 cm ³ /sec
0.45 atm	5.137E-08 cm ³ /sec	2.569 E-08 cm ³ /sec
0.65 atm	8.185E-08 cm ³ /sec	4.093 E-08 cm ³ /sec
0.85 atm	1.263E-07 cm ³ /sec	0.632 E-07 cm ³ /sec
1.00 atm	1.897E-07 cm ³ /sec	0.949 E-07 cm ³ /sec

¹ Max. Leak Rate is taken from Table 4.3.1-2 at T=273K

8.3.2.1 Explanation of the Gap Between Lead and the External Shell

Prior to lead pouring, the cask body components that form the mold for lead pouring are heated to approximately 350°C (662°F). The components include the inner shell, outer shell, inner bottom plate and upper flange. The thermal expansion for each of these components is calculated using the thermal expansion coefficient for the materials used in the fabrication of the individual component.

$$D_m(T_2) = D_m(T_1) \cdot [1 + \lambda \cdot (T_2 - T_1)]$$

$$e(T_2) = e(T_1) \cdot [1 + \lambda \cdot (T_2 - T_1)]$$

$$H(T_2) = H(T_1) \cdot [1 + \lambda \cdot (T_2 - T_1)]$$

$$D_m(T_2), D_m(T_1), e(T_1), e(T_2), H(T_1), H(T_2)$$

Are the mean diameters, thicknesses and lengths at the temperature T_2, T_1

λ Is the stainless steel linear thermal expansion coefficient

Liquid lead is poured in the gap between the two (2) pre-heated shells. At this stage, the lead fills the cavity completely (within the specified geometry tolerances). The manufacturing tolerances ensure that the gap between the inner shell and the outer shell is 90 +5/-4 mm.

As described in Section 8.1.6, the gap between the inner and outer shells is measured to be at least 86 mm prior to lead pouring operations. Therefore, the thickness of liquid lead is at least 86 mm and there is no gap between the liquid lead and the shells.

After filling the entire annulus between inner shell and outer shell with liquid lead, the lead solidification is controlled by carrying out a progressive water rise on both the external surface of the outer shell and the internal surface of the inner shell. This process ensures that the lead solidifies beginning at the bottom of the lead column. Solidification occurs when the temperature of the shells cools to 327°C. Lead solidifies initially at the upper flange (bottom for lead pour) then progressing upward along the inner and outer shells. Liquid lead forms a 'V' shape in the vertical section of the lead column in the area of solidification.

The lead shrinkage during solidification due to the difference of densities of liquid and solid lead

at 327°C does not result in the creation of a gap between the shells and the lead because the gap formed by solidification is immediately compensated by the liquid lead from inside of the 'V' (see Figure 8.3.2-1). Therefore, the effect of lead solidification is the lowering of the liquid lead level. This is compensated by addition of liquid lead throughout the solidification process.

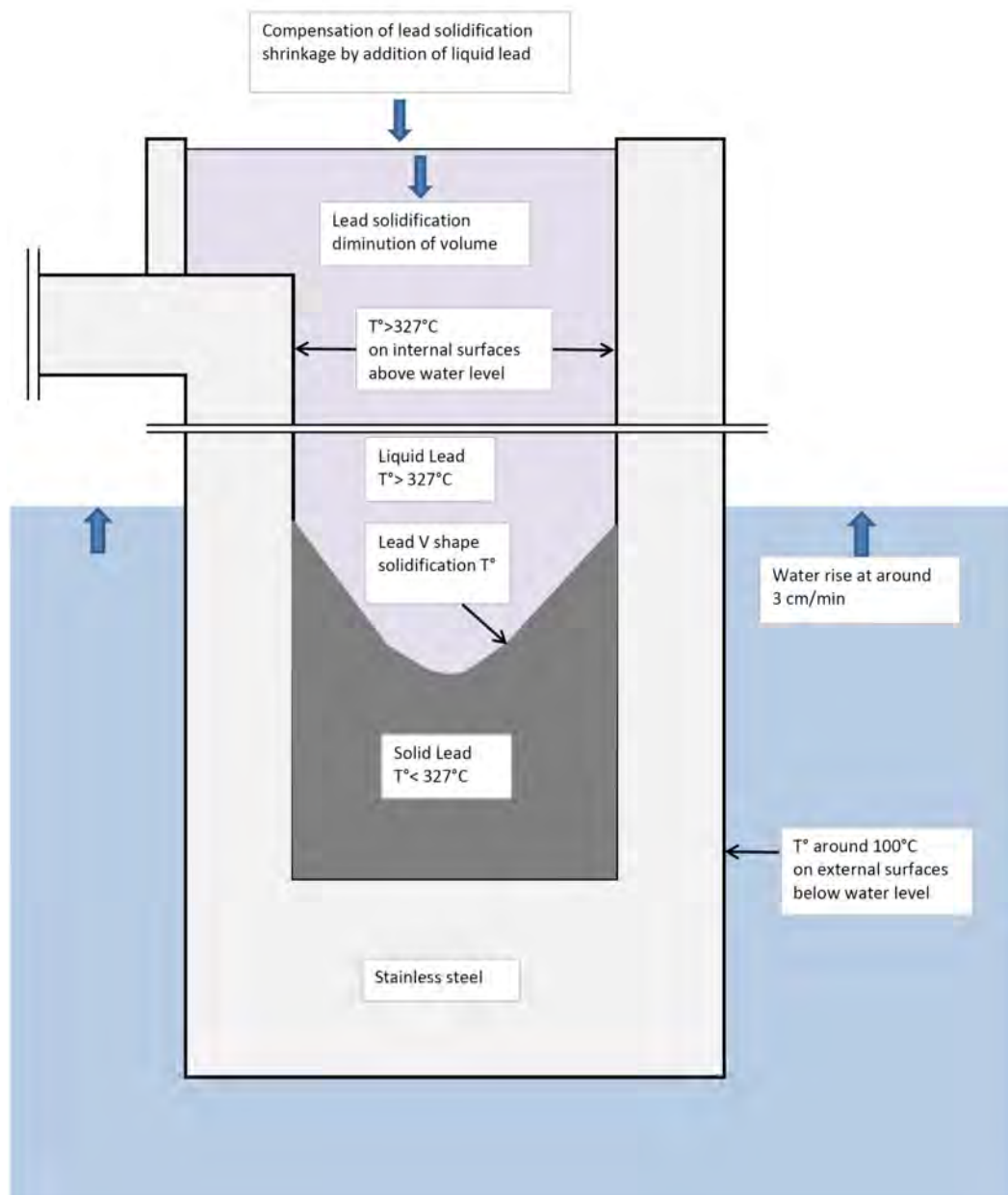


Figure 8.3.2-1 Lead Solidification Diagram

As the lead continues to cool below the solidification temperatures, a gap between the outer shell and the lead is created. This is due to the fact that the thermal expansion coefficient of lead is higher than for stainless steel. During the cooling process, the inner and outer shells shrink according to the stainless steel expansion coefficient. The lead shrinkage, which has a greater thermal expansion coefficient than the stainless steel, cannot be calculated the same way. In fact,

the lead cannot shrink freely on its inner annular surface because the inner shell (having far higher yield and tensile strength) precludes this. As a result the inner annular surface of the lead presses against the inner shell and consequently the lead shrinkage is constrained by the inner shell. It is assumed that all this missing lead shrinkage is transferred to the lead thickness only. Thus, a lead section perpendicular to the cask vertical axis shrinks following the formula:

$$S(T_2) = (1 + \lambda)^2 \cdot S(T_1) \cdot (T_2 - T_1)$$

The internal lead diameter being the outer diameter of the internal shell.

$S(T_2)$, $S(T_1)$ are the lead section areas at the temperatures

$(1 + \lambda)^2$ is the surface thermal expansion coefficient of lead.

When solidification occurs from bottom to top, the height shrinkage is compensated by addition of liquid lead on the top surface. So, vertical shrinkage is not taken in account in the gap estimation. The annular gap is created because of thermal expansion differences between lead and stainless steel as previously described.

In the calculation, the lead linear thermal expansion coefficient found in the literature is 28.9E-6 mm/mm/°C. The linear thermal expansion coefficient of stainless steel is 16E-6 mm/mm/°C which is less than what was found in the literature (average between 0° and 300°C is around 16.33E-6 mm/mm/°C according to DOT/FAA/AR-MMPDS-01 – Metallic Materials Properties Development and Standardization (MMPDS) January 2003, page 2-224 (see Figure 8.3.2-2) [Ref. 11].

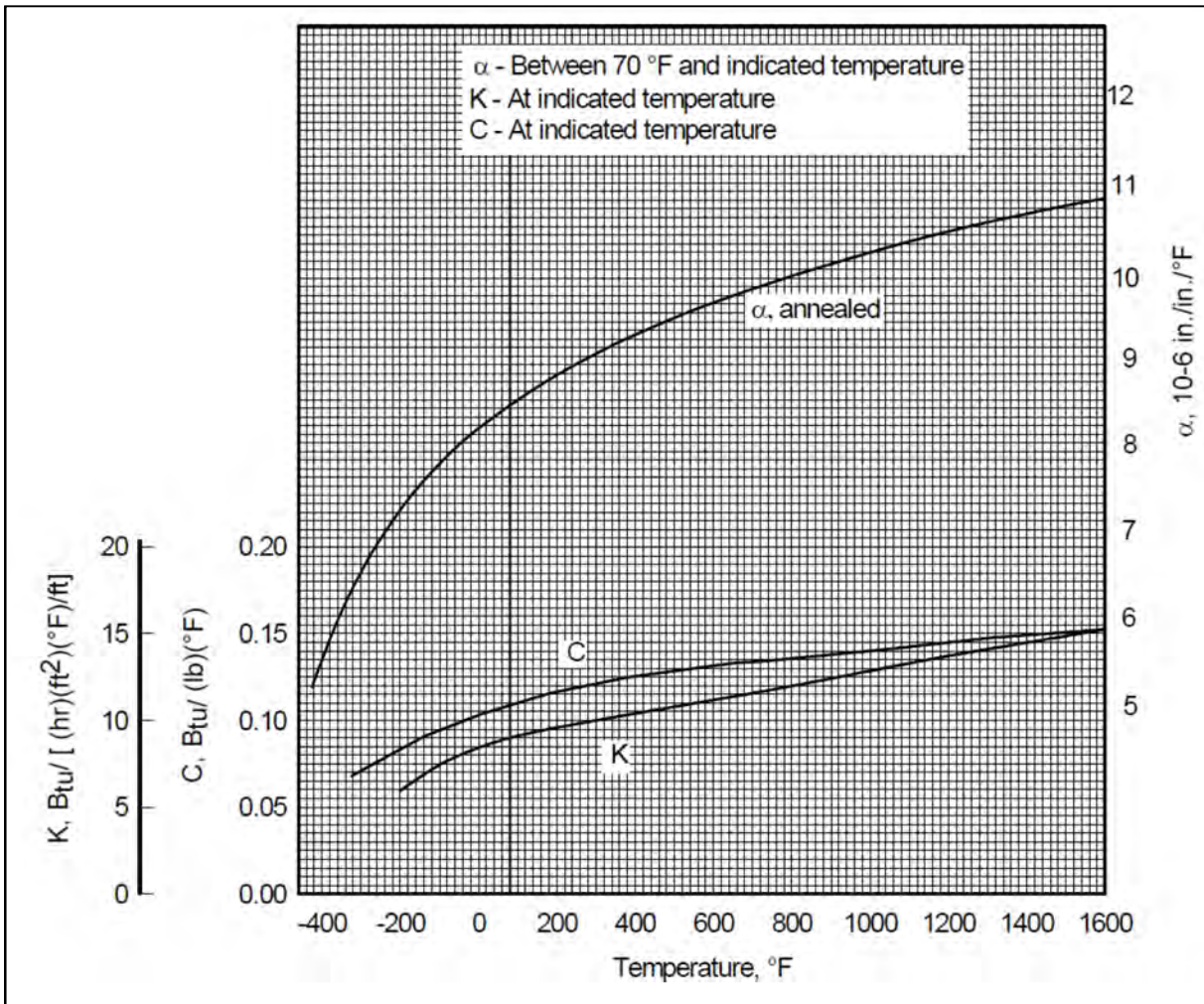


Figure 8.3.2-2 **Effect of temperature on the physical properties of AISI 301 stainless steel**
[Ref. 11]

Data

$\lambda_{\text{lead}} := 28.9 \cdot 10^{-6} \cdot \text{mm} \cdot \text{mm}^{-1} \cdot \text{K}^{-1}$	linear expansion coefficient of lead
$\lambda_{\text{steel}} := 16 \cdot 10^{-6} \cdot \text{mm} \cdot \text{mm}^{-1} \cdot \text{K}^{-1}$	linear expansion coefficient of stainless steel
$\theta_0 := 20^\circ\text{C}$	reference temperature
$\text{Dm}0_i := \frac{1790 + 1730}{2} \text{mm}$	mean diameter of inner shell at θ_0
$\text{Dm}0_o := \frac{2040 + 1970}{2} \text{mm}$	mean diameter of outer shell at θ_0
$t0_i := 30 \text{mm}$	thickness of inner shell at θ_0
$t0_o := 35 \text{mm}$	thickness of outer shell at θ_0
$\theta_s := 327^\circ\text{C}$	lead melting point

Diameter and thickness of shells at temperature θ

$$\begin{aligned}
 \text{Dm}_i(\theta) &:= \text{Dm}0_i \cdot [1 + \lambda_{\text{steel}} \cdot (\theta - \theta_0)] & \text{Dm}_i(\theta_s) &= 1.769 \times 10^3 \text{ mm} \\
 \text{Dm}_o(\theta) &:= \text{Dm}0_o \cdot [1 + \lambda_{\text{steel}} \cdot (\theta - \theta_0)] & \text{Dm}_o(\theta_s) &= 2.015 \times 10^3 \text{ mm} \\
 t_i(\theta) &:= t0_i \cdot [1 + \lambda_{\text{steel}} \cdot (\theta - \theta_0)] & t_i(\theta_s) &= 30.147 \text{ mm} \\
 t_o(\theta) &:= t0_o \cdot [1 + \lambda_{\text{steel}} \cdot (\theta - \theta_0)] & t_o(\theta_s) &= 35.172 \text{ mm}
 \end{aligned}$$

Outer diameter of inner shell and inner diameter of outer shell

$$\begin{aligned}
 D_i(\theta) &:= \text{Dm}_i(\theta) + t_i(\theta) & D_i(\theta_s) &= 1.799 \times 10^3 \text{ mm} \\
 D_o(\theta) &:= \text{Dm}_o(\theta) - t_o(\theta) & D_o(\theta_s) &= 1.98 \times 10^3 \text{ mm}
 \end{aligned}$$

Section of liquid lead at lead solidification temperature θ_s

$$S_{\text{lead.liq}}(\theta_s) := \pi \frac{D_o(\theta_s)^2 - D_i(\theta_s)^2}{4} \quad S_{\text{lead.liq}}(\theta_s) = 0.537 \text{ m}^2$$

Section of solid lead at reference temperature θ_0

$$S_{\text{lead}}(\theta) := S_{\text{lead.liq}}(\theta_s) \cdot [1 + \lambda_{\text{lead}} \cdot (\theta - \theta_s)]^2 \quad S_{\text{lead}}(\theta_0) = 0.527 \text{ m}^2$$

Inner and outer diameter of solid lead at reference temperature

$$\begin{aligned}
 D_{\text{lead.i}}(\theta) &:= D_i(\theta) & D_{\text{lead.i}}(\theta_0) &= 1.79 \times 10^3 \text{ mm} \\
 D_{\text{lead.o}}(\theta) &:= \left(\frac{4}{\pi} S_{\text{lead}}(\theta) + D_{\text{lead.i}}(\theta)^2 \right)^{\frac{1}{2}} & D_{\text{lead.o}}(\theta_0) &= 1.969 \times 10^3 \text{ mm}
 \end{aligned}$$

Gap between lead and outer shell

$$j(\theta) := \frac{D_o(\theta) - D_{\text{lead.o}}(\theta)}{2} \quad j(\theta_0) = 0.687 \text{ mm}$$

8.3.2.2 Conclusion

Drawing RT100 PE 1001-1, Rev. H (Chapter 1, Appendix 1.4, Attachment1.4-2), specifies that the gap between the inner and outer shells prior to lead pouring is required to be $90 +5 / -4$ mm. This dimension is measured during the fabrication process to ensure that the minimum lead thickness of 85 mm will be maintained including the subsequent lead shrinkage during cooling, given that the thickness prior to lead pour is ensured to be at least 86 mm. The evaluation of lead shrinking during the cooldown process described above shows a final calculated gap between the outer shell and the lead of 0.687 mm.

8.4 References

1. Robatel Technologies, LLC, Quality Assurance Program for Packaging and Transportation of Radioactive Material, 10 CFR 71 Subpart H, Rev. 2, Dated November 10, 2017 and NRC Approved on March 21, 2012
2. U.S. Nuclear Regulatory Commission, 10 CFR Part 71--PACKAGING AND TRANSPORTATION OF RADIOACTIVE MATERIAL
3. U.S. Nuclear Regulatory Commission, REGULATORY GUIDE 7.9 – Standard format and content of Part 71 applications for approval of packages for radioactive material, dated March 2005
4. U.S. Nuclear Regulatory Commission, Standard Review Plan for Transportation Packages for Radioactive Material, NUREG-1609, March 31, 1999
5. ASME Boiler & Pressure Vessel Code 2007 Edition, Section III – Division 1 – Subsection ND, "Class 3 Components", The American Society of Mechanical Engineers, Three Park Avenue, New York, NY, www.asme.org.
6. ANSI N14.5-2014, "American National Standard for Radioactive Materials – Leakage Tests on Packages for Shipment," American National Standards Institute, Inc., 11 West 42nd Street, New York, NY, www.ansi.org.
7. ASTM E 499-1996, "Standard Test Methods for Leaks Using the Mass Spectrometer Leak Detector in the Detector Probe Mode," ASTM International, 100 Barr Harbor Drive, West Conshohocken, PA, www.astm.org.
8. ANSI N14.6-1978, "American National Standard for Special Lifting Devices for Shipping Containers Weighing 10000 pounds (4500 kg) or More for Nuclear Materials," American National Standards Institute, Inc., 11 West 42nd Street, New York, NY, www.ansi.org.
9. ASME Boiler & Pressure Vessel Code 2007 Edition, Section III – Division 1 – Subsection NF, "Supports", The American Society of Mechanical Engineers, Three Park Avenue, New York, NY, www.asme.org.
10. SFPE Handbook of Fire Protection Engineering, "Thermal Decomposition of Polymers," C.L. Hirschler, M. Marvelo, Chapter 7 of 3rd Edition, NFPA, 1 Batterymarch Park, Quincy, MA, 2001, www.nfpa.org.
11. DOT/FAA/AR-MMPDS-01, "Metallic Materials Properties Development and Standardization (MMPDS)," U.S. Department of Transportation – Federal Aviation Administration, Washington, DC, www.ntis.gov.
12. 102885 EQN 001, Rev C, "Equivalence Table – ASNT / COFREND – Qualification and Certification of NDE Personnel" (PROPRIETARY)
13. Recommended Practice No. SNT-TC-1A-2006: Personnel Qualification and Certification in Nondestructive Testing. Columbus, OH: The American Society for Nondestructive Testing, Inc.